FLUIDIZED BED GASIFICATION OF BIOMASS

KYRIAKOS MANIATIS
Doctor of Philosophy

THE UNIVERSITY OF ASTON IN BIRMINGHAM

October 1986

To my parents and Tassos

The University of Aston in Birmingham.
Fluidized bed gasification of biomass.
Kyriakos Maniatis
Doctor of Philosophy
1986.

SUMMARY

A fluidized bed process development unit of 0.8 m internal diameter was designed on basis of results obtained from a bench scale laboratory unit. For the scaling up empirical models from the literature were used. The process development unit and peripheral equipment were constructed, assembled and commissioned, and instruments were provided for data acquisition.

The fluidization characteristics of the reactor were determined and were compared to the design data. An experimental programme was then carried out and mass and energy balances were made for all the runs. The results showed that the most important independent experimental parameter was the air factor, with an optimum at 0.3. The optimum higher heating value of the gas produced was 6.5 MJ/Nm^3, while the thermal efficency was 70%.

Reasonably good agreement was found between the experimental results, theoretical results from a thermodynamic model and data from the literature. It was found that the attainment of steady state was very sensitive to a continuous and constant feedstock flowrate, since the slightest variation in feed flow resulted in fluctuations of the gas quality.

On the basis of the results a set of empirical relationships was developed, which constitutes an empirical model for the prediction of the performance of fluidized bed gasifiers. This empirical model was supplemented by a design procedure by which fluidized bed gasifiers can be designed and constructed. The design procedure was then extended to cover feedstock feeding and gas cleaning in a conceptual design of a fluidized bed gasification facility. The conceptual design was finally used to perform an economic evaluation of a proposed gasification facility. The economics of this plant (retrofit application) were favourable.

KEYWORDS

Fluidized bed, biomass gasification, empirical model design procedure, conceptual design.

ACKNOWLEDGEMENTS

I would like to thank the several people who helped and assisted me during the execution of this work and I am obliged for their kindness. More in particular:

- I want to express my graditute to Dr. A.V. Bridgwater for his continuous support, advice, guidance as well as for his unyielding efforts to make this PhD take place. Had it not been for him, this work would never have been completed.
- I am deeply obliged to Professor Dr. Ir. A. Buekens for supporting this postgraduate study at Aston University, while the actual work took place in the CHIS laboratory at the Free University of Brussels.
- I wish to thank Dr. Ir. J. Schoeters for his friendship, good-fellowship, advice and support during the long late evenings at the CHIS laboratory. He always had "a minute" to discuss for hours the complicated behaviour of fluidized bed gasifiers.
- Professor S. Wajc, Professor G. Baron and all my other colleagues at the department of Chemical Engineering and Industrial Chemistry of the Free University of Brussels for their friendship and support for this work.
- Mr D. Vyncke for his kind permission to use part of the results of the Vyncke Warmtetechniek N.V. - VUB - IWONL project for this thesis.
- Mr D. Van Engeland, Mr M. Cortenville of the R&D department of this company and the several technicians who assisted during the construction, commissioning, maintenance and experimentation of this work.
- Mrs L. de Nijs for the painstaking typing of the thesis and Dr. A.J. Whitten for his kind disposition of the computer facilities.
- Last but not least my wife for she provided the support and push during the difficult moments when decisions were critical and Danae who had to share me with this work during her first four years.

CONTENTS

LIST OF TABLES

APPENDIX - TABLES

LIST OF FIGURES

CHAPTER TWO : LITERATURE REVIEW

CHAPTER ONE: INTRODUCTION

It has been estimated that about 2070 million tons of waste were produced in the European Economic Community in 1982, equivalent to nearly 5.7 million tons per day (1). The annual total consists of the components and arisings shown in Table 1.1. Moreover the stream of waste is expected to increase by 2 to 3 % annually - although there are variations from country to country - in spite of the low rate of growth in industrial production and in gross national product (1).

Table 1.1: 1982 estimated arisings of wastes in EEC (1).

Component	tons x 10^6
Household waste	120
Agricultural waste	950
Industrial waste	160
Sewage sludge	300
Waste from extractive industries	250
Demolition waste and debris	170
Consumer waste (used vehicles, tyres, etc)	120

It is obviously worthwile therefore to develop technologies which can use these waste materials to the full (produce energy or reclame usefull components) and reduce the volume of waste arising from today's communities; in particular because these recycling processes can to some extent help to solve increasingly serious environmental problems.

Now that energy is no longer cheap, it ranks in importance with the classical factors of production (land, labor and capital) and its supply and cost must be given due weight in planning on national as well as industrial level. These considerations apply not only to forms of energy that are traded internationally, but also to energy that is produced and consumed domestically, and to traditional as well as commercial fuels, because the prices, availability and consumption levels of all forms of energy are inextricably interrelated. The world commercial energy consumption for the years 1975 to 1990 is shown in Table 1.2.

Table 1.2: World commercial energy consumption, 1975-90 (2).
(Million barrels a day of oil equivalent)

	1975	1980	1985	1990	Average annual growth percent 1950-74	1975-80	1980-90
World	122.1	137.8	166.0	201.5	5.0	2.5	3.9
Developing Countries	13.9	16.7	22.3	30.6	6.9	3.7	6.2
Oil Importing Dev. Coun.	10.4	12.4	16.8	22.8	6.9	3.6	6.3

1985, 1990: estimated data.

Energy consumption in developing countries accounts for a small part of the world total, but has been growing much faster than in the developed countries (2). During the 1980s commercial energy consumption in these countries is projected to grow at 6.2 % a year. It is obviously a matter of great urgency that all countries take effective measures to reduce their energy consumption, but no country can afford to wait for a unified global effort. It is crucial both to continue to expand efforts to use energy efficiently and to increase domestic production. Under this realistic scenario energy containing wastes can be considered as a low grade fuel.

Since this work is concerned with energy from biomass in particular, the estimated arisings of the principal biomass sources in countries of the European Community and their energy content are shown in Table 1.3.
The EEC is characterized by low land availability and high density of population; therefore the utilization of the energy in the higher energy content wastes could not only alleviate the energy shortage, but also help solve some of the associated disposal problems.

Thermal, thermochemical and biochemical processes are available for this purpose with the added benefit that the final volume for disposal is only a fraction of the volume of waste (usually less than 10 % for the first two and less than 40 % for the biochemical processes!). Combustion is the most developed process for utilizing biomass (4); however, the utilization of the energy produced is either limited to production of steam, hot water or hot air. Pyrolysis, gasification and biomethanation are particularly attractive

processes as they all produce storable and transportable fuels in either gaseous, liquid or solid form. These fuels can, in principle, be burned efficiently with only minor modifications to existing equipment. Thermochemical processes are generally more efficient than biological ones.

Table 1.3: 1979 Estimated overall national arisings of potential energy from principal agricultural residues (millions of GJ/yr. unless otherwise stated) (3).

	Cereal, Maize and Rice Residues	Livestock (1) Wastes	Green Plant (2) Matter	Total	Total in Mtoe
Germany	327.1	129.7	40.0	496.8	11.29
France	556.6	171.2	59.3	787.1	17.89
Italy	233.7	81.7	37.3	352.7	8.02
Holland	16.4	45.6	17.7	79.7	1.81
Belgium and Luxembourg	27.1	27.3	12.3	66.7	1.52
U.K.	191.4	99.2	20.7	311.3	7.08
Ireland	21.9	38.1	3.3	63.3	1.44
Denmark	98.7	29.2	6.4	134.3	3.05
	1,472.9	622.0	197.0	2,291.9	52.10

(1) Presented as biogas available from pig, cattle and poultry by anaerobic digestion, not as gross energy, animal bedding excluded.

(2) Presented as biogas available by anaerobic digestion: other conversion routes are available. No data available for Greece, Spain and Portugal.

This is because in biological processes only a fraction of the waste, that is the biomass components which can be attacted by bacteria (such as hemicellulose, sugars; whereas lignin cannot be converted by methanogenic bacteria) (5), is converted to energy leaving a residue which is often used as compost.

However not all types of waste can readily be used in the above mentioned processes without some pretreatment. The crop residues, animal wastes and unused forestry byproducts shown in Table 1.3 offer an immediate opportunity to meet about 3 % of the 1980 EEC energy demand (1200 Mtoe) by the year 2000 (3). With the introduction of energy crops (perennials on available land and catch crops with little disturbance to existing agriculture

and forestry), some local energy needs can be covered and the potentional contribution could be about 45 Mtoe by the year 2000 : a total of 7.5 % of the 1980 EEC energy demand (6). Table 1.4 shows the maximum energy content of the various types of biomass, which could be harvested as energy feedstocks by the year 2000 in the European Community (7). If that degree of utilization (75.1 Mtoe) could be attained, it would represent 6 % of the estimated consumption (EC 9) by the year 1985.

Table 1.4: Maximum energy content of dry and wet crop residues, animal wastes (bedding included), forestry and wood wastes, dry and wet biomass from energy productions, which could be harvested as energy feedstocks by the year 2000 in the European Community (9 members states)(7).

	Animal wastes (1) CH_4 Mtoe (3)	Wet crop residues (1) CH_4 Mtoe	Dry crop residues (2) Mtoe (3)	Forestry and wood wastes (2) Mtoe	Firewood (2) Mtoe	Total harvest-able	Energy product-ion wet CH_4 Mtoe	Energy product-ion dry Mtoe	Total Biofuels Mtoe
UK	2.0	0.1	1.1	0.3	0.2	3.7	1.0	7.2	11.9
EIR	0.6	-	-	-	-	0.6	0.1	2.4	3.1
DK	0.5	-	1.1	0.1	-	1.7	0.5	0.5	2.7
NL	0.6	0.1	-	0.1	-	0.8	0.1	-	0.9
B&L	0.5	0.1	-	0.3	0.3	1.2	0.2	-	1.4
D	2.4	0.2	2.5	1.3	1.9	8.3	1.6	1.9	11.8
F	3.7	0.6	4.8	4.5	2.8	16.4	3.4	12.7	32.5
I	1.2	0.4	1.5	1.3	1.4	5.8	1.6	3.4	10.8
CE 9	11.5	1.5	11.0	7.9	6.6	38.5	8.5	28.1	75.1(4)

No data available for Greece, Spain, Portugal.

(1) As net production of methane, 40% of the production being used to heat the digestor

(2) Energy content of the solid fuel

(3) Straw used as bedding incorporated in animal wastes

(4) 6% of the estimated consumption (EC 9) by the year 1985

The potential for biomass is significant not only for the industrialized world but even more for the developing countries. Their economy is mainly based on intensive labour agriculture and foresty (8) - practices which produce

considerable quantities of wastes. If the energy content of biomass could be converted to fuels and chemicals, it would offer significant reduction in their energy demand and consequent problems of lack of foreign exchange.

Biomass is renewable and often abundant. Photosynthesis produces an amount of 'stored energy' in the form of biomass which is about ten times the world's annual use of energy (6). Thus the stored biomass on the earth's surface at present is equivalent to the proven fossil fuel reserves. This massive-scale capture of solar energy and conversion into a "stored product" occurs with only a low overall efficiency of about 0.1 % on a world-wide basis, but because of the adaptability of plants it takes place and can be used over most of the earth (6). Studies on tree growth and production methods as "wood fuel farms" or "energy plantations" are in progress with promising results (9,10), while the competition for available land between energy plantations and agriculture for food production in some cases can be overcome by the utilization of aquatic biomass.

1.1 PROPERTIES OF BIOMASS RELEVANT TO GASIFICATION

Plants are made up of individual cells, each of which has elaborated a cell wall that together serve to define the morphology of the plants, provide its structural support and control the passage of water and nutrients. They all consist predominantly of polysaccharides, of which cellulose is the most abundant, and in case of woody plants they contain another important component : lignin (4).

1.1.1 Chemical composition

Cellulose comprises approximately 50 % of all biomass while lignin comprises about 25 % (7). The third major cell wall component is hemicellulose which is closely associated with the skeletal polysaccharide cellulose, comprising approximately the remaining 25 % of the cell wall material. The specific composition of seven species along with their energy content is presented in Table 1.5 (9).

Table 1.5 : Chemical composition of wood species (9)

Tree species	Cellulose wt %	Lignin wt %	Hemi-celluloses wt %	Higher heating value MJ/kg
Beech	45.2	22.1	32.7	19.6
White birch	44.5	18.9	36.6	19.3
Red maple	44.8	24.0	31.2	19.4
White cedar	48.9	30.7	20.4	19.4
Hemlock	45.2	32.5	22.3	20.6
Jack pine	45.0	28.6	26.4	20.7
White spreuce	48.5	27.1	21.4	20.6

The different chemical compositions are responsible for varying heat contents among wood fuels. Holocellulose (cellulose and hemicellulose) and lignin offer significantly different heats of combustion: 17.46 MJ/kg for holocellulose and 26.63 MJ/kg for Douglas fir lignin. As Table 1.5 shows, there is some association between the lignin content and calorific value. As the lignin content of wood species rise, so does the higher heating value of the wood.

A more traditional approach to combustible fuels evaluation employs the ultimate analysis of the material. Table 1.6 presents the ultimate analysis of numerous biomass and coal fuels on a dry weight basis (9).

These data demonstrate generally that wood is a highly oxygenated fuel with about two-thirds the energy content of coal. Softwoods (Douglas Fir and Redwood) generally contain more energy than hardwoods (Beech and Maple) on a dry weight basis due to higher lignin (hence carbon) content. The ultimate analysis shown in Table 1.6 strongly indicates a relationship between carbon content and higher heating value. These data also suggest that wood is the transition fuel between the waste materials (4.7 - 13.1 MJ/kg) and coal (30.3 - 33.4 MJ/kg).

Table 1.6 : Ultimate analysis of selected fuels (9).

Fuel	Ultimate analysis dry wt %						
	C	H	O	N	S	Ash	HHV.MJ/kg
Utah coal	77.9	6.0	9.9	1.5	0.6	4.1	32.8
Pittsburgh coal (a)	75.5	5.0	4.9	1.2	3.1	10.3	31.6
Pittsburgh coal (b)	73.3	5.3	10.2	0.7	2.8	7.6	30.3
Wyoming coal	70.0	4.3	20.2	0.7	1.0	13.8	33.4
Douglas fir.	52.3	6.3	40.5	0.1	0.0	0.8	20.9
Red wood	53.5	5.9	40.3	0.1	0.0	0.2	20.9
Beech	51.6	6.3	41.5	0.0	0.0	0.6	20.3
Maple	50.6	6.0	41.7	0.3	0.0	1.4	19.9
Bagasse	47.3	6.1	35.3	0.0	0.0	11.3	21.2
Rice husks	38.5	5.7	39.8	0.5	0.0	15.5	15.3
Rice straw	39.2	5.1	35.8	0.6	0.1	14.2	15.1
Municipal solid waste	33.9	4.6	22.4	0.7	0.4	38.0	13.1
Sewage sludge	14.2	2.1	10.5	1.1	0.7	71.4	4.7

1.1.2 Moisture content

Wood has the disadvantage of the presence of moisture in significant quantities in relation to coal. Fresh wood may contain upward of 22 to 55 wt % moisture and at times may contain as much as 70 wt % moisture on as received basis. The moisture successfully denotes the many variations in wood fuel because the moisture content significantly influences the net heating value of wood fuels, the ignition properties and the overall efficiency of fuel utilization (4).

The influence of moisture on higher heating value can be calculated by the following conceptual formula :

$$NHV = HHV - (Lw + LHV) \qquad \text{equation 1.1}$$

where NHV is the net heating value, HHV the higher heating value, Lw the loss in weight of combustible products as water replaces wood and LHV the loss due to heat of vaporization required to remove the water. The above conceptual formula leads to a more precise formula which is :

$$HHV = HHV - [0{,}0114\,(HHV) \times M] \qquad \text{equation 1.2}$$

where M is the moisture content expressed as a percent of total as received fuel material (9).

1.1.3 Potential pollutants analysis

Traditionally, sulphur and ash are considered the principal impurities in combustible fuels. The sulphur on combustion forms sulphur dioxide which is a pollutant. It also can combine with rain to form dilute sulphureous acid. The ash results in the release of particulates up the smokestack. These pollutants can be controlled by devices such as gas scrubbers, cyclones and baghouse installation. All such installations, however, reduce the energy efficiency of a given operation.

The ultimate analysis presented in Table 1.6 shows wood to be very low in sulphur and ash. These values demonstrate that wood is essentially pollution free in relation to the other fuels, although wood thermochemical processing plants require some particulate control. From the point of view of controlling formation of sulphur dioxide and prohibiting the release of particulate matter, wood is a more desirable fuel than any of the other solid fuels of Table 1.6. In an era of environmental consciousness, this advantage is a compelling attraction for the biomass energy source.

1.2 NATURE OF GASIFICATION

Gasification of biomass is a combination of several individual processes which take place in series and or in parallel in a gasifier. Five different stages can be broadly distinguished in the gasification of biomass (7).

1. Drying of the biomass: moisture is evaporated.
2. Pyrolysis or thermal degradation: volatile components are distilled off to produce char, condensibles (tar) and non condensible gases.
3. Gasification of the char: reactions of steam and carbon dioxide with the char that yield hydrogen and carbon monoxide.

4. Combustion of the remaining char to produce carbon dioxide and water and to supply the energy required for sustaining a certain operating temperature.
5. Gas phase pyrolysis/gasification of tars.

However, there is usually no clear distinction between the various stages especially with reactors which under normal operating conditions exhibit high local heating rates (above 100° C/s, see section 2.2.2).

1.3 DEFINITIONS

In the literature on waste disposal the terms" pyrolysis" and "gasification" are regularly used. Their significance is however often blurred and not well understood. This is also the case for the term "biomass" which is used among others for wood and municipal solid waste. The following definitions will apply for this thesis:

Biomass is the wide range of products which have been derived from the process of photosynthesis. These include standing forests and crops; products, wastes and residues from forestry and agricultural processes; aquatic plants and weeds; as well as the lignocellulosic fraction of urban waste. Thus everything which has been derived from the process of photosynthesis is a potential source of energy.

Pyrolysis is the thermal degradation of organic matter in the absence of an oxidizing reactant (anaerobic atmosphere). [illegible] pyrolysis the volatiles are driven-due to thermal effects - out of the substrate, resulting in char condensable liquids or tars and gaseous products.

Gasification or partial oxidation is the combination of thermal decomposition of organic matter followed by reactions of the char, tar and primary gases with oxidizing reactants, yielding mainly low molecular weight gaseous products (aerobic atmosphere).

In this thesis the term Pyrolysis will refer to strict thermal decomposition processes in anaerobic conditions and will be considered as a precursor to gasification; while gasification is the entire process of thermochemically converting biomass into a predominantly gaseous fuel with an oxidant.

1.4 BACKGROUND

During the initial stages of this work and through an extensive literature review on the gasification of biomass with special emphasis on fluidized bed reactors, it became clear that although considerable work had been carried out, this was often incomplete and with contradicting conclusions and results. After studying the theory of gasification as well as the available models for fluidized bed gasifiers, it became apparent that no work had been carried out which considered gasification of biomass in a fluidized bed reactor with a comprehensive methodology for reactor design. Most of the works either studied the gasification process while ignoring the engineering and feasibility study, or economics and feasibilities studies were presented based on experimental assumptions. In addition, no direct comparison appears to have been made between the various available models (empirical or analytical) for the design of fluidized bed gasifiers, and it was not possible to generalize the available ones for the design of gasification plants.

Another potential limitation on the reliability of those models was the relatively small size of reactors generally used in those studies, which could result in uncertainty on scaling up. It became evident that the gasification of biomass and the conceptual design of a fluidized bed gasifier plant had to be studied together in order to obtain a detailed and comprehensive design procedure. In order to achieve this objective, a reasonably large scale reactor (pilot plant) had to be used to obtain reliable results for scaling up purposes.

1.5 METHODOLOGY

A fluidized pilot plant gasifier was designed on the basis of previous laboratory experiments and subsequently constructed, tested and commissioned. A substantial experimental programme was performed and a large data bank of results was created. The results obtained were then compared to those from the literature, and from the experimental results an empirical model was derived for the prediction of the performance of fluidized bed gasifiers. Then a design procedure, covering feeding, fluidized bed gasifier and particulates removal, was developed. Finally a conceptual design of a fluidized bed gasifier plant was made, which examines all major aspects of engineering and characteristics of the reactor and peripheral equipment. Where possible, alternative solutions are presented, so that a

comprehensive conceptual design is obtained. This is considered to be the main contribution of this work to the field of biomass gasification.

1.6 OBJECTIVES

The objectives of this thesis are:

I) to describe the design of the fluidized bed pilot plant and its subsequent construction, commissioning and testing;

II) to study the product characteristics from air gasification of wood and to assess the influence of the operating parameters (such as temperature, air to feedstock ratio, feedstock flowrate) on the gasification process and product characteristics;

III) to develop and compare a new design procedure for fluidized bed gasifiers based on empirical correlations, so that this type of gasifier can be designed and scaled with greater confidence and without reliance on computer packages;

IV) to exemplify the new design procedure with a conceptual design for a specific fluidized bed gasification process.

CHAPTER TWO: LITERATURE REVIEW

2.1 INTRODUCTION

In this chapter the literature on the subject of biomass gasification in fluidized bed reactors is reviewed. This begins with a discussion of the general principles of thermochemical conversion of biomass and the differences between pyrolysis and gasification. Then the advantages and disadvantages of the various types of gasifiers are examined. The review considers the principles and theory of fluidized bed reactors and a comprehensive review of published data on the subject of biomass gasification in fluidized bed reactors is presented. Although special emphasis is given to the subject of air gasification of biomass in single fluidized bed reactors operating at atmospheric pressure, both oxygen and catalytic gasification in single and dual bed systems are also reviewed since they can be used for comparison and suggest possible extensions to this work.

The chemistry of biomass gasification is then examined and the different approaches (thermodynamic, kinetic rate laws and empirical models) for modelling biomass gasifiers are presented and evaluated, with special reference to fluidized beds.

Another aim of this chapter is to evaluate published data which are needed for designing and operating fluidized bed gasifiers. These are compared to the results obtained from the experimental programme later in this thesis. These data and results are then incorporated into the conceptual design of a fluidized bed biomass gasification plant.

2.2 THE THERMOCHEMICAL CONVERSION OF BIOMASS

There are three thermochemical processes by which biomass can be converted into useful products: gasification, pyrolysis and liquefaction. The general principles of these processes are presented in Figure 2.1.

Of these three processes, the liquefaction process is beyond the scope of this thesis, since it produces predominantly liquid products under particular processing conditions in an essentially liquid phase process.

The gasification route is shown to be the more versatile one in view of possible products and applications. This characteristic of gasification offers

the advantage that in principle a single reactor concept could be used in more than one gasification route (for example fluidized beds can be operated either with air, oxygen, steam or mixtures of these oxidants to produce low or intermediate higher heating value gas under different operating conditions).

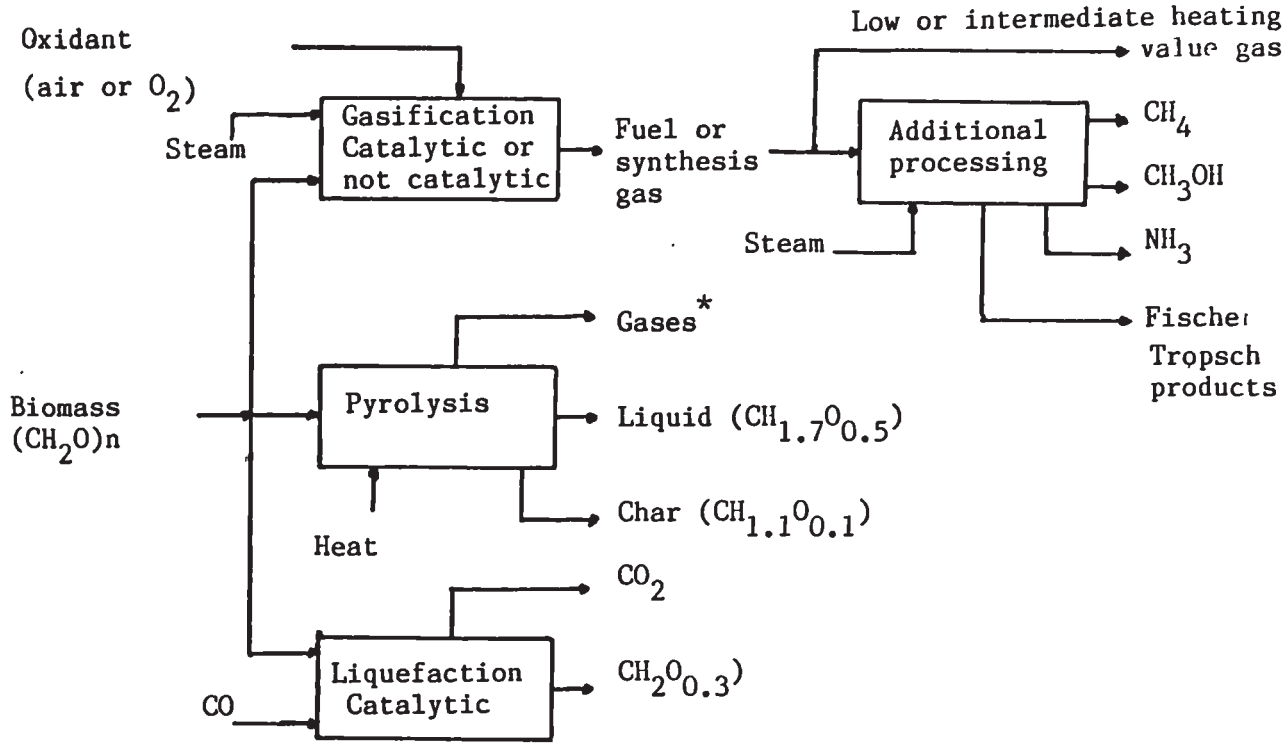

* H_2,CO,CO_2,H_2O,CH_4,C_2H_4,C_3H_6

Figure 2.1: Generalized block diagram for the thermochemical conversion of biomass (11).

2.2.1 Pyrolysis and gasification-general principles

Prolysis and gasification are two thermochemical processes by which solid organic materials can be converted into useful products. Pyrolysis is the thermal degradation of organic materials in the absence of oxygen (see section 1.3). It is a relatively low temperature process (300 °C to 700 °C) with pyrolytic oil and solid char residue as the main products, while some gas is also produced which can be used as fuel. Pyrolysis is also a precursor to gasification.

Gasification on the other hand, is the thermochemical conversion of organic materials in the presence of oxidizing gases. This process takes place at relatively high temperatures (650 °C to 1300 °C) and can be used to convert biomass virtually completely to combustible gas or synthesis gas. The

former can be utilized as fuel, while the latter as feedstock for chemical synthesis or fuel synthesis (ammonia, methanol) as well as in the petrochemical industry (12,13).

The relative yields of the products of both processes depend upon many factors, the most important of which are the physical properties of the feedstock, the rate of heating, the initial and final temperatures, the type of contacting device used, and in the case of gasification the gasifying medium as well (11, 13). Furthermore in the case of gasification, these changes are accompanied by chemical reactions amongst the volatiles, the char residue and the gasifying medium (see sections 2.5.3, 2.5.5), which influence the characteristics of the product gas (composition, yields). Thermodynamics also have a significant influence on the final composition of the product gas (see section 2.5.4), since under most high temperature operating conditions thermodynamic equilibrium is closely approached (15). Some of the chemical changes occuring during pyrolysis and gasification can be shown in a ternary diagram (16), see Figure 2.2.

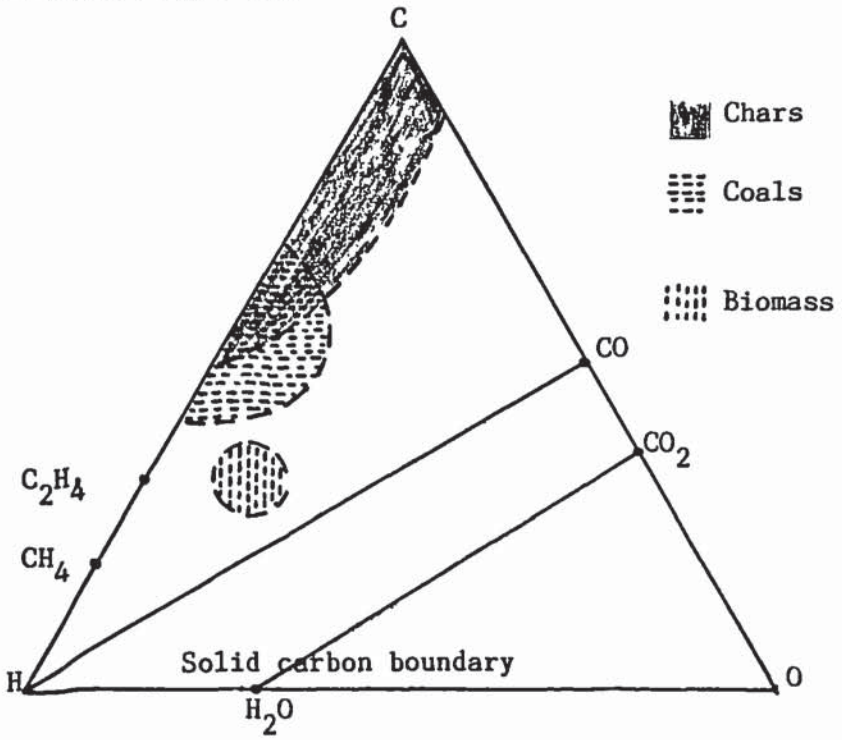

Figure 2.2: Chemical changes during biomass gasification or pyrolysis

Although this presentation is somewhat simplified, it is useful for showing the possible process routes and products.

Since gasification cannot proceed unless pyrolysis has taken place, the latter process must also be included in any analysis. A more detailed description of the chemical changes occuring during pyrolysis and gasification is given in sections 2.5.3 and 2.5.5. This discussion is included in the section concerning modelling of fluidized bed gasifiers for subject cohesion (see section 2.5). Since fluidized beds are only one type of gasifiers, first the different reactor concepts are discussed and then fluidized bed reactors are presented in detail.

2.2.2 Types of reactors used in thermochemical conversion of biomass

Many different kinds of contacting devices such as moving bed, entrained bed, fluidized bed and rotary kilns have been proposed and used for the pyrolysis and/or gasification of carbonaceous feedstocks (13, 16-18). A variety of methods have been used to classify the different types of reactors.

In this work gasifiers are classified in terms of the amount of biomass present in the reactor under normal operating conditions relative to the total reactor volume. This density factor is an important characteristic of gasifiers. Hence gasifiers can be clasified as lean and dense phase reactors (19). The ratio of the volume of biomass over the volume of reactor can be used as an illustrative parameter. Typical values are in the range of 0,05-0,2 and 0,5-0,8 respectively for lean and dense phase gasifiers (20). In general lean phase reactors have a low solid to reactor volume ratio, with relatively small amounts of feedstock occupying only a small fraction of the total reactor volume. In dense phase reactors the feedstock occupies most of the reactor volume.

2.2.2.1 Dense phase reactors

The most common reactors of this type are the co-current downdraft and the counter-current updraft (21, 22, 23). The names co-current and counter-current indicate the relative motion of the gases and the biomass bed in respect of each other, while the names updraft and downdraft indicate the relative motion of the gases in respect of the gasifier. The biomass bed is generally supported on a grate and always moves downwards by gravity.

Dense phase reactors have a long history and were the first types of gasifiers produced commercially. Their main advantages are simplicity in construction

and operation. One important characteristic of dense phase reactors is that distinct reaction zones of drying, pyrolysis, oxidation and reduction exist within the reactor (21, 22). A relatively new concept of stratified downdraft gasifier has been reported recently (23), in which only two zones can be distinguished, one of flamming pyrolysis and the other of char gasification.

The co-current downdraft gasifier features a co-current flow of gases and solids through a descending packed bed for a major part of its volume. The pyrolysis gases pass through the hot char bed which is supported on the grate, and this cracks the larger, more complex compounds into non condensible gases and water (16, 17, 24).

In the counter-current updraft configuration, the flow of gases and solids is in opposite direction. The pyrolysis gases which ascend, do not pass through the hot bed of char or through a high temperature gasification zone and consequently the product gas contains a high level of tar and organic condensibles (22, 24).

The operating principles, together with typical temperature and conversion profiles, are given in Figure 2.3 for both types of gasifiers. From this figure it can be seen that typical operating temperatures are about 1000 °C and 1200 °C for the counter-current updraft and the co-current downdraft respectively. Conversion of feedstock into gas for both types generally approaches 100%. Figure 2.3 also depicts a common feature of co-current downdraft gasifiers, being a "throat" or restriction. This is normally at or below the inlet of the oxidizing medium and its main purpose is to avoid channeling and bypassing of pyrolysis products through the oxidation zone. These pyrolysis products are cracked to lower molecular weight hydrocarbons as they pass through the high temperature zone at the throat (25-28).

Co-current downdraft gasification is simple, reliable and proven for certain fuels, such as relatively dry (about 15 wt % moisture) with low ash content (below 1 wt %) and neither fine nor coarse particles (chips not smaller than about 2 cm and not bigger than about 10 cm longest dimension (23)). Due to the low content of tars in the gas, it is generally favoured for electricity generation via an internal combustion engine and is usually promoted for Third World applications, since gasifiers of this type can easily be fabricated and operated and relatively small scale units are feasible for low shaft

power generation (e.g. irrigation pumps) (29). There are however difficulties in scaling up, but this can be overcome with multiple units if economics permit. Producer gas from counter-current updraft gasifiers requires substantial clean up if further processing is to be performed.

This configuration is therefore more suitable for close coupled combustion applications and retrofitting boilers as no clean up is then required (30-32), since tars are fully burned out.

Finally another type of dense phase reactor is the crossdraft gasifier (34, 35), with many similarities to the co-current downdraft but a shorter response time to load changes. This characteristic is useful in traction applications. The product gas is however high in tars and requires cleaning.

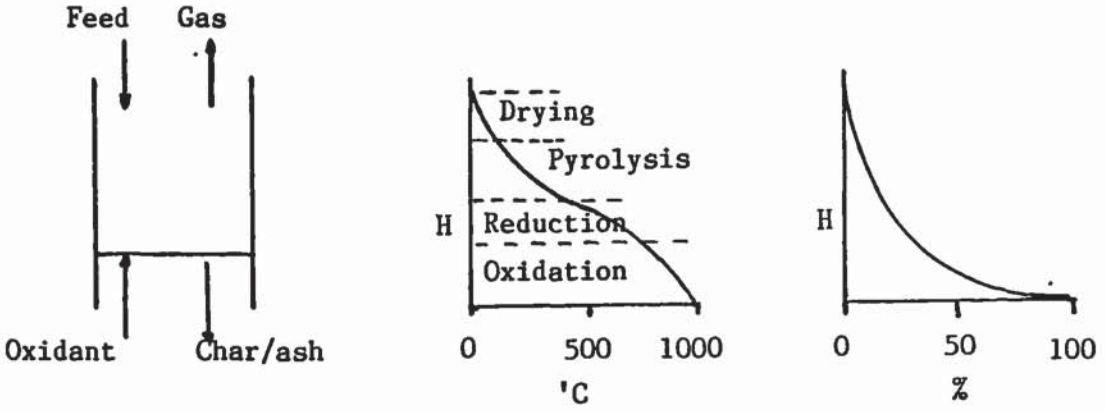

Updraft counter-current

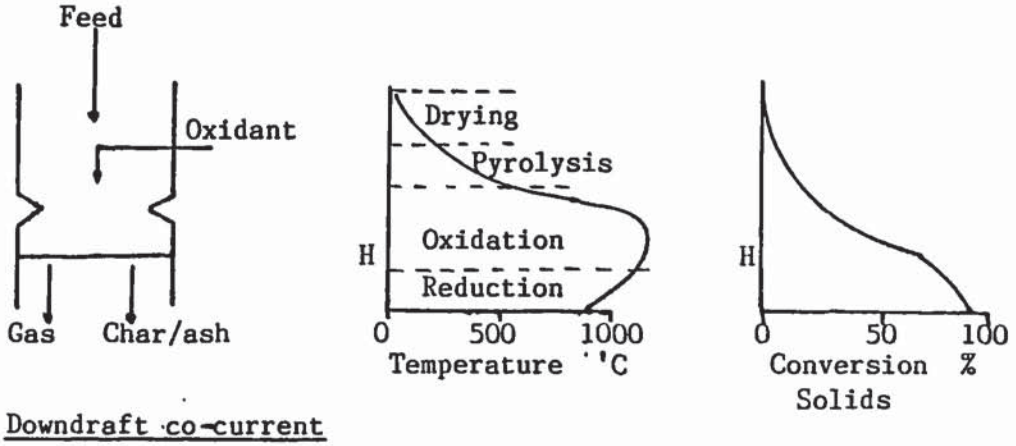

Downdraft co-current

Figure 2.3: Principles of dense phase gasifiers (10, 11).

2.2.2.2 Lean phase reactors

Lean phase gasifiers were originally developed for coal gasification and have only recently been adapted for biomass conversion. Contrary to dense phase reactors, no distinct reaction zones exist within the gasifier and drying, oxidation, pyrolysis and reduction take place effectively in the same region. Fluidized bed and entrained bed are the most commonly used lean gasifiers.

Fluidized beds are attractive as gasifiers as they provide many features that are not present in the dense phase types, including high rates of heat and mass transfer and well mixing of the solid phase, which means that reaction rates are high and the temperature is more or less constant in the bed. A relatively smaller particle size than for dense phase gasifiers is necessary and this may require additional size reduction. Due to the small particle size many types of feeding devices can be used; solids are thus easily introduced and ash generally is removed as fine particulates entrained in the off gas (18, 33). Fluidized beds generally have the attraction of being easy to scale up and operate at lower maximum temperatures (in the range of 700-850 °C) than dense phase gasifiers. It is also possible to separate the pyrolysis and the char gasification processes by using a dual bed system. One fluidized bed is commonly used as a combustor (e.g. char) and the other as pyrolyser. The heat for the pyrolysis reaction is most commonly provided by circulation of hot sand from the combustor to the pyrolyser (24). A more detailed review and problems associated with fluidized bed gasifiers are presented in later sections (see sections 2.3, 2.4).

In entrained bed gasifiers no inert material is present but a finely reduced feedstock is required. This type of lean phase reactor is still under development and problems such as scaling up and feeding have still to be overcome.

The principles of lean phase gasification with temperature and conversion profiles are shown in Figure 2.4. From this figure it can be seen that fluidized beds are the only gasifiers with isothermal bed operation. Typical operating temperatures for biomass gasification are about 800 °C. Most of the conversion of the feedstock to product gas takes place within the bed. However conversion to product gas continues in the freeboard section and in most cases approaches 100%, unless excessive carry over of fines takes

place. Entrained bed gasifiers however operate at much higher temperatures of about 1500 °C and hence the product gas has low concentrations of tars and condensible gas. However, this high temperature operation creates problems of materials and ash melting. Conversion in entrained beds can also approach 100%.

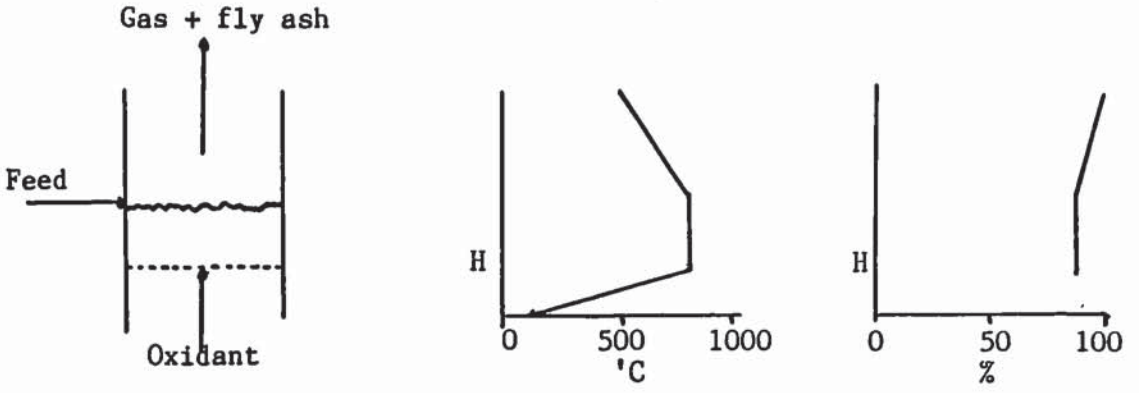

Fluidized bed

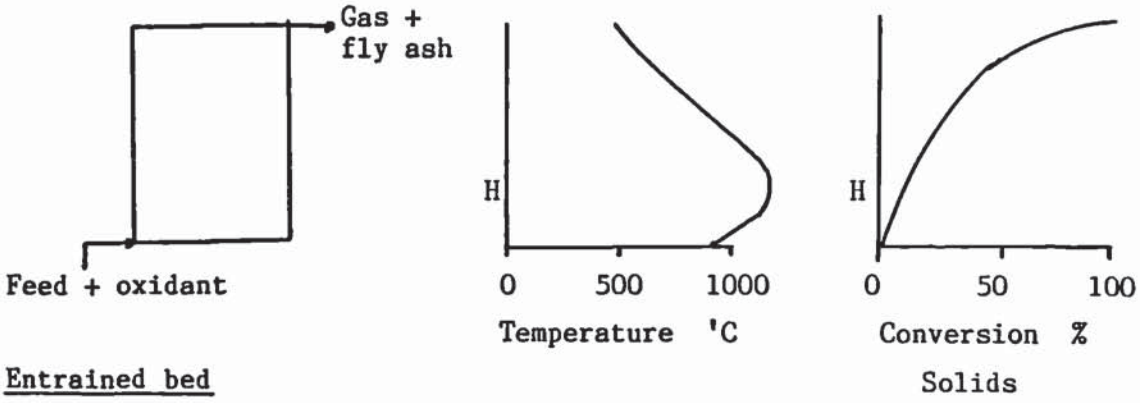

Entrained bed

Figure 2.4: Principles of lean phase gasifiers (23-25).

Table 2.1 summarizes the general advantages and disadvantages of dense and lean phase gasifiers reviewed in this section, while fluidized bed reactors in particular will be described in more detail.

Table 2.1: Comparison of various gasifiers.

Dense phase gasifiers		Lean phase gasifiers	
Updraft	Downdraft	Fluidized bed	Entrained bed
Low gas outlet temperature	Low tar yield High thermal efficiency	Good temperature control Low tar yield Can tolerate variation in quality of fuel. Can operate at part load, started and stopped easily.	Produces tar free gas and little methane High feedstock utilization due to high reaction rates.
High carbon conversion. Low ash carry over. Large residence time of solids. Relatively simple construction.		Very good gas-solid contact and mixing. High throughputs.	
High tar yield		Carbon loss with ash. Low operating temperature.	Refractories and materials of construction. High outlet gas temperature. Slagging.
Low specific capacity. Poor turn down capability. Uniformly sized feedstock with mimimum of fines required. Ash fusion and clinker formation on grate.		Low feedstock inventory. Extensive particulates clean up is required.	

2.2.2.3 Other types of gasifiers

Many other types of reactors, such as rotary kiln, multiple hearth and cyclonic reactors have been tested or are under development for biomass conversion. Their success has been however limited, unless for very specific applications and their inclusion is beyond the scope of this thesis.

2.3 FLUIDIZED BED GASIFIERS

The contacting pattern between biomass and gasifing medium is a very important aspect of any gasifier. Fluidized bed reactors are considered to be two phase systems in both the contacting pattern and flow of reactants and products, since two distinct phases (solid and gas) exist (36). In this section the phenomenon of fluidization and the various models describing the hydrodynamic behaviour of fluidized bed reactors are discussed.

2.3.1 The phenomenon of fluidization

If a fluid passes upwards through a bed of solids, the fluid first percolates through the voids of the particles and a pressure drop builts up across the bed (36, 37). As the fluid flow is increased, the pressure drop increases roughly proportionally, but when the frictional drag on the particles becomes equal to their apparent weight (actual weight less buoyancy), the particles become rearranged, to offer less resistance to the flow of the fluid and the bed starts to expand. Eventually, as the fluid flow rate is increased, the bed begins further to expand until a point is reached when the particles are all just suspended by the upward flowing fluid. At this point the bed is said to be at the point of "incipient" fluidization. If the fluid flow is further increased, the particles seperate still further and the pressure drop remains approximately equal to the bed weight per unit area of the bed.

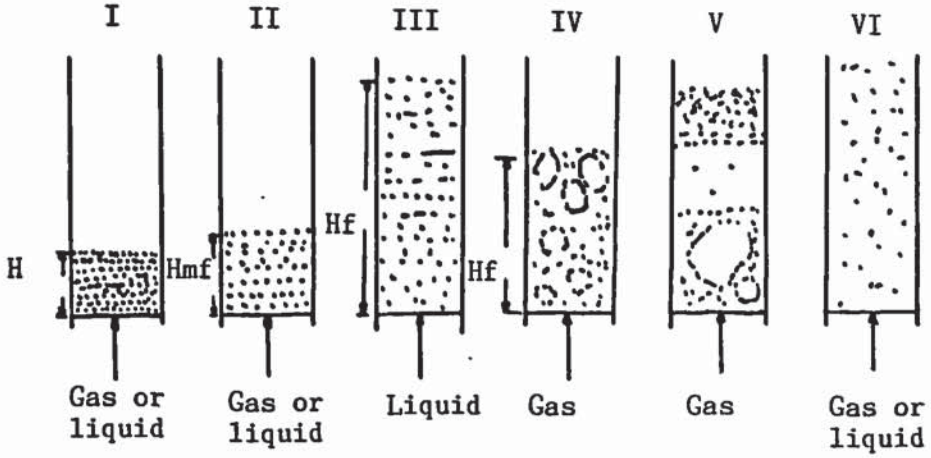

I. Fixed bed
II. Incipient or minimum fluidization
III. Particulate or smooth fluidization
IV. Aggregative or bubbling fluidization
V. Slugging
VI. Lean phase fluidization with pneumatic transport

Figure 2.5: Various kinds of contacting of a batch of solids by fluid (36).

Up to this point the system behaves in a similar way whether the fluid is liquid or gas. With a liquid the bed continues to expand with increasing flowrate and the fluidization is known as "particulate" fluidization (36, 37). With a gas, however, at high velocities two separate phases are formed; the continuous phase, which is known as the dense or emulsion phase and the discontinuous phase known as the lean or bubble phase. The fluidization is then said to be "aggregative". Bubbles are formed at the distributor and rise up the bed. As they rise, they coalesce with other bubbles and become larger. If the bed is sufficiently deep and narrow, the bubble may become large enough to spread across the entire bed section. Then as it rises, it moves the solids upwards until it collapses. Then the bed is known to be "slugging". These various kinds of contact regimes are shown in Figure 2.5.

2.3.2 Definition of the minimum fluidization velocity and types of fluidizations

The minimum fluidization velocity, Umf, is the theoretical fluid flow velocity, at which the pressure drop through a bed is just enough to support the weight of the bed. The ideal fluidization characteristics can be shown on a graph of pressure drop against air flow for a bed consisting of one mono sized component, see Figure 2.6 (38). The broken line parallel to the abscissa represents the weight of solids per unit cross sectional area of the bed and in this idealized case, according to the definition, it is exactly equal to the pressure drop required for Umf. Line ABDE represents increasing gas flow rates and EDC represents decreasing rates. After fluidization, the particles are more loosely packed and therefore the pressure drop for each particular flowrate is lowered, giving the hysteresis loop ABDC. Any further increase in air flow, however would produce a pressure drop on the path CDE (36).

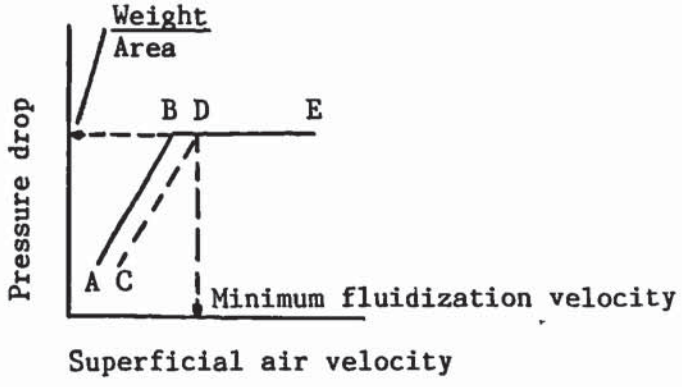

Figure 2.6 : Idealized pressure drop-flow characteristics for a fluidized bed.

In this ideal case, U_{mf} would be defined uniquely as the point D, which in fact is the intersection of the two straight lines CD and DE representing respectively the fixed bed and the fluidized bed. But such an idealized pressure drop versus air flow rate is never obtained in practice. A typical real system is shown in Figure 5.4 (see section 5.4.3), where the Umf of the fluidized bed pilot plant reactor was determined.

There are several regions under which fluidized beds can operate. These regions are roughly separated in terms of the slip velocity, which characterizes the motion of particles in a fluidized bed, and are defined by equation 2.1 (38).

$$U_{sl} = \frac{U_g}{e} - U_p \qquad \text{equation 2.1}$$

where U_g = the superficial gas velocity,
e = the bed voidage,
and U_p = the particle velocity.

The different regions are shown in Figure 2.7 (38).

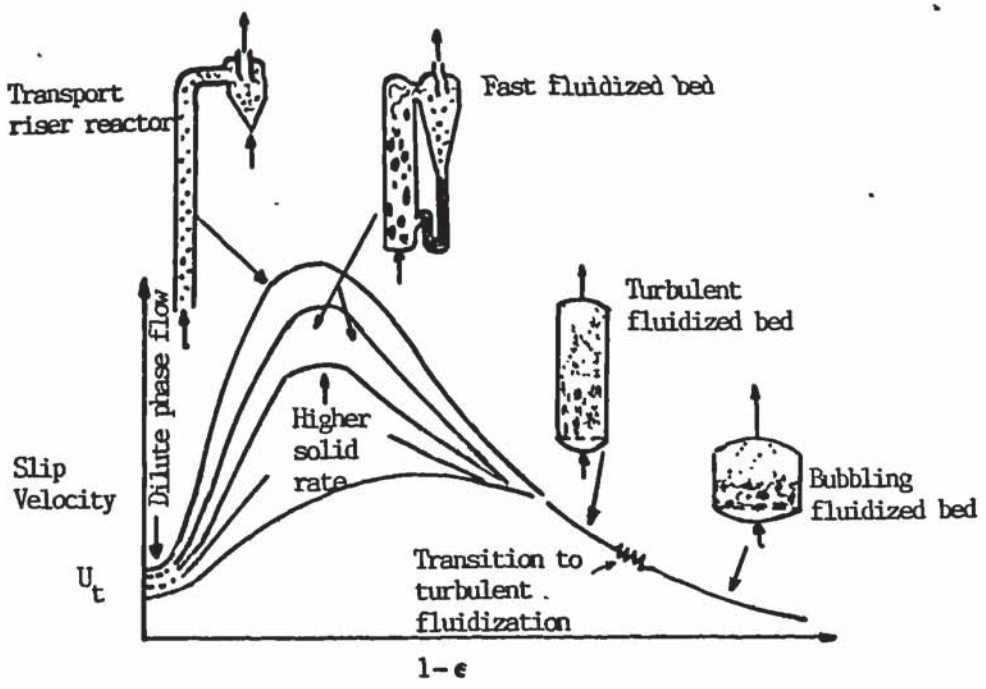

Figure 2.7: Basic regions of fluidization (38).

Under gas velocities slightly higher than the minimum fluidization velocity a "bubbling fluidized bed" is established and the voidage in the bed is close to $1 - e_{mf}$. Higher gas velocities will result in a "turbulent fluidized bed", where many solid particles are entrained with the gas. Nevertheless the bed maintains a certain height and the entrained particles are either discharged or fall back in the fluidized bed. However, when the gas velocities increase even further, then the slip velocity increases significantly and a "fast" or circulating fluidized bed is established. This is characterized by a high degree of particle turbulence with slip velocities, an order of magnitude greater than the terminal fall velocity of the individual particles (above this velocity, the particles are entrained from the bed (36)). The solids are almost uniformly distributed over the reactor height. The quantity of solids entrained by the gas increases, is separated in the recycle cyclone and recycled to the reactor. This leads to the recycle cyclone being a permanent constituent of the reactor system.

This phenomenon is feasible on hydrodynamic grounds, only if the individual particles form into relative stable agglomerates with correspondingly larger terminal velocities. When this is attained, it causes an extremely intensive mixing movement between gas and solids and considerable back mixing. Together with the solids recycle, inner circulation gives a uniform temperature across the overall circulating fluidized bed reactor.

At still higher velocities than those characterizing the 'fast' regime, the flow in fluidized beds passes into a dilute-phase region where, as it is generally agreed, the slip velocity approaches the "terminal fall" velocity of individual particles. This type of flow finds its main application in pneumatic conveying and entrained bed reactors.

It is also possible to combine two or more fluidized beds by using 'risers' and 'down comers' (by which the solids are transported from one bed to the other), as has been successfully demonstrated by the petrochemical industry (36). Such systems have also been considered for biomass gasification. Typically each fluidized bed is used for a different process, for example, catalytic cracking and catalyst regeneration, or gasifier and combustor (see section 2.4.5).

2.3.3 Models describing the behaviour of fluidized bed reactors

In order to describe the behaviour of a fluidized bed, a model to represent the flow of gas through the bed and its contacting of solids is required. This is especially necessary for gasification reactions, which are heterogeneous in nature (more than one phase are present: solid and gas). Therefore the contact and interactions between the phases strongly influence the rates of the chemical reactions (see sections 2.5.5 and 2.5.6). Considerations of bubble flow are therefore central to the design of any gas-solid fluid-bed process and some aspects of bubble behaviour will be discussed. The earliest theory to be proposed for the division of gas between the bubble phase and the emulsion phase of a bubbling bed was the "Two Phase theory".

2.3.3.1 Two phase theory

This theory was proposed originally by Twoomy and Johnstone (39) and states that all gas in excess of that necessary to just fluidize the bed, passes through in the form of bubbles. Thus if Q_t is the total volumetric flowrate into the bed, Q_{mf} the minimum fluidization flowrate and Q_b the bubble flowrate:

$$Q_t = Q_b + Q_{mf} \qquad \text{equation 2.2}$$

Dividing equation 2.2 by the bed area, A, gives the bubble flow in terms of the superficial velocities U and U_{mf}:

$$\frac{Q_b}{A} = U - U_{mf} \qquad \text{equation 2.3}$$

In recent years, however, a large number of experimental studies have been reported (40), in which the flow of bubble gas has been measured and the general conclusion drawn has been that in the majority of systems the two-phase theory overestimates the actual bubble flow. In other words, in these systems a larger quantity of gas flows through the emulsion phase than is predicted by equation 2.2. It has been suggested therefore that equation 2.3 be rewritten in the following form (38):

$$\frac{Q_b}{A} = U - U_{mf}\,(1 + nf_b) \qquad \text{equation 2.4}$$

where n is a positive number and f_b is the volume fraction of bed occupied by bubbles.

2.3.3.2 General approach to fluidized bed modelling

Most models are based on the two-phase theory of fluidization, but differ considerably in the assumptions they make regarding the exact nature of the phases, the mode of inter-phase gas exchange and the degree of gas mixing in the phases among others.

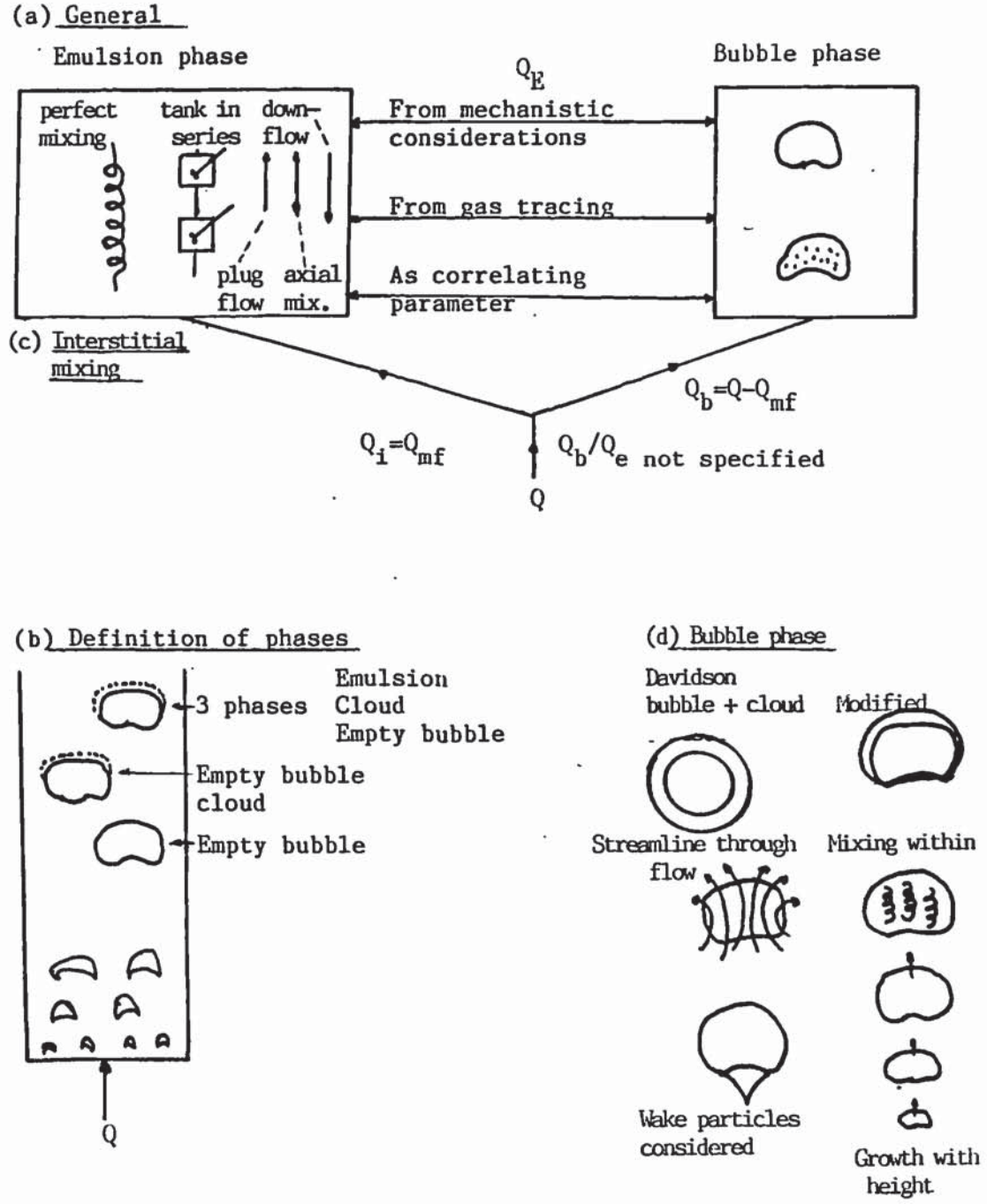

Figure 2.8 : Fluidized bed reactor models assumptions: a) general; b) phases; c) bubble phase. (51).

The Davidson-Harrison (37) and the Kunii-Levenspiel (36) models have received most attention, since they can predict the hydrodynamics of fluidized beds better than other models (38).

In both these two phase theory models the bed is depicted as two regions, a bubble and an emulsion phase with gas interchange between phases, while the Kunii-Levenspiel model also considers a third phase - the cloud phase. This third phase is made of a "cloud" of gas which surrounds the bubble and moves with it. Both postulate plug flow for the bubble phase, while for the emulsion phase the D-H model postulates it as well mixed and the K-L model as stationery. Numerous extensions and alternative analyses for both models have been published in recent years (41-49) and some of the options are shown in Figure 2.8. A detailed description and comparison of the various models is beyond the scope of this thesis as several reviews (38, 50-52) of the various models have recently been published.

The two phase theory is a very useful concept in understanding the behaviour of fluidized bed reactors. This is essential, besides the chemical and/or physical processes taking place in the reactor, since unless efficient fluidization is established, the other processes cannot proceed according to the desired specifications and rates. Later in this work, principles of the two phase theory are used in evaluating the operation of the process plant fluidized bed reactor (see section 3.6).

2.3.3.3 Multiple region models

During a model comparative study, Chavarie and Grave (53) concluded that fluidized bed reactor models take insufficient account of reaction in the entry and exit regions of the bubbling bed, i.e. in the region close to the distributor and in the freeboard space above the bed surface. There is widespread agreement (38, 54-56) with this conclusion, since a number of authors have commented on the abnormally high rate of reaction near the distributor, where interphase mass transfer appears to be very fast and gas-solid contact most pronounced. Similarly, observations have been made concerning freeboard space temperature increases in the case of exothermic

gas - solid reactions, indicating an extra degree of reactant conversion in this region (57, 58).

It would thus seem more realistic to model fluidized bed reactors on the basis of three consecutive regions: the grid region, the bubbling bed itself and the freeboard (45). On the other hand the consideration of three different regions would increase the complexity of an overall model and design.

2.4 APPLICATIONS OF FLUIDIZED BED GASIFIERS

The interest in using fluidized bed systems for thermochemical processing of solid feedstocks has steadily increased over the last decate due to their attractive features. A comprehensive review and assessment of the large variety of ideas, proposals and plants is beyond the scope of this thesis, since that would include the gasification and combustion of coal, peat, biomass and municipal solid waste. Only gasification of woody biomass in fluidized bed reactors is thus reviewed.

It is necessary to obtain a clear understanding of the process, the problems encountered by other research groups and to identify the limitations of fluidized bed gasifiers, in order to interpret the results obtained from the process development unit, and develop empirical correlations and conceptual design for fluidized bed gasifiers. Some parameters not directly relevant to the aim of this work (for example oxygen gasification, use of catalysts, pyrolysis and dual bed systems) are also identified and reviewed, since they provide the basis for further work.

In order to present and compare the numerous publications in this area, it was decided to classify them according to reactor specifications (for example, existence of inert bed) and gasifying medium (for example, air/steam) and to use summary tables. Significant features, results and contradictions as well as status and scale of operation are identified and discussed. In the summary tables the information is presented in groups of research, thus several publications of one research center are given together. The publications of each group are presented in chronological order, as well as the work of the various groups.

2.4.1 Early work with fluidized bed systems (pre 1970)

Early work on the thermochemical processing of biomass in fluidized bed reactors was aimed at producing useful chemicals such as aldehydes, phenols and waxes. Little information was given concerning the reaction conditions, gas composition and higher heating value of the product gas. Only four publications were found on this topic of chemicals production and they are summarized in Table 2.2. Their value is limited in the general scope of this thesis, which considers the production of fuel gas, but their inclusion is justified since they indicate process routes which are different from these of present work on the same subject.

Dimitri et al. (59) are the first to have been found working on biomass in fluidized bed reactors. They described the destructive distillation of powdered wood in a low temperature fluidized bed with nitrogen (see Table 2.2). The main products of interest were acetic acid, methenol and tars. Although their work was not aimed at producing fuel gas product, it is of interest to note that they were able to identify and propose several process parameters of interest in fluidized bed biomass gasification processes, some of which are currently under study and development by various group (see sections 2.4.3-2.4.6). These process parameters are:

a) they suggested the use of recycle gas as the fluidization gas. This could be secured from combustion and recycle of gas leaving the chemicals recovery system, or by manufacturing producer gas from some of the charcoal product,
b) they proposed a two stage fuildized bed system: "the first to distill most of the volatile matter at a relatively low temperature with a minimum of thermal decomposition of acid, alcohol and tar; and the second, operating at a higher temperature, to strip residual volatile matter from the charcoal".
c) they identified "charcoal as a promising raw material for activated carbon. Activation could be done conveniently by the fluidized-powder technique".
d) it was determined that "rates of distillation are far higher than those reported for other methods". This and the higher yields of chemicals were attributed to the "exceptional uniformity of temperature and the absence of localized overheating".
e) studying the rate of distillation, they proposed that "the high heat-transfer rates secured in fluidized bed make it possible to heat all the wood to carbonization temperatures almost instantaneously".

This work was extended later (61) in order to improve the yields of acetic acid and methanol by using several refinements to the gas cleaning system (such as cyclone, condenser, mist trap, cold trap and carbon dioxide scrubber).

Table 2.2 : Early work with fluidized bed systems

Author	Internal bed diameter m	Bed materials	Feedstock	Fluidizing medium	Temperature range of experiments °C	Applications, purpose
Dimitri et. al. (59)	0.05	biomass char	sawdust	nitrogen	250-400	chemicals from biomass
Morgan et.al. (61)	0.05	"	hardwood	nitrogen	400	"
Vroom (60)	0.07	"	bark	nitrogen steam	260-460 260-460	fuel gas production/ fuel for internal combustion engine.
Shuster (62)	0.05	biomass char. + inert bed	paper leaves	air + nitrogen	260-880 260-810	qualitative fundamental, high temperature experiments.

However, the authors reported for the first time the composition of the fuel gas and identified three stages for the pyrolysis reaction at 400°C: a) a first stage of less than a minute during which little products are collected, b) a second stage of about 4 minutes during which the reaction proceeds rapidly and c) the final long period in which the reaction continues at a slow and gradually decreasing rate. Their results indicated that at 400°C, carbon monoxide is the only non-condensable gas formed by primary decomposition of hardwood and that it is not formed by secondary reaction, while carbon dioxide and residual gas were associated with secondary reactions.

This analysis is in contradiction with recent results (see section 2.4.6), which show that carbon dioxide as well as hydrogen, methane and C_2, C_3 hydrocarbons are produced along with carbon monoxide at the early stages of

pyrolysis. These discrepancies are probably due to the gas sampling method used in their experiments. The sampling point was downstream the charcoal filters. The charcoal may have retarted somewhat carbon dioxide. It is known (63) that various forms of activated carbon have separating capabilities and are used as packing material in gas-solid chromatography.

The first work found in the field of biomass gasification in fluidized bed systems, aiming at producing a fuel product, was carried out by Vroom (60). He studied the pyrolysis and gasification of bark and examined the possible use of the product gas as fuel in internal combustion engines. He also concluded that burning the charcoal produced by the pyrolysis in pulverized coal boilers might produce as much steam as that obtained from the combustion of wet bark in industrial ovens.

Several efforts (62) were also made to identify the components of tar and gas produced by the gasification of paper and leaves (see Table 2.2). Several analytical techniques were employed including wet chemical methods, gas chromatography, infrared and mass spectroscopy. However, the most important contribution of this work was the identification of defluidization in case of biomass beds with no inert material and the improvement in fluidization by the addition of an inert bed such as silica sand.

2.4.2 Gasification with no inert bed

The unique features of fluidized bed reactors are mainly due to the bed material and its efficient fluidization (see section 2.3). The bed may either be an inert material such as sand, or it can be a reactant (such as char) or a catalyst (such as alkali metals). Since the fluidization properties of a reactor are strongly influenced by the physical and/or chemical properties of the bed (29-31), the selection of a suitable material is of considerable importance, otherwise defluidization or elutriation of the bed may occur.

When biomass is gasified, the char residue can form a bed material of its own. Hence char fluidization can reduce the complexity of the gasification process by eliminating the inert bed. This idea was "borrowed" by the research community of coal gasification in fluidized bed systems, where beds of ash and char are often used. However, one condition for formation of a fluidized bed is a certain degree of homogeneity of the bed. Biomass char fluidization is very difficult due to the relatively low bulk weight and the

variation in its specific gravity. Thus, most of the processes under development use a system with an inert bed, usually silica sand. It is, however, possible to fluidize a bed of coal ash/char which has specific gravity about 2 to 3 times higher than biomass char/ash beds (64).The available literature on fluidized bed gasification of biomass with a char bed is summarized in Table 2.3.

Table 2.3 : Gasification of biomass in fluidized bed with char as bed material.

Institute/ Author(s)	Internal bed diameter m.	Feedstock	Oxidizing medium	Temperature range °C	HHV MJ/m^3
Texas Tech. University (65-69)	0.05	manure	air + steam	680-800	2.6-5.0*
	0.15	manure	air + steam	517-670	10.1-15.8*
	0.15	oak sawdust	air + steam	600-800	11.2*
	0.15	various agric. wastes + biomass	air + steam	600-800	9.0-14.1*
Saskatchevan Power Corp. (70-71)	1.2	spruce, poplar chips	air	400-1000	3.4-5.7
Technical Research center of Finland (72-73)	0.15	peat	air + steam	650-900	3.0-6.6
IGT (74)	0.25	peat char	oxygen + steam	915-1043	N.G.
Liu et.al (75)	0.60	hemlock sawdust	air + steam	550-1100	5.8*

*) indicates units in MJ/N m^3 . N.G. = Not given.

It is of interest to note that of the research projects shown on Table 2.3, all but two were abandoned when if became evident that it was not possible to fluidize efficiently the bed of char. In all publications, severe temperature gradients were reported between the distributor and surface of the bed (from 50 to 200 °C), a proof that the bed of char was not well fluidized. Some authors (65, 70, 71) concluded that since loss of fluidization occured, the reactors were effectively operated as an updraft gasifier. They also noted that excessive amounts of tars were produced, which supported their conclusions. Another complication of char beds is the necessary continuous

mechanical removal of part of the bed (66, 69, 72, 74) in order to maintain a constant bed height. This can be achieved by means of screws or overflows, which is an added complexity to the design of a system and also increases the capital cost.

One of these projects (70-71) was the earliest (1978) demonstration of fluidized bed gasifiers (reactor diameter 1.2 m) in the rural communities of Canada. After about a year of operation the plant was abandoned and the project was continued with a downdraft gasifier. The work of the Texas Technical University (65-69) is the most extensive, since they were able to study several feedstocks and the influence of various parameters (such as equivalence ratio, temperature, gasifying agent). This led to the development of an empirical model, which is however of limited value (see section 2.5.7.2), as a mean solids residence time has to be assumed and the model did not predict either the calorific value of the product gas or the gas composition. This group also failed to go deeper in the principles of gasification and repetition is a common feature in their publications, because the main body of their work consisted of carrying out the same types of experiments on different biomass feedstocks.

It can be concluded that under normal operating conditions, it is not possible to fluidize efficiently a bed consisting of biomass char only. This problem can be overcome by using complicated mechanical char removal systems. However, for a gasification process - which main objective is to produce fuel gas - this loss of char would represent a significant reduction of the overall efficiency. Because this work aimed at studying the gasification process of biomass in a fluidized bed reactor, and since from the literature review it was deduced that good and stable fuidization of the bed is a prerequisite for achieving the advantageous properties (isothermal bed, high mass and heat transfer rate coefficients) of this type of reactor (see section 2.3), it was decided to use an inert bed (silica sand) in the process development unit (see Chapter 3).

2.4.3 Air gasification

Most processes under development use air as the fluidizing and oxidizing medium. Steam is sometimes added either to control the temperature of the reactor or to increase the fluidization velocity at low air flowrates. In this section those processes which use an inert bed (mostly silica sand) are

discussed. The largest number of references -28- have been found on this area so it is apparent that this is the most widely used configuration.

2.4.3.1 Early research activities

In this section only those works which reported the experimental conditions and discussed the results in detail will be presented. Several other works which published only results of general nature or incomplete analysis of data will be discussed in section 2.4.3.9.

Results on fluidized bed air gasification of biomass are summarized in Table 2.4. At the end of this table, earlier experimental activities of the author are also included.

Some of the earliest work was carried out at West Virginia University in the early 70s. Its main emphasis was on municipal solid waste pyrolysis/gasification (76, 77), although several biomass feedstocks were also independently studied (see Table 2.4). The results obtained were compared with data on other feedstocks such as coal and plastics. However, the most important contribution of this works is in the comparison of fluidized bed reactors with other systems.

They were also the first to report significant concentration - from about 2 volume % (cow manure) to 28 volume % (animal fat) (77) - of C_2 hydrocarbons in the product gas. They also reported that above 780 °C operating temperature, the yields of gas increased at the expense of solid and liquid yields. The authors found that for sawdust gasification in fluidized bed (at 850 °C operating temperature and an estimated heating rate of 800 °C/min), the gas yield was about 3.3 times higher than the gas yield resulting from the gasification of newsprint in a traditional retort, under similar operating conditions. They therefore concluded that fluidized bed reactors were the superior unit operation for solid waste gasification.

Table 2.4 : Air gasification with inert bed.

Institute/ Author(s)	Internal bed diameter m	Feedstock	Oxidizing medium	Temperature °C	Higher heating value MJ/m^3	Thermal efficiency %	Status
1	2	3	4	5	6	7	8
West Virginia University (76-77)	0.46+	sawdust			14.8 N		Programme terminated
		chicken-manure			11.5 N		
		cow-manure	methane + air	740-830	12.2 N	N.G.	
		tyre			24.6 N		
		sewage-sludge			13.4 N		
Eco research Omnifuel (78)	1.2+	woodwaste	air + O_2	N.G	1.4 N	70	Research of this group resulted in the 1st commercial plant.
(79-81)	1.2+	woodwaste	air	700-800	2.3	44	Work continuous on methanol.
Kansas State University							Research continues. Analytical models are developed.
(83)	0.22	manure	propane-air steam	630-705	12.5-21.8 N	20-58	
(84)	0.22	cane	"	620-710	10.0-14.5 N	N.G	
		sewage-sludge	"	710-820	19.0 N	N.G	
		tyres	"	700-800	19.0-38.0	N.G	
(85)	0.22	corn stover	"	560-800	13.6-16.5	N.G	
(86)	0.22	manure	"	530-780	8.0-19.0	N.G	
(87)	0.05	graindust	steam	590-760	9.4-11.5	8-55	
(88)	0.05	manure	steam	670-1100	10.0-15.0	N.G	
(89)	0.05	a-cellulose	steam	590-790	11.8	32-92	

University of Missouri Rolla.							Research continues. An
(90)	1.02	paper	air	650	3.7 N	75	empirical
		"	steam	540-730	7.4-13.6	N.G	model and
(91)	1.02	sawdust	air	500-840	0.4-9.7 N	50-70	design pro-
	0.56	woodwaste	"	"	"	"	cedure was
	0.15	"	"	"	"	"	developed.
(92)	1.02	woodwaste	air + recycle gas	N.G.	N.G.	N.G.	
(93)	0.15	sawdust	air + recycle gas	626-1110	4.4-4.1	20-85	Recycle gas was used but with
(94)	0.10	charcoal	air + steam	870-930	2.4-3.1	N.G	mixed results.
Twente University of Techno- logy							Research continues. A mathema- tical
(95,96)	0.3	beechwood	air	700-950	5.0-6.6	53-76	model has
(97)	0.3	rice husks	air	750-940	4.8-6.3	60-66	been developed.
Chou and Chang (98)	0.45	bagasse	air	280-750	N.G.	N.G.	-
Moreno/ Goss	1.3	cotton gin	air	760-845	4.8-6.1 N	N.G.	Research continued in
(99,100)		nut shells	air	750-850	6.7 N	N.G.	collabo- ration with University Davis California.
Salvi et al. (101)	0.35	agri- culture wastes	air	700-850	3.9-5.5 N	62-65	System developed on data from University Missouri- Rolla.
Free University of Brussels (Maniatis et al.) (102)	0.15	cacao pellets	air + seam	760-880	1.3-4.5 N	26-60	Research continues.
		wood shavings bark	air + steam	740-880	3.3-5.7 N	38-65	A mathema- tical model for char- coal was
			air + steam air	700-880	1-4.6 N	16-50	developed.

+ outside bed diameter;
N = units in MJ/Nm^3;
NG = not given.

2.4.3.2 Temperature

The operating temperature of a fluidized bed gasifier at steady state has attracted the greatest attention and has been studied by many of the research groups of Table 2.4 as an independent variable.

There is agreement in general that the gas yield, the heating value of the gas produced and the energy recovery increase as the operating temperature is increased in the range of 650-900 °C (77, 83, 86, 87, 90, 103). This is shown in Figures 2.9 to 2.11 for the gas yield, thermal efficiency and higher heating value of the product gas respectively. None of these groups has extended the temperature range to higher temperatures due to limitations of ash-sand bed sintering (see section 2.4.3.6).

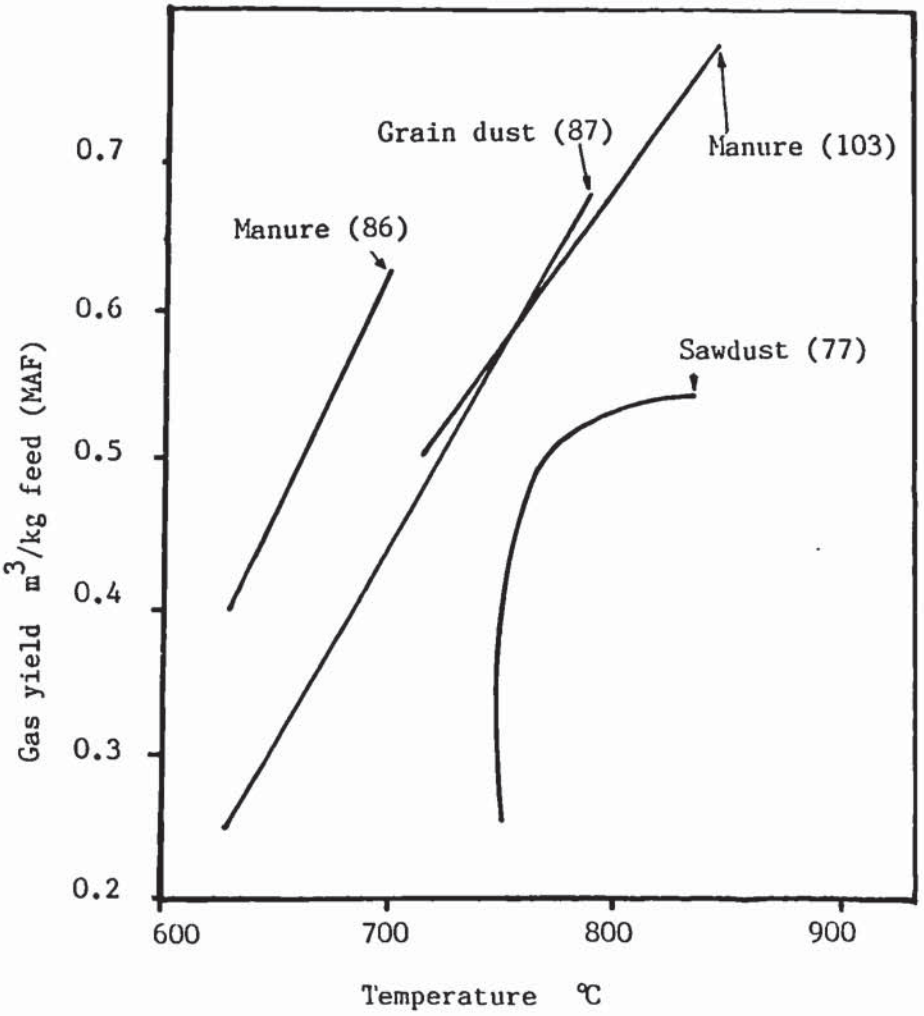

Figure 2.9 : Effect of temperature on gas yield

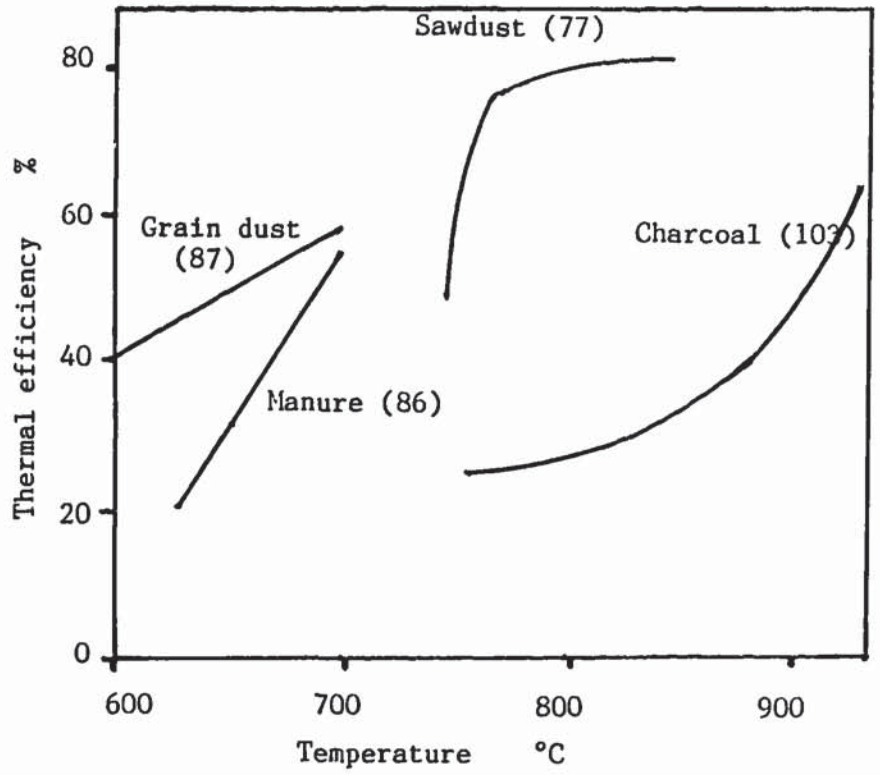

Figure 2.10 : Effect of temperature on thermal efficiency

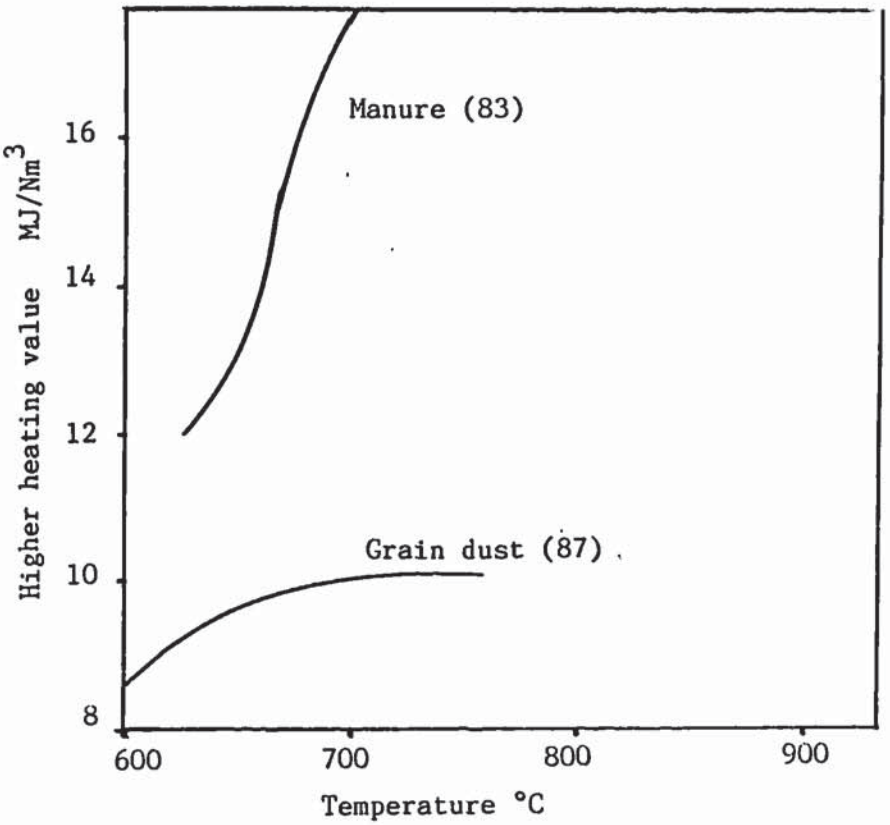

Figure 2.11 : Effect of temperature on the higher heating value

Since these results were obtained under different experimental conditions and with different feedstocks, it can be concluded with certainty that an optimum operating temperature should be around 800 ± 50 °C. Operation below this temperature range will result in low gas yields, low thermal efficiency and low calorific value of the gas. Operation close to 900 °C will cause the biomass ash to melt and consequently the bed will sinter. These observations are also supported by other research groups (77, 102, 108) (for further discussion see section 5.10). In contrast to systems operating without inert bed (see section 2.4.2) all publications of Table 2.4 reported isothermal conditions in the sand bed.

2.4.3.3 Air to fuel ratio

The amount of air in relation to the amount of biomass fed to a gasifier (sometimes termed equivalence ratio (109) or air factor (104)) is a parameter which strongly influences the performance of a system. It is defined as the amount of oxidant fed to the reactor devided by the amount required for stoichiometric combustion (see section 5.2). This ratio must be equal to 1 for complete combustion of the feedstock to carbon dioxide and water (109), though in practical application values greater than 1 (e.g. 1.2) are used. When this ratio is equal to 0, it corresponds to pyrolysis of biomass in the absence of oxygen (108). Commonly, fluidized bed gasifiers operate in the range of 0.2 to 0.5. Figure 2.12 shows the influence of the equivalence ratio to the adiabatic flame temperature. These results were computed with a thermodynamic model (109) and show the operational range of the different processes. They are supported by other authors too (15, 104, 68). It has been shown that as the air to fuel ratio increases, the temperature of reaction will also increase (96, 98,104, 108). Similarly, with higher values of air to fuel ratio, the gas yield (96, 99, 103, 105) and the heat of reaction (104, 105, 108) will increase as well.

In the same figure the char formation in relation to air factor is also shown. At 0 air factor, the maximum char production is predicted at about 0.34 kg char per kg of dry wood. However at an air factor of 0.23, the char formation drops to 0. This is an important conclusion, since operation at air factors above 0.23 would theoretically be beyond the carbon boundary in the gas phase region, see Figure 2.12. Thus thermodynamics predict no char above an air factor of 0.23 and the only possible products can be in the gaseous state.

However, this is not always the case in practice, as gasifiers often operate in the gas phase region and yet solid carbon is removed from the gasifier.

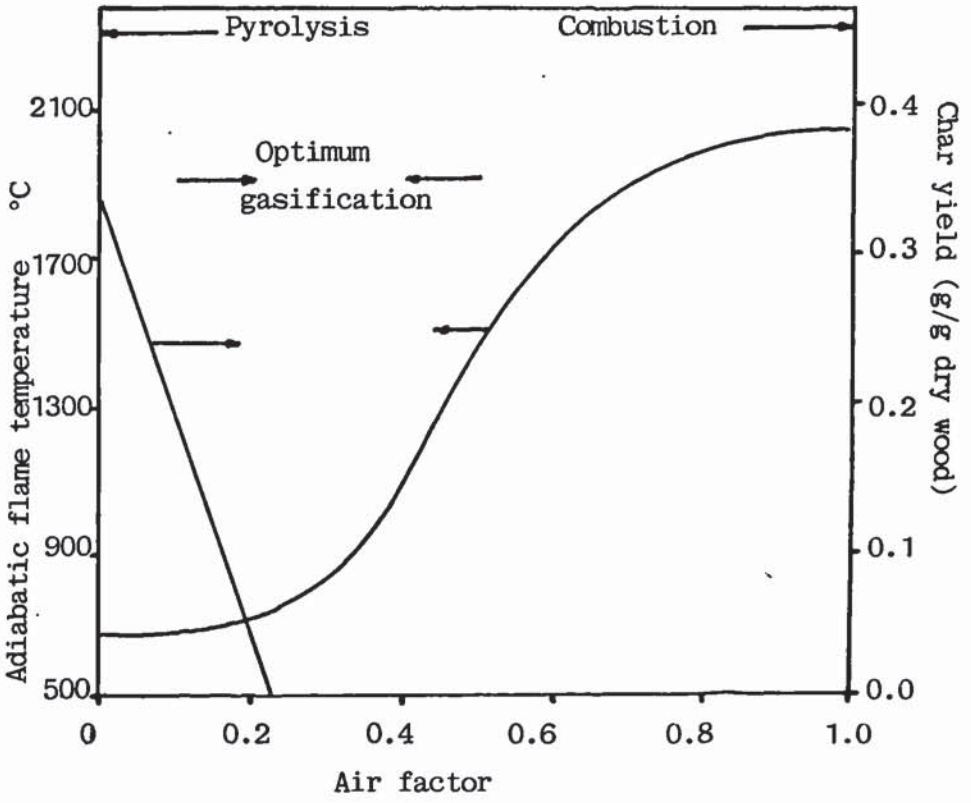

Figure 2.12 : Adiabatic air gasification of dry wood at 1 atm, effect of air factor on the adiabatic flame temperature.

The opposite also takes place experimentally (e.g. updraft gasifiers can operate in the solid carbon region while no solid carbon leaves the gasifier). These descrepancies have been analysed and explained by Shand and Bridgwater (24), who were the first to relate their thermodynamic model with the carbon boundary.

A common conclusion of the above articles is that the quality of the gas produced and the thermal efficiency (defined as the chemical energy - higher heating value - of the cool gas over the chemical energy of the feedstock; for detailed definitions see section 5.2.5) drop significantly above an air factor of 0.5, while below a value of 0,2 the yields of pyrolysis products (tars and pyroligneous acids) increase considerably. Figure 2.13 shows that the chemical energy of the gas decreases with air factors above 0.3 (109).

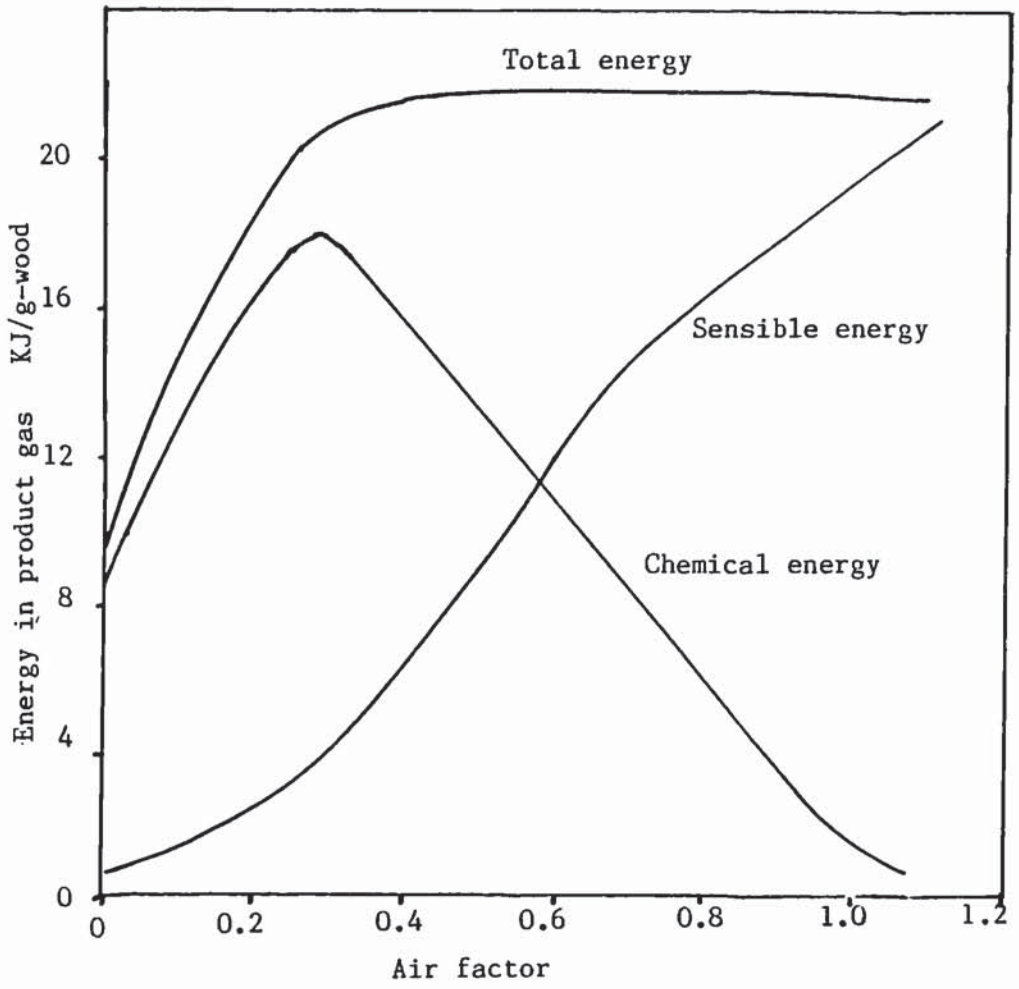

Figure 2.13 : Adiabatic air gasification of dry wood at 1 atm, effect of air factor on energy in product gas (109).

2.4.3.4 Gas composition

There is good agreement (variations less than 10 % under similar operating conditions) amongst the various publications of Table 2.4 concerning the gas composition of the product gas. Typical operating data for fluidized bed gasifiers are given in Table 2.5. (A common characteristic is that ethylene and ethane are typical components of the product gas. These gas components are not found in the product gas of dense phase reactors.

Table 2.5 : Typical operational data for fluidized bed gasifiers (102, 110).

Parameter	Units	Value
Grate energy release(a)	GJ/hm^2	6-9
Operating temperature	°C	700-850
Off gas temperature	°C	500-800
Moisture cont. max.	wt%	40
Fuel size max.	mm	60x60x30
Gas Composition	Vol.%	
N_2		50
CO_2		20
CO		14
H_2		9
CH_4		5
C_2 hydrocarbons		2

(a) Defined as the energy released by the feedstock per unit time and cross sectional area of reactor.

Although their concentrations are low (see Table 2.5) they significantly improve the higher heating value of the gas. Several groups have also reported low concentrations of C_3 and C_4 hydrocarbons (86, 102, 111). However, they are often ignored, as their detection is much difficult.

Evidence was recently produced by the group of the Free University of Brussels that the gas composition is greatly affected by the approach to equilibrium of the homogeneous water gas shift reaction by which the equilibrium conversion for hydrogen, water, carbon monoxide and carbon dioxide is set (105, 112, 15). It was found that at about 800°C the gas composition approaches the equilibrium position (see section 5.7.3 for detailed description). Lately this has been verified by others as well (89, 96). The same group also identified the temperature of the freeboard zone as a significant influence on the gas composition (108). The freeboard region of a fluidized bed gasifier assumes a great importance as a disengagement zone for entrained particles; as a cracking zone for tars and pyroligneous acids; and as a zone for continued gas phase reactions. The fact, that higher operating temperatures improve the gas quality, is in accordance with the conclusion of several works (see section 2.4.3.2).

2.4.3.5 Thermal efficiency

Thermal efficiencies as low as 15% have been reported when operating a fluidized bed gasifier at high air to fuel ratios of above 0.5 (83, 102). However under normal operating conditions thermal efficiencies in the range of 60-70% have been attained by several researches (78, 89, 91, 95, 102) (see Table 2.4.). A common conclusion is that the overall efficiency can be improved further if the sensible heat of the product gas could be recuperated in a heat exchanger.

The thermal efficiency is favoured by higher operating temperatures, dry feedstock and an air to fuel ratio in the range of 0.25 - 0.35 (91, 95, 102).

2.4.3.6 Bed sintering

Sintering and loss of fluidization have been reported by several groups as a major problem (102, 77, 88) with beds of silica sand. Bed agglomeration typically occurs at temperatures above 850 °C. The ash content and composition of the feedstock also play an important role in bed sintering, as well as the particle size and method of feeding. It has been reported (105) that slagging was experienced when feeding wood shavings in a fluidized bed above the surface of the bed. This was attributed to the "floating behaviour" of the wood shavings (the material was segregated at the top of the bed) which caused very high local temperatures.

In order to avoid bed sintering, several other materials such as limestone, quartz sand, alumina sand and even chromite sand have been tested by various groups as alternative bed materials (88, 114, 115, 116). In general alumina sand is considered a better bed material than silica sand, since the reactions between ash components and alumina proceed at a lower rate than those between ash and silica, to form low temperature melting eutectics. However, the author has reported (116) that even with a bed of alumina sand, it was not possible to operate a fluidized bed gasifier fed with Euphorbia Tirrucalli at temperatures above 650 °C, due to ash-sand agglomeration. Instead, chromite sand had to be used. The problem of ash-sand sintering and its causes are discussed in more detail in section 2.4.7.

2.4.3.7 Feedstock properties and feeding

Feedstock characteristics and properties influence the performance of a gasifier significantly (117-118). However, few studies have investigated these parameters. It has been shown (78, 123) that the calorific value of the product gas decreases more than 50 % as the moisture content of the feedstock increases from 20 to 50 wt %. Recently, equilibrium and non equilibrium thermodynamic models have been developed (see section 2.5.4.4), which studied the influence of the moisture content on the volume % concentration of the gas components (232). The volume % concentration of hydrogen, carbon monoxide, carbon dioxide and methane were all decreased by 2/3 for the moisture content range of 0-40 wt%. Reasonable agreement was achieved between the non equilibrium model and experimental results of Creusol Loire, except for methane. It has also been reported (86) that the feed size fraction of manure had a definite influence on the composition, heating value and gas yield of the product gas. It was also established that gas yield increased while the heating value of the gas decreased as the size fraction of the feedstock became smaller. However no conclusive arguments were presented to explain this behaviour. Feedstock characteristics also influence the selection of an appropriate feeding system. Several problems such as bridging in the feed hopper have been encountered with biomass feeding systems (78, 102, 120) and this led to the design and creation of special feeding units (118, 119). A center-bottom feed arrangement had to be developed (99,100) to feed cotton ginning wastes in a fluidized bed gasifier in order to eliminate freeboard combustion. In general there is no standard feeding system and the feeding arrangement is dictated by the properties of the feedstock. However, for easy to handle feedstocks (such as wood chips with dimensions 4x4x1 cm) above bed feeding with a screw conveyor is the preferred system, since they are reliable and relatively of low capital cost.

Problems of reduced efficiency due to high carbon losses (6-10 wt %) in the fly ash have also been reported (123) when feeding fine biomass (sawdust) above the surface of the bed. It was recommended to modify the feeding system for in-bed feeding to minimize the carbon losses with such feedstocks.

The content of inerts and/or ash in the feedstock also has to be considered. If this is significant (above 3-5 wt %) and it has the tendency to accumulate in the bed (102), then special provisions have to be made to ensure the continuous or semi-continuous removal of part of the bed material.

2.4.3.8 Scale of operation

The majority of studies have been carried out in relatively small laboratory units with inside bed diameters smaller than 0.40 m. Only two works have been found using reactors with internal bed diameter larger than 1 m (78, 80,99, 100). However, since both groups represented private concerns few results were published thus limiting evaluation of these systems.

The most comprehensive study concerning the scale of operation has been carried out at the University of Missouri Rolla (90-94), where units with internal bed diameters of 0.10, 0.15, 0.56 and 0.70 m have been tested and the results compared. Their results indicated that the quality of the dry gas produced was only slightly affected by the size of reactor and the location of the feed addition point. This conclusion gives credence to the results obtained by the other groups which used only small units. Nevertheless, it is apparent that much more research is needed with larger scale units in order to obtain reliable results over a wide range of values of all significant parameters.

2.4.3.9 Commercial groups

Little information is usually published by private companies which have developed and marketed fluidized bed units, especially as far as specifications, experimental data, modelling and design procedures are concerned. Table 2.6 (compiled from references 24, 110 and author's data) shows a list of the known installations utilizing a fluidized bed gasifier.

It has been reported that Ahlström and Energy Products of Idaho have sold one plant more each (125). Similarly Lurgi has sold two plants and Combustion Power Corporation one. However, since there are no more informations available about these plants, they were not included in Table 2.6.

The Omnifuel fluidized bed gasifier in Canada was the first large scale commercial biomass gasifier that should show stable operation and good

performance over an extended period of time (114, 121). Omnifuel supplied only the gasifier, cyclone and an air to gas heat exchanger. The raw hot gas was cleaned in the cyclone and cooled in the air preheater and then piped 250 m to be used in oil heaters. During 1982 a good availability - 87 % - of the gasifier was achieved. However, the unit is presently shut down due to problems with fuel

Table 2.6 : Fluidized beds : Present commercial suppliers with operating reference plant. (24, 110, author's data).

Manufacturer	Output GJ/h	No. of plants	Location	Feedstock	Comments/appl.
Ahlström OY, Finland	120	1	Shaumann Mill, Pietarsaari, Finland	Bark, wood waste	Lime kiln (fast fluid bed), continuous operation since November 1983.
Energy Products of Idaho, USA	57	1	Sacramento, USA	Wood waste	Boiler retrofit, discontinuous operation 1981.
Omnifuel, Canada	75	1	Hearst, Ontario, Canada	Wood waste	Hot oil dryer, not in operation today (online 1981).
Surlite	10, 30	3	Arizona, California, USA	Sawdust, cotton gin trash	Cotton dryer, one unit 10 GJ/h in discontinuous operation other pilot plant or not operating.
Fritz Werner	10	2	Germany	Wood waste	In start-up.

specification (widely varying moisture contents), clogging of the transfer pipe at low loads and ash handling problems. A total of about 8.000 h of operation has been achieved making Omnifuel's gasifier the installation with one of the longest operational times.

Recently shop fabricated small (small less than 30 GJ/h output; large more than 60 GJ/h output) to medium scale fluidized beds are coming on the market from several companies. For example, Surlite-Adenap (99, 100) is marketing a turn key unit, which has been applied to a cotton ginning facility. The 3-4 units run on cotton gin trash, but other fuels have caused startup problems due to their high ash content (>40-20 %). Similarly Fritz-

Werner is introducing a type which does not use a sand bed and does not condense the water before the engine (gas moisture content <20 %).

Another large scale (4.1 tons/h) installation in Sacramento (CA) is from Energy Products of Idaho. This is a fluidized bed fed from above the bed surface and close coupled to a boiler. The boiler provides heating and steam for state buildings and a nearby hospital (122, 123). The biggest and most successful of current large-scale biomass gasifiers is probably the Pyroflow gasifier installed by Ahlström at a pulpmill in Finland. Pyroflow is a fast fluidized bed with a simple one stage cleaning cyclone before an air preheating heat exchanger. The gas is fed directly into the lime kiln burner. Very low char losses and a small volume/high throughout, low tar yields, low direct heat losses and high efficiency (98 %) are claimed by the manufacturer. The plant was ready for startup in September 1983 and has run continuously since November 1983.

Some other companies have also developed fluidized bed systems, but have not succeeded in marketing them at the time of writing. A selection of these, for which some informations were found are summarized in Table 2.7 (24, authors data).

Table 2.7 : Fluidized beds : Suppliers without commercial plant

Manufacturer	Comments
ERCO USA	Extensive research with a pilot plant. Developed mobile units as well. Currently in receivership.
Rheinbraum/Uhde West Germany	Developed the high temperature Winkler process mainly for coal. Only recently working with biomass. Two operational plants, 25 t/day and 40 kg/h.
Vyncke Warmtetechniek Belgium	Currently developing air blown fluidized bed.
AVSA, Belgium	Developing a twin bed system.
TAG Trocknungs Anlagen GmbH	Developing an air blown fluidized bed.

2.4.3.10 Conclusions

Although there is a significant amount of information in the literature, it is limited to practical applications with a high level of empiricism. The most important parameters of biomass gasification in fluidized beds are efficient fluidization, temperature, air to fuel ratio, gas composition, thermal efficiency, feedstock properties and scale of operation.

Many problems have also been identified which demand careful attention and/or re-examination of the principles involved. These include : the need of an inert bed, the role of the freeboard region, bed sintering and efficient feeding of the biomass in the gasifier. .

2.4.4 Oxygen gasification

2.4.4.1 Introduction

Present R&D efforts both in North America and Europe are concentrating on Medium Heating Value Gasification for large scale application in methanol production (126). Oxygen is used as the oxidizing agent in most examples of this type of process, with the advantage that there is no nitrogen in the product gas which lowers the higher heating value.

Synthetic methanol production conventionally originates principally from natural gas feedstocks via steam-reforming and methanol synthesis. The synthesis technology has evolved from the high pressure technology of the 1920s-1960s, to the low pressure (i.e. 50 to 100 atms) technologies used today. Methanol synthesis catalysts also have evolved, as the development of sulphur purification processes for the synthesis gas permitted more active, sulfur-intolerant catalysts to be used (127).

The production of methanol from synthesis gas is a well proven technology, thus the remaining task in any wood to methanol proposal is to make synthesis gas from wood. The synthesis gas should in principle meet the standards shown on Table 2.8 (128).

Table 2.8: Required quality of synthesis gas (128).

Stoichiometric ratio	:	$(H_2 - CO_2) / (CO + CO_2) = 2 ....2.2$	equation 2.5
Sulphur content	:	< 0.1 ppm	

This section reviews the literature on the subject of oxygen gasification in fluidized bed systems and the possibilities of producing synthesis gas for methanol production. In addition, the oxygen donor gasification process which uses solid oxygen carrier is also covered here.

2.4.4.2 Single fluidized bed

This is a simple and flexible process which, if operated at 800-900 °C, produces a low tar but still methane rich synthesis gas. Much higher temperatures (above 950 °C) are not possible because of ash melting and bed sintering problems. The available results are summarized in Table 2.9. A common major problem in view of methanol synthesis is the high concentration of methane that is produced in such systems. Methane as well as any other hydrocarbons present in the gas (such as ethylene, ethane, propylene) are mostly produced during the pyrolysis of the feedstock. They all represent a loss in the conversion efficiency of carbon to methanol, since these compounds "fix" carbon and hydrogen. Conversion of these hydrocarbons to carbon monoxide and hydrogen is desirable and would result in a far better synthesis gas composition. The relevant conversion reactions for methane are:

$$CH_4 + H_2O \rightleftharpoons CO + 3H_2 \qquad \text{equation 2.6}$$

$$CH_4 + CO_2 \rightleftharpoons 2CO + 2H_2 \qquad \text{equation 2.7}$$

Thus all commercial processes under development (129-135) have added a methane reformer step to produce carbon monoxide and hydrogen.

Creusot-Loire (129-130) and Rheinbraun HTW (133, 134) plan to eliminate methane thermally, by introducing additional oxygen above the bed and raise the temperature up to 1300 °C. Rheinbraun HTW also plans to expand the freeboard zone in order to increase the residence time of the product gas at the high temperature region. On the other hand in the Mino process (134, 137) the gas is cleaned from dust in specially developed high temperature filters

and then catalytically reacted with oxygen at 900 - 1000 °C. The Biosyn/Omnifuel process (135) would also use a catalytic reformer.

Table 2.9 : Oxygen gasification in fluidized bed systems.

Process	Capacity kg dry-wood/hr	Pressure bar	Moisture wt %	Temper-ature °C	Thermal effic. %	Methanol yield kg MeOH / kg dry wood	Status
I. Single fluidized bed							
Creusot-Loire	100	1	20-40	850	53	0.42	oper.
(129-130)	2500	10-30	20-40	800-1000	53	-	oper.
Mino	10	30	10	700-850	54	0.56	oper.
(131, 132)	300	10-30	50	950	54	-	oper.
Rheinbraun HTW	1,300	10	10-40	1100	-	-	oper.
Biosyn/Omnifuel (135)	10,000	10-20	10-40	750-925	-	-	eng. study
IGT (136)	455	22	10	900	80	-	in con-struction
V.U.B. (116)	5-10	1	8	750-870	65-75	0.34	laboratory
INCO (115)	40	1	10	750-940	63.5	0.14	study.
II. Circulating fluidized bed							
Lurgi	50-250	1	20	760-840	75-	-	in operation
(139-141)	-	30	20	800	85	0.50	engineering
III. The oxygen donor process							
John Brown (142, 137)	900	1	11	-	75	0.50	engineering study, cold tests, and experi-mentation are completed

In the former reforming option, gas mixing and soot formation are critical points, while for the latter the high temperature filtering and possible catalyst deactivation by sulphur are steps that remain to be proven.

In a laboratory study (116), the author of the thesis examined the influence of the bed and freeboard temperatures on methane concentration. Higher bed temperatures resulted in somewhat lower methane concentration (temperature range 750-850 °C, methane concentration 8-6 Vol%, while the

freeboard temperature had no effect. It was concluded that for a methane thermal reforming step to have significant effect, the temperature has to exceed 900 °C. Since this cannot take place in the fluidized bed reactor because of ash/bed sintering, an additional reformer reactor must be added to the process.

Another drawback of this process is that, since they are basically autothermal (the heat necessary for sustaining gasification is provided by combusting part of the wood), the carbon dioxide content in the product gas will be relatively high (about 30 vol %).

Although some studies have been carried out in laboratory scale equipment (137-138) by research institutes at atmospheric pressure, all commercial processes are developing pressurized gasifiers. With the molar flow of the product gas about three times as large as the oxygen feed and with methanol processes operating typically at 50-70 bars, there is a economic incentive for pressurized gasifiers, not only for reducing the volume of the equipment but also for saving on downstream compression costs.

The differences in methanol yield between laboratory studies (116, 115) and commercial processes (see Table 2.9) are due to the addition of a methane reformer step by the latter processes (129-132).

2.4.4.3 Circulating fluidized bed

The circulating fluidized bed was originally developed by Lurgi (139-141) for alumina calcination (20 commercial plants) and coalcombustion (3 commercial plants), (see section 2.3.2). Application to wood gasification, however, is new. Compared to classical fluidized beds, this reactor is operated at much higher superficial gas velocities, although they are lower than in an entrained flow reactor. Since slip velocities between particles and gas are relatively high it is possible to operate at high temperatures (about 1100 °C) while preventing ash sintering. Thus Lurgi expects to obtain a practically tar free gas, with methane concentrations below 1 vol. %, in which case a reformer step would be avoided. Another advantage is the high specific reactor capacity obtained due to the high superficial gas velocity and high operating temperature. This process also offers an attractive methanol yield (see Table 2.9).

2.4 4 4 The oxygen donor process

In this double fluidized bed process (142, 137) a solid heat carrier is continuously circulated between two beds, one being an oxidizer and the other the gasifier, with the heat produced in the former being transferred to the latter. A unique feature of this process is that the heat carrier also acts simultaneously as an oxygen carrier from the oxidizer to the gasifier (122, 127). It is therefore the only process under development that uses neither air nor oxygen nor steam to produce medium heating value gas. Solid calcium sulphate acts as bed material, heat carrier and gasifying agent, while part of the product gas is recirculated to achieve fluidization. Another interesting feature is that the gasifier and oxidizer are integrated in a single vessel, thus minimizing heat losses and insulation requirements. Cold tests have been carried out to test the solid circulation system. However several engineering problems still have to be overcome (e.g. establishing a balanced solids circulation, minimizing fresh stone make up, minimizing methane and tar formation).

2.4.4.5 Cost considerations for methanol from biomass

Since cost is the ultimate criterion for implementation, it is of interest to compare the cost of producing methanol from wood and other conventional sources. Table 2.10 (143) shows that - for 1983 prices - methanol from wood was reasonably on a par with conventional sources.

Table 2.10: Cost of methanol from wood and from conventional sources (1983) (143).

Methanol (a)	£/t	£/GJ
- contract	150-160	6.5-7
- spot	120	6
- new plant	180	9
- wood	170	7

(a) Production in industrialised countries, assuming 1983 costs of natural gas.

It seems likely that future demand will be much less than the installed capacity. The possible supply and demand for methanol is given in Table 2.11 (129) (143).

Table 2.11: Possible supply and demand for Methanol up to 1990 (143).

Tons x 10^6	1980	1985	1990
Demand	12.2	17.4	29.0
Installed capacity	14.9	22.0	34.1

Therefore, the surplus capacity is estimated at about 5 million t/y by 1990 and this could lead to softening of prices. Several countries with low cost natural gas (such as Bahrain and Saudi Arabia) would probably construct the additional plants. The uncertainty in the future cost of methanol, combined with the additonal R&D work necessary to improve the reliability and performance of most of the proposed processes, casts doubts about the near future implementation of methanol from wood.

However, medium heating value gas can be used for other synthesis routes, such as for ammonia, which currently seems more promising (143). Nevertheless the author could not find any published work reporting actual experiments and results for such a process. Methane, which has the highest energy content of the product constitutents at 55 GJ/t, has also attracted some interest and several alternatives for processing the methane content of synthesis gas were recently proposed (144). Still, only one recent experimental work (145) could be found in this area, which presented very few results. Its main emphasis was in postulating some hypotheses concerning the methane yields. They postulated that the tar of the solids free gas undergoes thermal decomposition to soot in the reformer reactor. The tar and/or soot was consumed in two reactions: it was either steam reformed to carbon monoxide, carbon dioxide and hydrogen or hydrogenated to methane. The methane also decomposed thermally to yield a char with a higher activity than graphite and/or reacted with steam to form carbon monoxide and hydrogen. Their hypotheses were supported by experimental results which were comparable to published data.

2.4.4.6 Other processes

Another process (146) also proposed for methanol synthesis considered a triple fluidized bed reactor. The proposed reactor was divided into a combustion chamber and a gasification chamber. The ring-shaped gasification chamber was built around the combustion chamber in such a way, that the hot gases leaving the combustion chamber were led past the outer

wall of the gasification chamber before leaving the reactor. Part of the feedstock (26 wt %) would be fed in the combustion section and the rest in the gasifier section. It was also proposed that the heat for the gasification process could be generated from the synthesis gas produced by using an appropriate burner and thereby gasify practically all the biomass. In addition, the product gas was to be reformed thermally in a third fluidized bed cracking chamber built into the reactor, by adding oxygen. This chamber was to be installed at the top of the reactor and presumally the synthesis gas had to fluidize the bed. Several problems concerning the materials and the overall configuration exist for such a proposal. Such a complexity at present is considered unjustified by the author and at the best of his knowledge this remained at the drawing board.

2.4.4.7 Conclusions

Several processes are being developed based on different technologies. However most of them still have to overcome certain obstacles and obtain reliable data. The most reliable process seems to be the Lurgi circulating fluidized bed, since several units of this reacting system have been sold for various applications, two of which are operating as gasifiers (125); and low concentrations of methane and tars are expected.

The economics of these processes must be carefully evaluated to determine which technology will be the most prospective (138).

2.4.5 Steam gasification

2.4.5.1 Introduction

Steam is usually added as a thermal moderator and/or reagent in oxygen gasification. However, it can also be used as gasifying agent. In such a system, the energy is supplied by a steam reforming reaction which is only exothermic at high pressures (above 7 bars). (144). As with oxygen gasification, the dilution of the product gas by nitrogen is avoided and hence medium heating value gas can be produced. In addition, concentrations of carbon dioxide are less than in oxygen gasification since there is no free oxygen in the system.

Steam is also used in dual fluidized bed systems. In such systems, one fluidized bed is used as a gasifier and the other as a combustor. Steam is fed to the gasifier with the biomass, producing gas and char. The char is transferred in the combustor where it is burned with air. The hot sand is then transferred to the gasifier as a heat carrier and provides the heat necessary to sustain the gasification process. This section reviews the relatively few processes under development, using steam.

2.4.5.2 Steam gasification in single fluidized bed units

There is only one institution (87, 89) that has carried out extensive studies on steam gasification in a single fluidized bed. At the Kansas State University experiments have been performed with grain dust, manure and alpha-cellulose, in a small (0.05 m) fluidized bed (see Table 2.12). Operating temperatures were in the range 590-710 °C, with the exception of manure where temperatures as high as 1100 °C were obtained. The three feedstocks produced a gas with a calorific value around 10 MJ/m^3, while the thermal efficiencies ranged from 30-90%. In general similar results and trends were obtained as with air gasification (see section 2.4.3).

Table 2.12 : Steam gasification in fluidized bed systems

Process	Capacity dry wood kg/h	Pressure bar	Moisture cont. %	Temperature °C	Thermal eff. %	Status
Kansas State University (87-89)	0.5-2	1	5-10	600-1100	30-90	Operational
Battelle Columbus (147-148)	23-220	1	15-50	600-870	20-70	Operational test plant
Pollution Prevention (149)	750	7.8	20	720	-	Engineering study
AVSA (150)	830	1	20	700-750	-	Engineering study

2.4.5.3 Steam gasification in dual fluidized bed systems

In such a system the heat carrier is an inert material (sand or alumina) and heat is provided by combusting the product char that flows with the heat carrier to the combustor. The process has been strongly advocated in the literature (151) because of its advantages:

a) lower capital investment since no oxygen plant is needed;
b) lower operational expenses because no oxygen is used;
c) lower carbon dioxide content in product gas since gasification and combustion are separated.

This process has been proven commercially for municipal solid waste (151, 152).

For biomass, a system has been developed by Battelle Columbus (147, 148) during the last decade (see Table 2.10). The principle of the Multi-Solid fluidized bed is that very coarse particles which are ordinarily not fluidizable by gas, can be fluidized in a flowing gas solids suspension. With the coarse particles fluidized, backmixing is improved and the residence time of the solids is increased. In addition, the entrained solids penetrate the bubbles and hence the system operates with smooth fluidization. One of the advantages claimed of such a system is that higher specific throughputs can be achieved. Initial results from a 100 kg/h unit indicated that with increasing moisture levels lower carbon conversions were obtained, while increased temperatures resulted in increased carbon conversions, higher thermal efficiencies and higher heating values for the product gas, up to a temperature of 840 °C. It was also reported that the steam/wood ratio had no effect on the carbon conversion. Nevertheless the process is still under development and some problems such as fracture of silica pellets which comprised the dense phase have still to be solved. This process can also be applied for methanol synthesis. However the large yields of lower hydrocarbons (about 20 Vol.% (147)) and tars will require a secondary reforming reactor.

Two engineering studies have also been carried out (149, 150) utilizing dual bed systems for synthesis gas production. However, no experiments have been performed and thus they are not discussed any further.

2.4.5.4 Conclusions

Steam gasification has attracted some interest lately, since it produces a nitrogen free gas and low carbon dioxide yields. In addition, medium heating value gas can be produced without using oxygen, therefore significantly lowering the capital and operating costs of such a process by eliminating the oxygen plant. For methanol synthesis the high concentrations of hydrocarbons and tars is a drawback. Dual bed systems, employing downcomers, slots and risers, although commercially proven in catalytic cracking, increase considerably the mechanical complexity and investment costs of a gasification plant. The horizontal twin circulating beds of the oxygen donor gasification system offer a potentially significant advantage in this respect.

It is interesting to note that steam gasification has been shown (144) as the process by which the maximum energy efficiency could be obtained for both methane (77 %) and methanol (55 %) over three other processes (low temperature pyrolysis, high temperature pyrolysis and oxygen gasification). Although doubts were expressed on the authenticity of the source data, these results nevertheless demonstrate that more efforts on steam gasification R&D are justified.

2.4.6 Pyrolysis of biomass in fluidized bed systems

2.4.6.1 Introduction

Several recent research activities (153-163) have demonstrated that substantial yields of oil and tar can be obtained from biomass by very short residence time, rapid heating in non-oxidizing atmospheres and at moderate temperatures (400-700°C). Fluidized bed reactors can provide high heating rates and have been used with the objective of maximizing liquid yields by flash pyrolysis of biomass. Practically all studies use nitrogen or recycle gas as the fluidizing agent. This section reviews the relevant literature on this subject with main emphasis on the difference between products of gasification and pyrolysis.

2.4.6.2 Emphasis on maximizing liquid yields

The most extensive published work has been the flash biomass pyrolysis programme of the University of Waterloo (153-156) (see Table 2.13). The

process studied had as a primary objective to determine the conditions for maximum yield of liquids from biomass feedstocks. Results from a bench scale unit (15 g/h) operated in a nitrogen atmosphere over a temperature range of 400 °C - 650 °C indicated that, at apparent vapour residence times of about 0.5 seconds, organic liquid yields of 60-70% on a moisture free feed basis could be obtained from hardwoods (such as aspen-poplar and maple). Lower but still high yields of organic liquids could be obtained from agricultural wastes (40-60%) (wheat straw, corn stover and bagasse).

Table 2.13 : Biomass pyrolysis in fluidized bed systems

Institute Authors	Internal bed diameter	Feedstock and capacity	Gas medium	Temperature range °C	Yields % Char	Liquid	Gas	Status
University of Waterloo	0.02	Hybrid-poplar Aspen 0.015	N_2	450-650	6-16	7078	5-28	Bench scale work terminated.
(153-156)	0.1	Sugar Maple 1-3	Recycle gas	400-600	5-25	66-67	4-25	Pilot scale continues.
		Wheat straw 2-3	Recycle gas	500-580	16-25	35-58	8-20	
University of Waterloo	0.2	Cellulose	N_2	400-700	-	-	-	Work continues
(159-160)		Filter-paper	N_2	400-700	-	-	-	
Indian Inst. of Techn. (161)	0.05	Bovine waste	N_2	600-800	-	-	76-88	Unknown
Tokyo University (162)	0.03	Peanut-shells lanan-chips	N2	400-1000	18-50	5-55	10-90	Work continues
Arizone State Un. (163-164)	Dual system	86 different species	Air + recycle for regenerator recycle for pyrolyser	600-800	-	-	-	Work continues

In terms of calorific value and carbon to hydrogen ratio, the best quality liquids were obtained at conditions which also gave the maximum liquid yields. Similar results were demonstrated at a larger scale unit (1 - 3 kg/h of dry feed), operated with recycle gas with very good agreement in the yields of liquids and char with the bench scale unit.

.It was also concluded in the larger scale unit that in the temperature range of 450 - 550 °C neither particle size nor reaction atmosphere has a major influence on organic liquid yields. However this conclusion is in contradiction with other studies (157, 158) which reported that particle size has a strong influence on product yields. By carefully selecting sand size, biomass particle size, bed velocity and reactor configuration a "blow through" method of operation has been achieved in which practically no char remains in the reactor.

There are however several disadvantages in such a process. The loss of unreacted char represents a decrease in thermal efficiency, while the reactor has to be heated externally (e.g. electrical heating of the fluidizing gas). Since the feedstock has to be relatively finely grounded the biomass pretreatment costs will be high. Tests in a pilot plant or process development unit are needed as well as careful economic analysis before this process can be widely accepted.

2.4.6.3 Identification and yields of chemical feedstocks

In a completely different series of experiments, another group of Waterloo and Yokohama National Universities used the bench scale fluidized bed (0.002 internal diameter, see Table 2.13) with a pyroprobe (159, 160) in order to predict the yields of individual gaseous components from the pyrolysis of cellulose and filter paper. The aim of the research was to identify possible chemical feedstocks produced by flash pyrolysis of biomass. They identified a linear relationship between the logarithms of the gaseous products and carbon monoxide yields for the pyroprobe experiments of the form :

$$Y_{product} = A\,(Y_{CO})^{B}. \qquad \text{equation 2.8}$$

where Y_i = yield of component i

A,B = constants varying with component

They also determined the values of A and B for sixteen components. In addition to hydrocarbon gases (CH_4, C_2H_4, , C_2H_6, C_3H_6 and C_3H_8) important yields of acetaldehyde, furtural and levoglucosan were obtained (in the range of 10^{-2}-1; 10^{-1}-1 and 1-7 wt% of sample fed respectively). However, the authors did not consider the problems associated with seperating these components and the economics of such an upgrading process.

2.4.6.4 Emphasis on maximizing gaseous products

The pyrolysis of manure was studied (161) at fairly high temperatures (600-800 °C) for pyrolysis, in which very high gas yields were reported (76-88 wt%). However, the authors were unable to collect any liquids or condensate, so their mass balances are of limited value and their data questionable. Nevertheless they demonstrated that particle size can have a significant influence in a pyrolysis process, which is in agreement with generally accepted data.

In a comprehensive work at Tokyo University (162) the pyrolysis of wood residues was studied in a bench scale unit (see Table 2.13). In the initial experiments it was found out that the moisture content and the size of the feedstock had little or no effect on the constituents and the product pattern of the outlet gas. An important result was the measurement of the variations in the temperatures of the centres of 5 mm chip cubes after they were thrown into the fluidized bed. It was recorded that it took about 10 seconds for the centre of the chip to reach the maximum temperature. It was also reported that the yields of each product gas, as well as the total gas yield, increased with rising temperatures, while the char yield decreased as temperature rose. The yield of condensed material reached a maximum at around 600 °C and then decreased as the temperature increased. The authors concluded that there were no significant differences between the experimental data for wood chips (luan species) and those for peanut shells.

2.4.6.5 Diesel fuel from biomass

A project to convert various biomass materials to diesel type transportation fuel compatible with current engine designs and the existing distribution systems is under study (163, 164). A continuous thermochemical indirect liquefaction approach is used. The system consists of a circulating solid

fluidized bed gasification unit (dual bed) to produce a synthesis gas containing olefins, hydrogen and carbon monoxide, followed by a catalytic liquefaction step to convert the synthesis gas to liquid hydrocarbon fuel.

Numerous materials (87 individual species) had been processed through the conversion system without any significant change in product quality (essentially C_7-C_7 paraffinic hydrocarbons), while the major emphasis was to maximize product yield.

The gasification system - which is the part of main interest for this work - comprised two fluidized beds with connecting circulating solid transfer loops. One fluidized bed was used as a feedstock pyrolyser, while the second bed (regenerator) operated in a combustion mode to heat the circulating solids media. Both inert solids (sand) and catalytic material were investigated. Biomass feedstocks were continuously fed to the pyrolyser and flashed to a synthesis gas consisting of paraffins, olefins, carbon monoxide, carbon dioxide and hydrogen (residence time 2 seconds). The gas could be distributed via a compressor to the pyrolysed and/or the liquifaction reactor. Several types of liquifaction reactor are still under evaluation.

This overall approach offers the potential of producing a diesel type transportation fuel with relatively few processing steps. Relatively little information was given concerning the gasification system and as such it is of limited value to this work. An important remark however is that there is no significant influence in product quality by using different biomass feedstocks, which is an advantage for the commercialization of any process (see section 2.2).

2.4.6.6 Conclusions

Most current activities o the field of biomass pyrolysis aim at producing liquid fuelas or chemical feedstocks. With the exception of the work at Arizona State University, they so far have failed to demonstrate the viability of the process o a large scale reactor or even a process development unit. Another disadvantage for the ther studies is also the loss of char, which lowers the overall carbon conversion efficiency of a process.

A common problem is that ony one work (164) addressed the product quality and that in an unconvincing way (chromatograms from product oil produced by

feedstocks were compared to commercial no 2 diesel oil). All others failed to consider the quality of the products and to compare them to commercial ones. Several groups proposed possible thermochemical conversion routes for producing desirable products, but only one (163, 164) actually tried to produce these. Moreover, the other groups did not even identify the seperation and purification processes required to achieve the end products proposed. Similarly, with the exception of the Arizona State University group, none of the other clearly identified the applications and uses of the products of the proposed processes.

Besides the technical shortcomings and limitations, such processes are presently commercially unattractive due to the decrease of the price of oil. Since due to their nature only large scale plants can be economically sound for such processes, it is not believed that they could come on stream in the foreseeable future.

2.4.7 Gasification of biomass with bed materials other than silica sand, char and catalyst

2.4.7.1 Introduction

Most fluidized bed designs use an 'inert' solid material to make up the bulk of the bed. Silica sand is the most commonly used material being readily available and relatively cheap. However agglomeration problems due to ash-sand reactions have been experienced with sustained operation by many researchers (see section 2.4.3.6). Similar sintering problems have also been encountered when using catalysts as bed material, or when impregnating biomass with a catalyst in a silica sand bed (see section 2.4.8.2). Alternative bed materials that have been used widely include alumina, limestone or finely grounded metals.

It is believed (115, 116) that ash reacts readily with silica to form low melting silicates containing sodium and potassium resulting in sintering. This section reviews work done with other bed materials such as alumina and limestone to minimize or eliminate the problems of sintering and agglomeration which result in loss of fluidization.

In this thesis, agglomeration refers to the formation of clusters of particles which progressively become larger and cannot be fluidized after a certain size

(depends on density of solids, viscosity of gas and minimum fluidization velocity). The originally small particles of the bed are held together in the clusters by melted ash and tend to accumulate at the bottom of the bed. However, the rest of the bed continues to fluidize until all bed materials is fixed into clusters. Sintering on the other hand refers to the whole, or at least to a significant portion of the bed forming one mass consisting of bed particles, clusters and melted ash. This cannot be fluidized and when cooled hardens and is difficult to remove from the reactor. Sintering can damage internal devices such as thermocouples, heat exchangers and baffles.

2.4.7.2 Alumina sand

Alumina sand has been the most common alternative bed material to silica sand. An extensive study with this material was carried out by INCO Metals Company (115). During tests with silica sand and wood chips, severe fusing was observed, so the bed material was changed to alumina sand. It was found that alumina was a better material, however coarsening of the alumina particles was reported. This was attributed to reaction with alkali (sodium/potassium) and alkali earths (calcium, magnesium oxides) forming low melting compounds resulting in slow agglomeration. The mechanism of fusion was studied by metallographic and electron microprobe studies. It was shown that agglomeration occured by formation of a complex low melting silicate phase containing potassium which fused at high temperature and agglomerated. Thus a progressive sand agglomeration was observed which was very rapid after 5 hours of operation. Although the work was comprehensive, the authors failed to report any influence of the bed materials on the performance of the gasifier. Alumina sand was also tested at the free University of Brussels (116) during experiments with Euphorbia Tirrucalli. However, no major improvement was attained over silica sand. With both bed materials the bed sintered within 30 minutes of operation at 650 °C. The study had to be continued with metallic sand (see section 2.4.7.4).

2.4.7.3 Limestone

Limestone was investigated as bed material at the Kansas State University (165) and its influence on the performance of the gasifier was examined. With silica sand agglomeration occured about 15-30 minutes, with sintering of the bed 30 to 50 minutes after the initiation of feeding. Limestone was added to 25 wt% and during 13 hours of experiments no agglomeration was detected. It was

also reported that the gas components showed variations with operating temperature when limestone was present. Correspondingly the heating value of the gas depended on temperature for the sand bed, while it was invariant with temperature for limestone. Over the temperature range studied, the presence of the additive resulted in an average increase in the volumetric gas yield (m^3 gas/kg feed) of 33%. Since the heating value of the gas was constant over the temperature range, the efficiency also increased.

In the same study, satisfactory results were also obtained with dolomite and marble chips since the bed did not sinter after extended operation. However, no other information was given concerning the experiments with these two bed materials. Prelimenary tests with lime and gypsum were also successful, except that their beneficial effect did not last very long (2 hours). Potassium carbonate was also tested and it was observed that very severe agglomeration occured prior to the introduction of the feed. Thus it would appear that potassium salts play a key role in the agglomeration phenomenon, which is in accordance with the observation of INCO Metals Company (115).

On the other hand sintering was experienced at Kansas State University (165) with the gasification of manure and crop residues in a fluidized bed of quartz sand.

2.4.7.4 Metallic sand

Chromite sand was investigated at the free University of Brussels (115), after silica sand and alumina sand proved unsuitable because of the occurence of sintering in a series of experiments with Euphorbia. This fast growing species (166) demands particular attention due to the relatively high ash content (7-8 wt%) (167). The decision to use chromite sand was taken on basis of informations (168) provided to the Free University of Brussels.

However, gradual agglomeration was noticed although it never resulted in loss of fluidization. Tests on sintered chromite sand particles were carried out with energy dispersive X-ray micro-analysis (EDXM) and X-ray mapping (XM) for several elements, while photos from a scanning electron microscope (SEM) were taken. The photos from SEM clearly showed the sintering of the individual sand particles to larger aggregates. The XM analysis was carried out to identify the elements formed on the surface of the sand. These were mainly low alkali

metals (calcium and potassium), while some chlorine, phosphorus and iron were also detected. Then X-ray mapping was carried out on calcium and potassium, which proved that those elements were found all over the surface of the sand particles. From these analyses it was shown that sintering was caused by the alkali metals found in the ash of Euphorbia.

Additional tests were carried out with a Leitz heating microscope with different mixtures of sand and Euphorbia, which confirmed the previous results (ash content and composition of Euphorbia ash: 8 wt% ash; Ca = 11, Mg = 3.5, K = 30, Na = 1, Cl = 2.5 wt%; Al = 600, Fe = 1500, Mn = 625, Zn = 200 ppm) (167). It was also determined that the ash content of Euphorbia could be reduced through mechanical dewatering by which the latex was extracted. Analysis of the latex proved that about 50 wt% of the ash was removed. Subsequent experiments with biomass obtained after such a pretreatment showed no chromite sand agglomeration.

2.4.7.5 Conclusions

Bed agglomeration, sintering and consequent loss of fluidization is a serious problem which has not been thoroughly examined. Alternative bed materials such as limestone and chromite sand can improve the reliability of a system, while with alumina sand limited success has been achieved since the bed has to be removed, sieved and then returned to the reactor with fresh sand.

However, sintering has been observed only with some feedstocks, especially materials with a high ash content and it has been proven that with low ash feedstocks problems are seldom encountered even at commercial scale (see section 2.4.3.9). Nevertheless, sintering is more common in processes using catalysts or impregnated feedstocks. The pretreatment attempted at the Free University of Brussels (latex removal) might prove significant in reducing the ash content of a high ash feedstock to minimize agglomeration problems.

2.4.8 Catalysis of biomass gasification

2.4.8.1 Introduction

Despite substantial theoretical and experimental results most gasification systems presently under development do not use catalysts. The benefits from catalytic gasification can be summarized as follows (169):

a) increased reaction rates (greater throughput),
b) lowered operating temperatures (greater efficiency),
c) cracking of heavier hydrocarbons to form desirable products such as hydrogen and carbon monoxide,
d) increased yields of preferred species, such as methane.

The various catalysts available for biomass gasification can be classified in terms of their chemical composition into three groups; namely alkali carbonates, metallic oxides and metals and alloys. (168).

Alkali carbonates ($Na_2 CO_3$, $Li_2 CO_3$ and $K_2 CO_3$) increase reaction rates and gas production rates and decrease the yield of tars. The general consensus is that alkali carbonates catalyse the water gas shift and carbon-steam reaction (169-172).

Metallic oxides can be subdivided into:

a) cracking catalysts, which decompose high molecular weight hydrocarbons to products of lower molecular weight; they are predominantly synthetic products consisting of various mixtures of silica ($Si O_2$) and alumina ($Al_2 O_3$), or single compounds, such as limestone (CaO) and dolomite (MgO) which are considered good tar cracking catalysts (125), and
b) other metallic oxides (copper, iron, lithium, magnesium, molybdenun, potassium and zinc), which act similarly to alkali carbonates by favouring the production of lighter hydrocarbons and by catalysing the carbon-steam reaction. Although metallic oxides are considered to be good catalysts for the steam-carbon reaction, alkali carbonates are generally more economical to procure and slightly more efficient (148, 152). However these alkali carbonates are usually present in the ash content of biomass.

Metals and alloys can enhance the gas yields and gasification rates. The alkali and group VIII transition metals are of particular value and nickel has

been recognized as one of the most effective catalysts (169). The use of nickel results in a greater net yield of combustible gaseous products. However, nickel is costly and must be maintained in a highly reduced state; both factors rule against its commercial use in large-scale gasification. Cobalt has also proved to be a good catalyst, accelerating the rates and increasing the gas yield. There is also some evidence to encourage the use of such alloys as stainless steel and nichrome in gasification (174).

2.4.8.2 The use of catalysts for biomass gasification in fluidized bed systems

There are few research groups working on this field; their activities are summarized in Table 2.14. The earliest, longest and most extensive studies have been carried out at Pacific Northwest Laboratory, Battelle Memorial Institute. Several screening and preliminary experiments were carried out with a free fall reactor system (175). With this system and sodium carbonate ($Na_2 Co_3$) as reference catalyst, it was shown that the total gas production and the rate at which gas was produced, was significantly increased.

Table 2.14 : Catalytic gasification in fluidized bed units

Institute	Internal bed diameter m	Feedstock	Fluidizing medium	Catalyst	Temperature °C	Comments
Pacific Northwest (177-180)	0.61	Pine, Poplar Alder Bagasse	Steam	$K_2 CO_3$ $Na_2 CO_3$ N_i-C_u-M_o	730-740	Aimed at producing either methane or methanol. Serious differences between laboratory and pilot plant results
Forintek (180)	0.05	Powdered wood	N_2	$K_2 CO_3$ CaO	500	Short study to increase gaseous yields
Taiwan Nat. Univ. (181)	-	Rice husk	N_2, steam	Silica-aluminum zeolites metallic oxides	400-580	Screening experiments to identify most efficient catalyst

It was also concluded that the presence of alkali carbonate increased both char and gas production, while it decreased the amount of oil and tar produced.

The research was continued with a process development fluidized bed unit and focused on synthesis gas for methanol production (156-158) with new catalysts developed in the laboratory. A trimetallic catalyst, Ni-Co-Mo on silica-alumina doped with 2 wt% Na, was found to retain activity indefinitely for generation of a methanol synthesis gas from wood at 750 °C and 1 atm absolute pressure. However, catalysts for generation of a methane rich gas were deactivated rapidly and could not be regenerated as required for economic application.

When the same catalysts were used in the process development unit they display neither a long lifetime nor high activity, as was the case in the laboratory studies. The authors attributed these discrepancies to carbon deposition on the catalysts and to sintering.

Similar studies were carried out with bagasse using nickel and potassium carbonate catalysts (157). With the former catalyst deactivation occured rather rapidly and the experiments were terminated. While the latter catalyst did not lose its activity and functioned properly, severe problems were encountered with:
a) preparing the feedstock (impregnated with 10 wt %, $K_2 CO_3$),
b) preventing agglomeration in the fluidized bed, and
c) finding a suitable inert material for the bed.
Carbon conversion to liquids was always below 1 wt %, the balance being char.

In an other study (179), it was shown that as soon as the catalysts start loosing their activity, the yields of tars and other condensible hydrocarbons increased considerably. In a similar but much shorter study (180), the gasification of hybrid poplar was studied in a fluidized bed at 500 °C, using potassium carbonate and calcium oxide as catalysts. Both catalysts increased the liquid and gas yield at the expense of char, with a final product which was approximately 50% gaseous, 30% liquid and 20% solid. It was concluded that the carbonate catalyst enhanced the formation of hydrogen and methane and reduced the formation of carbon dioxide. The oxide catalyst had a similar but more pronounced effect.

The catalytic gasification of rice husks was investigated in Taiwan (181) using four amorphus (silica-alumina and zeolites) catalysts and five metal oxides catalysts. It was reported that the first group of four catalysts produced gaseous products of a moderate quantity and little hydrogen Nevertheless they produced more carbon monoxide, ethylene and propylene than the other five metal oxides catalysts The second group of five catalysts produced a hydrogen rich synthesis gas The gaseous products yields by these catalysts were much higher than those of the amorphus catalysts Very little information was given in this publication concerning detailed composition of catalysts used, experimental conditions and procedures, thus making comparison with other work difficult and the data of limited value

2.4.8.3 Conclusions

It has been demonstrated that certain catalysts can enhance the formation of certain components in biomass gasification Most commonly the yields of gaseous compounds are increased at the expence of liquid or solid products However, at present there exists no catalyst which has been proven for commercial applications Problems of poisoning by carbon deposition, sintering and rapid deactivation of some catalysts still have to be solved Gasification catalysts are therefore at an early stage of development

There are no commercial companies marketing biomass gasifiers operating with catalysts, indicating that further efforts have to be made at R&D level to improve the existing knowledge on this subject

Commercial processes using catalysts should aim at improving the yields of desired products For fuel gas production alkali carbonates are well suited for maximizing gas yields. Other catalysts such as nickel can be used when a specific gas product distribution is desired Alternatively, a dual catalyst system may be required one to maximize gas yields and the other to tailor the gas composition for synthesis gas Ideally, commercial catalysts should be developed, that can resist poisoning from various elements (such as sulphur, chlorine) and/or deactivation by deposition of carbon and/or tar In case of poisoning or deactivation, it would be desirable and for some catalysts (those composed of compounds of expensive, elements such as nickel, cobalt et al) an economic necessity, to reactivate them or at least

recover the expensive compounds. More specifically for fluidized bed reactors, if the catalysts are to be used as bed material, they should withstand temperatures in excess of 850 °C in order to avoid melting and consequently bed sintering (melting points of sodium carbonate = 851 °C; potassium carbonate 891 °C)(182). Finally the cost of procurement and reactivation or recovery of the catalyst should not exceed the benefits achieved by them in the overall process.

Relatively cheap materials such as limestone and dolomite deserve better evaluation of their catalytic properties.

2.5 MODELLING OF FLUIDIZED BED GASIFIERS

2.5.1 Introduction

Modelling implies the representation of a chemical or physical system by a set of equations which in a limited way can represent the system under study. Relevant in reactor design, is a mathematical description that can predict reactor outlet concentrations and temperature from inlet concentrations, flows and reactor dimensions (183).

In general there are two approaches by which fluidized bed gasifiers can be modelled:
a) modelling a fluidized bed reactor which contains biomass and
b) modelling biomass gasification which happens to be in a fluidized bed.

In the former approach emphasis is given on the hydrodynamics of the reactor, while biomass is considered as non reacting (such as modelling of the fluidization characteristics of a char bed). In the latter approach, the fluidization characteristics of the bed are set constant while the gasification of biomass is modelled. It is this second approach that is of particular interest for this work, since fluidized bed reactors have been extensively covered in the literature (see section 2.3.3.2) and gasification of biomass taking place in a fluidized bed reactor is the main subject of this thesis.

There are two aspects to any theoretical investigation of gasifier behaviour (109, 184). The first is a thermodynamic approach which gives information on gas composition and its dependance on feed and oxidant compositions. The

second is a kinetic approach which considers the effects of rate laws of chemical reaction and heat and mass transfer. Finally the behaviour of a gasifier can also be studied on the basis of empirical models. These principles are shown in Figure 2.14.

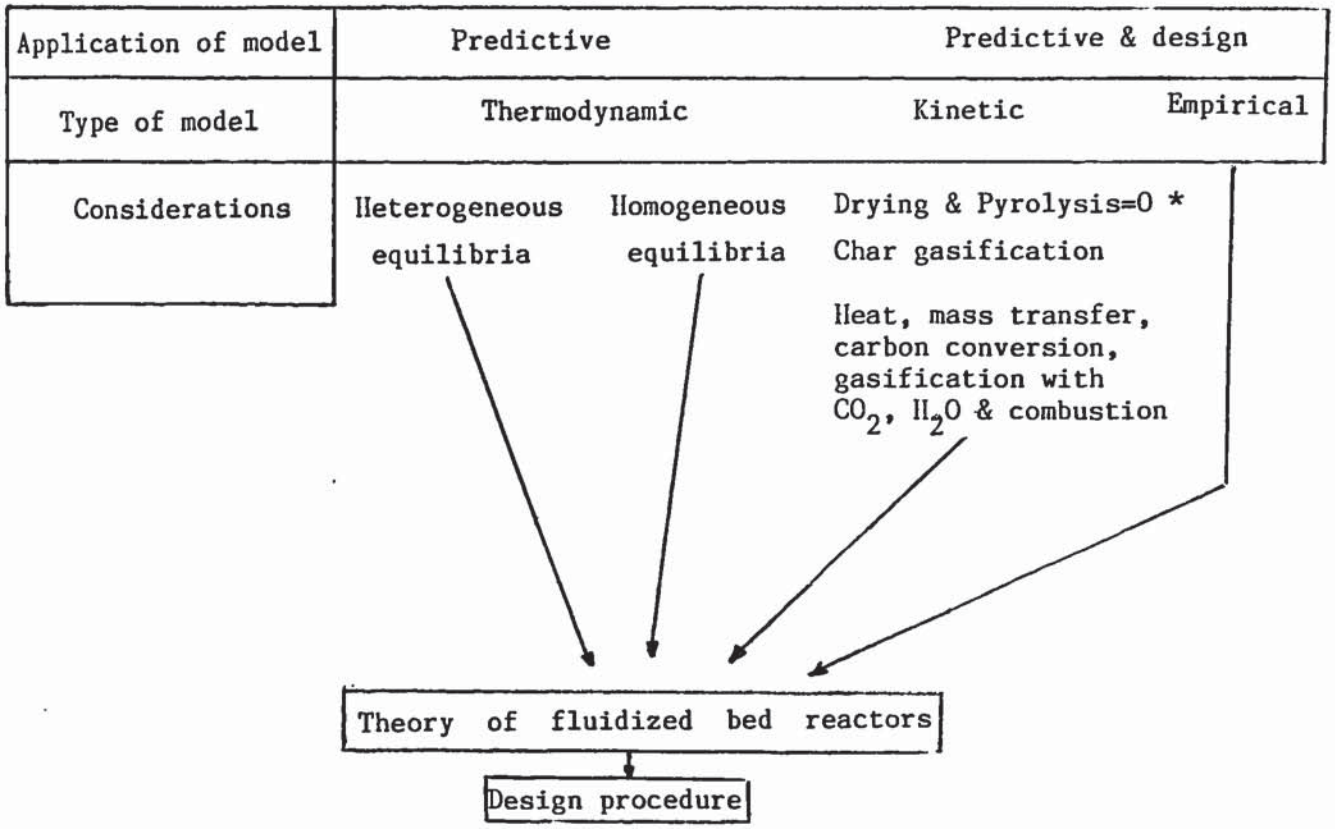

Figure 2.14 : Various aspects of modelling fluidized bed gasifiers

Fluidized bed reactors are considered to be multiphase systems in terms of the contacting pattern and flow of reactants and products since several phases (bubble, emulsion and cloud) exist (50) (see section 2.3.3 and Figure 2.15). Gasification reactions are heterogeneous (the reaction requires the presence of at least two phases - gas and solid - to proceed at the rate that

it does (183, 185) (see section 2.5.5)). Therefore this type of gasifier is complex as far as the contacting patterns and chemical reactions are concerned.

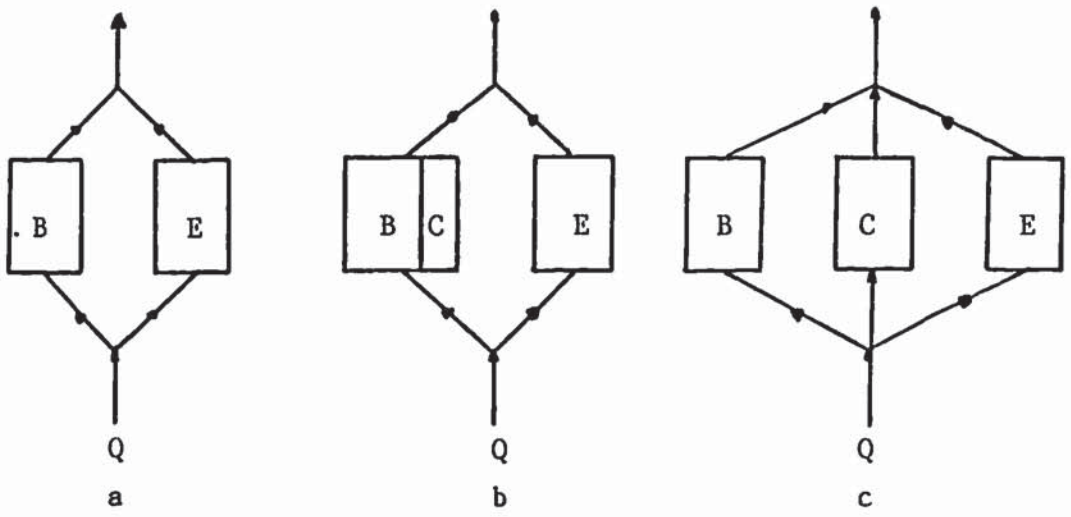

Figure 2.15 : Schematic of two phase and three phase representation of fluidized beds: B, bubble phase; C, cloud phase ; E, emulsion phase.
Two phase models a and b, three phase models (50).

For such reacting systems there are two complicating factors that must be accounted for in addition to the reaction rate used in simple contacting systems such as homogeneous reactors:

a) in ideal contacting of heterogeneous systems, each phase may be in plug or mixed flow (see. Figure 2.8.). Thus many combinations of contacting patterns are possible. Further, if one of the phases is discontinuous, as are bubbles or discrete solid particles, its characteristics will have to be accounted for (38). Thus each of the many methods of contacting of two phases has a specific form of performance equation associated with it. For fluidized bed gasifiers,the hydrodynamics of the bed and thus the contact pattern have to be accounted for (see section 2.3.3.2);

b) in gasification reactions, since more than one phase is present, the movement of material from phase to phase must be considered in the rate equation. Thus the rate equation in general will incorporate mass transfer terms in addition to the usual chemical kinetic term (185).

In this section the different modelling approaches for a fluidized bed gasifier will be reviewed, while the advantages and disadvantages of each method will be discussed. Attention is paid to the applicability of each method and its complexity in view of developing design procedures .

The underlying science of thermochemical conversion of biomass materials to useful fuels is not adequately understood. Recent experimental research in the USA (187) and Sweden (157) concluded that biomass gasification occurs in three steps: 1) drying and pyrolysis producing volatile matter and char; 2) secondary reactions of the evolved volatile matter in the gas phase and 3) char gasification with steam and carbon dioxide.

Figure 2.16 (188) is a state of the art depiction of the stages through which each biomass particle and intermediates must pass during a typical thermochemical process. In principle all stages could be separated in different reactors; however, in practice, they are taking place in a single reactor (e.g. moving bed reactors, single fluidized bed), or in two reactors (dual fluidized bed systems) where the pyrolysis and gasification stages are separated.

A more detailed analysis of the gasification stages of biomass particles is proposed in Figure 2.17. This considers the reactions of tars and volatiles and internal recycle of the product of pyrolysis to the pyrolysis stage (this actually takes place in most reactors but especially in fluidized beds since, due to intense mixing, biomass particles undergo pyrolysis all over the bed), as well as the exchange and reaction between the three different products of pyrolysis; e.g. primary gas components, such as carbon dioxide and carbon monoxide, can react with char or tar.

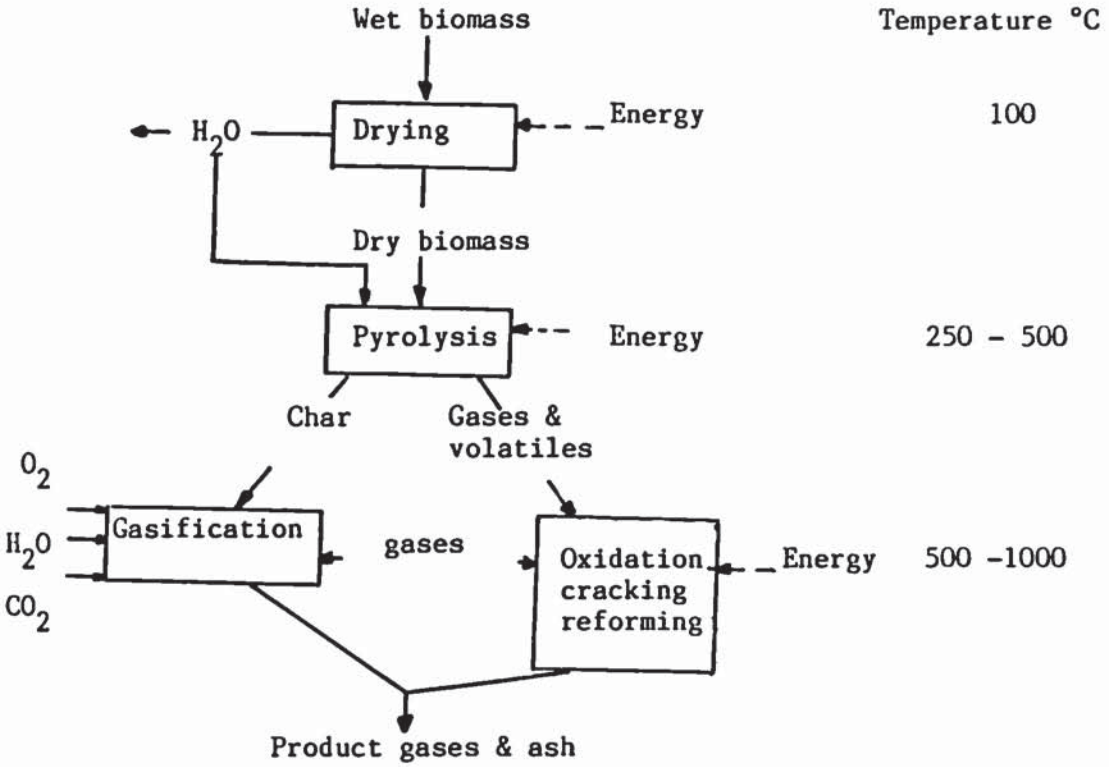

Figure 2.16 : Stages in thermochemical processing of biomass (188).

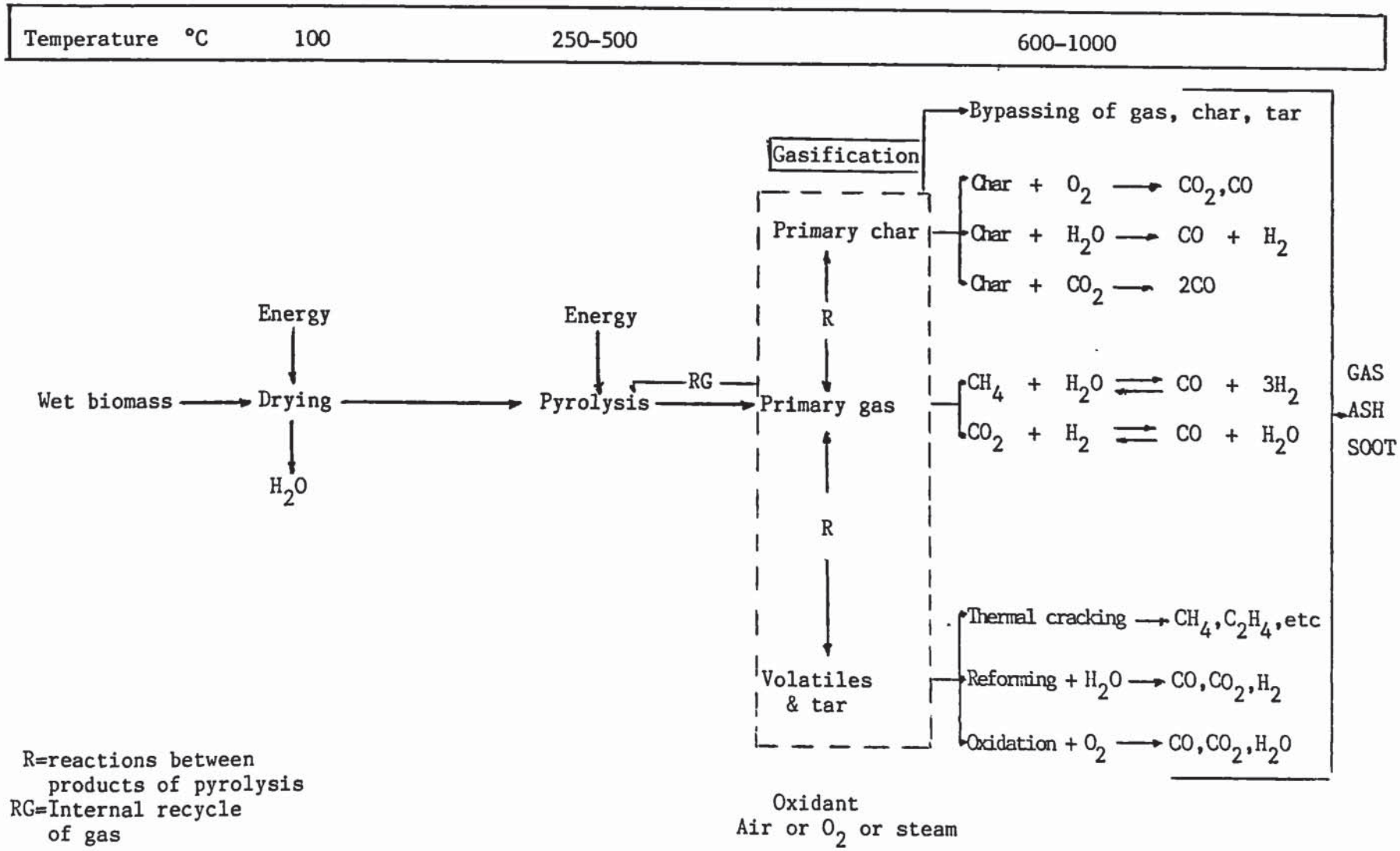

Figure 2.17 : Steges in biomass gasification

2.5.2 Drying of biomass

2.5.2.1 Introduction

Removal of water reduces the weight of material that must be transported or handled in a processing plant, thereby lowering operating costs and it generally improves the quality of wood for thermochemical processing. On the other hand, the disadvantages of drying-equipment and operating costs must be carefully evaluated in any process.

2.5.2.2 Periods of drying

When a material is dried, a drying curve can be plotted as moisture content (dry basis) versus time, as shown in Figure 2.18a (189). This curve represents the general case, when wet biomass loses moisture first by evaporation from a saturated surface on the solid, followed in turn by a period of evaporation from a saturated surface of decreasing area and finally by a period when the water evaporates in the interior of biomass (for a realistic example see Figure 5.2).

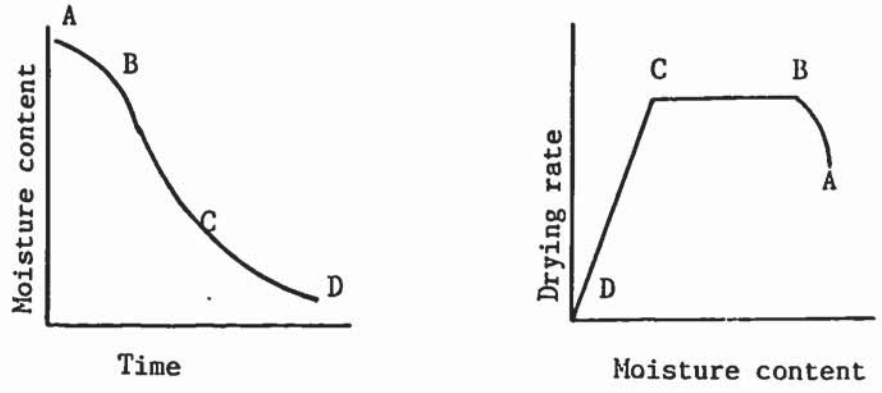

Figure 2.18 : The periods of drying

The variation in drying rate can be better illustrated by plotting the drying rate versus moisture content (Figure 2.18b). The rate curve shows that drying is not a smooth, continuous process in which a single mechanism controls throughput. Section BC represents a constant rate period, the portion CD is termed "the falling rate period" and section AB is the heating up period (189).

During the constant rate period, drying proceeds by diffusion of vapour from the saturated surface of the material across a stagnant-air film into the environment. Moisture movement within the solid is rapid enough to maintain a saturated condition at the surface and the rate of drying is controlled by the rate of heat transfer to the evaporating surface. The rate of mass transfer balances the rate of heat transfer and the temperature of the saturated surface remains constant (190). Point C, where the constant rate ends and the drying rate begins to fall, is termed "the critical moisture content".

If heat is transferred solely by convection, the temperature of the surface approaches the wet-bulb temperature (defined as the dynamic equilibrium temperature attained by a water surface, when the rate of heat transfer to the surface by convection equals the mass transfer away from the surface) (190). However, when heat is transferred by radiation, conduction, or a combination of these and convection, the temperature of the saturated surface is between the wet-bulb temperature and the boiling point of water. Under these conditions the rate of heat transfer is increased and a higher drying rate results.

The falling rate period begins at the critical moisture content. If the final moisture content is above the critical moisture content, the whole drying process will occur under constant rate. If, on the other hand, the initial content is below the critical moisture content, the entire drying will occur in the falling rate period. This period is usually divided into two zones a) the unsaturated surface drying and b) the zone where internal moisture movement controls. In the first zone, the evaporating surface can no longer be maintained saturated by moisture movement within the solid. The drying rate decreases and moisture from the solid to the surface and transfer diffusion of moisture away from the surface become rate controlling. As drying proceeds, the point is reached where the evaporating surface is unsaturated and the place of evaporation moves into the solid and the drying

enters the second falling rate period (189). The drying rate is now governed by the rate of internal moisture movement.

Studies of internal moisture movement indicate the possibility of several controlling mechanisms, the most important ones being postulated as diffusion, capillarity and pressure gradients caused by shrinkage (191).

Another complication lays in the important differences between 'free' and 'bound' water in wood. Free water is found in the cell cavity and can be moved reasonably rapidly from wood, whereas bound water is in the cell wall and its rate of movement is of the order of 100 to one 1000 times slower than free water (192).

Specifically for biomass, the moisture movement during the falling rate period is controlled by diffusion. Since the rate of drying during the constant rate period is proportional to the temperature difference,

$$\text{rate of drying} = \frac{h_t A \Delta t}{l} = k_g A \Delta p \qquad \text{equation 2.9}$$

where h_t = heat transfer coefficient (KJ/hm^2 °C)

A = area for heat transfer (m^2)

l = latent heat of evaporation (KJ/kg)

k_g = mass-transfer coefficient (Kg/hm^2 atm.)

$\Delta t = t - ts$ where t = gas temperature (°C)

ts = temperature of surface (°C)

$\Delta p = Ps - p$ where Ps = vapour pressure of water at surface temperature (atm.)

p = partial pressure of water vapour in the gas (atm.)

Under normal operating conditions of gasifiers (700-1200 °C) drying of biomass attains very high rates (184).

In dense phase reactors (see section 2.2.2.1) the operating temperatures in the drying zone are relatively low (100-350 °C), (11-15) while in lean phase reactors, since distinct zones do not exist, the temperature is relatively high (600-950 °C). Thus for lean phase gasifiers (see section 2.2.2.2.) the rates of heating and drying attain very high rates and these processes are generally considered to be instantaneous in view of a model development (184).

Therefore these processes can safely be ignored in the formulation of a model. However, this assumption does not hold for dense phase reactors, since the preheating and drying zone represents a significant fraction of the total reactor volume.

2.5.3 Pyrolysis of biomass

2.5.3.1 Introduction

Different components of biomass (cellulose, hemicellulose, lignin) display different thermal properties and the thermal properties of the aggregate represents the sum of its major organic components (193). Furthermore, the thermal properties of the components and aggregate are influenced by the presence of inorganic materials and pretreatment methods. These phenomena have been demonstrated by thermal analysis of cottonwood and its components, as shown in Figure 2.19 (194).

The primary transformations in pyrolysis are thermally driven; as the temperature wave propagates into the solid, moisture evaporates and the breakdown of the more unstable polymers begins; as the local temperature increases so does the rate of degradation and more stable components of the heterogeneous biomass decompose (195). The volatile products of primary pyrolysis flow out of the solid matrix and may participate in secondary reactions. The volatiles then flow away from the carbonizing particle and may react further as they pass through the bed (see Figure 2.17).

2.5.3.2 Effect of temperature

Pyrolysis of biomass materials occurs under normal conditions at relatively low temperatures (300 °C to 500 °C) (193). Very rapid heating causes pyrolytic weight loss to occur at somewhat higher temperatures (450 to 700 °C) (196). In general, the volatile matter content of cellulosic materials is approximately 90 % of the dry weight of the initial feedstock, while woody materials contain between 70 and 80 % volatile matter (197). However,

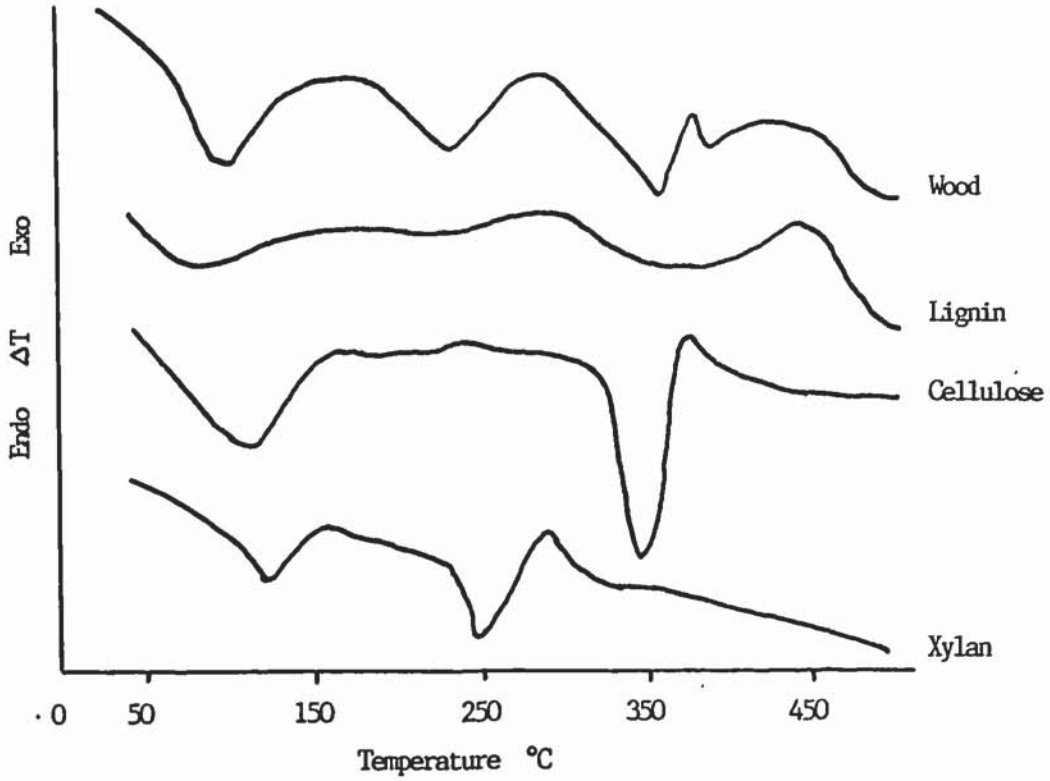

(a) Differential thermal analysis of wood and its components

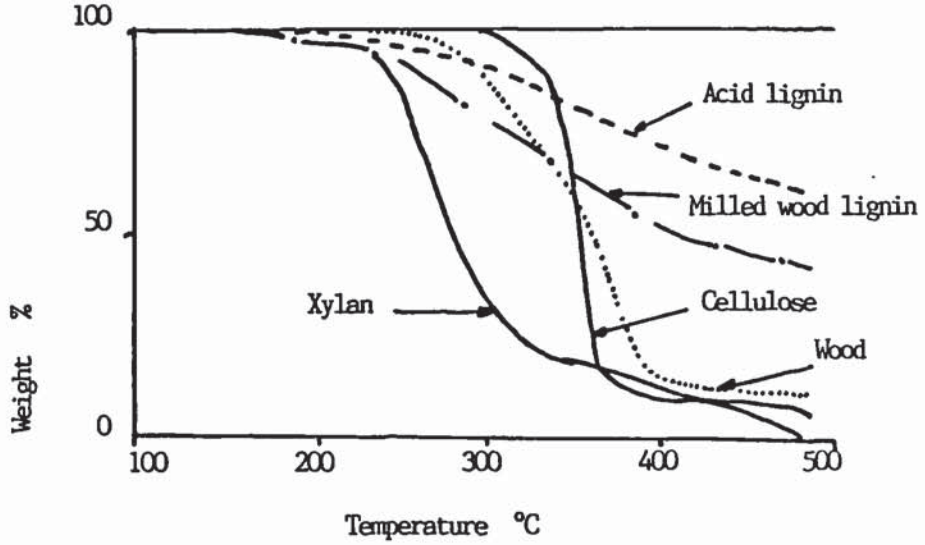

(b) Thermogravimetry of wood and its components

Figure 2.19 : Thermal analysis of cotton wood and its components (194).

it has been demonstrated (198) that cellulosic materials can be completely volatilized when subject to very rapid heating (above 10,000 °C/s).

Volatile matter produced by pyrolysis of biomass begins to participate in secondary gas phase reactions, such as oxidation and reduction (see Figure

2.17) at temperatures exceeding 650 °C. These reactions occur very rapidly and yield a hydrocarbon rich gas (199). At still higher temperatures (above 700 °C) pyrolytic char reacts with steam and carbon dioxide to produce hydrogen, carbon monoxide and carbon dioxide. Rates of gasification and combustion of biomass derived chars are known to be higher than coal derived chars. Nevertheless, much higher temperatures are required to achieve char gasification than biomass pyrolysis (200).

2.5.3.3 Other parameters affecting pyrolysis

During thermal degradation of biomass various amounts of gas, volatiles and char are produced, the relative product distribution of which is a sensitive function of many factors including temperature, physical size and state of material, temperature history, inorganic impurities and heating rate (193, 199). The gaseous environment seems to be relatively unimportant (193). Secondary reactions take place which are related to contact with char, temperature, pressure, dilution, and residence time, while the gaseous environment is again of secondary importance with the exception of oxygen (201).

As the degradation proceeds, more volatiles leave the char and its carbon content increases while the hydrogen and oxygen contents decrease. This process is significant since some of the products of pyrolysis leave the reactor unchanged and thus are reported downstreams, e.g. tars. As with drying in lean phase reactors, small particles with attendant fast heating rates (it has been reported that typical heating rates in fluidized bed units are in the order of 1000 °C/s (153, 156, 159, 160)) will be subjected to short residence time. Therefore the degradation process has an extremely high rate and it can be assumed to be instantaneous. Thus the rate of pyrolysis could be disregarded in the formulation of a biomass gasification model for such systems. However, for dense phase reactors, pyrolysis has to be accounted for.

2.5.3.4 Cellulose pyrolysis

The pyrolysis of biomass has a strong influence on the overall gasification process. The primary products of pyrolysis contribute to the gas composition as well as the products of their secondary gas phase reactions. Moreover, tar

which is produced during the pyrolysis stage can have a negative influence on gas quality if excessive amounts of this component are produced.

The thermal decomposition rate of wood closely follows that of cellulose, whereas hemicellulose decomposes faster and lignin slower (see Figure 2.19) (202). Thus the majority of the experimental work has been done with cellulose to better understand the pyrolysis of wood and other biomass materials (198, 202). Also cellulose has the advantage that it can be made into homogeneous samples, having a wide choice of closely controlled densities and physical constants.

Several global models have been postulated for the chemistry of cellulose pyrolysis (205, 202, 198) (see Figure 2.20).

The first widely adopted scheme which provided a conceptual framework for many observations was proposed by Kilzer and Broido in 1965 (205). They postulated that pyrolysis proceeds by two reactions:
reaction 1: Dehydration and charing at low temperatures: this reaction proceeds more rapidly than reaction 2, forming char, water, carbon monoxide, carbon dioxide and other light gases from the cellulose substrate.
reaction 2: Levoglucosan formation: this reaction produces tar and under faster heating rates, reaction 2 becomes more important than 1.
Shafizadeh (202) elaborated on this scheme and proposed the mechanism shown in Figure 2.20b. Reactions 1 and 2 are similar to the Kilzer-Broido model.
reaction 3 : Fission and disproportionation: this reaction takes place at high temperatures (higher than 500 °C) and high heating rates (higher than 10 °C/s) and produces additional gases and low molecular weight products.

Lewellen et al. (198) proposed the third scheme in Figure 2.20. According to their mechanism, cellulose could decompose rapidly to an intermediate, tentatively identified as levoglucosan. The levoglucosan may then (1) be transported from the cellulose matrix to give tar; (2) repolymerize, crack or be cross-linked, to yield char; (3) be pyrolysed to lighter volatile products including carbon monoxide, carbon dioxide, permanent gases, organic acids, ketones, esters, aldehydes and free radicals, some of which could (4) inhibit char formation or (5) autocatalyse step (3). Lighter stable products could also (6) escape the matrix to yield volatiles.

(a) Kilzer & Broido (205)

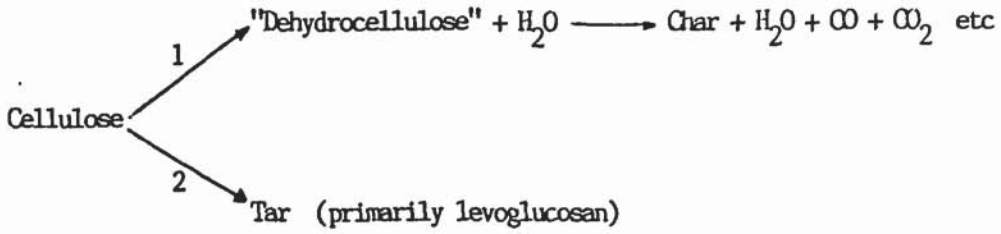

(b) Shafizadeh (202)

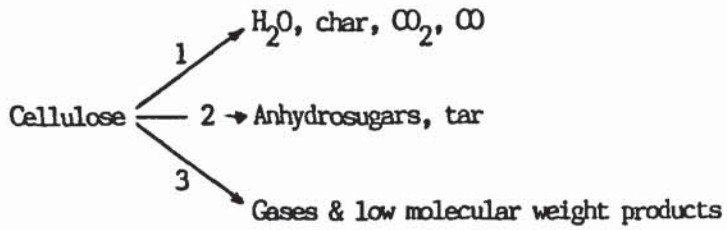

(c) Lewellen et al (198)

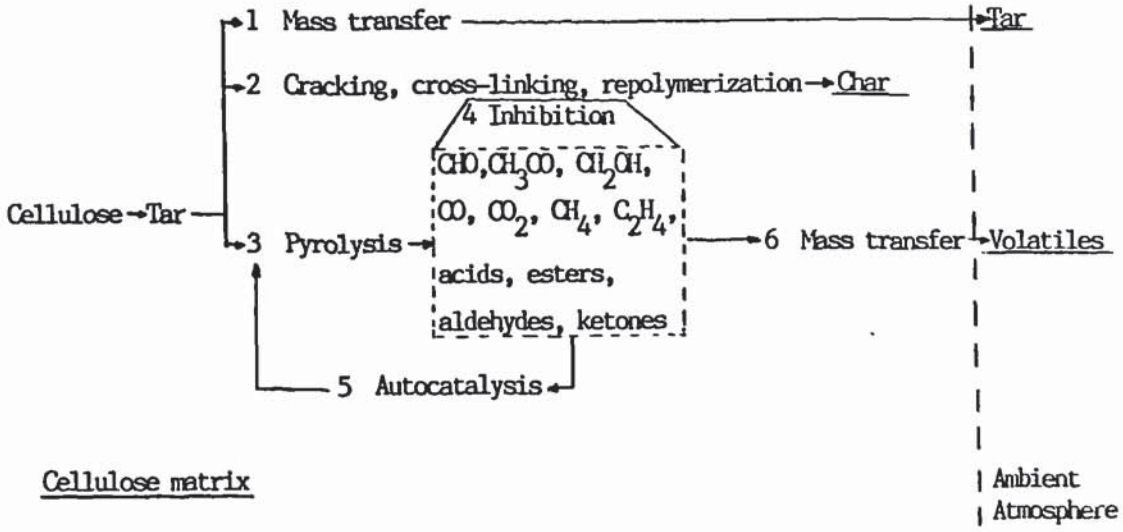

Figure 2.20 : Comparison of the various mechanisms for cellulose pyrolysis.

The most thorough mechanism seems to be the one of Lewellen et al. (198), but it is also the most complicated to model. However, the most widely used mechanism is the one of Shafizadeh (202).

Several kinetic models have appeared in the literature for cellulose pyrolysis below 500°C (206-212). High temperature pyrolysis kinetics (above 500 °C) must necessarily reflect the rates of lower temperature pathways and consequently the competitive reaction 3 of the Shafizadeh mechanism (see Figure 2.20). In addition, the elucidation of a comprehensive high temperature rate law also requires a determination of the rate law associated with the postulated high temperature fission pathway (reaction 3). A comprehensive rate law for the high temperature fission pathway has not been determined yet due to the complexity of pyrolysis under such conditions.

However, two techniques can be used to overcome this problem:

a) the assumption of a single reaction first order decomposition model

$$\text{cellulose} \longrightarrow a\text{CO} + b\text{CO}_2 + d\text{H}_2\text{O} + e\text{tar} + f\text{char} + \ldots\ldots \qquad \text{equation 2.10}$$

b) the assumption that cellulose decomposes directly to each reaction product i by a single independent reaction pathway also designated i:

$$\text{cellulose} \xrightarrow{k_i} \text{product i} \qquad \text{equation 2.11}$$

and the kinetics of the process can be modelled by a unimolecular first order reaction (209, 212).

The application of the above techniques cannot predict tar yields adequately, furthermore other sets of quite different rate parameters can regenerate the measured data. Therefore these techniques cannot be used widely and their reliability is questioned.

The mechanisms and kinetics of hemicellulose and lignin have not received strong interest and inconclusive results have been obtained. The hemicelluloses have received less study partly because of their lesser abundance in wood and partly because of their variety of constituents. All studies (194, 213, 214) indicate that they are the most unstable major

component of wood. Lignin is the most complicated, least understood, hardiest to extract without change and most refractory component of wood. Consequently the interpretation of experiments with lignin is the most empirical and shows the most variable behaviour of the wood constituents (12, 215, 216). Thus a more detailed discussion of the pyrolysis of hemicellulose and lignin is unjustified in terms of this work.

2.5.3.5 Wood pyrolysis

Studies on wood pyrolysis have only recently appear in the literature (217-227). The majority of this work is of qualitative nature, in trying to identify the primary and secondary products of pyrolysis and their yields. Although these are of interest in understanding wood pyrolysis, they are however of limited value to this thesis.

Due to the complicated nature of wood pyrolysis, it has been attempted to predict its pyrolysis behaviour - under a given set of reaction conditions - from corresponding information on woods constituents, cellulose, hemicellulose and lignin (221). A pyrolysis simulation model was proposed assuming that the simulated integral yield $Y_{iw}(t)$ of a given product i from pyrolysis of this wood up to time t is given by:

$$Y_{iw}(t) = \sum_{J=1}^{3} W_j \; Y_{i,j}(t) \qquad \text{equation 2.12}$$

where w_j is the weight fraction of constituent j in the wood, and $Y_{i,j}(t)$ is the integral yield of product i from pyrolysis of constituent j up to time t. Complete results were not available yet at the time of writing to evaluate this approach.

Though this analysis may be usefull in simulation of wood pyrolysis, it overlooks the fact that wood constituents are usually chemically bonded and physically intermixed. Moreover, the detailed molecular structures particularly of hemicellulose and lignin can vary among different biomass types.

2.5.3.6 Conclusions

Pyrolysis is a very important process in thermochemical processing of biomass. It is a complicated process and despite serious efforts by several groups it is still not very well understood. Low temperature pyrolysis of cellulose has been extensively studied and some success in modelling has been achieved in this area. However high temperature pyrolysis of cellulose is still not adequatelly covered and no reliable models exist in this field.

Pyrolysis of hemicellulose, lignin and wood are understood even less than pyrolysis of cellulose. More specifically, in relation to this work, pyrolysis of wood at high temperatures (above 500 °C) and at high heating rates (higher than 1000 °C/s) is poorly understood and its mechanisms and kinetics still have to be extensively examined, before they could be successfully used in design.

However it can be safely assumed that the rate of pyrolysis is faster than the rate of char gasification by at least an order of magnitude (193) and especially for lean phase reactors, it does not have to be accounted for in a model (15). The same is also true for drying of biomass. Therefore, since this thesis is concerned with the development of an empirical model and design procedure for fluidized bed gasifiers, emphasis will be given in the next section to char gasification only.

2.5.4 Thermodynamic models

2.5.4.1 Introduction

Thermodynamic prediction is the most widely used technique to model the performance of gasifiers (24).

In the foregoing discussion, pyrolysis and gasification were identified as the two major stages in biomass gasification. The products of pyrolysis and char gasification reactions are not in chemical equilibrium because gas phase reactions are slow below 500 °C; there is great complexity in terms of product formations and temperatures gradients exist in and around the pyrolysing particle. However, at temperatures above 500 °C, chemical equilibrium is approached fast enough, so that thermodynamic calculations

can be increasingly accurate in predicting important trends and in some cases the gas composition to be expected from biomass gasification (228).

The conditions at which all the carbon in the char is theoretically gasified is called the solid carbon boundary (see Figure 2.2). To one side of this boundary some charcoal is predicted, to the other side no solid carbon leaves the gasifier (94). Such a system represents an idealized case and operation of a thermodynamically equilibrated gasifier on the solid carbon boundary results in maximum thermal efficiency. However, in practice a range of factors including the temperature, residence times and gas-solid contacting methods employed in gasification reactors, significantly affect the degree of attainment of equilibrium. The uniformly high temperatures in a fluidized bed offer favourable conditions for equilibrium but the degree attained depends on gas residence time. However, this is also the case with downdraft gasifiers.

2.5.4.2 Heterogeneous and homogeneous reactions

The most important char gasification reactions are listed in Table 2.15. The first two reactions which are irreversible, represent the oxidation of char with oxygen and the heat released by these reactions drives subsequent processes.

Table 2.15 : Gasification reactions (184, 229).

Equation	Reaction		Heat of reaction (KJ/mole) 20 °C
	Heterogeneous		
2.13	$C + 1/2\ O_2$	$\longrightarrow CO$	- 110.6
2.14	$C + O_2$	$\longrightarrow CO_2$	- 393.8
2.15	$C + CO_2$	$\Longleftrightarrow 2CO$	+ 172.6
2.16	$C + H_2O$	$\Longleftrightarrow CO + H_2$	+ 131.4
2.17	$C + 2H_2$	$\Longleftrightarrow CH_4$	- 74.9
	Homogeneous		
2.18	$CO + H_2O$	$\Longleftrightarrow CO_2 + H_2$	- 41.2
2.19	$CH_4 + H_2O$	$\Longleftrightarrow CO + 3H_2$	- 201.9
2.20	$2H_2 + 2CO$	$\Longleftrightarrow CO_2 + CH_4$	+ 321.3

High temperatures favour the Boudouard (eq. 2.15) and water gas (eq. 2.16) reactions - both kinetically and thermodynamically - which are highly endothermic. Conversely the methane reaction (eq. 2.17) is not favoured by high temperatures (230, 231). In order to compute the equilibrium composition, only two methods of approach can be applied a) the equilibrium constant method of Gumz (183) and b) the rarely applied approach of minimizing the total Gibbs free energy of the reacting system. Both methods have been extensively discussed and analysed in the relevant literature (15, 24, 184, 228-232).

The former method uses the equilibrium constants of a set of reactions, which represent the reacting system and with material balances a set of equations is formed, the solution of which gives the equilibrium composition (see following section). The second method applies the total Gibbs function for the given system:

$$nG = \Sigma (n_i \overline{G_i}) \qquad \text{equation 2.21}$$

where nG = total Gibbs function, n_i moles of component i and $\overline{G}_i$ is the partial molar Gibbs function of component i. The problem then is to find a set of n_i's which minimizes nG at constant temperature and pressure subject to the restrains of the material balances. This is solved by the method of Lagrange's undetermined multipliers. It is important to note that in this procedure the question to know which chemical reactions are involved never enters directly into any consideration. However, the choise of a set of species is entirely equivalent to the choise of a set of independent reactions among the species. A disadvantage of this procedure is that the standard Gibbs heat of formation of the components must be known at the temperature of the system. However in both cases some assumptions have to be made:

a) all gases are ideal
b) the only gaseous products are H_2, CO, CO_2, H_2O, CH_4, and N_2, while O_2 is fed in the gasifier (in the form of air or oxygen).

2.5.4.3 Illustrative example

In this section a thermodynamic model on the carbon solid boundary is developed. It is postulated that all fuel fed to the gasifier is gasified (it

contains no ash), while the assumptions a) and b) of the previous section are valid. The homogeneous reactions 2.18 and 2.20 are considered to be at equilibrium. Such a set of equations is more suited for lean phase gasifiers than heterogeneous reactions, since the excess of carbon in lean phase gasifiers is not always certain. On the other hand dense phase gasifiers operate always with excess of carbon and a set of heterogeneous equilibrium reactions is valid. When the heterogeneous equilibria are established, the homogeneous equilibria are automatically attained. However the reverse is not always true (15).

The corresponding equilibria constants of reactions 2.18 and 2.20 at atmospheric pressure are:

$$K_w = P_{CO2} \times P_{H2} / P_{CO} \times P_{H2O} \qquad \text{equation 2.22}$$

$$K_m = P_{CO2} \times P_{CH4} / P^2_{H2} \times P^2_{CO} \qquad \text{equation 2.23}$$

where K_w and K_m = equilibrium constants of reactions 2.18 and 2.20 respectively
and P_i = partial pressure of component i.

These constants were evaluated from standard thermodynamic relationships (233).

Using a fuel of known elemental composition and a blast consisting of a mixture of air and steam, the only variable parameter is the operating temperature. The mass conservation equations for each element are:

$$\text{for C}: F_{fC} = G\,(M_{CO2}\ 12/44 + M_{CO}\ 12/28 + M_{CH4}\ 12/16) \qquad \text{equation 2.24}$$

$$H: F_{fH} + B\,b_{N2} = G\,(M_{N2} + M_{CH4}\ 4/16 + M_{H2O}\ 2/18) \qquad \text{equation 2.25}$$

$$O: F_{fO} + B\,(b_{O2} + b_{H2O}\ 16/18) = G\,(M_{CO2}\ 32/44 + M_{CO}\ 16/28 + M_{H2O}\ 16/18) \qquad \text{equation 2.26}$$

$$N: F_{fN} + B\,b_{N2} = G\,M_{N2} \qquad \text{equation 2.27}$$

Total : $M_{N2} + M_{H2} + M_{CO2} + M_{CO} + M_{H2O} + M_{CH4} = 1$ equation 2.28

where F = amount of feedstock consumed in kg/h
G = amount of gas produced kg/h
B = amount of blast gas consumed kg/h
f_i = mass fraction of component i in fuel
b_i = mass fraction of component i in blast
M_i = mass fraction of component i in gas produced

Substituting the volume fraction of each compenent i in the gas (using $P_i/P_t = V_i$), and assuming atmospheric pressure, equations 2.22 and 2.23 can be written as:

$V_{CO2} \cdot V_{H2} - K_w \cdot V_{CO} \cdot V_{H2O} = 0$ equation 2.29

$V_{CO2} \cdot V_{CH4} - K_m \cdot P_t^2 \cdot V_{H2}^2 V_{CO}^2 = 0$ equation 2.30

Substituting equation 2.31

$V_i = (M_i/\rho_i) \cdot \bar{\rho}$ equation 2.31

where ρ_i = specific weight of component kg/m³
$\bar{\rho}$ = specific weight of product gas kg/m³

equations 2.29 and 2.30 become:

$M_{CO2} M_{H2} - K_w (\rho_{CO2} \rho_{H2}/\rho_{CO} \rho_{H2O}) M_{CO} M_{H2O} = 0$ equation 2.32

$M_{CO2} M_{CH4} - K_m P_t^2 (\rho_{CO2} \rho_{CH4}/\rho_{H2}^2 \cdot \rho_{CO}^2) M^2_{CH4} M^2_{CO} \bar{\rho}^2 = 0$

equation 2.33

$\bar{\rho}$ is obtained from equation 2.34

$1/\bar{\rho} = M_{N2}/\rho_{N2} + M_{H2}/\rho_{H2} + M_{CO2}/\rho_{CO2} + M_{CO}/\rho_{CO} + M_{CH4}/\rho_{CH4} + M_{H2O}/\rho_{H2O}$

equation 2.34

Thus a set of 8 equations (2.24 - 2.28, 2.32, 2.33 and 2.34) with 8 unknows M_{N2}, M_{H2}, M_{CO}, M_{CO2}, M_{H2O}, M_{CH4}, G, and $\bar{\rho}$ is formed. This set was solved numerically by means of subroutine VA05A obtained from the Harwell library

with the following feedstock and blast data, and over the temperature range 600-1300 °C:

feedstock flowrate : 299 kg/h

feedstock composition : C =45.3 wt %
H = 5.8 wt %
O = 48.8 wt %
N = 0.0 wt %

Blast flowrate 474 kg/h

blast composition : H_2O = 7.6 wt %
O_2 = 21.5 wt %
N_2 = 70.9 wt %

(Note: the above conditions were selected since they correspond to actual gasification experiments performed on the process development unit)

The results are shown in Figure 2.21

2.5.4.4 Evaluation of thermodynamic models

From Figure 2.21 important conclusions can be derived concerning that particular set of conditons. However, such a model is of limited value if it is to be used in a design procedure, since a) it contains no heat balance (the equilibrium is calculated on set temperatures), b) it is non specific as far as gasifier configuration is concerned, c) it cannot predict concentrations of hydrocarbons higher than CH_4 (C_2, C_3), d) it cannot be used for detailed gasifier design because it ignores the effect of internal processes, e) it ignores kinetics, rate processes and heat losses from the system, f) it ignores ash and tars and other pyrolysis products and g) it assumes ideality and that equilibrium is attained.

Efforts have been made to overcome the above drawbacks; for example several models have appeared which include a thermal balance (24, 228, 232, 234, 235). With such models the operating temperature of a gasifier is specified by thermodynamics only. All the above models predict equilibria with only solid carbon present, while others have extended the analysis to both sides of the carbon boundary (15, 236).

Two more rigorous approaches have been suggested in the literature (24, 232), which combine theoretical and empirical relationships. In the former,

gasification is assumed to take place in two successive steps: first pyrolysis of wood, followed by oxidation and reduction reactions of pyrolysis products.

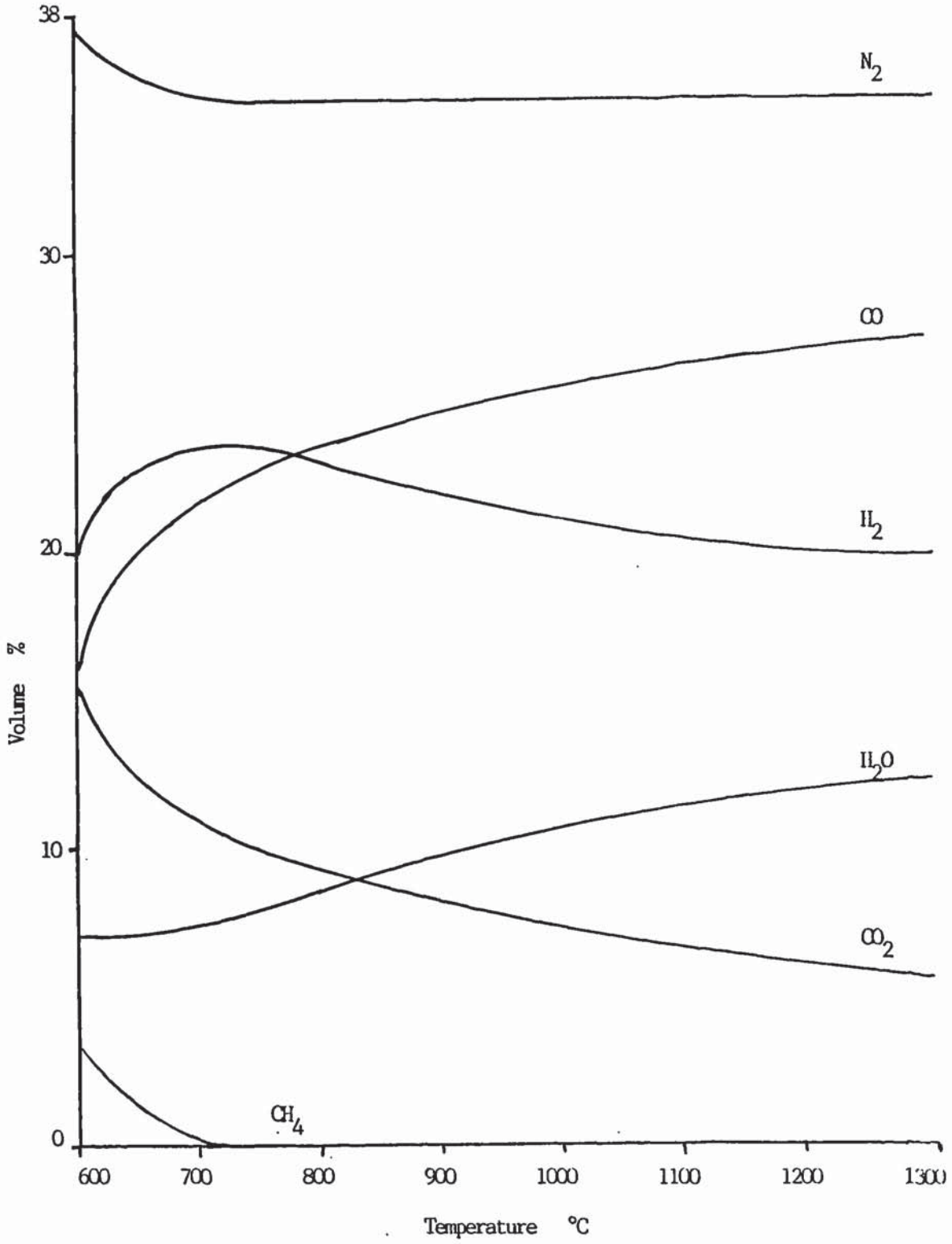

Figure 2.21 : Equilibrium composition of a gasifier as a function of temperature.

In such an approach thermodynamic equilibrium between gases is not needed and the model is referred to as non-equilibrium. According to the hypothesis of such a model, the outlet gas of the gasifier is the result of mixing of burnt and unburnt pyrolysis gases and the gases produced by the reactions of the char and tars due to combustion as well as to reduction. A limitation of such a procedure is that it is not known which component consumes the oxygen: the char and tar or the pyrolysis gas itself. Nevertheless, it is possible to assume that oxygen reacts either with one or the other product in which case solutions can be derived. The authors (232) found that the non-equilibrium model gave better results than an equilibrium model in comparison with pilot plant results.

In the latter work (24), the authors justified deviations between equilibrium and experimental data on the following factors: a) incomplete reactions, b) heat losses from the reactor, c) variations in moisture content and equivalence ratio, d) by-pass or channeling of pyrolysis products through the oxidation/reduction zone and e) kinetic requirements. On the basis of these factors, they proposed an approach at which a fraction of pyrolysis products would by-pass the oxidation and reduction zone and join the rest of the gas at the exit of the gasifier, see Figure 2.22.

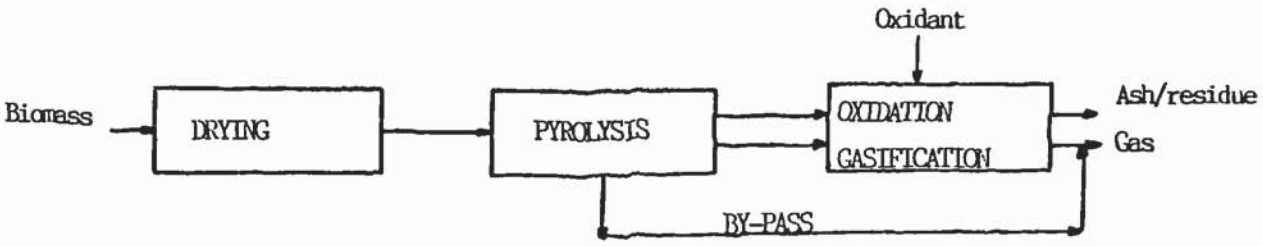

Figure 2.22 : By-passing of pyrolysis gases.

Such a semi-empirical equilibrium model incorporating by-passing can be proved accurate in predicting gas compositions of gasifiers, since the fraction and composition of by-pass can be varied accordingly to match exit gas composition. This approach was expanded to accomodate several possible by-passing pathways in an updraft gasifier (237). The model assumes that fractions of tars and or gas can move upwards (with the gas) or downwards (with the char) or even recycle in the gasifier. The unknown factors in the

model, being the fractions of gas and tar that move up or down, are difficult to estimate but can be matched empirically. The concept can be equally well applied to any other type of gasifier.

2.5.4.5 Conclusions

Thermodynamic models are widely used for predicting the performance of gasifiers based either on heterogeneous or homogeneous equilibria. However, the higher concentrations of methane and other hydrocarbons found in actual gasifiers cannot be predicted by thermodynamic models. These discrepancies can be attributed either to the fact that gasifiers operate far from equilibrium, or to physical and operational limitations of such systems, such as by-passing or channeling of pyrolysis products, variations in the composition of the feed, heat losses which change the temperature and hence the oxygen requirement and kinetic limitations. Recent results (15, 24, 112, 116) however support the latter.

The development of semi-empirical models can overcome some of the disadvantages of thermodynamic models. At present, however, thermodynamic models cannot be used in designing gasifiers. This is a fundamental limitation of thermodynamic models, since they can only be used for prediction of the performance of a gasifier but not for its design. For design, analytical or empirical models have to be used (see following sections).

2.5.5 Kinetics of char gasification

2.5.5.1 Introduction

If the assumption is maintained that drying and pyrolysis are instantaneous (see section 2.5.2.2 and 2.5.3.6), then the char gasification reactions control the overall rate of the gasification process (238). The char produced from pyrolysis can be gasified via the heterogeneous reactions, with carbon dioxide, steam, oxygen and hydrogen. The overall rate of char gasification is affected by several factors including chemical kinetics and intraparticle and external mass transfer resistances. Due to the exothermicity of some of the reactions, the reaction rate can also be influenced by temperature gradients within the char particle as well as between the char surface and the

surrounding gas (200, 239). Therefore the effects of mass and heat transfer must be considered when rate laws are used in modelling.

In this section the main principles of char gasification reactions are discussed as an introduction to kinetic modelling (see section 2.5.6). Most of the relevant literature is based on gasification of coal chars, which exhibit a much smaller surface area than biomass chars (down to 200 times less) (200, 238). It has been shown (157) that surface area and reaction rate are closely related during gasification. Since the char gasification reactions strongly influence the overall rate of gasification it would be unrealistic to derive a model or any theoretical approach of biomass char gasification, on data obtained from coal chars an approach like this would lead to an underestimation of the reaction rate and hence an overestimation of the reactor dimention, resulting in failure of the model. Therefore biomass char gasification kinetics must be considered in any kinetic model for biomass gasification.

2.5.5.2 Effects of mass and heat transfer on reaction rate

A single particle char gasification system is depicted in Figure 2.23

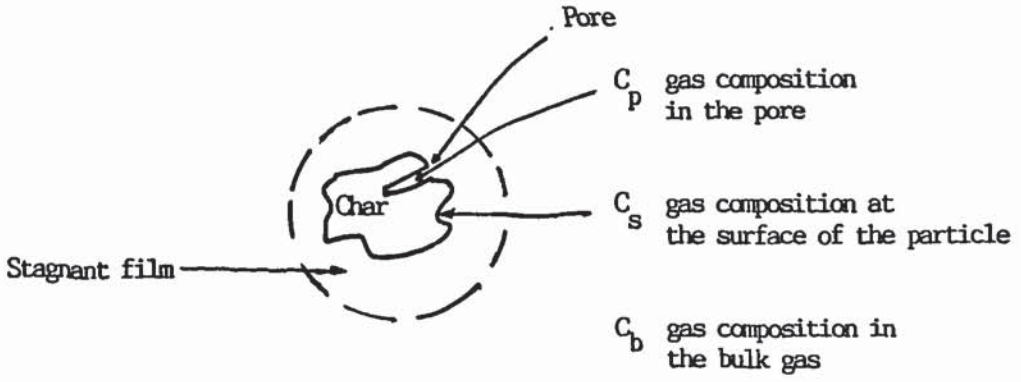

Figure 2.23 : Single particle char gasification

In a system such as the one shown in Figure 2.23, the following reaction steps can be considered to occur in series (185):

a) diffusion of reactant from main body of gas through the gas film to the surface of the particle
b) diffusion of the reactant gas into the pores of the particle
c) adsorption on the pore wall
d) surface reaction
e) desorption on the pore wall
f) diffusion of the products out of the pore
g) diffusion of the products acrosss the stagnant film back to the main body of gas.

However, a reaction system as the one described above is an idealized case and several deviations exist from actual reacting systems. For example surface adsorption, reaction and desorption can also take place on the outer surface of the char particle. In practice, there are more than one reacting gases, hence different components of the gas (e.g. carbon dioxide, steam, oxygen) and the different products of their reactions with char have to compete with each other in all of the above reaction steps.

The reacting system becomes more complicated when pyrolysis has not been completed. This is the case especially with large particles of biomass where char gasification reactions are initiated while pyrolysis still continues at the inner core of the particle. In such a particle, there would be competition between the diffusion of the pyrolysis products through the pores and the diffusion of the char gasification reactants and products. In addition, pyrolysis products such as carbon dioxide may react with the char before reaching the pores of the particle, while tars may crack on contact with the char particle which is at high temperature and deposite carbon on the surface of the pore.

Ash and its catalytic efforts on char gasification reactions are also excluded from the above reaction steps. Hence char gasification is a very complex process and at present it is not possible to account for all possible steps in a model. Thus kinetic models usually assume that the char particle consists of carbon only and that there is only one reacting gas (steam or carbon dioxide or oxygen), while the reaction takes place isothermally. Under these assumptions the reaction steps a to d are valid and they truly represent the reacting system.

The resistances of the different steps usually vary considerably and in such cases the step with the highest resistance may be considered to be rate controlling. This is illustrated in Figure 2.24 which depicts the influence of the various processes on the activation energy.

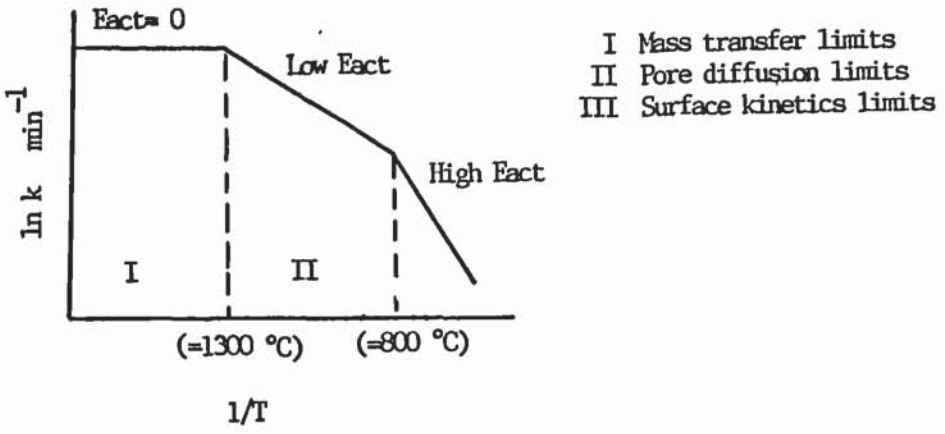

Figure 2.24 : The effect of temperature on reaction rate.

At low temperatures below 600 °C, the kinetic rate constant of the char gasification reactions approaches zero. The pore diffusion and mass transfer processes are fast relative to the kinetics and the concentration of the reactant gas is practically the same throughout both the particle and the bulk of the gas. Thus the kinetic step of the surface reaction is the rate limiting one. As the reaction temperature increases, the rate of the char gasification reactions increases and the reactant gas is depleted within the particle. Hence the rate is controlled by the supply of reactant gas in the pore and internal pore diffusion becomes important. At even higher temperatures (above 1300 °C) the reactant gas effectively reacts as it reaches the surface of the particle and then external mass transfer becomes the dominant step (238).

Several equations concerning mass and heat transfer to a char particle under gasification conditions have appeared in the literature. Most of these relationships are empirical (based on experimental results), while a few have been derived from first principles. Since their inclusion here is beyond the scope of this thesis, the reader is directed to several reviews available and original papers (228, 238-242).

2.5.5.3 Effect of conversion

Several studies (238, 240, 243) have been made on the effect of the extent of carbon conversion (expressed as weight loss) on gasification rates in different atmospheres. They all show that there is a complex relationship between carbon conversion and reaction rate. In general the rate of gasification is expressed as a function of carbon conversion, temperature and partial pressure of reactant and product gases.

$$r = F\ (M_C)\ .\ f\ (P_i, T) \qquad \text{equation 2.35}$$

or

$$r = F\ (x)\ .\ f\ (P_i, T) \qquad \text{equation 2.36}$$

where r = intrinsisic reaction rate mol C/h

M_C = residual amount of carbon kg C

x = fractional carbon conversion, $x = \dfrac{M^0_C - M_C}{M^0_C}$ equation 2.37

M^0_C = initial amount of carbon

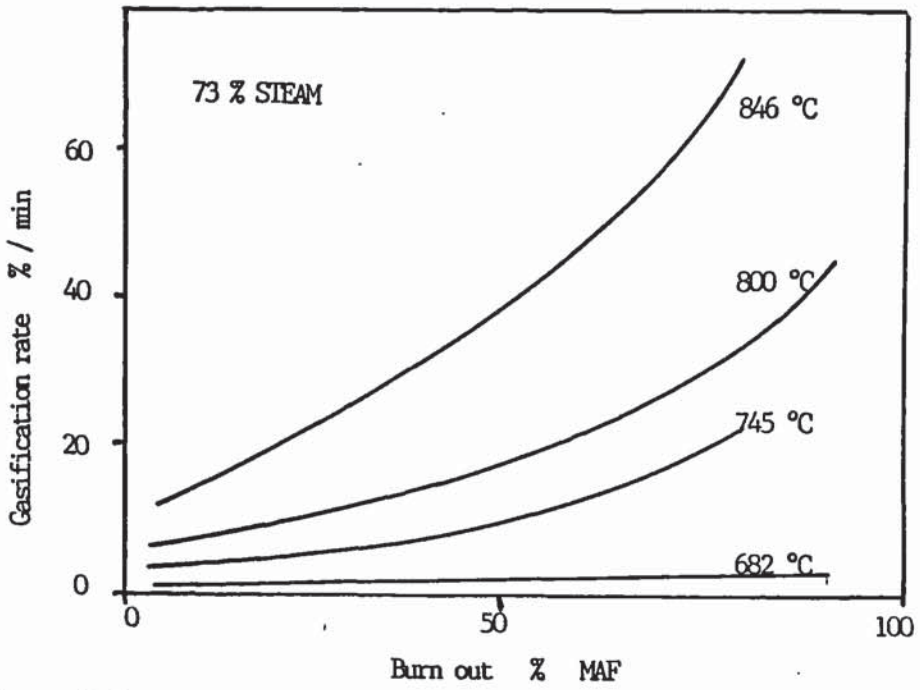

Figure 2.25 : Influence of carbon conversion and temperature on the gasification rate of poplar wood in steam argon mixtures (157).

The carbon conversion or burn off alters the pore size distribution, pore volume and hence surface area available for reaction. The rate of reaction depends on the carbon conversion to the extent that burn off alters the structure of the char particle. This has been demonstrated experimentally and is shown in Figure 2.25 (157).

2.5.5.4 Effect of surface area

The rate of gasification depends on the nature and origin of the char. In addition, the reactivity and pore structure depend greatly on the history of its formation, such as temperature of pretreatment, rate of heating, its environment during pretreatment and many others. Most of the surface area is provided by the micropores and a small fraction by the macropores (244, 245).

It has been found that the surface area initially increased with gasification and then dropped sharply at higher conversion. The increase in the surface area is due to the formation of new pores by preferential removal of carbon atoms or opening of new pores, which existed originally but were closed, and the enlargement of pores which existed or were newly opened. At the same time, there is a decrease in surface area due to the collapse of two pores by gasification of the pore wall. The increase in surface area dominates at low carbon conversions (246-249). Consequently the surface area has a strong influence on the rate of gasification (244-248) (see section 2.5.5.2).

2.5.5.5 Char gasification with carbon dioxide and steam

Both reactions have been studied extensively since they are the most important in char gasification (see section 2.5.5.1). It is generally accepted (157, 238, 240, 248, 250) that both reactions have similar kinetics, which can be described by Langmuir (eq. 2.27) type rate equations. Mechanistic models as well as Langmuir type rate expressions for both reactions are given in Table 2.16. Mechanistic studies (251, 252) indicate that for the char-carbon dioxide reaction the exchange of oxygen (eq. 2.27) occurs reversibly. Later as the gas pressure is increased, surface decomposition of the oxide species (eq. 2.38) takes place. It was suggested (251) that reaction 2.38 was rate controlling since the oxygen exchange (reaction 2.37) was potentially faster.

Table 2.16 : Char gasification with CO_2 and steam

Char + CO_2	equation
1. Mechanistic model	
$C_f + CO_2 \underset{k'_1}{\overset{k_1}{\rightleftharpoons}} C(O) + CO$	2.37
$C(O) \underset{k'_2}{\overset{k_2}{\rightleftharpoons}} CO + nC_f$	2.38
2. Langmuir model	
$-r_C = \dfrac{k'_1 C_{tot} \cdot P_{CO2}}{1 + \frac{k'_1}{k_2} P_{CO} + \frac{k_1}{k_2} P_{CO2}}$	2.39

Char + steam	equation
1. Mechanistic model	
$C_f + H_2O \underset{k'_3}{\overset{k_3}{\rightleftharpoons}} C(O) + H_2$	2.40
$(CO) \underset{k'_4}{\overset{k_4}{\rightleftharpoons}} CO + nC_f$	2.41
2. Langmuir model	
$-rc = \dfrac{K_3 C_{tot} \cdot P_{H2O}}{1 + \frac{k'_3}{k'_4} P_{H2} + \frac{k_3}{k_4} P_{H2O}}$	2.42

where
- $C(O)$ = represents a surface oxide
- C_f = free carbon sites
- C_{tot} = total number of active carbon sites
- P_i = partial pressure of component i
- rc = char gasification reaction rate

as the gas pressure is increased, surface decomposition of the oxide species (eq. 2.38) takes place. It was suggested (251) that reaction 2.38 was rate controlling since the oxygen exchange (reaction 2.37) was potentially faster.

The Langmuir type rate equation 2.39 indicates that CO_2 and CO can suppress the overall reaction. Also the rate is proportional to C_{tot}, the total number of active carbon sites available. It has been suggested (252) that the number of exposed active carbon sites is small compared to the total number of exposed sites.

For the char steam reaction there is less information available due to the possible side reactions resulting from the production of hydrogen and carbon monoxide which complicates the analysis. It has been proposed (200) that steam deposits oxygen on the active carbon surface at temperatures below those required for gasification (eq. 2.40). This oxygen may be removed by reaction with either carbon monoxide or hydrogen at these temperatures; however, the surface oxide decomposes to liberate carbon monoxide (eq. 2.41). As with rate expression for carbon dioxide gasification, in steam gasification the rate is proportional to C_{tot}, while hydrogen and steam can suppress the reaction.

2.5.5.6 Reaction rate constants and rate expressions for biomass chars.

Although extensive data are available for gasification of coal chars, limited information was found in the literature for biomass chars and this is all relatively recent. In general, with biomass chars it has been found (157) that the reaction rate increased with conversion for most types of char (see section 2.5.5.3).

Since pretreatment has a strong influence on the reaction rate (see section 2.5.5.4), some studies have been devoted to this area.

Thus it has been reported (253) that the reactivity of "in-situ" prepared chars was higher than that of stabilized and aged chars, while the total pressure did not affect the rate of the reaction with the latter type of chars. However, the addition of hydrogen decreased the char gasification rate. This is shown in Table 2.17 which summarizes the data on reaction rate parameters found in the literature for biomass chars. Also if the pretreatment temperature exceeds the char gasification temperature, a reduction in reaction rate occurs (254). This pretreatment effect was correlated in terms of a thermal annealing contributing to the apparent activation energy:

$$E = E(\text{true}) + E(\text{pretreatment}) \qquad \text{equation 2.34}$$

Table 2.17 : Reaction rate parameters for the gasification of biomass chars

Author(s)	Fuel	Reactant	Mole % reactant	Type of rate equation	Activation energy KJ/mole	Rate constant value	Rate constant units	Comments
Rensfelt et.al. (157)	Poplar	Steam	73	1st Order	182	1.2×10^{6}		Temperature range of
	Straw	Steam	73	1st Order	182	5.9×10^{7}		
	Bark	steam	73	1st Order	178	9.1×10^{7}	min^{-1}	
	Peat	Steam	73	1st Order	169	5.1×10^{6}		792-843 °C
Nandi and Onischak (253)	Maple	Steam	50	1st Order	176	3.3×10^{7}		Previously stabilized chars, in temperature range of 760-815 °C
	Maple	Steam+H_2	50+5	1st Order	195	1.8×10^{8}		
	Jack pine	Steam	50	1st Order	170	1.0×10^{7}	min^{-1}	
	Jack pine	Steam+H_2	50+5	1st Order	178	1.7×10^{7}		
	Maple	Steam	50	1st Order	166	2.4×10^{7}		In situ carbonization, gasification, temperature range of 760-815 °C
	Maple	Steam+H_2	50+5	1st Order	167	2.2×10^{7}		
	Maple	steam+H_2	50+10	1st Order	194	2.7×10^{8}		
	Maple	Steam+H_2	50+25	1st Order	262	4.1×10^{11}	min^{-1}	
	Jack pine	Steam	50	1st Order	163	1.3×10^{7}		
	Jack pine	Steam+H_2	50+5	1st Order	176	1.1×10^{8}		
	Jack pine	Steam+H_2	50+10	1st Order	206	8.0×10^{8}		
	Jack pine	Steam+H_2	50+25	1st Order	266	4.5×10^{11}		
Edrich et.al (254)	Pine	CO_2	100 -	Langmuir	-	-	-	Temperature range of 850-1000 °C

Groeneveld (228)	Wood	H_2O+CO_2	Various	$d(C_{CO2}+C_{H2O})^{0.7}$	217	10^6-10^7	$s^{-1}m^{2.1}mol^{-07}$	Temperature range 800-1000 °C
Van den Aarsen (255)	Beech wood	CO_2	-	$d\,C_{CO2}^{0.83}$	166	1.4×10^6	min^{-1}	-
Bjerle et al. (256)	Sawdust	CO_2	-	1st Order	249	1.8×10^9		Chars produced in N_2atm. at 900 °C Temperature range 700-900 °C
	Sawdust	H_2O	-	1st Order	240	1.8×10^{10}		
	Halm	CO_2	-	1st Order	210	1.8×10^8		
	Halm	H_2O	-	1st Order	198	3.5×10^9		
	Peat	CO_2	-	1st Order	196	9.0×10^6		
		H_2O	-	1st Order	168	4.0×10^7		
De Groot and Shafizadeh (257)	Douglas fir	CO_2	33	Zero order	221	1.4×10^{10}		Chars prepared at 1000 °C in N2 atm., initial reaction rates at 950-1000 °C.
		H_2O	7.7		258	4.8×10^{11}		
	cotton-wood	CO_2	33	-r=kwo	197	9.7×10^9	min^{-1}	
		H_2O	7.7	-r=kwo	188	8.8×10^8		
Schoeters (15)	Char	CO_2	-	1st Order	220	7.7×10^7	mole/(kg C.h. P_a)	Temperature range of 823-894 °C
	Char	H_2O	-	1st Order	177	4.9×10^5	"	
	Char	H_2O	-	Langmuir	-	-	-	

A zero order dependence of the observed rate on carbon inventory (defined as the amount of carbon present in the reacting system) has been found (254) suggesting that if mass transfer limitations exist they are confined to the micropore structure of the solid. It has also been reported (256) that for stream gasification, the reaction rates were more than an order of magnitude larger than those of carbon dioxide gasification.

More specifically for this thesis concerned with fluidized bed gasifiers, it has been found (15) that inhibition by steam of the steam char gasification

reaction was small and decreased with increasing temperatures, so that for temperatures and partial pressures of practical importance its effect was almost negligible. Hydrogen, however, inhibited the reaction markedly. Table 2.18 summarizes the available rate expressions for biomass char gasification reactions.

Table 2.18 : Rate expressions for biomass char gasification

	Ref.	Eq.	Rate expression	Comments
Char + CO	255	2.44	$-r_C \propto C_{CO2}^{0.83}$	Reaction determined as surface reaction
	254	2.45	$-rC = \frac{k_1 P_{CO2}}{1 + k_2 P_{CO}}$	Inhibition by CO insignificant.
	15	2.46	$-rC = a_2 . P_{CO2}$	For low P_{CO_2}, negligible CO, pseudo first order.
Char + steam	15	2.47	$rC = \frac{a_1 P_{H2O}}{1 + b_1 . P_{H2O} + C_1 P_{H2}}$	Inhibition by steam small. Inhibition hydrogen significant.
	257	2.48	$rC = kW_0$	Zero order.
	253	2.49	$rc = k(1-X_C)$	1st order rate expression; assumed.
Overall	228	2.50	$rc \quad [C_{CO2} + C_{H2O}]^{0.7}$	Overall rate equation.

where
- rc = rate of char gasification
- P_i = partial pressure of component i
- K_i = reaction i rate constant
- a, b, c = constants
- W_0 = initial weight of char
- C_i = concentration of component i
- X_C = carbon conversion

It is evident from Table 2.18 that the rate expressions depend strongly on the experimental conditions under which they were obtained and that no generalization is possible. Thus their utilization is limited and they may not be applied in general biomass gasification models. For general biomass gasification models empirical relationships are better suited. Another limitation is that the rate expressions of Table 2.18 were developed using idealized systems (e.g. only one or two gas reactants) and thus the deviations from actual systems discussed in section 2.5.5.2 are valid.

2.5.5.7 The combustion of char

Under normal operating conditions gasifiers operate autothermally (i.e. no additional fuel is added in the system, but part of the char is combusted to provide the energy necessary to maintain the process). Therefore the consumption of char by oxygen must be taken into account in a model, otherwise excessive amounts of char will be assumed available for gasification by other reactants such as steam, carbon dioxide and hydrogen. The combustion of char has been studied extensively in the combustion literature and several reviews have been recently published (e.g. 258-260), so its discussion here is considered out of the scope of this work. However, the rate of char combustion is much faster than char gasification and in most models it is considered to be instantaneous (see for example 15). For fluidized bed units in particular, where the air is fed at the bottom of the reactor, it has been proven that all oxygen is consumed within a very thin layer above the distributor (36, 38). Therefore, since drying, pyrolysis and combustion are considered instantaneous the char gasification reactions are the most important in determining the overall rate of the gasification process.

2.5.5.8 Conclusions

Char gasification reactions are very important in understanding the overall biomass gasification process. However, their rates are strongly influenced by several parameters and there is a serious variation of rate expressions in the literature. Therefore in general the published data can only be used under identical experimental conditions and with the same type of chars. Since most of these studies are carried out in reactors other than actual gasifiers,

their direct inclusion in a model is not justified. For similar reasons they can contribute little to a design procedure.

However, work such as that discussed in section 2.5.5 on kinetic modelling is very valuable in advancing the understanding of char gasification. Contributions in this field are important since the kinetics of char gasification reactions, if obtained under realistic gasifier conditions, can determine the amount of carbon inventory and hence the relative dimensions of the reactor. .

2.5.6 Analytical models

2.5.6.1 Introduction

Analytical models include fluidized bed hydrodynamic equations as well as kinetic or other expressions for predicting the performance of a gasifier. This is the most rigorous approach as well as the most complex one since several parameters have to be accounted for. In the literature of coal gasification, several such models have been published recently (261-264), while only a few have appeared for biomass feedstocks. Since the reactivities of these materials are very different (see section 2.5.5.2), models developed for coal cannot be readily applied to biomass gasification.

In section 2.3.3 the various models describing the hydrodynamic behaviour of fluidized bed reactors were introduced. All are based on the two phase theory which considers two phases, the bubble and emulsion phase. Several modifications have been made on the two phase theory regarding the exact nature of the phases (e.g. some consider a third phase, the cloud (36)). This section begins with a brief description of the complicating factors involved in a fluidized bed modelling. Then the governing equations of a simple reacting system in a fluidized bed are derived and the most common assumptions made are listed. This section discusses the available analytical models which have been published on biomass gasification in fluidized bed reactors.

In analytical models firstly the hydrodynamic parameters must be specified since they define the fraction of bubble and emulsion phase, the size and velocity of bubbles, the velocity of the gas in the emulsion phase and the

height in the reactor (50, 51) (see sections 2.3.3.1, 2.3.3.2). When these parameters are known, on the basis of previously made assumptions, a set of equations has to be solved to calculate the gas composition and carbon hold up. The complexity of a realistic fluidized bed model is enormous as will be shown in the following subsections.

2.5.6.2 Backmixing

A typical model is shown in Figure 2.26 (38). This considers three phases: bubble, emulsion and cloud. The wake, being the amount of solids carried with the bubble upwards, is responsible for the intense solids mixing. Generally the wake is considered as part of the cloud. However, in a more rigorous approach, the wake could be considered as a fourth phase, since it has distinct characteristics. It is probably due to the complexity of such a system, that no model has appeared in the literature yet with the wake as the fourth phase.

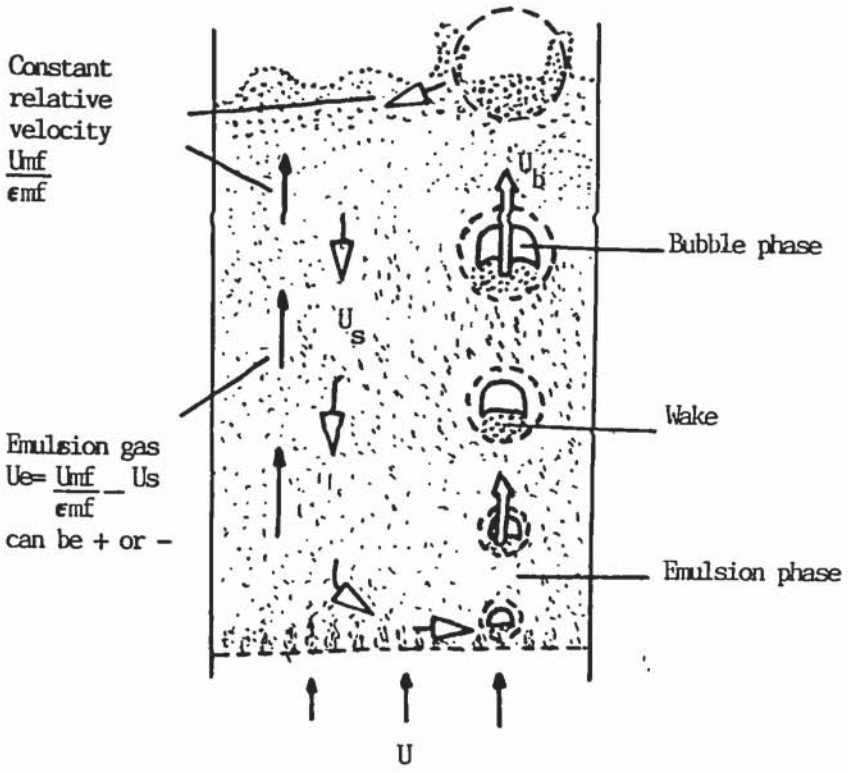

Figure 2.26 : Main features of solid movement and gas flow in the bubbling bed model.

On the basis of Figure 2.26, Kunii and Levenspiel (36) showed that flow reversal of the gas flowing interstitially in the emulsion leading to

backmixing is possible. They predicted backmixing for fluidizing gas velocities of between six and eleven times the minimum fluidization value.

2.5.6.3 Interchange of solids between emulsion and wake

As a bubble rise in a fluidized bed, it encounters solids continuously and there is an interchange of solids between the emulsion and wake. Figure 2.27 shows postulated movements of solids into and out of the wake.

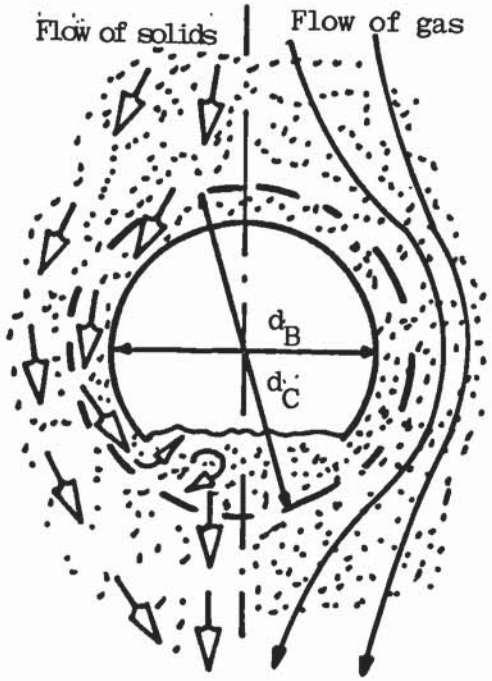

Figure 2.27 : Movement of solids into and out of the wake.

The bubbles also push the emulsion aside and the solids passing close to the bubble enter its cloud and are drawn into its wake, the breadth of which is roughly that of the bubble. Solids are mixed in the wake and this gives rise to lateral mixing as well as axial dispersion of solids (38).

2.5.6.4 Interphase gas exchange

There is no coherent surface and no surface tension force surrounds a gas bubble in a fluidized bed and as a result it is possible for gas within a bubble to flow through the interstices between the particles, and to exchange with gas in the emulsion phase. This exchange has an important influence on the extent of gas-solid contact and hence on the chemical conversion that can be achieved under given conditions.

There are three classical approaches (36) to the problem of predicting mass transfer from single bubbles as depicted in Figure 2.28.

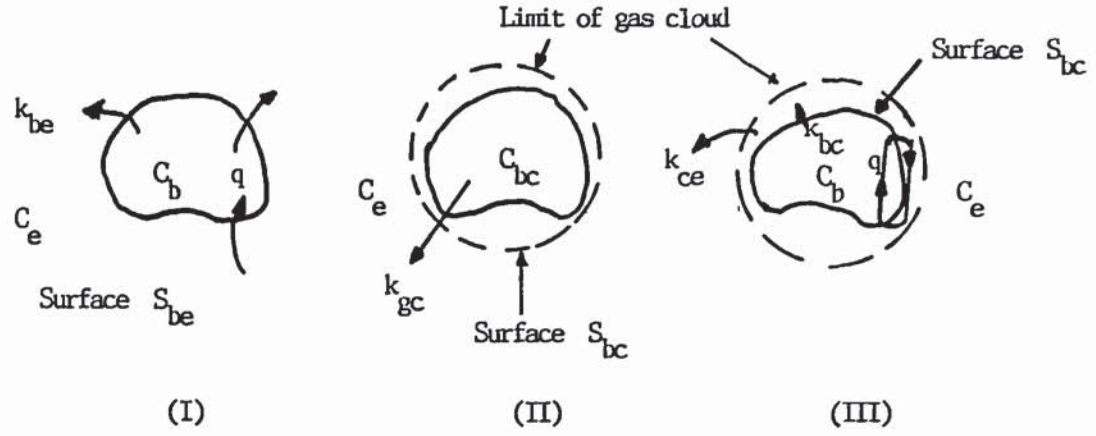

i I Direct bubble to emulsion
II Bubble cloud to emulsion
III Bubble to cloud to emulsion

Figure 2.28 : Models of interphase gas transfer.

Each approache results in different governing equations. However, the overall transfer rate of model C is given by equation 2.51

$$\frac{1}{k_{be}} = \frac{1}{k_{bc}} + \frac{1}{k_{ce}} \qquad \text{equation 2.51}$$

where k_{ij} = gas exchange rate between i and j per unit bubble volume

i, j = bubble, cloud, emulsion.

In most practical cases however, the transfer from cloud to emulsion is rate controlling :

$$k_{be} \approx k_{ce} \qquad \text{equation 2.52}$$

For both solids and gas interchange between the various phases, another complicating factor is that the size (and hence the surface area) of bubbles is increasing with hight in a complicated manner. Since solids and gas interchange are related to the surface area of bubbles, the rates of these processes vary with height in the bed.

2.5.6.5 The jetting region

When a perforated or a multinozzled plate is used as the distributor in a fluidized bed, gas jets are observed to form just above the distributor as depicted in Figure 2.29 (38).

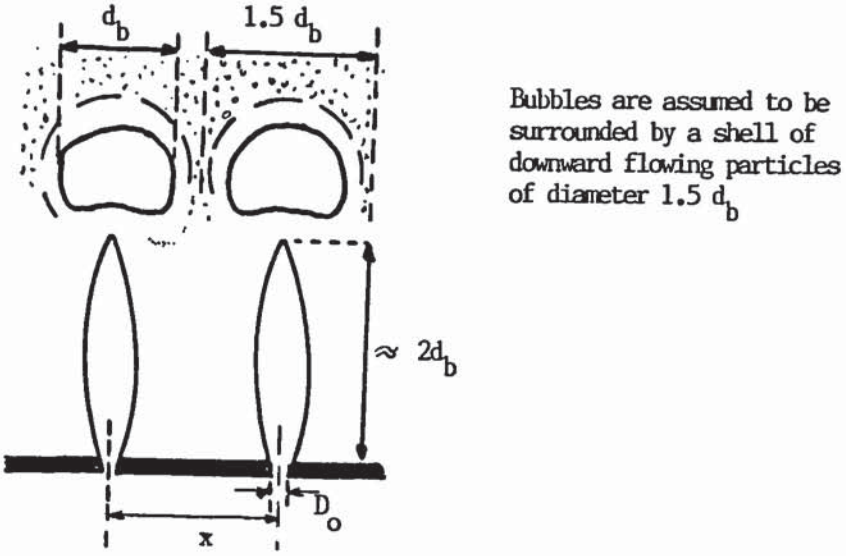

Figure 2.29 : Idealized jet to bubble emergence pattern

Thus there is a relatively thin area just above the distributor which is inherently different from the rest of the bed. In case of a reacting system, the concentration gradient of the reactant is highest in this area. More specifically with fluidized bed gasifiers operating with air or oxygen, the jetting region is of particular importance, since it is in this area that most of the oxygen is depleted by the combustion of char and possibly gases (such

as methane, carbon monoxide et. al) and the heat required to sustain the process is released.

However, only recently this topic attracted the interest of the research community (42, 45, 265, 266).

2.5.6.6 Governing equations

Due to the importance of solid-catalysed reactions in fluidized bed reactors, the majority of published models are designed for application to these systems, although in recent years a number of studies of non catalytic processes have been reported. Furthermore, the complexities introduced by reactions which do not have first order kinetics or have reversible or consecutive steps or result in volume changes, are commonly ignored. In general attempts are made to obtain model equations that are capable of analytical solution.

The classical approach is based on the general one dimensional two phase model shown in Figure 2.30 (38). For the case of an irreversible, first order gas solid reaction with no volume change, a mass balance on reactant A moving through the emulsion phase involves five terms as follows (38).

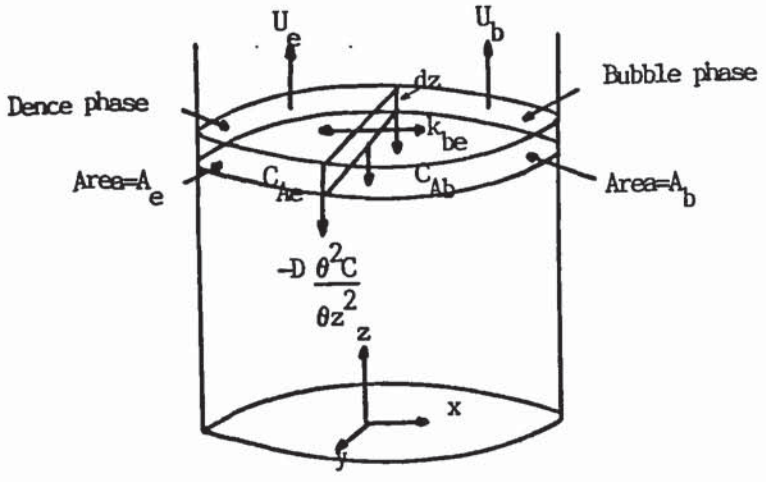

Figure 2.30 : The general one-dimensional two phase model (38)

$$\frac{\partial C_{Ae}}{\partial t} - E\frac{\partial^2 C_{Ae}}{\partial z^2} + U_e\frac{\partial C_{Ae}}{\partial z} + k_{be}(C_{Ae}-C_{Ab}) + k_e C_{Ae} = 0 \qquad \text{equation 2.53}$$

where C_{Ab} = concentration at A in the bubble phase
C_{Ae} = concentration of A in the emulsion phases
U_e = linear velocity of emulsion gas
E = gaseous diffusion coefficient
k_{be} = interphase mass transfer rate per unit volume of bubble gas
k_e = reaction rate constant for the emulsion phase
t = time

The corresponding equation for the bubble plus cloud phase is :

$$\frac{\partial C_{Ab}}{\partial t} - D\frac{\partial^2 C_{Ab}}{\partial z^2} + U_b\frac{\partial C_{Ab}}{\partial z} + k_{be}(C_{Ab}-C_{Ae}) + k_b C_{Ab} = 0 \qquad \text{equation 2.54}$$

These equations can be simplified by the following assumptions:
a) the reactor operates in steady state; hence the first term is 0
b) gas is in plug flow in both phases; hence the back diffusion term is 0
c) no reaction occurs in the bubble phase; hence the last term of equation 2.54 is 0.

The resulting simplified relationships are simultaneous linear first-order differential equations which can be solved analytically:

$$U_e\frac{dC_{Ae}}{dz} + k_{be}(C_{Ae}-C_{Ab}) + k_e C_{Ae} = 0 \qquad \text{equation 2.55}$$

$$U_b\frac{dC_{Ae}}{dz} + k_{be}(C_{Ab}-C_{Ae}) = 0 \qquad \text{equation 2.56}$$

Char gasification, however, is a complex system with complicated kinetics (see sections 2.5.5.5 - 2.2.5.7); reactions resulting in volume change; reactions influenced catalytically by the ash of the char; reversible reactions in the gas phase (e.g. watergas shift) and several reactants are present. Therefore for each gaseous component (eg. methane, ethylene, ethane, nitrogen, carbon dioxide, carbon monoxide, steam and oxygen) mass balance equations must be written for both emulsion and bubble phases. In addition to the above considerations, the additional gas produced by the pyrolysis stage - which also takes place in the bed - must be accounted for, in the mass balance equations of the pyrolysis gas components. Since the kinetics of tar reactions are not known, this important product of gasification can not be considered in such an analytical model.

2.5.6.7 General assumptions

Most common assumptions in the various models (15, 267-270) for the determination of fluidization parameters are:

a) the two phase theory: the basic assumptions of the theory are that the bed consists of two phases, the bubble and emulsion phases; the flow of gas in excess of minimum fluidization (see section 2.3.2) passes through the bed in the form of bubbles which are free of solids; and the emulsion phase has characteristics of a bed at minimum fluidization;
b) solids in the emulsion phase are well mixed;
c) the pyrolysis products are determined by empirical equations;
e) there is no resistance to mass transfer at the interphase between cloud and emulsion;
f) all excess gas generated in the emulsion is immediately transferred to the bubble phase.

Usually the solution of the overall model starts by the determination of the fluidization parameters. Thus on the basis of the assumptions made, the bubble diameter, bubble and emulsion gas velocities and the interphase mass transfer rates are determined. These data are incorporated in the mass balance equations and the system of differential equations is solved by computer techniques.

The set of differential equations to be solved for the gas composition may depend upon thermodynamic equilibria (270) (see section 2.5.4) or kinetic

expressions (15, 267-270) (see section 2.5.5). However, in both cases mass balances must be made for both emulsion and bubble phases (51).

2.5.6.8 Entrainment and elutriation

In most practical applications, fluidized beds are operated at gas velocities well in excess of the minimum fluidization velocity, U_{mf}, and under these circumstances it is common for bed particles to be blown from the bed into the freeboard space above it. This phenomenon is known as "entrainment" and it becomes more severe as the fluidizing gas velocity, U, increases. If U becomes so high that it equals the terminal fall velocity of the particles, U_t, then particles will be 'elutriated', i.e. carried out of the system completely. Normally there is a range of sizes of particles in a fluidized bed and since smaller particles have lower values of U_t, they will be elutriated first, although the larger ones can be entrained for a certain distance above the surface before falling back to it. Thus, it is common for a particle concentration gradient to exist in the freeboard as depicted in Figure 2.31 (36, 38, 43, 58).

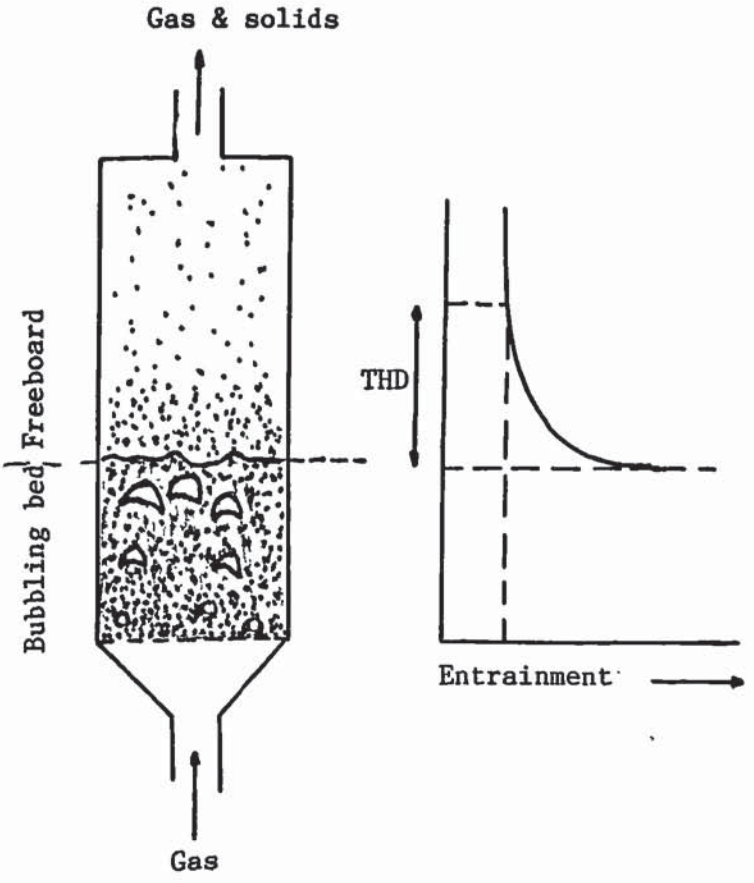

Figure 2.31 : Entrainment and elutriation (38).

The height above the bed surface at which the high velocity gas jets produced by the erupting bubbles, have become dissipated and the gas velocity has returned to U, is called the "transport disengaging height" or TDH, see Figure 2.31. The particles elutriated from the system are then only these whose terminal fall velocity is less than U, all other particles falling back to the bed.

However in the case of a reacting system, the entrainment and elutriation of fine particles can lead to a greater conversion than that achieved in the fluidized bed itself due to freeboard reactions. More in particular with biomass gasification, the fine char particles having a lower density than the inert material of the bed will be entrained and possibly elutriated. In the freeboard the heterogeneous char gasification as well as the homogeneous reactions continue and greater conversion is obtained. The reacting particle in the freeboard is depicted in Figure 2.32 on the basis of a simple model (38).

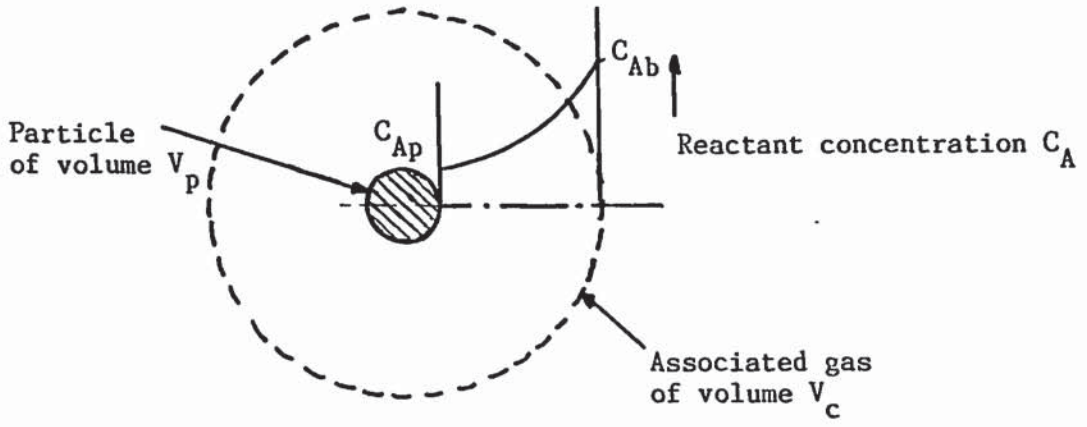

Figure 2.32 : Simple freeboard reaction model.

Therefore, the freeboard region t, is an integral part of a fluidized bed reactor, in which important processes are taking place and it should be accounted for as realistically as possible in a model. In addition to the char gasification reactions and other homogeneous reactions taking place, it is in

this region that the cracking of tars takes place. This is especially true with fluidized bed gasifiers in which the feeding takes place above the surface of the bed. Since pyrolysis is a very fast process (see section 2.5.3.6), most of the pyrolysis products are produced above the surface of the bed or in its upper layers and thus escape in the freeboard. Therefore a reliable model for biomass gasification must account successfully for the reactions taking place in the bed as well as in the freeboard .

The typical approach is to assume that the freeboard is in plug flow and that the concentrations of the various products at its inlet are defined by the reactions taking place in the bed. However it is usually assumed that only homogeneous reactions take place in the freeboard and that char is either consumed completely in the bed, or escapes to the cyclones.

In general for a plug flow reactor, the material balance of component A is given by (185):

input = output + disappearance by reaction + accumulation

$$FA = (FA + dFA) + (- r_A \, dV) \qquad \text{equation 2.57}$$

where FA = molar flowrate of A, moles/time
V = volume of system

Since

$$dFA = d\,[FAo\,(1 - XA)\,] = -FAo\,dXA \qquad \text{equation 2.58}$$

where FAo is the molar flow rate of A at the inlet and XA is the conversion of A_X. By substitution in equation 2.57 the following expression is obtained:

$$FAo\ d\,XA = (-rA)\ dV \qquad \text{equation 2.47}$$

Integration of this equation would result in mathematical expression relating the conversion of A to the volume of the freeboard zone and to the gas composition of the upper limit of the sand bed.

The overall approach in analytical models is shown in Figure 2.33

Definitions and
assumptions

Determination of
fluidization parameters

Solution of system of
differential equations
for the bed from two
phase theory

Solution of
equations for the
freeboard

Gas composition at
reactor outlet

Figure 2.33 : Overall approach in analytical models.

2.5.6.9 Analytical models for biomass gasification

The available models are summarized in Table 2.19

2.5.6.9.1 The Bacon model

In the only model incorporating thermodynamic equilibria (270), a computer simulation was developed to assess the performance of a fluidized bed gasifier. The overall gasification process was described by assigned degrees of approach to equilibrium and was based on heterogeneous equilibria. The modified bubble assemblage model (42) was used to describe the bed hydrodynamics. They concluded that the composition of the product gas was very sensitive to the assigned degree of approach to equilibrium and that the air to dry wood ratio determines the calorific value of the product gas. The design variables had no direct effect on gasification, therefore the fluidized bed may be designed solely from the standpoint of achieving stable fluidization. This conclusion is rather striking since theoretically the design variables have a direct effect on the gasification process. However, it will be considered again in the context of the results of this work (see Chapter 5).

Table 2.19: Modelling of fluidized bed gasifiers for biomass

Author(s)	Operating state	Freeboard	Energy balance	Phases	Comments
Bacon et. al. (270)	Transient	Not considered	Considered	Two phase, Bubble Assemblage	Thermodynamic theory and fluid bed hydrodynamics. No experimental work.
Raman et. al. 268)	Steady	Not considered	Not considered	Two phase with plug flow	Pyrolysis kinetics incorporated in the model. Supported by experiments in fluidized bed.
Chang et.al. (269)	Transient, steady	Not considered	Not considered	Two phase	Simulation. No experimental data.
Schoeters a)		-		None	Thermodynamic theory, kinetics
(15) b)	Steady	-		CSTR	supported by experiments in fluidized bed.
c)		-	Not considered	Plug flow	Single phase, perfectly mixed
d)		Assumes only water gas shift reaction		Two phase model with plug flow	reactor. Plug flow reactor plug flow in both emulsion and bubble phase
Van den Aarsen et. al. (267)	Steady	Not considered	Not considered flow	Two phase with plug	Thermodynamic and kinetics. Usage of empirical relationship for pyrolysis in mathematical model, experimental data.

2.5.6.9.2 The Raman model

In an isothermal transient two phase model for the gasification of feedlot manure, it was assumed that pyrolysis was instantaneous and that it occured homogeneously over the whole bed (268). The distribution of the pyrolysis products was determined experimentally (83). The kinetic expressions for the carbon-steam and carbon-carbon dioxide gasification reactions, as well as the water gas shift reaction, were taken from the literature (271). The simulation results were compared with experimental data. This comparison suggested that cracking and reforming reactions, involving the volatiles produced during degradation, should be included in the model. An estimation of the gas and liquid yields incorporating the thermal cracking reactions of the heavy volatiles compared more favorably with the data.

It was concluded that the water gas shift reaction was the significant reaction in the range of the experimental conditions and not the char gasification reactions.

2.5.6.9.3 The Schoeters model

In the most comprehensive work on fluidized bed gasification (15), the gasification of biomass char was studied in a fluidized bed reactor. The feedstock of char was selected in order to simplify the expressions for the pyrolysis step, although the pyrolysis of charcoal was studied and empirical relationships were incorporated in the model. The char gasification reactions (see section 2.5.5) were studied in detail and all necessary kinetic parameters were determined.

The predictions of four reactor models, namely homogeneous equilibrium (HE), well mixed (WM), plug flow (PF) and two phase (TP) were determined and compared on the basis of the equilibrium constant of the homogeneous water gas shift reaction. It was found that all four models could fairly well predict the gas composition at the outlet of the reactor. Since the water gas shift reaction fixes the concentrations of the four most important gas components (water, hydrogen, carbon monoxide and carbon dioxide), this method is rather well suited for comparison purposes. It was concluded that the gas composition was mainly determined by this reaction in the freeboard zone and that processes occuring in the sand bed do not affect it significantly,

which is in accordance with the Raman model's conclusions (see previous section).

Moreover, it was shown that the plug flow model predicted the lowest char hold up in the bed and thus the highest overall reaction rate, while the well mixed and two phase models gave identical results.

Schoeters explained this behaviour on basis of the gas exchange rate between bubble and emulsion phase, concluding that the similar results for the well mixed and the two phase model were coincidential and that in general these models will predict different char hold ups. In larger reactors where the size of bubbles is bigger, the gas exchange rate will decrease and the two phase model will approach the prediction of the plug flow model.

The experimental results were then compared with the predictions of the four models and it was found that the two phase model (TP) with plug flow in emulsion and bubble phase gave the best representation of the fluidized bed charcoal gasifier. It was concluded that the water-gas shift reaction, the wake fraction of a bubble and the average bubble size, used to calculate the bed voidage and bed height, did not significantly affect the char hold up.
The char hold up was, however, strongly influenced by the gas exchange rate between the bubble phase and emulsion phase. He finally concluded that the homogeneous equilibrium model could fairly well predict the gas composition at the outlet of the reactor and thus this model was sufficient for predictive purposes. However, this is only true for charcoal gasification since the volatiles content of charcoal is very small (about 5 wt%) compared to biomass (about 80 wt%) and since thermodynamics cannot predict the pyrolysis products.

2.5.6.9.4 The Van den Aarsen model

In this model (267) developed for the gasification of beech wood, wood pyrolysis product yield, char gasification kinetics and bubble to dense phase mass transfer kinetics were separately determined and incorporated in the model. In this model a separate oxidation zone was distinguished where part of the wood is combusted by the complete supply of oxygen. The gas composition and mass flowrate leaving that section was derived from thermodynamic considerations. A reactor height, required for completing the fast pyrolysis process, was determined which depended on the particle

pyrolysis time and solids mixing time. This reactor height was estimated by an empirical equation.

As with Schoeters, they considered the two phase model with plug flow in the bubble and emulsion phase. In the model calculations it was also assumed that the homogeneous water gas shift reaction attains equilibrium in both dense and bubble phases, after each differential conversion. Their model predicted fairly well experimental exit gas compositions and char hold up as function of the operating variables (temperature, throughput and bed height). However in the char gasification kinetics, they did not calculate the exact values of the Langmuir Hinshelwood kinetic expressions, but used instead global kinetics.

2.5.6.9.5 The Chang model

The most recent model (209) was a computer simulation for the gasification of feedlot manure. The model examined both transient and steady state operation and was compared to previous experimental results (83, 84). The model considered three general steps: a) pyrolysis of biomass to produce volatiles and char, b) cracking and other reactions of the volatiles and c) char gasification reactions incorporating the water gas shift reaction. The steady state results predicted by the model agreed well with the available experimental data. However, at higher operating temperatures there were discrepancies, which were attributed to incomplete information concerning the cracking and other reactions of the volatiles (a rough empirical assumption that only 20% of the volatiles are decomposed, due to cracking and other reactions to a gaseous product with the same product distribution as that of pyrolysis, was employed in the model calculations).

The transient results showed that pyrolysis was fast and the transient period of the gas short; the gas composition which included C_2 hydrocarbons was stabilized in about 5 seconds. The char produced accumulated in the gasifier due to the low rate of char gasification, even at the highest operating temperature of 710 °C. The concentration profiles indicated that gases passing through the emulsion and bubble phases reached equilibrium prior to their exit from the gasifier.

The transient data could not be compared against experimental information which was not available. However, the authors concluded that before the

model could be used for design purposes, additional information was needed on:

a) pyrolysis data including composition of gas and rate expression with enhanced accuracy,
b) incorporation of cracking and other reactions of the volatiles into the governing equations and
c) securing transient experimental data.

2.5.6.10 Conclusions

The analytical models which have been proposed offer significant insight into the gasification of biomass in fluidized bed reactors and their sophistication is continually increasing.

The most important parameters which have to be considered in a comprehensive model are: a) kinetics of biomass pyrolysis, b) char gasification kinetics, c) tar cracking kinetics, d) compartmental fluidized bed, consisting of a jetting region just above the distributor, where most of the oxygen is consumed, and four phases: bubble, emulsion, cloud and wake in the rest of the bed, e) backmixing, f) interchange of solids between emulsion and wake, g) interchange of gas between emulsion, cloud and bubble phases, h) entrainment and elutriation and i) heterogeneous and homogeneous reactions in the freeboard. From these, backmixing is the least important and could be excluded from a model without compromising it significantly.

However, it is impractical yet to include all these parameters in an analytical model, since the set of governing equations to be solved would become severely complicated and information is often missing. Therefore various assumptions are made concerning the bed hydrodynamics, pyrolysis, cracking of pyrolysis products, thermodynamics and kinetics in order to simplify and solve the model.

Reasonable assumptions are that pyrolysis and char combustion are instantaneous processes, that the two phase theory applies, that the bed is isothermal and well mixed and that the emulsion and bubble phases are in plug flow. However, it is unreasonable to assume that bubbles have an average diameter all through the bed, that the additional gas produced by the gasification process automatically goes in the bubble phase, that there are no resistances for transfer of gas and solids amongst the various phases, that

no conversion takes place in the freeboard, that the products of pyrolysis do not undergo secondary reactions and that tar does not crack, that char particles have the same dimensions (no population balance) and that no entrainment and elutriation takes place. Although certain features of the reactor performance and behaviour can be predicted (e.g. exit gas composition), these are limited and the shortcomings of the models are explained on the basis of some of the assumptions made at their derivation.

It is of interest to notice that the complexity of an analytical model is not a prequisite in predicting the performance of a gasifier. Thus it has been concluded (270) (see section 2.5.6.9.1), that bed hydrodynamic design variables have no effect on gasification and the reactor could be designed solely from the standpoint of achieving stable fluidization. Similarly (15), it has been shown that the gas composition at the exit of a gasifier can be predicted fairly well irrespectively of the reactor model applied (homogeneous equilibrium, well mixed, plug flow and two phase theory of fluidization) (see section 2.5.6.9.3).

Similar observations have been made in the literature for coal gasification, for example it has been shown (262) that no appreciable difference in the total carbon conversion for average bubble sizes smaller than 0.1 m, can be found by comparing the completely stirred tank reactor model to a modified Davidson-Harrison model (37). Similarly, no appreciable (within $\pm$ 10 %) differences were found with regard to the predicted carbon conversion and the gas heating values by comparing the completely stirred tank reactor model to the two phase bubble assemblage model (42).

It can be concluded that although analytical models are significant from the scientific point of view, they can contribute little to a design procedure.

2.5.7 Empirical models

2.5.7.1 Introduction

Empirical models are based on mathematical correlationships which have been derived from experimental results. Usually a set of independent variables is defined and from these empirical correlations are developed, from which dependent variables can be calculated. On the basis of the

dependent and independent variables it is often possible to derive a design procedure.

The most suitable independent variables are:
a) the feedstock flowrate
b) the equivalence ratio (or air factor)
c) the temperature.

However, the total carbon to nitrogen ratio has also been used as an independent variable (see section 2.5.7.4)

Usually only 1 or 2 independent variables are used in a model.

The following dependent variables are usually obtained:
a) gas composition
b) higher heating value of the product gas
c) thermal efficiency
d) gas yield
e) condensate yield
f) freeboard temperature.

Three such models have recently appeared in the literature and are discussed in this section.

2.5.7.2 The Beck model

The first of these models (66) was derived from experiments for the gasification of feedlot manure in a laboratory reactor with no inert material in the fluidized bed (see section 2.4.2 and Table 2.3).

Empirical correlations were derived for product gas yield, hydrogen to carbon monoxide mole ratio and carbon conversion as a function of gasifier temperature, oxygen to wood ratio, steam to wood ratio and mean solid residence time. Apart from the fact that only a few parameters (3) could be determined by application of the model, these did not include the calorific value or the composition of the gas, which are the most important in predicting the performance of the gasifier. Another limitation of the model is that the mean solid residence time has to be used as an independent variable, while there is little information in the literature about this parameter. However, the most serious drawback of this model is that it was derived from a reactor, which did not operate as conventional fluidized bed, but as a semi updraft- semi fluidized bed unit. Its validity for fluidized bed

design is doubtfull and in any case, the authors made no attempt to propose a design procedure.

2.5.7.3 The Hoveland model

In this work (87) a set of seven equations were proposed by which the gas yield, calorific value and gas composition could be estimated, with operating temperature as the only independent variable. The results were obtained for the gasification of grain dust in a small laboratory fluidized bed unit (ID 0.05 m) (see Table 2.3). The disadvantages of this model, besides the small scale of operation, is that temperature was selected as an independent variable. This is not true in practice, since the operating temperature is determined by the air factor. Also no attempt was made to correlate the data with any other variables and no design procedure was proposed for its application. Therefore it is not considered a reliable model.

2.5.7.4 The Flanigan model

The most comprehensive empirical model was derived at the University of Missouri Rolla, based on numerous experiments made in three fluidized beds of different dimensions (91) (see Table 2.4).

Several attempts were made to derive correlations by using both linear and non-linear equations, semi-empirically based on equilibrium or rate type equations. Little success was obtained with non-linear types of correlations and only slight improvements were obtained by including several variables in the linear equation. These trials also indicated that the ratio of total carbon to nitrogen in the dry gas correlated better than any other variable, with the important variables of the product gas, including total carbon in the dry gas, higher heating value and total hydrogen in the dry gas. Their results indicated that at a given total carbon to nitrogen ratio, the gas quality was only slightly affected by wide variations in the type of reactor, the existence of a thermal state, the type of feed, the moisture content, the residence time or the bed temperature. However, these variables do affect char and tar formation and the total carbon to nitrogen ratio.

A set of ten equations were proposed by which the fraction of char and tar, the total carbon in dry gas, the higher heating value of the gas, the total hydrogen in the dry gas and the composition of the gas (H_2, CO, CO_2 and CH_4

only) could be determined. A design procedure was also developed. However for the application of the model the total carbon to nitrogen ratio on the gas must be known. This requires detailed pyrolysis studies to determine the fraction of char and tar and their elemental composition, as well as the elemental composition of the feedstock, before this parameter can be determined. This is a serious limitation of the Flanigan model since usually these data are not available, thus its applicability is restricted. Moreover, by basing the model on the total carbon to nitrogen ratio, the possibility to extend it for oxygen gasification is excluded.

2.5.7.5 Conclusions

It is possible to develop empirical or semi-empirical models based on experimental results. Although these kind of models are generally applicable only for similar experimental conditions under which they were developed, they can be very useful in scaling up the reactors with a good degree of performance prediction and simpler and more reliable computational procedures.

A common drawback for all the above models is that they include no information whatsoever concerning the design and determination of the hydrodynamics of the fluidized bed or how they could be predicted. Good and stable fluidization is necessary if a gasifier is to operate successfully.

2.5.8 Conclusions of the literature review

Biomass gasification has been studied extensively during the last decade and commercial units have already appeared. From the different types of gasifiers, fluidized bed units offer several advantages over the other types; the most important of which are versatility, easy to scale up to very high capacities and good turn down ratios.

The best opportunities are identified for fluidized beds, which operate with an inert bed in the reactor with air as the gasifying medium. Oxygen, steam and pressurized gasification are important for synthesis gas production. However market indications of the last two years show that a methanol synthesis plant would not be economically viable at current prices. Similarly interest in pyrolysis of biomass in fluidized bed units for producing liquid fuels or chemicals has decreased recently, due to the reduction of the price

of oil. Further, a serious effort in academic research is required before such a process can reach commercialization.

Catalysts could play an important role if the problems associated with their poisoning and short lifetime could be overcome. It is however clear that more research and development of new catalysts are needed.

The underlying nature of pyrolysis, a precursor to gasification, is still poorly understood although important findings have been reported. The complexity is such, that practically all available models either do not include pyrolysis at all or use rude empirical relationships to account for the process.

Thermodynamic models have been successfully employed in predicting the performance of gasifiers and new techniques such as non-equilibrium models and by-passing of pyrolysis products can improve their accuracy. However, at the present stage of sophistication they cannot be used for design purposes.

Analytical models which include char gasification kinetics as well as fluidized bed hydrodynamics have provided an important insight in the overall process, its limitations and the sensitivity of performance on several parameters. However, complicated approaches have to be followed without necessarily improving the accuracy of the final prediction.

Empirical models on the other hand are relatively simple, but numerous experiments are needed before they can be derived with an acceptable degree of accuracy. The scale of operation is also a very important factor. None of these models offered any information or predictions of the fluidized bed hydrodynamics, while only one proposed a relative complicated design procedure for predicting the performance of the gasifier.

It is evident that a complete design procedure incorporating:
a) a model to predict the performance of a fluidized bed gasifier,
b) a method to determine the fluidization parameters and characteristics for designing the fluidized bed gasifier and
c) a conceptual design of a fluidized gasification plant

is missing from the literature.

It was therefore decided :

I) to design and build a process development unit fluidized bed gasifier for the gasification of biomass at atmospheric pressure employing an inert bed of sand on the basis of previous laboratory results and experience;

II) to commission the plant and provide detailed and accurate measurements of all important parameters;

III) to perform an experimental programme for the acquisition of suf-ficient data;

IV) to develop an empirical model and design procedure, and

V) to supplement such a model and design procedure with a conceptual plant design.

CHAPTER THREE : DESIGN AND CONSTRUCTION OF THE FLUIDIZED BED PROCESS DEVELOPMENT UNIT

3.1 INTRODUCTION

The literature review indicated that the majority of work on fluidized bed gasification had been carried out in laboratory scale pilot plants, while only two studies were executed in reactors with internal diameter larger than1 m (see section 2.4.3.8). It was also noted that none of the empirical or analytical models published resulted in the design and construction of a scaled up version of the original reactor. It also became apparent that no work had been carried out which considered gasification of biomass in a fluidized bed reactor with a comprehensive methodology for reactor design.

Thus, it was manifested that the gasification of biomass had to be studied in a relatively large scale reactor, so that reliable results for scaling up purposes could be gathered. On the basis of these results a design procedure and a comprehensive methodology for the design of fluidized bed gasifiers would then be derived.

This chapter presents the design and engineering specifications of the process development unit fluidized bed gasifier. At the time of design - January 1982 - only two empirical models had been published and none were applicable to the system being studied. The first provided for no inert bed in the reactor and was developed for feedlot manure (66) (see section 2.5.7), while the second was based on steam gasification and provided very little information (87) (see section 2.4.5.2). Therefore the design procedure for the process development unit was based on previous results (102) (see also Appendix'I, article 1, which presents some of the results from (102)) and on empirical models for fluidized bed reactors, which are described later in this chapter.

The aim of the project was to design and construct a multipurpose flyidized bed reactor, which would be employed for gasification of biomass feedstocks. It would be used at the premises of Vyncke Warmtetechniek at Harelbeke Belgium, a boiler manufacturer, as a process development unit for a variety of gasification processes. In addition, the characteristics of the reactor as a fluidized bed, the problems associated with different biomass feedstock properties, such as high inerts and/or ash content and particle size (see section 2.4.3.7) had also to be considered. Hence the reactor characteristics

had to provide for versatile operation under a wide range of operating conditions.

This chapter begins with a summary of results from previous research on wood gasification, which is followed by the calculation of throughputs at maximum and minimum operating conditions. Since no appropriate design procedure existed, a high degree of empirism was unavoidable. After establishing the throughputs of the reactor, the fluidization parameters of importance are calculated and the design is verified for optimum operation, on the basis of empirical models published for fluidized bed reactors. The overall approach is depicted in Figure 3.1.

1. Set specifications
   a) type of gasifier
   b) feedstock
   c) reagents
   d) operating conditions
2. Calculation of throughputs
   calculate at max and min conditions:
   a) air input
   b) feedstock input
   c) dry gas output
   d) steam output
3. Design of distributor
   calculate:
   a) minimum ΔP distributor
   b) Re for flow approaching distributor
   c) velocity of gases through orifice
   d) number of orifices
   e) diameter of orifices
4. Pressure drop for the compressor
5. Size of sand
   calculate mean particle diameter
6. Fluidization parameters
   calculate:
   - minimum fluidization velocity
   - Reynolds number at conditions of minimum fluidization
   - particles terminal falling velocity
   - size of bubbles at max and min conditions
7. Verification of design
   calculate:
   - amount of gas flowing interstitially
   - residence time of gas flowing interstitially
   - bubble velocities at max and min conditions
   - the ratio of bubble velocity to interstitial gas velocity
   - the fraction of bubbles in contact with particles
8. Construction of fluidized bed

Figure 3.1 : The various steps used in the design of the process development unit.

It is surprising to note that, although an enormous amount of research has been carried out on fluidized bed systems, the actual design of the reactors is still largely empirical. The case of the design of the distributor, which is one of the most important components of a fluidized bed, is characteristic of empiricism, since it is still based on a rule of a thumb (see section 3.3.2). In addition, no unified approach for the determination of the fluidization parameters and their verification had been published, so more than one source were used for this purpose.

3.2 REVIEW OF PREVIOUS WORK

The design of the pilot plant at Vyncke Warmtetechniek was based on data obtained previously from a bench scale unit using linden tree shavings (102). This earlier work was used as basis for designing the new plant as considerable experience had been obtained. This approach helps to achieve one of the objectives of the project which is to examine scale-up.

One of the most important single parameter in biomass gasification is believed to be the air factor (for definition see section 5.2.2). In practice optimum values of air factor are found in the range of 0.2-0.4 (see section 2.4.3.3). In the design calculations an air factor of 0.233 was assumed, since this had been found to be the most satisfactory value for gasification of linden tree shavings (102). At this value of air factor, the results presented in Table 3.1 were derived from this earlier work.

Table 3.1 : Experimental results for an air factor value of 0.233 (102); basis for design.

Parameter	Value	
Gas yield	2	kg gas/kg feedstock*
Average density of gas	1.3	kg/Nm^3
Condensate yield	0.35	kg condensate/kg feedstock*
Air flowrate per feedstock flowrate	1.35	kg air/kg feedstock*
Heat of reaction	4.98	MJ/kg+
Bed temperature	800	°C

Note: * on dry and ash free basis.

+ absolute value; calculation based on higher heating value of the components.

3.3 THE DESIGN OF THE FLUIDIZED BED

The design was based on the results presented in Table 3.1 and on empirical models found in the literature (36) and in an undergraduate course (273).

3.3.1 Calculation of throughputs

On the basis of the literature review, it was decided to construct a fluidized bed reactor of significantly larger dimensions than the bench scale unit in which the previous work had been carried out (102) (see section 3.1). However, financial limitations at Vyncke Warmetechniek, set certain restrictions regarding the scale of the process development unit. Thus a compromise was made between the available budget and the scale of reactor that was considered necessary in order to obtain meaningful and reliable results. On the basis of the experience gained with the bench scale unit, (0.15 m diameter and 0.2 m height, bed dimensions), it was decided to set the dimensions of the bed at minimum fluidization conditions, at 0.6 m diameter and 0.6 m height.

Thus, the diameter of the bed of the bench scale reactor was scaled up by a factor of 5.3, while the height was scaled up by a factor of 3 (note: the diameter and height of the bed are never scaled up proportionally since this would result in excessive pressure drop for the compressor) (273).

The dimensions of the bed are related to the reactor load (or feedstock flowrate) on the basis of equation 3.1 (273).

$$\text{Reactor load} = \frac{\text{capacity of bed} \times \text{volume of bed at } U_{mf}}{\text{Heat of reaction}} \qquad \text{equation 3.1}$$

However, the maximum bed capacity (or heat release per unit volume) for fluidized bed reactors based on wood is generally considered to be 4189 MJ/h m^3 bed (274). Substituting values for expanded bed volume and heat of reaction from Table 3.1, with the specific energy capacity given above in equation 3.1 gives:

$$\text{Reactor load} = \frac{4189 \times (0.6 \times 0.6^2 \times \pi) \times 1/4}{4.98} = 253.7 \text{ kg/h}$$

Thus, the maximum feedstock flowrate under the conditions set above is 253.7 kg/h.

It is possible to determine the minimum feedstock flowrate on the basis of the turn down ratio, which is generally defined as the ratio of the normal maximum flowrate through a system to the minimum controlable flowrate. However in the case of gasifiers, the turn down ratio is defined as the ratio of the normal maximum feedstock flowrate to the minimum feedstock flowrate that would result in the same performance of the gasifier. Although turn down ratios higher than 5:1 have been quoted, it is safer to use a value of 3:1 (273). With this value, the minimum feedstock flowrate is found to be 253.7/3 = 84.6 kg/h. Using the experimental results of Table 3.1, it is possible to calculate the maximum and minimum mass and volumetric throughput, by the application of equations 3.2 to 3.4 below:

Air flowrate = feedstock flowrate x 1.35 equation 3.2

Product gas flowrate = feedstock flowrate x 2 equation 3.3

Condensate flowrate: = feedstock flowrate x 0.35 equation 3.4

Thus, for maximum feedstock flowrate:

Air flowrate = 253.7 x 1.35 = 342.5 kg/h of air
or 342.5/1.293 = 264.9 Nm^3/h of air,
where 1.293 is the density of air in kg/Nm^3 (189).
Product gas flowrate = 253.7 x 2 = 507.4 kg/h dry gas,
or 507.4/1.3 = 390.3 Nm^3/h dry gas,
where 1.3 is the density of dry gas (Table 3.1).
Condensate flowrate = 253.7 x 0.35 = 88.80 kg/h condensate
or 88.8/0.811 = 109.49 Nm^3/h (189),
where 0.811 is the density of steam in kg/Nm^3 (189).

The same approach can be applied for the minimum feedstock flowrate and thus the input and output mass and volumetric throughputs can be computed as shown in Table 3.2

It has to be stated that it was assumed that the condensate consisted only of water and that no tar and/or oil were present. This was necessary since no information had been collected concerning tar and/or oil yields.

Table 3.2 : Calculated mass and volumetric throughputs.

Component	Input				Output			
Flowrate	Min.		Max.		Min.		Max.	
Units	kg/h	Nm^3/h	Kg/h	Nm^3/h	Kg/h	Nm^3/h	kg/h	Nm^3/h
Feedstock	84.6		253.7					
Air	114.2	88.3	342.5	264.9				
Gas dry					169.2	130.2	507.4	390.3
Condensate					29.6	36.5	88.8	109.5
Total	198.8	88.3	596.2	264.9	198.8	166.7	596.2	499.8

Although this is not true in practice, however, for the purpose of the design this assumption was justified, since the tar-oil yields at 800 °C (the assumed operating temperature) are significantly reduced (85-97).

3.3.2 Design of distributor

3.3.2.1 Introduction

It has been shown (275) that the quality of bubbling fluidization is strongly influenced by the type of gas distributor used. This is illustrated in Figure 3.2 as follows (36): for few gas inlet openings the bed density fluctuates appreciably at all flow rates, although more severely at high flow rates. The bed density varies with height and gas channeling may be severe. For many gas inlet openings the fluctuation in bed density is negligible at low air flow rates, but again increases significantly at high flow rates. However, the bed density is more uniform throughout the bed, the bubbles are smaller and the gas-solid contacting is more intimate with less channeling of gas.

Although contacting is better when sintered plates or plates with several orifices are used as distributors, such distributors have the disadvantage of relatively high pressure drop from the standpoint of industrial or large scale

operations. This may significantly increase the power requirements for the blowers, often a major cost factor.

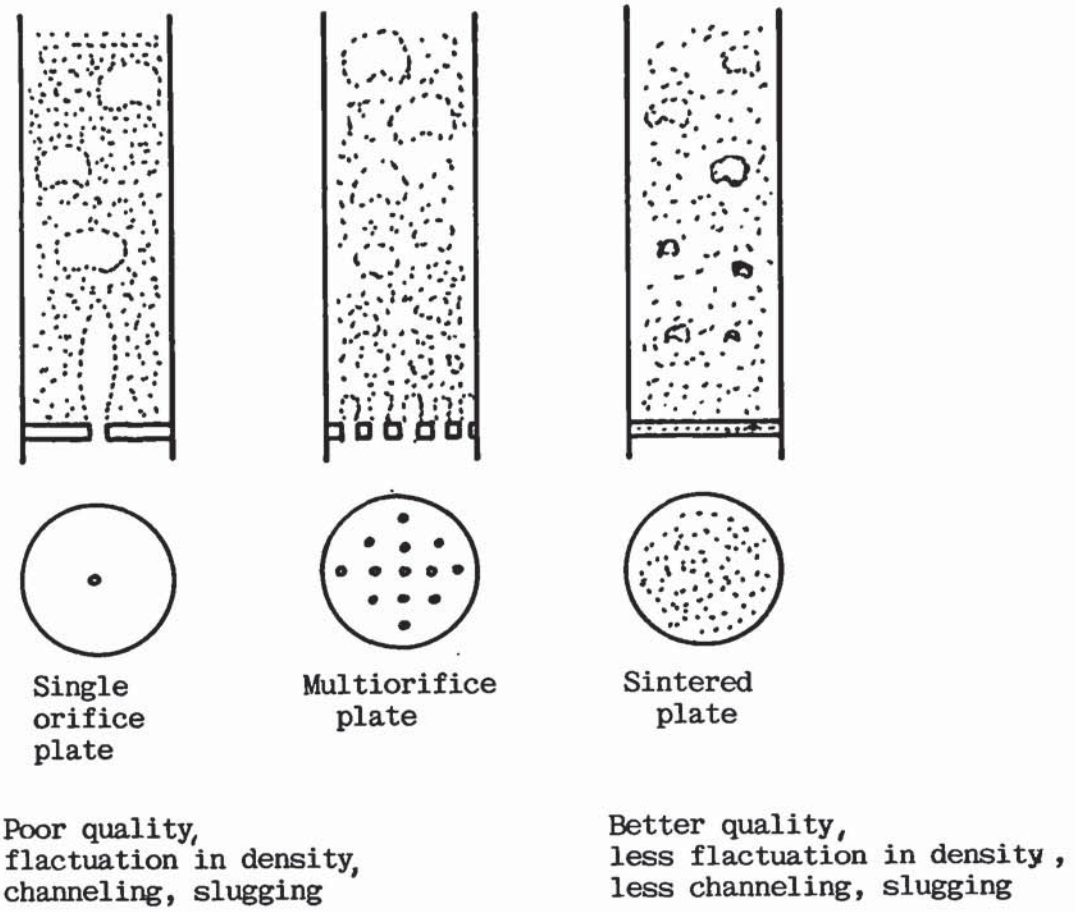

Figure 3.2 : Quality of fluidization as influenced by the type of gas distributor (36).

In general distributors have two functions: a) to support the bed and b) to distribute the gas equally all over the cross sectional area of the bed. In addition, as stated above, they also have the requirement of low pressure drop. It is evident that distributors should be selected and designed with care, for this is the first step to the successful application of a fluidized bed process.

3.3.2.2 Design procedure

It is rather surprising that although the distributor is one of the two most important components of a fluidized bed along with the bed material, its design is still largely empirical.

Experience shows that distributors should have a sufficient pressure drop to achieve equal flow through the openings. Therefore the pressure drop across the distributor should be considerably larger than the inherent resistance to distribution of the incoming gas. As a generous estimate, the rearrangement resistance can be taken as the expansion loss when flow passes from the inlet connection into the vessel (36).

It has been suggested that the ratio of distributor to expansion loss be taken as 100 (276). It has also been recommended (36) that the pressure drop across the distributor plate be about 10 % of the pressure drop across the bed, with a minimum in all cases of about 35 cm H_2O. The above conditions can be summarized by :

ΔP_{dmin} = Max (0.1 ΔP_b; 35 cm H_2O;100 ΔP expansion into vessel) equation 3.5

where ΔP = pressure drop
$_d$ = denotes distributor
$_b$ = denotes bed

According to equation 3.5 the minimum pressure drop over the distrtibutor should be the highest value of the three parameters given in this equation. However, in practice, the pressure drop over the distributor is dictated by the power requirements of the blower and industrial units have been reported with pressure drop over the distributor as low as 25 cm H_2O (36).

Distributors can be designed directly from orifice theory and since the orifice pressure drop is only a small fraction of the total pressure drop, the following procedure has been suggested (36).

1) determine the necessary pressure drop across the distributor from equation 3.5;
2) calculate the Reynolds number for the total flow approaching the distributor and select the corresponding value for the orifice coefficient Cd from standard figures (eg. Figure 12, chapter 3, p. 88 (36));

3) determine the velocity of fluid through the orifices, measured at the approach density and temperature :

$$U_{or} = Cd \frac{(2g_c \Delta P_d)^{1/2}}{\rho_g} \qquad \text{equation 3.6}$$

where U_{or} = the velocity of fluid through the orifices
ρ_g = the density of the fluid
g_c = conversion factor = 980 g cm/ g s^2

The ratio of the approach velocity of the fluid to the velocity of fluid through the orifices gives the fraction of open area in the distributor plate.

4) decide on the number of orifices per unit area of distributor and find the corresponding orifice diameter as followed:

$$U_o = \frac{\pi}{4} d^2_{or} U_{or} N_{or}. \qquad \text{equation 3.7}$$

where U_o = the velocity of the fluid approaching the distributor
d_{or} = the diameter of the orifices
N_{or} = the number of the orifices

Other design procedures more or less rigorous have also been suggested; however, they are all empirical and even the most rigorous design procedure gives results that differ not more than a few per cent from equation 3.7 (36, 189). It was therefore decided that for the purpose of the design, the procedure outlined above was sufficiently accurate and it was applied for the design of the distributor of the process development unit. Since the application of this procedure incorporates a lot of basic engineering calculations, the various computations are given in Appendix II, while the most important results are summarized in Table 3.3.

Table 3.3: Summary of distributor results

Component	Value
ΔPd (min)	15.6 cm H_2O
ΔPd (max)	140.4 cm H_2O
Re_t	2758 -
Cd	0.6 -
U_{or}	29.4 m/s
N_{or}	240.0 $1/m^2$
$N_{or,a}$	120 -

where N_{or} = number of orifices per unit area
$N_{or,a}$ = actual number of orifices on distributor.

3.3.3 Pressure drop for the compressor

The compressor should supply at least enough pressure to ensure that the pressure drop over the distributor and the bed is overcome. For the former, the computations should be based on the maximum air flow conditions, i.e. 140.4 cm H_2O (see Table 3.3), since under these conditions the pressure drop is the highest, for the latter, the pressure drop at conditions of minimum fluidization should be considered, since even if the air flowrate increases significantly above the minimum fluidization flowrate, the pressure drop over the bed remains relatively constant (see section 2.3.2 and Figure 2.6).

The pressure drop over a bed at conditions of minimum fluidization is given by equation 3.8(38):

$$\Delta P_{bed} = H(1 - e_{mf})(\rho_s - \rho_g)\frac{g}{g_c} \qquad \text{equation 3.8}$$

where ΔP_{bed} = pressure drop over the bed
H = height of bed
e_{mf} = bed voidage at conditions of minimum fluidizatiion
ρ_s = density of solid bed material
ρ_g = density of fluidizing gas
g = acceleration due to gravity
g_c = conversion factor 9.80 kg. m/kg. s^2

Assuming e_{mf} = 0.5 which is a generally accepted value for sand beds (38); and p_s = 2450 kg/m³ (38), then p_g can be considered negligible. Substitution in equation 3.8 gives:

$$\Delta P_{bed} = 735 \text{ kg/m}^2$$
$$\text{or} \quad \Delta P_{bed} = 73.5 \text{ cm } H_2O$$

Hence the total minimum pressure drop the compressor should overcome is (189):

$$\Delta P_{total} = \Delta P_d + \Delta P_{bed} \qquad \text{equation 3.9}$$

The pressure drop over the distributor is calculated in Appendix II, section II.2 and its value is given in Table 3.3. Thus:

$$\Delta P_{total} = 140.4 + 73.5 = 213.9 \text{ cm } H_2O.$$

In practice and with commercial fluidized bed, it is found that there is an increase - although relatively small - in the pressure drop over the bed, as the gas flow increases above the minimum fluidization conditions (273, 280). However, this increase in pressure drop cannot be predicted, since it is strongly influenced by the actual system. Common values have been reported in the range 20-30 % above the pressure drop at minimum fluidization (273). It is therefore necessary to consider this in the considerations for the total pressure drop.

In addition, it had to be envisaged at the design stage that other types of bed material such as alumina sand could be employed in the reactor, since it was a process development unit and would be used with different feedstocks and processes. The density of alumina is 4200 kg/m³ (189). Substitution in equation 3.8 gives:

$$\Delta P_{bed} = 1260 \text{ kg/m}^2$$
$$\text{or } \Delta P_{bed} = 126 \text{ cm } H_2O$$

and therefore from equation 3.9: ΔP_{total} = 266.4 cm H_2O for alumina sand.
In addition, the non uniformity of sand (sand of a narrow size fraction is relatively expensive) has to be accounted for. Thus, although the design may specify a particular mean particle size (see following section), this is rarely

used in practice. Instead a wide size fraction is taken and this usually contains particles with larger size than the mean. These particles are more difficult to be fluidized and hence require higher pressure drop.

It was therefore decided to increase the total pressure drop, for safety reasons, by 40 % in order to ensure that efficient fluidization could be attained under all experimental conditions. Thus,

ΔP_{total} = 300 cm H_2O.

An air compressor capable of delivering a pressure of 300 cm H_2O and a maximum air flowrate of 300 m^3/h was required.

3.3.4 Calculation of the particle size of sand

The average particle size of sand must be determined subject to the constrains of ensuring good fluidization and the various parameters determined above. This is usually done by employing empirical equations for the determination of the minimum fluidization velocity, which includes the average particle diameter as a term. In general (36):

$$U_{mf} \propto d_p^x \qquad \text{equation 3.10}$$

where U_{mf} = the minimum fluidization velocity
d_p^x = the average particle diameter
x = an exponent.

Several equations have been proposed for the calculation of the minimum fluidization velocity all of which are of the form of equation 3.11

$$U_{mf} = k\, g\, (\rho_s - \rho_g)^a\, d_p^b\, \rho_f^c\, \mu^d \qquad \text{equation 3.11}$$

where k = a constant
g = acceleration due to gravity
ρ = density (s for solid, g for gas)
μ = viscosity of fluidizing gas

The most commonly used are summarized in Table 3.4.

Table 3.4 : Constants and exponents of the different equations for the calculation of the minimum fluidization velocity (273).

Name of researcher	K Constant	a	b	c	d	Re increasing
Stokes	0.0008	1	2	0	- 1	↓
Carman kozeny	0.0006	1	2	0	- 1	
Leva	0.805	0.94	1.83	0	- 0.88	
Newton	0.066	0.5	0.5	-0.5	0	
Ergun	-	0.5	0.5	-0.5	0	

From the above equations, the one of Leva (279) is the most commonly used for Reynolds numbers : $Re_{mf} < 10$. Leva's equation is given by equation 3.12.

$$U_{mf} = 0.805 \times 10^{-3} \times g \times (\rho_s - \rho_g)^{0.94} \times dp^{1.83} \times \mu^{-0.88} \qquad \text{equation 3.12}$$

(the difference in the value of the constant k being in the units for m/s)

Equation 3.12 should be applied at actual reaction conditions and for the minimum input air flowrate, which is derived from Table 3.2 as $Q_{air,min}$ = 88.3 N m^3/h. The design operating temperature was set at 800 °C on the basis of previous experience (see section 3.2 and Table 3.1). Thus, the volumetric flowrate at the temperature of the reactor, $Q_{air,T}$ can be estimated by assuming ideality of gases and using equation 3.13 :

$$Q_{air,T} = Q_{air} \times \frac{273 + T_r}{273} \qquad \text{equation 3.13}$$

where : T_r = reactor temperature

Q_{air} = air flowrate at normal conditions.

Substituting the appropriate values equation 3.13 gives :

$Q^{800}_{air,min}$ = 347.0 m^3/h.

In order to ensure efficient fluidization, the velocity of the gas in the bed should satisfy the commonly adopted condition set by equation 3.14 (36, 279):

$$\frac{U}{U_{mf}} > 2.5 \qquad \text{equation 3.14}$$

where U = the actual superficial gas velocity in the bed
U_{mf} = the minimum fluidization velocity.

In general, the volumetric flowrate of a gas in a pipe is given by equation 3.15

$$Q = U \times A \qquad \text{equation 3.15}$$

where Q = volumetric flowrate of gas
U = velocity of gas
A = cross sectional area.

Assuming a value of $U/U_{mf} = 2.5$ from equation 3.14 and substituting for the cross sectional area (internal diameter = 0.8 m, see section 3.3.1) and the volumetric flowrate of gas at reaction conditions, equation 3.15 becomes:

$$\frac{347}{3600} = 2.5\, U_{mf} \times \frac{\pi \times 0.8^2}{4} \qquad \text{equation 3.16}$$

Substituting equation 3.12 as well as the following appropriate values for ρ_s, ρ_g and μ ; (189) ;

$\rho_s^{800} = 2450$ kg/m^3
$\rho_g^{800} = 0.329$ kg/m^3
$\mu_g^{800} = 4.3 \times 10.^{-5}$ kg/m.s

equation 3.16 becomes:

$$\frac{347}{3600} = 2.5 \times 7.9 \times 10^{-3} \times d_p^{1.83} \frac{(2450-0.329)^{0.94}}{(4.3 \times 10^{-5})^{0.88}} \times \frac{\pi \times 0.8^2}{4}$$

Solving for dp gives:

$$d_p = 499 \times 10^{-6} \text{ m}$$

or $d_p = 499\ \mu$

or $d_p \simeq 500\ \mu$

Therefore the mean particle size of the sand should be 5×10^{-4} m according to the design basis.

3.4 CALCULATION OF THE FLUIDIZATION PARAMETERS

On the basis of the above results, the following fluidization parameters can be determined, which can then specify the design parameters. These parameters are later used to verify the design in terms of contact efficiency (see section 3.6). The necessary fluidization parameters are: 1) the minimum fluidization velocity; 2) Reynolds number; 3) terminal falling velocity of particles, and 4) the size of bubbles.

3.4.1 Minimum fluidization velocity

With the same data for ρ_s, ρ_g and μ_g reported in section 3.3.4 and with a mean particle diameter of 4.99×10^{-4} m calculated in section 3.3.4, Leva's equation (3.19) gives :

$U_{mf} = 0.076$ m/s

However, for a bed of sand with wide size distribution, the minimum fluidization velocity will vary from the design value and the only accurate way to determine it, is to measure it experimentally.

3.4.2 Reynolds number at minimum fluidization conditions

The Reynolds number at minimum fluidization conditions is given by equation 3.17:

$$Re_{mf} = \frac{d_p \times \rho_g \times U_{mf}}{\mu_g} \qquad \text{equation 3.17}$$

where : d_p = mean particle diameter

P_g = density of fluidizing gas
μ_g = viscosity of fluidizing gas
U_{mf} = minimum fluidization velocity

Substituting the appropriate values from section 3.3.4 and the value of U_{mf} from section 3.4.1 equation 3.17 gives:

$Re_{mf} = 0.291$

This value of Reynolds number indicates laminar flow (see Appendix II), which is typical of fluidized beds of fine particles (36) and justifies the application of Leva's equation 3.12 for the calculation of the U_{mf}, since this equation is applicable for $Re_{mf} < 10$.

3.4.3 Particles terminal falling velocity

The particles terminal falling velocity specifies the velocity, which if exceeded, the particles of the bed will be entrained and elutriated (see section 2.5.6.8).

When $Re_{mf} < 1$, the terminal falling velocity, U_t, is given by equation 3.18 (273):

$U_t = 70 \times U_{mf}$ equation 3.18

Hence $U_t = 70 \times 0.078 = 5.32$

To avoid the possibility of slowly moving particles forming clusters and to ensure good heat transfer from the walls, it was considered - as has been proposed (273) - that gas velocity at the bottom of the bed (where it is lowest) must not be less than $2.5 \times U_{mf}$. To minimize particle carry over and to reduce the necessary freeboard, it was specified that gas velocity at the bed surface should not exceed 0.5 x Ut. Hence for efficient fluidization at the bottom of the bed:

$U_{op} \geq 2.5\, U_{mf}$ equation 3.19

where U_{op} = operational velocity
or $U_{op} \geq 0.19$ m/s

and at the surface of the bed:

$$U_{op} < 0.5\, U_t \qquad \text{equation 3.20}$$

or $U_{op} < 2.66$ m/s

Therefore the operational velocities should be in the range:

$$0.19 < U_{op} < 2.7 \text{ m/s} \qquad \text{equation 3.21}$$

However, equation 3.21 is only valid for an operating system if actual reactor conditions are considered. In the case of fluidized bed gasifiers, two factors must be considered : a) the increase in the volumetric flowrate, due to raising the temperature of the air from ambient to the operating and b) the increase in the volumetric flowrate, due to the formation of gas by the gasification process. In the design equations above, the first factor was taken into account since the mean particle size of sand was determined at the actual operating volumetric flowrate (see section 3.3.4, equations 3.13 and 3.16). This value was used in Leva's equation (3.12), while the value of ρ_g and μ_g were determined also at the operating temperature.

The second factor, however, has to be evaluated. From Table 3.2 the maximum output volumetric flowrate (which takes into account the increase in the volumetric flowrate due to the gasification process) is $Q_{gas,max}$ = 499.8 Nm^3/h. Using equation 3.13, at 800 °C this becomes :

$Q_{gas,max}$ = 1964 m^3/h or
$Q^{800}{}_{,gas,max}$ = 0.546 m^3/s.

Dividing this value with the cross-sectional area of the bed, A = 0.503 m^2, the actual operational velocity can be found :

U_{op} = 1.08 m/s

The above value of the operational velocity satisfies equation 3.21 and thus the design is acceptable.

3.4.4 Size of bubbles

Bubbles grow in size by coalescence, as they rise through the bed and correspondingly, diminish in number to maintain a roughly constant flowrate of gas in the bubble phase (see section 2.3.3.1). The type of distributor determines the initial size of bubbles, but thereafter has no influence. Provided the vessel is big enough, bubbles grow according to equation 3.22 (280).

$$d_B = g^{-0.25} \times (U-U_{mf})^{0.5} \times (h+ho)^{0.75} \qquad \text{equation 3.22}$$

where d_B is the average diameter of bubbles at any height, h above the distributor, where the gas velocity is U.ho corresponds to the initial bubble size and is that imaginary distance beneath the distributor, where the bubbles would be of zero diameter. ho can only be determined empirically on the basis of the initial bubble size. When the latter is known, then a value for ho is set on basis of experimental results (273).

Assuming an initial bubble diameter of 0.005 m (which is a generally accepted value for orifices), then ho corresponds to 0.10 m (280).

Under normal operating conditions (which should satisfy equations 3.19 and 3.20), there is an appreciable expansion of the bed (see section 2.3.2). For beds consisting of sand particles, this expansion is usually 30% (273). Thus:

$$h = h_{mf} + 0.3\, h_{mf} \qquad \text{equation 3.23}$$

where h_{mf} = the bed height at conditions of minimum fluidization,

or $h = 0.6 + 0.3 \times 0.6$

$= 0.78$ m

The operational velocity at reaction conditions was determined in the previous section;

$U_{op} = 1.08$ m/s.

Substitution of the appropriate values in equation 3.22 gives:

$d_{B\,max} = 0.515$ m

Similarly, under conditions of minimum input flowrates, the output gas produced is 166.7 Nm^3/h (see Table 3.2).
Under actual operating conditions this corresponds to:

$$Q^{800}_{gas,min} = 655 \ m^3/h$$
or $$U^{800}_{gas,min} = 1302 \ m/h = 0.362 \ m/s$$
$$d_{Bmin} = 0.274 \ m.$$

When the bubble diameter is equal to or higher than the reactor diameter at the top of the bed, the bubbles will become slugs some way down the bed. This will cause large amplitude heaving of the bed surface, excessive carry over of particles and probably swamping of the cyclones. An empirical rule to avoid this problem is to ensure that the mean bubble size at the top of the bed is no more than half the vessel diameter, especially if the freeboard is not of the expanded variety (273). Thus :

$$\frac{d_b}{d_B} \geq 2 \qquad \text{equation 3.24}$$

where d_b = diameter of bed
d_B = average diameter of bubbles

In the case of maximum flowrate of product gas

$$\frac{d_b}{d_B} = \frac{0.8}{0.515} = 1.55$$

and for minimum flowrate of product gas

$$\frac{d_b}{d_B} = \frac{0.8}{0.274} = 2.92$$

The restriction of equation 3.24 is satisfied only at the minimum flowrate of product gas. At the maximum flowrate, the above restriction is not satisfied. However, the bubbles do not become slugs ($d_b = d_B$), which would certainly cause problems. Since no slugs would be formed and the operational gas

velocities were determined to be acceptable in terms of the terminal falling velocity of the particles (see section 3.4.3), it was decided on the basis of previous experience not to modify the design of the fluidized bed, but instead to construct the freeboard with an expanded diameter in relation to bed diameter, in order to minimize any possible entrainment of bed particles (see section 3.7).

3.5 DESIGN DATA

The design data are summarized in Table 3.5. From these only the bed diameter and height were fixed. The flowrates of the reactants were determined on the basis of the experimental parameters given in Table 3.1, while the other data were determined on the basis of empirical relationships (36, 273).

Table 3.5 : Summary of design data

Input/output	at normal conditions		at 800 °C	
Volumetric flowrate at bottom of bed = Q^b_{max}	264.9	Nm^3/h	1041.0	m^3/h
= Q^b_{min}	88.3	Nm^3/h	347.0	m^3/h
Volumetric flowrate at top of bed = Q^t_{max}	499.8	Nm^3/h	1964.2	m^3/h
= Q^t_{min}	166.7	Nm^3/h	655.1	m^3/h
Gasvelocity at distributor = U^d_{max}	0.146	m/s	0.575	m/s
= U^d_{min}	0.049	m/s	0.192	m/s
Gasvelocity at top of bed = U^t_{max}	0.276	m/s	1.08	m/s
= U^t_{min}	0.092	m/s	0.362	m/s

Distributor parameters		
Maximum pressure drop, Δpd (max.)	140.4	cmH_2O
Minimum pressure drop, Δpd (min.)	15.6	cmH_2O
Gasvelocity in orifices U_{or}	29.4	m/s
Number of orifices per unit area N_{or}	240.0	$1/m^2$
Number of orifices on distributor N^a_{or}	120.0	-

Fluidization parameters			
Bed diameter	d_b	0.8	m
Bed cross sectional area	A_r	0.503	m^2
Bed height : static	h_b	0.6	m
: fluidized	h_b	0.78	m
Mean particle diameter	d_p	499×10^{-6}	m
Minimum fluidization velocity	U_{mf}	0.076	m/s
Reynolds number at mf	R_{emf}	0.291	-
Particle terminal falling velocity	U_t	5.32	m/s
Operational velocity range	-	$0.19 < U_{op} < 2.7$	m/s
Size of bubles, initial	d_{Bi}	0.005	m
maximum	d_{Bmax}	0.515	m
minimum	d_{Bmin}	0.274	m

3.6 DESIGN VERIFICATION

3.6.1 Introduction

Since several assumptions were made in the design calculations and some parameters were arbritrarily chosen, it was necessary to evaluate the results obtained. A simple but reliable model was used to verify the design (273).

The two most important parameters, which must be determined according to this model, are the residence time of gas flowing interstitially and the fraction of bubble gas in contact with particles. The former indicates whether there is enough time for the reactions to proceed to a certain degree, while the latter represents the contact efficiency and whether the gas enclosed by the bubbles will react with the particles of the bed and up to which degree. Both must be within certain generally accepted values to ensure satisfactory operation. Application of this model also completes the design of the fluidized bed as a reactor.

3.6.2 Residence time of gas flowing interstitially

To a first approximation the amount of gas flowing interstitially at all levels of the bed, Q_{ig}, is given by equation 3.25, according to the two phase theory (see section 2.3.3.1).

$$Q_{ig} = U_{mf} \times A_r \qquad \text{equation 3.25}$$

For the fluidized bed designed in this chapter:

$$Q_{ig} = 0.076 \times 0.503$$
$$= 0.038 \text{ m}^3/\text{s} \quad \text{or} \quad 136.8 \text{ m}^3/\text{h}$$

This value is compared to the total gas flowrate for both minimum and maximum output in Table 3.6.

Thus at maximum gas flowrate, 13.14 % of the total gas flows interstitially at the bottom and 6.96 % at the top of the bed. Similarly, at minimum gas flowrate these values are 39.42 and 20.88 % respectively. An average of 10 and 30 % can be taken for the maximum and for the minimum flow respectively, of all flow occurring interstitially.

Table 3.6 : Comparison of interstitial flow to total flow of gas

	Percentage of gas flowing interstitially	
	Minimum	Maximum
Bottom bed	39.42	13.14
Top bed	20.88	6.96

The residence time of this gas in the bed is given by equation 3.26:

$$(tr)_i = \frac{h_b}{U_{mf}} \qquad \text{equation 3.26}$$

$$= \frac{0.78}{0.076} = 10.26$$

This means that the contact time between the gas and bed particles in the emulsion phase, will be about 10 seconds. Although this is not very high, however, if the rate of reaction of oxygen with char is considered at 800 °C , then it is clear that this residence time is sufficient to ensure complete consumption of oxygen in the bed (see section 2.5.5.7).

3.6.3 Contact efficiency

The bubble diameter at the bottom of the bed is 0.05 m and at the top 0.515m and 0.274m for the maximum and minimum flow respectively (see 3.4.4). Hence, it can be assumed that the mean size of bubbles over the bed is 0.283m and 0.162m for maximum and minimum flow rates respectively. Similarly, the mean velocity of the gas in the bed is 0.827 and 0.277 m/s respectively for the maximum and minimum flow conditions. The bubble velocity is given by equation 3.27 (279).

$$U_B = \frac{\sqrt{g\, d_B}}{2} + (U - U_{mf}) \qquad \text{equation 3.27}$$

Substituting the appropriate values in equation 3.27, the bubble velocity is found to be 1.93 and 1.09 m/s respectively for maximum and minimum flow. The residence time of bubbles in the bed is:

$$(tr)_B = \frac{h_b}{U_B} \qquad \text{equation 3.28}$$

and $(tr)_B$ = 0.404 s for maximum flow,
$(tr)_B$ = 0.715 s for minimum flow.

The ratio at bubble velocity to interstitial gas velocity is (273):

$$a = \theta \frac{U_B}{U_{mf}} \qquad \text{equation 3.29}$$

Assuming a voidage value of 0.5 (acceptable value for sand particles (36)), the above ratio was found to be 12.70 and 6.99 respectively for maximum and

minimum flow. The fraction of bubble gas in contact with particles is given by equation 3.30 (280):

$$\frac{V_{cp}}{V_B} = \frac{1.17}{a-1} \qquad \text{equation 3.30}$$

where V_{cp} = volume of particles in the cloud
V_B = volume of the bubble

Thus, $\frac{V_{cp}}{V_B} = 0.10$ for maximum flow

and $\frac{V_{cp}}{V_B} = 0.195$ for minimum flow

The above values are roughly equivalent to a contact efficiency of 10.0 and 19.5 % for the maximum and minimum flow respectively. These results are satisfactory, since in general a contact efficiency of 10 % is considered acceptable (273).

3.6.4 Discussion

The above verification method is mainly based on empirical equations. Nevertheless it is valuable since it allows for a reliable check up of the design of a fluidized bed reactor. The residence time of the gas flowing interstitially was estimated to 10.26 s, which in principle allows sufficient time for oxygen to be completely consumed by the combustion of char. Similarly the fraction of bubbles in contact with particles was equal or above (see previous section) the minimum acceptable value of 10 % (10.0 and 19.5 % for the maximum and minimum flow). These data indicate that the fluidized bed could achieve stable fluidization under these design parameters and that the oxygen would be consumed within the bed.

3.7 CONSTRUCTION OF THE FLUIDIZED BED

Since the reactor was a process development unit, it would be operated under different - even extreme conditions - in order to identify its limitations.

These would help define the range of operating parameters which could ensure trouble free operation. The construction had to provide for a) versatility in operation, b) measurement of all parameters of importance, c) operating with different feedstocks, d) easy removal of inerts from the bed, e) inspection of distributor and walls of reactor and f) easy access to the internals for repairs and maintenance. In this section the construction of the distributor is first discussed and then the shell of the fluidized bed and its various provisions.

3.7.1 Construction of the distributor

The quality of fluidization is strongly influenced by the type of gas distributor used (see section 3.3.2.1).

Operating problems (such as bed sintering and accumulation of inerts in the bed) arising from the utilization of feedstocks with high ash/inerts content (above 5 wt%), had to be considered and provisions also made for the removal of the foreign bed material. In studies investigating the segregation of particles in a fluidized bed (281, 282), it has been concluded that in a bed of similarly shaped particles, the heavy (larger density) and big (larger size) congregate at the bottom of the bed (Jetsam), while the light and small particles congregate at the top of the bed (Flotsam). Since the inerts in some feedstocks include stones bulky solids and sometimes pieces of iron as well as ash (e.g. the ash content of rice husk is about 20 wt%), these would accumulate at the bottom of the bed.

There are several types of distributors, some of them are applicable to standard fluidized beds, while others have been especially designed for special applications. The most commonly used types of distributor are shown in Figure 3.3 (36).

Type (a), a flat perforated plate or wire mesh, is usually applied for laboratory-scale units; it has the disadvantage that fine solids can fall through the orifices when the gas flow is stopped. This, however, can be countered by using two staggered perforated pates, (b). This can also be applied for industrial applications, since it is easy to design and construct and offers good gas distribution.

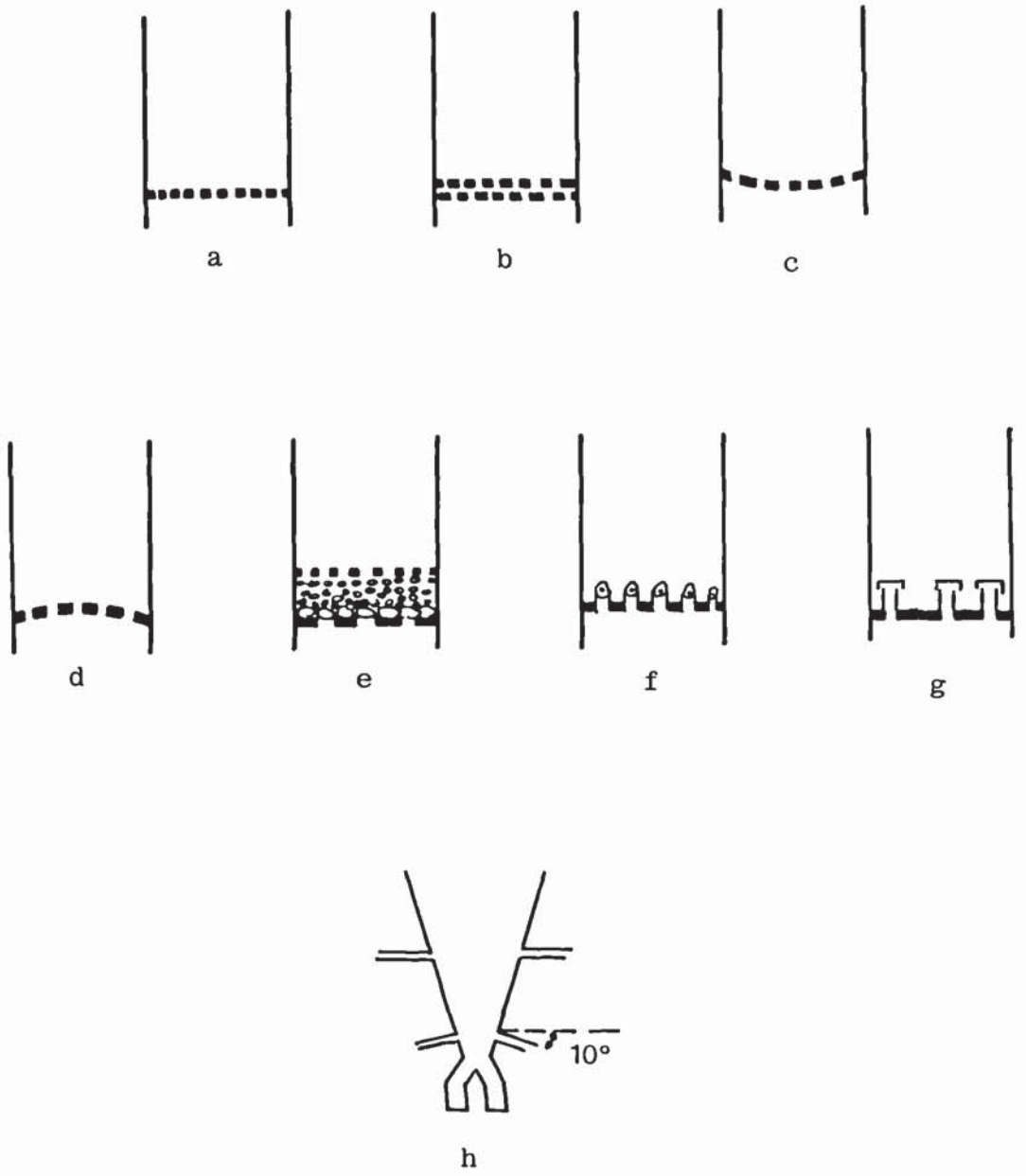

Figure 3.3 : Examples of various distributors for fluidized beds (36).

With the heavy load in large diameter beds, flat plates deflect appreciably and hence curved plates (c and d) which withstand heavy loads and thermal stresses are used. However, in order to ensure good gas distribution non-uniform orifice spacing is required, which is a disadvantage from the point of view of fabrication. When the inlet gas is free of solids, then a packed bed of granular material sandwiched by two perforated plates (e) is a good distributor and an excellent thermal insulator protecting low temperature gases from a hot bed. In addition, the packing can be used to mix feed gases. Thus injecting a second gas in the packed bed, where the first gas is flowing, results in good design for explosive reactant gas mixtures. Nozzles (f) and bubble caps (g) have also been used to prevent solids from falling through the distributor. In spite of their complicated construction they do not offer better gas distribution than (b) and (e), while solids tend to settle on the distributor. However, none of these distributor types shown in Figure 3.3 permit easy removal of inerts from the bed. This can be overcome by using a distributor of type (h), which was used in a modified design of the Winkler generator. No plate or distributor is used, but the gas is introduced through six side mixing nozzles into a teetered bed. However, the hydrodynamics of such a bed are difficult to describe and predict, since there is no uniform distribution of gas. The only type of distributor that allows for a classic fluidized bed as well as for easy removal of bed material is the type shown in Figure 3.4 (36). It was therefore decided to use the "pipe grid" concept as a gas distributor. This configuration permits efficient distribution of gas and the simultaneous passage of Jetsam in between the pipes of the grid.

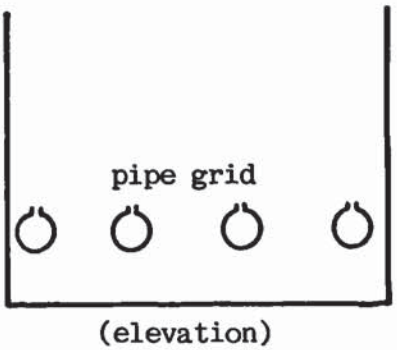

Figure 3.4 : Configuration of pipe grid distributor (36).

3.7.2 Configuration of the distributor

The author is not permitted to present a detailed figure of the distributor and any more details of its design and construction, than the following ones due to commercial interests and the possibility of a patent application.

For simplicity in inspection and maintenance the pipe grid was composed of two identical parts. The incoming gas was split into two flows, each of which passed through a gas collector pipe of 0.125 m diameter and parallel around the reactor. The gas flow from each collector was then introduced into the bed through seven pipes with a total of 60 orifices of 3 mm for each side (total design number of orifices = 120).

The number of orifices per pipe were : 6 orifices in pipes 1 and 7, 8 orifices in pipes 2 and 6, 10 orifices in pipes 3 and 5 and 12 orifices in pipe 4 respectively. The distance between the pipes was 0.11 m. To avoid blockage of the orifices by sand particles or other foreign material, the orifices were drilled in pairs on the pipes, facing downwards at 90° of each other, in a modified version of pipgrid than the one shown in Figure 3.4. The pipes were 25 mm inside diameter and were introduced into the bed through a pipe of 0.05 m. Flingerit rings were used between the flanges to prevent gas leaks.

3.7.3 Material of construction

Both metallic and ceramic materials can be used for distributors and have certain advantages. Ceramics are more resistant to corrosive gases and to high temperatures, but they have a low strength against thermal shock or expansion stresses (275). Ceramics are also eroded relatively easily, resulting in a gradual widening in the orifice openings. Metallic distributors are very good for expansion stresses or thermal shocks and in the case of a solids free gas have a high resistance to erosion. However unless special alloys (such as inconel) are used, metallic distributors are susceptible to corrosive gases. It was therefore decided to use refractory steel pipes. This type of pipe is very good for high temperature applications and is difficult to erode.

3.7.4 Construction of the fluidized bed

The reactor is a 1.6 m diameter cylindrical tube of 4.5 m height, outside dimensions. The shell is composed of carbon steel. It has been found (15) that the freeboard region is of great importance in a fluidized bed gasifier. It not only serves as a solids disengagement zone, but it is in this part of the reactor that the tars are believed to be cracked and the water gas shift reaction attains equilibrium at higher temperatures.

In order to allow for a good disengagement of solids due to a relatively large diameter of bubbles at the surface of the bed (see section 3.4.4), the reactor was constructed with an expanded freeboard. The bed diameter was set at 0.8 m as described in section 3.3.1 as a basic parameter. Some of the parameters had to be set arbitrarily. Thus the diameter of the freeboard was chosen arbitrarily as 150 % of the bed diameter, or 1.2 m. Emphasis was given in ensuring stable fluidization and providing a relatively large freeboard for the cracking of tars.

3.7.5 Insulation

A layer of refractory bricks forms the inner lining of the shell to give a finished diameter of 0.8 m bed and 1.2 m freeboard. This layer is 0.15 m at the freeboard and 0.35 m at the bed. At the top of the reactor, the horizontal surface is protected inside by a layer of 0.15 m of steelmix (refractory material). Sandwiched between the carbon steel outer shell and the refractory is a 0.05 m layer of rock wool, which acts as a further insulating medium. The conical reduction between the freeboard and the bed was constructed by refractory cement. Details about the fluidized bed insulation are given in Figure 3.5.

3.7.6 Details of construction

These are shown in Figures 3.6 and 3.7. The fluidized bed is supported on four legs of 1.3 m height. A square cone forms the bottom of the reactor. The cone ends in a square opening 0.83 m, OP1, below the distributor level, on which a manual gate valve was installed. The Jetsam is collected in this part of the reactor which otherwise contained sand.

The gases are introduced from the pipe grid, PG, and exit from a side opening, OP2, at the top of the reactor of 0.6 m diameter. Two wells, OP3, OP4, for overbed preheating burners of 0.22 diameter are forseen. Since some feedstocks with a high content of fines (e.g. wood shavings) were to be used, two horizontal feeding ports FP1, FP2, of 0.22 diameter are provided. Two observation wells, OW1, OW2, are constructed at the top of the bed. In total there are 12 ports for thermocouple TP or pressure drop measurements (see sections 4.1.2.1 and 4.1.2.2). Finally a rectangular well, RW, of 0.28 - 0.60 m is provided for the installation of a cooling system in the bed. It is possible to enter the reactor vessel by removing the conical square bottom of the reactor and one side of the pipe grid distributor.

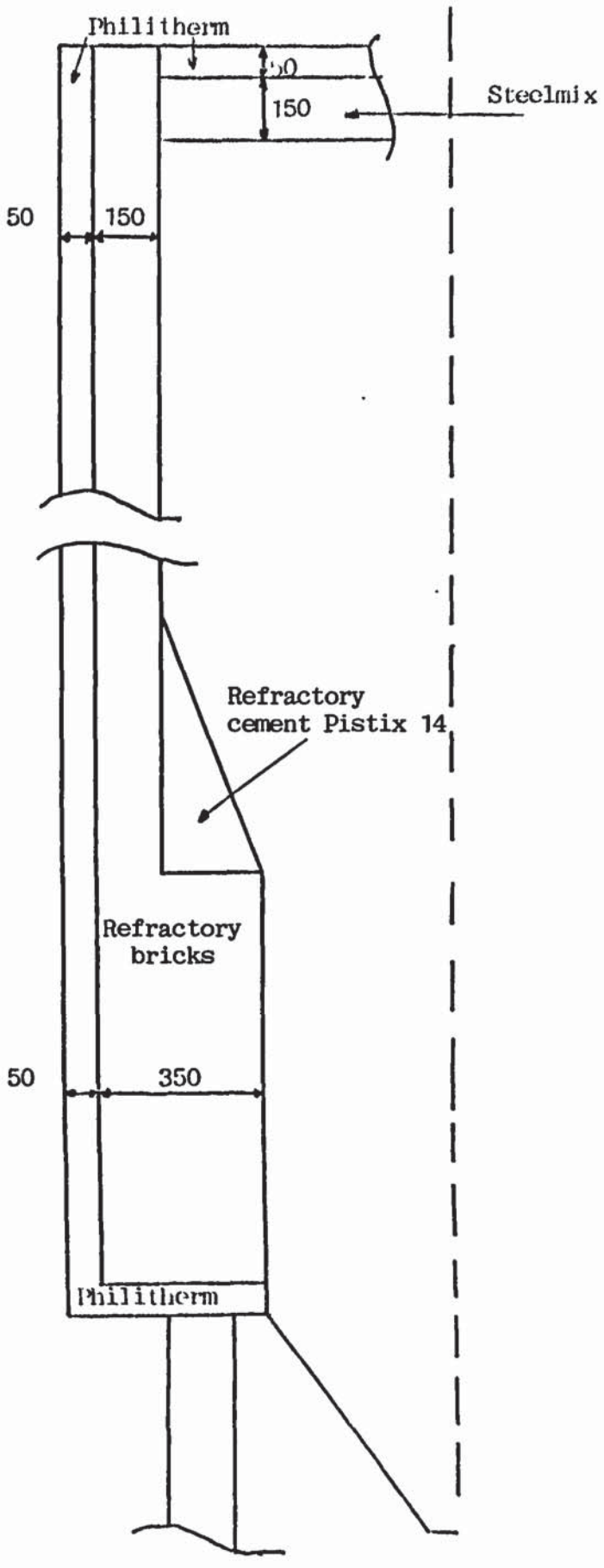

Figure 3.5 : Insulation of fluidized bed

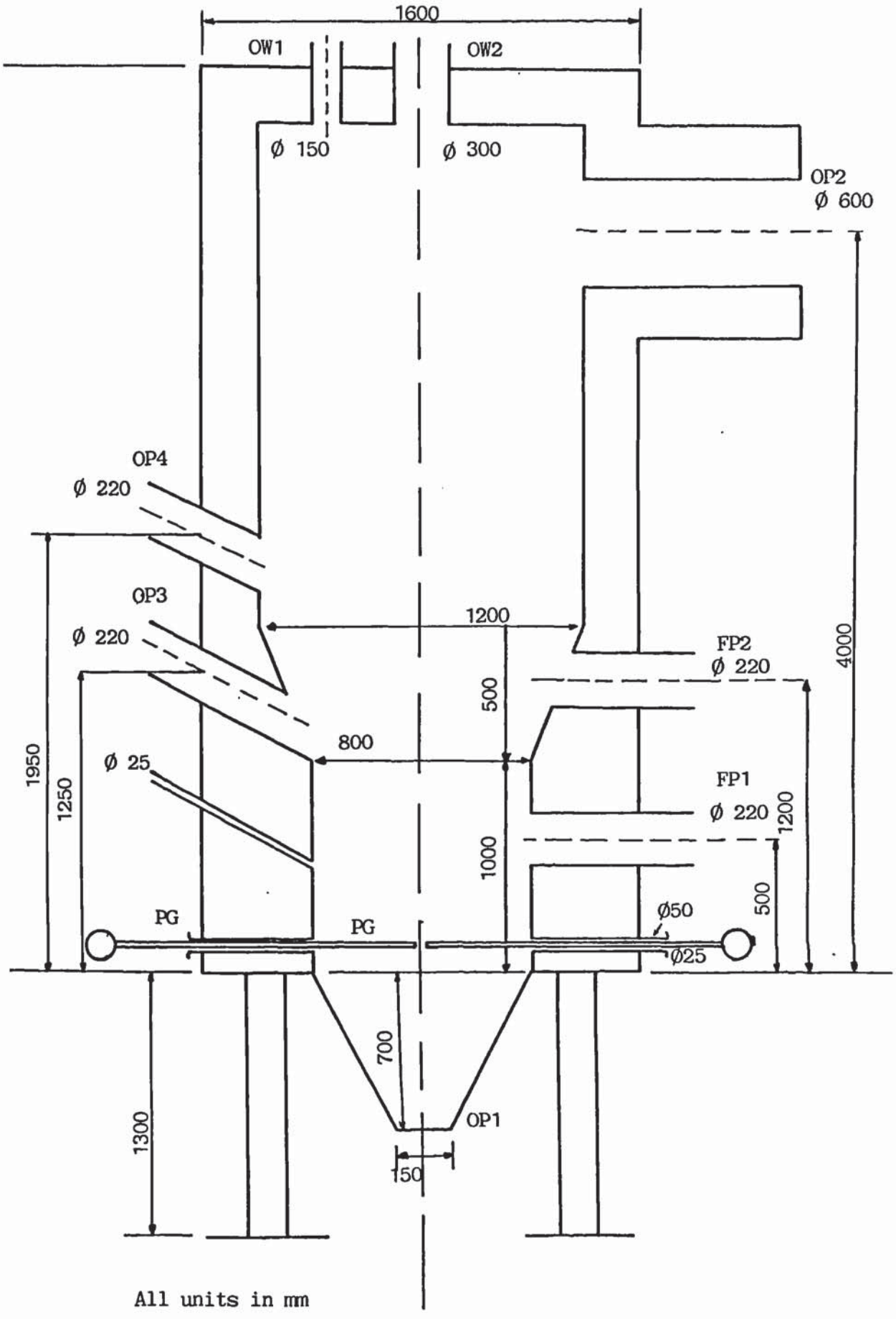

Figure 3.6 : Configuration of fluidized bed

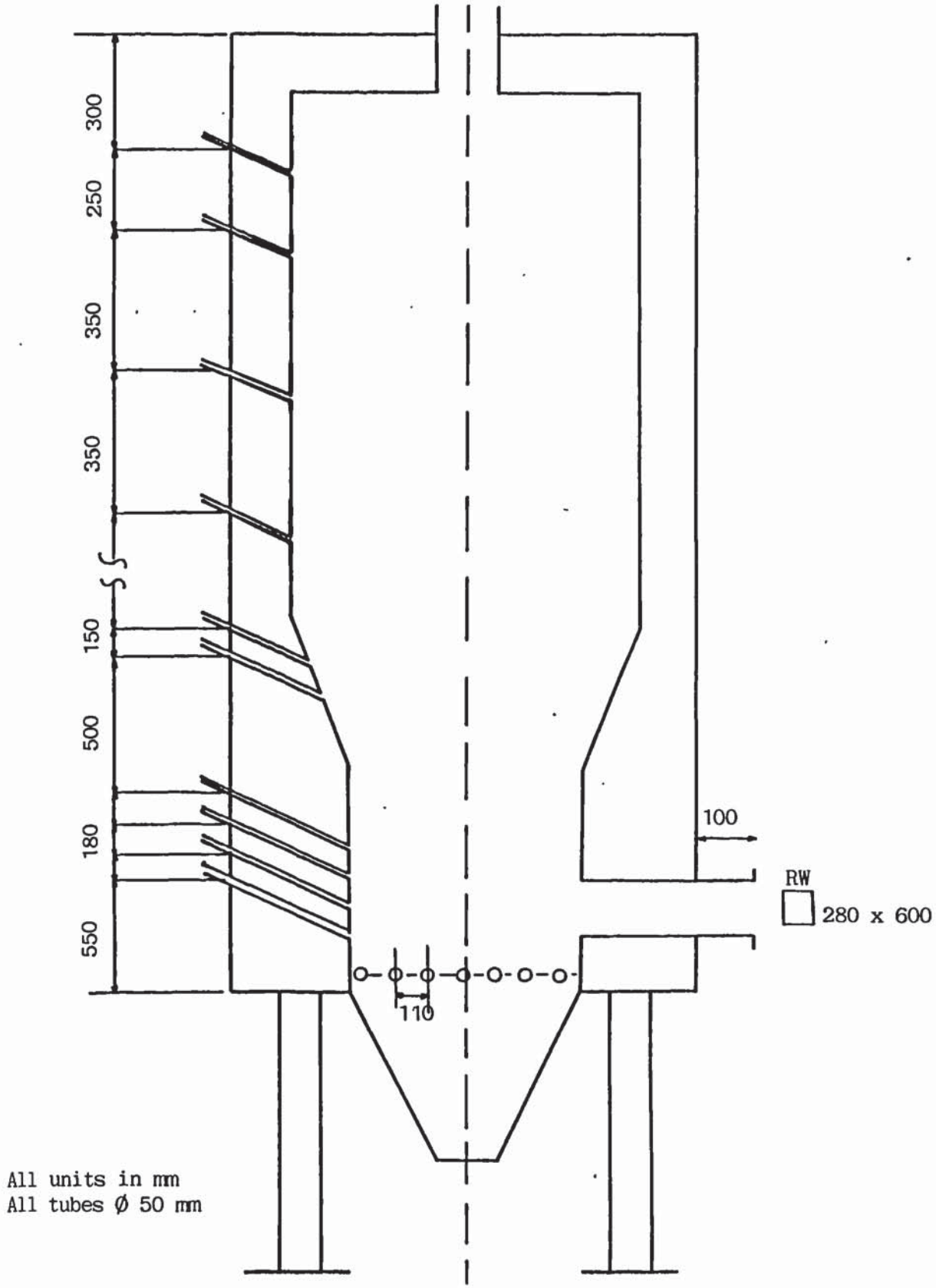

Figure 3.7 : Details of construction and measuring ports for thermocouples and U-tube manometers.

CHAPTER FOUR : EXPERIMENTAL PROGRAMME

4.1 INTRODUCTION

In this Chapter the pilot plant is described in detail with all peripheral equipment and apparatus. This is followed by a discussion of the commissioning of each item of equipment and the plant as a whole including the shortcomings and limitations of the plant. The experimental procedure follows with experimental analysis and the Chapter concludes with a discussion of the experimental programme.

4.1.1 Resources at the project site

The pilot plant, its supporting equipment and apparatus had to be constructed or procured within the budgetary limitations of the project. These limitations were rather serious and as a result only the fluidized bed reactor and the cyclone were constructed according to specifications of a design. All other equipment were either procured on second hand basis (compressor, temperature recorder, gas chromatograph, heat exchanger) or were constructed by Vyncke Warmtetechniek on basis of their experience (feeding system, preheating burner, product gas burner) (see Figures 4.1 - 4.3).

Some of these equipment functioned satisfactorily, others not, but it was not possible to replace the misfunctioning equipment with new ones. It was therefore necessary either to modify them until acceptable operation was achieved (eg. the product gas burner), or to abandon them and modify the data acquisition process (eg. the temperature recorder). These problems will be discussed further in the sections concerning the commissioning of the equipment.

Although the project was not carried out under optimum conditions in terms of resources, every effort was made to provide for the shortcomings of the plant by continuous attendance of the troublesome equipment; and although this was not very efficient in terms of manpower requirements, these shortcomings did not influence the value of the results of this work. Finally only one assistant was provided, whose main activity was to control the feeding system. All other experimental activities during the runs were carried out by the author.

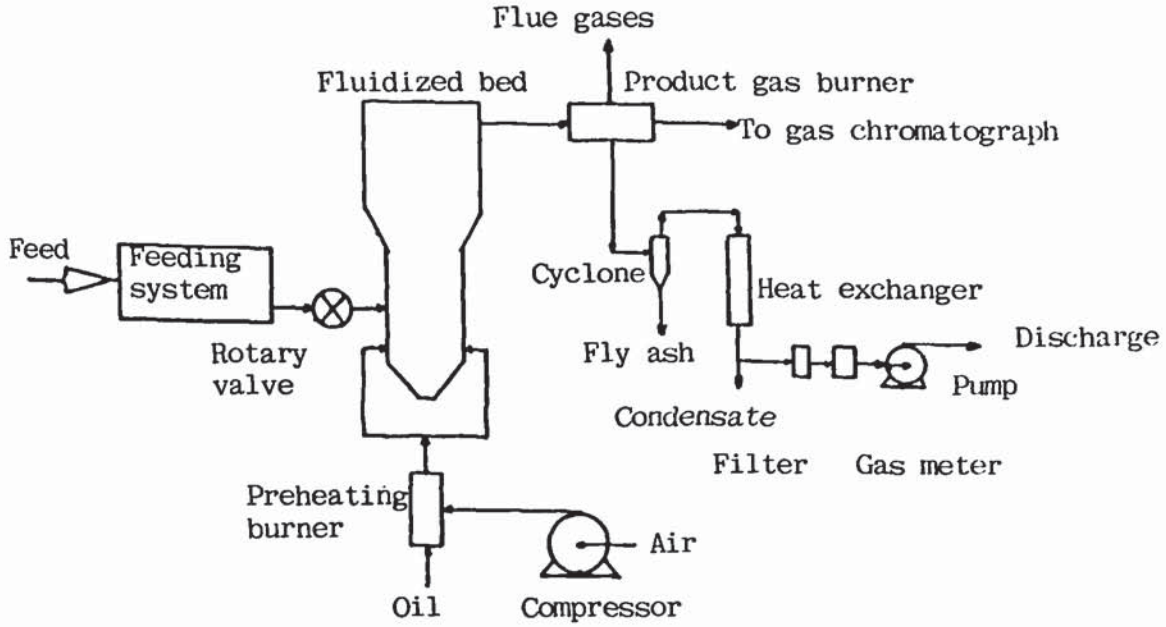

Figure 4.1 : Process flowsheet

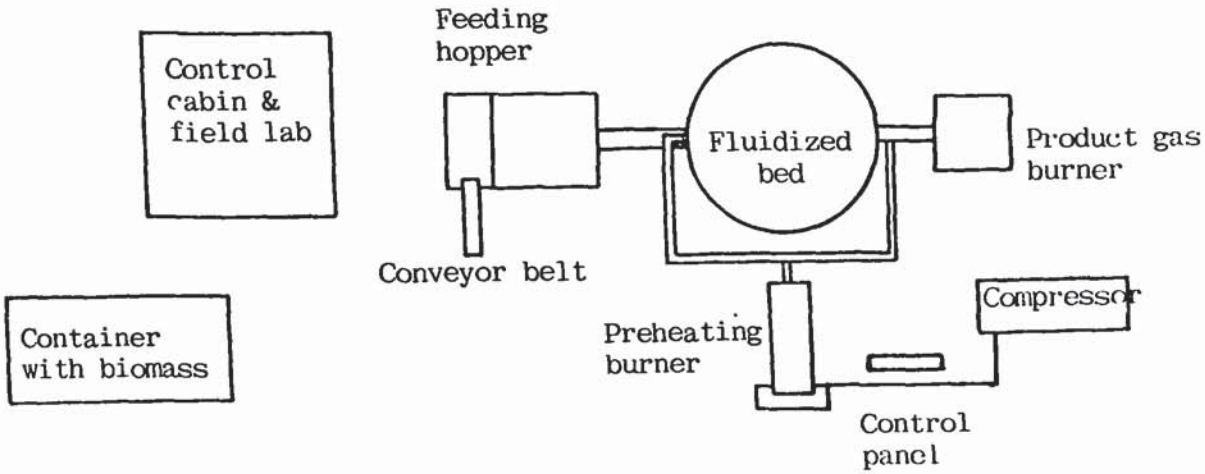

Figure 4.2 : Process development unit plan

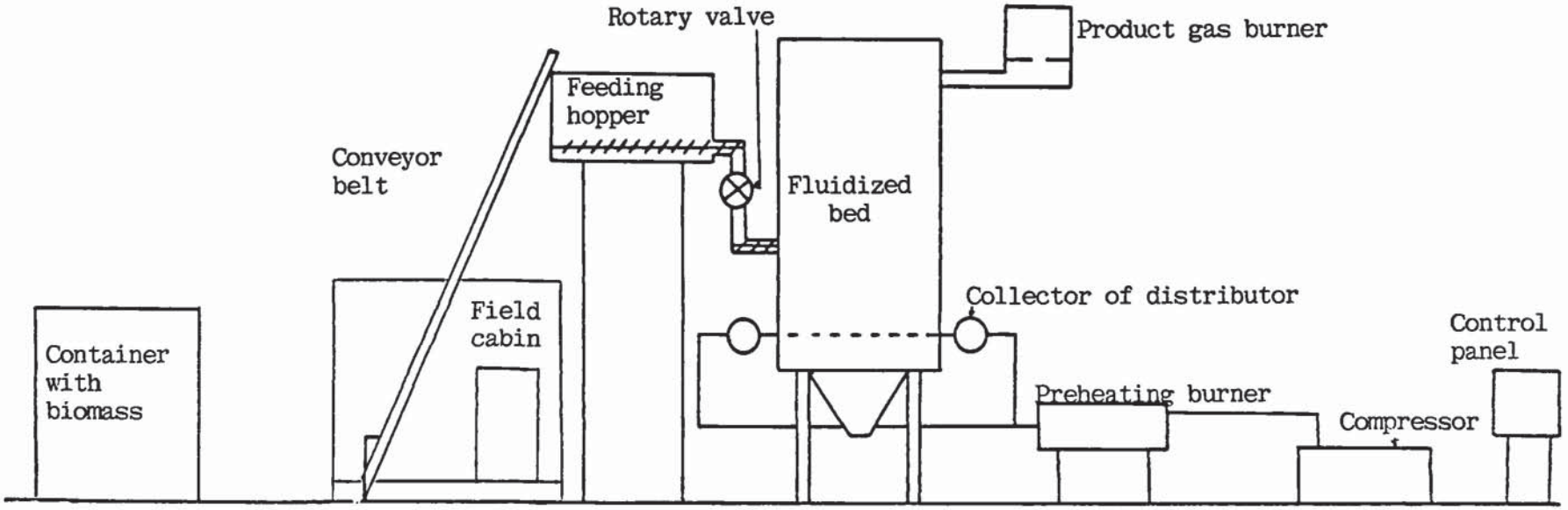

Figure 4.3 : Process development unit elevation

4.1.2 Objectives of the pilot plant and experimental programme

The objectives of the pilot plant were :

a) to provide for a multipurpose fluidized bed process development unit
b) to facilitate the acquisition of all necessary data and parameters required for its evaluation
c) to demonstrate in process development unit scale that fluidized bed gasification of biomass is a viable technology.

To meet these objectives, an experimental programme was derived (see section 4.5). This programme had to be specified within the financial restrictions and the actual limitations of the process development unit. The experimental programme was derived on the basis of the objectives of this work, the most important of which are (see Chapter 1) :

a) to determine the fluidization characteristics of the reactor
b) to study the air gasification characteristics of chopped wood
c) to assess the influence of the operating parameters on the gasification process
d) to develop new design procedures for scaling up fluidized bed gasifiers, by using empirical models
e) to develop a conceptual design for a fluidized bed gasification plant.

4.2 DESCRIPTION OF THE PILOT PLANT

4.2.1 Equipment

Figure 4.1 shows a flowsheet of the gasification facility, while Figures 4.2 and 4.3 are respectively a plan and an elevation of the major equipment of the process development unit. The system consisted of a materials handling and feeding unit, a fluidized bed reactor, an air supply system complete with start up burner, a product gas burner and a gas sampling line with appropriate instrumentation. A switch board and electrical panel was provided for the control of the above items (see Figures 4.2 and 4.3). The pilot plant was instrumented for data recording and analysis in a small cabin, which was used as a field laboratory for gas analysis.

Since a number of items (the preheating burner, the product gas burner and the feeding system) were of novel design and subject to patent application or licencing agreements, full details could not be disclosed at the time of writing, but as they were peripheral to the project and as there was no

influence on the results, ommission is not deleterious to the value of the project. All were designed and constructed by Vyncke Warmtetechniek.

4.2.2 Process description

The process is depicted in the process flowsheet, Figure 4.1. The feedstock was delivered to the plant from a particle board manufacturer in closed containers. A front end loader transported the feedstock to the conveyor belt for loading the hopper. This was fitted with a primary screw feeder, a rotary valve and a secondary screw to feed in the reactor.

The feedstock entered the reactor above the surface of the bed. A compressor supplied the air required to fluidize the bed. The air was fed through the preheating burner to the collectors of the distributor and from there it entered the bed.

The feedstock pyrolysed as soon as it fell in the fluidized bed to produce pyrolysis gases and char. The char was gasified and the pyrolysis gases participated in secondary reactions (see sections 2.5.3). The product gas and fly ash were then fed in the product gas burner where the gas was combusted.

A small fraction of the gas was removed from the product gas burner and passed through the cyclone to remove the fly ash and the heat exchanger to condense the steam and tars. Another sample was taken from the product gas burner to the gas chromatograph for gas analysis.

4.2.3 Material handling and feeding unit.

The speed of the primary screw of the feeding hopper was continuously variable, while the rotary valve and the secondary screw were operated under constant speed by different motors (see Figure 4.3). At the base of the second screw an opening was provided for calibration of the feedstock flowrate.

4.2.4 The fluidized bed reactor

Details about the construction of the fluidized bed are given in section 3.7.6 and are summarized in Table 4.1.

The measurement of temperature is imperative in a fluidized bed gasifier. This is the best indicator of steady state attainment and efficient fluidization (there should be no temperature gradient in the bed).

Table 4.1 : Characteristics of the fluidized bed reactor.

Parameter	Data	
Outside diameter	1.6	m.
Inside diameter a) bed	0.8	m.
b) freeboard	1.2	m.
Total height	5.8	m.
Height from distributor	4.37	m.
No of distributor tubes	7 x 2	- (2 gas collectors)
No of distributor orifices	120	-
Thickness of insulation a) bed	0.4	m
b) freeboard	0.2	m

Pressure drop measurement over the bed is essential to measure the minimum fluidization velocity. The measurement of temperature and pressure are discussed in sections 4.2.4.1 and 4.2.4.2 respectively.

4.2.4.1 Temperature measurement

Five thermocouples were installed in the reactor (see Figure 4.4). One for the temperature of gases before entering the distributor, two in the bed - the first 0.18 m above the distributor and the second 0.36 m above the distributor-and two in the freeboard region - the first just above the bed at fluidizing conditions or 0.86 m. above the distributor and the second below the exit of the gases or 3 m above the distributor. In order to establish a better temperature profile in the reactor, a sixth thermocouple was added later in the freeboard at 2.5 m above the distributor.

Apart from the thermocouple for the preheating gases which was iron-constantane, all others were nickel-chrome. The iron-constantane thermocouple was of 0.012 m outside diameter and 0.5 m long, while the nickel-chrome ones were of 0.025 m outside diameter and 1 m long.

Due to unreliability of the temperature recorder and unavailability of replacement (see section 4.1.1) , it was necessary to manually record temperatures every 10 minutes from visual observation using digital

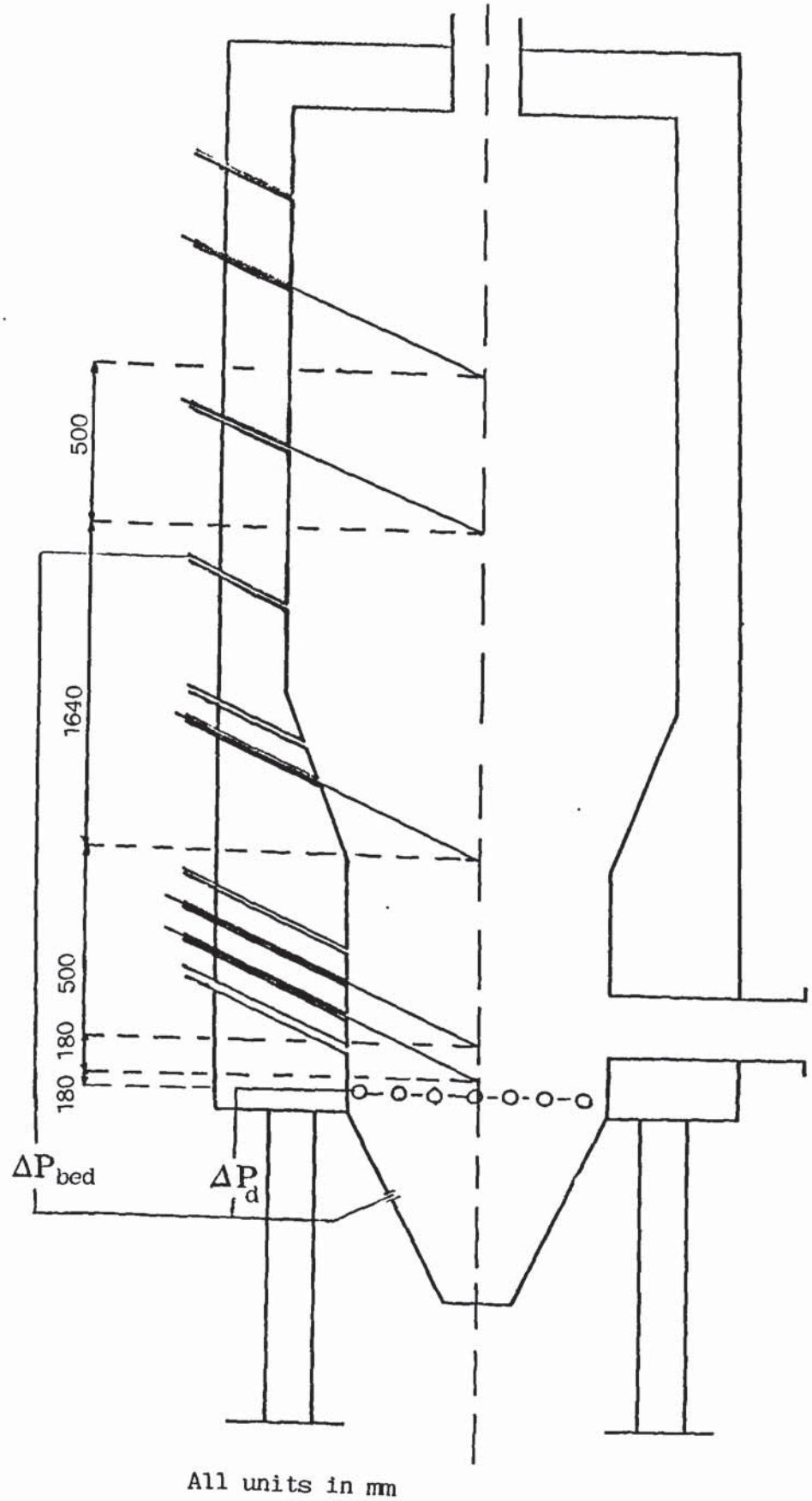

Figure 4.4 : Temperature and pressure drop measurements.

indicators. The indicators were compatible to the type of thermocouples used and as such did not require any calibration. However, the reading of the indicators was periodically checked (about once a month) by means of a portable calibrated temperature indicator borrowed on these occasions from the Free University of Brussels. The temperature difference between the digital indicators installed at the plant and the calibrated one was never higher than 2 °C and hence the available indicators were considered accurate enough.

This procedure, although time consuming, was more accurate. Also from previous experience and actual observations during the commissioning of the pilot plant, it was appreciated that temperature fluctuations do not occur in fluidized bed reactors under normal operating conditions. Therefore it was considered that this method of temperature recording was quite acceptable for the purpose of the experiments, although the temperature indicators of the bed section were practically continuously watched.

4.2.4.2 Pressure drop measurement

Two U-tube water manometers were used to measure the pressure drop across the distributor and over the complete bed. These manometers were also used for the measurement of the minimum fluidization velocity. Their exact positions are also indicated in Figure 4.4.

4.2.4.3 Fluidizing medium

Although there have been studies (see section 2.4.2) on the use of wood char and ash as bed material, an inert bed such as sand has been found to improve wood mixing, heat transfer and permit higher throughputs to be attained (15, 75-108).

Also the use of an inert bed increases the residence time of wood in the reactor. The inert bed also acts as a heat sink for smoother temperature control of the fluidized bed, since the materials used usually have higher heat capacity than that of wood char.

Silica sand was selected as the inert material. The selection was based on the relatively low price and availability of this material and on the fact that no agglomeration and sintering of the bed was expected with the feedstock to

be used. The bed had a height of about 0.60 m above the distributor under static condition, while the specifications of the sand used is discussed in section 5.4.2.

4.2.5 Air supply and preheating system

This system consisted of a screw compressor, a rotameter, temperature and pressure indicators, a diesel oil burner with the appropriate control unit, a control needle valve and a vent pipe with a restriction gate valve at its end. This arrangement is shown in Figure 4.5. It was not possible to directly regulate the air flowrate supplied by the compressor, hence a vent line and a control valve was used to regulate the air flowrate by bleeding part at the air. The restriction vent valve was used to equalize the pressure differential between the bleed flowrate and the flowrate of air supplied to the reactor. This was necessary since when the pressure drop over the fluidized bed and the product gas burner became excessive, the air preferentially flowed through the vent pipe, (see following section).

The rotameter indicated flowrates in the range of 40 - 340 Nm^3 air/h. The calibration conditions of the rotameter were 1.481 bar absolute and 60 °C. The data from the temperature and pressure indicators, being different from the calibration conditions of the rotameter, were thus used to convert the experimental flowrate into Nm^3/h assuming ideality of air. Two gate valves were also used to regulate the primary and secondary air fed to the tubular direct fired burner, which was used only for preheating the reactor during start up. The gas stream leaving the preheater was divided equally for each arm of the distributor (see section 3.7.2). During actual operation of the fluidized bed the oil burner was turned off, however the air fed to the reactor passed through the burner all the time. During preheating the flue gases also passed through the reactor.

4.2.6 The product gas burner

This was placed above a rectangular product gas collector through which the gases flowed on leaving the reactor (see Figure 4.6). The gases were ignited with a torch at the outlet of the burner and were combusted upon leaving the burner's inner configuration . There was no air supply in the burner other than by natural convection from the opening to the atmosphere. A more detailed description of the internals of the burner was not possible at the time of writing (see section 4.2.1).

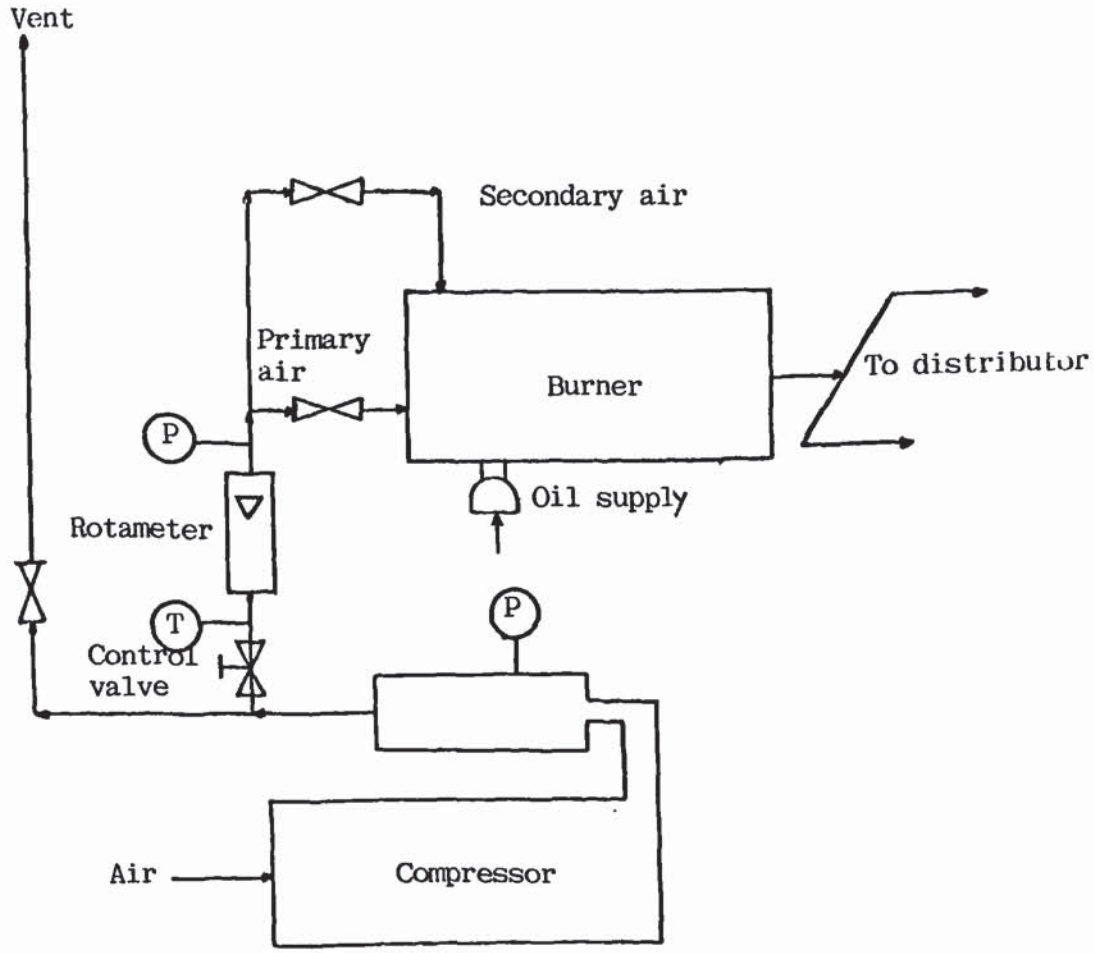

P=Pressure measurement
T=Temperature measurement

Figure 4.5 : The preheating arrangement

The pressure drop across the product gas burner was, however, high resulting in gas leaks through the wood feeding system and in unsteady air flowrate, due to oscillating flow through the vent of the air regulation system (see Figure 4.5). This took place whenever the pressure drop became extreme and the air flowed preferentially to the vent pipe upstream the rotameter. When the pressure drop in the vent pipe became high, the air flowed through the fluidized bed and the product gas burner. Usually there were several oscillations per minute. Initially this was not serious and it was possible to obtain stable air flowrates down to 80 Nm^3/h. However, over a long operating time the open area of the product gas burner became smaller due to deposition of ash and char and eventually it became impossible to obtain stable air flowrates lower than 180 Nm^3/h, even though the burner was regularly cleaned. In the end it was decided to remove the gas burner completely and replace it by a vertical pipe of 1.3 m high and 0.3 m diameter, which was placed on the rectangular collector as shown in Figure 4.6. With this configuration and the vent pipe it was possible to obtain stable air flowrates as low as 120 Nm^3/h. The product gas was flared at the end of this pipe.

4.2.7 The gas sampling system

Due to economic constraints, it was not possible to construct a downstream treatment plant for the total flow of the product gas stream. The system described below and shown in Figure 4.7 was designed to clean and sample a representative portion of the total flow. This was needed in order to measure the mass flowrate of fly ash and condensate, which were later employed in the mass and energy balance. The sampling point was about 0.15m from the inlet of the gases in the collector and in the center line of the pipe connecting the fluidized bed and the gas collector (see Figure 4.6). The location of the sampling point, the high pressure drop over the burners (and later to a lesser extent over the vertical pipe) and the amount of gas sampled (see section 4.2.7.4) ensured that this was a representative fraction of the total flow.

The sample was taken from the gas collector (see Figure 4.6) through a heated pipe, a cyclone, a shell and tube heat exchanger, a filter, a gas meter and finally a suction pump. The cleaned gas was then vented. A shut off valve was initially used to isolate the gas sampling system when not in operation, to avoid accumulation of ash and tar in the line system. Even when

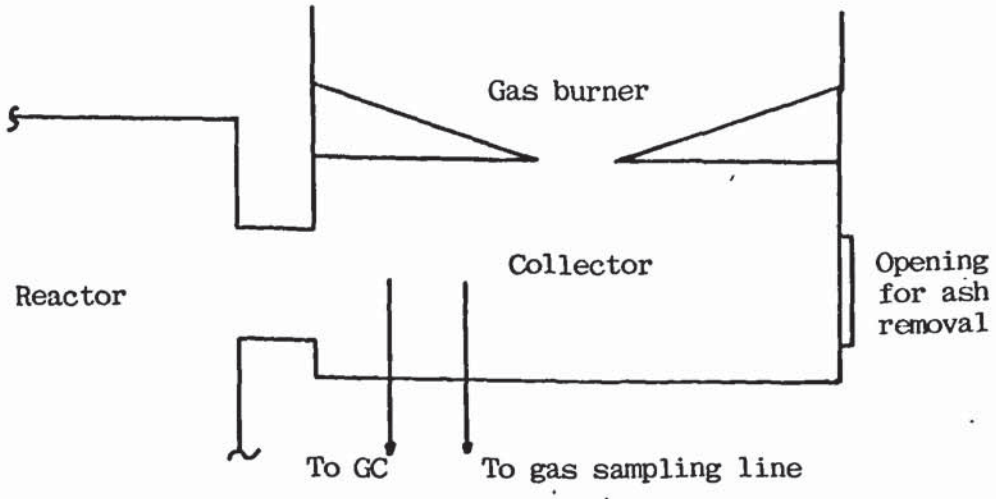

Initial configuration

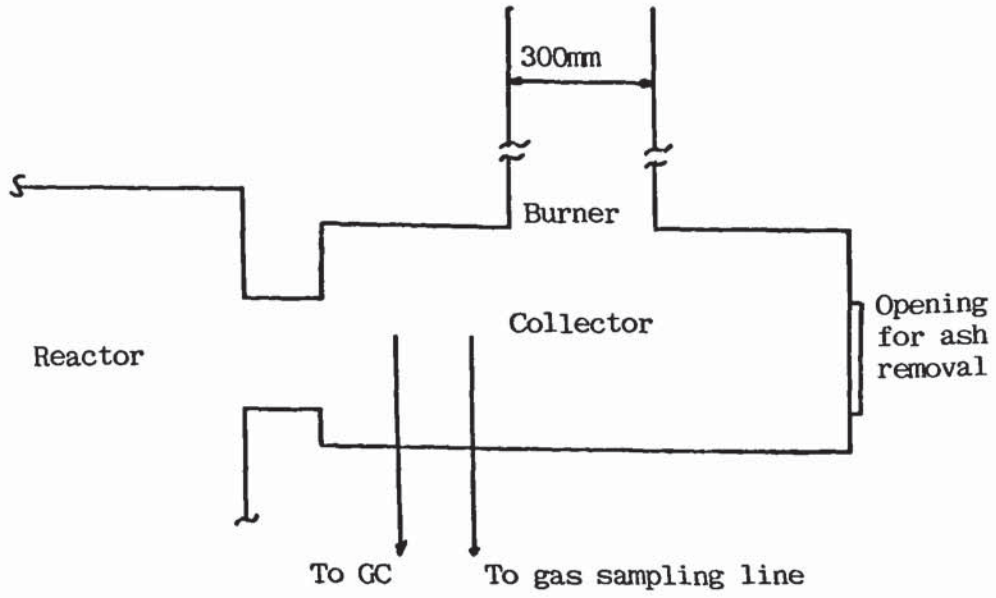

Final configuration

Figure 4.6 : The product gas burner.

the pump was not operating, gas flowed through the gas sampling system due to the high pressure drop over the product gas burner. When the product gas burner was replaced by a vertical pipe, this problem was solved and the shut off valve then remained open continuously.

4.2.7.1 Heated and insulated components

The line from the product gas collector to the cyclone and from the cyclone to the heat exchanger was heated to about 300 °C by means of an electrical ribbon and was also insulated with ceramic wool. This was done to avoid condensation of water and tars in this section. A drain valve was provided before the cyclone, to drain any condensate accumulated during the beginning and the end of a run when the lines had not been heated to operating temperature yet.

The heating ribbon had a maximum temperature of 300 °C and was controlled by a proportional controller. The latter was set at its maximum. The temperature attained by the ribbon was checked periodically with a portable temperature indicator (see section 4.2.4.1) connected to a nickel-chrome thermocouple. This was always in the range of 300 $\pm$ 15 °C, depending on the flow of gas and the operating conditions of the reactor. In general this system functioned properly.

4.2.7.2 The cyclone

This was designed and constructed by a standard procedure (189). By assuming a total flow of gas and an operating temperature the dimensions of the cyclone were calculated. The design specifications and construction of the cyclone are given in Appendix III.

However, 800 °C was considered as the design temperature which was not the case in practice (about 300 °C). This gave lower gas velocities in the cyclone and thus reduced its efficiency giving only small fraction of separation of the fly ash. This was collected in a fly ash receiver below the cyclone, from which samples were removed and kept for carbon content determination.

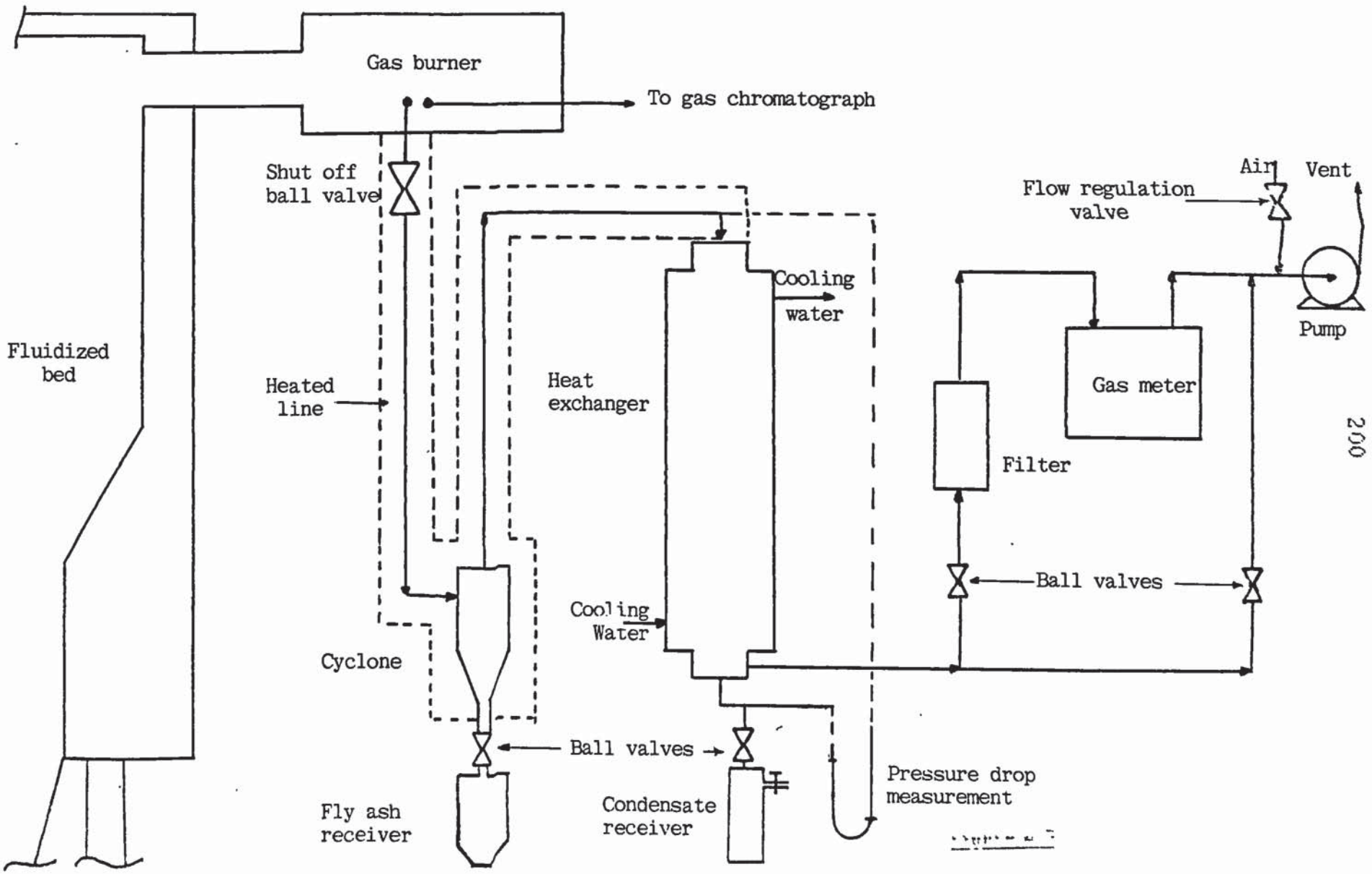
Gas burner
To gas chromatograph
Shut off ball valve
Fluidized bed
Heated line
Heat exchanger
Cooling water
Air
Vent
Flow regulation valve
Pump
Gas meter
Filter
Ball valves
Cooling Water
Cyclone
Ball valves
Fly ash receiver
Condensate receiver
Pressure drop measurement

4.2.7.3 The heat exchanger

The gases leaving the cyclone flowed into the heat exchanger, which was taken from a unused pilot plant installation of the V.U.B. The specifications of the heat exchanger were :

material of construction	: stainless steel	
length	: 2000	mm
outside diameter	: 300	mm
number of tubes	: 15	
diameter of tubes	: 10	mm
length of tubes	: 1800	mm
cooling medium	: water	
capacity	: 1-15 m^3/h	

The heat exchanger was a shell and tube type, with the water flow in the shell installed vertically.

It was necessary to clean the heat exchanger periodically with compressed air in order to remove the fly ash and tar accumulated in the tubes. This was achieved by removing both ends of the heat exchanger and injecting the air by means of a short metal tube (length 0.5 m, diameter 0.8 mm) attached on a rubber hoose directly into the tubes of the heat exchanger. This procedure was very efficient in removing all accumulated material and was performed whenever the pressure drop over the heat exchanger (measured by a U-tube water manometer, see Figure 4.7) exceeded 0.1 m water. The condensate was collected in special receivers constructed from glass which could be isolated by means of a ball valve and which could be removed. Samples were kept for subsequent analysis (such as pH.and carbon content).

4.2.7.4 The filter and the gas meter

The flowrate of the gas flowing through the gas sampling system was measured by a dry gas meter. Due to economic restraints a wet gas meter was not provided, thus special precautions were necessary to ensure proper operation of the dry gas meter. A cylindrical glass wool filter (dimensions : height 0,40 m, diameter 0.30 m) was employed to remove any remaining tars or fly ash from the gas stream (see Figure 4.7). After the filter, the gas passed through the dry gas meter and then through the pump. A by-pass over

the filter and gas meter was provided, so that the gas meter was used only when it was necessary to measure the flowrate of the gas. This was achieved by means of ball valves BV4 and BV5.

In order to regulate the flowrate of the gas sucked through the gas sampling system, a valve connected to the atmosphere was used. By opening this valve the gas flowrate through the gas sampling line was decreased and vice-versa. However, the flowrate was always kept in the range of 9 - 13 Nm^3/h (measured by the gas meter) to ensure that measurable and realistic quantities of fly ash and condensate would be collected (see also section 4.3.3). The maximum flowrate of gas through the sampling system was limited by the capacity of the heat exchanger (see previous section). This flowrate represented about 3-10 % of the total flow, depending on the experimental conditions. Although 3 % of the total flow for some of the experiments was rather limited this was of no major concern since the sample was representative. In addition, the yields of condensate and fly ash obtained were comparable to previous results from a laboratory unit where the complete flow of gas was treated (102). Thus this procedure was considered reliable and the results representative of the total flow.

4.2.8 Analytical methods

The gas composition was determined by gas chromatography. A suction pump was used to supply a continuous untreated gas sample directly from the product gas collector and not from the gas sampling system (see Figure 4.7). This was done so as to obtain a representative sample in terms of gas composition at the moment the gas left the gasifier. Since the line of the gas sampling system was heated and the temperature of the gases at the exit of the reactor were above 500 °C, it was possible for the gas phase reactions to proceed further while in the gas sampling system, even though at a low rate. Thus an independent, not heated, not insulated line was opted for in order to make the sampling of the gas chomatograph, in which the gas was quenched as soon as it left the gas collector. In addition, the sampling for the gas chromatograph could be done independently from the gas sampling system which did not operate during the start up and shut down of the reactor. However, often the gas composition was determined during the above operational stages (see section 4.4).

Thermal conductivity detectors were employed with two columns; one with molecular sieve 13 x and another with chromosorb 106. Two columns were

necessary for the detection of all gas components of interest, since no single column could achieve this. In the former H_2, O_2, N_2, CH_4 and CO were analysed, while in the latter H_2, a composite peak of O_2 + N_2 + CO, CH_4, CO_2, C_2H_4 and C_2H_6 were analysed. Nitrogen was used as internal standard in subsequent calculations for the mass balance.

4.2 8.1 <u>The gas chromatographs</u>

Initially two gas chromatographs, each equipped with one of the above columns were installed with automatic injection valves. A plotter-integrator was used for the recording of the gas chromatogram and the calculation of the gas composition. An interface was used to automatically select the appropriate programmes (one programme per gas chromatograph) on the recorderintegrator and to actuate the injection valves. This system proved to be troublesome, since condensation of tars and water as well as deposition of fly ash (carried with the sample) caused problems in the injection valves, which were installed in series and had to be frequently cleaned by injecting acetone. The use of a glass wool filter upstream of the first valve, did not improve the overall performance of the system, since tars were not retained in it. The columns also lost part of their analytical efficiency when tars were deposited on the packing. This was a major problem with the molecular sieve column which was the first, as the gas chromatographs were connected in series. This arrangement is shown in Figure 4.8a.

Another problem faced with this arrangement was that the analysis over the two columns was never from exactly the same sample, since both injection valves had to be activated simultaneously, but only one chromatogram was recorded. The selections of the gas chromatogram to be recorded was achieved by the interface; when the calculations over the first gas chromatograph were finished, the injection system was activated again in order to have the analysis of the other gas chromatograph.

As there was a differenceof 4 minutes between sampling in the two instruments, it was necessary to check if the results were comparable. This was achieved by comparing the ratios of the concentration of hydrogen and methane from both samples. When the ratios were close to unity this indicated that the samples were comparable. In case the ratios of the concentrations deviated from unity then the samples were not considered directly comparable and the results were disregarded.

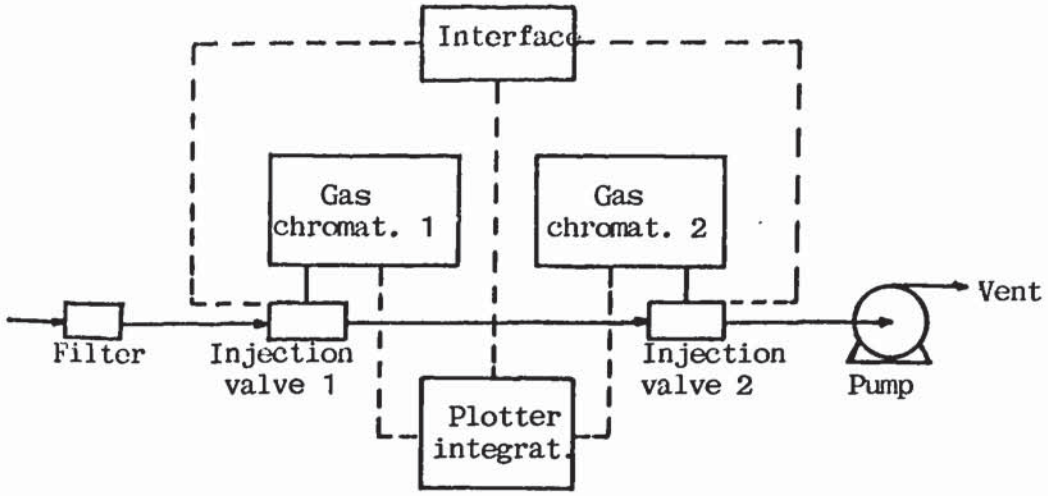

4.8 a) Initial apparatus configuration

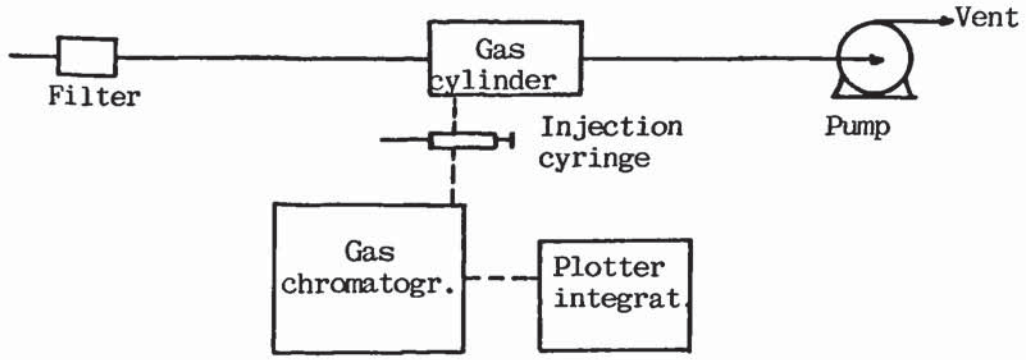

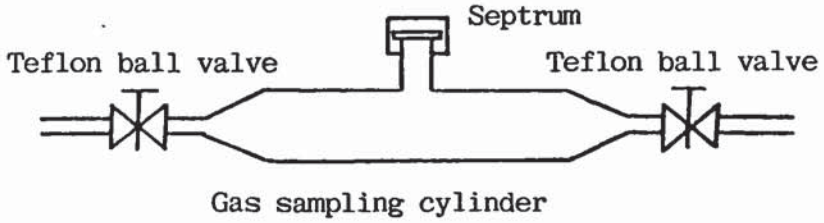

4.8 b) Final apparatus cofiguration

Figure 4.8 : Configuration of gas chromotographic analysis

Due to these problems a new gas chromatograph with two thermal conductivity detectors and two flame ionization detectors was installed. A short filter and a moisture trap were used to separate fly ash and to collect any condensate. Instead of injection valves, a sampling cylinder (see detail in Figure 4.8) was employed and the injections to the gas chromatographs were made with a syringe, while the same recorder-integrator was used (see Figure 4.8.b). This system proved much more efficient and versatile. The injection to the two different columns of the gas chromatograph was made with the same sample, while previously a different sample had to be used. It was also possible to collect several samples within few minutes by changing the gas sampling cylinder and to check the analysis by injecting the same sample to the gas chromatograph at the field lab and to another used as a reference at the laboratory at the Free University of Brussels. Even more important, the two columns remained clean and still functioned properly up to the end of the experimental programme. No cleaning had been necessary. In general it took about 15 minutes to complete a gas analysis cycle.

4.3 COMMISSIONING OF THE PILOT PLANT

Each piece of equipment was tested as soon as it was constructed and/or assembled. Minor problems (fuel ignition due to the distance between the two electrodes) were faced with the preheating burner which were soon resolved. It was soon realized that the feeding system could not function properly without attendance. Because of financial restrictions (see section 4.1.1), a new one could *not be built and only later did it become clear that* continuous manual intervention was necessary in order to ensure proper feeding. The problems encountered with the feeding system and their solution are discussed in detail in section 4.3.2. No problems were, however, encountered with the operation of the fluidized bed reactor.

When the reactor had been constructed and the preheating burner tested, several commissioning runs were carried out to determine the unit's operating characteristics. In most cases the fluidized bed was used as a combustor with manual feeding. During the same trials the air preheating system characteristics were also determined.

4.3.1 Procedure for preheating the reactor

With the preheating burner on, the fluidizing air was heated to about 500 °C (maximum temperature at the collectors of the distributor, see Figure 4.4).

The temperature of the bed reached about 400 °C within one and a half to two hours. Figure 4.9 shows temperature-time relationships during the preheating of the reactor.

Feedstock was then added to the reactor intermittently while the air flowrate was set at its maximum. Intermittently feeding was necessary since at low temperatures continuous feeding could choke off the bed. Due to the heat liberated by the combustion of the feedstock, the temperature of the bed increased rapidly to 650 °C (within about 45 to 60 minutes); when this temperature was reached, the feedstock could be added continuously (by the screw feeder) at the desired flowrate without any danger of choking the bed. The preheating burner was then turned off, since from that point the reactor could be heated solely by the combustion of biomass. When the temperature reached about 800 °C, the desired air flowrate was set on the rotameter and the mode of operation of the fluidized bed changed from combustion to gasification. Then the system was left to attain steady state.

It took about two to two and a half hours in total to bring the reactor to the desired temperature. When an experiment had taken place the day before, the following morning the reactor was usually at about 550 °C so that experiments could start almost immediately.

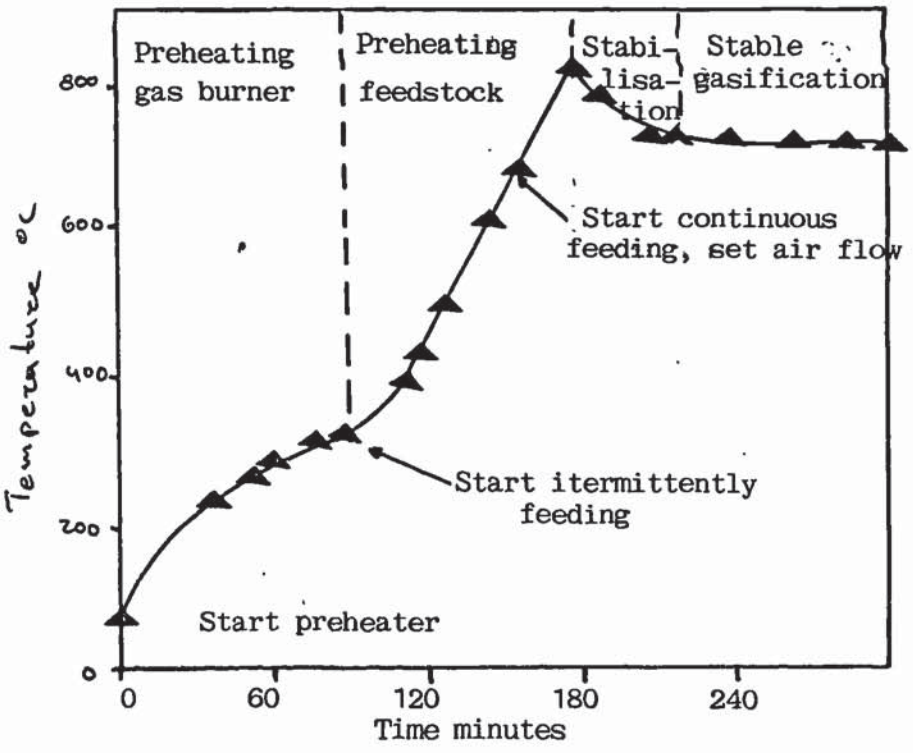

Figure 4.9 : Preheating of the reactor, temperature-time relationship.

4.3.2 The biomass feeding system

4.3.2.1 Introduction

The biomass feeding system proved to be the most troublesome part of the pilot plant. Bridges were formed practically continuously in the hopper, which resulted in loss of steady state operation in the reactor This was indicated by significant variations in the bed temperature and product gas quality (see section 5.12). These problems became apparent during the commissioning experiments and subsequently an assistant was required for all experiments to break any bridges formed. Even this procedure sometimes proved ineffective.

4.3.2.2 Nature of problems

The bridging was caused by inappropriate design of the hopper which is shown in Figure 4.10. The hopper had a triangular cross section and the screw was installed at the bottom which had a circular cross section. Thus only half of the screw was really exposed to the feedstock. The other half could only transport whatever biomass could fall between the screw and the walls of the bottom (radial space ± 30 m). Another drawback was that the bed above the screw was very short since the hopper was horizontal.

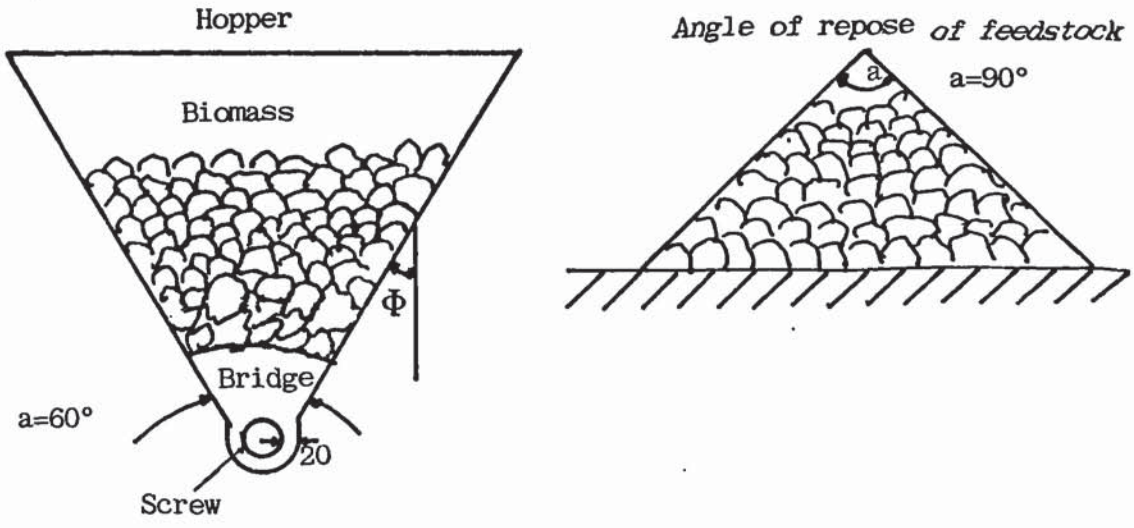

Figure 4.10: Details of hopper and bridging

These problems were caused by inappropriate hopper design. In general, for flow through a bin opening, materials that can be compacted (as opposed to being free flowing) will be compacted because of storage vessel shape and packing characteristics of the material. When this happens, the material forms an arch that is capable of withstanding considerable stress Since the arch transfers the load to the hopper walls and in doing so applies so much pressure to them, the kinematic coefficient of friction, F, (the angle of kinematic friction, see Figure 4.10 is a measure of the friction coefficient between the solid and the material of construction used for the conical shaped hopper) becomes high. The net result is that the bridge formed prevents any flow from the vessel. Force must then be applied to the arch so that it will collapse and flow will begin. When the strength of the arch, f, is exceeded by the internal stress, S, generated by a force applied above the arch, flow takes place. Summarizing (189) :

when $f < S$ flow occurs

$f > S$ no flow occurs

$f = S$ critical point is reached.

None of the above parameters were determined by Vyncke Warmtetechniek and in addition the hopper was designed with the wrong angle.

In case the kinematic angle of friction, F, cannot be determined, then the common criterion is to measure the angle of repose of the material (defined as the angle at which the material will rest on a pile, see Figure 4.10) and use this value as the hopper angle. The angle of repose of the feedstock was about 90 °C while the hopper angle was 60 °C. This also aggravated the formation of bridges.

It is believed that these problems could have been overcome by using an arrangement as shown in Figure 4.11. In this configuration 3 screws are used in parallel in a flat bottom cylindrical hopper. The utilization of 3 screws and the expansion of the space above the screws would eliminate bridge formation. In addition the extra weight provided on the vertical bed would break any bridge formed. A semi-conical ending at the discharge end of the hopper, as shown in Figure 4.11, would also improve the discharge of the feedstock. However, due to financial limitations (see section 4.1.1) it was not possible to construct a new hopper as discussed above.

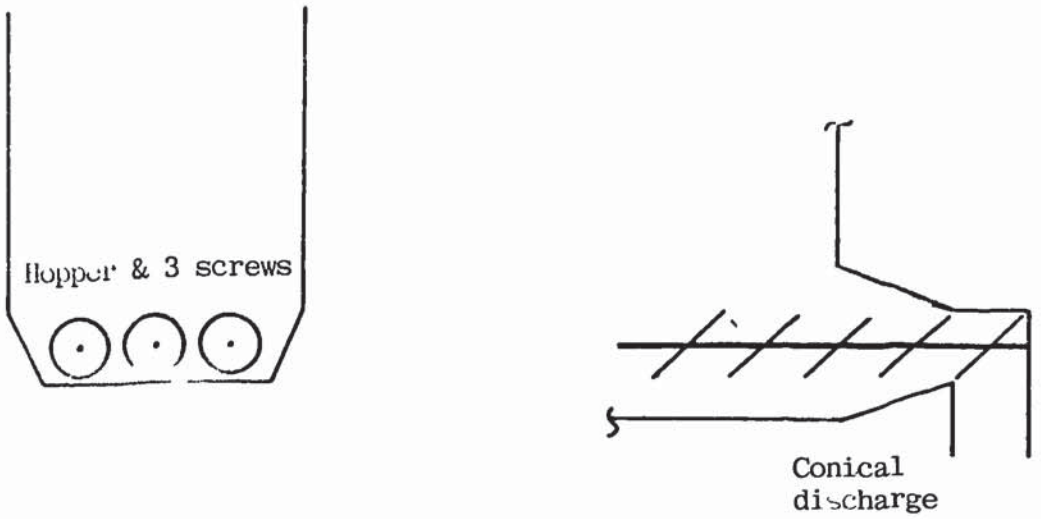

Figure 4.11 : Alternative hopper configuration.

4.3.2.3 Procedure followed

As the commissioning experiments continued, poor closure of the mass and energy balances suggested that the actual feedstock flowrate was lower than that calibrated. To solve this problem, the feedstock had to be preweighted and then fed in the reactor via the feeding system. At the end of the experiment the total weight fed was divided by the operating time giving the feedstock flowrate. This necessarily assumed a constant flowrate with time. Even with this method it was only possible to obtain a feedstock flowrate with about $\pm$ 5 % accuracy.

This should not be seen as a bad result, since in the literature even higher inaccuracies in feedstock flowrates ($\pm$10%) due to impropriate hopper design have been reported (65, 66, 80). This problem seems to be general to all new fluidized bed pilot plant reactors unless a proven feeding system is used. It has even obliged some researchers to calculate the mass and energy balances from the product gas composition (80, 91, 92) and not from the feedstock and air mass flowrates.

4.3.2.4 Calibration of the biomass feeding system

During calibration, the cover of the opening provided at the bottom of the second screw (see section 4.2.3) was removed and the feedstock was collected in preweighted barrels for weighting, as depicted in Figure 4.12.

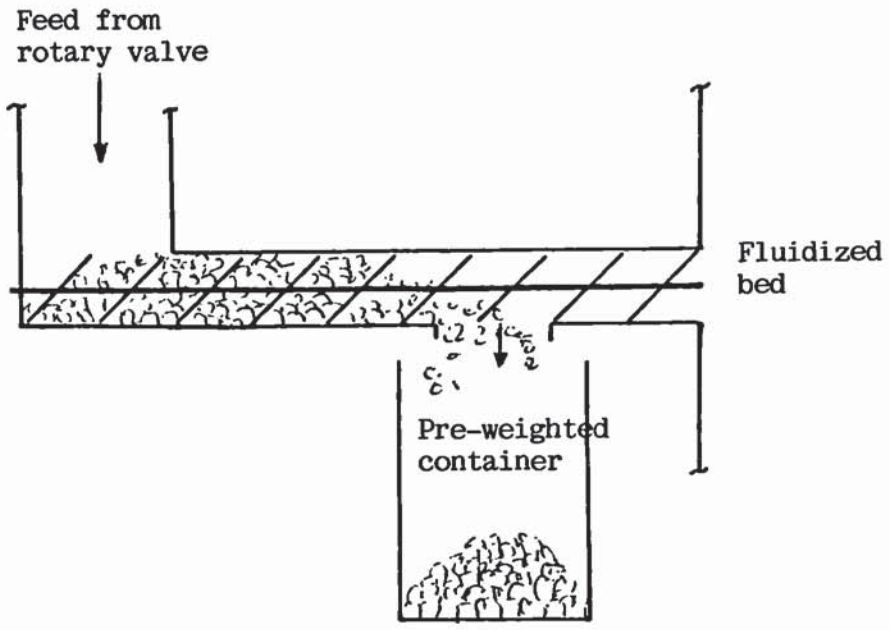

Figure 4.12 : Feedstock calibration

Many trials were made to calibrate the feeding system by establishing a relationship (rpm) of the screw in the hopper and feedstock flowrate. It was found that after several days of operation at the same setting, the speed of the screw had decreased by about 10 % thus reducing the feedstock flowrate. This was probably caused by vibrations which caused the relative position of the motor to the screw to change, resulting in different rpm.

It was possible to alter the speed of the screw in the hopper, by controlling the position of the motor relative to the position of the screw (fixed). The motor was connected with the screw by means of a belt, which was attached to a standard gear on the motor and to a gear of variable diameter on the screw (see Figure 4.13). By moving the motor (by means of a mechanical screw) away from the screw, the two movable conical plates of the variable

diameter gear were displaced further apart, thus decreasing the diameter of the gear (see detail of Figure 4.13). Since the motor was operating at a constant speed, this resulted in an increase of the speed of the screw.

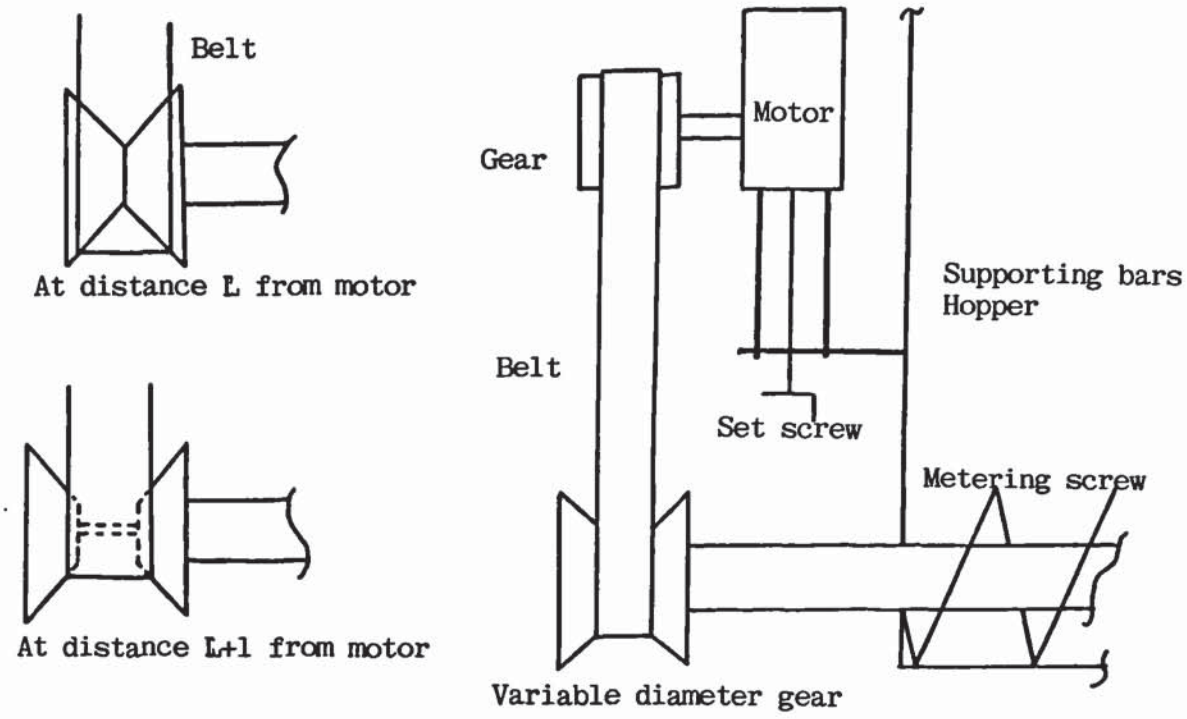

Figure 4.13 : Control of feeding screw

The rotary valve and the second feeding screw were coupled on a second motor and run continuously at a constant speed. The rpm of the second screw which fed into the reactor was set at 350 rpm (which was always higher than the speed of the first screw in the hopper) to avoid any blockage of material in the pipe feeding the reactor. Both screws had the same design and dimensions.

To ensure that the correct feedstock flowrate was measured, it was decided to measure the flowrate before and after each experiment. If the same flowrate was used for more than one experiment, then the feedstock flowrate was checked every second day. However, in order to improve the reliability

of the measurements, it was also desided to preweight the feedstock fed in the hopper by the conveyor belt (see Figure 4.3). This procedure - although time consuming - proved to be adequate and sufficiently accurate - with a ± 5 % maximum error. This was indicated by the mass balances, the closures of which improved significantly.

4.3.3 The commissioning of the gas sampling system

This was performed during the commissioning experiments by activating the suction pump shown earlier in Figure 4.4. Initially, neither a by-pass round the gasmeter (precalibrated; accuracy 0.1 %) nor a filter was provided, but, after only a few minutes of operation some condensate and fly ash had accumulated in the dry gas meter. After cleaning, it was decided to add a glass wool filter together with a by-pass (see section 4.2.7.4), so that the gas would flow through the gas meter only when it was desired to measure the gas flowrate. This configuration ensured more reliable operation and a longer life for the gas meter. During each experiment the flowrate of the gas was measured about 3 to 4 times to obtain a reliable result. Each measurement of the gas flowrate took about 1 to 2 minutes to be performed.

The length of measuring time was compromised due to the fact that the gas was not dry. For larger measuring times a wet gas meter should have been used, but this could not be provided due to its higher cost (see section 4.1.1. and 4.2.7.4). Extended operation with a wet gas would certainly damage the gas meter. This happened once after about five commisioning experiments and the dry gas meter had to be replaced. However, during these experiments it was realised that as long as a constant flowrate had been attained in the gas sampling line (see following section), a length of measuring time of 1 minute was sufficient for an accurate measurement. No measurable difference could be recorded between lengths of measuring times of 1 to 6 minutes (6 minutes was the longest measuring time tried during the commissioning experiments).

During these tests it was also realized that the cyclone had not been designed appropriately, since it could remove only about 50 % of the ash load of the gases because of higher design temperature than the operating temperature (see section 4.2.5.2). Due to financial restrictions a new one could not be built.

Another problem which arose during the commissioning of the gas sampling line was blockage of the heat exchanger by ash and tar. It was relative easy to clean the heat exchanger by blowing compressed air through the tubes. However, in order to avoid significant errors with the measurement of the a various parameters, a U-tube water manometer was installed to measure the pressure drop over the heat exchanger. When the pressure drop increased above about 100 mm water, indicating that the tubes were getting blocked, the heat exchanger was cleaned at the end of that particular experiment. Also after about ten experiments, the gas meter was removed and the complete gas sampling system was cleaned by compressed air to remove any ash or tar deposits. After cleaning the lines, the glass wool of the filter was also replaced.

4.4 EXPERIMENTAL PROCEDURE

The experimental procedure is summarized in Table 4.2.

Table 4.2 : Experimental Procedure.

Step		See Section
1.	Determination of feedstock flowrate	4.3.2.4
2.	Air flowrate at maximum	4.2.5
3.	Heating up of reactor	4.3.1
4.	Temperature measurements	4.2.4.1
5.	At 650 °C air flowrate at actual experimental conditions	4.4
6.	Gas analysis	4.2.6
7.	Constant bed temperature, gas analysis - gives steady state	Figure 4.9
8.	Activation of gas sampling line pump	4.2.7
9.	After 20 minutes steady state attained	4.4
10.	Condensate flowrate measurement	4.2.7.3
11.	Fly ash flowrate measurement	4.2.7.2
12.	Gas analysis during gas sampling	4.2.6
14.	Temperature recording during gas sampling	4.2.4.1
15.	Gas sampling line pump turned off	4.4
16.	Air is left to burn off char	4.4
17.	When bed temperature <700 °C, air is turned off	4.4

The biomass feeding system was calibrated to the desired feedstock flowrate. When this was established, the air flowrate was set at its maximum and the reactor was heated as described in section 4.3.1. When the

temperature in the bed reached about 650 °C, the desired air flowrate was set and the reactor was left to reach steady state as determined by the bed temperature (shown in Figure 4.6). Gas samples were analysed by means of gas chromatography during the last stage of heating the reactor and when no major variations (below 2 Vol. % in the gas composition were found, it was then considered, in combination with the bed temperature, that a steady state had been attained.

When steady state was obtained, the gas sampling system pump was activated and a flow of about 15 Nm^3/h of product gas was established. The sampling system was left for about 20 minutes to stabilize. This was indicated by constant condensate flowrate and bed temperature. Then the fly ash and condensate flowrates were measured. This was achieved by isolating the cyclone or the heat exchanger by means of ball valves (see Figure 4.4), sampling the ash and condensate receiver and then opening again the ball valves, so that samples of ash and condensate could accumulate in their respective receiver. When the valves were closed a timer was started so that sampling time could be registered. From the weight of the sample and the sampling time the mass flowrates of condensate and fly ash were determined. Fly ash flowrates were measured over half hour, so that measurable quantities of fly ash were collected, while condensate flowrates were measured over 5 to 10 minutes.

During sampling, the gas flowrate through the gas sampling system was measured by means of the gas meter, at least twice if good agreement between the results was obtained, or up to four times if poor agreement resulted. In the latter case, the average of the four values was used for the subsequent calculations. In parallel with these measurements several gas analyses were made with the independent sampling line (see Figure 4.4) and all the temperatures were recorded.

When all parameters had been measured and recorded, the gas sampling system pump was shut off while further gas analyses could be performed if desirable. When it was concluded that all measurements had been carried out successfully, the biomass feed was turned off and the air was left on to burn the char; the bed temperature increased more than 100 °C above the steady state gasification temperature. When the char was burned off, the temperature of the bed dropped and when it reached below 700 °C, the air supply was stopped by turning off the compressor.

In general it took about 5 to 6 hours to perform one experiment. Approximately 45 minutes were spent on measuring the feedstock flowrate, 150 minutes on preheating the fluidized bed, 30 to 45 minutes to allow the reactor to reach a steady state, 15 to 30 minutes for the gas sampling line to attain steady state, 40 to 60 minutes for sampling the various parameters and 30 to 40 minutes for the burn off of the char bed in the reactor.

4.5 EXPERIMENTAL PROGRAMME

4.5.1 Introduction

The most important experimental parameters for fluidized bed gasifiers are listed in Table 4.3.

Table 4.3 : Experimental parameters in fluidized bed gasification

Parameter		Comments
1. Oxidizing (fluidizing) gas	:	Nature (air, steam, O_2 ..) and flowrate.
2. Feedstock	:	Characteristics and flowrate.
3. Temperature	:	In bed and freeboard.
4. Pressure	:	In reactor.
5. Hydrodynamic characteristics	:	In bed and freeboard.

Most of these were set in the specification and design of the plant. Only the air and feedstock flowrates, and the feedstock characteristics could be altered. The temperature in the bed and freeboard depends upon the air and feedstock flowrates since they define the degree of gasification or combustion.

It was decided to use only one feedstock with constant properties, so that the results would be comparable and could form the basis for the development of a design procedure, which was the main objective of this work.

Previous experience had shown that other feedstocks with similar physico-chemical properties, such as ultimate analysis, ash content, particle size and moisture content, would not affect the design to any significant extend (102).

However, the design procedure developed later in this work is not applicable for feedstock inherently different (eg. municipal solid waste) from the feedstock used in this work.

4.5.2 Programme specifications

The fluidization characteristics were determined during the commissioning experiments, while the second and third objectives were determined by the execution of 36 individual experiments which are listed in Table 4.4. The

Table 4.4 : Summary of experimental programme

Part	Feedstock flowrate kg/h	Air flowrate Nm^3/h	Run	Specifications
One	92	151.5	4	Commissioning experiments.
		194.8	3	In total 12 runs were made; runs 1, 2, 5, 6 and 9
		194.8	8	had to be stopped since various problems were
		196.2	10	encountered.
		196.2	11	
		242.3	7	
		239.7	12	
Two	78	101.7	14	The main body of experiments, in total 23 runs were
	78	143.7	13	made but run 17 had to be stopped due to inadequate
	78	188.5	15	gas analysis.
	78	233.3	16	This was caused by tars and ash deposition at the inlet
	160	145.3	21	of the molecular sieve column.
	160	187.4	19	The feedstock flowrates were choosen to cover the
	160	226.7	18	design flowrate range (and even exceed it).
	160	275.8	20	Then air flowrates were selected to cover selected and
	190	250.5	28	specific air factor (for definition see Chapter 5)
	210	166.0	22	ranges.
	210	187.4	23	
	210	277.9	24	
	210	231.2	25	
	220	218.3	26	
	220	245.5	27	
	226	202.7	35	
	232	250.4	34	
	285	248.0	29	
	279	300.4	30	
	277	305.6	33	
	277	347.6	32	
	283	357.3	31	
Three	340	338.8	37	To repeat a specific run.
	340	333.8	38	To repeat a specific run.
	230	249.2	36	A long duration run.
	350	188-348	39	Constant feedstock flowrate variable air flowrate.
	350-400	318.8	40	Constant air flowrate variable feedstock flowrate.
	320	289.6	41	Measurement of flame burn out and gas composition.
	320	289.6	42	Measurement of char bed.

experiments were planned in such a way that the verification of the design of the reactor would be possible (eg. establishment of turn down ratio, operating temperature, the gas flow ratio of U/U_{mf} and products flowrates).

The air flowrate varied in the range of about 100 to 300 Nm^3/h, while the feedstock flowrate varied in the range of about 78 to 400 kg/h. With one feedstock flowrate several air flowrates were tried at different runs. The 36 experiments can be separated into three main parts. The first part consists of 7 successful commissioning experiments (five more were made, but were not completed due to various problems such as gas leaks, and unsteady feedstock flowrate). In part two, 22 experiments were made. The results of these experiments form the basis of the derivation of the design equations, as well as of the conclusions concerning the overall performance of the fluidized bed gasifier. In part three, 7 experiments were performed, each to identify or clarify uncertainties or problems which appeared during part two.

CHAPTER FIVE : RESULTS AND DISCUSSION

5.1 INTRODUCTION

In this chapter the experimental results are presented, discussed and compared with the published data. The general approach to the presentation and discussion of the results is depicted in Figure 5.1. The results are given in computer print outs in Appendix V.

Section	Subject	
5.1	Introduction	General discussion and approach
5.2	Definitions	
5.3	Feedstock properties	
5.4	The fluidization characteristics of the reactor	
5.5	Commissioning experiments	
5.6	Summary of primary results	
5.7	Gas composition	
5.8	Mass balances	
5.9	Energy balances	
5.10	Temperature profiles	
5.11	Influence of Air factor	
5.12	Extended runs	Specific investigation, secondary results
5.13	Reproducibility of a specific system	
5.14	Operating limits of the system	
5.15	Flame burn out	
5.16	Char bed	
5.17	Ratio of U/unit	
5.18	Mean particle size of sand	
5.19	Turn down ratio	
5.20	Condensate yield	
5.21	Retention time of gases in reactor	
5.22	Conclusions	

Figure 5.1 : General approach to the presentation and discussion of the results.

5.2 DEFINITIONS

The following definitions of terms apply for this Chapter and for this thesis in general.

5.2.1 Air factor (or equivalence ratio) "S"

This is the ratio of the amount of oxidant fed to the reactor over that required for stoichiometric combustion (104). For this work in particular the oxidant was air. The amount of air required for stoichiometric combustion was determined on base of the elemental analysis of the feedstock. Thus:

$$S = \frac{G_{air}}{(X_i \times q_i^{air}) \,.\, G_{feed(MAF)}} \qquad \text{equation 5.1}$$

where G_{air} = mass flow rate of air per unit time, in kg/h
X_i = fraction of component i (O, H, C) in the feedstock
and q_i^{air} = amount of air required for stoichiometric combustion of component i, in kg/kg feed
$G_{feed(MAF)}$ = mass flowrate of feedstock, in kg/h

$$\text{and } S = \frac{G_{air}}{(X_C \times q_C^{air} + X_H \times q_H^{air} - X_O \times q_O^{air})\, G_{feed\,(MAF)}} \qquad \text{equation 5.2}$$

In case the oxidant is oxygen, equation 5.2 becomes:

$$S = \frac{G_{air}}{X_C \times q_C^{O2} + X_H \times q_H^{O2} - X_O \times q_C^{O2}} \qquad \text{equation 5.3}$$

where q_i^{O2} is the amount of oxygen required for stoichiometric combustion of i, in kg.
The parameters q_i^{air} and q_i^{O2} were determined from stoichiometry.

Thus for q_C^{O2} :

$$C + O_2 \longrightarrow CO_2 \qquad \text{equation 5.4}$$

or 1 gr. atom carbon requires 1 gr-mole oxygen for combustion to carbon dioxide, and

$$q_C^{O2} = \frac{32.0}{12.01} = 2.665 \text{ kg } O_2/\text{kg C} \qquad \text{equation 5.5}$$

Thus q_C^{air} can be determined as follows:

$$q_C^{air} = q_C^{O2} \times \frac{\text{fraction of N in air}}{\text{fraction of O in air}} + q_C^{O2} \qquad \text{equation 5.6}$$

$$= 2.665 \times \frac{0.767}{0.233} + 2.665 = 11.480$$

The oxygen fraction of the feedstock is substracted in equation 5.2 and 5.3, since it can also react with carbon and hydrogen. This is supported by pyrolysis studies which have shown that carbon dioxide, carbon monoxide and water are amongst the primary products of pyrolysis (153-162).

The values of q_i^{O2} and q_i^{air} are given in Table 5.1. In this table only carbon, hydrogen and oxygen were considered, since these were the only elements measured in the elemental analysis of the feedstock (see section 5.3.5).

Table 5.1 : Stoichiometric requirements for the combustion of C, H and O by oxygen and air.

Element	q^{O2}	q^{air}
C	2.665	11.480
H	7.936	34.194
O	0.0	4.308

5.2.2 Higher heating value "HHV"

This is the higher heating value of all cool and clear gas product components added together (the higher heating value is numerically equal to the standard

treat of combustion of a component but of opposite sign), with all the water initially present as liquid in the fuel and that present in the combustion products, condensed to the liquid state, at constant pressure and at temperature of 25 ^{0}C (220) :

$$HHV = \sum_{1}^{n} wt\%\ i \times H_{Ci} \qquad \text{equation 5.7}$$

where H_{Ci} is the standard heat of combustion of component i in MJ/kg.

The standard heat of combustion of the components found in the cool and clean gas are given in the Table 5.2 (229) (for the components of the product gas, see section 5.7).

Table 5.2 : Standard heat of combustion of product gas component (229).

Component	Standard heat of combustion (MJ/kg)
H_2	141.80
CH_4	55.50
CO	10.11
C_2H_4	50.30
C_2H_6	51.87

Thus the higher heating value of a gas consisting of the above five (amongst others) components is given by equation 5.8 :

$$HHV = (wt\%\ H_2) \times 141.80 + (wt\%\ CH_4) \times 55.5 + (wt\%\ CO) \times 10.11 + (wt\%\ C_2H_4) \times 50.3 + (wt\%\ C_2H_6) \times 51.87 \text{ in MJ/kg} \qquad \text{equation 5.8}$$

5.2.3 Gas yield, "Y"

This is ratio of weight (kg) of gas produced over that of feedstock (kg) (moisture and ash free basis) fed to the reactor per unit time. Thus :

$$Y = \frac{\text{weight of gas produced per unit time}}{\text{weight of feedstock (MAF) fed per unit time}} \qquad \text{equation 5.9}$$

5.2.4 Heat of reaction, "H_R"

This is defined as the change in enthalpy resulting from the reaction taking place under a pressure of 1 atm., starting and ending with all materials at a constant temperature of 25 ^{0}C (229).

For a reaction between organic compounds the basic thermochemical data are generally available in the form of standard heats of combustion. The standard heat of reaction where organic compounds are involved, can be calculated by using directly the standard heats of combustion instead of standard heats of formation (229). An energy balance is employed (see equation 5.10) where the standard reference state is not the elements, but the products of combustion at 25 °C and 1 atm. in the state of aggregation specified by the heat of combustion data. For example, the enthalpy of methane relative to its products of combustion, gaseous carbon monoxide and liquid water, is equal to the negative value of its standard heat of combustion or 55.5 MJ/kg. Therefore in any equation involving combustible materials the formula of a compound may be replaced by its enthalpy relative to its products of combustion. The enthalpy of the products minus the enthalpy of the reactants, or the standard heat of combustion of the reactants minus the standard heat of combustion of the products, is equal to the standard heat of reaction, ΔH_2, (229). Thus,

$$(\Delta H_r = \Sigma\ \Delta H_C \text{ (reactantants)} - \Sigma\ \Delta H_C \text{ (products)}\ )\ 25\ ^\circ C \qquad \text{equation 5.10}$$

where ΔH_C is the standard heat of combustion of the reactants and products in MJ/kg.

The heat of reaction H_R is then calculated by dividing the standard heat of reaction ΔH_r by the amount of feedstock (MAF) fed in the reactor per unit time. Thus:

$$H_R = \frac{\Delta H_r}{G_{\text{feedstock (MAF)}}} \qquad \text{equation 5.11}$$

The overall gasification reaction can be written as:

$$\text{Feedstock} + O_2 \longrightarrow aH_2 + bCH_4 + cCO + d\,CO_2 + e\,C_2H_4 + fC_2H_6 + g\,H_2O + h\,C_w + i\,C_mH_nO_z \qquad \text{equation 5.12}$$

where C_w represents carbon in the fly ash and
$C_mH_nO_z$ represents tar

In terms of mass, equation 5.12 becomes:

$$X_1 \text{ kg feedstock (MAF)} + X_2 kgO_2 \longrightarrow X_3 kgH_2 + X_4 kg\,CH_4 + X_5 kgCO + X_6 kgCO_2 +$$

$$X_7 kgC_2H_6 + X_8 kgC_2H_6 + X_9 kgH_2O + X_{10} kgC_w + X_{11} kgC_mH_nO_z \qquad \text{equation 5.13}$$

where X_{1-11} represent the amount for each component, in kg.

Substituting in equation 5.10 gives :

$$\Delta H_r = (X_1\,\Delta H_{C\ \text{feedstock(MAF)}} + X_2 \Delta H_C O_2) - (X_3\,\Delta H_C\,H_2 + X_4\,\Delta H_C CH_4 + X_5 \Delta H_C\,CO + X_6 \Delta H_C\,CO_2 + X_7\,\Delta H_C\,C_2\,H_4 + X_8\,\Delta H_C\,C_2\,H_6 + X_9\,\Delta H_C\,H_2O + X_{10}\,\Delta H_C\,C_w + X_{11}\,\Delta H_C\,C_mH_nO_z) \qquad \text{equation 5.14}$$

$$\text{But } \Delta H_C O_2 = \Delta H_C\,CO_2 = \Delta H_C\,H_2O = 0 \qquad \text{equation 5.15}$$

Substituting equation 5.15 into 5.14 gives :

$$\Delta H_C = X_1\,\Delta H_{C\ \text{feedstock (MAF)}} - X_3\,\Delta H_C\,H_2 - X_4\,\Delta H_C\,CH_4 - X_5\,\Delta H_C\,CO - X_7\,\Delta H_C\,C_2H_4 - X_8\,\Delta H_C\,C_2\,H_6 - X_{10}\,\Delta H_C\,C_w + X_{11}\,\Delta H_C\,C_mH_nO_z \qquad \text{equation 5.16}$$

$$\text{and } H_R = \frac{\Delta H_r \text{ MJ}}{X_1 \text{ kg feedstock (MAF)}} \qquad \text{equation 5.17}$$

5.2.5 Thermal efficiency, "Y"

This is defined as the ratio of the chemical energy in the cool, clean gas produced to that of the chemical energy in the feedstock per unit time, expressed in percentage (229).

$$Y = \frac{G_{gas} \times HHV_{gas}}{G_{feedstock} \times HHV_{feedstock}} \times 100 \qquad \text{equation 5.18}$$

where G is mass flowrate on as received basis.

5.2.6 Heat losses (unaccounted), "HL"

These are defined as the ratio of energy balance over the reactor (total energy input in the reactor - total energy output from the reactor) devided by the total energy input in the reactor, expressed in percentage.
Thus :

$$HL = \frac{\text{total energy input - total energy output reactor}}{\text{total energy output reactor}} \times 100 \quad \text{equation 5.19}$$

The total energy input and total energy output from the reactor are given respectively by equations 5.20 and 5.21.

Total energy input = sensible heat in air + energy in feedstock
equation 5.20

Total energy output = sensible heat in product gas + sensible and latent heat in steam + sensible heat in fly ash + chemical energy in product gas + chemical energy in fly ash and tar + heat losses from reactor walls. equation 5.21

Equations 5.20 and 5.21 are presented in detail in Appendix IV, where an example of mass and energy balance is computed.

5.3 FEEDSTOCK PROPERTIES

In order to eliminate problems of variations in the properties of the feedstock, it was desided to use a standard material which could be supplied in sufficient quantities and with constant properties. Thus the feedstock was supplied by a particle board manufacturer in closed containers. It consisted of chopped wood from a variety of species. Efforts were made to characterize the feedstock in terms of composition (softwood, hardwood, bark) and size (longest dimension). The former is important since it has been shown that different species of wood have different thermal properties (9) (see also section 1.1.1), while the latter provides informations concerning the fractions of fines and large particles. Since the feeding inlet was above

the surface of the bed (see Figure 3.6), the fines would be blown in the freeboard while very large pieces of wood would accumulate in the bottom of the bed. Other feedstock properties such as moisture content, ash content, elemental analysis and heating value were also determined.

5.3.1 Composition

Three samples of 1 kg were taken (one from three different deliveries) and they were judgementally separated manually into softwood, hardwood and bark. The results are summarized in Table 5.3.

Table 5.3 : Composition of feedstock (in wt%).

Sample	Softwood	Hardwood	Bark
1	52.1	35.3	12.6
2	53.0	33.8	13.2
3	56.6	35.3	8.1
Average	53.9	34.8	11.3

A small error, less than 5 wt%., may exist in the results, especially in separating between hardwood and softwood. The bark fraction was determined accurately, since it was easily distinguished from the wood fraction.

5.3.2 Size

The same samples, used in the determination of the feedstock composition, were analysed by measuring the longest dimension of every piece after being sieved to separate the fines. The average results of the three samples are given in Table 5.4. Since the size distribution of the feedstock is only important for mixing considerations, the size distribution of the feedstock components (softwood, hardwood, bark) was not determined separately.

Table 5.4 : Size characterization of feedstock

Longest dimension	mm	0-1	1-30	30-50	50-70	70-150
Weight	%	1.2	11.5	60.1	15.3	11.9
Variation in samples	%	1.5	3.3	2.5	1.9	8.4

The fraction in the dimension range 0-1 mm were the fines and this fraction of feedstock would be blown in the freeboard before reaching the bed. However, since it has been shown that fluidized beds attain very high heating rates (about 1000 °C/s) (153, 157, 160) and the residence time of the gases in the freeboard was in the range of 7-40 s (this was determined by substracting the residence time of the gas flowing interstitially in the bed (see Table 5.9) from the total experimental gas residence time, see section 5.21.2), it was considered that the fines would be completely gasifical in the freeboard.

The next size range, 1-30 mm, was determined on the basis of previous experimental work (102, 105), where it was shown that particles in this range were segregated in the upper sections of the bed and "floated" on the surface of the bed. When the fraction of feedstock in this size range is high (above 50 wt%) then agglomeration and sintering can take place (see section 2.4.3.6). However, with this particular feedstock which had a fraction of only 11.5 % in this size range, no agglomeration or sintering was expected. The execution of the experimental programme confirmed this as no sintering took place.

Usually, biomass particles with longest dimension in the range of 30-70 mm,, mix well in a fluidized bed (102) and this range was separated into two, 30-50 and 50-70 mm, for better accuracy. Finally, no particle larger than 15 cm was found in the feedstock and thus the last range was 70-150 mm. Since the other two dimensions of the particles were never larger than 20 mm (the feedstock had the shape of splinters), it was believed that the particles in this range would also mix satisfactorily in the lower region of the bed about 20 cm above the distributor and would not accumulate on the distributor. However, as their gasification would proceed, their size would be reduced and gradually they would also mix in the upper regions of the bed (273).

From Table 5.4 it can be concluded that 60 wt% of the feedstock was in the size range of 30-50 mm, while the other size ranges had practically the same weight percentage except the fines, which were only 1.2 wt%. Thus it was expected that the feedstock would mix well in the fluidized bed, while excessive carry over of fines would be minimal.

5.3.3 Ash content

The ash content was determined by heating samples in a muffle oven at 800 °C for 24 hours. This proved to be a good method with excellent reproducibility. Several samples (at least four per container) were analysed (four analyses per sample) and it was found that the ash content was consistently in the range 1.5-1.7 wt% with an average of 1.6 wt%. Thus there was no variation in the ash content with the various deliveries. This indicates that the composition of the feedstock, at least in this respect remained practically constant.

Care was taken to ensure that the samples were representative. Thus about half a liter of feedstock was collected in plastic sacks from different places in the container. The content of the sacks were then placed in four crusibles of 150 ml for ash content determination. Since the ash content is used in the mass balances only, it was not necessary to determine it separately in forms of feedstock composition or size.

5.3.4 Moisture content

According to the supplier the feedstock had a controlled moisture content of 12 wt% on wet basis. This was checked by measuring the moisture content of several samples (at least four per container and four analyses per sample). The samples were heated at 105 °C for 24 hours in the oven of a gas chromatograph which provided for accurate temperature control.

The moisture content of the feedstock for most of the deliveries was 12 $\pm$ 0.5 wt%; this value was used in the analysis of experimental results (runs 1-28). Because of a water leak in one of the containers (they were covered with plastic hoods), the moisture content of the biomass of this particular container increased to 14.1 wt%; this value was used in the computations of later runs 29-36. Finally the moisture content of the last delivery was found to be 10.6 wt% and this feedstock was used for runs 37-42.

In order to check whether the above procedure for measuring moisture content was sufficiently accurate, a drying curve was obtained by measuring the moisture content of two samples over 55 hours drying period. The results of both samples were identical and are shown in the Figure 5.2. A drying period of 25 hours appeared to be sufficient for accurate moisture content determination, since the weight percent loss after 25 hours was below 0.5 %.

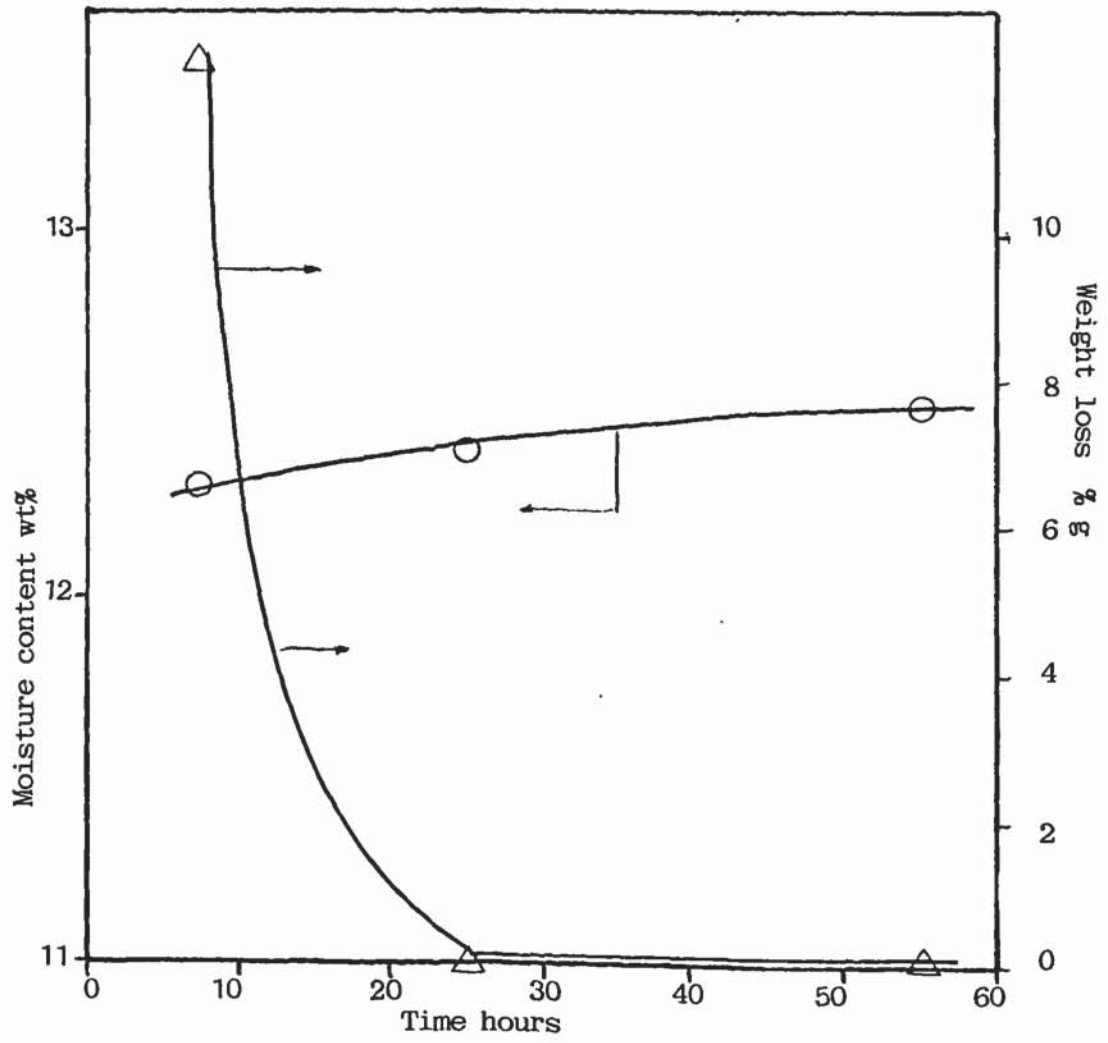

Figure 5.2 : Drying curve of the feedstock.

5.3.5 Elemental Analysis

The determination of the elemental analysis of a feedstock is of great importance, since the calculation of the heating value is based on it. The elemental analysis also indicates whether the thermochemical processing of the feedstock would result in environmental pollution in terms of sulphur dioxide and nitrogen dioxide.

Two representative samples were sent to Depauw and Stokoe S.A., Antwerp to determine the elemental analysis of the feedstock. The average results were:

C = 45.3 wt%
H = 5.8
O = 48.8
N <0.01
S <0.01

The variation between the two samples was below 1 % for all elements.

5.3.6 Heating value

The determination of the heating value of the feedstock presented some problems. Usually, the sample is grinted to powder and a pellet (cylindrical in shape, d = 1 cm, l = 1 cm, weight = ± 1 g) is made in a press. This pellet is then ignited in an atmosphere of oxygen in a calorimetric bomb.

Due to the nature of the feedstock it was very difficult to select a representative sampe of 1 g. Initially, the heating value was determined at the VUB laboratories. Since no apparatus was available and in order to facilitate grinding, only softwood was used in that determination (see Table 5.5). However, that sample was not really representative of the feedstock, so a sample was sent to Depauw and Stokoe S.A., where it was possible to grind about 2 kg of the feedstock and to carry out the heating value determination on a representative sample (see Table 5.5).

Table 5.5 : Higher heating value of feedstock

Measured at the VUB (softwood)	4680	kcal/kg
Depauw and Stokoe S.A. (1st) MAF basis	4400	
Tillman eq.	4326	
SERI eq.	4354	
IGT eq.	4128	
Depauw and Stokoe S.A. (final) MAF basis	4300 ± 20	

Equations:

Tillman : $HHV = 188\,C - 718$

SERI : $HHV = (141\,C + 615\,H - 10.2\,N + 39.95S) - (1 - Ash)\left(\frac{17244\,H}{C}\right) + 149$

IGT : $HHV = 146.58\,C + 568.78\,H + 29.45 - 6.58\,Ash - 51.53\,(O + N)$

All in Btu/lb.

Btu/lb x 0.5547 = kcal/kg equation 5.20

In order to check these results, the heating value was also calculated using the equation of Tillman (9), SERI and IGT (64). This approach gave lower

heating values than the ones measured by Depauw and Stokoe S.A. After discussion with the representatives of this company on this discrepancies, they indicated that their measurements could have up to 2 % error and, after checking their results once more, a value of 4300 ± 20 kcal/kg was agreed to be the most representative.

From the equations given in Table 5.5, the equation developed by SERI is considered as the most accurate for biomass (wood) feedstocks (64), yielding errors of only ± 230 kcal/kg. Although the IGT equation was developed on the basis of coals and coal chars, it can also predict the higher heating value of biomass and biomass chars rather accurately with an error of about 400 kcal/kg. However, for coal and coal chars the IGT equation is the most accurate (64).

The errors of the above equations are related to experimentally determined higher heating values, which is considered the most accurate method of determining this parmeter. Since the final experimental value provided by Depauw and Stokoe S. A. was relatively close to all these values determined by the various equations (maximum difference 172 kcal/lkg with IGT equation), it was considered as the most representative of the feedstock and thus used in mass and energy balances.

5.4 THE FLUIDIZATION CHARACTERISTICS OF THE REACTOR

Before the actual experiments started, the fluidization characteristics of the reactor were determined. This are discussed in the following sections.

5.4.1 Pressure drop over the distributor

The pressure drop over the distributor was measured by means of a U-tube manometer (see section 4.2.4.2). This pressure drop was initially measured with no bed in the reactor and later with a 600 mm unexpanded bed. The results are shown in Figure 5.3 and are compared to the calculated values in Table 5.6. However, only the results with the 600 mm bed are comparable to the calculated values, since in the latter the existence of a bed is assumed and it is unrealistic to consider an empty bed.

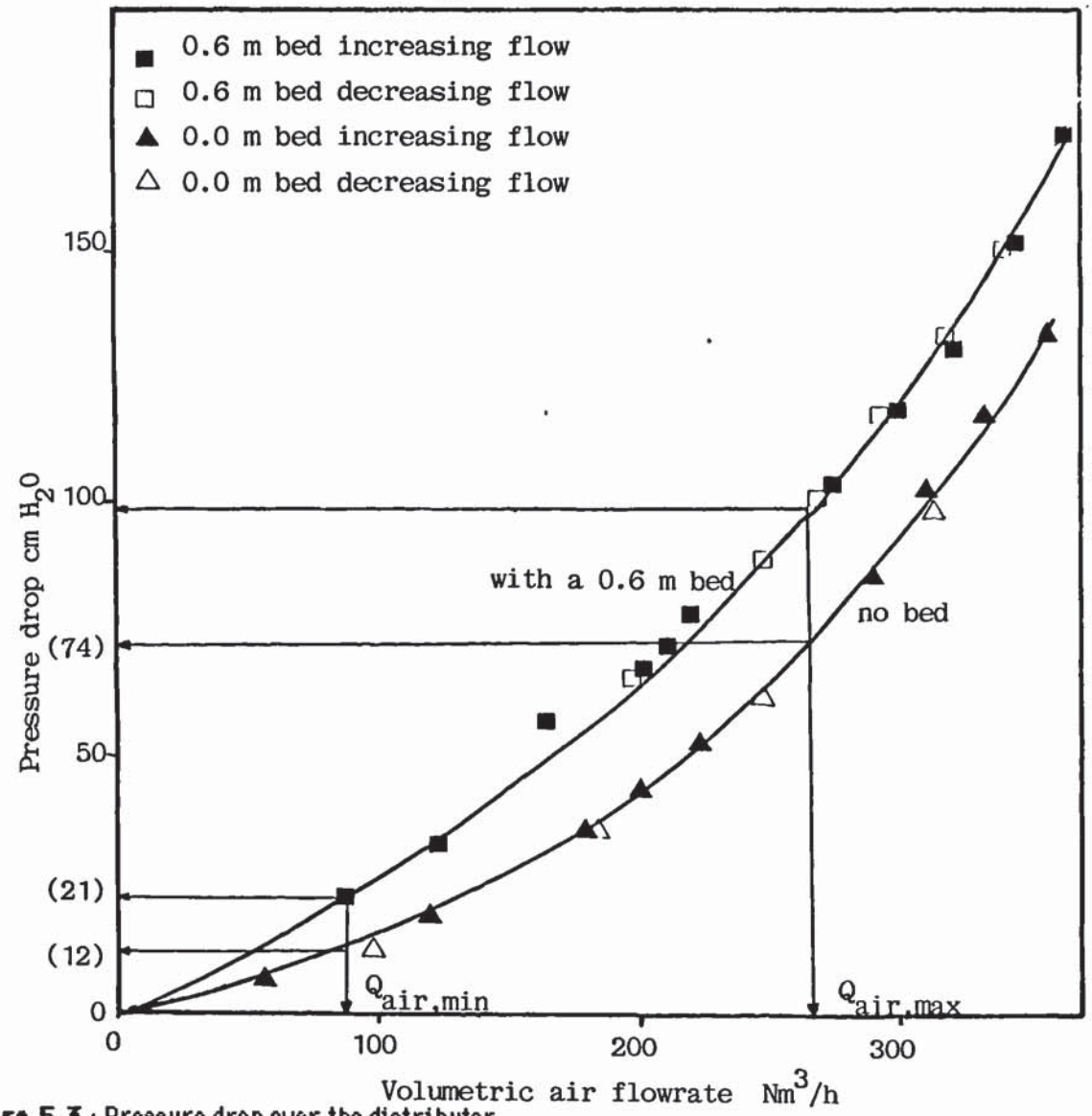

Figure 5.3 : Pressure drop over the distributor

Table 5.6 : Calculated and measured pressure drop over the distributor.

ΔPd mm H_2O	Minimum air flowrate ($88.3\ Nm^3/h$)	Maximum air flowrate ($264.9\ Nm^3/h$)
1. Calculated (see Tabel 3.3)	156	1404
2. Measured, no bed	120	740
3. Measured 600 mm bed	210	1000
Difference 1-3 %	34	29

From Figure 5.3 it can be seen that there was no hysterisis loop of pressure drop for either the empty bed or the 600 mm bed. There is a difference of 34

% between the calculated and measured pressure drop values for the minimum air flowrate. This difference was attributed to the fact that the distributor orifices were not constructed with a conical opening (see Figure 5.4), but with a cylindrical opening. The design procedure followed in Chapter 3 considers orifices with conical opening.

Since the choice of the distributor was the pipe grid (see section 3.7.1) and the diameter of the pipes used was 25 mm, it was not possible to drill orifices with a conical opening. In addition, orifices are always considered to be made from a flat plate while in the pipes used, the surface was curved (see Figure 5.4). Also an orifice is always placed perpendicular to the direction of the fluid flow, while in the pipe of the distributor the orifices were parallel to the direction of the air flow (see Figure 5.4). The construction resulted in a higher pressure drop than that assumed in the design calculations.

There was also a difference of 29 % between the calculated and measured pressure drop over the distributor for the maximum air flowrate. The measured value was lower than the calculated. This was caused by assuming that for the maximum air flowrate, the pressure drop would follow equation II.13 of Appendix II, which is a rough approximation.

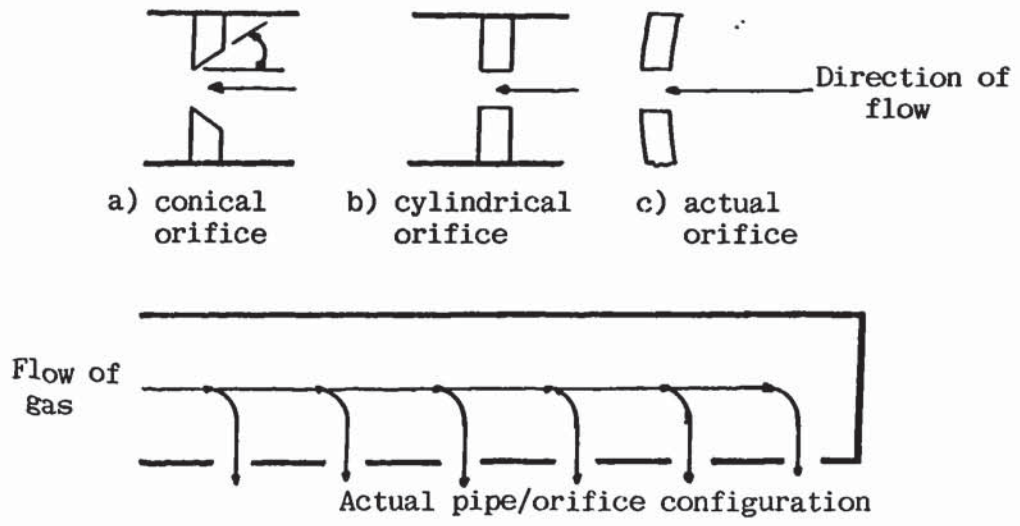

Figure 5.4 : Type of orifices.

5.4.2 Mean sand particle size diameter

In order to operate a fluidized bed under optimum conditions, a bed material of a narrow size distribution is required, since the particle diameter would be well defined and representative of the complete bed. The particle diameter strongly influences the calculated value of the minimum fluidization velocity, see equation 3.12. Due to the budget restriction (see section 4.1.1), it was not possible to obtain sand at a narrow size distribution. Thus a sample was obtained from a sand supplier and its size distribution was determined by sieving at the free University of Brussels. The results are given in Table 5.7.

Table 5.7 : Size distribution of sand

dp range mm	dpi mm	weight fraction in interval x_i	$\underline{X}$ dpi
0.075-0.150	0.1125	1.7	0.153
0.150-0.250	0.2	11.3	0.565
0.250-0.300	0.275	6.3	0.231
0.300-0.425	0.3625	26.2	0.724
0.425-0.710	0.5675	33.1	0.583
0.710-1.0	0.855	7.5	0.088
1.0 -2.0	1.5	7.3	0.049
2.0 -3.5	2.75	3.5	0.013
3.5 -5.0	4.25	3.0	0.007
		99.9	$\Sigma(\underline{X})$ = 2.413 dpi

$$\bar{dp} = \frac{1}{\Sigma(\underline{x})} \text{ dpi}$$

$$= \frac{1}{2.413}$$

$$= 0.414 \text{ mm}$$

equation 5.21

The mean particle size (0.414 mm) was somewhat smaller than the design value of 0.499 mm, but this difference was not considered significant and the sand was obtained from that supplier. Indeed, the effect on the design and performance of the bed by using this sand is summarized in Table 5.8, where the most important design parameters are compared for both sand diameters.

Table 5.8 : Comparison of performance of fluidized bed for two different particle diameters

Parameter		Particle diameter mm Design	Actual	% Difference
		0.499	0.414	17.0
1. U_{mf}	m/s	0.076	0.054	29.0
2. R_{emf}	-	0.290	0.171	41.0
3. U_t	m/s	5.32 3.78	29.0	
4. U_{op}	m/s	$0.190<U_{op}<2.66$	$0.135<U_{op}<1.89$	-
5. $\overline{d}_{Bmax}$	m	0.515	0.520	1.0
6. $\overline{d}_{Bmin}$	m	0.274	0.284	3.6
7. $d_b/\overline{d}_{Bmax}$		1.55	1.53	1.3
8. $d_b/\overline{d}_{Bmin}$		2.92	2.82	3.4
9. Q_{ig}	m^3/h	136.8	97.2	29.0
10. $(t_r)_i$	s	10.3	14.4	39.8
11. U_{Bmax}	m/s	1.93	1.94	0.5
12. U_{Bmin}	m/s	1.09	1.13	3.7
13. $(t_r)_{Bmax}$	s	0.40	0.40	-
14. $(t_r)_{Bmin}$	s	0.72	0.69	4.2
15. Q_{max}		12.7	18.0	42.0
16. Q^{min}		7.0	10.5	50.0
17. $(V_{cp}/V_B)_{max}$		0.1	0.07	30.0
18. $(V_{cp}/V_B)_{min}$		0.19	0.12	37.2

From Table 5.8 it can be seen that the minimum fluidization velocity, the Reynolds number at minimum fluidization conditions and the terminal fall velocity are significantly affected by a reduction of 17 % in the mean diameter of particles. However, the bubble parameters (5-8, 11-14) remain relatively the same. The most important parameters related to performance are nevertheless the residence time of gas flowing interstitially $(t_r)_i$ and the contact efficiency (V_{op}/V_B). The former was increased by about 4 seconds, which would ensure complete combustion of oxygen in the bed, while the latter was decreased; however, it remained around 10% which is considered acceptable (see section 3.6.3). It was therefore considered that the

utilization of sand with mean particle diameter of 0.414 mm would not effect adversely the performance of the reactor.

5.4.3 The minimum fluidization velocity

The design value of the minimum fluidization velocity was calculated as 0.076 m/s at particle size of 0.499 mm (see section 3.4.1). Under the same conditions, at particle size of 0.414 mm, the minimum fluidization velocity is 0.054 m/s.

However, the minimum fluidization velocity was measured experimentally by means of a U-tube manometer (see section 4.2.4.2 and Figure 4.4) and found to be 0.16 m/s. The results of these measurements are shown in Figure 5.5. The difference between calculated and measured minimum fluidization velocity was due to the nature of the bed. Thus, the sand used had a wide size distribution (see Table 5.7), while the calculated value was based on the mean particle diameter. Hence the calculated value represents the minimum fluidization velocity of a bed of monosized particles. Each size fraction of the bed had a different minimum fluidization velocity, thus for example the fraction with an average size of 0.363 mm (weight fraction = 26.2, see Table 5.7) had a minimum fluidization velocity of 0.043 m/s (calculated under same conditions), while the fraction with an average size of 0.568 mm (weight fraction = 33.1, see Table 5.7) had a minimum fluidization velocity of 0.097 m/s. Indeed equation 5.22 has been derived from first principles (283), by which the minimum fluidization velocity of a mixture of particles of the same density but different diameter can be determined on the basis of the properties of different fractions:

$$U_c = U_1 \left[\left(\frac{e}{e_1}\right)^3 \cdot \left(\frac{1-e_1}{1-e}\right)^{0.947} \right]^{0.940} \left[X_1 + \frac{d_1}{d_2} X_2 + \ldots \right]^{-1.85} \qquad \text{equation 5.22}$$

where U_c = minimum fluidization velocity of mixture
U_1 = minimum fluidization velocity of fraction 1
e = voidage of mixture
e_1 = voidage of fraction 1
X_1 = weight fraction of 1
d_1 = diameter of particles of fraction 1

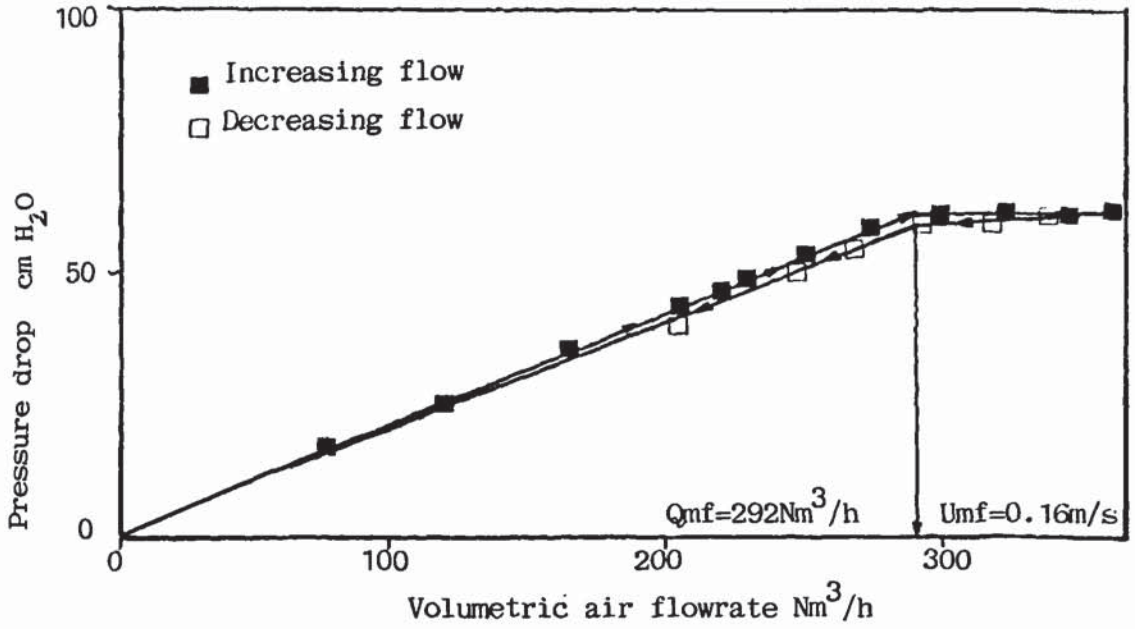

Figure 5.5 : The minimum fluidization velocity

Table 5.9 : Performance of the fluidized bed for U_{mf} = 0.16 m/s

1.	R_{emf}		0.507
2.	U_t	m/s	11.20
3.	U_{op}	m	$0.4 < U_{op} < 5.6$
4.	$\overline{d}_{Bmax}$	m	0.487
5.	$\overline{d}_{Bmin}$	m	0.231
6.	$d_b/\overline{d}_{Bmax}$	-	1.64
7.	$d_b/\overline{d}_{Bmin}$	-	3.46
8.	Q_{ig}	m^3/h	289.7
9.	$(t_r)_i$	s	4.9
10.	U_{Bmax}	m/s	1.82
11.	U_{Bmin}	m/s	1.20
12.	$(t_r)_{Bmax}$	s	0.43
13.	$(t_r)_{Bmin}$	s	0.66
14.	a_{max}	-	5.7
15.	a_{min}	-	3.7
16.	$(V_{cp}/V_B)_{max}$	-	0.25
17.	$(V_{cp}/V_B)_{min}$	-	0.43

However, experimental work (284) could not confirm the validity of equation 5.22. It can therefore be concluded that unless the bed consists of narrow size distribution, its minimum fluidization velocity cannot be calculated accurately at present and has to be determined experimentally. The effect on the performance of the fluidized bed due to experimentally measured minimum fluidization velocity is given in Table 5.9.

As in the previous section, the parameters of importance in relation to performance are the residence time of the gas flowing interstitially $(t_r)_i$ and the contact efficiency. With this minimum fluidization velocity (0.16 m/s), the contact efficiency increases significantly, while $(t_r)_i$ is reduced to about 5 seconds. However, even at this residence time, complete consumption of oxygen can be achieved (see section 2.5.5.7).

5.5 COMMISSIONING EXPERIMENTS

The complete process development unit was commissioned with a series of twelve experiments, runs 1 to 12. However, from these only seven experiments (runs 3, 4, 7, 8, 10, 11, 12) could be completed, the others had to be stopped halfway due to various problems (such as insufficient gas analysis due to badly conditioned columns, diffusive air leaks in the sampling system, break down of the motor in the rotary valve and problems with the preheating burner). During these experiments, the behaviour of the reactor under normal operating conditions was established.

The results are summarized in Tables 5.10 to 5.12. During these experiments, it became apparent that several modifications were necessary in order to facilitate the collection and improve the accuracy of the various results.

Mass balance closures well in excess of 100% (see Table 5.11) suggested that some erroneous data were used in the calculations. More specifically the mass balance closure of H, O and fly ash were always well above 100% while the one for C was below 100%. This consistancy of errors indicated that the problem was with the measurement of the gas sampling line flowrate. It was soon realized that the gas meter was connected erroneously, so that the indicated flowrate was significantly lower than the actual one. Since this parameter is used in calculations, for example:

$$\text{total fly ash flowrate} = \frac{\text{total gas flowrate}}{\text{sampling gas flowrate}} \times \text{sampling gas fly ash flow-rate}$$

equation 5.23

the error was significant and accounted for the discrepancies in the mass balance and subsequently the energy balance.

Table 5.10 : Summary of results of commissioning experiments

Run	Mass flow-rate solids kg/h	Volu-metric flow-rate air Nm^3/h	Air factor -	Bed temp. (average) °C	Higher heating value MJ/Nm^3	Gas yield kg/kg f	Thermal efficiency %	Heat of reaction MJ/kg	Heat losses by difference MJ/h
3	94	194.7	0.51	916	3.4	4.0	53.9	10.1	13.1
4	94	151.5	0.40	898	3.2	3.1	38.5	11.3	33.2
7	94	242.3	0.64	944	3.2	4.9	62.3	11.9	-15.0
8	94	194.8	0.51	977	2.7	3.8	40.3	13.3	9.9
10	94	196.2	0.52	927	2.3	3.7	32.4	12.8	30.6
11	94	196.2	0.52	958	2.9	4.0	45.4	9.7	17.7
12	94	239.7	0.64	996	0.7	4.2	11.3	13.5	46.2

Table 5.11 : Mass balances of commissioning experiment

Run	Input kg/h			Output kg/h				
	feed	air	total	gas	condensate	fly ash	total	balance %
3	94	251.8	345.8	330.0	59.1	3.7	392.8	113.5
4	94	195.9	289.9	255.6	50.9	3.5	310.0	106.9
7	94	313.3	407.3	406.0	107.9	6.4	520.3	127.7
8	94	251.8	345.8	308.7	108.1	6.4	423.2	122.4
10	94	253.6	347.6	305.1	76.4	4.6	386.1	111.1
11	94	253.6	347.6	323.6	59.8	3.9	387.3	111.4
12	94	310.0	404.0	344.2	68.2	5.8	418.2	103.5

Table 5.12 : Energy balances of commissioning experiments

Run	3	4	7	8	10	11	
Input							
Sensible heat air	11.0	8.5	15.4	21.9	10.0	10.0	13.5
Energy in feed	1581.4	1581.4	1581.4	1581.4	1581.4	1581.4	1581.4
Total	1592.3	1589.9	1596.8	1603.3	1591.3	1591.4	1594.9
Output							
Sensible heat gas	273.5	221.9	380.0	314.8	259.1	311.2	347.8
Sensible, latent heat steam	228.6	200.9	437.8	455.5	301.6	247.0	293.3
Sensible heat fly ash	2.4	2.4	4.7	5.1	3.2	3.0	4.9
Heat loss, reactor walls	28.0	28.4	29.8	32.0	28.8	31.2	33.2
Energy in gas	851.4	607.8	984.6	636.4	512.0	717.8	178.3
Total	1383.9	1061.3	1836.9	1443.8	1104.6	1310.2	857.5
Balance %	13.0	33.2	-15.0	10.0	30.6	17.7	46.2

The calorific value of the gas was found to vary significantly (see Figures 5.6a and 5.6b) indicating unsteady feedstock flowrate. This was checked and it was found that bridges were often formed in the hopper (see section 4.3.2), especially when it was practically full. The situation was improved slightly by having only a small amount of feedstock in the hopper, but the problem remained. It was solved satisfactory when an assistant remained in the hopper continuously to break down the bridges with a shovel.

In addition a serious air leak was found at the valve for the removal of inerts at the bottom of the ractor. This was made gas tight by using a metal plate to close the valve exit, with a rubber sheet between the flanges.

Finally during runs 1 and 2 a very high oxygen content in the product gas (6-9 vol.%), indicated the existence of air leaks into the sampling system of the gas chromatographs, which were remedied.

Although the results of these initial experiments cannot be used with any confidence, they indicate trends. Thus, they were considered in the discussion of the influence of the various parameters on the performance of the reactor, wherever it was appropriate, though they were not explicity mentioned due to the uncertainties because of the above reasons. Moreover, during runs 8, 11 and 12 (see Table 5.10) bed temperature in the range of 950-1000 °C were recorded while the bed did not sinter. This is an

important result, since bed agglomeration and sintering has been reported at temperatures of 800 °C (see section 2.4.3.6).

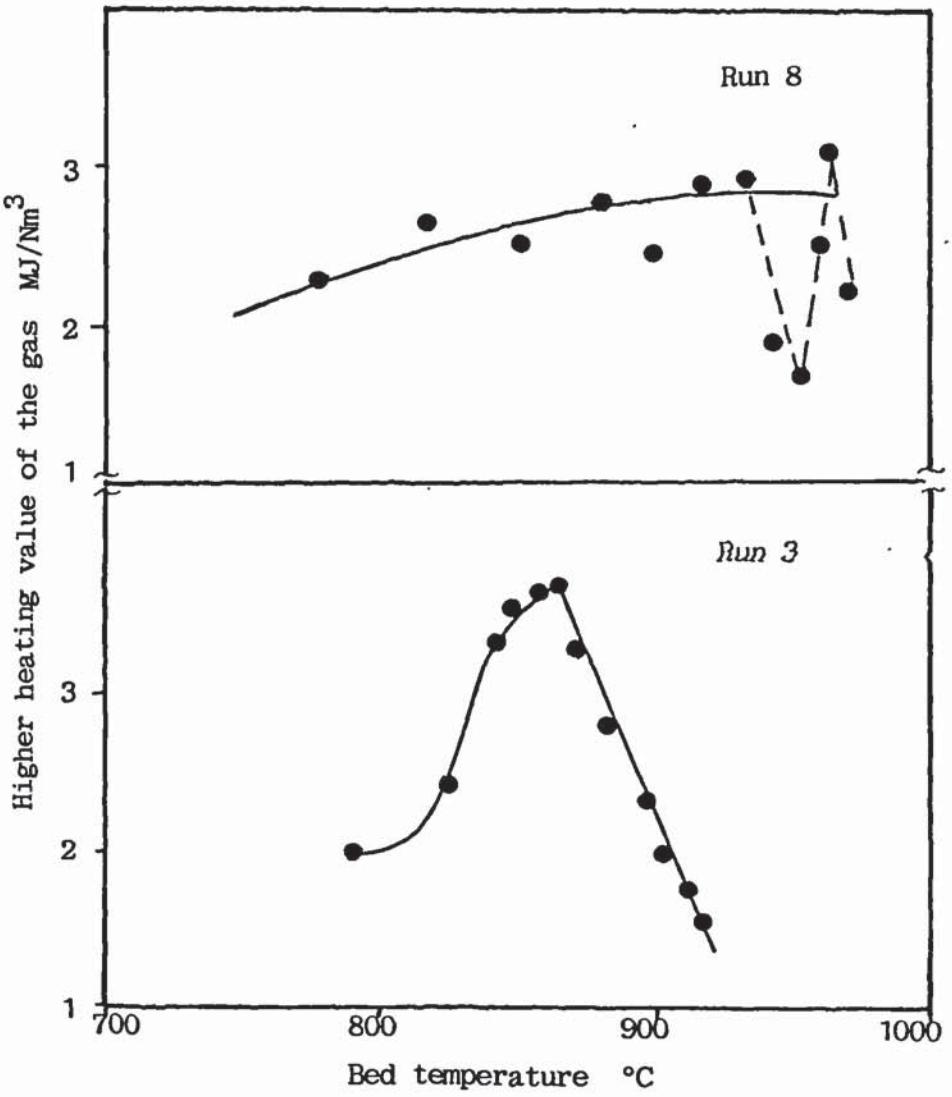

Figure 5.6 a,b : Unsteady feedstock flowrate indicated by the higher heating value of the product gas.

5.6 SUMMARY OF RESULTS OF MAIN EXPERIMENTS

In order to provide a quick reference and comparison of the results, the most important parameters i.e. feedstock flowrate, air flowrate, air factor, temperature of bed, higher heating value of gas, gas yield, thermal efficiency, heat of reaction and unaccounted heat losses are summarized in Table 5.13.

Table 5.13 : Summary of results of main experiments

Run no.	Mass flow-rate solids	Volu-metric air flow-rate	Air factor	Bed tempera-ture average	Higher heating value	Gas-yield	Thermal efficien-cy	Heat of reaction	Un-accoun-ted heat losses	Subjective assessment of confidence High H Moderate M Low L
	kg/h	Nm^3/h	–	°C	MJ/Nm^3	kg gas/ kg feed-stock	%	MJ/Kg	%	
13	78	143.1	0.53	860	3.11	3.28	43.3	11.5	10.8	H
14	78	101.7	0.38	774	4.39	2.55	48.0	10.1	14.0	H
15	78	188.5	0.70	942	2.18	4.21	36.3	12.2	12.1	H
16	78	233.3	0.87	970	0.31	4.62	5.8	16.3	35.2	L
18	160	226.7	0.42	917	3.13	2.63	34.9	10.9	24.9	M
19	160	187.4	0.34	827	4.14	2.52	44.2	10.6	23.6	M
20	160	275.8	0.50	986	2.45	3.05	31.3	10.8	25.5	M
21	160	145.2	0.26	817	5.68	1.99	50.7	8.6	16.8	H
22	210	187.4	0.25	774	5.38	1.89	46.2	9.3	25.3	M
23	210	166.0	0.23	799	5.31	1.71	44.8	7.6	26.6	M
24	210	277.9	0.38	927	4.05	2.51	44.7	8.2	16.8	H
25	210	231.2	0.32	876	5.21	2.56	53.3	7.2	12.8	H
26	220	218.3	0.29	746	6.35	2.24	63.5	8.1	11.8	H
27	220	245.5	0.32	780	6.48	2.62	75.9	6.9	-5.8	H
28	189	250.5	0.38	811	5.37	2.88	69.9	7.6	0.3	H
29	285	248.0	0.26	706	6.57	2.29	65.4	8.2	11.8	H
30	279	300.4	0.32	722	5.41	2.53	59.6	8.7	14.9	H
31	285	357.3	0.38	803	4.75	2.59	64.8	8.3	16.3	M
32	277	347.6	0.37	837	4.99	2.61	57.8	8.3	10.9	H
33	277	305.6	0.33	814	5.86	2.61	68.4	7.8	1.4	H
34	232	250.4	0.32	735	4.38	2.96	45.8	11.4	23.6	L
35	226	202.7	0.27	699	5.86	2.12	54.2	9.3	17.9	H
36	230	249.2	0.32	760	6.95	2.60	82.7	6.9	-13.9	L
37	340	338.8	0.29	871	6.76	2.02	70.1	6.7	- 0.1	H
38	340	333.8	0.29	865	7.01	1.99	72.9	6.2	- 3.0	H

Run 17 was interrupted due to blockage of the feeding system before any analysis could be made.
Note: Results from runs 39-42 are not included as they were not comprehensive, being designed for specific problems (see sections 6.13-6.24)

These parameters and their influence on the performance of the fluidized bed gasifier are discussed in subsequent sections. Full details (print outs) of results are given in Appendix V, while in Appendix VI the programme used for the calculation is presented. A Tectronix desk top computer was used for this purpose.

The major performance factors of a fluidized bed gasifier are the higher heating value of the gas and the thermal efficiency. In addition, the composition of the product gas can provide considerable information on the gasification process, while mass and energy balances indicate whether the system was operated under reliable conditions. After carefully examining

the mass and energy balances as well as the gas composition of the gas, the performance factors are plotted against the air factor and discussed.

5.7 PRODUCT GAS COMPOSITION

5.7.1 Introduction

In total eight compounds were identified with concentrations higher than 0.1 vol. % (for method of identification see section 4.2.6.1), namely, nitrogen, oxygen, carbon dioxide, carbon monoxide, hydrogen, methane, ethylene and ethane.

The last two compounds were produced in small amounts in most runs. Despite their low concentrations, these compounds have a significant influence on the higher heating value of the gas: an increase in ethylene content of 1 vol % corresponds to a 10% increase of the higher heating value. In some experiments propylene as well as a C_4 hydrocarbon (probably butadiene) were also identified at very low concentrations of below 0.1 vol. %. The average specific weight of the product gas was 1.27 kg/Nm^3.

In Table 5.14 the higher heating value of the gas (the most important property of the product gas which also reflects its composition) is compared to published results from pilot plant units of similar scale of operation. The results of this work compare well with other published data especially for air gasification.

Significantly higher values of HHV have been reported by Welch (90) for the steam gasification of paper, which is an expected result since the product gas is not diluted by nitrogen. However, the air gasification of the same material gave significantly lower values than the ones obtained during this work. Similarly Burton and Bailie (77) reported a higher heating value of 14.8 MJ/Nm^3, but they did not measure the nitrogen concentration of the product gas (and hence did not consider it in their calculations). Thus their value is unrealistically high and if the nitrogen concentration was accounted for, then the higher heating value should be in the range of 4.5-6.5 MJ/Nm^3.

Table 5.14 : Comparison of higher heating value of product gas with published results (under comparable conditions)

Author	Internal bed diameter, m.	Feedstock	Oxidizing medium	H.H.V. MJ/Nm^3
This work	0.8	chopped wood	air	2.2-7.0
Black et.al. (38)	1.2 outside	wood waste	air + O_2	1.4-8.0
Garey et.al. (79)	1.2 outside	wood waste	air	2.3 (a)
Black (114)	3.6	mill waste	air	1.9 minimum
Welch (90)	0.7	paper	air	3.7
	0.7	paper	steam	7.4-13.6
Flamigan et.al. (92)	0.7	sawdust	air	0.7-9.3(a)
Van den Aarsen et.al. (95-97)	0.3	beach wood	air	5.0-6.6
	0.3	rice husk	air	4.8-6.3
Moreno (99)	1.3	cotton ginning	air	4.8-6.1
	1.3	nut shells	air	6.7
Burton, Bailie (77)	0.46	sawdust	air + CH_4	14.8

(a) In MJ/m^3

The results also compare very well with the first commercial fluidized bed gasifier (100). It was reported that the higher heating value of the gas produced from that plant had a minimum value of 1.9 MJ/Nm^3, while the maximum value did not exceed 4.8 MJ/Nm^3.

5.7.2 Carbon conversion

This carbon conversion can be determined from the product gas composition, the elemental composition of the feedstock and their respective flowrates. This parameter represents the efficiency of conversion of the carbon present in the feedstock, to gas. Figure 5.7 shows the amount of carbon recovered in the product gas as a function of bed temperature for air factor in the range 0.30-0.39, the narrowest range with most experiments. The last scatter of data, which is attributed to experimental errors in determining the gas composition, renders any conclusion difficult. It can be tentatively proposed that the carbon conversion decreases with increasing temperature. This is shown more clearly for temperatures above 800 °C.

This is in contradiction with the two studies found in the literature of fluidized bed gasifiers discussing this parameter (15, 89), where it was shown that the carbon conversion increases with temperature. In the former

work, the increase in temperature was achieved with external means (electric heating elements) and the increase in carbon conversion was attributed to higher conversion of carbon in the electricated particles. Electric heaters were also used in the latter work, but the authors provided no explanation concerning the increase in carbon conversion. The results of Figure 5.7 can be explained by examining the means by which the increase in temperature was achieved. In this work, no electrical heating was provided and thus the temperature could only be raised by obtaining a higher degree of combustion. This can be achieved by increasing the air flowrate or decreasing the feedstock flowrate. However, since the control of air flowrate was simpler and more reliable, this parameter was mainly used to control the bed temperature. As a consequence of higher air flowrates, higher linear velocities were attained in the reactor resulting in reducing the retention time of gases and enhancing the electrication and carry over of fine char particles from the bed.

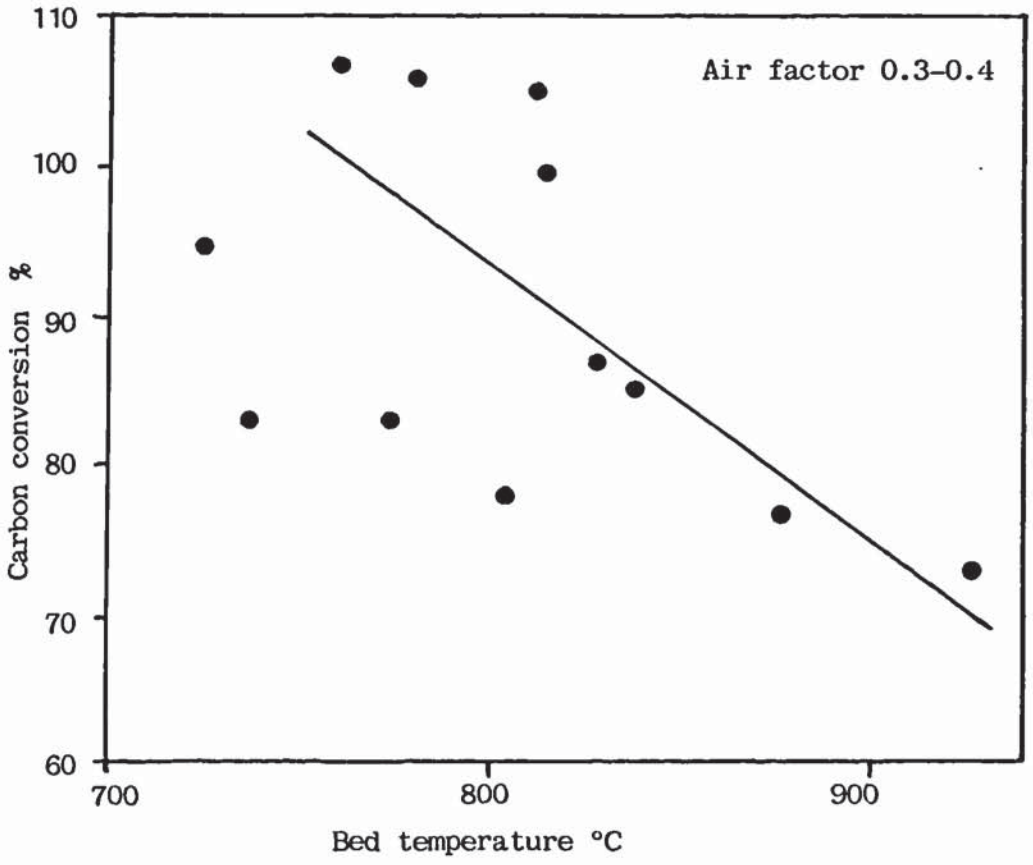

Figure 5.7 : Carbon conversion to gas versus bed temperature

Since the fines could escape from the reactor with incomplete conversion, this resulted in a decrease of carbon conversion. The average carbon content of the fly ash (see section 5.8.2) was determined at about 70 wt%. This value is rather high in comparison to the laboratory pilot plant (104-108), where values in the range of 30-50 wt% were typical. Similarly, shorter retention time of pyrolysis gases decreases the extent of the cracking reaction, which take place to connect tars and other higher hydrocarbons to low molecular weight product which can be determined by gas chromatography.

The latter view is supported by Figures 5.8 and 5.9, which show the effect of temperature on the concentration (vol.%) of methane and the carbon conversion to methane (defined as the efficiency of conversion of the carbon present in the feedstock to methane) respectively. Figure 5.8 indicates that there is no major variation of the concentration of methane with temperature over the range 700-950 °C, which is supported by thermodynamics (109). However, the carbon converted to methane decreases with temperature as indicated in Figure 5.9, especially over the temperature range 750-950 °C. There is also a large scatter of data in Figure 5.9; however, if the data of run 34 (T_b = 735, % C in CH_4 = 7.17), for which the subjective assessment of confidence was low (see Table 5.13), are excluded from Figure 5.9, then the scatter is significantly reduced, and a straight line can be tentatively drawn.

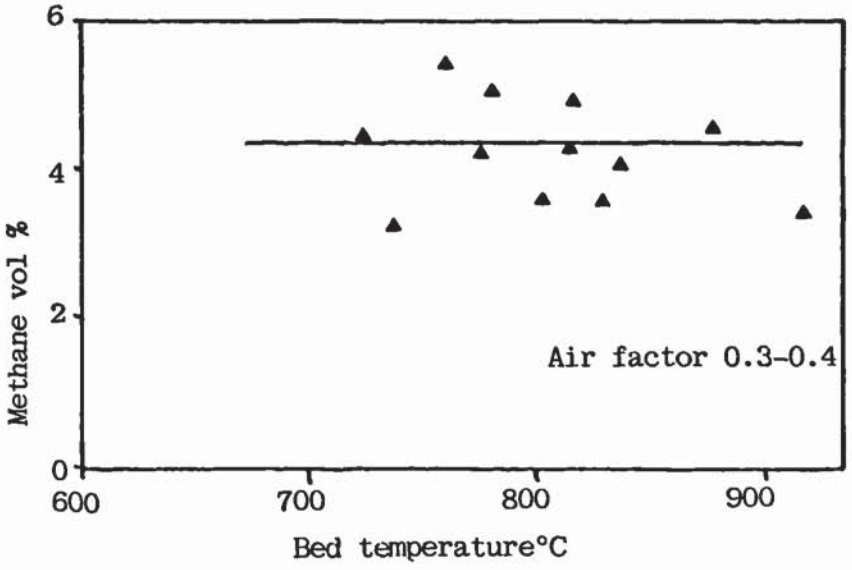

Figure 5.8 : Methane vol.% as a function of bed temperature.

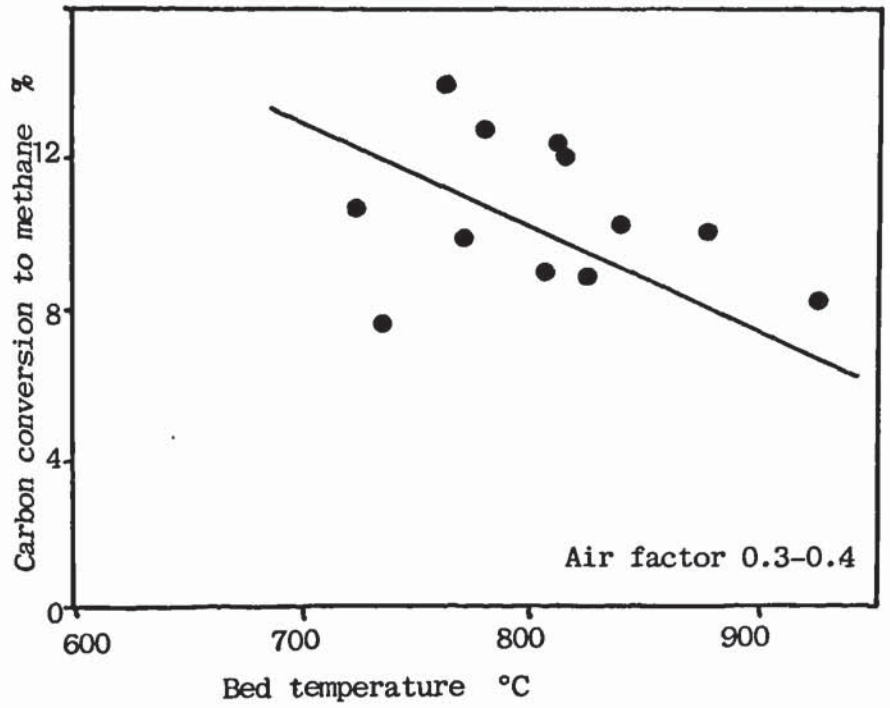

Figure 5.9 : Carbon conversion to methane as a function of bed temperature

5.7.3 Water gas shift equilibrium

The main components of producer gas are hydrogen, carbon dioxide and carbon monoxide. Thermodynamically, their relative quantities are governed by the chemical equilibrium of the water gas shift reaction :

$CO + H_2O \rightleftharpoons CO_2 + H_2$ (see section 2.5.4.2, Table 2.15)

There is some controversy in the literature concerning the equilibrium of this reaction in fluidized bed gasifier modelling, as discussed below. In most models for fluidized bed gasifiers, it is assumed that a) the water gas shift reaction attains equilibrium and b) the equilibrium composition is frozen at the exit of the reactor (15, 255). Some authors (231, 233) however argue that equilibrium will not be attained, since residence time and reaction temperature are low compared to those in a dense phase gasifier.

Previous experience with the laboratory fluidized bed pilot plant with other fuel (sawdust, refuse derived fuel (105, 112)), has shown that this reaction attains equilibrium, provided the reaction temperature is sufficiently high (above 800 °C).

The standard Gibbs function of the homogeneous ideal gas reaction :

$$aA + bB \longrightarrow c\,C + dD \qquad \text{equation 5.24}$$

is given by equation 5.25 (285)

$$-\Delta G = RT \ln k_p \qquad \text{equation 5.25}$$

where ΔG = change of the standard Gibbs function
R = ideal gas constant
T = temperature of the reacting system
and k_p = equilibrium constant in terms of partial pressures.

The equilibrium constant in terms of partial pressures is (285) :

$$K_p = \frac{(p_C)^c - (p_D)^d}{(p_A)^a - (p_B)^b} \qquad \text{equation 5.26}$$

where p_i = partial pressure of component I
and a, b, c, d stoichiometric numbers.

Thus, for the water gas shift reaction, equation 5.26 becomes:

$$K_{PW} = \frac{P_{CO2} \cdot P_{H2}}{P_{CO} \cdot P_{H2O}} \qquad \text{equation 5.27}$$

For the experiments of this work, the experimental value of equation 5.27 was calculated as a function of various process parameters and compared to theoretical values from the literature (233). Figures 5.10 and 5.11 show the effect of bed and exit gas temperatures respectively on K_{PW}. In most experiments it was found that the experimentally determined value of K_{PW} is well below the equivalent theoretical prediction, when related to the bed temperature. However as the bed temperature increases, the differences between experimental data and theoretical predictions of K_{PW} reduce, especially above 850 °C. At higher bed temperatures above 900 °C very good agreement is reached because of a higher rate of reaction. Hence it can be concluded that equilibrium is only attained at temperatures above 900 °C.

The same approach can be applied to Figure 5.11. However, since the freeboard temperature rarely exceeded 750 °C the agreement between experimental and theoretical predictions of k_{pw} is poor.

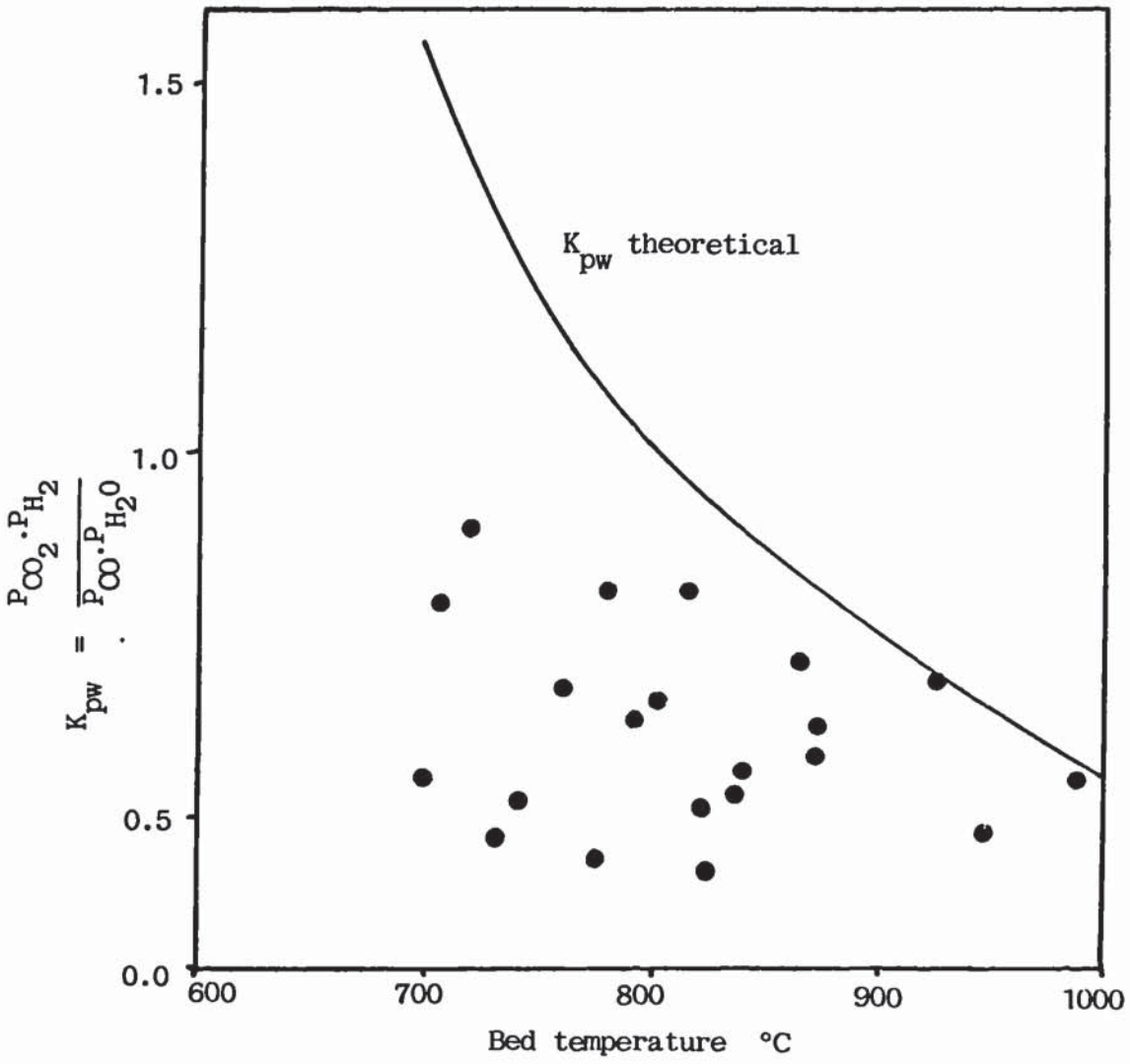

Figure 5.10 : Effect of bed temperature on K_{pw}.

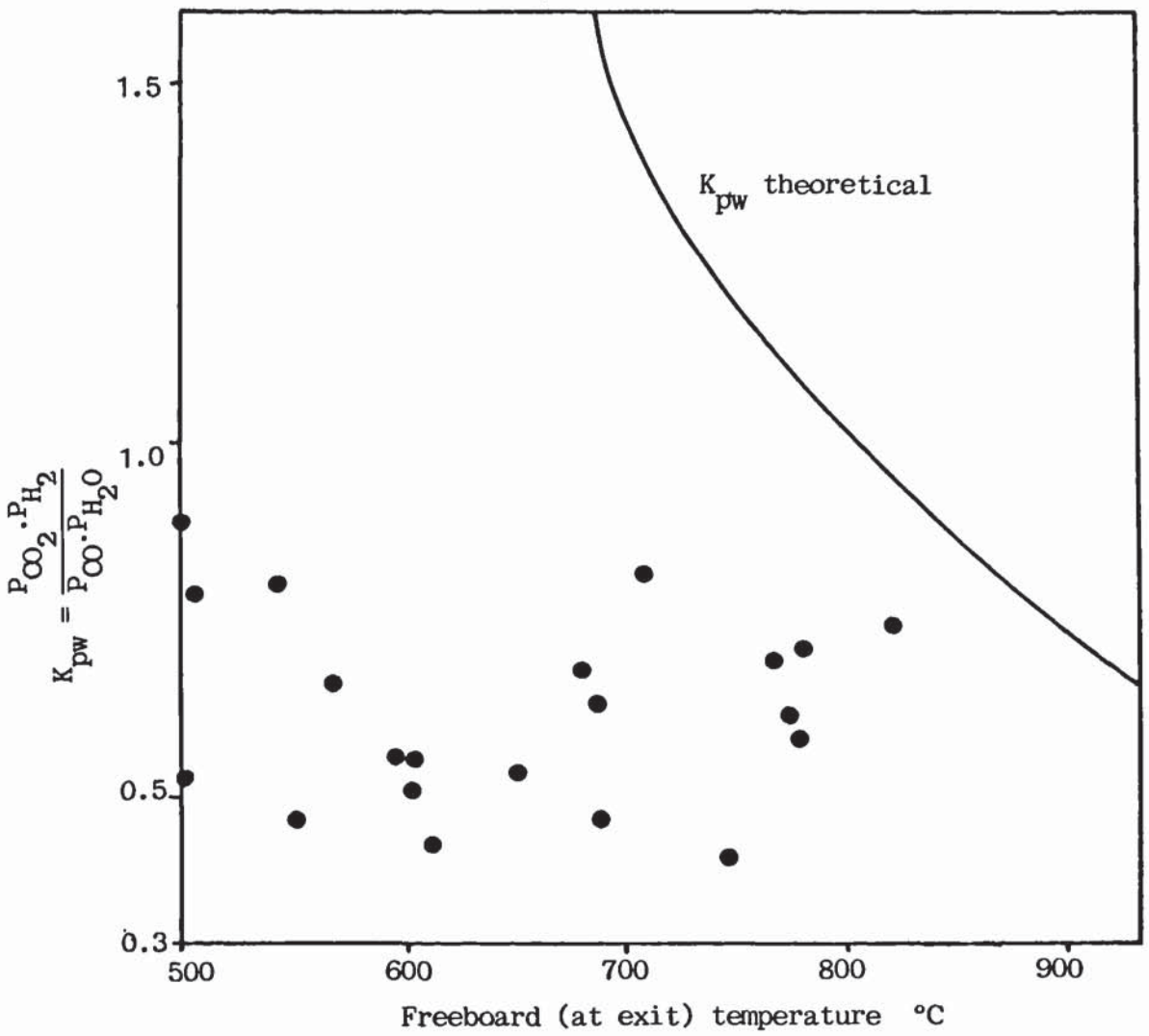

Figure 5.11 : Effect of exit gas temperature on K_{pw}.

5.7.4 Comparison of gas composition to thermodynamic predictions

In section 2.5.4.3 a thermodynamic model was developed on the basis of homogeneous equilibrium. This was used to simulate the gas composition of the fluidized bed gasifier (for example see Figure 2.21). Table 5.15 compares thermodynamic equilibrium compositions to actual experimental ones for some of the runs at both bed and freeboard temperature. The runs were selected to cover a wide temperature and air factor range.

The results of Table 5.15 indicate that the thermodynamic model cannot predict accurately the gas composition of the fluidized bed gasifier. This is especially true for methane, ethylene and ethane for which the model predicts significant concentrations.

Table 5.15 : Comparison of thermodynamic (T) and experimental (E) dry gas compositions, Vol.%.

Run	13			15			25			28			35			38		
Component	E	T_B	T_F	E	T_B	T_F	E	T_B	T_F	E	T_B	T_F	E	T_B	T_F	E	T_B	T_F
O_2	8.0	-	-	0.0	-	-	0.1	-	-	0.0	-	-	0.7	-	-	1.4	-	-
N_2	67.2	58.0	57.4	70.0	67.7	65.4	54.9	42.7	41.3	51.7	47.2	47.1	50.6	36.1	38.2	48.1	38.4	37.7
H_2	3.8	12.8	14.5	3.6	6.5	7.5	10.1	22.6	23.7	10.6	19.9	19.5	8.9	27.7	23.1	9.9	24.9	25.8
CO_2	16.2	15.0	16.6	17.9	16.9	17.5	15.4	9.8	10.9	16.7	12.4	17.3	20.7	12.2	17.4	16.8	9.4	10.8
CO	9.5	14.1	11.5	6.4	8.8	7.3	14.5	24.8	23.6	16.4	19.7	13.7	12.4	23.6	17.2	16.2	27.2	25.2
CH_4	2.8	0.0	0.0	1.8	0.0	0.0	4.7	0.0	0.0	4.3	0.0	1.7	4.6	0.4	3.9	5.3	0.0	0.1
C_2H_4	0.4	-	-	0.3	-	-	0.3	-	-	0.3	-	-	1.7	-	-	2.0	-	-
C_2H_6	0.1	-	-	0.0	-	-	0.1	-	-	0.1	-	-	0.3	-	-	0.3	-	-
Air factor		0.53			0.70			0.32			0.38			0.27			0.29	
T_B °C		860			942			876			811			699			865	
T_F °C		696			779			777			594			593			775	

--- : Not determined

T_B : Bed temperature

T_F : Freeboard temperature

However, there is a good agreement between theoretical and measured gas composition for run 15, for both bed and freeboard temperature. This is in agreement also with the results concerning the water gas shift reaction (see previous section), where the experimental equilibrium constant of this reaction approached the theoretical equilibrium constant only at temperatures above 900 °C.

It can be concluded that pure thermodynamic models are unsuitable for the prediction of the gas composition of fluidized bed gasifiers operating at temperatures below 900 °C. The same has also been concluded by others (24, 232). These discrepancies are commonly attributed among others to the relatively short residence time of gas and biomass in this type of reactor. However, thermodynamic models can be empirically modified to account for the descrepancies at temperatures below 900 °C, as has been recently demonstrated (24) (see also section 2.5.4.4). Alternatively empirical correlations can be developed by which the gas composition can be determined, as shown in Chapter 6.

5.8 MASS BALANCES

5.8.1 Introduction

The total quantity of gas produced was calculated from a nitrogen balance over the air input (which was accurately measured and corrected for temperature and pressure) and the nitrogen content of the product gas analysis.

$$\text{Total product gas flowrate kg/h} = \frac{\text{Total amount of nitrogen fed to reactor (from air flowrate), kg/h}}{\text{weight \% of nitrogen in product gas analysis}} \times 100$$

equation 5.28

It was assumed that nitrogen did not react with oxygen at these temperatures (below 950 °C) to any significant extent (229).

The mass flowrate of condensate and fly ash measured with the gas sampling line (see section 4.2.7) were corrected to the total gas flowrate by multiplying them by the following correction factor:

$$\text{correction factor} = \frac{\text{total product gas flowrate}}{\text{sampling line gas flowrate}} \qquad \text{equation 5.29}$$

Thus the quantities of condensibles and fly ash were prorated up from the sampling line flowrate to total product gas flowrate in direct proportion, assuming that the sample line product was representative of the full reactor product (see section 4.3.3).

The total product gas flowrate varied in the range of 190-650 kg/h depending on the air flowrate and experimental parameters, while the sampling line gas flowrate varied in the range of 12 to 18 kg/h. Thus the above correction factor varied in the range of 15-36.

5.8.2 The fly ash

As explained in section 4.2.7.2, the sampling line cyclone did not function very well. Hence assumed values were used in the calculations (most of them producing ash balances in the range of 80-100%).

The carbon content of the fly ash was measured and the average value of 70 wt% carbon content was used in the calculations.

From Appendix V it can be seen that the carbon reported to the fly ash represented a loss of carbon of about 6-10 % of the carbon present in the feedstock. This was a significant amount and it is further discussed in section 5.8.4. The fly ash had an average bulk density of 210 kg/m^3.

5.8.3 Dissolved hydrocarbons in condensate

Samples from the condensate were analysed with a Coulometer and it was found that the average (of six samples) carbon concentration in the condensate was 0.013 kg C/kg condensate. This value was incorporated in the calculations for the carbon balance. The condensate had an average density of 985 kg/m^3.

5.8.4 The mass balances and closures

A detailed calculation of the mass and energy balances is given in Appendix IV (for run 38). The mass balances of all runs (except commissioning experiments and runs 39-42, which were not made due to the nature of the run) are given in Table 5.16, while in Table 5.17 the closure of the mass balance of the individual components is given. In the latter table some results from previous work at the laboratory pilot plant are also included for comparison. The total mass balance closure was in the range of 83.6-106.6 %, only one run (run 23) was below 90.5 %. The average closure was 98.29%. The range and average values of mass balance closure for the individual components are shown in Table 5.18 (see also Appendix V).

Table 5.16 : Mass balances

Run	Input in kg/h			Output in kg/h					Subjective assessment of errors
	Feed	Air	Total	Gas	Condensate	Fly ash	Total	Balance %	
13	78	185.0	263.0	220.9	40.1	3.9	264.8	100.7	L
14	78	131.5	209.5	171.9	31.5	3.0	206.3	98.5	L
15	78	243.7	321.7	284.0	37.3	3.1	324.5	100.9	L
16	78	301.6	379.6	311.1	36.8	2.9	350.8	92.4	M
17	160	295.7	455.7	262.9	63.8	9.9	436.6	95.8	M
19	160	242.3	402.3	348.3	50.5	7.4	406.2	100.9	L
20	160	356.6	516.6	421.4	49.4	10.7	481.4	93.2	M
21	160	187.8	347.8	274.9	43.3	6.1	324.2	93.2	M
22	210	242.3	452.3	343.4	63.5	8.0	415.0	91.8	H
23	210	214.6	424.6	310.0	36.2	8.7	345.9	83.6	H
24	210	359.3	569.3	454.6	44.4	15.9	515.0	90.5	H
25	210	298.9	508.9	407.9	50.5	13.5	471.8	92.7	H
26	220	282.3	502.3	425.8	68.4	7.8	502.0	99.9	L
27	220	317.4	537.4	498.1	54.2	8.7	561.0	104.4	L
28	189	323.9	513.4	471.3	51.7	10.3	533.4	103.9	L
29	285	320.7	605.7	552.5	64.5	10.3	627.3	103.6	L
30	279	388.5	667.5	595.4	73.9	11.8	681.1	102.0	L
31	283	462.0	745.0	618.7	81.2	11.6	711.6	95.5	M
32	277	449.5	727.0	611.2	87.8	13.8	712.8	98.1	L
33	277	394.2	672.2	609.3	83.8	12.1	705.2	104.9	L
34	232	323.7	555.7	480.6	90.7	8.4	579.7	104.3	L
35	226	262.1	488.1	404.6	69.9	8.5	482.9	98.9	L
36	230	322.3	552.3	505.1	72.8	10.9	588.8	106.6	M
37	340	438.1	778.1	685.9	82.6	21.6	790.2	101.5	L
38	340	431.5	771.5	678.3	65.1	24.0	767.4	99.5	L

Low L - Medium M - High H.

Table 5.17 : Mass balance closure for the individual components

	Balance %				
Run	Total	C	H	O	Ash
13	100.7	98.1	121.9	101.7	95.9
14	98.5	91.0	104.9	99.6	73.8
15	100.9	107.7	113.7	199.5	127.8
16	92.4	79.0	89.4	88.4	115.5
18	95.8	85.0	95.4	93.7	119.7
19	100.9	96.1	90.3	105.6	89.0
20	93.2	88.8	78.4	84.3	129.1
21	93.2	82.8	88.8	91.5	74.1
22	91.8	75.7	92.9	90.9	69.7
23	83.6	71.7	68.3	74.4	75.1
24	90.5	89.1	74.2	77.6	137.8
25	92.7	89.7	87.5	84.9	116.3
26	99.9	95.4	108.1	102.1	69.8
27	104.4	114.0	107.2	106.0	76.3
28	103.9	116.8	105.1	103.9	105.7
29	103.6	106.7	91.9	105.8	70.1
30	102.0	101.9	96.1	105.5	82.1
31	95.5	84.6	95.8	94.2	89.8
32	98.1	94.8	101.7	96.6	96.8
33	104.9	109.5	110.5	109.1	84.6
34	104.3	90.2	103.9	116.7	70.4
35	98.9	90.3	97.3	102.7	72.0
36	106.6	117.7	123.3	108.0	114.3
37	101.5	109.0	98.9	99.8	119.3
38	99.5	109.4	92.4	94.1	132.6
Average	98.3	95.7	97.5	97.5	95.2
Cacao pellets	94.3	82.8	81.6	91.1	36.5
Wood shavings	102	89	87	100	136
Bark (88)	98	77	69	106	107

Table 5.18 : Mass balance range and average closure of individual components

Component	Range	Average
C	71 - 117	95.7
H	68 - 123	97.5
O	74 - 116	97.5
Ash	68 - 132	95.2

Not only the errors associated with the measurement of the various parameters must be considered, but also the fact that two of the parameters (condensate and fly ash) were measured only from a small amount of gas and then were converted to the total flowrate. Thus, an error of 0.01 kg in the

measurement of the condensate in the sampling line would represent an error of 0.2 kg for the total flow, assuming a correction factor of 20 (see section 5.8.1), or 0.4 kg assuming a correction factor of 40. However, it is believed that the gas treated in the gas sampling line was a representative sample of the total flow (see section 4.2.7.1).

The unsteady feedstock flowrate was another source of error which was revealed in the mass balance calculations. In addition, higher hydrocarbons than C_4 were sometimes detected (but not in sufficient concentrations to allow for accurate qualitative and quantitative determination), but could not be used in the calculations. Also, the fly ash was assumed to be consisting of ash and carbon only, while oxygen and hydrogen could also be present. Due to budgetary limitations (see section 4.1.1), it was not possible to perform an ultimate analysis of the fly ash.

It was generally accepted (78, 84-87, 87, 99) that, if the mass balance closures are in the range of 110-90%, the results can be considered acceptable. On this principle, only the results of run 23 closure of 83,6% should be rejected. Considering the various uncertainties explained above, the results of the mass balance were fairly good.

5.8.5 Comparison with published results

From Table 5.17 it is clear that the average results of the process development unit (P.D.U.) are better than the ones of the laboratory pilot plant, in particular the carbon and hydrogen balance was much improved. This can be attributed to two reasons:

a) since the P.D.U. is a larger reactor and the feedstock was fed just above the bed and not from the top, the relative loss of unreacted solids and fines carried away with the product gas would be reduced;
b) the hydrocarbons reporting to the condensate were only considered in the mass balance calculations for the P.D.U., with an average value of 0.013 kg C/kg cond.

However, the carbon content of the fly ash and the consequent loss in carbon was higher in the process development unit than in the laboratory pilot plant.

The following are some possible ways to improve reactor efficiency with regard to loss of carbon in the fly ash :

a) a higher bed with the adverse consequence of higher pressure drop

b) lower air velocity with the adverse consequence of loss of efficient fluidization
c) separation and recirculation of part of the fly ash back into the bed
d) feeding below the surface of the bed.

The last two (or a combination of both) are believed to be the most promising methods to be investigated.

Major losses due to carbon loss with the ash have been reported (99). However, these experiments were made with cotton gin wastes which have an ash content of about 25 wt%. It was reported that with a feedstock flowrate of 2000 kg/h, the ash rejected by the system was 500 kg/h together with about 100 kg of char. Similarly, the carbon content of fly ash for wood was approximately 50 % (70 % for this study).

In another work (92) the product composition was used to calculate the feedstock flowrate, on the assumption that the carbon reported in the product gas should correspond to carbon in the feedstock. The other authors of Table 5.14 did not publish or comment on their results concerning the mass balances.

Therefore the results of this work are comparable to published data, though care should be taken to improve the efficiency of the system.

Thus run 13 produced 3.86 kg/h fly ash of which 2.67 kg/h was carbon (see Appendix V). If 50% of this could be converted to methane, the mass flowrate of methane would increase from 3.36 kg/h to 5.13 kg/h, while the higher heating value of the gas would increase by 26% (from 2.38 MJ/kg to 2.80 MJ/kg).

5.9 ENERGY BALANCES

5.9.1 Introduction

The energy balances are summarized in Table 5.19. The energy input to the reactor consists of two parameters: the sensible heat of air and the energy of the feedstock:

Energy in feedstock = $G_{feedstock}$ X $HHV_{feedstock}$ equation 5.30

where $G_{feedstock}$ = mass flowrate of the feedstock, on as received basis kg/h

and $HHV_{feedstock}$ = higher heating value of the feedstock, MJ/kg

The energy output consists of six parameters:
a) the sensible heat of the product gas
b) the sensible and latent heat of steam
c) the sensible heat of fly ash and tars
d) the heat losses from the reactor walls
e) the chemical energy in the product gas
f) the energy in fly ash, tars and carbon in the condensate.

The general balance over the reactor is given by equation 5.31.

$$C_{Pair} \times G_{air} (T_R - 20) + HHV_{feedstock} \times G_{feedstock} = \Sigma C_{Pi\,out} \times G_{i\,out} (T_E - 20) + L_{H2O} \times G_{H2O\,out} + HHV_{gas} \times G_{gas} + H_W + H_F + H_C$$

equation 5.31

where G_{Pi} = specific heat capacity of gas component i
G_i = mass flowrate of gas component i
HHV = higher heating value
T_R = temperature of reactor
T_E = temperature of gases at exit of reactor
H_W = heat losses from reactor walls
H_F = higher heating value fly ash
H_C = energy in the condensate.

A detailed analysis of energy balance is given in Appendix IV.

Table 5.19 : Energy balances

Run	13	14	15	16	18	19	20	21	22	23	24	25	26	27
INPUT														
Sens. heat air	5.4	2.7	10.4	12.8	14.2	8.2	17.5	6.6	7.7	7.3	15.3	11.7	12.9	14.5
Energy in feed	1213.9	1213.9	1213.9	2490.1	2490.1	2490.1	2490.1	2490.1	3268.2	3268.2	3268.2	3258.2	3423.8	3423.9
TOTAL	1219.4	1216.6	1224.3	1226.7	2504.3	2498.3	2507.6	2496.7	3275.9	3275.5	3283.5	3279.9	3436.8	3438.4
OUTPUT														
Sens. heat product gas	178.6	138.7	253.1	311.4	305.3	249.8	398.6	258.9	266.6	289.0	420.1	399.0	270.9	347.8
Sens. lat. steam	153.9	119.6	149.7	157.9	248.7	184.0	202.4	170.7	233.4	138.3	170.6	202.6	234.7	191.1
Sens. heat fly ash	2.5	1.8	2.3	2.41	6.5	4.0	8.0	4.2	4.5	5.4	11.2	9.6	3.5	4.3
Heat loss reactor walls	106.4	99.3	119.2	130.1	111.5	95.8	125.9	106.4	94.5	108.7	115.3	112.8	83.2	89.7
Energy in gas	525.4	582.8	464.7	70.2	867.1	1100.2	778.9	1262.3	1508.5	1483.3	1481.9	1741.1	2173.8	2596.8
Energy in fly ash, tars	101.1	77.9	64.9	59.7	245.5	183.5	258.1	153.2	209.5	214.9	387.0	330.9	200.0	214.6
TOTAL	1067.7	1020.2	1053.9	731.7	1784.6	1817.3	1772	1955.7	2317.1	2192.2	2572.2	2795.8	2965.9	3444.2
Heat loss by difference	151.7	196.5	170.3	495.0	719.6	680.9	735.6	548.9	358.9	1083.3	711.3	484.2	470.8	-5.9
% unaccounted heat loss	10.8	14.0	12.1	35.2	24.9	23.6	25.5	18.7	25.3	28.0	18.8	12.8	11.9	-0.1
Thermal efficiency %	43.3	48.0	38.3	5.8	34.8	44.2	31.3	50.7	46.2	44.8	44.8	53.3	63.5	75.9
Heat of reaction MJ/kg	11.6	10.1	12.2	16.3	10.9	10.6	10.8	8.6	9.3	7.6	8.2	7.2	8.1	6.9

All units in MJ/h unless otherwise stated; the same subjective assessment of errors per corresponding run applies in this table as in Table 5.14.

Table 5.19 : continued

28	29	30	31	32	33	34	35	36	37	38
12.7	14.0	19.9	22.6	30.9	23.7	15.17	11.4	15.5	17.2	23.0
2949.2	4327.6	4236.5	4297.3	4213.7	4206.2	3522.8	3431.7	3492.5	5299.4	5291.4
2961.9	4341.6	4256.4	4319.9	4244.6	4229.9	3538.0	3443.2	3507.9	308.6	5314.5
349.3	350.6	354.3	445.4	489.9	553.2	314.1	301.5	45.3	679.1	681.2
187.6	221.8	250.4	293.1	328.4	324.5	319.8	253.7	276.7	330.2	260.8
5.6	4.7	5.11	6.3	8.2	7.8	4.2	4.5	6.8	15.3	17.1
95.3	81.9	81.2	94.4	100.7	103.7	85.9	87.6	98.1	112.1	111.9
2061.7	2829.0	2522.2	2355.0	2434.8	2873.3	1614.4	1859.7	2885.0	3707.5	3855.3
251.7	255.3	292.6	294.7	336.7	295.6	212.4	208.4	278.9	524.7	574.1
2951.3	3743.4	3505.8	3488.8	3698.8	4158.1	2552.7	2715.4	3995.8	5368.7	5500.4
10.58	596.2	750.6	831	545.8	71.8	985.3	717.8	-487.8	-60.2	-185.4
0.3	11.7	14.9	16.3	10.9	1.4	23.6	17.9	-13.9	-0.9	-3.0
70.0	65.4	59.6	54.8	57.8	68.4	45.8	54.2	82.7	70.1	72.9
7.6	8.2	8.7	8.3	8.3	7.8	11.5	9.3	6.9	6.7	6.2

5.9.2 The heat of reaction

The heat of the gasification reaction as defined by equation 5.12 has been derived from the heat of combustion of the feedstock and from this of the individual reaction products (see section 5.2). The heat of reaction was in the range of 6.2 to 16.3 MJ/kg. Figure 5.12 shows the influence of the air factor on the heat of reaction.

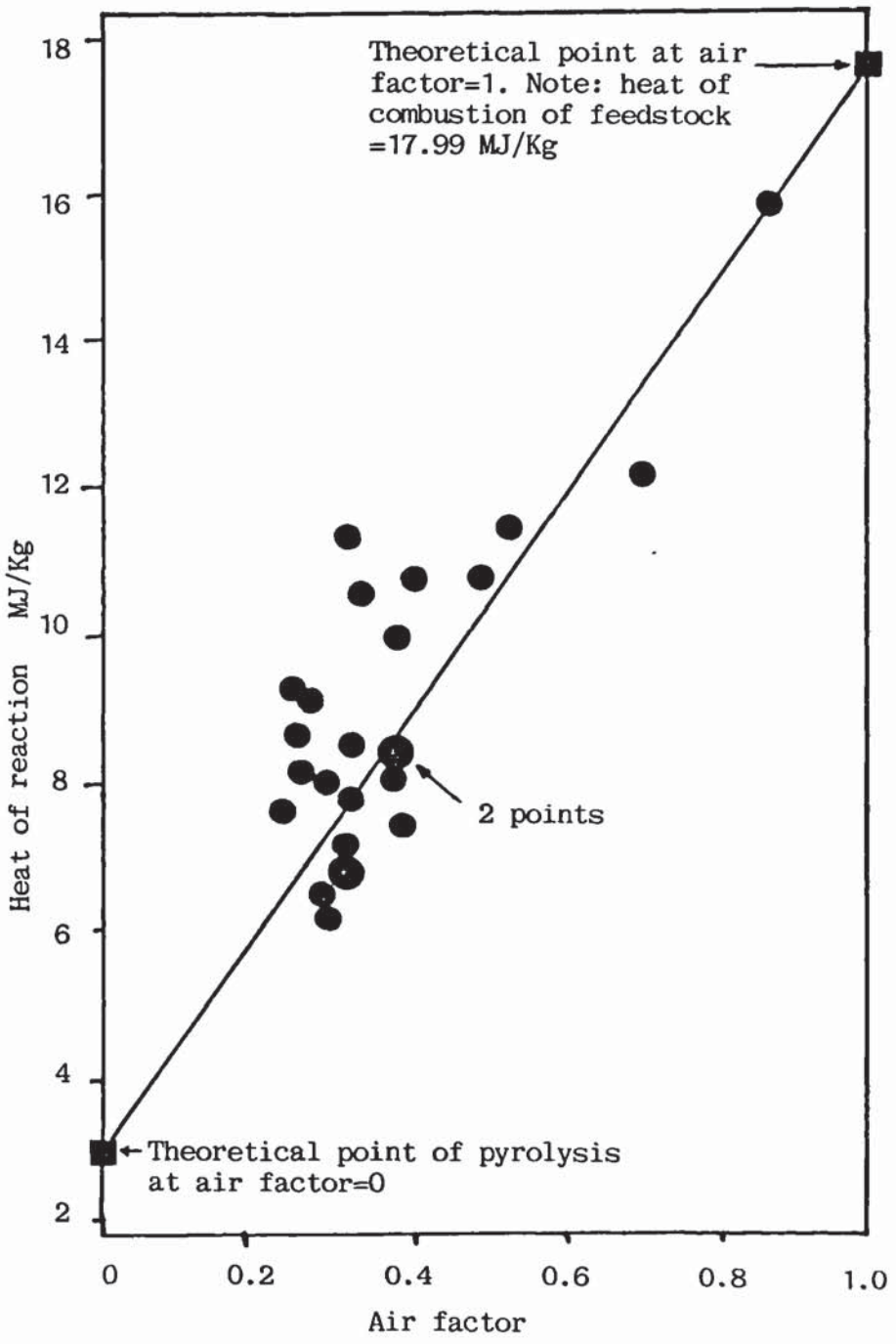

Figure 5.12 : Influence of the air factor on the heat of reaction

Although the results are somewhat scattered, there is a clear trend that the heat of reaction increases with increasing air factors. This is readily explained by the occurence of more complete combustion as the oxygen content increases in relation to the feedstock flowrate. Under such conditions the concentrations of hydrogen, methane, carbon monoxide, ethylene, ethane and tars decrease, while the concentration of the products of combustion (carbon dioxide and water) increase.

The data of Figure 5.12 were extrapolated to find the heat of reaction at a zero air factor. This is assumed to be the heat of pyrolysis in the absence of oxygen. These results indicate that the overall pyrolysis reaction with this feedstock is mildly exothermic, with a heat of reaction of about 3 MJ/kg. For a feedstock with high moisture content the heat of pyrolysis would become endothermic, while for a dry feedstock the exothermicity of the heat of pyrolysis would increase. These results are consistent with published results (68).

5.9.3 Heat losses through reactor walls

In the energy balance the heat losses through the reactor walls were considered. These were calculated using equation 5.32 (190):

$$\text{Heat loss reactor walls} = \frac{K \times S \times \Delta T}{X} \qquad \text{equation 5.32}$$

where K = thermal conductivity of insulation
S = surface area
X = thickness of insulation
ΔT = temperature difference between inside and outside walls.

The thermal resistances were calculated and supplied by the manufacturer of the insulating material. The following values were given :

for the bed walls : k_b = 0.3125 kcal/m²h °C
for the freeboard walls : k_f = 0.6313 kcal/m²h °C
for the ceiling of the bed: R_c = x/k = thermal resistance = 1.0144 m²h °C/kcal

To account for the heat losses through all measuring ports and openings, the manufacturer of the insulating material and Vyncke Warmtetechniek

recommended that the calculated heat losses through the reactor walls be increased by a factor of 2. Also to account for the heat losses to the non-fluidized sand bed below the distributor and through the non-insulated conical wall at the bottom of the reactor, it was recommended to further increase the heat losses by a factor of 2.

The heat losses through the reactor walls calculated by equation 5.28 were in the range of 81-130 MJ/h with an average of 102 MJ/h. The heat losses correspond to 1-10% of the energy in the feedstock. However, if only the experiments with air factor in the range of 0.2 to 0.4 (which is the optimum range for gasifiers) are considered, then the heat losses through the reactor walls accounted for 1%-3.5% of the energy in the feedstock, with an average of 2.2 %. This is generally considered an acceptable value.

5.9.4 Unaccounted heat losses

The application of equation 5.31 resulted in unaccounted heat losses which were in the range of -14 to 35% of the total energy input, while the average value was 13.38 %. This is rather high. However, if only runs 27 to 38 (during which care was taken to measure the feedstock flowrate more accurately, see section 4.3.2.3) are considered, then the average unaccounted heat losses are reduced to 9.35 % which is more acceptable (within about 10% variation). Also runs 13 to 28 were made with low feedstock flowrates, hence the heat losses were relatively high. This is clearly shown in Table 5.19, where the heat losses are much higher for runs 13 to 26 than for the rest of the runs.

Moreover, any increase in the accounted heat losses (see previous section) would reduce the unaccounted heat losses accordingly.

It has been reported (79) that from a reactor of 12 m outside diameter with 1 ton/h capacity, the heat losses through the reactor walls were 29.1 % of the output energy from the gasifier with 6.9 % unaccounted heat losses.

Figure 5.13 indicates that there is no significant influence of the reactor bed temperature on the unaccounted heat losses. This supports the reasoning that these heat losses are mainly due to low feedstock flowrates (for the initial runs) and to high heat losses through the reactor walls, since the heat losses are a function of the operating temperature (189).

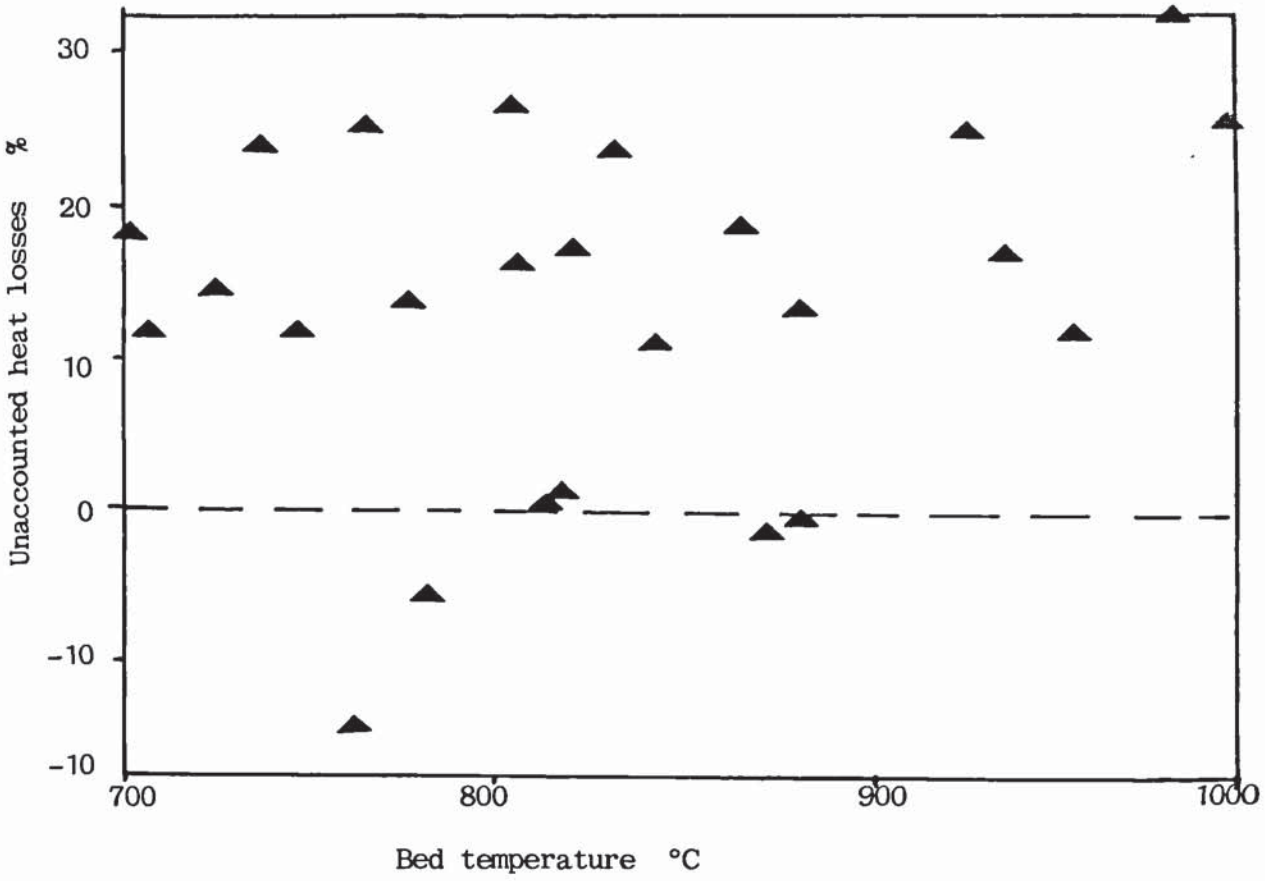

Figure 5.13 : Influence of reactor temperature on the heat losses

5.9.5 Thermal efficiency

The calculated thermal efficiencies were in the range of 5.8 to 82.7 % with an average of 51.8 % (see Table 5.19). However, if only the experiments with feedstock flowrates higher than 160 kg/h are considered (which are the flowrates the gasifier would operate with under normal conditions; the others being tested for the influence of the turn down ratio), then the range of thermal efficiencies is 45 to 83 % with an average of 61 %. This is a good result, since it indicates that under normal operating conditions the thermal efficiency would be around 60% and if the sensible heat of the product gas would also be recuperated, then the overall efficiency of the gasification process in the fluidized bed could increase to about 80% (for example the overall efficiency of run 33 improves from 68.4% to 89.4%, while for run 32 from 57.8% to 77.1% if the sensible heat of the product gas, the sensible and

latent heat of steam and the sensible heat of fly ash are also included in equation 5.18, see section 5.2.5).

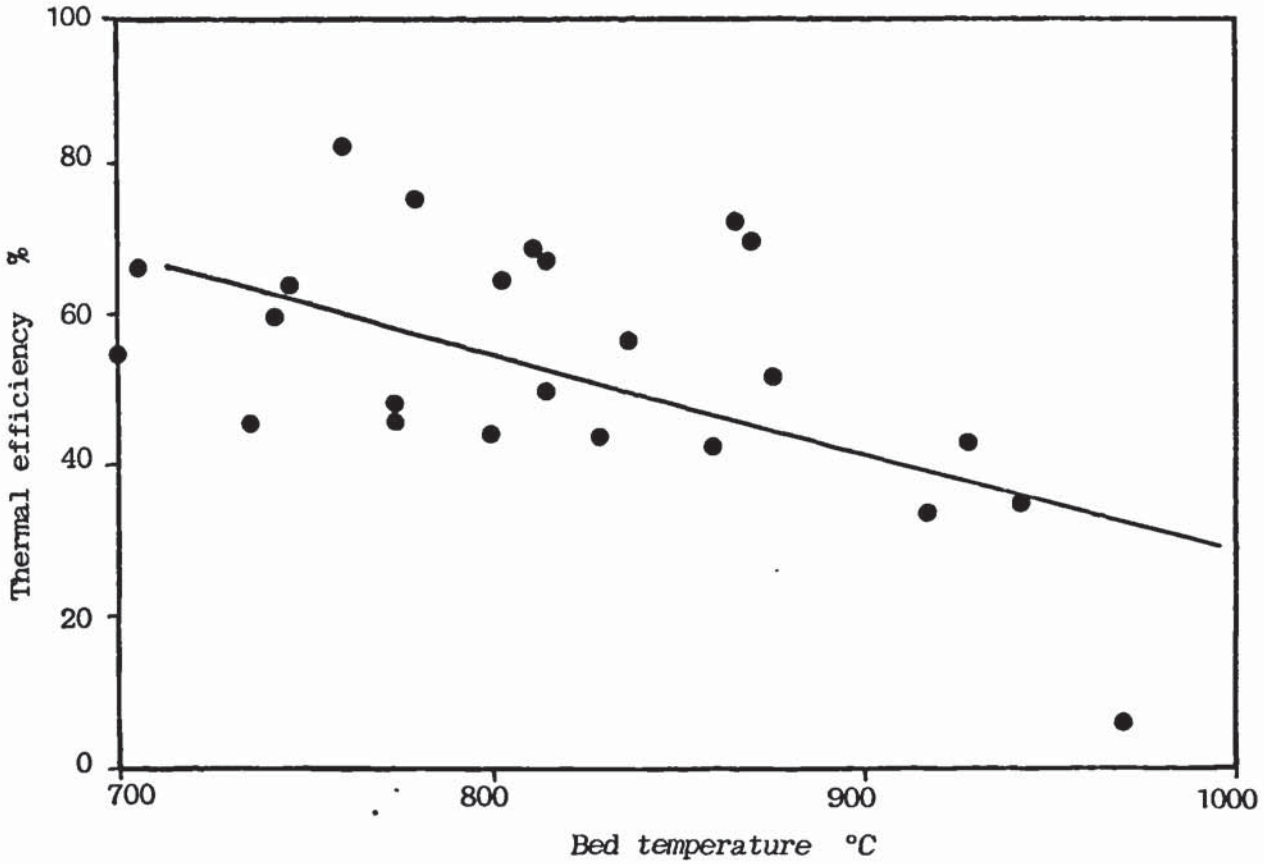

Figure 5.14 : Influence of bed temperature on the thermal efficiency of the gas.

Figure 5.14 shows the influence of bed temperature on the thermal efficiency. Although the data are scattered due to a range of air factors and other reaction parameters, it can be claimed that the thermal efficiency decreases with higher bed temperatures. *This behaviour is explained later in section* 5.11, where other data can also be incorporated in the discussion which gives a better coherence.

5.9.6 Comparison with published results

Table 5.20 shows a summary of the energy balance (see Table 5.19) along with results obtained from the laboratory pilot plant (104, 105, 108) and other published data from plants of similar scale of operation.

Table 5.20 : Comparison of energy balances, with published results

Author	Internal bed diam. m	Feedstock	Oxidizing medium	Unaccounted heat losses %	Thermal efficiency % cold gas
this work	0.8	chopped wood	air	(-14)-35	5.8 - 82.7 35-82.7(b)
V.U.B. (104)	0.15	cacao pellets	air + steam	20 - 40	40 - 60
V.U.B. (105)	0.15	wood shavings	air + steam	23 - 43	38 - 65
V.U.B. (108)	0.15	bark	air + steam	-	16 - 50
Flanigan et al. (92)	0.7	sawdust	air	1 - 43	50 - 70
Moreno (99)	1.3	cotton ginning	air	-	75 - 85(a)
Gurnik et al. (79)	12 outside	wood waste	air	6.9	44

(a) the sensible heat of the product gas is included.
(b) excluding run 16 in which the air factor was deliberatly set at 0.87 and thus the process was more combustion (starved air) than gasification.

The results of this work compare well with the published data, especially if run 16, which was at extreme (combustion) conditions, is excluded.

5.10 TEMPERATURE PROFILES IN THE REACTOR

In total there were four thermocouples installed in the reactor, two within the bed and two in the freeboard (for exact position see section 4.2.4.1 and Figure 4.4). Due to the high heat transfer rate in a fluidized bed, there should be no temperature gradients in the bed. Thus the two thermocouples in the bed should indicate approximately the same temperature. For all runs, the temperature profile is shown on the computer printouts in Appendix V. However, for illustrative reasons, some of the temperature profiles are also shown in Figures 5.15 and 5.16.

As the air factor increases, the bed temperature also increase. This is readily explained by the higher amounts of energy (heat) released due to more complete combustion of the feedstock, since the oxygen concentration in the system is increased.

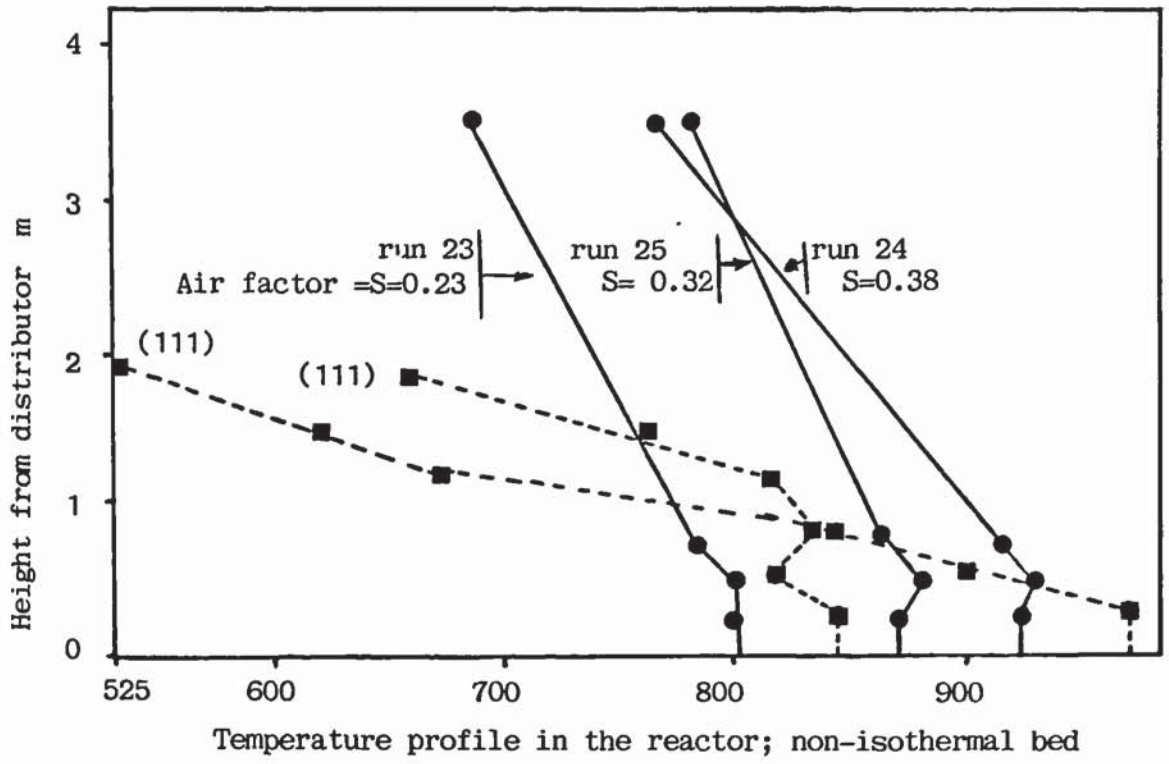

Figure 5.15 : Temperature profile in the reactor, non-isothermal bed.

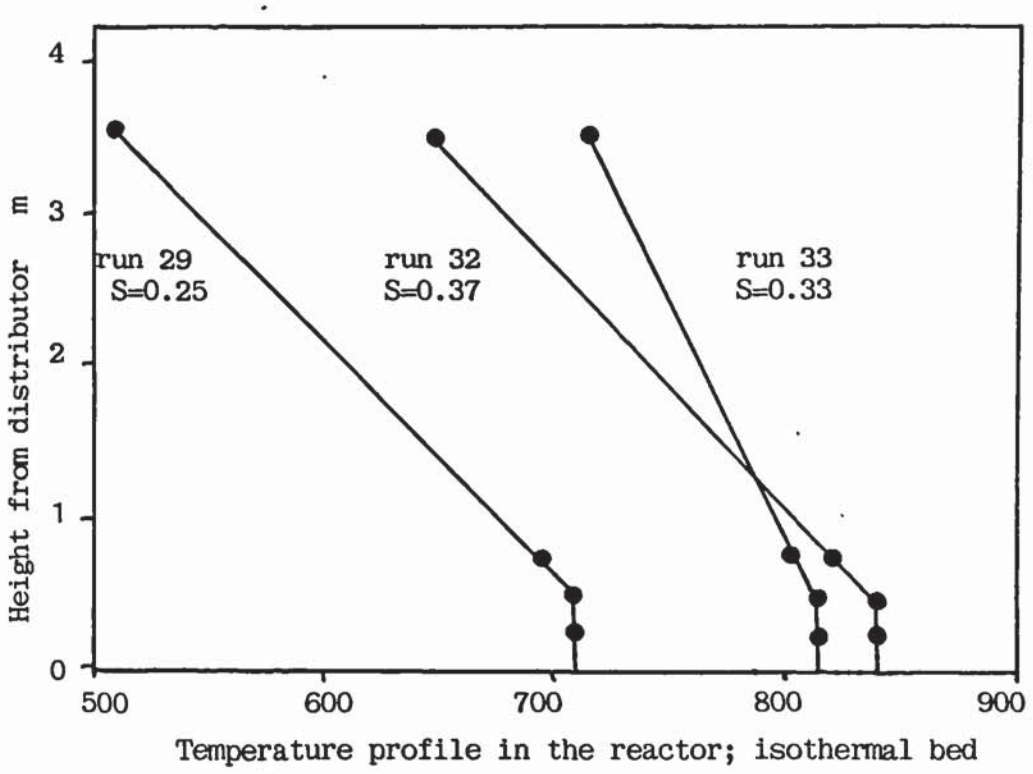

Figure 5.16 : Temperature profile in the reactor, isothermal bed.

In Figure 5.15 an anomaly in the temperature profile is indicated for runs 24 and 25, where a peak of temperature is shown at about 0.45 m above the distributor. Since there is no question about the degree of fluidization (these temperatures were stable whereas when the bed starts to de-fluidize the temperatures drop considerally), the only explanation can be the existence of a hot spot. This can occur when relatively fine and light particles of biomass tend to float at the top of the bed (105, 282) and their mixing is inadequate; several investigators have reported similar results (80, 86, 91, 99). Indeed, in Figure 5.15 the temperature profile of two runs from the literature are also shown (dotted lines with no data points) (111), where it is clear that the bed (1 m height) did not operate isothermally. However, this phenomenon occured rarely in this work and it can be tentatively explained by a smaller particle size and a higher fraction of fines than usually in the feedstock used for these experiments. Indeed, it was noticed that often the material at the end of the container had a higher fraction of fines than the front. This was probably caused because the bottom layer of the feedstock accumulated in the container to be used at the end (it was difficult to be picked up by the fork lift). The fines segragated to the bottom layer during transportation and handling of the container because of vibrations.

As shown in Figures 5.15 and 5.16 the temperature drops significantly in the freeboard region of the reactor. In order to improve the temperature profile, a fifth thermocouple was placed within the reactor at a height of 25 m above the distributor (see section 4.2.4.1 for the last two runs (41, 42). The temperature profiles of these two runs are shown in Figure 5.17. They are very similar to the temperature profiles of Figures 5.15 and 5.16. Similar results have also been reported by others (67, 68, 83) and practically identical profiles were obtained at the laboratory pilot plant (104-108), upon which the present P.D.U was designed.

Twice it has been reported, however, that the temperature of the product gas leaving the reactor was only 10-30 °C lower than the bed temperature, (99, 114). Apparently in both studies fluidized beds without an expanded freeboard and with a relatively high bed and short reactor were used. This is justified by the need to continuously replenish the sand (the bed material was carried over to the cyclones) for one of these studies (114); while for the other (99) there were size limitations, since that company was developing mobile fluidized bed gasification units and the design had to comply with highway safety standards.

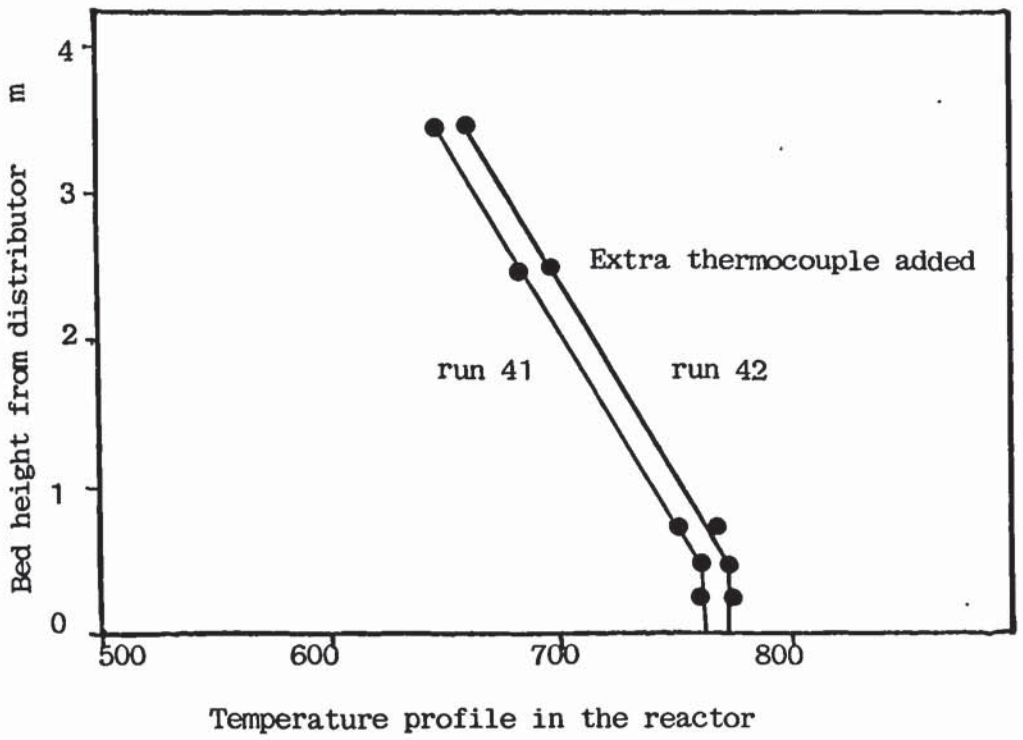

Figure 5.17 : Temperature profile with extra thermocouple in the freeboard.

5.10.1 Influence of bed temperature on gas composition

The influence of the bed temperature on the gas composition is shown in Figure 5.18, in which the results of runs 22-27 and 35-36 are given. These runs were performed with a feedstock flowrate in the range of 210-232 kg/h and an air factor range of 0.23-0.38.

It is shown that the volume percent concentration of carbon monoxide and hydrogen pass through a maximum at about 820 °C, while the concentration of carbon dioxide has a minimum at about the same temperature. Methane has practically a constant concentration of about 5 vol.% till about 820 °C and drops thereafter. Ethylene and ethane have constant concentrations till about 780 °C and fall thereafter to concentrations below 0.5 and 0.1 vol.% respectively for the former and the latter. A similar behaviour is presented by the higher heating value of the gas, which has an average value of 6 MJ/Nm^3 till about 820 °C but drops thereafter.

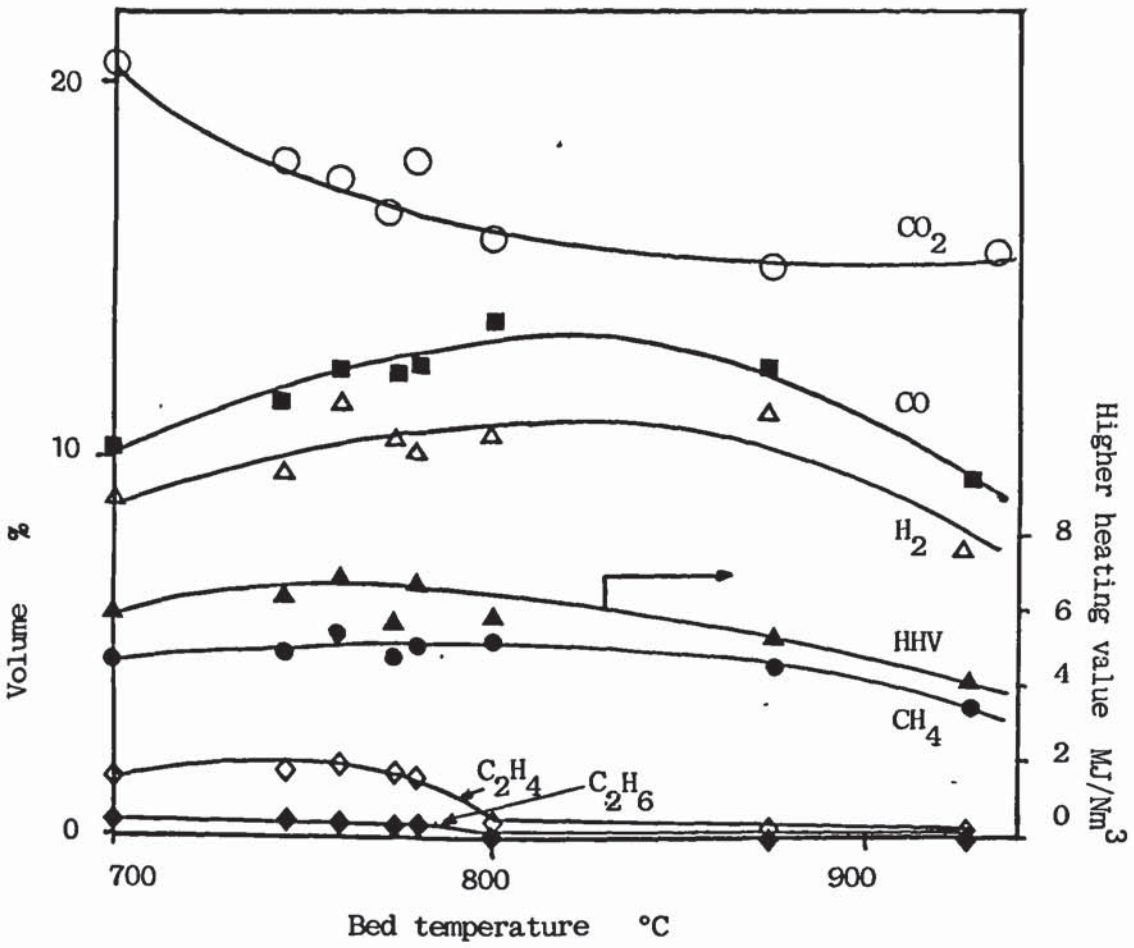

Figure 5.18 : Variation of volume % concentration of gas components with bed temperature.

The decrease in the concentrations of carbon monoxide and hydrogen below 800 °C can be tentatively explained by the assumption that below this temperature the pyrolysis products (tars and condensable organic vapours) predominate due to the low temperature and hence the cracking reactions (which could transform the pyrolysis products to lower hydrocarbons) are very slow. Moreover, as has been shown in section 5.7.3 and Figure 5.10, the water gas shift reaction does not approach equilibrium at these temperatures.

Above 830 °C however, more feedstock has to be combusted to maintain the temperature of the bed at that high level and thus the concentrations of the gasification products decrease, while the concentration of carbon dioxide increases.

In Figures 5.19 - 5.23,the concentrations of the individual gas components and the higher heating value of the gas are compared to thermodynamic prediction and published data (93). The thermodynamic data can be found in Appendix VII ,where the model developed in section 2.5.4.3 is applied for the experimental conditions of runs 13-38. The published data were obtained from sawdust. In general there is relatively good agreement between the published data and the results of this work with the exception of carbon monoxide and to a lesser extend carbon dioxide. Another difference is that in the published data, the concentrations of ethylene and ethane remain virtually constant up to about 1000 °C, which is not the case with the results of this work. However, this is acceptable considering the differences in the various parameters (such as feedstock properties, air factor, reactor design et al.). Moreover, both sets of data have the same characteristic curve.

This is also the case with the thermodynamic predictions. Although the experimental data deviate from thermodynamic predictions (which was expected), nevertheless they follow the same pattern of maxima and minima around 820 °C.

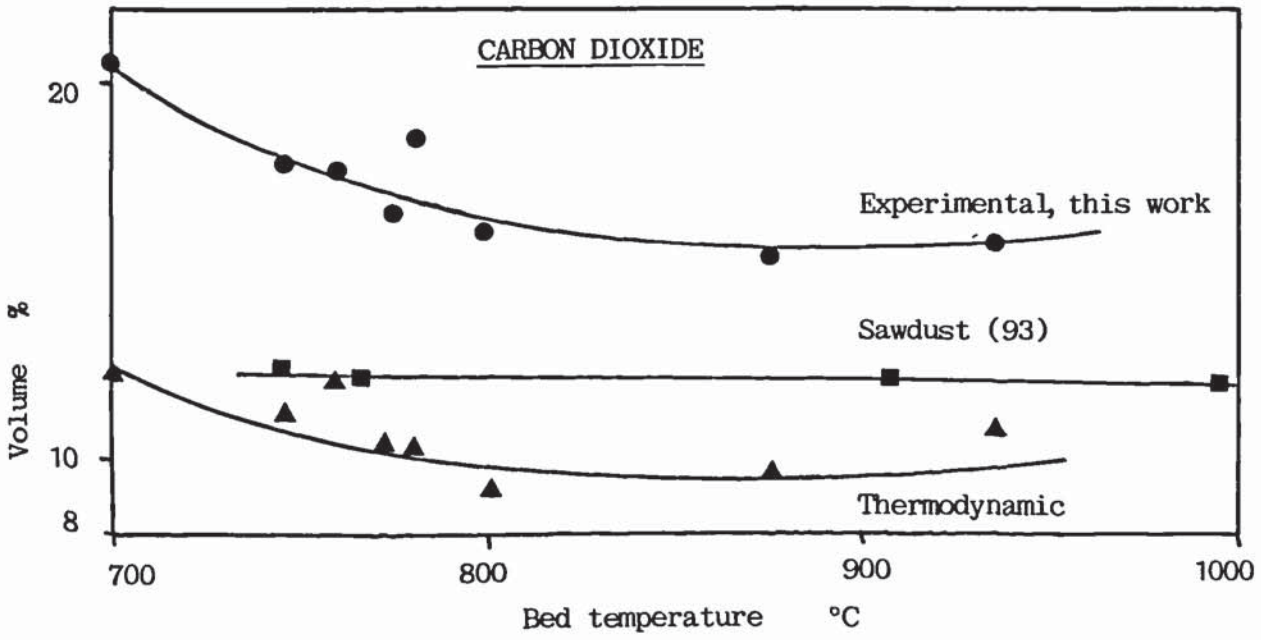

Figure 5.19 : Volume % concentration of CO_2 versus bed temperature.

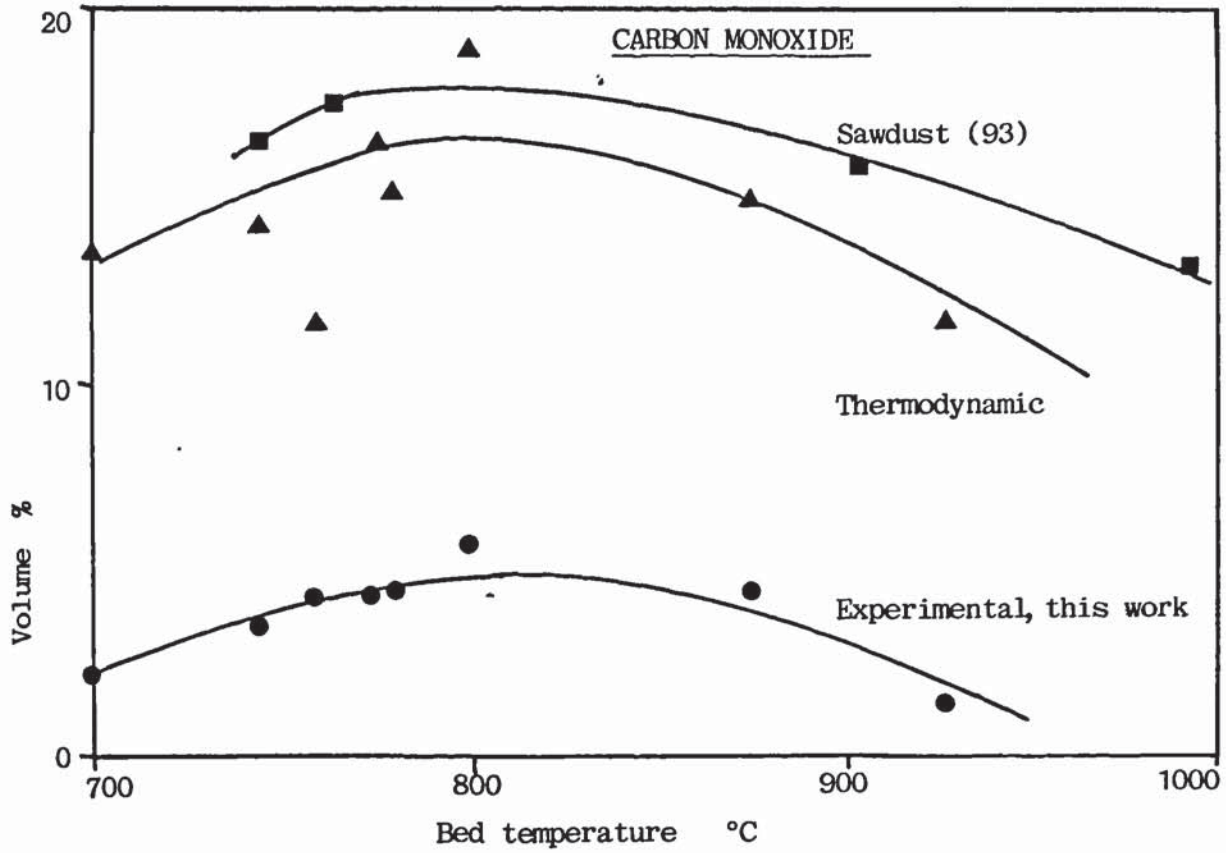

Figure 5.20 : Volume % concentration of CO versus bed temperature

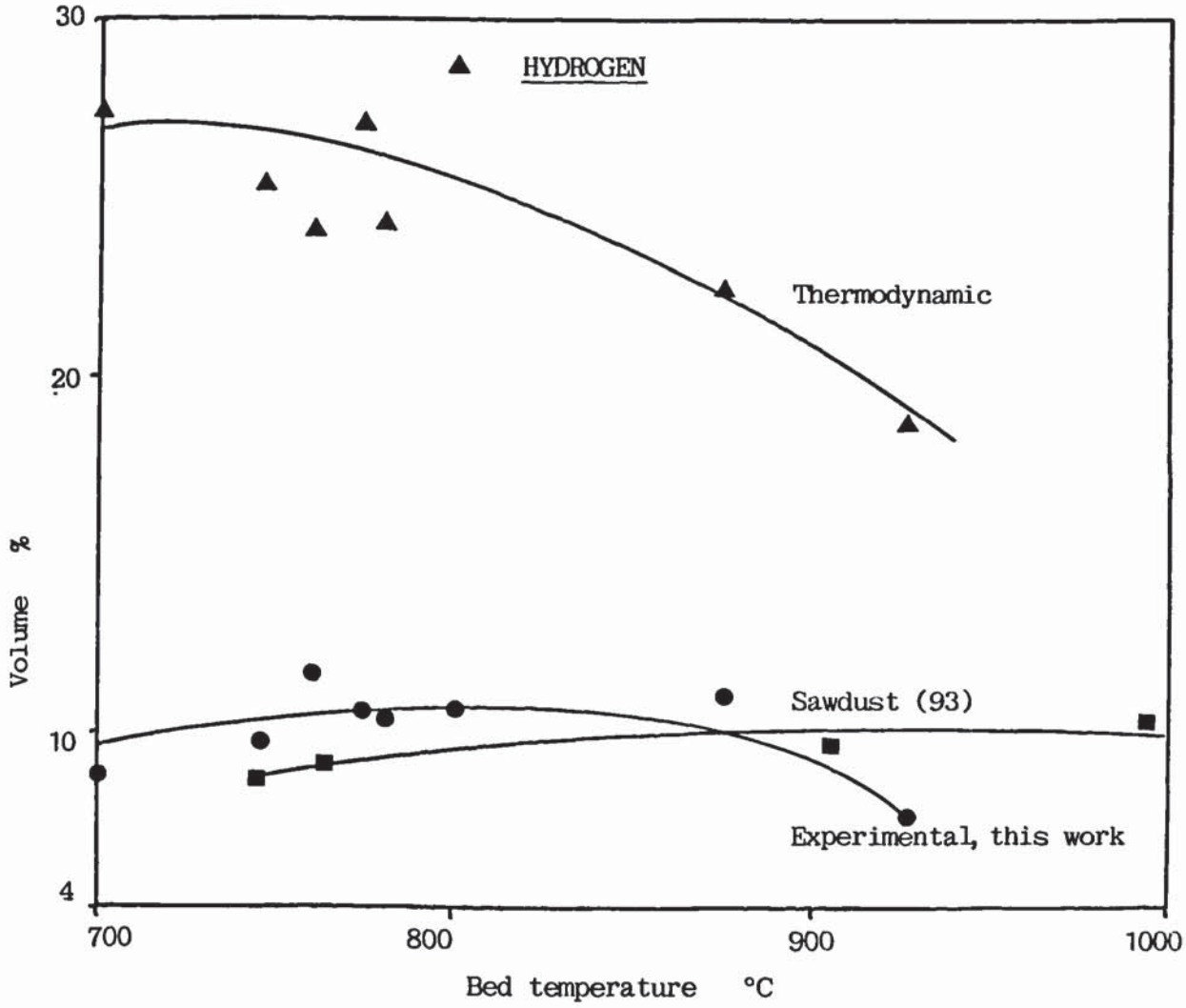

Figure 5.21 : Volume % concentration of H_2 versus bed temperature

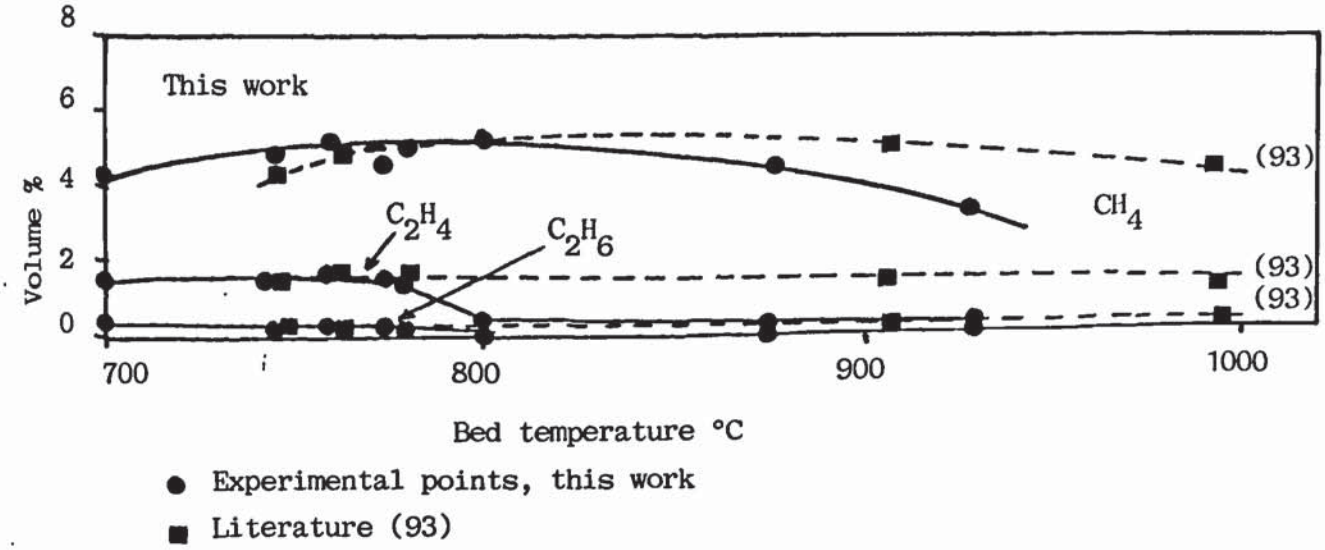

Figure 5.22 : Volume % concentration of CH_4, C_2H_4, C_2H_6 versus bed temperature.

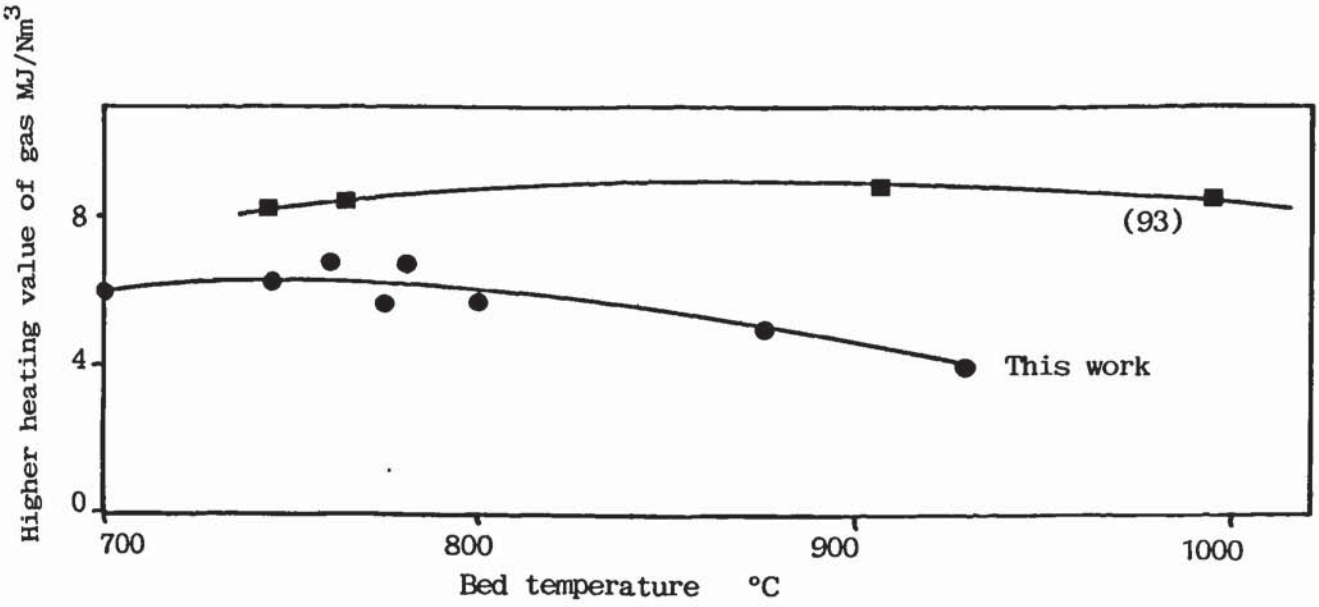

Figure 5.23 :. Higher heating value of gas versus bed temperature

However, several others (66-69,83-89 and 104-108) have reported results in which the concentrations of the components of the gas increase with increasing bed temperatures. Nevertheless, these authors increased the bed temperature by means others than the feedstock and air flow rates (which is the case in actual fluidized bed gasifiers), eg. with electrical heating blankets. Therefore their results are correct and indicate that, if higher temperatures are reached - with all other variables constant -, then the rate of the gasification reactions will increase (see section 2.5.5), as well as the concentrations of the gasification products.

It can therefore be concluded that there is no contradiction between the conclusion of the first and second group of authors.

5.10.2 Influence of bed temperature on the higher heating value of the gas

As the concentrations of the gasification products decrease with higher temperatures, the heating value of the gas will also decrease, since it is calculated on the basis of the gas composition (see section 5.2). This is shown in Figure 5.24, where the higher heating value of the gas is plotted against average bed temperature for all runs.

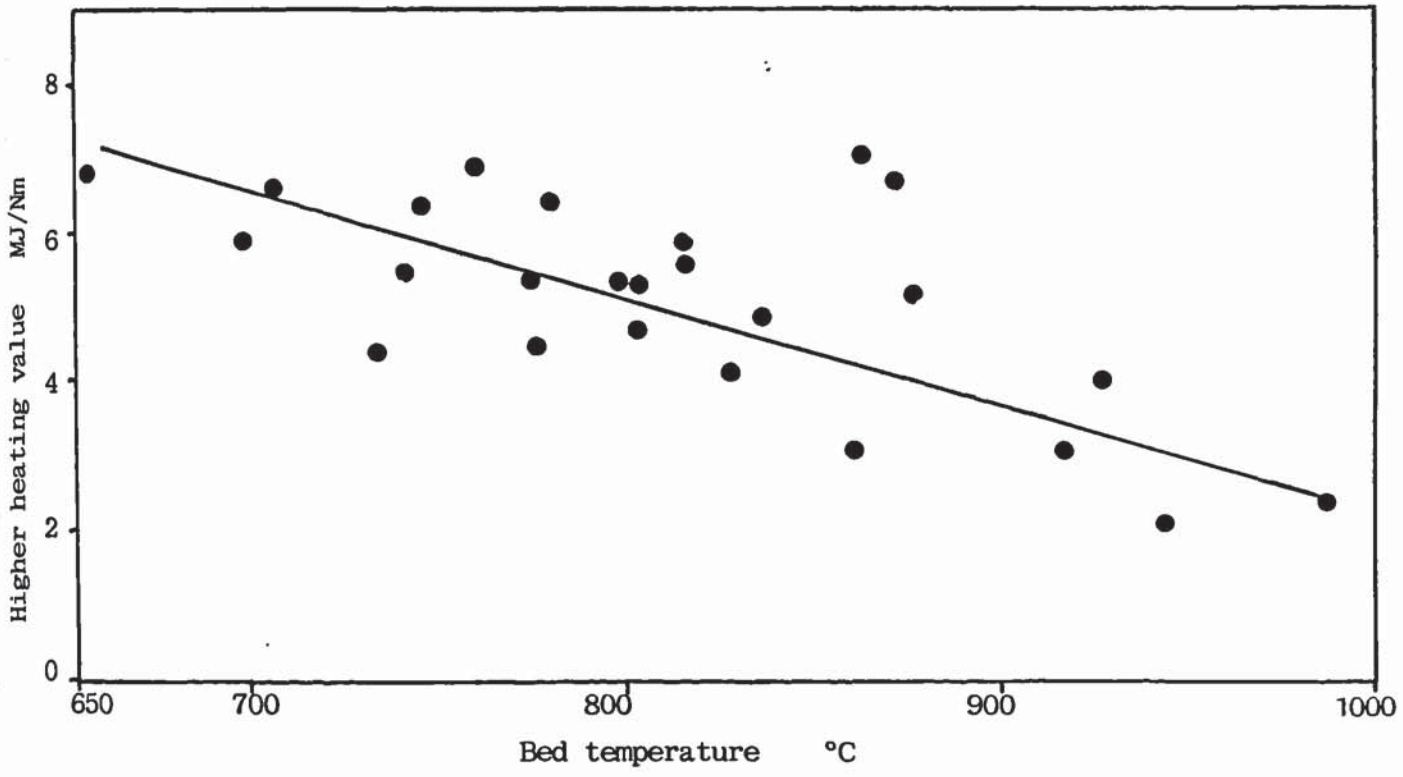

Figure 5.24 : Influence of bed temperature on the higher heating value of the gas.

5.11 THE AIR FACTOR

5.11.1 Introduction

The air factor or equivalence ratio is the most important operating parameter in gasification (see section 2.4.3.3). In addition, this parameter can be directly related to thermodynamic predictions and it is the only independent

variable (as far as feedstock and oxidant flowrates are defined) of the gasification process. Its importance in a fluidized bed gasifier is enhanced since it is also a control variable and is determined by the air flow rate for the fluidization process.

The air factor varies in the range of 0-1; at 0, where no oxidant is added to the system, pure pyrolysis takes place and the product characteristics depend on the thermal degradation of biomass (see section 2.5.3). However, at an air factor of 1, thermodynamics predict almost complete combustion of the feedstock to carbon dioxide and water. In between 0 and 1 gasification takes place and the product characteristics depend on several factors (such as temperature, heating rate, gaseous atmosphere, size of feedstock, type of gasifier, presence of catalyst et al. - see also section 2.2.1), with the air factor having the strongest influence on the process. In this region an optimum range must be found in which a gasifier could operate efficiently and the product gas meet the required specifications.

When the air flowrate is increased, the amount of available oxygen and therefore the degree of oxidation also increases. Additional heat is liberated and the temperature in the bed rises. In consequence more carbon dioxide is formed and the concentration of nitrogen in the product gas stream also increases. Conversely, when the air flowrate is decreased the temperature is reduced and the concentrations of the pyrolysis products, including tars and condensible organic vapours will increase. Therefore certain compromises need to be made in order to determine the optimum operating value for the air factor.

These compromises largely depend on the application of the product gas. If for example, the gas is to be combusted in a generating set to produce electricity, tars cannot be tolerated. Thus, it is advisable to run the gasifier at a higher air factor, which will result in higher temperatures at which the tars may crack to lighter hydrocarbons. However, operation at higher air factors will also result in reduced higher heating value of the gas, which will reduce the thermal efficiency of the process. If the gas is to be combusted in a boiler, then tars present no problem and the gasifier can be operated at the air factor for which maximum thermal efficiency is obtained.

Thermodynamic considerations define the optimum air factor range for gasification between 0.2 and 0.4, while the maximum chemical energy in the

product gas is obtained at an air factor of 0.28 (for air gasification of dry wood at 1 atm.) (109) (see section 2.4.3.3 and Figure 2.19). This range of air factor has also been confirmed experimentally (104-108).

No other group has been correlating their research results with the air factor, except the group of the free University of Brussels. Two other groups (Missouri Rolla and Twente University) correlated few of their results with the air (kg) to fuel (MAF) (kg) ratio. Although this parameter has the same effect on the gasification process as the air factor, it cannot be related directly to generalized thermodynamic predictions as there is no information about stoichiometry. Hence, it is advantageous to use the air factor in correlating gasification data. However, only limited comparison of the results with published data was possible.

5.11.2 Influence of the air factor on bed temperature

When a higher degree of combustion is attained, the rate of heat generation increases and as a consequence the bed temperature also increases. This is shown in Figure 5.25a, where the temperature of the bed is plotted against the air factor. At high values of air factor where complete combustion is approached, the heat generation and thus the bed temperature level off, since practically all biomass is consumed in the combustion process.

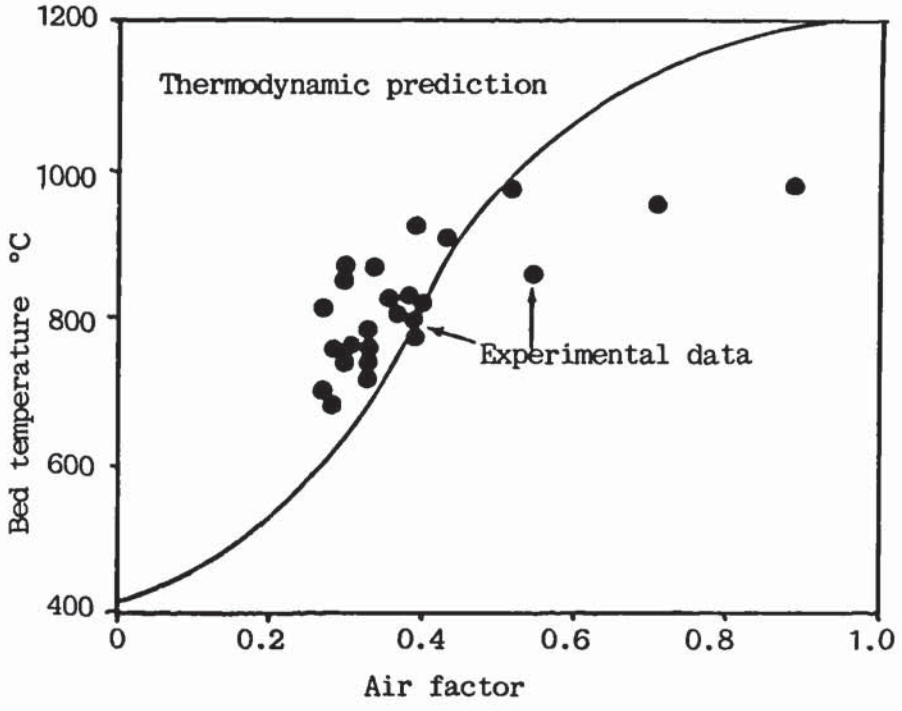

Figure 5.25a : Influence of air factor on the bed temperature.

As a result the chemical energy in the product gas drops to zero, since theoretically the only possible products at an air factor 1 is carbon dioxide and water. The line covering the complete range of air factor 0.0 to 1.0 corresponds to thermodynamic predictions (109). Good agreement exists between the results of this work and thermodynamic predictions for the range 0.2 to 0.5. However, above an air factor of 0.5 thermodynamics predict higher temperatures than the experimental ones. This difference is due to deviations from ideality, since at an air factor of 1.0 thermodynamics predict almost complete combustion to carbon dioxide and water, which is never the case in practice.

Similar results have been reported in the literature. Since the literature results were quoted on basis of air (kg) to fuel (MAF) (kg) ratio, the results of this work were converted to the same ratio for comparison and are shown in Figure 5.25b. There is very good agreement between the results of this work and the work of Twente University (96, 97) for air to fuel ratios in the range of 1 to 35. However, the results of Missouri Rolla University show good agreement with this work and the data of Twente University (if extrapolated) in the air to fuel ratios of 1-2, while above this range, they deviate significantly showing lower bed temperatures.

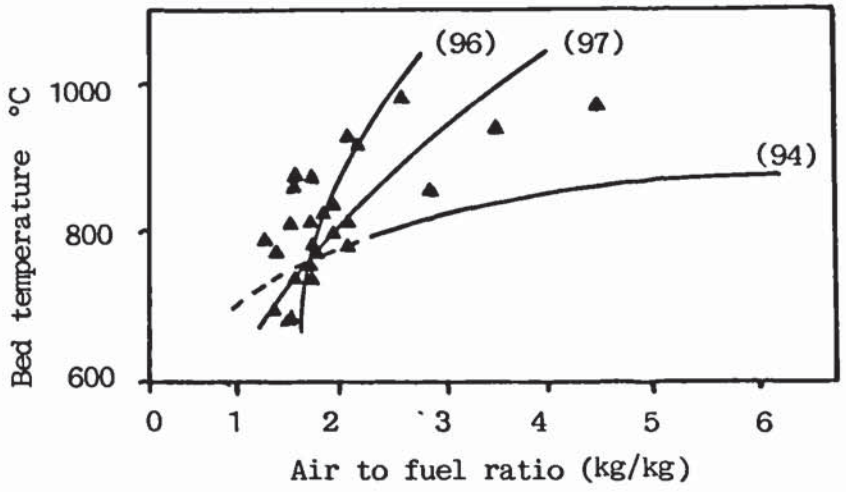

Figure 5.25b : Influence of air to fuel ratio on bed temperature, comparison with published data.

The temperature of the gases at the outlet of the reactor should also increase as the bed temperature increases, assuming that heat is lost only through the reactor walls. This is shown in Figure 5.26 from which can be concluded that

the temperature of the gases at the outlet is proportioned to the temperature of the bed.

In only one reference (111) it was possible to find data relating bed and outlet temperatures. These are also shown in Figure 5.26. In general there is acceptable agreement between the results of this work and the published data. The agreement is further improved in the range of 700 to 850 °C, if the published data are extrapolated below 800 °C (broken line).

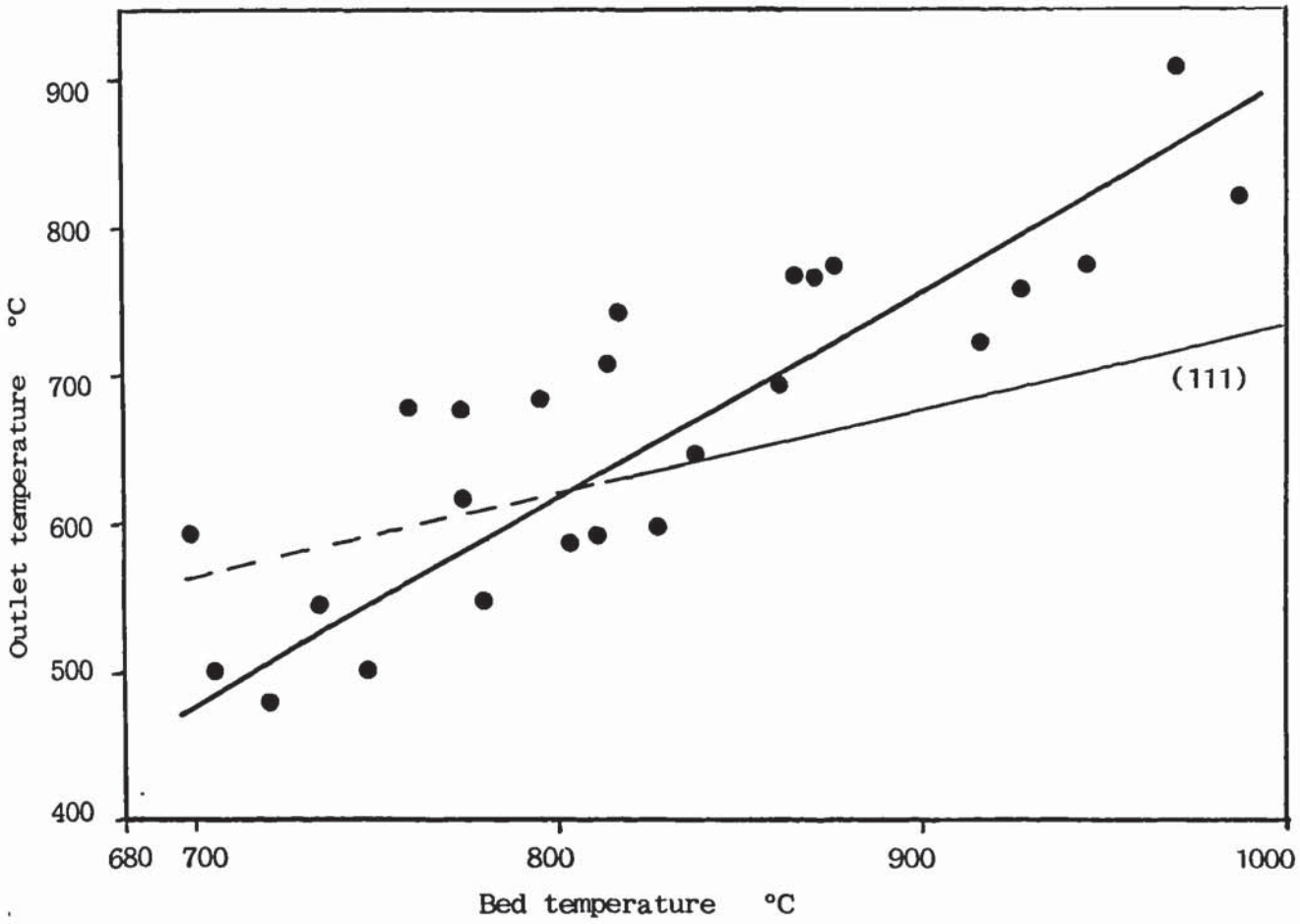

Figure 5.26 : Relationship between temperature of gases at the exit and bed temperature.

5.11.3 Influence of the air factor on the higher heating value of the gas

The influence of the air factor on the higher heating value of the gas is shown in Figure 5.27. The maximum higher heating value 7.0 MJ/Nm^3 was obtained at air factor 0.29 (run 38), while the minimum 0.31 MJ/Nm^3 at air factor 0.87 (run 16). The minimum was, however, obtained at an unrealistically high

air factor, where a fluidized bed gasifier would never operate (unless during heating up or shutting down). Thus for the practical range of interests - that is air factor between 0.2 and 0.4 - the higher heating value of the gas varied between 4.0 and 7.0 MJ/Nm^3.

These results indicate that the optimum operating range is between air factors 0.2 and 0.4. Moreover, the air factor at which the maximum higher heating value was obtained, 0.29, agrees very well with the thermodynamic prediction of 0.28 (see Figure 2.12). This result as well as the results of Figures 5.19-5.21, indicate that although there is a significant difference between experimental results and thermodynamic prediction, the trend is the same as well as the maxima and minima. This is an important conclusion, since thermodynamic prediction can be directly linked to experimental results as far as trends maxima and minima are concerned.

In Figure 5.27 some of the results obtained from a laboratory pilot plant at the Free University of Brussels (105, 108, 112) are also plotted for comparison. The data with wood shavings (105) and refuse derived fuel (112) agree relatively well with the results of this work. However, the data with bark (108) are significantly lower than those obtained at the process development unit.

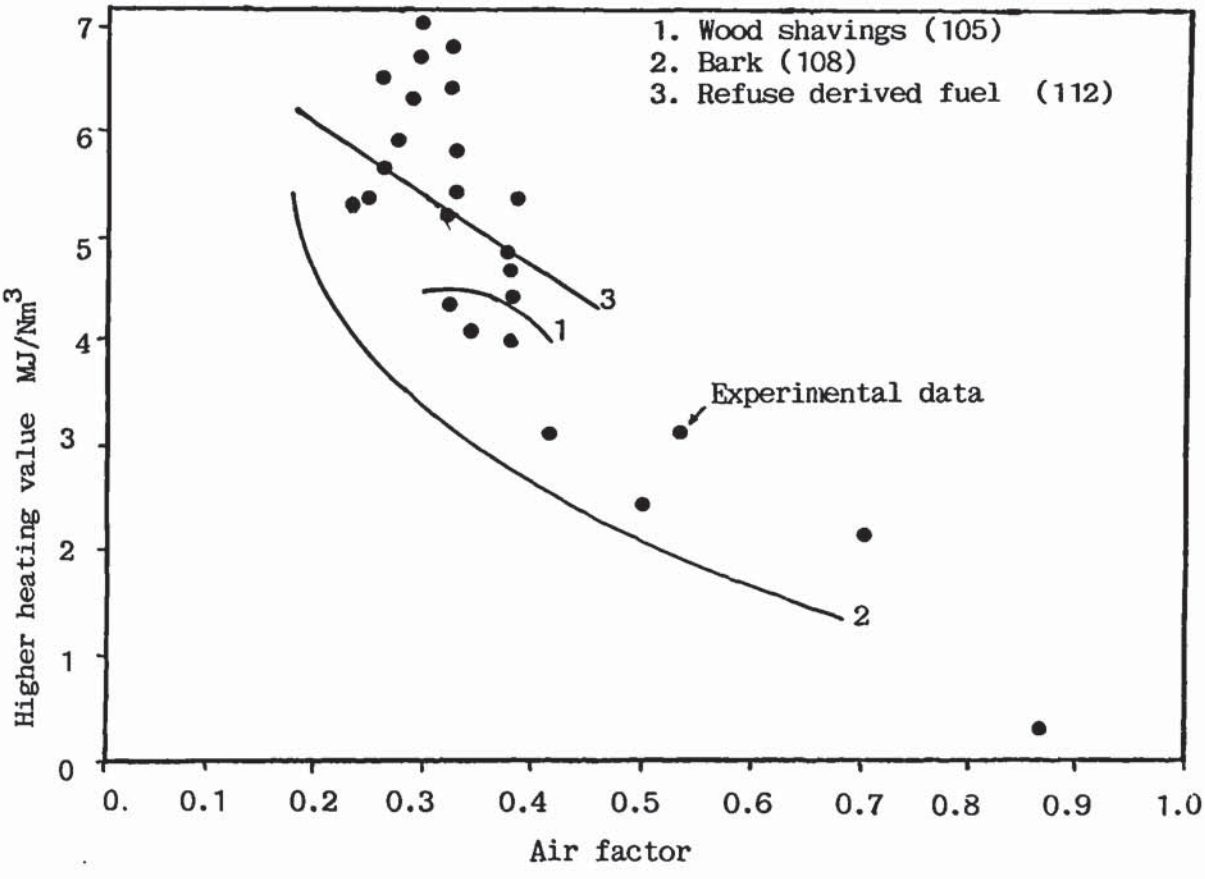

Figure 5.27: Influence of the air factor on the higher heating value of the gas

This difference is due to the very high ash/inerts content (24 wt%) of the bark which resulted in a gas of inferior quality. Nevertheless, the trend is the same, i.e. highest values were obtained in the air factor range of 0.2-0.4, while above this range the higher heating value of the gas drops significantly.

The results are compared to thermodynamic predictions in Figure 5.28. The thermodynamic data were obtained from Appendix VII. Surprisingly there exists good agreement between the two sets of data. This can tentatively be attributed to the fact that thermodynamics predict very small (below 1 Vol.%) concentrations for methane, while they cannot predict at all ethylene and ethane. Thus the existence of these gas components compensate for the lower concentrations of hydrogen and carbon monoxide in the product gas than predicted by thermodynamics (see Figures 5.20 and 5.21).

In order to facilitate comparison of the results of this work to other published data, the air factor was converted to air to fuel ratio and the higher heating value of the gas was plotted versus this parameter, along with data from the literature (93, 111). These data are shown in Figure 5.29, from where it can be concluded that although different feedstocks were used, there is an acceptable agreement amongst the various data.

5.11.4 Influence of the air factor on the gas yield

The gas yield (defined in section 5.2.3) is an important parameter, since it can predict the total flow of gas from the feedstock flow. The gas yield obtained in this work is plotted versus the higher heating value of the gas in Figure 5.30. Due to the higher degree of combustion at high air factor valves the gas yield increases.

These results are supported by published data of the Free University of Brussels (105, 108). As with the higher heating value of the gas the agreement with the wood shavings (105) is very good, while bark (108) gave higher gas yields. This is again attributed to the high ash/inerts content of the bark used. No other published data were found correlating the gas yield with the air factor or air to fuel ratio. By extrapolating the curve in Figure 5.30 till an air factor of 0.0, the experimental gas yield pure pyrolysis can be estimated. Thus about 0.4 kg gas/kg feed MAF can be produced by the thermal degradation of the feedstock. This value agrees very well with experimental data obtained from the pyrolysis of the softwood fraction of the feedstock in

a pyroprobe (158) (e.g. gas yield at 700 °C = 0.30, 850 °C = 0.40, 900 °C = 0.48 kg/kg feed MAF).

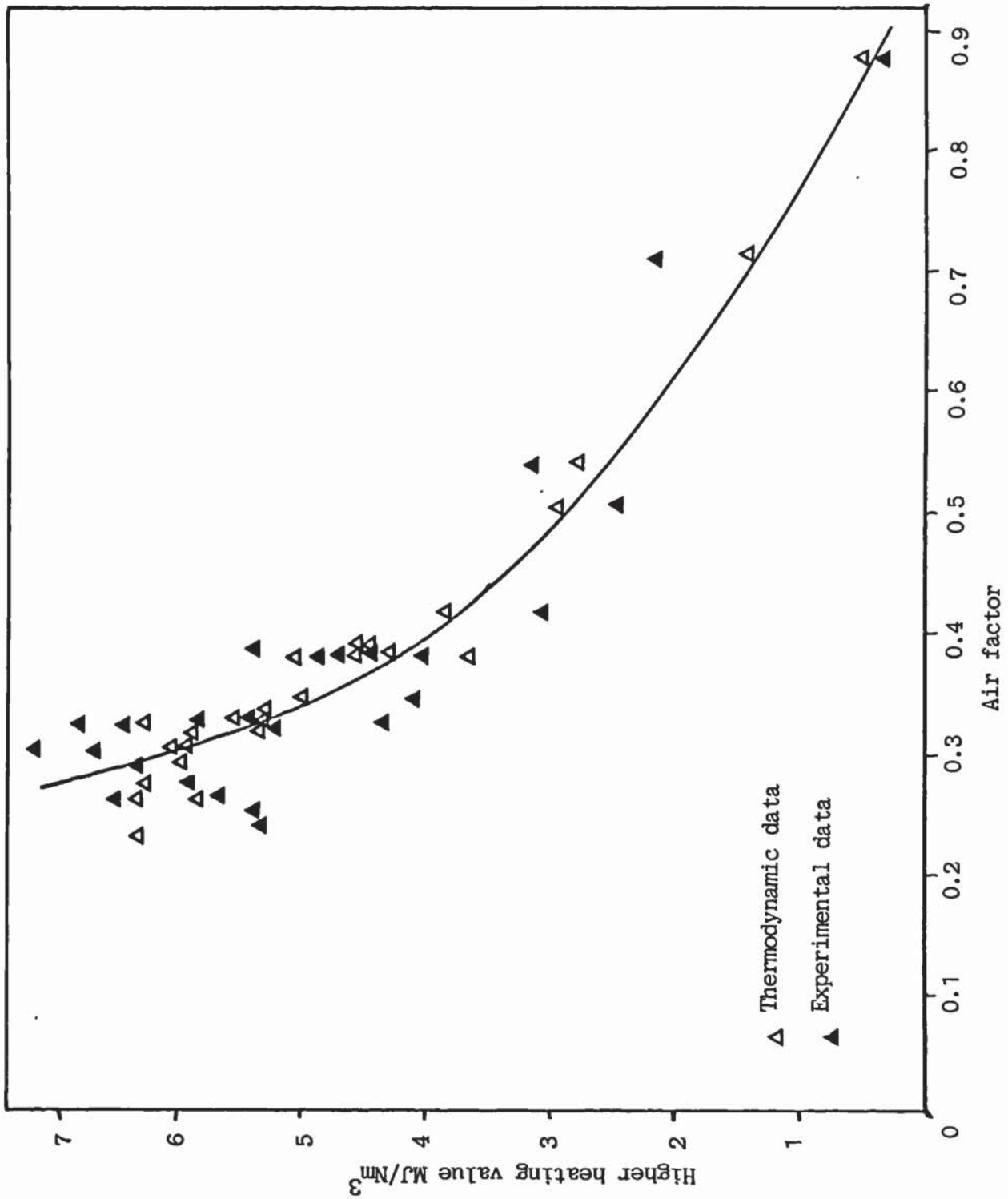

Figure 5.28 : Influence of the air factor on the higher heating value of the gas comparison with thermodynamic predictions.

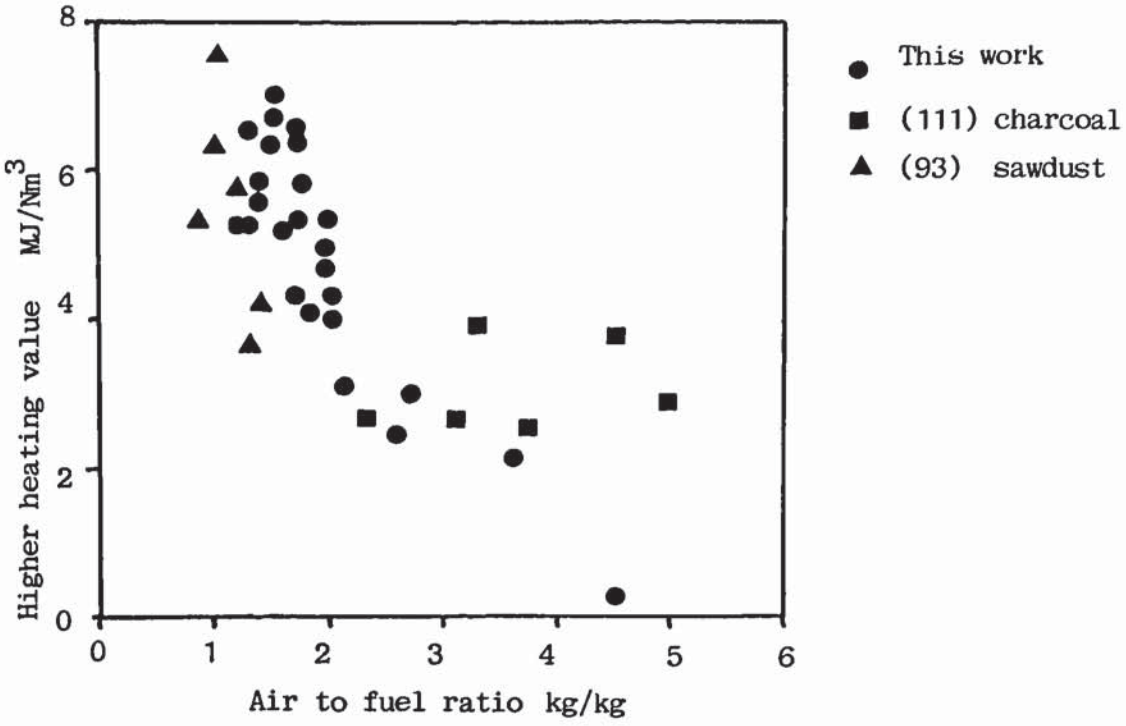

Figure 5.29 : Higher heating value versus air to fuel ratio, comparison with published data.

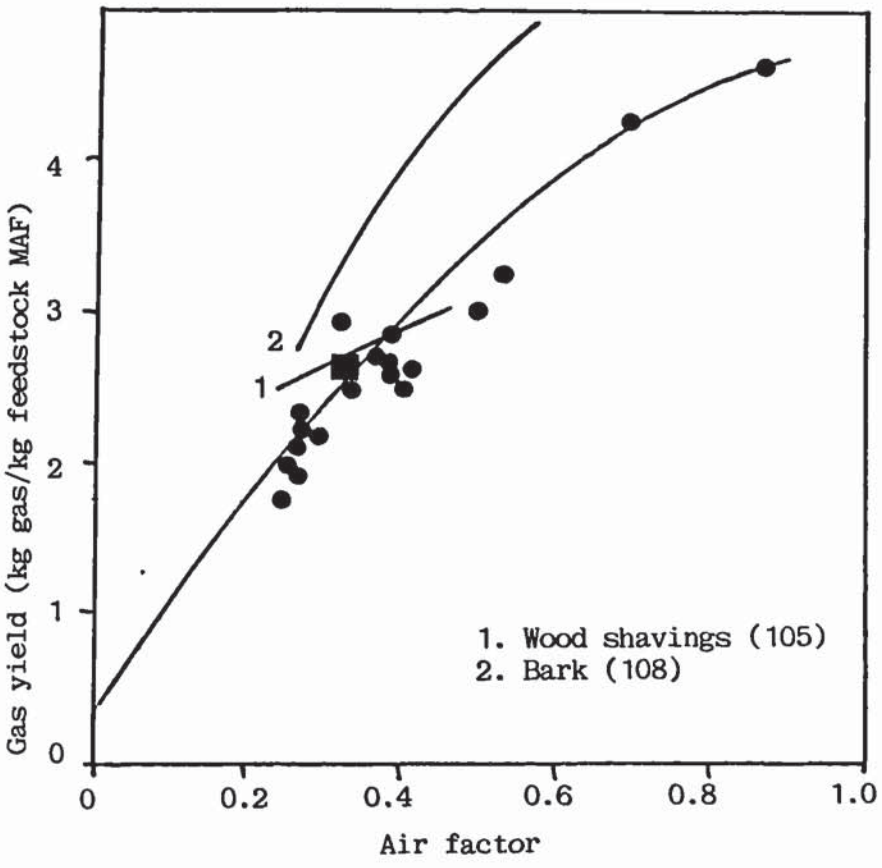

Figure 5.30 : Influence of the air factor on gas yield.

In general a gas yield between 2 and 3.5 kg gas/kg MAF feedstock was achieved in the air factor range of interest (0.2-0.4). When specifing the optimum air factor for a specific reactor and feedstock, the gas yield must be taken into consideration, since it is increasing with higher values of air factor while the higher heating value of the gas is decreasing. Thus on basis of these results, operation at an air factor of 0.2 would produce the following amount of gas.

$$G_g = G_f \times Y \qquad \text{equation 5.33}$$

where G_g = mass flowrate of gas in kg/h
G_f = mass flowrate of feedstock in kg/h
Y = gas yield

from Figure 5.30 the gas yield at air factor 0.2 is 1.8 kg gas/kg MAF feedstock and

$$G_g = 1.8\, G_f \qquad \text{equation 5.34}$$

The energy content of this amount of gas can be found from Figure 5.27. At an air factor of 0.2 the higher heating value of the gas is about 6.9MJ/Nm^3.

Thus:

$$\text{Total energy} = G_g \times \frac{1}{\rho_g} \times HHV \qquad \text{equation 5.35}$$

where ρ_g = specific gravity of the gas
HHV = higher heating value.

Substituting the appropriate values in equation 5.35 gives

$$(\text{Total energy})_{0.2} = \frac{12.4\, G_f}{\rho_g} \qquad \text{equation 5.36}$$

Repeating the same procedure for an air factor 0.4 gives :
$Y_{0.4}$ = 2.8 kg gas/kg feedstock (MAF), $HHV_{0.4}$ = 4.4 MJ/Nm^3)

$$(\text{Total energy})_{0.4} = \frac{12.3\ G_f}{\rho_g} \qquad \text{equation 5.37}$$

Dividing equation 5.37 by 5.36 and assuming that the specific gravity of the gas is the same in both cases, which is a valid assumption (see data on specific gravity of the gas in the printouts of the experiments in Appendix V),gives :

$$\frac{(\text{Total energy})_{0.4}}{(\text{Total energy})_{0.2}} = 0.99 \qquad \text{equation 5.38}$$

Therefore, operation at an air factor of 0.4 will result in practically the same overall efficiency due to higher gas yield, although the higher heating value of the gas will be decreased.

5.11.5 Influence of the air factor on the thermal efficiency

Since the higher heating value of the gas decreases as the air factor is increasing (see section 5.11.2), it follows that the thermal efficiency (see section 5.25) will also decrease.

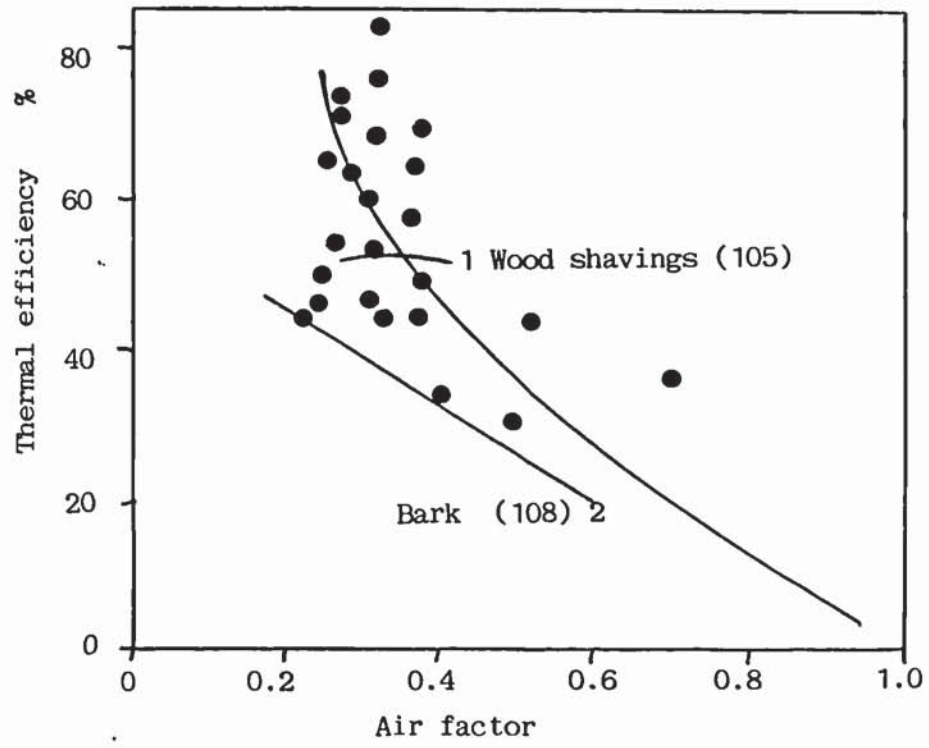

Figure 5 31 : Influence of the air factor on thermal efficiency

This is shown in Figure 5.31 where the thermal efficiency is plotted versus the air factor; for the practical air factor range of interest, the thermal efficiency was mainly in the range of 40 to 80 % while a maximum of 82% was obtained (run 36).

In Figure 5.31 some data from the literature are also compared to the results of this work. Relatively good agreement exists amongst the various data. The results are also compared to thermodynamic predictions in Table 5.21.

Figure 5.32 shows the results of this work in terms of air to fuel MAF ratio and compares them to other published data on the same basis.

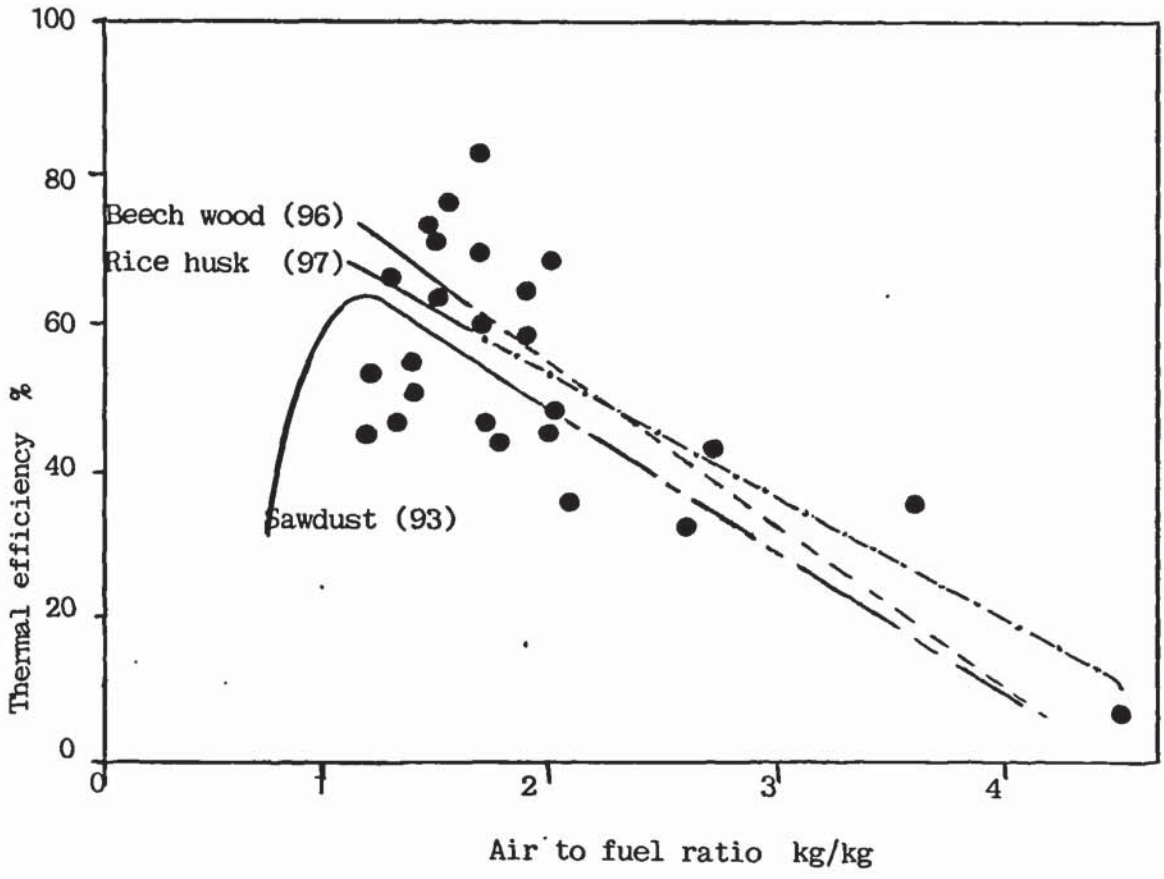

Figure 5.32 : Influence of the air to fuel ratio on thermal efficiency.

There is acceptable agreement amongst the data, especially if the data from the literature are extrapolated to higher air to fuel MAF ratios as the ones used in this work.

Table 5.21 : Comparison of experimental and thermodynamic results of the thermal efficiency of the gas

Run	Experimental Thermal efficiency %	Thermodynamic Thermal efficiency %	Ratio (exp/therm)
13	43.3	48.7	0.89
14	48.0	42.3	1.13
15	36.3	31.0	1.17
16	5.8	13.7	0.42
18	34.9	60.8	0.57
19	44.2	68.7	0.64
20	31.3	52.0	0.60
21	50.7	75.4	0.67
22	46.2	75.7	0.61
23	44.8	80.2	0.55
24	44.7	64.1	0.69
25	53.3	71.9	0.74
26	63.5	74.9	0.84
27	75.9	73.1	1.03
28	64.9	63.9	1.02
29	65.4	71.4	0.91
30	59.6	69.1	0.86
31	64.8	63.6	1.02
32	57.8	62.5	0.92
33	68.4	68.5	0.99
34	45.8	69.2	0.66
35	54.2	74.3	0.72
36	82.7	68.9	1.20
37	70.1	76.1	0.92
38	72.9	76.6	0.95

From Table 5.21 it can be deduced that reasonable agreement (ratio exp/therm. $\geq$ 0.85) between experimental and thermodynamic data of the thermal efficiency was obtained in most of the experiments.

It can be concluded that under optimum conditions (air factor about 0.28), thermal efficiencies above 60% can be expected in industrial fluidized bed gasifiers.

5.12 EXTENDED RUNS

5.12.1 Introduction

Usually it took about 5 to 6 hours to carry out one experiment (see section 4.4), while the actual gasification period was about 2 to 3 hours, depending on the thermal state of the reactor at the beginning of the experiment. With other activities carried out at the plant (cleaning up, maintenance, supply of

feedstock and gases for gas chromatography, moisture and ash determination for the feedstock, administration, et al.) the normal 8 working hours were completed. Since there was only one technical assistant (who controlled the feeding hopper, see section 4.3.2), the author took all measurements and made the gas analyses during the experiments. No other assistance was provided by Vyncke Warmtetechniek unless in case of a breakdown or maintenance of equipment. Thus it was not possible to extend the actual operating time beyond six hours.

In order to obtain data on extended runs, the author tried to carry out an experiment (run 36) for about 5 hours gasification times, on his own. However, analysis of the results showed that there were significant variations in the feedstock flowrate which resulted in unsteady state operation (see subsequent discussion in this section). Thus permission was requested for the technical assistant to stay for some days few hourslonger, so that two extended time runs could be performed. This was granted by Vyncke Warmtetechniek. A request later for the provision of three shifts for a 24 hours experiment was not approved by this company. Hence two runs (37, 38) were made which lasted in total for about 10 hours, from which 4 hours were actual gasification operation.

Figures 5.33 - 5.38 show respectively the variation with time of the bed temperature (average), the freeboard temperature (at the exit), the higher heating value of the gas and the gas composition of runs 36, 37 and 38.

5.12.2 Bed temperature

From Figure 5.33, it can be deduced that from 0 to 2 hours, the temperature of the bed increases towards the steady state value. After about 2 hours, the temperature of the bed levels off and it should not increase appreciable unless there is an interruption of the feeding.

For run 36 a drop in bed temperature is noticed at 3/4 and 2 3/4 hours, while for the last 1 1/2 hour the bed temperature stabilized in the range of 750 to 755 °C. The bed temperature of run 37 stabilized after 2 hours in the range of 850 - 855 °C; however, it increased from this temperature to 884 °C within half hour (at 3.0 hour) and then dropped to 865 °C at the end of the run. For run 38, which was performed under identical experimental conditions with run 37, the bed temperature stabilized after 2 1/4 in the temperature

range of 830 to 835 °C for 1 hour; however, at 3 1/2 hours it started increasing till it reached 858 °C at the end of the run.

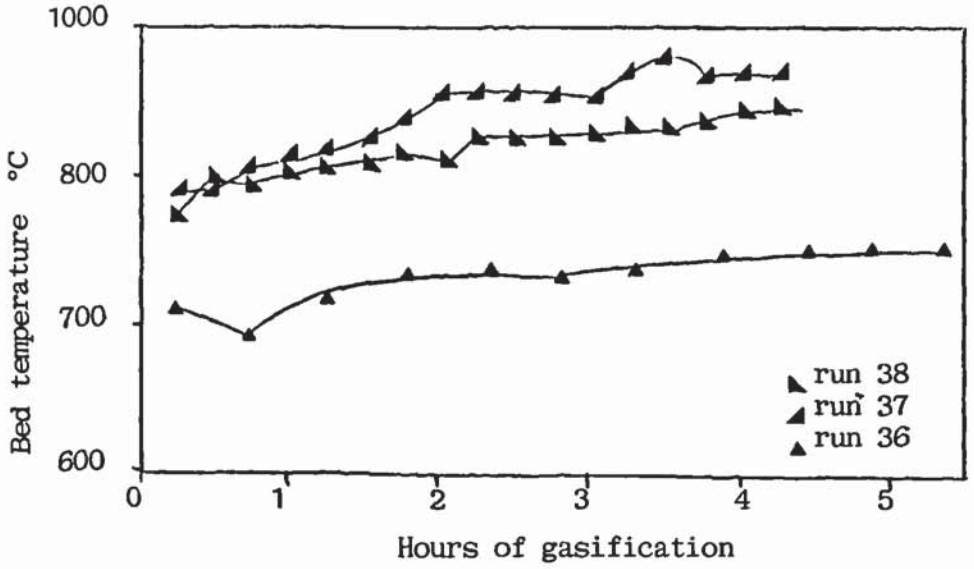

Figure 5.33 : Variation of bed temperature with time.

The variations in bed temperature with time, when a steady state has been attained after about 2 hours gasification, are attributed to unstable feedstock flowrate. Indeed, if the feedstock supply is increased, the temperature of the bed will drop due to the higher degree of pyrolysis taking place (the air factor will decrease) for which higher quantities of heat are required to pyrolyse the feedstock. Since the oxygen supply remains constant, the extra char produced cannot be combusted/gasified to provide the additional energy requirements, hence the temperature drops. Conversely, if the feedstock supply is decreased, less heat is consumed by the pyrolysis process and less char is produced. This results in a higher degree of combustion of the char bed and the temperature rises. It can nevertheless be concluded that a constant bed temperature is attained after about 2 hours of gasification. The unstable feedstock flowrate also affects the gas quality as discussed later in this section.

5.12.3 Freeboard temperature

From Figure 5.34 it is shown that the freeboard temperature did not attain steady state within the operating time. If the curves for runs 36-38 are extrapolated, then stable temperatures would have been attained at 750 °C and 850 °C respectively for run 36 and runs 37, 38, after about 8 hours of gasification (about 100 °C higher for each experiment).

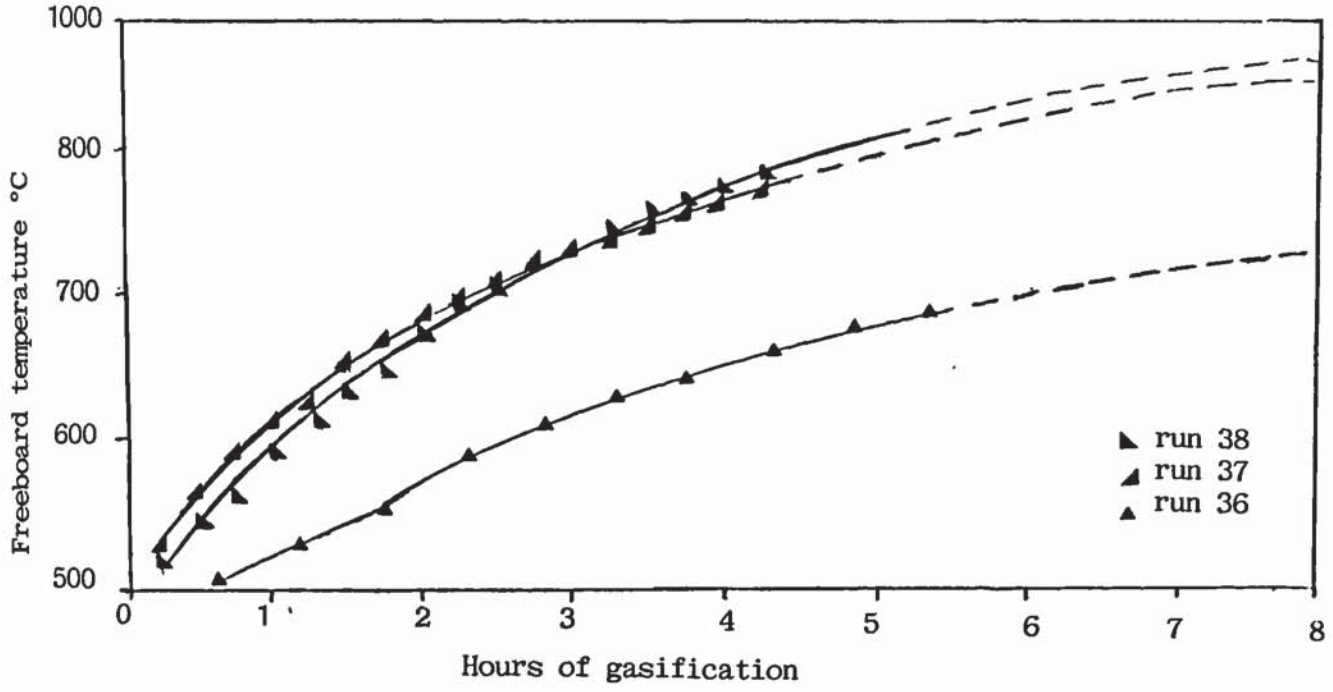

Figure 5.34 : Variation of freeboard temperature (at the exit).

The attainment of a constant freeboard temperature would have been of experimental interest; however it would not have affected the gas composition to any significant extent, since the equilibrium gas composition is not approached even at temperatures of 850 °C (see section 5.7.3).

5.12.4 Higher heating value of the gas

The time higher-heating value relationship is shown in Figure 5.35. The effect of unsteady feedstock flowrate on the higher heating value of the gas are clearly shown in this figure.

While for run 38 there were no apparent variations in the feedstock supply, which is shown by the absence of any fluctuations in the bed temperature-time and higher heating value of the gas-time relationships, there were however variations in the feedstock flowrate for run 37. This is shown at 2 hours when the higher heating value of the gas drops and the bed temperature rises (see Figure 5.33). The rise in bed temperature at 3 1/2 hours is not shown in Figure 5.35, since no gas analysis was made at that hour; (note: for runs 37 and 38 only five gas analyses could be made since the field laboratory run out of Argon, the carrier gas used for gas chromatography (see

section 4.2.6) and the gas sampling cylinders had to be taken to the Free University of Brussels for analysis).

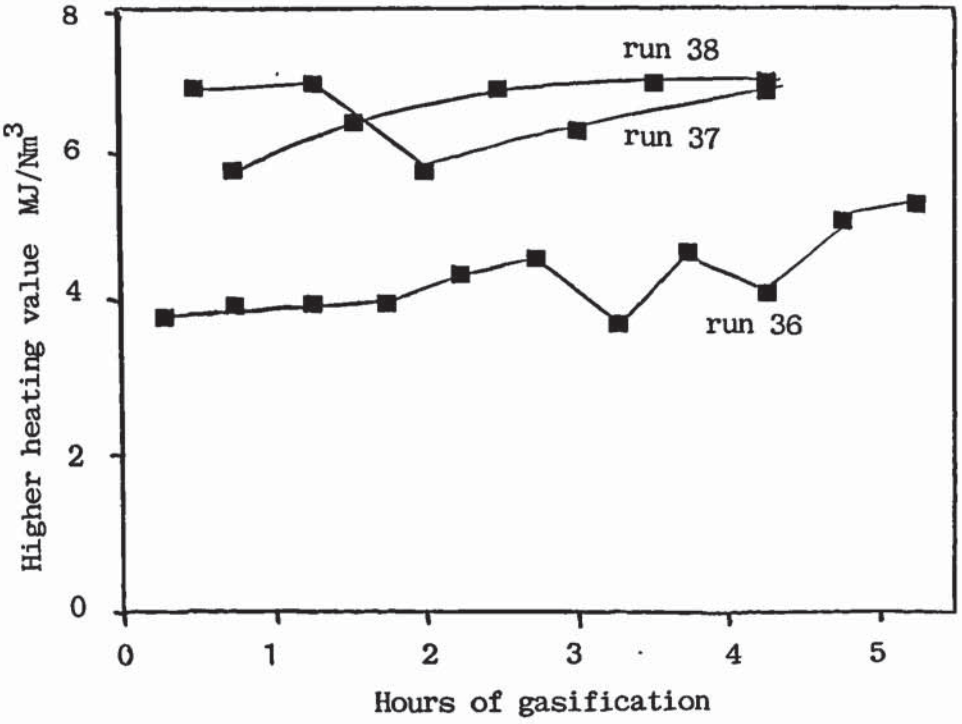

Figure 5.35 : Variation of higher heating value of the gas with time.

The same is shown for run 36 at 2 3/4 hours when the higher heating value of the gas registered a maximum and the bed temperature (see Figure 5.33) showed a minimum. The fluctuations of the higher heating value of the gas after 3 1/2 hours are also attributed to unstable feedstock flow, but are not registered by the bed temperature time curve of Figure 5.33. This can be tentatively explained by assuming that the gas composition - and hence the higher heating value of the gas - is very sensitive to a continuous and constant feedstock supply. However, since there is always a char hold up in the bed, the bed temperature is not that sensitive to small feedstock supply variations.

5.12.5 Gas composition

The variation of the gas composition with time is shown in Figures 5.36 - 5.38 respectively for runs 36-38. As with the higher heating value of the gas, fluctuations are shown whenever there was an interruption in the feedstock supply. The fluctuations of all gas components shown in Figure 5.36 indicated that during this specific run a steady state was not reached. For this reason, the author requested the assistant to stay overtime in order

to control and destroy any bridges that might be formed in the hopper during runs 37 and 38.

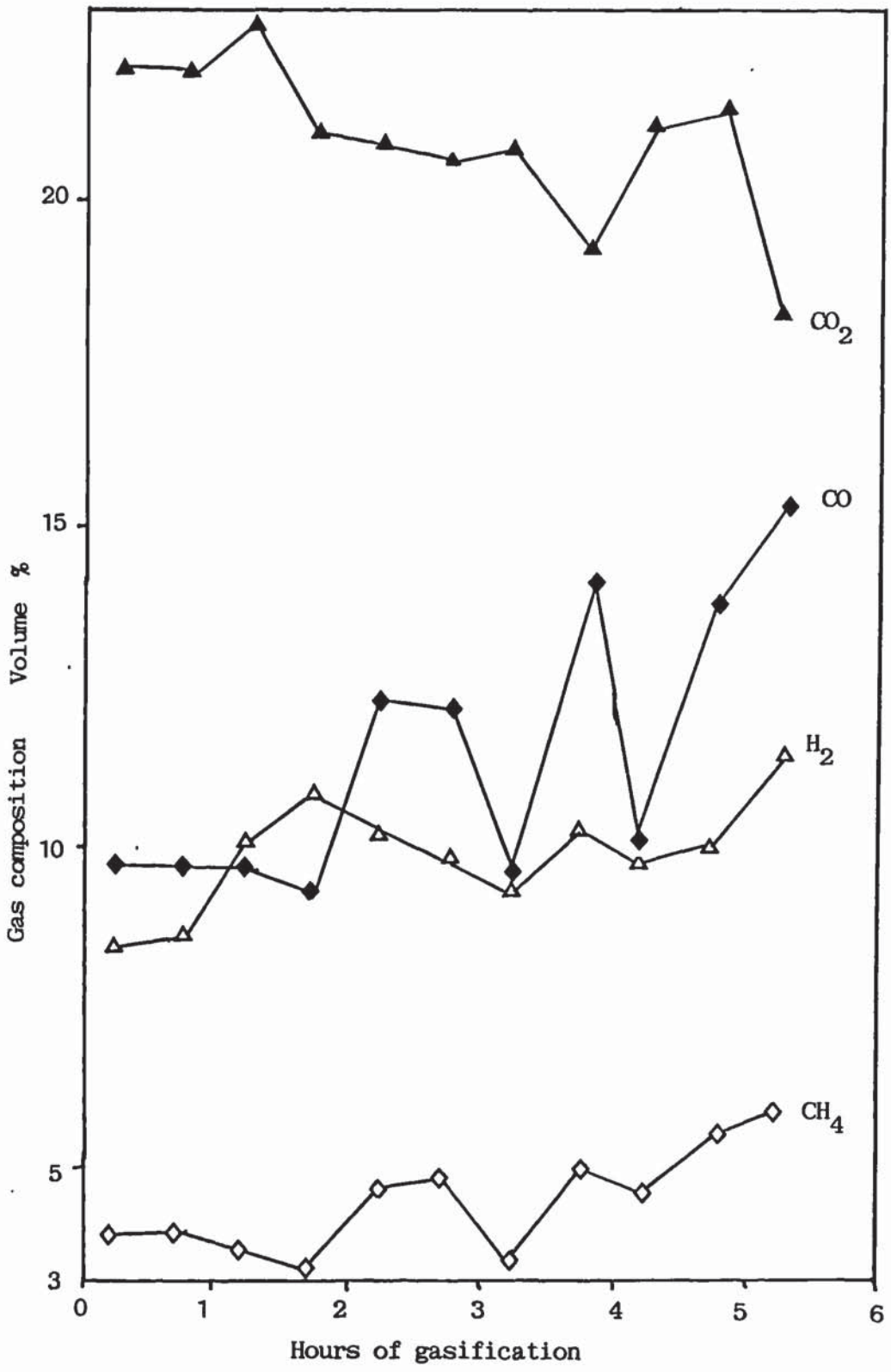

Figure 5.36 : Variation of gas composition with time, run 36.

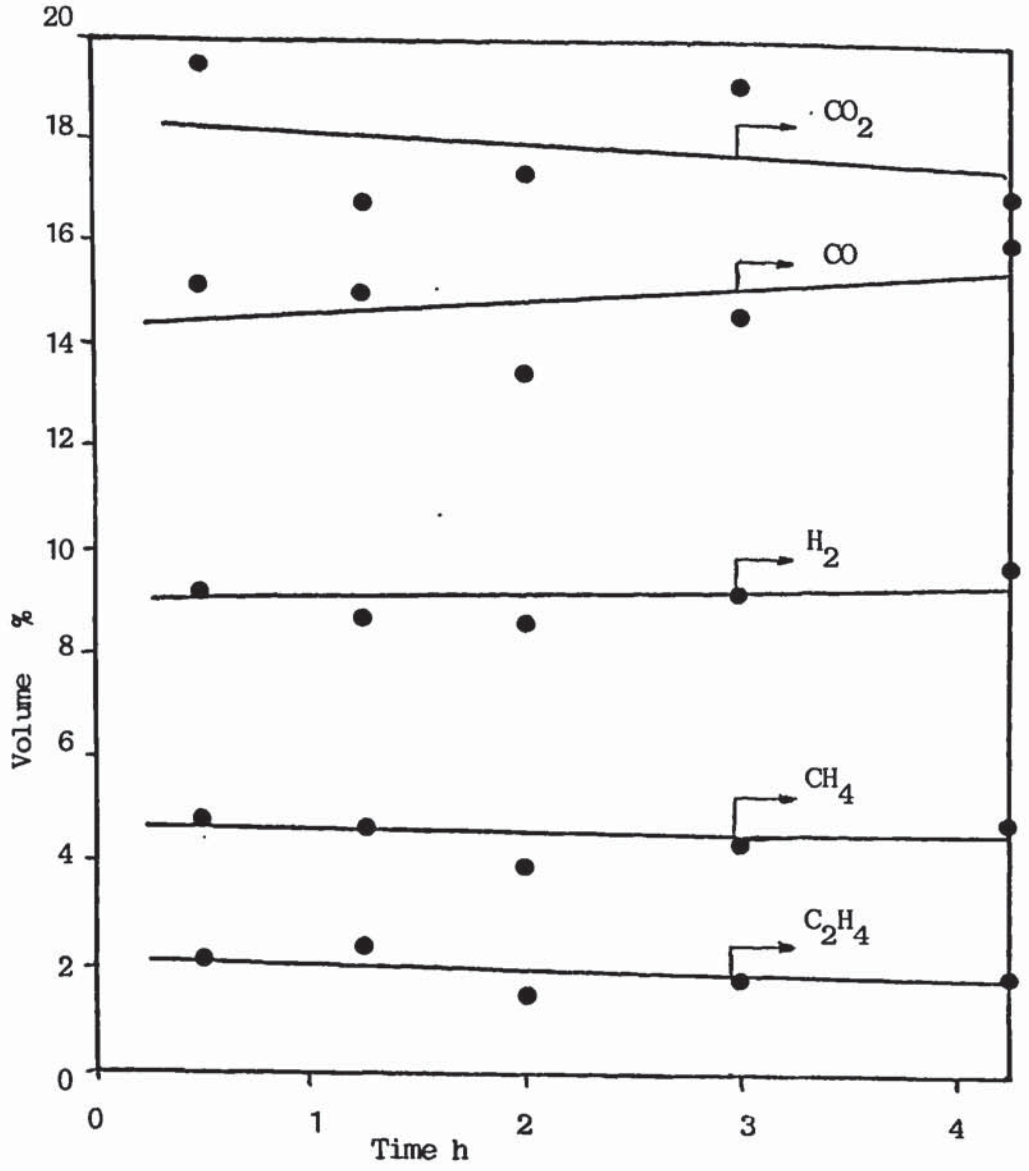

Figure 5.37 : Variation of gas composition with time, run 37.

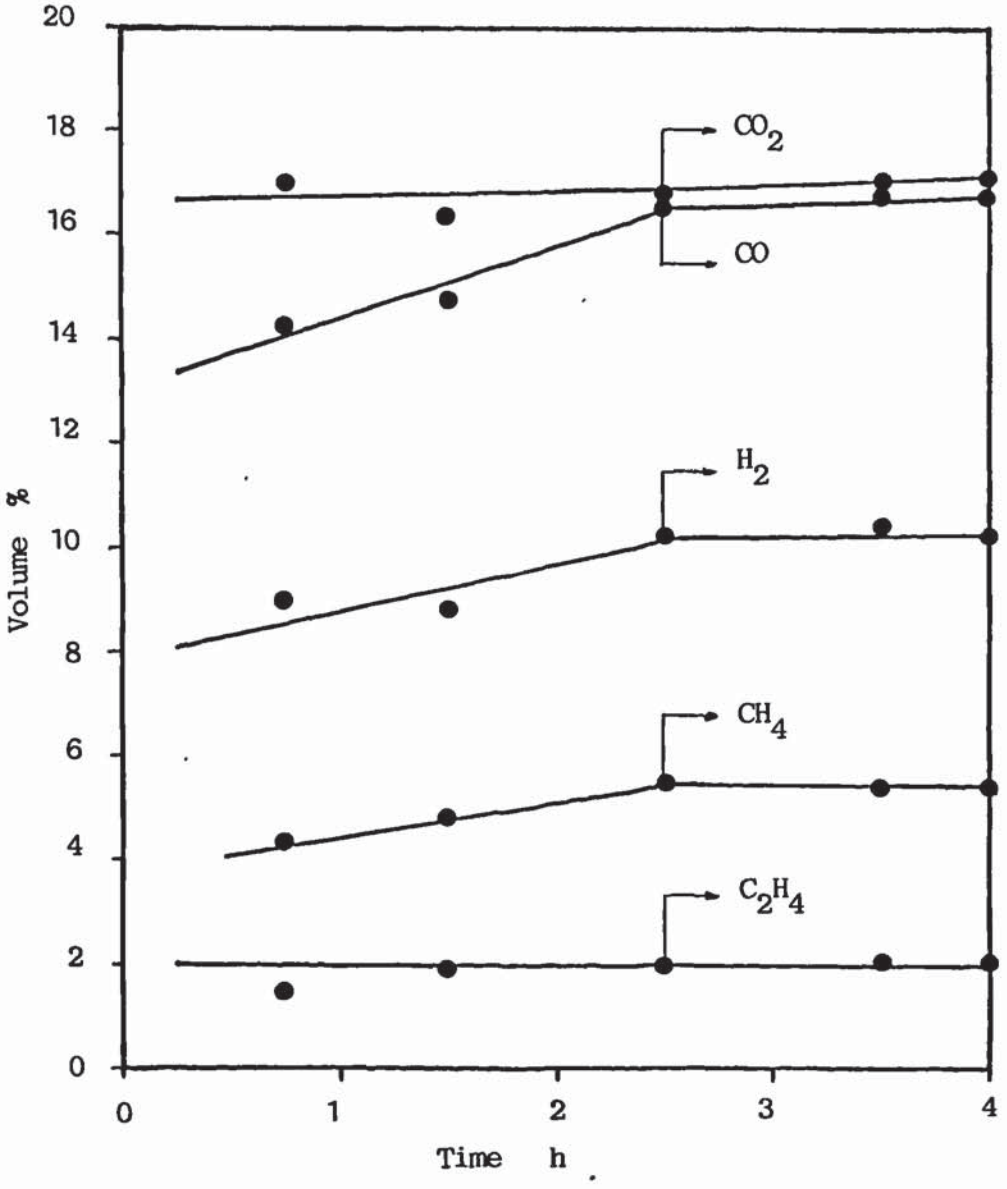

Figure 5.38 : Variation of gas composition with time, run 38.

From Figures 5.37 and 5.38 it can however be concluded, that the concentrations of methane and ethylene reach a steady state within 2 hours of gasification and remain constant unless there is an interruption in the supply of the feedstock.

The concentrations of carbon monoxide and hydrogen increase with time, as shown in Figures 5.36 and 5.37 for runs 36 and 37 respectively. The increase in the concentration of carbon monoxide could have been attributed to the water gas shift reaction,

$$H_2O + CO \rightleftharpoons CO_2 + H_2.$$

assuming that the above reaction is favoured from right to left. Nevertheless, since the concentration of hydrogen increased as well and the condensate flowrate did not change with time, this explanation must be disregarded.

The only other possible explanation for the increase in the concentration of these components is the cracking of tars and pyroligneous acids.

From these three runs, only run 3.8 was carried out with practically a constant feedstock flowrate. This is proven by the constant gas composition after 2 1/2 hours as shown in Figure 5.38 and summarized in Table 5.22.

Table 5.22 : Variation of gas composition with time, run 38.

Time	2 1/2	3 1/2	4 1/4
Component Vol. %			
Ethylene	2.0	2.1	2.0
Methane	5.5	5.4	5.3
Hydrogen	10.3	10.5	10.3
Carbon monoxide	16.7	16.9	17.1
Carbon dioxide	16.9	17.0	16.9
Higher heating value	7.0	7.1	7.0

However, this leads to the conclusion that after 2 1/2 hours the gas attains a constant composition, assuming that a constant feedstock supply to the reactor is maintained, while the freeboard temperature has little if any influence on gas quality.

5.12.6 Comparison with published results

In only one work carried out in a reactor of comparable size (80) some data on the stability of the reactor were found and listed in Table 5.23. In a reliability test of 26 1/2 hours, seven hours were needed to preheat the reactor from 260 °C to 700 °C. Then the preheating burner was shut off and it took one hour for the system to stabilize at 730 °C, with a feedstock flowrate at 630 kg/h. The bed temperature and gas composition remained constant for 1 1/2 hours and later increased over 4 1/2 hours to 785 °C. After changing the feedstock, the bed temperature varied in the range of 750 to 740 °C over 13 1/2 hours.

Table 5.23 : Reliability test (80).

Time h	Operational sequence	Reactor condition	Bed temp. °C	Gas Analysis mol % CO_2	O_2	N_2	CH_4	CO	Feed rate kg/h
- 8.00	Start pre-heater	Combustion	260	3.2	17.0	78	-	-	0
- 5.00	Start wood feed	Combustion	425	14.4	1.0	65	0.1	1.6	210
- 1.00	Shut down preheater	Gasification	700	14.5	1.8	61	0.4	2.2	485
0.00	Start run	Stable gasif.	730	12.5	1.1	46	1.2	3.0	660
1.30		Stable gasif.	730	12.5	1.1	49	1.1	3.3	660
6.00		Stable gasif.	785	12.3	1.1	49	1.1	5.4	660
12.00	Change feedstock	Stable gasif.	750	12.0	2.2	53	1.6	5.5	800
18.00		Stable gasif.	750	12.2	2.4	51	1.6	5.6	800
24.00		Stable gasif	740	14.1	2.6	51	1.8	6.0	800
25.30	Stop feedstock	Venting	740	4.0	9.0	72	-	-	800
26.50	Reactor shut down	-	640	-	-	-	-	-	-

In that work, only the outside diameter of the reactor was reported, 1.2 m, (see Table 2.4); and hence the bed diameter must have been larger than the one used in this work. This is also proven by the high feedstock flowrate attempted: 800 kg/h. Thus the results are not directly comparable.

From Table 5.23 it can be concluded that within one hour the reactor attained a steady state . The authors reported that all other gasification runs were extended only between 1 and 2 1/2 hours of actual operation under gasification conditions. The above conclusion validates the supposition in the previous section that for the reactor used in this work, two hours were sufficient for the bed to reach a stable temperature and gas composition in case there were no variations in the feedstock flowrate.

However, it is surprising that the authors (80) did not report any fluctuations in the bed temperature and gas composition since they did report unstable feeding, thus there is some suspicion that the data quoted were average values and not actual ones.

It has been reported by several authors (84, 97, 98, 102), that for laboratory scale fluidized bed gasifiers one hour is sufficient for the attainment of a steady state. However, no data were given for extended runs or for time-

temperature and time-gas composition relationships. Only one work was found (100) where the variability of gas composition and lower heating value of the gas with time were presented. Figure 5.39 shows these data. It is clear that the fluidized bed of the University of Davies (100) never approached a steady state. These large variations were attributed to a) variability in the composition of the feedstock (walnut shells), b) variability in the feedstock flowrate and c) automatic control of the fluidized bed.

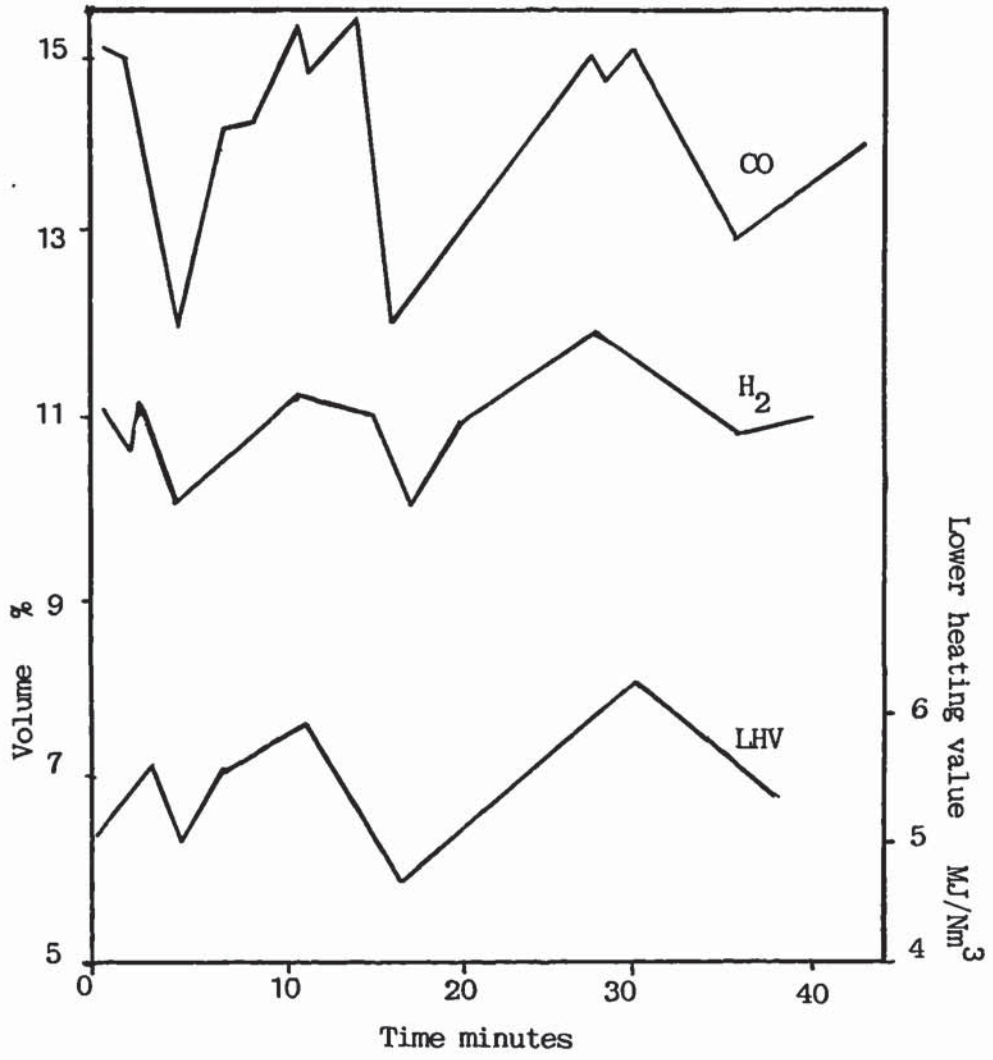

Figure 5.39 : Variability of gas composition and LHV with time (100).

5.12.7 Conclusions

The bed temperature stabilizes after about two hours, while much longer time is required for the freeboard to attain a stable temperature. This is estimated at about eight hours.

The gas composition and higher heating value of the gas stabilize after about 2 1/2 hours in case there is a constant feedstock flowrate. If there are interruptions in the supply of the feedstock, the gas composition fluctuates appreciably. Thus, it can be tentatively concluded that the gas quality is very sensitive to a continuous and constant supply of feedstock. However, although the bed temperature varies in case of unstable feedstock flowrate, it is not that sensitive as the gas composition. This is due to the existence of the char hold up in the bed.

No correllation could be found between the freeboard temperature and gas composition in terms of gas quality.

Results from the literature show that these conclusions are valid and that fluctuations in the gas composition and bed temperature are characteristics of all experimental fluidized bed gasification facilities.

5.13 REPRODUCABILITY OF A SPECIFIC EXPERIMENT

Since runs 37 and 38 were performed under identical experimental conditions, their results can be used to check the reliability of the fluidized bed gasifier in case of periodic operation (8-10 hours per day). The results of these two runs are shown in Figures 5.33-5.38 and discussed in the previous section. They are also summarized in Table 5.24.

Table 5.24 : Comparison of results of runs 37 and 38

Component	Units	run 37	run 38	difference	% Variation
Feedstock flowrate (average)	kg	340	340	0	0
Air flowrate	Nm^3/h	338.8	333.8	5	1.5
Air factor	-	0.289	0.285	0.004	1.4
Bed temperature (average)	°C	871	865	6	0.7
Higher heating value	MJ/Nm^3	6.76	7.01	0.25	3.5
Gas yield	$\frac{kg\ feed}{kg\ dry\ gas}$	2.02	1.99	0.03	1.5
Thermal efficiency	%	70.1	72.9	2.8	3.8
Heat of reaction	MJ/kg	6.67	6.17	0.5	7.5
Heat losses	%	-0.1	-0.3	0.2	66.6
Length of run	hours	4 1/4	4 1/4	0	0

There is good and acceptable agreement between these runs. The small difference in the air flowrate was due to a difference in ambient air

conditions, which produced a small difference in the air factor, although the indicated air flowrates were identical.

It can be concluded that the fluidized bed gasifier will produce identical results under identical experimental conditions.

5.14 OPERATING LIMITS OF THE SYSTEM

All previous experiments were executed in the air factor range of 0.23-0.87, since no operating problems with the fluidized bed were anticipated in this range. However, in order to determine the operating limits of the reactor it was decided to carry out experiments by varying the feedstock or air flowrates until failure of the system would occure. The break point was arbitrarily defined as the air factor beyond which the bed would not obtain a constant temperature. For this purpose, two more runs (39 and 40) were performed.

The first was carried out with a constant feedstock flowrate of 350 kg/h, while the air flowrate was varied in the range of 348.3 to 188.5 Nm^3/h. These capacities corresponded to air factors in the range of 0.250 to 0.135. The following procedure was followed: after the reactor was preheated and the temperature of the bed stabilized at a flowrate of 348.3 Nm^3/h air, the flowrate of the latter was decreased to 313.5 Nm^3/h. Stabilized bed temperatures were considered these which did not vary more than 10 °C within a period of about 30 minutes. Since the reactor was well preheated the - gasification run took 5 1/2 hours - this definition was considered sufficient for the purpose of the experiment. When the temperature of the bed was stabilized, the air flowrate was decreased again to 290.5 Nm^3/h and then to 260.2, 219.3 and 188.5 Nm^3/h.

The results are shown in Figure 5.40 along with the higher heating value of some gas samples. From this figure it can be seen that at an air factor of 0.208 the bed temperature stabilized at 788 °C with a gas higher heating value of 6.9 MJ/Nm^3. At an air factor of 0.187, the bed temperature initially dropped, then stabilized around 770 °C but started to drop again. This can also be seen by the higher heating value of the gas which dropped from 6.9 to 4.7 MJ/Nm^3. At a still lower air factor (0.157) the bed temperature failed to stabilize. Over 1 3/4 hours the bed temperature dropped from 760 to 700 °C.

At the lowest air factor obtained (0.135), the rate of temperature decrease increased as indicated by the gradient of the line in Figure 5.40.

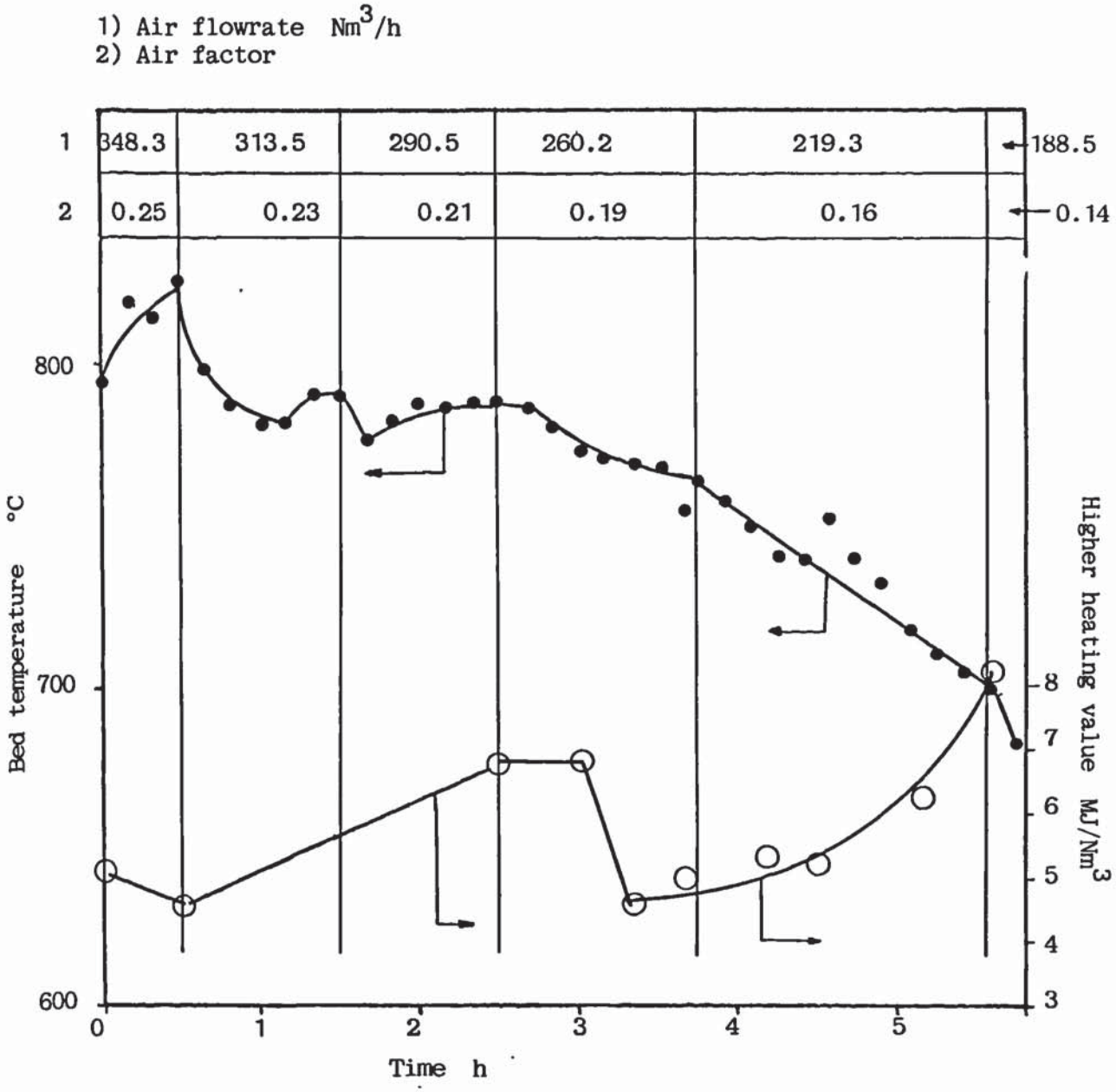

Figure 5.40 : Operating limits of reactor: variation of air flowrate at constant feedstock flowrate.

However, the higher heating value of the gas increased from 5.4 to 8.3 MJ/Nm^3. This increase was due to high concentrations of carbon monoxide and methane which increased from 14.0 to 20.9 and 5.7 to 10.5 Volume % respectively (see computer printouts in Appendix V).

From the above results, it can be concluded that the lowest air factor at which a stable bed temperature was obtained was at 0.2. At air factors below this value the bed temperature did not stabilized.

Run 40 was executed at a constant air flowrate of 320.7 Nm^3/h and by varying the feedstock flowrate from 350 to 400 kg/h. The feedstock flowrate was changed when a steady temperature was recorded for the previous setting over half an hour. The highest feedstock flowrate possible was 400 kg/h.

The results are shown in Figure 5.41. The temperature of the bed stabilized at 745 °C even at the highest feedstock flowrate. The same is indicated also by the higher heating value of the gas which stabilized around 7.5 MJ/Nm^3. This last set of conditions corresponds to an air factor of 0.20. Combined with the results of Figure 5.40, it further supports the conclusion that stable bed temperatures and higher heating value of the gas will be obtained by operating a fluidized bed gasifier at an air factor of 0.2.

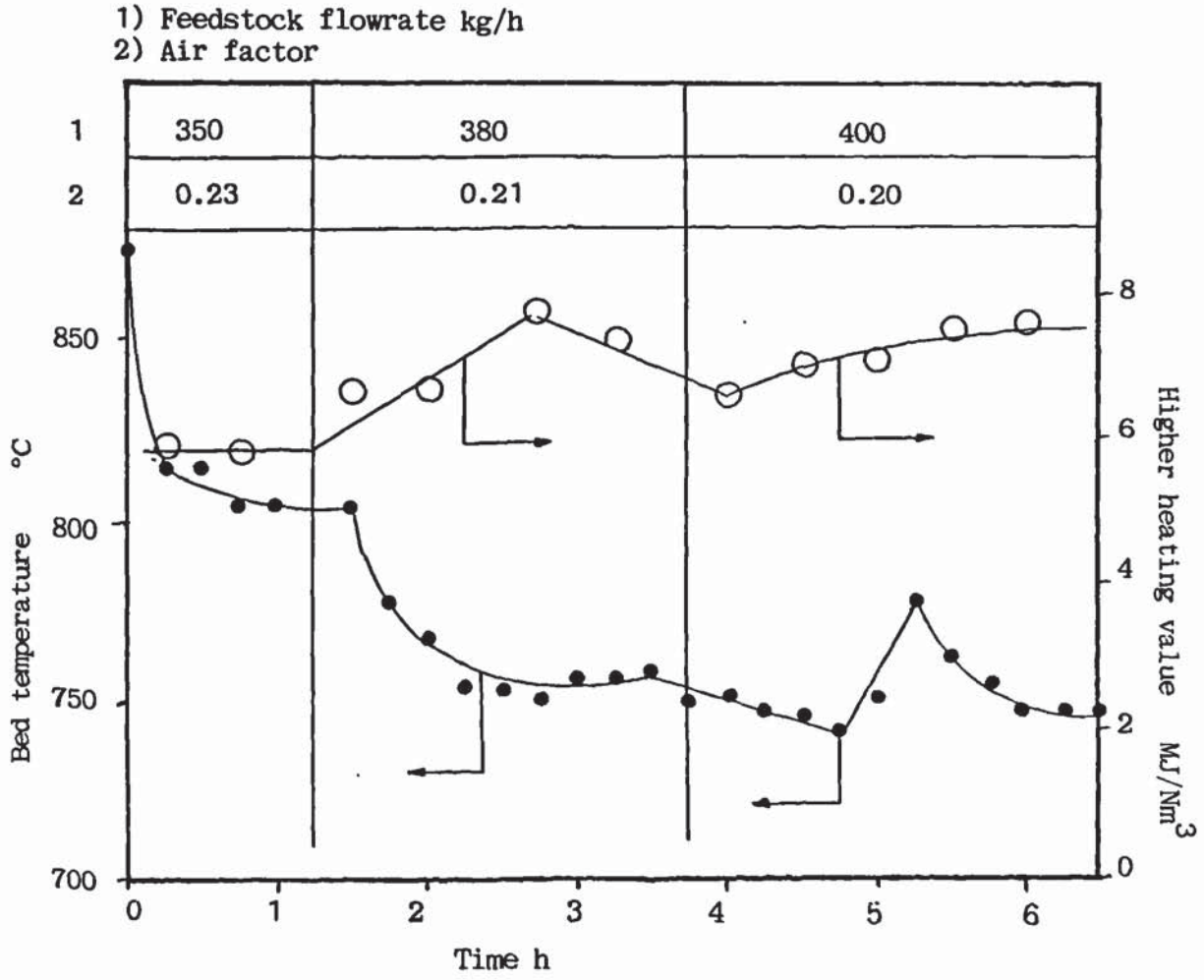

Figure 5.41 : Operating limits of the reactor: variation of feedstock flowrate at constant air flowrate.

Due to limitations in the feeding system, it was not possible to continue run 40 at even a higher feedstock flowrate. However, at still higher feedstock flowrates, eg. 430 kg/h, which corresponds to an air factor of 0.18, the temperature of the bed would have probably dropped below 700 °C and since the gasification reaction rates would decrease significantly, the char bed would continue increasing until loss of fluidization and complete choking of the bed would take place. This is supported by the results of run 39 as well as by thermodynamic considerations (see section 2.4.3.3), which predict the carbon boundary at an air factor of 0.23. Indeed during this work an experiment was made at this air factor (run 23, see Table 5.13) without any problem; however, runs 39 and 40 proved that a fluidized bed gasifier can be operated at an air factor of 0.2 and attain a stable performance.

If the maximum feedstock flowrate obtained is divided by the cross sectional area of the bed, then the maximum specific capacity of the bed per hour and unit cross sectional area for these experimental conditions can be found. Thus,

$$\text{maximum specific capacity} = \frac{\text{maximum feedstock flowrate}}{\text{cross sectional area of the bed}}$$

equation 5.39

$$\text{or} \quad \text{maximum specific capacity} = \frac{400 \text{ kg/h}}{0.503 \text{ m}^2} = 795 \text{ kg/hm}^2$$

On a moisture free basis :

$$\text{maximum specific capacity} = \frac{357.6}{0.503} = 711 \text{ kg/hm}^2$$

5.15 FLAME BURN OUT

As described in section 4.2.6 the gas was flared at the exit of the product gas burner. During the last experiments (starting from run 30), when the gas burner was removed (see section 4.2.6) and replaced by a vertical pipe, the flame was clearly visible. It had a red-orange colour caused by the combustion of carbon carried away with the ash (there was no cyclone). The burning ashes were clearly visible at the border of the flame. In most of the runs the flame had a height in the range of 0.5-1 m.

At the end of run 37 when the feedstock flowrate was stopped, it was accidentally observed that the flame burned out in less than a minute. In subsequent runs the burn out time of the flame was measured and the results are shown in Table 5.25.

Table 5.25 : Flame burn out

Run	Time of burn out sec.
37	less than 60
38	32
39	29
40	30
41	27
42	26

In order to investigate this phenomenon, the gas composition of run 41 was measured on the first minute and thereafter every two minutes after the feedstock flowrate was stopped. The results are shown in Figure 5.42 where the major components of the gas are presented in function of time. It was not possible to take any gas samples between 13 and 25 minutes after the feedstock flowrate was stopped, since there were only 7 gas sampling cylinders available and it took about 15 minutes for one gas analysis (see section 4.2.6). At time 0 the steady state gas composition is plotted, before the feedstock flowrate was stopped.

Within one minute, the volume % concentration of hydrogen, carbon monoxide, methane and ethane had been reduced considerably. Only the carbon monoxide partially recovered after about 3 minutes, while the others dropped to zero. While for the first 12 minutes, the concentration of oxygen was below 1 volume %, indicating complete consumption due to the combustion of the char bed, at 25 minutes its concentration had increased to 7.5 volume %.

These results suggest that the gas composition is very sensitive to continuous feedstock flowrate. The gasification of char is of secondary importance as far as gas composition is concerned, while the degradation of biomass is of primary importance, since according to the above results it is the main parameter affecting the gas composition. Run 41 was made with 320 kg/h or 5.3 kg/min and if the gasification of char was of primary importance, then the gas quality would not have degraded so much within one minute.

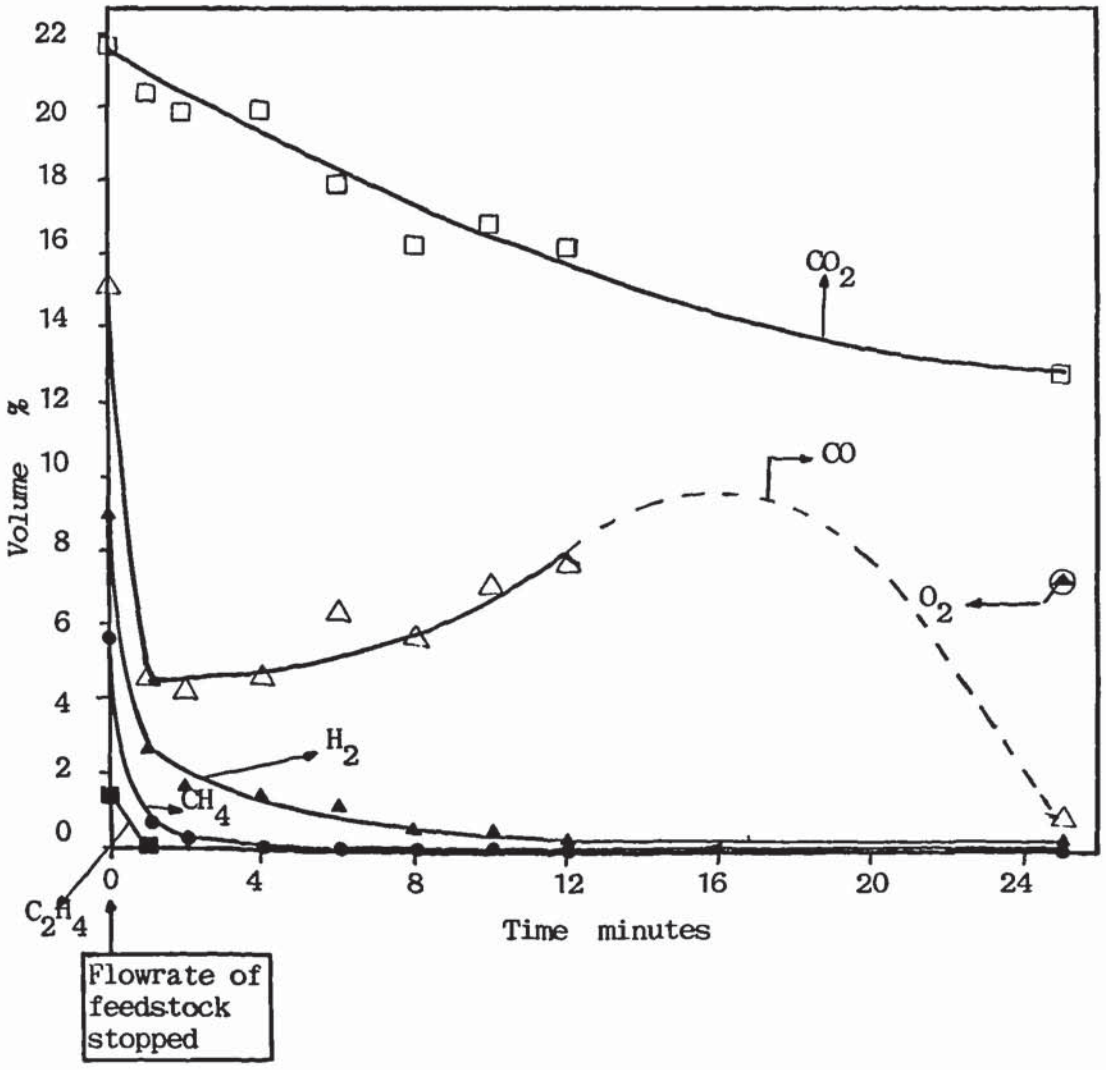

Figure 5.42 : Variation of gas composition with time after termination of feedstock flowrate, run 41.

No other vaiables related to the flame burn out could be found.

Assuming that the volume % concentration for carbon dioxide would decrease linearly with time, the burn out time of the char bed can be estimated at about 70 min. (see Figure 42). Using a theoretical procedure described in Appendix IX (294) the burn out time for a char bed of 8.25 kg (see following section) was calculated in the range of 75-109 min. In view of the assumptions and uncertainties involved, the differences between estimated and calculated burn out time are considered acceptable.

While the nature of the reactions occuring in the fluidized bed reactor involve a number of stages which have major affects on the gas composition, these changes are all very rapid. Factors which can affect the gas composition within the system are the air factor, bed temperature, composition of the

feedstock including moisture content and amount of feedstock reacting in the bed. With the exception of the amount of feed reacting in the bed, there is evidence that all these factors were essentially constant. It can therefore be concluded that the time of flame burn out is related only to the feedstock termination.

Only one group examined the sensitivity of the gas quality in terms of the feedstock flowrate (80). Initially it was found that there were significant variations in the gas composition. The only data reported were that while the daily average of the higher heating value of the gas for all samples was 2.3 MJ/m^3, the average of selected samples was 3.7 MJ/m^3. These data indicate that the higher heating value of the gas actually varied in the range of about 1.5-4.5 MJ/m^3. It was found that the particular feeding system used in that work, a fast acting lock hopper, in effect supplied the feedstock to the fluidized bed in a cyclic period of 20 seconds. The fluctuations of the gas quality were attributed to this periodic supply of feedstock to the reactor. The authors came to the conclusion that true gasification was probably occuring for part of the time. They postulated the following sequence:

a) vaporization of the appreciable water content (35-60%)
b) combustion of part of the wood to maintain the bed temperature
d) pyrolysis of the remainder of the wood under conditions of oxygen deficiency
c) in the absence of any further pyrolysable feed until injection of the next slug of feedstock, combustion of part of the products of pyrolysis.

However, their postulated sequence cannot be justified for several reasons. Wood first pyrolyses before it can be combusted; the pyrolysis gaseous products would escape the bed and combust in the freeboard or even at the exit of the reactor; they assumed no char hold up although the feedstock flowrate was varied in the range of 325 to 776 kg/h. It is believed, that the cyclic feeding produced a cyclic production of pyrolysis gases which resulted in cyclic fluctuations in the gas composition, while the temperature of the bed was maintained by gasification/combustion of the char hold up.

Nevertheless, the overall conclusion is that indeed the gas quality is very sensitive to a constant supply of feedstock in the fluidzed bed reactor.

5.16 THE CHAR BED

5.16.1 Introduction

The char bed, defined as the weight of char hold up in the bed at steady state, must be considered in any fluidized bed gasifier application. If the char bed attains very high values, then loss of fluidization may occur due to excessive pressure drop over the bed. Thus in applications of steam gasification, where the overall reaction rate is not as fast as with air gasification, the char bed must be removed mechanically (see section2.4.5). With air gasification the problem becomes important at low air factors, 0.2-0.3. At high air factors, above 0.4, the char bed is minimal if existing at all, since the char reacts very fast with the higher concentration of oxygen present. However, at an air factor 0.2, thermodynamics predict a 0.04 kg char/kg dry feed char yield which increases rapidly below an air factor of 0.2 (109). It was therefore decided to determine the char bed at this value of air factor.

5.16.2 Experimental

Several attempts were made to measure the char built up in the fluidized bed, based on the differential pressure drop measurement between the bed and the freeboard (36). For reasons yet unexplained, it was not possible to register any significant difference in the pressure drops over the bed and between the bed and the freeboard.

After the results of run 41, it was decided to measure the char bed with a more direct method. Run 42 started immediately after run 41 on the same day; after the measurements of run 41 had finished, the feedstock and air flowrates started again and the bed was left for 1 1/2 hours to stabilize. Since the reactor had stabilized during run 41, that period of time was considered sufficient for the attainment of a constant char bed. However, that particular day the section pump of gas sampling line did not function properly and no condensate and fly ash flowrates could be determined; hence no mass and energy balances could be made for these two runs. Before run 41 started, the observation port at the top of the reactor was opened (see Figure 3.6) and the height of the surface of the bed to the top of the reactor was measured. The height from the centre of the distributor tubes to the top of the reactor was then measured from the outside of the reactor (see Figure 5.43) and thus the static bed height H_b was found to be 43.5 cm (the thickness of insulation was taken into consideration).

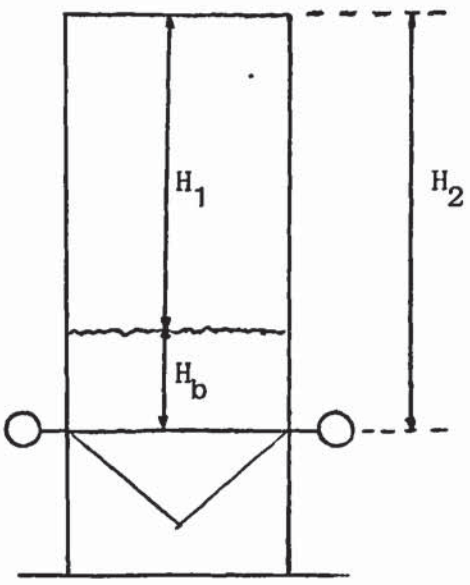

Bed height=$H_b=H_2-H_1$

Figure 5.43 : Measurement of bed height

Then run 42 was carried out under exactly the same conditions as run 41. When a steady state was attained, the feedstock and air flowrates were cut off simultaneously and then the height from the surface of the bed to the top of the reactor was measured again and the bed height was found to be 54.5 cm. Hence the char bed height at static conditions was :

$$54.5 - 43.5 = 11 \text{ cm.}$$

However, it was not possible to exactly calculate the amount of char present, since the bulk density of the sand-char mixture was not known, and since the bed was not left to cool down (it takes about 3-4 days), the mixture could not be removed for seiving and analysis (281, 282).

It can be assumed that the char floats on the surface of the bed in which case the extra bed (11 cm) could be considered of being composed by char only. By assuming a bulk density (ρ_{ob}) of the char of 150 kg/m^3 (255) an estimation of the weight of the char bed can be made.
The cross sectional area A of the bed is:

$$A = \frac{\pi \times 0.8^2}{4} = 0.503 \text{ m}^2$$

Thus the char bed volume V_{cb} was:

$$V_{cb} = A \times H \qquad \text{equation 5.40}$$

where H = height,
and $V_{cb} = 0.503 \times 0.11$
$= 0.055\ m^3$

The weight of the char bed W_{cb} is then given by:

$$W_{cb} = V_{cb} \times \rho_{cb} \qquad \text{equation 5.41}$$
$$= 0.055 \times 150$$
$$= 8.25\ kg$$

Therefore, since the feedstock flowrate was constant at 320 kg/h, only 2.6 wt% of the feedstock accumulates as char bed in the reactor.

5.16.3 Comparison with published data

Run 42 was carried out at an air factor of 0.2. At this value thermodynamics predict (see Figure 2.12) a char yield of 0.04 kg char/kg dry wood. Thus for the run in consideration,

Dry wood flowrate = 320 x 0.104 = 286.7 kg/h
Char yield = 286.7 x 0.04 = 11.5 kg.

The difference of 28% with the experimental determination can be considered acceptable if all the uncertainties in determining the weight of the char bed are considered.

Only one work (15) was found in which the char hold up had been determined. However, since those experiment were carried out with charcoal, which has a low volatiles content, the reported data are not directly comparable to this work. It was found that the average char bed weight was 0.474 kg. The air to fuel ratio was 3.33 and 1.32 respectively for the published data and this work. However, if the experiments with charcoal would have been carried out at the same air to fuel ratio as in this work, then much higher char hold up capacities would have been obtained, since biomass has higher content of volatiles than charcoal by a factor of about 7.

5.16.4 Conclusions

It can be concluded that at an air factor of 0.2 a char bed of 8.25 kg was obtained. This amount of char does not pose any problem for efficient fluidization and hence this result strengthens the conclusion that fluidized bed gasifiers can be operated with confidence at this low value of air factor.

5.17 THE SUPERFICIAL GASVELOCITY OVER THE MINIMUM FLUIDIZATION VELOCITY RATIO

In fluidized bed systems solid circulation is negligible at low gas velocities, while at high gas velocities the circulation of solids becomes appreciable (273). Thus the ratio of superficial gas velocity over the minimum fluidization velocity U/U_{mf} is a measure of solids mixing in a fluidized bed. For effective solids mixing equation 5.43 should hold (36)

$$\frac{U}{U_{mf}} \geq 2.5 \qquad \text{equation 5.43}$$

In order to check whether the above condition was met during the experiments of this work the ratio of U/U_{mf} was calculated and the results are given in Table 5.26. For this calculation, the volumetric flowrate of air (see Table 5.13) was converted to the actual operating flowrate at reactor temperature. From this value the air velocity was calculated and then divided by the minimum fluidization velocity (see section 5.4.3) corrected for the viscosity effect due to temperature.

From Table 5.26 it can be seen that all runs did meet the condition of equation 5.43. The ratio of U/U_{mf} was in the range of 2.85 to 10.97, while the average value was 7.54. It can therefore be concluded that during the experiments of this work efficient solids mixing was achieved.

The U/U_{mf} ratio has an effect on the entrainment and elutriation of particles from the bed. As this ratio increases, the superficial velocity in the bed rises and hence larger particles are entrained (see section 2.5.6.8). However, since the complete product gas stream could not be treated in a cyclone and since the cyclone of the product gas sampling line had a low seperation efficiency (see section 4.2.7.2), no correllation could be found between U/U_{mf} and fly ash flowrate.

No published data could be found on the U/U_{mf} ratio.

Table 5.26 : The ratio U/U_{mf}

Run	U/U_{mf}
13	4.55
14	2.85
15	6.75
16	8.70
18	7.86
19	5.67
20	10.69
21	4.30
22	5.28
23	4.84
24	9.73
25	7.55
26	5.80
27	6.96
28	7.38
29	6.13
30	7.63
31	10.46
32	10.61
33	9.04
34	6.58
35	4.97
36	6.87
37	10.97
38	10.75

5.18 MEAN PARTICLE SIZE OF SAND

The problems associated with sand sintering have been discussed in section 2.4.3.6. In order to ascertain if similar problems would be encountered in this fluidized bed, sand samples from the bed were removed periodically and analysed for size distribution. About one liter of sand was each time removed from the bed at static conditions and was subjected to sieve analysis at the Free University of Brussels.

Figure 5.44 shows the meanparticle size of sand as function of time, while Figure 5.45 gives the variation of the weight % in each sieve with time from both figures it is char that there was no noticable increase either in the mean particle size or in the fraction of sand in each size of particles. In Figure 5.45 an anomaly is shown for the fraction of sand in the 0.075 mm size. The fraction of this particle size started at 9.3 wt% and after 21.5 hours it dropped to 0.5 wt%. This was caused by the elutriation of this fine

fraction of sand by the gas (see section 2.5.6.8). However at 26.5 hours, it was measured to 3.3 wt%. This was probably due to experimental errors in the sieve analysis. The f;uctuations in the curves of Figure 5.45 were due to the relatively small size of samples taken for analysis. However, it was not posible to remove significantly larger samples since that would require the addition of fresh sand which would defeat the purpose of the experiment.

In Figure 5.45 published data (115) are also presented, which show a significant increase (about 40%) for the 0.200 mm size. Those tests were carried out with alumina sand for the oxygen gasification of wood. However, for the air gasification of wood it has been reported (80) that after 15.00 hours of operation the fraction of silica sand between 0.8 and 0.5 mm decreased from 85% to 54%. The proportion of sand of less than 0.5 mm had risen from 10 to 28% and that over 0.8 mm had increased from 4 to 28%. The increase in oversize sand was attributed to crushed stones from the feed receiving pad, picked up as the feedstock was removed by front and loaders.

It can be concluded that during the period of measurements in this work no appreciable enlargment of the sand particles due to agglomeration took place.

The bed material was replaced at least once a month, since Vyncke Warmtetechniek often carried out test runs with a variety of feedstocks (bark, carpet waste, plastic waste et al.) for prospective clients. The sand was always replaced after an experiment with feedstocks other than chopped wood.

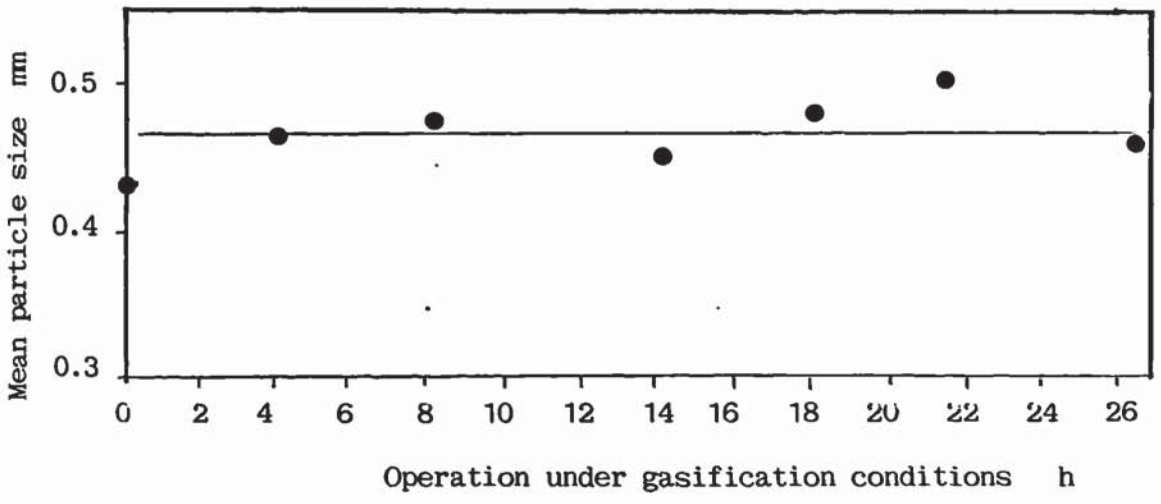

Figure 5.44 : Mean particle size of sand versus time of operation.

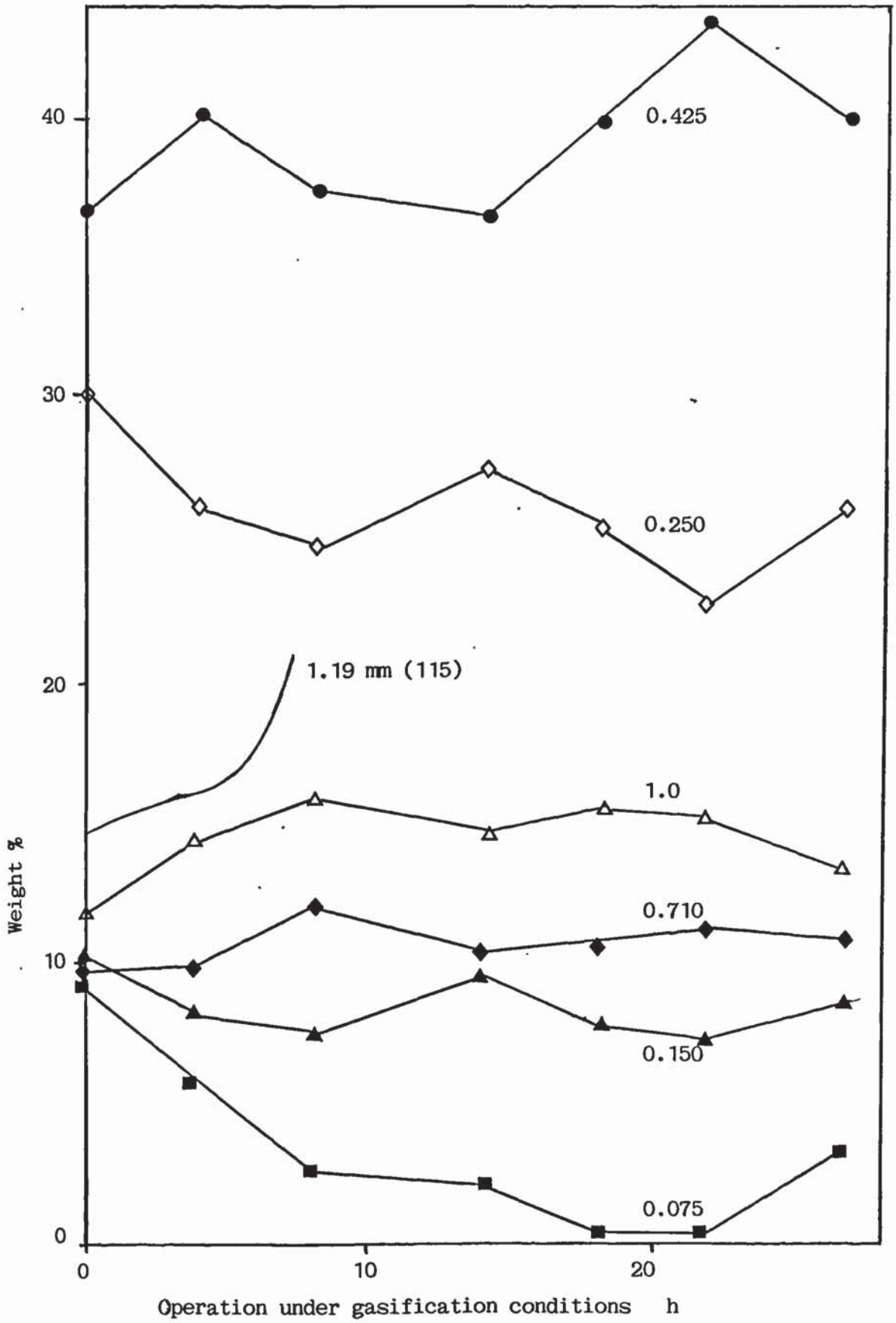

Figure 5.45 : Variation of weight % of different sizes of sand with time of operation.

5.19 TURN DOWN RATIO

The fluidzed bed gasifier was designed for a turn down ratio of 1:3 (see section 3.3.1). The lowest feedstock flowrate used during these experiment was 78 kg/h and run 14 (at such a feedstock flowrate) produced a gas with a higher heating value of 4..39 MJ/Nm^3 at an air factor of 0.38 (see Table 5.13). At three times higher feedstock flowrate, or about 232 kg/h, run 34 produced a gas with a higher heating value of 4.38 MJ/Nm^3 at an air factor of 0.32.

This is an important result since it can be concluded that it is possible to meet the 1:3 turn down ratio without any deterioration in gas quality or in the operation of any downstream application of the product gas, except in terms of capacity since the product gas flowrate would decrease. However, if the gas quality is not considered, then a turn down ratio of 5:1 was obtained since during run 40 stable operation was achieved at a feedstock flowrate of 400 kg/h. At an air factor of 0.2 the higher heating value of the gas was 7.5 MJ/Nm^3.

No published data on the turn down ratio could be found.

5.20 CONDENSATE YIELD

The yield of condensate is in general a function of the moisture content of the feedstock and the degree of combustion or air factor. The former is due to the moisture content of the feedstock, which is evaporated as it dries and thus the water is reported in the gas, while the latter is due to water produced by the combustion process of part of the feedstock. However, since in this experimental programme the moisture content did not vary significantly, the condensate yield should be a function at the air factor only.

This is shown in Figure 5.46 where the experimental as well as the thermodynamic yield condensate is plotted versus the air factor.

Both sets of data show that the condensate yield increases linearly with the air factor; however, the experimental data show a higher condensate yield, by about 0.115 kg/kg feedstock MAF or 11 % than thermodynamics predict.

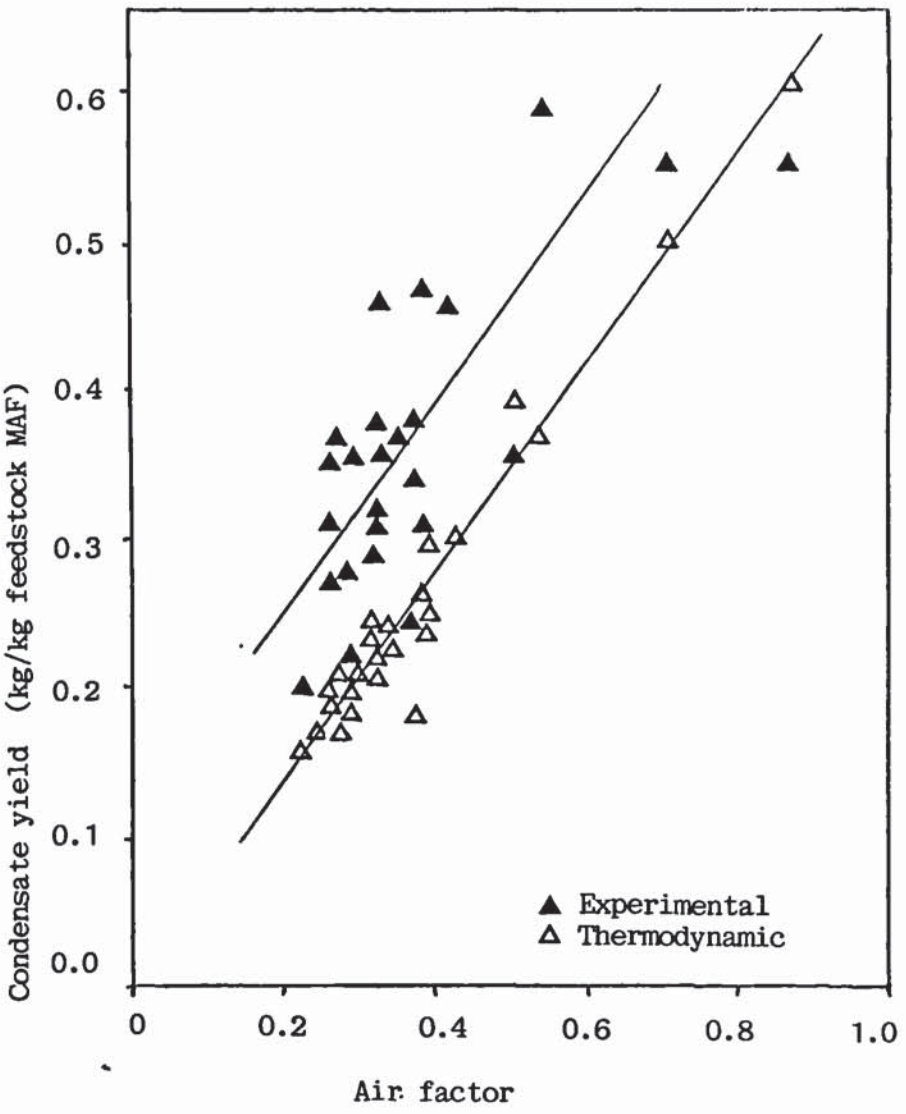

Figure 5.46 : Condensate yield as function of air factor.

In the air factor range of interest for fluidized bed applications, 0.2-0.4, experimental condensate yields between 0.25 and 0.35 kg/kg feedstock MAF were obtained.

Considering the limitations of thermodynamic models (see section 2.5.4.5) and the experimental uncertainties in determining accurately the condensate flowrate, it can be concluded that reasonable agreement exists between the two sources of data.

5.21 RETENTION TIME OF GASES IN THE REACTOR

5.21.1 Introduction

The retention time of gases in a fluidized bed gasifier is a parameter of significance for two reasons. Firstly at higher retention times more time is provided for the gases to remain in the reactor and thus for the different reactions to proceed further. Also, the tars remain longer in a high temperature environment and therefore the yields of their cracking products should increase. Moreover for the elutriated char particles, their degree of gasification will increase with longer retention time and this would improve the carbon conversion efficiency as well as the overall quality of the gas.

Secondly, the retention time is a useful tool for scaling up purposes, since it is used to determine the volume of the reactor under similar operating conditions.

5.21.2 Determination of the retention time

The retention time of the gases in the reactor is a function of the gas flowrate, since retention time is equal to the volume of the reactor divided by the volumetric flowrate (229). When reactions which result in a change of volume - as with gasification - take place, the increase or decrease of the volumetric flowrate should be accounted for.

It is very difficult - and there is lack of data - to predict the volumetric flowrate with accuracy in each region of a fluidized bed gasifier. Consider a reactor where air is introduced at the bottom of the bed and feedstock above the bed: initially the volumetric flowrate will increase considerably across the bed due to the combustion and gasification of char. Above the bed, the volumetric flowrate should also increase upto a certain height, due to the degradation of the biomass and formation of organic gases and vapours. However, above this region cracking reactions take place which further increase the volume of the gas, but the temperature is lower than the bed and thus the volumetric flowrate decreases due to lower temperatures. It is therefore evident that the prediction of the actual flowrate of the gases in a fluidized bed gasifier is rather complex and difficult for an accurate determination of the retention time. The kinetics of both biomass pyrolysis and gasification must be known in order to determine the rate and yields of the various products in the bed and the region around the feeding port. For the freeboard, the kinetics of tar cracking must also be evaluated and the

mass flowrates of the entrained and elutriated particles which react in the freeboard should be determined. Finally the catalytic effect of biomass ash should also be considered, since it can influence the yields of the gasification reactions (see section 2.4.8).

In order to calculate the retention time of the gases, an average gas volumetric flowrate was used. It was simply assumed as the average of the air flowrate at bed temperature and the product gas flowrate at freeboard temperature.

The influence of the normal air flowrate at actual reactor temperature on the average retention time of the gases is illustrated in Figure 5.47. As expected, by increasing the air fowrate, the retention time decreases significantly. The retention times deduced in this work thus ranged from about 10 to 50 seconds.

The higher the retention time of gases in the reactor, the higher is the possibility that the gasification reactions will attain equilibrium, since the gases remain at high temperatures longer and since more time will be provided for fines and tars to be gasified or cracked. In principle this should affect the higher heating value of the gas, since at longer retention time the yields of the gasification products are supposed to increase. This is shown in Figure 5.48, where the higher heating value is plotted versus retention time. It is evident that for each feedstock flowrate, the higher heating value of the gas increases with longer retention times as predicted.

This is due to higher concentrations of methane, hydrogen and carbon monoxide as the retention time increases. This is shown in Figure 5.49 for runs 18-21, which were performed with a feedstock flowrate of 160 kg/h. Since the feedrate was constant and the volatiles contact of the system did not change, the higher concentrations of these components can only be attributed to higher conversion of carbon and to the cracking of tar.

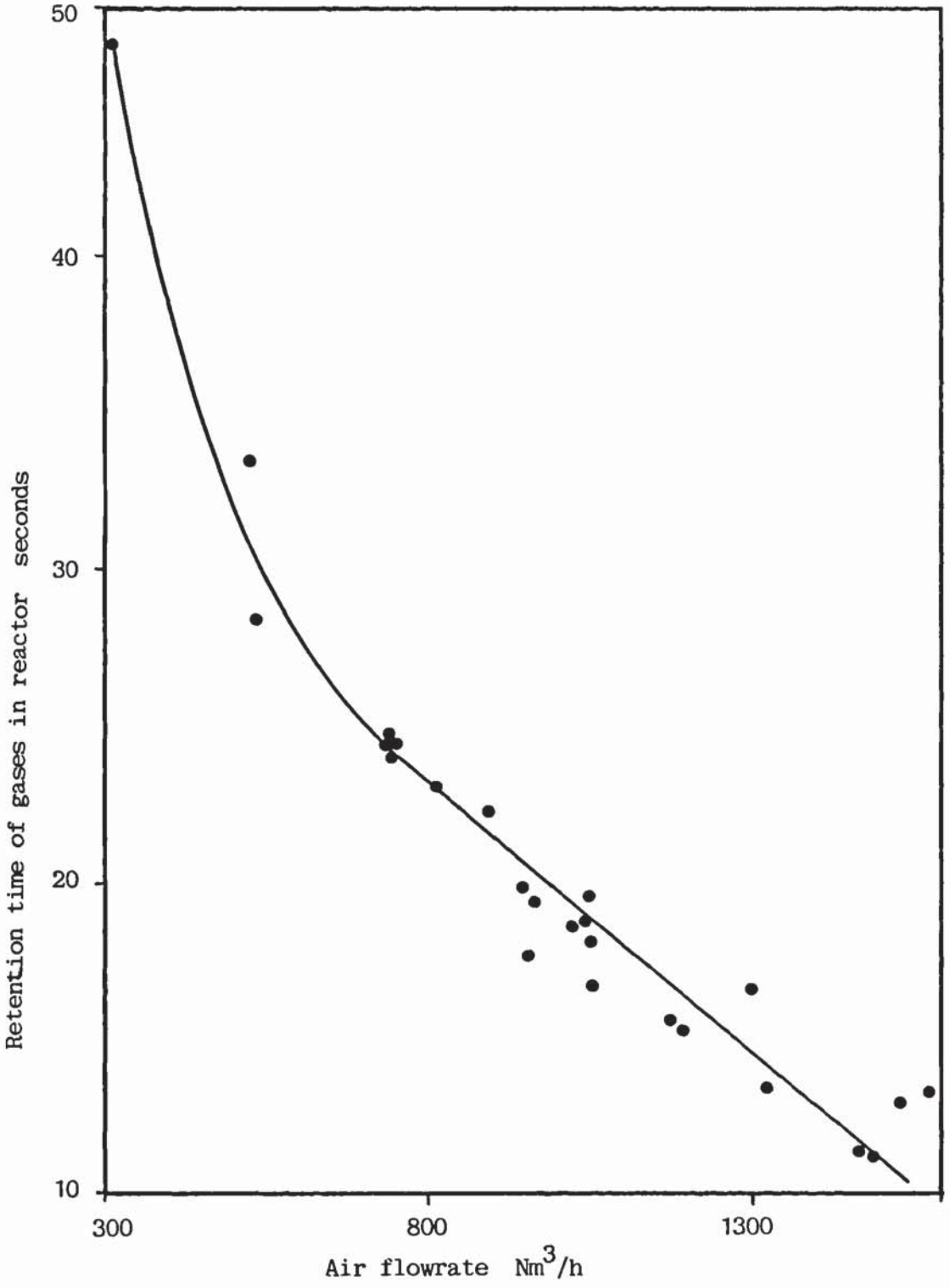

Figure 5.47 : Retention time of gases versus air flowrate.

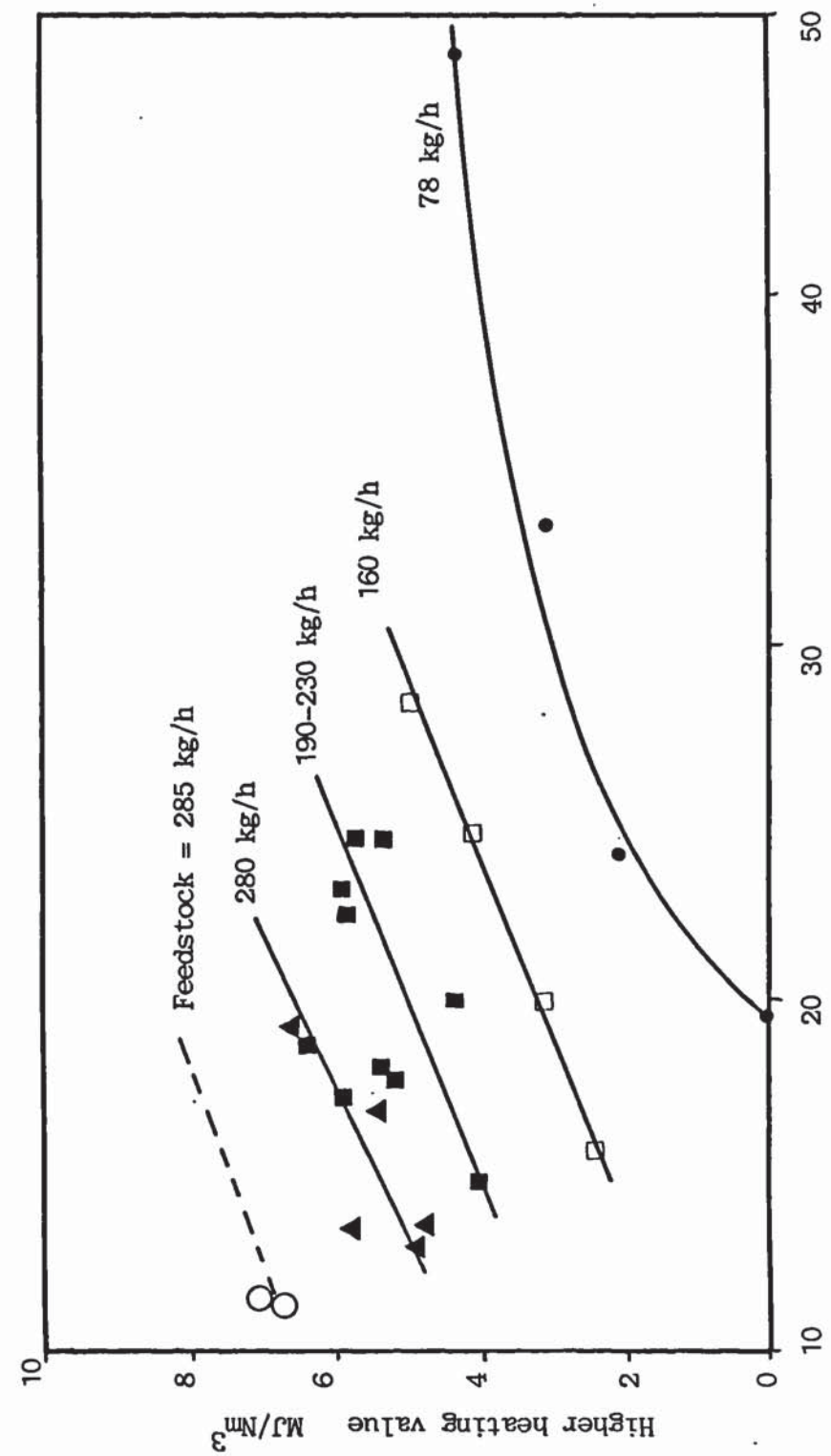

Figure 5.48 : Relationship between higher heating value of the gas and retention time.

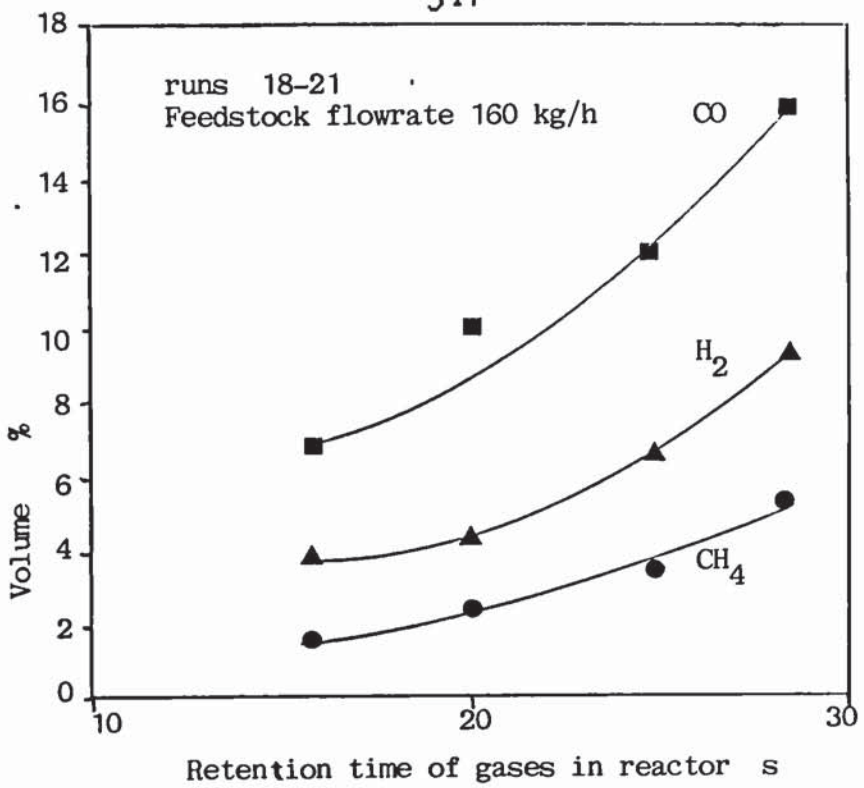

Figure 5.49 : Volume % of CO, H_2,CH_4 versus retention time.

5.21.3 Comparison with published results

The effect of retention time of gases on the performance of the fluidized bed had been examined only by the group of the Missouri Rolla University. However, conflicting results were reported. In two publications (93) (103), they reported most of their results of sawdust gasification as a function of gas residence time and showed that the performance of the reactor worsened as residence time increased. However, in two other articles carried out with charcoal, the performance of the same reactor improved with lower retention time (94, 111), as shown in Figure 5.50.

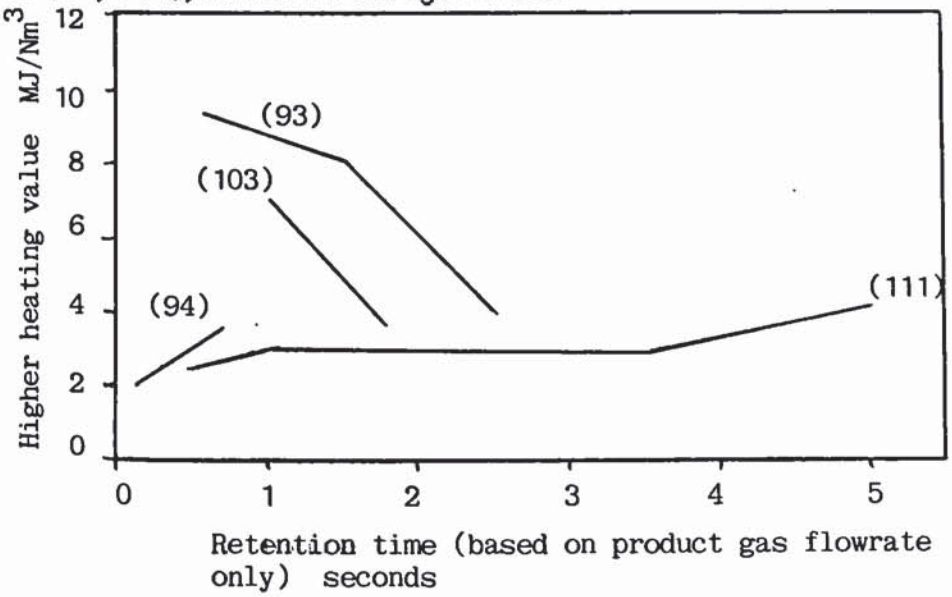

Figure 5.50 : Gas higher heating value versus retention time, published data (93, 94, 103, 111).

The above confusing data can be explained if the reactors and feedstocks used are examined. The reactor of references (93) and (103) was a 0.15 m internal diameter reactor with the feeding port just below the exit of the gases. The very small reactor (there was no expanded freeboard) resulted in very short residence times (0.5-2.55). Under these experimental conditions, the biomass pyrolysed as soon as it entered the reactor, but the pyrolysis products as well as most of the charred sawdust were carried out of the reactor. With longer residence times, however, the pyrolysis products probably reacted with oxygen from the air feed and were converted to carbon dioxide and water; hence the gas quality dropped. Thus the authors reported mainly pyrolysis gas compositions and not gasification. In reference (94) a 0.10 m internal diameter reactor was used, but the feedstock was introduced just above the bed. Since charcoal has a lower volatiles content than biomass, gasification of the char took place and the performance improved at longer retention times. In yet another small scale reactor of 0.10 m internal diameter, they introduced the feedstock below the surface of the bed and the performance improved significantly with lower retention times due to the reasons explained in the previous section.

5.22 CONCLUSIONS

Despite the limitation of resources at the pilot plant location, an extensive experimental programme was carried out, which evaluated the influence of most of the important parameters in fluidized bed gasification. It was demonstrated that fluidized bed gasification of biomass is a viable technology and the process can be commercialized after a design procedure has been postulated.

The fluidization characteristics of the reactor shown in Table 5.27, were within acceptable limits and the differences between experimental and design values were justified on basis of slightly different properties between actual and design data concerning the distributor and the sand bed.

Table 5.27 : Fluidization characteristics of reactor, experimental data at maximum flowrates.

Pressure drop over distributor	140 mm H_2O
Pressure drop over distributor and bed 0.6 m	1000 mm H_2O
Minimum fluidization velocity	0.16 m/s

The commissioning experiments identified the problems with the various equipment and apparatus and these were addressed accordingly, so that satisfactory operation of the pilot plant could be attained.

The experiments confirmed that the air factor has a strong influence on the performance of the reactor and that all others variables being constant, it sets the temperature of the bed and gas composition of the product gas. In those experiments the air factor varied in the range of 0.2 to 0.87; however, in the range of practical interest, 0.2 to 0.4, satisfactory results were obtained as summarized in Table 5.28. Reasonable agreement was obtained between the results of this work and published data.

Table 5.28 : Summary of most important results in the air factor range of 0.2-0.4.

Parameter		Range	Realistic *optimum*
Bed temperature	°C	700-917	850
Higher heating value of gas	MJ/Nm^3	30-70	6
Gas yield	kg/kg feed MAF	1.5-3.0	2.5
Thermal efficiency	%	40-85	70

The results confirmed the conclusions of the literature survey that thermodynamic predictions are useful in identifying the general trends; however, there are significant differences with actual experimental data. Nevertheless, it was shown that the predicted trends are the same with the experimental trends.

Several parameters which are often ignored in the literature, such as char bed, flame burn out, retention time, U/U_{mf} ratio and turn down ratio, were identified and examined. These can improve the understanding of the gasification process in a fluidized bed. The operating limits of this system were evaluated and it was found that the minimum air factor at which stable operation can be achieved is 0.2.

It can be concluded that the experimental programme yielded valuable results, which can form the basis of a design procedure for fluidized bed gasifiers.

CHAPTER SIX : EMPIRICAL MODEL FOR FLUIDIZED BED GASIFIERS

6.1 INTRODUCTION

In this chapter the results from the experimental programme are correlated by empirical relationships, which comprise an empirical model for the performance of a fluidized bed gasifier. This model is then extended to include feedstocks with moisture contents in the range of 15-50 wt%. Both models can be applied for simulation of the performance of fluidized bed gasifiers.

6.2 REGRESSION ANALYSIS

6.2.1 Introduction

Modelling is defined as the representation of a physical system by a set of equations. Relevant to reactor design, is the prediction of outlet products concentrations and temperature from inlet reactant concentrations and reactor dimensions. Thus in the case of a fluidized bed gasifier, a model is a set of equations by which the performance of the reactor can be determined on basis of the air and feedstock inlet concentrations. The term performance applies to the composition of the product gas, its mass and volumetric flowrate, higher heating value of the gas, thermal efficiency and temperature of the gases at the exit, as well as any other useful information concerning the products.

6.2.2 The independent variable

In the derivation of the empirical relationships, all data from the twenty five primary runs of the experimental programme (part II, see section 4.5.2) were used. However, non uniform feed rates were encountered in some of the experiments, in which cases the air factor varied. If the feed rate is reduced, the concentrations of hydrogen and methane, which are produced primarily from wood pyrolysis, are reduced more than the carbon oxides formed by the gasification of the char built up in the bed (see section 5.12.5). The reverse occurs if the feed rate is increased. Thus some unsteady state data were produced which are included in the derivation of the empirical relationships. This is believed to be the major reason for the scatter of the data.

The evaluation of the results concluded that the air factor is the most important parameter in gasification (see section 5.22), as it defines the temperature of the bed, the gas composition, and consecutively the higher

heating value of the gas and the thermal efficiency. It was therefore decided to try to correlate the results with the air factor and wherever possible with the bed temperature, which is the second parameter of importance in gasification (see sections 5.10.1 and 5.10.2).

6.2.3 Regression of data

Linear regression was used whenever possible to derive correlations. It can be shown (183) that the fit with the highest probability of being correct, i.e. the "best fit" of an equation to a set of experimental points which includes a normally distributed random error, is the equation that minimizes the sum of squares of the discrepancies between model predictions and measured values:

$$\sum_{i=1}^{n} (y_i - y_i^*)^2$$

where there are n experiments with experimental results y_i and model predicted values y_i^*.

However, with a non-linear model, the model is so free that there is no way of analytically determining the value of the parameters that will give the lowest least square fit, as there is with linear regression. In ths case the optimum parameter values must be obtained by a non-linear minimization procedure, using the parameters as the optimization variables and

$$\Phi = \sum_{i=1}^{n} (y_i - y_i^*)^2$$

as the objective function to be minimized (183). Non-linear regression packages therefore have as their first step an optimization routine to locate the parameter values. The optimization algorithm of Marquardt (287) has been specially developed for non-linear regression and is often successfully employed. Marquardt's is a derivative method (i.e. in the search for a minimum of Φ, the partial derivatives of Φ with respect to y_i^* must be calculated), which in principle combines the steepest ascent optimization method and Newton's method. This method was used for the non-linear regression analysis.

6.2.4 Procedure

The experimental data were plotted on arithmetic coordinate paper to examine if there was approximately a straight line or a curve. If a straight line was apparent, linear regression to an equation $y = a + bx$ was performed; but if the data appeared to approximate a smooth curve, then several relationship were assumed which could fit the data and regression analysis was performed with Marquardt's method until an optimum of Φ was obtained. It was found that six equations, given in Table 6.1, were sufficient in fitting the data of practically all curves and this was also confirmed by the literaure (287).

Table 6.1 : Equations used in regression analysis

6.1	$Y = \frac{1}{a + bx}$
6.2	$Y = a + \frac{b}{x}$
6.3	$Y = \frac{x}{a + bx}$
6.4	$Y = ax^b$
6.5	$Y = ab^x$
6.6	$Y = a + b \log^x$

6.3 EMPIRICAL MODEL

6.3.1 Best correlations

For each of the functions of Table 6.1 the final sum of squares, the standard deviation, the values of the parameters a and b, as well as the errors in these parameters and the partial correlation between the parameters, were computed and are given in Appendix VIII. The equations with the minimum final sum of squares and standard deviation were considered to fit the results best. A further improvement was then considered by including a third parameter (for example $1/y = a + bx + cx^2$), but in all except one correlation no significant improvement (in terms of final sum of squares and standard deviation) was obtained. The best correlations which constitute the empirical model are given in Table 6.2.

Table 6.2 : Best correlations, empirical model

Equation		Coefficient of correlation	Units	Number
HHV	$= 5.322 - 3.932 \log S - 6.088 S$	0.995	MJ/Nm^3	6.7
Y	$= 5.087 S^{0.6536}$	0.914	$\frac{kg\ gas}{kg\ MAF\ feed}$	6.8
η	$= 83.038 - 79.556 S$	-0.685	%	6.9
T_B	$= 1012.2 + 411.9 \log S$	0.959	°C	6.10
XCON	$= 0.1723 + 0.5114 S$	0.729	$\frac{kg\ condensate}{kg\ MAF\ feed}$	6.11
H_R	$= 4.429 + 12.561 S$	0.815	MJ/kg	6.12
YH_2	$= 0.0216 - 0.0206 S$	-0.626	$\frac{kg\ H_2}{kg\ MAF\ feed}$	6.13
YCH_4	$= 0.0873 - 0.082 S$	-0.720	$\frac{kg\ CH_4}{kg\ MAF\ feed}$	6.14
YCO	$= 0.4356 - 0.3710 S$	-0.644	$\frac{kg\ CO}{kg\ MAF\ feed}$	6.15
YC_2	$= 0.0487 - 0.0562 S$	0.414	$\frac{kg\ C_2}{kg\ MAF\ feed}$	6.16
YCO_2	$= 0.3852 + 0.9068 S$	0.802	$\frac{kg\ CO_2}{kg\ MAF\ feed}$	6.17
HHV	$= 16.463 - 0.014 T_B$	-0.683	MJ/Nm^3	6.18
η	$= 153.2 - 0.121 T_B$	-0.577	%	6.19
T_0	$= -198.6 + 1.174 T_B$ *	0.855	°C	6.20

where HHV = higher heating value
S = air factor
Y = gas yield
η = thermal efficiency
T_B = temperature of bed
T_O = temperature of outlet
XCON = condensate yield
H_R = heat of reaction
Y_i = yield of gaseous component i

*The original intercept for the T_O, T_B correlation (equation 6.20) was -298.6. This was increased by 100, to -198.6, to account for the temperature rise in the freeboard when steady state is attained (see section 5.12.3).

Thus, if the air factor, S, is known, then it is possible to predict the performance of the reactor by the application of the above empirical model.

6.3.2 Limits, optimum and confidence of the model

During the experimental programme, experiments were carried out in the air factor range of 0.2 - 0.9. However, only five experiments were performed at air factors higher than 0.4, while the bulk of the experiments 80% were in the air factor range of interest, 0.2 - 0.4 (see section 5.6). Thus, although equations 6.7 to 6.17 can be applied to the air factor range of 0.2 - 0.9 higher confidence exists in the range of 0.2 - 0.4. Table 6.3 gives the limits, optimum and confidence for each of the correlations of Table 6.2, so that the model can be applied with greater security for the air factor range of 0.2 - 0.4.

The model is limited at the lowest air factor of 0.2. Below this value, it was not possible to achieve a steady state during the experiments (see section 5.14) and thermodynamics predict that the performance of a reactor below this value of air factor will drop significantly (see section 2.4.3.3). Thus the model cannot be applied for the air factor range of 0.0 - 0.2. However, this is not a serious drawback for the model, since in practice no fluidized bed gasifier would operate in the air factor range of 0.0 - 0.2. However, for pure theoretical reasons and simulative excercises, the thermodynamic model developed in this work can very well be applied to predict the performance of a fluidized bed gasifier, in this lower range of air factors.

Table 6.3 : Applicability of model at constant feed moisture.

Parameter	equation	Typical range	Realistic optimum	Confidence
HHV	6.7	4.5-6.5	6.0 MJ/Nm^3	H
Y	6.8	1.9-3.5	2.5 $\frac{kg\ Gas}{kg\ MAF\ feed}$	H
η	6.9	50-70	65 %	H
T_B	6.10	724-850	800 °C	H
XCON	6.11	0.27-0.38	0.32 $\frac{kg\ condensate}{kg\ MAF\ feed}$	H
H_R	6.12	6.8-10.0	8 MJ/kg	H
YH_2	6.13	0.013-0.017	0.016 $\frac{kg\ H_2}{kg\ MAF\ feed}$	L
YCH_4	6.14	0.050-0.070	0.065 $\frac{kg\ CH_4}{kg\ MAF\ feed}$	L
YCO	6.15	0.290-0.360	0.35 $\frac{kg\ CO}{kg\ MAF\ feed}$	L
YC_2	6.16	0.026-0.037	0.035 $\frac{kg\ C_2}{kg\ MAF\ feed}$	L
YCO_2	6.17	0.22-0.42	0.24 $\frac{kg\ CO_2}{kg\ MAF\ feed}$	L
HHV	6.18	5.2-6.5	6.0 MJ/Nm^3	H
η	6.19	55-69	65 %	H
T_O	6.20	650-800	750 °C	H

where H = high
L = low

It is stipulated that the degree of confidence of the realistic optimum is a subjective evaluation of the author on basis of experience and the results obtained.

6.4 MOISTURE CONTENT OF THE FEEDSTOCK

6.4.1 Introduction

During the execution of the experimental programme, it was not possible to obtain feedstock of significantly different moisture contents in order to evaluate the effect of this feedstock characteristic on the performance of the fluidized bed gasifier. Therefore, the application of the empirical model of Table 6.2 is limited for feedstocks with a moisture content in the range of 10-15 wt%. In order to overcome this limitation, data from the literature were used to extrapolate the applicability of the model for feedstocks with moisture content in the range of 15-50 wt%.

6.4.2 Development of model

The moisture content of biomass is one of the more important parameters in biomass gasification (see section 1.1.2). However only one reference (78) could be found, which presented experimental data on the influence of the moisture content on the higher heating value of the gas only. These were correlated by linear regression and were used to extent the empirical model. The resulting relationship is given by equation 6.21:

$$HHV = 6.51 - 0.0844\ M \qquad \text{equation 6.21}$$

where the coefficient of correlation was 0.941 and M is the moisture content in %. However, this information is not sufficient to derive a model for the prediction of the performance of a fluidized bed gasifier.

To accomplish this the following assumptions are made :

1) It is assumed that the performance of a gasifier with a feedstock of 14 wt% is the basic representation of the system (a moisture of 10 wt% is considered representative of the results, since runs 29 to 36 were carried out with feedstock of this moisture and in the optimum air factor range of 0.2-0.4. With feedstocks of higher moisture content, it is assumed that the extra moisture (M-14) does not affect the performance of the reactor (higher

heating value, gas yield, thermal efficiency and heat of reaction), but leaves the reactor as steam. It has been shown experimentally that the addition of steam has little (105) or no influence at all (104) on the above parameters in the air factor range of 0.2-0.6.

However, thermodynamics predict that steam can strongly affect the performance of a gasifier in the air factor range of 0-0.15 (109). At such low air factor the yield of char increases (see Figure 2.12) and steam can accelerate the gasification of char, resulting in higher heating values and temperature (109). However, this effect diminishes at air factor ranges above 0.15 and according to thermodynamics (109) is eliminated above air factors of 0.25. Since also at temperatures below 900 °C, the composition of the product gas is significantly different from the equilibrium composition of the water gas shift reaction (see section 5.7.3) under normal operating temperatures (750-850 °C) and air factor (0.2-0.4), steam can be considered as an inert in the gasification process. However, it is possible that increasing the overall water content of gasification by raising the moisture content of the feed, can result in somewhat different performance. Since drying and pyrolysis occur almost simultaneously in a high heating rate reactor such as a fluidized bed (see section 2.5.3.2), it can be envisaged that moisture can affect the structure of the final char (e.g. larger pores), which can affect reaction rates (see section 2.5.5.2). However, no published data were found on this aspect.

For the purpose of design, however, it can be assumed that increasing the overall water content of gasification either by steam addition or higher moisture content will have no effect on performance.

2) Equation 6.21 indicates that as the moisture content of the feedstock increases (while all other parameters remain constant), the higher heating value of the gas will decrease. It is assumed, that lower higher heating values of the gas will be obtained by operation at a higher air factor. However, the bed temperature will decrease because of the additional heat required to maintain the steam at reactor temperatures. It is likewise assumed, that all additional energy released by operating at a higher air factor (see section 2.4.3.3) will be consumed to maintain the temperature of the additional steam at bed temperature. Bed temperature will be considered the temperature of the bed of a gasifier operating at an air factor of 0.32 (average value of runs 29 to 36) with a feedstock of 14 wt% moisture (see

Table 5 and section 5.3.4). Thus a constant bed temperature of 800 °C is postulated. This is maintained by increasing the air factor when the moisture content of the feedstock raises. Since the bed temperature is maintained constant, it follows that the outlet temperature of the gases will also remain the same. For bed temperature 800 °C, equation 6.20 gives:

$T_0 = 740$ °C

3) It is assumed that increased moisture content of the feedstock of this work would have the same effect on the higher heating value of the gas as the published data (78). Since the published results gave consistantly lower higher heating values of the gas than the values obtained in this work, the y intercept of equation 6.21 was extrapolated to the results of this work, as given by equation 6.22:

$$HHV = 6.77 - 0.0844\,M \qquad \text{equation 6.22}$$

This is determined by calculating the average higher heating value of runs 29 to 36, all of which were carried out with a feedstock of 14.1 wt% moisture content. This is equal to 5.59 MJ/Nm^3, while equation 6.21 for the same moisture gives 5.33 MJ/Nm^3. The difference 0.26 MJ/Nm^3 is added to the intercept and the sum 6.77 is considered as the new y-axis intercept. It is assumed that the slope of the line remains the same. This extrapolation is justified since different feedstocks were used in the two works, and the results of this work are more representative for the feedstock used.

4) The condensate yield is assumed to be the same under the experimental conditions at an air factor 0.32 plus the additional steam (M-14) produced by the extra moisture. Equation 6.11 for this air factor gives:

$$XCON = 0.33\ \frac{\text{kg moisture}}{\text{kg MAF feed}}$$

Thus the condensate yield for feedstocks at higher moisture content is:

$$XCON = 0.33 + \frac{M-14}{G_f} \qquad \text{equation 6.23}$$

where M = moisture content %
and G_f = the mass flowrate of the feedstock.

5) Equation 6.7 does not allow for an exact solution in terms of the air factor of the form:

$S = f(HHV)$ equation 6.24

Thus in order to determine the operating air factor, a new correlation of the results of this work was made between thermal efficiency and higher heating value as given by equation 6.25:

$\eta = 8.024 + 9.288\ HHV$ equation 6.25

where the coefficient of correlation was 0.91.
The air factor can then be determined by first determining h and solving equation 6.9 for S. Thus:

$$S = \frac{83.038 - \eta}{79.556}$$ equation 6.26

The equations for the performance of a fluidized bed gasifier with feedstock moisture content in the range of 15-50 wt% are given in Table 6.4

Therefore if the moisture content of the feedstock is known, it is possible to determine the performance of the gasifier, by applying consecutively the above equations.

Table 6.4 : Empirical model for performance of fluidized bed gasifier, moisture content.

	Equation	Units	Number
HHV	$= 6.77 - 0.084\,M$	MJ/Nm^3	6.22
η	$= 8.02 + 9.288\,HHV$	%	6.24
S	$= \frac{83.038 - \eta}{79.556}$	-	6.25
XCON	$= 0.33 + \frac{M-14}{G_f}$	$\frac{kg\ H_2O}{kg\ MAF\ feed}$	6.23
T_B	= 800	°C	
T_o	= 740	°C	
Y	$= 5.087\,S^{0.6536}$	$\frac{kg\ gas}{kg\ MAF\ feed}$	6.8
H_R	$= 4.429 + 12.561\,S$	MJ/kg	6.12
YH_2	$= 0.0216 - 0.0206\,S$	$\frac{kg\ H_2}{kg\ MAF\ feed}$	6.13
YCH_4	$= 0.0873 - 0.082\,S$	$\frac{kg\ CH_4}{kg\ MAF\ feed}$	6.14
YCO	$= 0.4356 - 0.3710\,S$	$\frac{kg\ CO}{kg\ MAF\ feed}$	6.15
YC_2	$= 0.0487 - 0.0562\,S$	$\frac{kg\ C_2}{kg\ MAF\ feed}$	6.16
YCO_2	$= 0.3852 + 0.9068\,S$	$\frac{kg\ CO_2}{kg\ MAF\ feed}$	6.17

6.4.3 Limits and confidence

The lower feed moisture content to be encountered in practice for biomass fluidized bed gasification is about 10 wt%. However, fresh biomass can have moisture up to 95 wt% (e.g. water hyacinth) (5). It has been shown experimentally that an upper limit of 50 wt% moisture content must be considered, since at this value the higher heating value of the gas decreased to about 1 MJ/Nm^3 (78).

Since in the range of 10-15 wt% moisture content the empirical model at constant moisture, EMCM, can be used with greater confidence, the applicability of the empirical model incorporating the moisture content of the feedstock, EMM, is restructed in the moisture content of 15-50 wt%.

The EMM model should be applied very cautiously as there is only moderate confidence for it. This is because it was developed by the combination of results from this work and data from the literature.

6.5 DISCUSSION

In order to illustrate the EMCM and EMM models, the EMCM was simulated for air factors of 0.2, 0.3 and 0.4, while the EMM was simulated for feedstocks of 20, 30, 40 and 50 wt% moisture content. The results are shown in Table 6.5.

The effect of the air factor and moisture content on performance (higher heating value and thermal efficiency) is illustrated in Figures 6.1 and 6.2 respectively for the EMCM and EMM models. Figure 6.1 and 6.2 show that the EMCM and EMM models can predict the performance of a fluidized bed gasifier. The predicted results are in general agreement with experimental data (see sections 5.11.3 and 5.11.5).

Table 6.5 : Simulation of EMCM and EMM models

	EMCM			EMM				
Moisture wt%	10 - 15			20	30	40	50	Units
Air factor	0.2	0.3	0.4	0.35	0.45	0.54	0.64	
HHV	6.85	5.55	4.45	5.09	4.25	3.41	2.57	MJ/Nm3
Y	1.78	2.32	2.79	2.56	3.02	3.40	3.80	kg gas/kg MAF feed
η	67.1	59.2	51.2	55.3	47.5	39.7	31.9	%
T_B	724	797	848	800	800	800	800	°C
XCON	0.275	0.325	0.377	$0.33+\frac{6}{G_f}$	$0.33+\frac{16}{G_f}$	$0.33+\frac{26}{G_f}$	$0.33+\frac{36}{G_f}$	kg condensate/kg MAF feed
H_R	6.94	8.20	9.45	8.82	10.08	11.21	12.46	MJ/kg
YH_2	0.017	0.15	0.013	0.014	0.012	0.010	0.008	kg H_2/kg MAF feed
YCH_4	0.066	0.063	0.055	0.058	0.050	0.043	0.035	kg CH_4/kg MAF feed
YCO	0.361	0.324	0.287	0.306	0.268	0.235	0.198	kg CO/kg MAF feed
YC_2	0.037	0.032	0.026	0.029	0.023	0.018	0.013	kg C_2/kg MAF feed
YCO_2	0.566	0.657	0.748	0.703	0.793	0.875	0.965	kg CO_2/kg MAF feed
T_o	651	737	797	740	740	740	740	°C

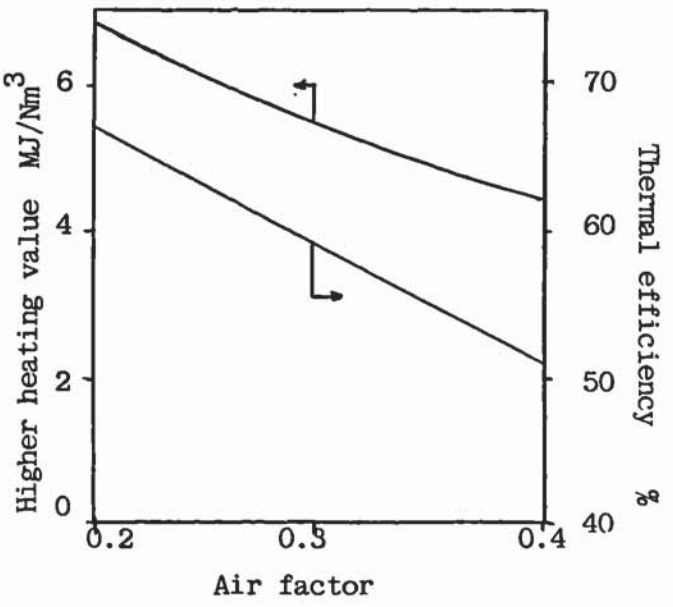

Figure 6.1 : EMCM model. Performance of fluidized bed gasifier.

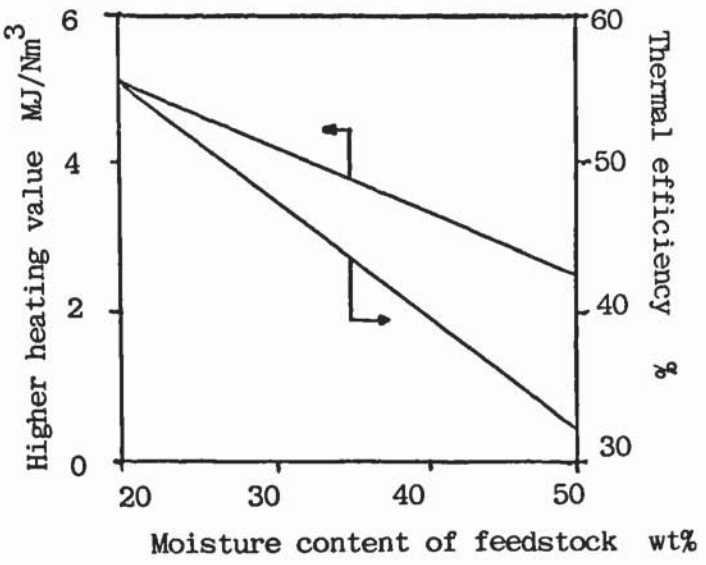

Figure 6.2 : EMM model. Performance of fluidized bed gasifier.

However, the EMM model has the limitation that moisture content and air factor cannot be varied independently. Instead the model is based on the assumption that the air factor is raised to compensate for the increase in moisture content. This assumption is partially valid, since it is not possible to operate a gasifier at an air factor of 0.2 with a feedstock of 50 wt% moisture. This would result in very low bed temperature, below 650 °C and probably it would not be possible for the system to operate autothermally but additional fuel should be added. Additional experimental work with moist feedstocks is required to improve the knowledge of this parameter (see section 10.2.).

6.6 CONCLUSIONS

Two empirical models were developed which can predict the performance of fluidized bed gasifiers. The EMCM, or empirical model at constant moisture, was developed exclusively on basis of results of this work. For the EMM, or empirical model moisture, data from the literature had to be used, while various assumptions were made. Since it was not possible to experimentally verify the model, it should be applied very cautiously.

CHAPTER SEVEN : DESIGN PROCEDURE FOR FLUIDIZED BED GASIFICATION PLANTS

7.1 INTRODUCTION

A model for fluidized bed gasifiers is commonly used to simulate the performance of this type of reactor under different operating conditions and/or air and feedstock flowrates. However, the simulation results are not directly applicable for specifications concerning the construction of the reactor, or the peripheral equipment. For this purpose, additional information and/or relationships are needed, the combination of which can lead to specifications of the reactor and peripheral equipment. This derivation of specifications is commonly termed design procedure. Thus a design procedure is the process that starts with an objective (in this work to design a gasification plant), proceeds through a sequence or set of mathematical, empirical or other relationships and ends with a specification which can be transferred to a fabricator, for the construction of the equipment.

In order to devise a design procedure, its objective must be clearly defined and all data required for the specifications of equipment must be identified. Then relationships must be developed by which the specifications can be determined on the basis of the definition of the objective. A well defined procedure must then be developed, which clearly shows all sequential steps that must be undertaken in order to determine the specification.

During this work, and especially in the literature review, the most common applications of fluidized bed gasifiers were identified. Thus the objectives of gasification plants are well understood and can be defined (see section 7.2). Furthermore, by the execution of the experimental programme the influence of all major parameters on performance was examined and the operation of large scale fluidized bed gasifiers was experienced. This led to the development of two empirical models by which the performance of this type of gasifiers can be simulated. The above information, supplemented by data from the literature can lead to the development of a design procedure for fluidized bed gasification plants.

This chapter begins with definitions of the most common objectives of fluidized bed gasification plants. Then, for each of the major parts of the plant - feeding system, reactor and gas cleaning - a design procedure is developed which leads to the determination of specifications.

7.2 OBJECTIVES OF GASIFICATION PLANTS

The general objective of gasification plants is to process biomass into a combustible gas to be used in a downstream process. Usually, the downstream process or "back-end" is a well proven process; however, on the other hand, the thermochemical processing or "front-end" is often unproven and there is a technological uncertainty (144).

The thermochemical processing can be subdivided into feedstock pretreatment, reaction and gas post-treatment, as shown in Figure 7.1 (144). However, the objectives of a gasification plant usually reduce the available options to just a few; for example, by defining the oxidant of the reaction as air, the reaction alternative operations in the system reduce to air gasification only.

		[Conditioning
		[Drying
		[Handling
	[PRETREATMENT	[Pelletisation
	[	[Screening
	[	[Size reduction
	[	[Storage
	[	
	[	[Air gasification
	[	[Oxygen gasification
THERMOCHEMICAL	[REACTION	[Liquefaction
PROCESSING	[	[Pyrolysis
	[	[Steam gasification
	[	
	[	[Absorption
	[	[Cyclone
	[	[Distillation
	[	[Electrostatic pptn.
	[	[Filtration
	[POST-TREATMENT	[Heat exchange
		[Oxidation
		[Phase separation
		[Reforming
		[Scrubbing
		[Waste treatment

Figure 7.1 : Alternative operations in thermochemical processing (144).

The most common specific objectives of a gasification plant are:

a) to recuperate the energy content of a well defined (availability, quality) feedstock, that either is produced as waste (e.g. wood waste from a furniture factory) or is available as raw material (e.g. energy plantation) and

b) to provide for the energy or power requirements of a plant with fuel gas, which can be produced by gasification of biomass. The former specific objective is "front-end" related, while the latter is related to the "back-end" of the total system. However, in both cases, one more parameter must be considered: the cost of the front and back-end.

7.3 AIR GASIFICATION PLANTS

7.3.1 Introduction

Air gasification plants are currently sold commercially by several companies and offer the best possibility for a wider application, due to their relative simplicity and acceptable cost (see section 2.4.3.9). Oxygen gasification has the drawback that it is only interesting for large scale pressurized applications for synthesis gas, which are relatively expensive and the present and near future market situation do not justify the cost (see section 2.4.4.4). Liquefaction pyrolysis for liquid fuels (with the exception of charcoal production which is a well proven and widely practiced process) and steam gasification still have to undergo development for proven and economically viable systems. Since the main objective of this thesis is to study the air gasification of biomass, only this type of reaction will be considered in the development of the design procedure. However, certain parts such as feedstock pretreatment and gas post-treatment can be valid for other types of thermochemical processing plants.

7.3.2 Alternative operations of an air gasification plant

Air gasification produces a low heating value gas and since the energy density (defined as the energy content per unit weight of material) is low, economics put some restrictions on the possible operations of such a plant (288).

7.3.2.1 Pretreatment

Provisions must be made to receive the feedstock. These usually include weighing, storage, retrieving and handling. For large scale plants (capacity

higher than 5 dry t/h) silos and live bottom bins linked to the gasifier feeder system are justifiable, while this is not the case for small scale plants. Specification of appropriate units also depend on the type of biomass, capacities and sophistication required.

The feedstock characteristics and the requirements of the gasifier will specify any processing such as densification or size reduction. Similarly, the sophistication of the feedstock size control operation strongly depends on the scale of the process, since screening and pelletizing are only economically justified for large scale units. In the case of wood, it is usually expected that it will be supplied as ready chipped material since this considerably reduces transport, handling and capital costs. However, the most economical gasification plant will not require any size control operation.

Drying of feedstock improves the gasifier performance in terms of gas quality and thermal efficiency. Drying is however an expensive operation and should only be applied when essential (e.g. biomass with moisture content higher than 10 wt%) and cost effective. This limits drying for large scale plants only.

7.3.2.2 Reaction

The objectives of the thesis (see section 1.6) specify the air gasification of biomass in fluidized bed systems as the thermochemical reaction. Thus, the pretreatment and post-treatment should be designed subject to the requirements of this reaction.

7.3.2.3 Post-treatment

For air gasification of biomass only cyclone, filtration scrubbing and exchange are cost effective operations. However, the most cost effective and simplest operation is to burn the hot raw gas, since no sensible heat is lost (which is about 10 % of the feed heating value); gas cleaning requirements and costs are minimal and there are no waste water treatment, disposal problems and costs.

Table 7.1 : Advantages and disadvantages of wet and dry collection (First, 1953)

WET	DRY
Advantages	
- Can collect soluble gases and particulates at the same time.	- Recovery of dry materials may give final product without further treatment.
- Cooling and washing of high temperature gases.	- Corrosion free in most cases.
- Corrosive gases and mists can be recovered and neutralized.	- Less storage capacity required for product.
- Plants are generally small in size compared to dry collectors.	- Particles greater than 0.05 µm may be collected with long equipment life and high collection efficiency.
Disadvantages	
- Insoluble material requires settling in filtration plant.	- Hydroscopic materials may form solid cake and are difficult to shake off.
- Soluble material must be concentrated and recrystalized.	- Maintenance of plant and disposal of dry dust may be dangerous to operators.
- Waste liquids require disposal which may be difficult.	- High temperature may limit means of collection.
- Mists and vapours may be entrained in the effluent gas stream.	- Limitations of use for corrosive mists.
- Washed gases will be saturated with liquid vapour, have high humidity and low dewpoint.	- Creation of secondary dust problem.
- Very small particles (sub-micron sizes) are difficult to wet, and so will pass through the plant.	
- Corrosion problems.	
- Liquids may freeze in cold weather.	

Hot gas cylcones are usually used to remove the particulates from the gas, however these devices will only reduce large particles above about 500 microns by up to about 75%. Gas scrubbers are relatively efficient units and can simultaneously remove particulates and cool the gas (289). However, they produce waste water which contains phenols and tar and has to be purified before discharge. Since the gas contains large amounts of water and

tars, mist filters are used in filtration of coolgas. However, filtration is only required if the gas is to be used in an internal combustion engine or turbine. Finally recuperation of the sensible heat of the gas is an interesting option and can be used either to produce steam in a waste heat boiler or preheat the oxidizing gas in order to improve the efficiency of the process.

The advantages and disadvantages of wet and dry collection are given in Table 7.1 (290). It can be concluded that dry collection, or cyclones, are more acceptable from the environmental point of view. Since cyclones have no operating costs they are the preferred operation whenever the gas does not have to be cooled. Moreover, when economics and scale of operation permit, a cyclone may proceed a scrubber to remove the coarser particles.

7.3.2.4 Operations for air gasification plants

Figures 7.2 and 7.3 summarize the possible operation for the air gasification of biomass in fluidized bed reactors, respectively for large and small scale operation .

Pretreatment	Handling Size control Screening Drying Storage in vessels Feeding
Reaction	Air gasification
Post-treatment	Cyclone Scrubbing Filtration Heat exchange Waste treatment.

Figure 7.2 : Operations at a large scale plant (capacity higher than 5 t/h MAF).

Pretreatment	Handling Storage Feeding
Reaction	Air gasification
Post-treatment	Cyclone Heat exchange Filtration.

Figure 7.3 : Operations at a small scale plant (capacity below 5 t/h MAF).

7.4 DESIGN OF AIR GASIFICATION PLANTS

7.4.1 Introduction

Present market evaluations (see section 2.4.3.9 (24), (290)) indicate that there is higher demand for low capacity gasifiers in the range of 1-5 ton/h MAF. Thus the design procedure will be developed on the basis of Figure 7.3.

7.4.2 Pretreatment

7.4.2.1 Handling and storage

The handling and storage of the feedstock are relatively simple for small scale gasification plants. Provisions must be made that the trucks transporting the biomass can have easily access to the storage place where they can unload the feedstock. Weighing of the feedstock delivered is not necessary and the deliveries can be recorded in terms of the volume of the truck.

The storage place should be on ground level to facilitate retrieving of the biomass and closed in order to protect the feedstock from rain and snow. The walls and ceiling can be constructed by pre-fabricated materials, while sliding doors can provide access for the trucks. The doors and ceiling must have sufficient height for the unloading of the trucks. Alternatively, the feedstock can be delivered in closed containers - as was done during this work - which needs no building for storage. Preferably the access roads and storage facilities should be covered by asphalt or cement.

The most easy and reliable way to transport the feedstock from storage to the feeding system is by means of a forklift equipped with a front-end loader.

7.4.2.2 Feeding

Feeding biomass in the gasifier is very important, since a continuous and constant flowrate must be maintained (see sections 2.4.3.7, 5.15). Therefore, biomass feeders are critical components of any energy conversion system and must operate automatically with minimal attention. However, most feeding problems can be avoided by careful characterization of the feedstock and proper matching of equipment to the required duty. During the commissioning of the process development unit, it was realized that the feeding system provided by Vyncke Warmtetechniek was inadequate (see section 4.3.2). Thus

it became clear that self designed systems, unless backed up by several years of experience, usually fail to operate satisfactorily. Considering that Vyncke Warmtetechnieck had about 50 years experience in the field of biomass boilers and feeders and still having failed to design an appropriate feeding system, it is evident that it is better not to design feeding systems but instead to rely on commercially proven systems.

However in the selection of an appropriate feeding system several parameters must be considered and evaluated. These are discussed in the following sections, 7.4.3 and 7.4.4.

7.4.3 Fluidized bed requirements

7.4.3.1 Introduction

The single most important characteristic of the fluidized bed gasifier pertaining to feeders is whether the reactor operates under conditions that produce a slight vacuum in the freeboard, or whether the system operates under positive pressure. The former case allows for simplified design of the feeder and there are several types available. However, the latter case imposes the limitation of appropriate sealing of the feeder to ensure that gases do not leak from the reactor.

Typically fluidized bed gasifiers are fueled by feedstocks ranging in size from 6 to - 80 mm with moisture content up to 50 wt%.

Fluidized beds are inherently well mixed and have a high thermal capacitance that makes them tolerant to non uniform feeding compared to fixed bed gasifiers. However, if hot and cold spots exist in the bed, then sintering can take place. Thus the distribution of fuel across and within the fluidized bed must be carefully addressed. The distribution within the bed is controlled by the ratio of the superficial velocity over the minimum fluidization velocity, which usually must be higher than 2.5 (see equation 3.14 and section 5.17). However, the distribution across the bed is controlled by the number of feeding ports. It is generally accepted that for fluidized beds up to 1 m diameter, a single feeding port is sufficient, while for larger beds additional feeding ports must be provided.

7.4.3.2 Determination of the distance between feeding ports

In the literature on biomass gasification no information could be found concerning this problem. However, from the coal gasification literature (291) the following simplified procedure can be applied. If S is the distance between two feeding ports, then the time required for complete mixing of the feedstock is (291):

$$M_t = \frac{S^2}{U_l} \qquad \text{equation 7.1}$$

where M_t = mixing time
U_l = lateral mixing velocity

In general, for sand-char mixtures fluidized beds, $U_l = 0.1\ m^2/s$ (291). Also it can be assumed that for single, fine biomass char particles, the burn out time is 30 seconds (291). Thus, solving for S and substituting these data in equation 7.1 gives:

$$S = \sqrt{M_t \times U_l} \qquad \text{equation 7.2}$$

$S = 1.7$ m.

It can therefore be concluded that in general feeding ports should be placed at about 1.7 m from each other.

Two feeding ports should be designed diametrically opposite; while three or four feeding ports should be designed at 120° and 90° respectively from each other.

7.4.4 Properties of biomass relative to feeding

7.4.4.1 Introduction

This section deals with the physical properties and flow behaviour of biomass, which in conjunction with fluidized bed gasifiers determine the types of feeders that should be used. The physical properties important to feeder design, that will be considered here, are: chemical composition, size distribution, bulk density, abrasiveness, corrosiveness, angle of repose, friction coefficient and stickiness. Of these properties, the single most

important one is size distribution, because of the inherently difficult task of obtaining anything near a consistent size distribution for a biomass fuel stream produced as a mill-by product. Related to size is the normally poor flowability of wood residues, which leads to bridging in bins and jamming of conveying and feeding equipment.

Because of the wide variety of species, shapes and sizes of biomass fuels, it is not possible to state specific values for physical properties. However, industrial experience has led to a definition of typical ranges of properties and it is these that have been extracted from published data and summarized in this section.

7.4.4.2 Chemical composition

The chemical composition of biomass was discussed in section 1.1.1. However, with respect to feeder selection, the influential contents of biomass are resins, intrinsic and extrinsic ash, and moisture. Extrinsic ash is usually associated with bark, since it can pick up sand and dirt during transport from the forest to the mill. Intrinsic ash is also important, since it must be removed from the product gas. Typical data are given in Table 7.2 (292).

Table 7.2 : Ranges of moisture and ash content for common mill residues (292).

Residue type	Moisture content wt% wet basis	Ash and dirt content wt% dry basis
Bark	25-75	1-5 *
Chips	25-60	0.1-0.2
Log yard residues	40-60	5-50
Sanderdust	2-8	0.1-2.0
Sawdust	25-40	0.1-2.0
Shavings	10-20	0.1-2.0
Slabs and Trim ends	25-50	0.5-2.0

* Clean softwood barks have ash contents of up to 3 wt%, while hardwood barks usually contain 5 wt% ash.

Resinous woods usually have high volatile contents and high heating values (see Table 1.5, e.g. pine). These resins promote sticking of the wood and dirt in feeding equipment and, consequently, cause feeder operating problems and higher maintenance. Therefore, feeders for resinous material should allow easy access for cleaning. Hardwoods are not commonly resinous and related feeding problems are not likely.

The moisture content of biomass is also an important parameter in gasification (see sections 1.1.2 and 6.4) and is in general undesirable. Contrarily, in relation to feeders, the presence of moisture reduces friction and, thus, can help reduce wear.

7.4.4.3 Size distributon

The size of particles in biomass fuels depends on the sources and whether there is one or several possible residues that make up the fuel. Typical size ranges are given in Table 7.3 (292).

Table 7.3 : Size distribution of common mill residues (292).

Residue	Size range mm
Bark	1-100
Chips, pulp	13-50
Hogged fuel	1-100
Log yard residues	>100
Sanderdust	0.01-1.0
Sawdust	1-10
Shavings	1-13
Slabs and Trim ends	>100

The structure of wood promotes the formation of elongated piece sizes during comminution, which may not fall within the specified limits. It is inevitable that some elongated particles or sticks will pass through all storage and handling systems and reach the feeder. The feeder must be designed to cope with the occasional undesired feed materials.

Prior to selection of any handling and feeding equipment a thorough sampling of the wood residue should be conducted. Size characterization of these samples would determine the size range, as well as the maximum possible piece size. Pieces that are too large should be removed upstream the feeder. Care should also be taken to remove any metals, stones and other foreign materials that cannot be accommodated by the feeder and can cause equipment failure.

7.4.4.4 Bulk density

The variability of the composition of residue fuels can easily lead to the use of incorrect densities for sizing feeder equipment. The bulk density of biomass fuels depend on the size, shape and moisture content of individual fuel components, the species of the wood residues and the relative proportions of wood and bark. The bulk density of any biomass fuel can be estimated simply by using the following relationship:

$$\text{Bulk density} = \frac{\text{Weight of biomass}}{\text{Total volume}} \qquad \text{equation 7.3}$$

The volume fraction of solid wood in a bulk sample for common wood residues is given in Table 7.4, along with typical ranges of bulk density.

Table 7.4 : Volume fraction of solid wood and bulk densities of common wood residues (292).

Residue	Volume fraction solid wood (m^3/m^3)	Typical bulk density (kg/m^3)
Bark	0.37-0.43	160-480
Chips compacted	0.4	160-400
uncompacted	0.35-0.36	160-350
Hogged fuel	0.33-0.37	200-400
Planer shavings	0.23-0.25	110-140
Sanderdust	-	160-200
Sawdust	0.36-0.40	200-350

7.4.4.5 Abrasiveness and corrosiveness

Most of the abrasiveness and corrosiveness of biomass fuel is due to the presence of foreign materials. Hog fuel can be extremely abrasive if it contains mixed soil and sand, usually associated with the bark component. If in significant concentration, these abrasive materials can quickly wear moving components of most feeders. The preferential cure for the problem is screening of the feedstock to reduce sand and dirt content. Alternatively, slow moving feeders, possibly with friction reducing or sacrificial wear surfaces can be used.

Corrosion of feeder systems can be a problem when handling the residues of high salt content that result from sea transport of logs. Moisture, of course, will promote some corrosion.

7.4.4.6 Angle of repose

Most wood fuels have steep angles of repose, often from 40°-60° to the horizontal, for free falling materials put in piles and against walls. Lightly compacted materials placed in bins frequently can form nearly vertical and sometimes overhanging surfaces when part of the material is removed. This leads to bridging and termination of feed transport to the gasifier. Both of these behaviours require special consideration, when designing bin discharge outlets and feeder inlets to ensure a continuous flow of feed. Especially with compacted fibrous wood which has a strong tendency to bridge, the feeder inlets must be designed with equipment to collapse bridges or so that no stable bridges can form against the bin walls, (see also section 4.3.2.2).

7.4.4.7 Friction coefficient

The kinematic coefficient of friction (see section 4.3.2.2) is the cause of wear in feeders and increases the power required for operation. Very little information is available concerning the friction coefficient of wood on metal and other surfaces common to feeder systems. Sliding friction coefficient of 0.16 for wet wood on steel and a value of 0.2-0.35 for dry wood on steel and a coefficient of 0.35-0.45 for wood chips on steel in a flight conveyor have been reported (33). In the absence of more specific data, a friction coefficient of near 0.4 appears realistic for most typical biomass feedstocks in feeder systems.

7.4.4.8 Stickiness

Stickiness of fine biomass particles on metal surfaces in a feeder depends on the resin content (see section 7.4.4.2) and the moisture content of the feed. Moisture can cause sticking in poorly cleared areas of feeders, although this is not a major problem.

7.4.4.9 Flow behaviour

Flow behaviour of solids is complex, related to size, shape, size distribution, density and several other physical characteristics. It must generally be assessed empirically and qualitatively. The qualitative nature of flowability makes it impossible to state categorically what the flowability of a certain biomass feedstock will be under all conditions. The following general comments are the best possible at present (33).

Table 7.5 shows general flowability characteristics of common biomass residues. All biomass feeds can, under certain circumstances, be sluggish materials prone to hangups, bridging and consolidation. The relative ease of handling ratings given in Table 7.5 are general guidelines and must be used with discretion since local and equipment conditions can reverse some of these.

The flowability of wood residues can be improved by agitation as done with bin activators. Dry residues consistently flow more easily than wet residues because of their lower shear strength.

Table 7.5 : Shape and flowability of biomass feedstocks (33).

Residue	Shape	Relative ratio, surface to volume	Relative ease of handling 1-Best 6-Worst	Flowability
Bark	Irregular lump	1	3	Sluggish
Chips	Irregular chip	1	1	Flows
Hogged fuel	Fibrous irrigular	-	2	Sluggish
Planer shavings	Curly wafer	5	6	Very sluggish
Sanderdust	Spherical, cubic	10	5	Very sluggish
Sawdust	Cubic	6	4	Sluggish

Wood residues consolidate upon application of pressure. Consolidation occurs with depth in piles and bins, as well as during extrusion-type conveying. Consolidation results in worsened problems with bridging and, of course, reduces flowability.

Consolidation can also occur because of freezing of water in and between biomass residues that unites them into a large mass. This can be a serious problem in cold climates.

7.4.4.10 Discussion

From the above section it is evident that the flowability of each biomass feedstock must be determined empirically and qualitatively. However, a careful examination of Tables 7.2 to 7.5 indicates that the preferred biomass feedstock for thermochemical conversion is wood chips. This type of feedstock has the best flowability.

7.4.5 Feeder systems for fluidized bed gasifiers

7.4.5.1 Introduction

Feeders as considered in this thesis encompass equipment that withdraws material from temporary storage, transports it and discharges it into a gasifier. The feeder must therefore be effective at recovering material steadily from storage, regulating the flow of material, discharging and if possible distributing the material in the reactor. One piece of equipment can rarely accomplish all of these tasks. Instead, up to three pieces of equipment must be used, one each for metering, conveying and distribution. However, distribution of the feed in the reactor is rarely attempted with gasifiers due to the relatively small scale of operation. Emphasis in this section is given on metering and conveying feeders that are suitable for fluidized bed gasifiers.

Generally, there are two types of feeders, volumetric and gravimetric feeders (189). Virtually all feeders in common use for biomass feedstocks are volumetric feeders, which regulate the volume of material conveyed. Gravimetric feeders regulate the rate of transport according to weight and are used where accurate feed rates are essential.

7.4.5.2 Metering

Both volumetric and gravimetric feeders can be effective at regulating the flowrate of material fed to a conversion system. However, gravimetric feeders can meter within plus or minus 2% of the desired flowrate, whereas volumetric feeders are much less accurate, particularly when the bulk density and the moisture content of the material are variable, (up to plus or minus 10% of the desired flowrate).

The metering system can be controlled manually or automatically, each depending on the size of the unit, the constancy of the fuel characteristics, the steadiness of the load on the conversion unit and the degree of sophistication of the plant. An automatic control system must be as simple and rugged as possible and may alternatively operate using on-off or proportional feedback controllers (189).

Regulation of feed rate for both volumetric and gravimetric feeders is accomplished either by controlling the size of the bin opening, while retaining an essentially constant discharge velocity of solids, or by controlling the discharge velocity of the material, while retaining a constant bin opening.

The metering portion of the feeder should extract material through the entire bin opening and produce nearly uniform flow of material through the bin to the outled. The type of feeder and the design of the bin and bin opening will influence the flow pattern of materials in the bin and determine whether the flow is non uniform or uniform.

7.4.5.3 Conveying

The metering portion of the feeder system regulates the flow of material and discharges into conveying equipment, that transports these materials to and discharges them within the gasifier. The metering and conveying functions may or may not be combined in one piece of equipment. Feeders can, therefore, be either conveying or non-conveying types.

7.4.5.4 Distribution

Most commercial feeders are not capable of distributing material across the area of the gasifier. Distributors can be used to achieve this. The need for a distributor increases with the cross-sectional area of the gasifier. However, distributors can be eliminated by multiple feeding ports (see section 7.4.3.2).

7.4.5.5 Types of feeders

A comprehensive list of all proven and commercially available feeders for biomass feedstocks is given in Table 7.6 (33). It is evident from this table that no single feeder satisfies all functional requirements. These feeders were evaluated on the basis of the requirements of fluidized bed gasifiers, being (see section 7.4.3):

- ability to operate under low positive pressure (up to 50 kPa)
- operate with feedstocks ranging in size from 6 to - 80 mm and 50 wt% moisture.

Table 7.6 : Comparison of feeder characteristics (33).

Type	Suitable sizes of wood residues cm	Differential pressure kPa	Comments
Belt feeder	<10 all types of feedstocks	0	- Best for non-sticky, non-abrasive materials - Inclines <15° - Belt cleaners preferred.
Feed chute	all sizes, all types	0	- Avoid direction changes. - Diverging sides preferred.
Flight conveyor feeder	all sizes, all types	0	- Poor for stringy residues. - Inclines <35°
Gate feeder	<5, all types	0	- Must be used with other feeders or flow-inducer for wood residues.
Lock hopper feeder	<15, all types	3,200 (8,500 max.)	- Feeders available with gravity, pneumatic and screw discharge. - Problems with jamming valves, bridging and venting of gases.
Pneumatic feeder	<5, all types	70	- Requires use of rotary air lock. - Poor for abrasive or stringy materials. - Good arrangement flexibility. - High noise and power levels. - Good for conveying long distances.

Table 7.6 - continued

Ram feeder	<7.5, wood	3	- Best for underfire stoker. - High power requirement to shear residues. - Poor for fine particles.
Rotary feeder a) general duty	<7.5, wood chips	0	- Used for metering. - Problems with jamming - Poor for wet, sticky solids.
b) low/medium pressure	<5, wood chips sawdust	1,030	- Requires venting. - Wear increases leakage. - Problems with jamming. - Low space requirements.
c) high pressure	<5, wood chips	2,400	- Suffers from problems noted above - Not attractive for most conversion systems.
Rotary table feeder	<5, all types	0	- Used successfully to unload wood chips from bins.
Screw feeder a) general duty	<7.5, wood chips sawdust	0	- Poor for stringy residues. - Well proven.
b) low/medium pressure	<5, wood chips	1,030	- Units used for metering and de-watering chips for processing. - Poor for stringy residues. - Several designs available.
c) high presure	<5, wood chips	2,400-20,000	- Poor for stringy residues. - Problems with jamming. - High cost.
Vibrating feeder	<20, all types	0	- Problems with powders. - High capacities. - Low power.

Since fluidized beds inherently provide good mixing up to 1 m diameter (see section 7.4.3.1) distribution was not considered as an important function. Also for simplicity, preference was given to feeders that provide metering and conveying of biomass. The feeders which are considered acceptable for fluidized bed gasifiers are of the general types, screw feeders or a combination of these and others, e.g. piston feeders. Since the other types of feeders are out of the scope of the thesis, emphasis will be put on the screw feeders only in the following section.

7.4.5.6 Screw feeders

A screw or auger feeder consists of helical flight attached to a rotating shaft, usually contained in a tube or through housing. The rotating flights trap material in the screw threads and advance it by a screwing motion resulting in feed rate regulation on a volume basis. The feed rate is determined by the helix pitch, depth, speed of rotation and percent loading.

Screw feeders may be classified as : constant cross section screws, variable cross section screws, choked screws, multiple screws and combination and/or modifications of these basic classes of screws. Multiple screws may be further subdivided into: non-intermeshing screws, conventric double screws, twin counter rotating screws or twin co-rotating screws (33).

From these types of screws only the variable cross section screw, choked screw, plug screw and constant cross section screw with reciprocating piston fulfil the requirements of fluidized bed gasifiers (see section 7.4.5.5), have been proven for biomass feedstocks and are commercially available. These are summarized in Table 7.7.

Table 7.7 : Comparison of screw feeders.

Type	Size of screw mm	Feed material	Feed size mm	Capacity range t/h	Differential pressure kPa	Comments
Variable cross section	337	wood chips	50	9.5	275	- meters,
	400	wood chips	50	22.8	275	- de-waters
	425	bark	50	4.5	275	- sawdust may plug drain holes.
Choked screw	100	wood chips	<75	0.38	49.8	- relatively reliable feeders.
	250	wood chips	<75	2.27	49.8	
	400	wood chips	<75	5.41	49.8	
	600	wood chips	<75	10.57	49.8	
Plug screw	225	wood chips	12-50	5.3	1034-1379	- meters.
	300	wood chips	12-50	25.4	1034-1379	
Constant section screw with reciprocating piston	-	straw	-		2413-5515	- new technology,
	-	bagasse	-		"	- meters
	-	wood-powder	-		"	- potential to de-water.
	-	bark	-		"	
	40	wood chips & sawdust	9.5	6.8	3102	
	50	wood chips & sawdust	0.6	9-22	low pressure	

a) variable cross section screws:

In this type of screw the diameter of the helix increases or decreases along the length of the screw. The shaft diameter may be constant or vary along the length. These tapered screws are frequently used for pressure applications. A diagram of this type of screw is shown in Figure 7.4. Variable cross section screws are well known and widely used for feeding wood residues. No major problems exist with this type of feeder.

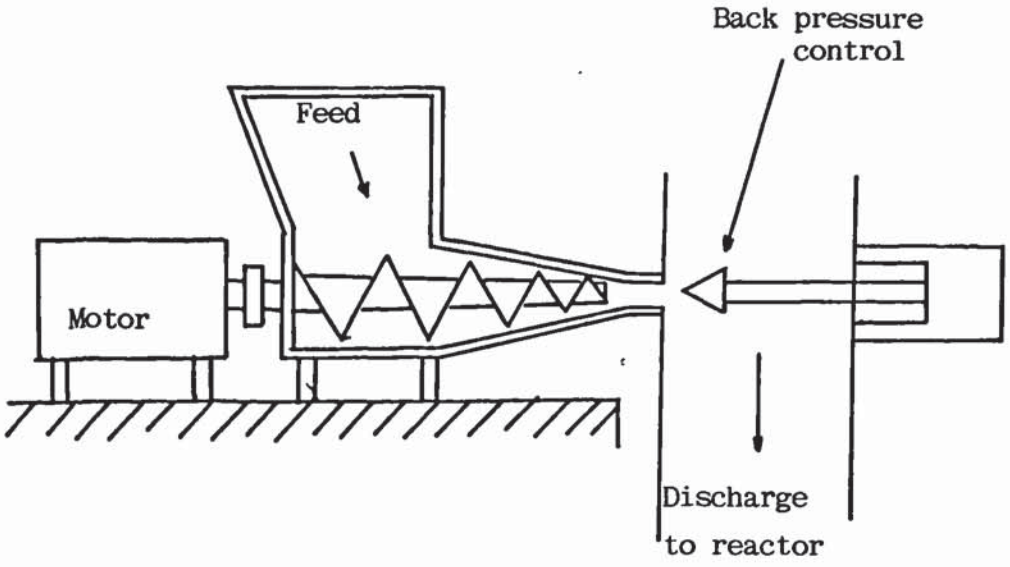

Figure 7.4 : Variable cross section screw feeder

b) Choked screws

In this configuration the feed material is discharged against a controllable back and pressure provided by some form of choke such as a weighted plate, hydraulically loaded cone, venturi type construction or some form of orifice plate. A typical weighted plate choked screw feeder is shown in Figure 7.5.

During operation the sealing chamber between the screw and the choke fills with material due to the forward conveying effect of the screw. The entire screw assembly is made to move axially by means of the sliding base and threaded adjusting rod, so that the length of the sealing chamber and hence the material plug is variable. The counter pressure of the damper plate is also adjustable by means of a counter weight arm and moveable weight. By

varying the length of the material plug and the counter pressure, a proper seal can be obtained.

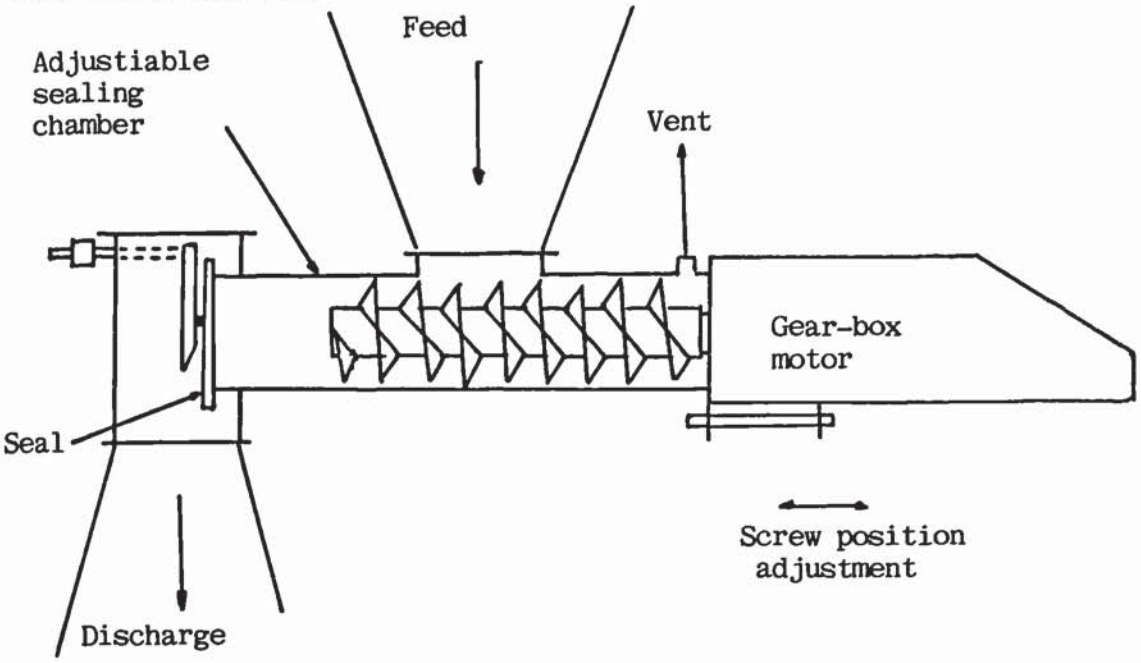

Figure 7.5 : Choked screw feeder

This type of feeder is of a promising design, which needs to be tested with various sizes of wood residues to determine the ability of the wood plug to seal against low gas back pressures.

c) Plug screw

In a plug screw feeder, a single screw is used to produce a plug of input material in a sealing section at the discharge end of the screw. This moving plug seal prevents back flow of gases from a pressurized reactor. The sealing section may have several different configurations such as a straight pipe with divergent outlet, a venturi, etc. These designs for the sealing sections have evolved to promote formation of the plug seal and steady flow of material through the sealing zone as shown in Figure 7.6.

The potential problems possible with this type of feeder are : a) jamming of the compression feed screw with oversized material and b) inability of the wood residue to seal against high back pressure

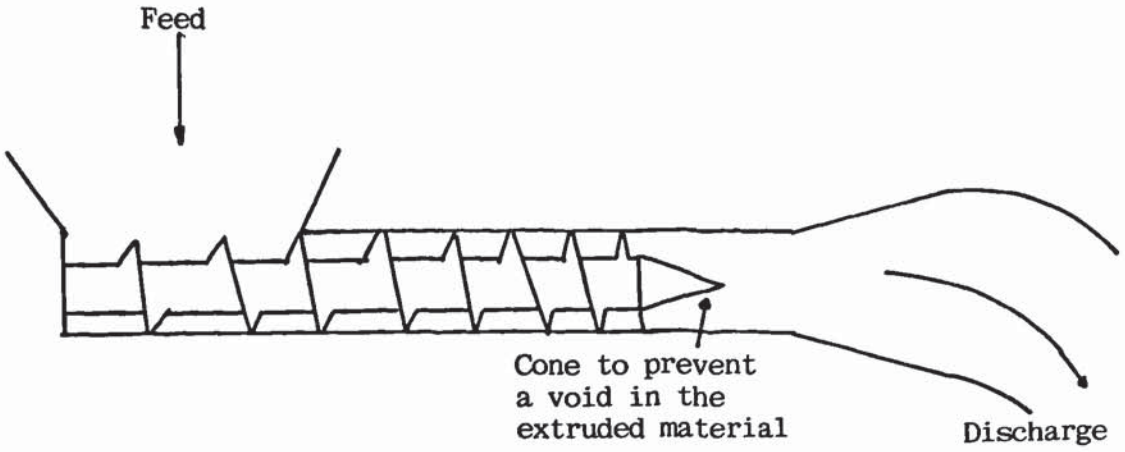

Figure 7.6 : Plug screw feeder

d) Constant section screw with reciprocating piston

A "co-axial" feeder has been developed in which material is metered to a single compression screw and the precompacted plug is moved forward against a choke by a reciprocating piston, see Figure 7.7. A screw conveyor is arranged to precompact loose wood residues and pass them to an intermediate chamber. Following this chamber, a piston reciprocating co-axially with the screw conveyor forces the material under high pressure in a direction co-axial with the screw and through a choker. A high degree of compactness is achieved primarily by the action of the piston.

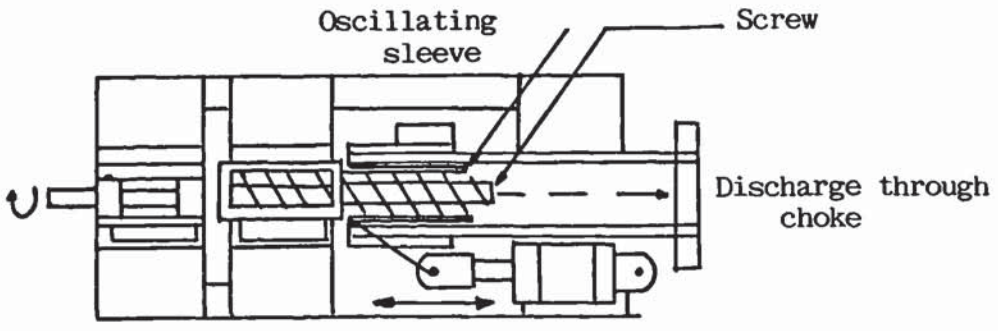

Figure 7.7 : Constant section screw with reciprocating piston feeder

A relatively high-volume, low-pressure unit was operated successfully on the low-pressure wood fluidized bed gasifier of Omnifuel in Hearst, Ontario (see Table 2.6). Potential problems envisioned are: a) jamming of the feeder screw feeding the co-axial reciprocating piston and b) jamming of larger wood particles in the seal section following the reciprocating piston.

7.4.5.7 Discussion

From the feeders discussed in the previous section, the choked screw feeder and the constant section screw with reciprocating piston feeder operate at low back pressures, while the variable cross section screw and the plug screw operate at high back pressures higher than 200 kPa and are applicable for pressurized fluidized bed or other types of gasifiers. However, this latter group can be used for low pressure gasifiers as well.

There exist several other types of feeders such as lock hoppers or piston feeders that would be applicable for feeding biomass materials into fluidized bed gasifiers. However, most of these have been developed for coal applications (e.g. piston feeders) or are still at the development stage (e.g. reciprocating screw plug feeder). A lock hopper with metering screws has been presented recently (293). However, problems such as poor lock valve performance due to tar accumulation have been reported (33) and since the maximum capacity is only 2 t/h, this type of feeder was not considered. It can also be envisaged that a combination of more than one feeders (e.g. a gas tight rotary feeder to fill a hopper and a metering screw to feed the gasifier) can be successful in feeding gasifiers. However, these combined systems are not offered commercially and have to undergo testing before they could be used commercially.

It can be concluded that the most appropriate biomass feeders for fluidized bed gasifiers are the choked screw feeder and the constant section screw with reciprocating piston feeder. However, all the types of feeders considered in section 7.4.5.7, except the plug screw feeder, feed the reactor intermittently, since a choke is used to prevent leaks of gases. This is a disadvantage for fluidized bed gasifier as has been reported in the literature (80) (see also section 5.15). The plug screw feeder feeds the reactor continuously, but a hopper inside the pressurized vessel may be necessary to

break up the compressed extruded product. It is also designed for high pressure applications (typical values are 1,034 kPa).

Moreover all these feeder designs are concerned with feeding biomass in a conversion system, but do not address the problem of bridging in the hopper and often bridging above the screw, at the outlet of the hopper, has been reported (33). In addition, feeders with moving parts, such as reciprocating pistons or screws, are prone to jamming. The author feels that although these feeders can feed fluidized bed gasifiers successfully, it would be better to develop a feeder that ensures no bridging in the hopper and can meet the requirements of fluidized bed gasifiers (see following section).

7.4.5.8 Proposal for feeder for fluidized bed gasifiers

On the basis of the foregoing and the experience of the author the feeder shown in Figure 7.8 is proposed for fluidized bed gasifiers.

It consists of three different feeders: a) a rotary feeder to supply material to b) multiple non intermeshing metering screws, which meter the feedstock to a vertical shaft and c) a simple screw conveying the material into the reactor.

a) Rotary feeder

Rotary feeders are pocket drums or vane type devices used to feed flowable materials (such as pellets, chips, sawdust). Material is trapped in the pockets at the feeder inlet and discharged from the bottom of the valve by gravity. Feed rate is determined by the volume of the pockets and drum rotation speed. For low to medium pressure applications the feeders use a tapered rotor and an appropriate liner to enable operation with minimal leakage under differential pressures up to 1,000 kPa. An example is shown in Figure 7.9. A rotor positioner is incorporated into the design to automatically adjust the clearence between the rotor and the liner to a valve resulting in minimum gas leakage. An exhaust vent relieves the gas pressure in the pockets exposed to the receiving vessel prior to their return to the feeder inlet.

The purpose of the rotary feeder is to supply the material to, and seal the hopper of the metering screws.

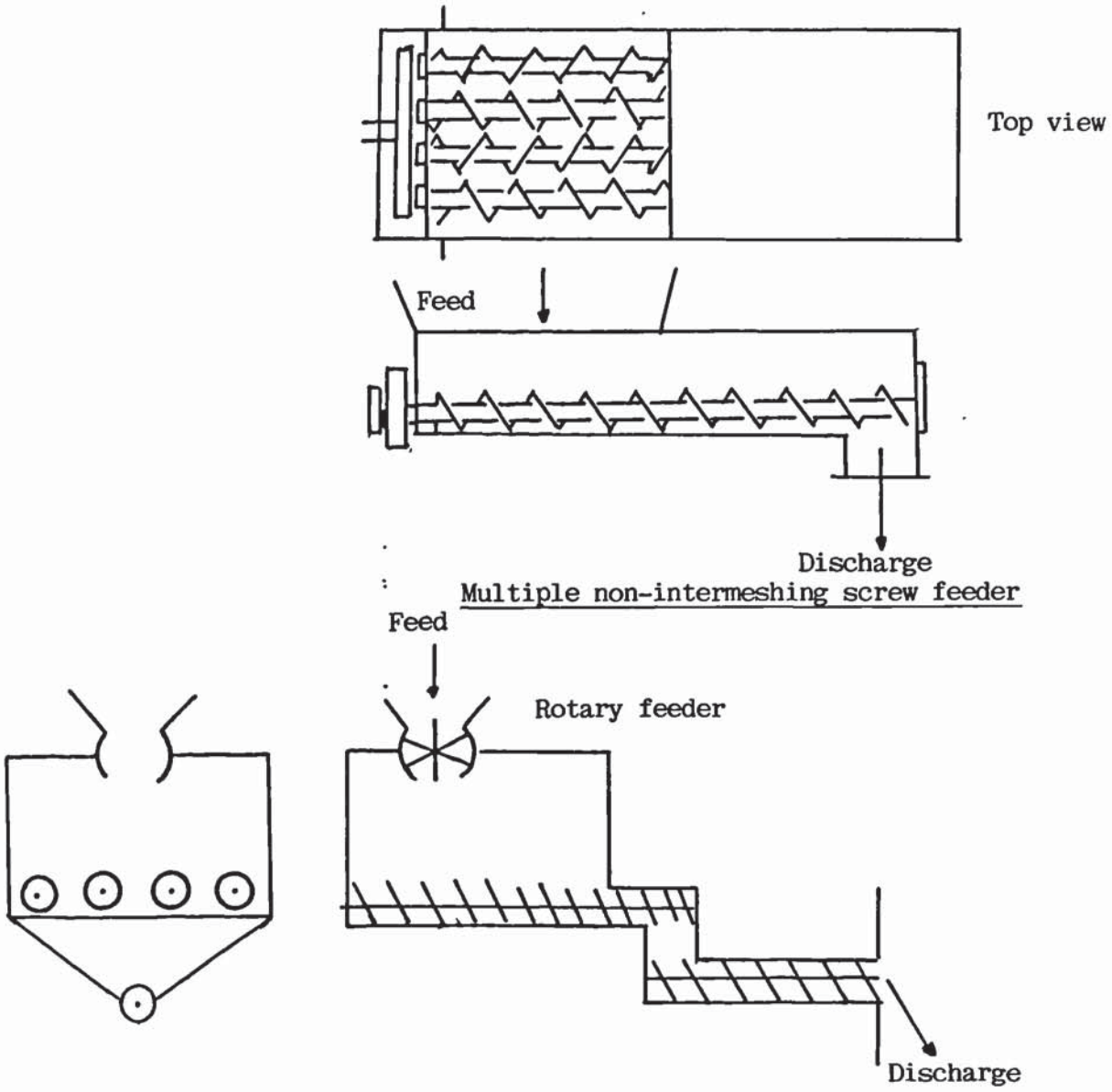

Figure 7.8 : Feeder for fluidized bed gasifiers.

b) Metering screws

Non intermeshing screws are multiple counter-rotaring screws operating in parallel. They feed material without surging and bridging. A typical multiple screw feeder is shown in Figure 7.8. In this design this multiple screw would meter the feedstock at relatively low speed.

c) Conveying screw

This is a simple screw which purpose is to convey the material to the

reactor. It operates at high speed relatively to the speed of the multiple metering screws.

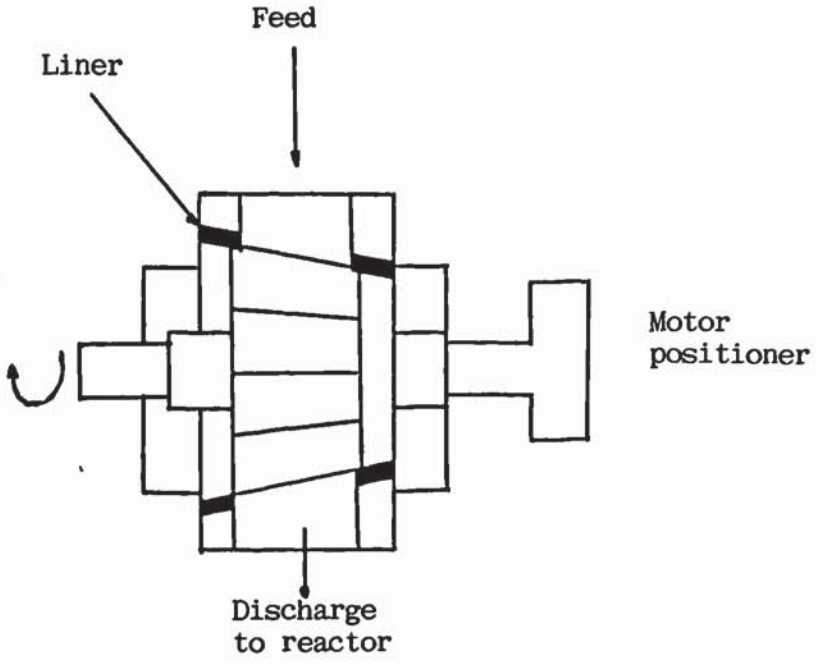

Figure 7.9 : Rotary feeder

The above configuration allows for continuous and constant rate feeding while a seal is provided for the gases. All three types of feeders proposed are commercially available and proven for their respective application. However, this configuration has not been tested exprimentally and trials must be made to ensure proper operation..

Indispensable of consideration in the final choice of a feeder are two more important parameters: the power requirements and the cost of the various feeders. The power requirements and the cost of screw feeders are given in Figures 7.10 and 7.11 respectively (33).

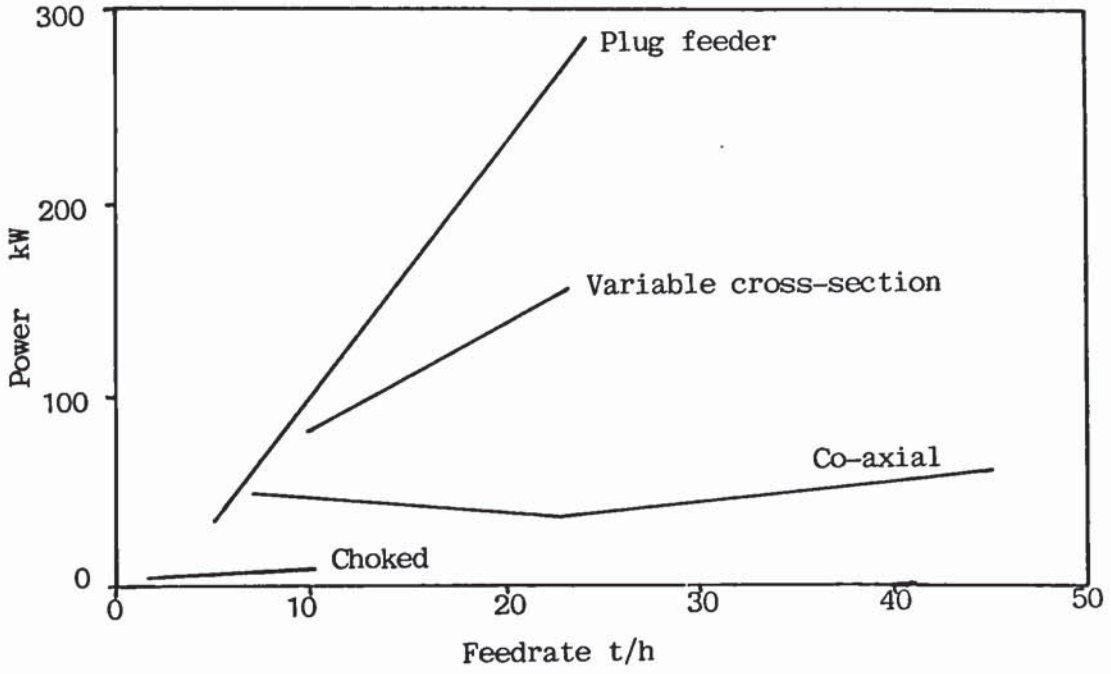

Figure 7.10 : Power requirements of screw feeders

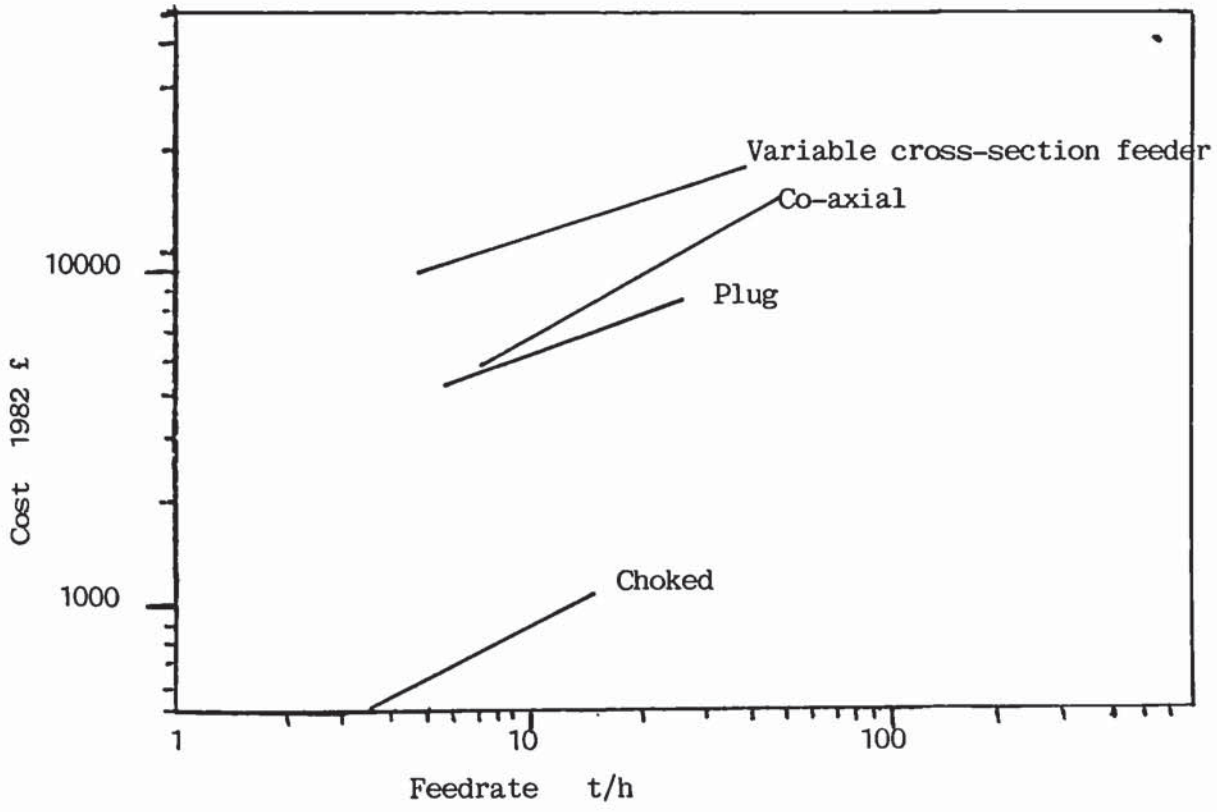

Figure 7.11 : Costs of screw feeders

7.4.5.9 Procedure for selecting a feeder for fluidized bed gasifiers

As discussed in section 7.4.4.10 the preferred biomass feedstock for thermochemical processing is wood chips. Therefore, wherever it is possible, this type of feedstock should be used in fluidized bed gasifiers. The procedure for selecting a feeder for fluidized bed gasifiers is outlined in Figure 7.12.

1) From a large amount of feedstock ($\pm$ 1 m^3) determine the following properties:
   - chemical composition, extrinsic and intrinsic ash content
   - size distribution
   - bulk density
   - angle of repose

2) Whenever possible and especially for hog feedstock determine the:
   - abrasiveness
   - corrosiveness

3) For resinous feedstocks the stickiness of the material should also be tested.

4) On the basis of the process specifications (e.g. operating pressure, sophistication, feedstock flowrate), power consumption and costs (Figures 7.10 and 7.11) select one of the following feeders:
   - variable cross section feeder
   - choked screw feeder
   - plug screw feeder
   - constant section with reciprocating piston feeder or the combined feeder proposed in section 7.4.5.8.

5) Supply all necessary informations (feedstock properties, reactor specifications, operating conditions et al.) to the selected feeder supplier and whenever possible arrange for a test with the feedstock and feeder in question.

Figure 7.12 : Procedure for selecting a biomass feeder for fluidized bed gasifiers.

In case the feeder proposed in section 7.4.5.8 will be selected, then test trials must be made to ensure proper operation.

7.4.5.10 Conclusions

As demonstrated in this work and by others (79, 80, 99, 102, 120) biomass feeders for fluidized bed gasifiers must be carefully selected to ensure trouble-free operation. Several systems have malfunctioned, not because of inadequate or bad design of the fluidized bed, but due to inappropriate design and selection of feeders. In the previous sections it was shown that the design of feeders is complicated and little is known about several properties of biomass relative to feeding (see section 7.4.4). It is therefore necessary to buy tested and proven feeder systems for fluidized bed gasification facilities. These feeders can even be bought from some companies with long experience on fluidized bed systems such as Lurgi, Foster-Wheeler et al., which have developed reliable systems.

7.4.6 Design procedure for fluidized bed gasifiers

7.4.6.1 Introduction

The most common objectives of a gasification plant are (see section 7.2):
a) to recuperate the energy content of a well defined feedstock, and
b) to provide for the energy or power requirements of a plant.

In combination with these objectives the following often have to be considered:

c) the quality of the fuel gas or its higher heating value,
d) the operating temperature in order to reduce the yield of tar

Finally the cost of any process must be carefully examined before a plant can be built.

In order to develop a design procedure, the engineer has the task to combine the objectives of the plant with engineering data and the performance of the reactor under the relevant conditions. The objectives of the plant usually define the starting point,while the performance data must be converted to mass flowrates and volumetric flowrates,so that the dimensions of the reactor and downstream equipment can be determined. Well defined and generally accepted engineering data are also used to determine several parameters.

For fluidized bed gasifiers the design must define the following parameters independently of the objectives of the plant:
a) feedstock flowrate
b) air flowrate
c) bed dimensions
d) operating temperature
e) product gas flowrate
f) higher heating value of product gas
g) condensate flowrate
h) fly ash flowrate
i) dimensions of reactor

The feedstock flowrate and air flowrate are related by the air factor (see section 5.11). The empirical models developed in Chapter 6 are based on the air fator since this parameter was shown to have the stongest influence on the performance of the fluidized bed reactor (see section 5.21). Thus, the air factor must be carefully selected for the design of fluidized bed gasifiers.

7.4.6.2 Independent design variables

These are based on the objectives of the plant and the application of the product gas. The objective of the plant can specify:
a) the feedstock flowrate, or
b) the energy (power) requirement of the "back-end" processing, and/or
c) the quality of gas required, and/or
d) the operating temperature.

The application of the gas can specify the air factor.

7.4.6.3 Selection of the air factor

The selection of the air factor is "back-end" related, that is, it depends on the application of the product gas. If the gas is to be combusted directly without cooling, then the problem of tar is elimitated (tar does not condense) and the air factor can be selected so that it would produce the highest possible higher heating value of the gas. If the gas is to be cooled and used in an application which cannot tolerate any tar, then the air factor has to be

selected so that it would result in high operating temperature in the bed and freeboard (see section 5.11.1) in order to crack the tar.

The objectives of the plant may also specify that the operation of the gasifier will be at the maximum output of energy. In order to identify the air factor which will result at maximum output of energy, the gas yield and higher heating value of the gas as predicted by the EMCM model are plotted versus the air factor in Figure 7.13. In the same figure, the energy output per kg of feedstock (gas yield x higher heating value of gas) is also plotted versus the air factor. It is clear that a maximum is reached at an air factor of 0.3. Thus, an air factor of 0.3 will result to the maximum energy output.

These considerations as well the recommended air factors are summarized in Table 7.8.

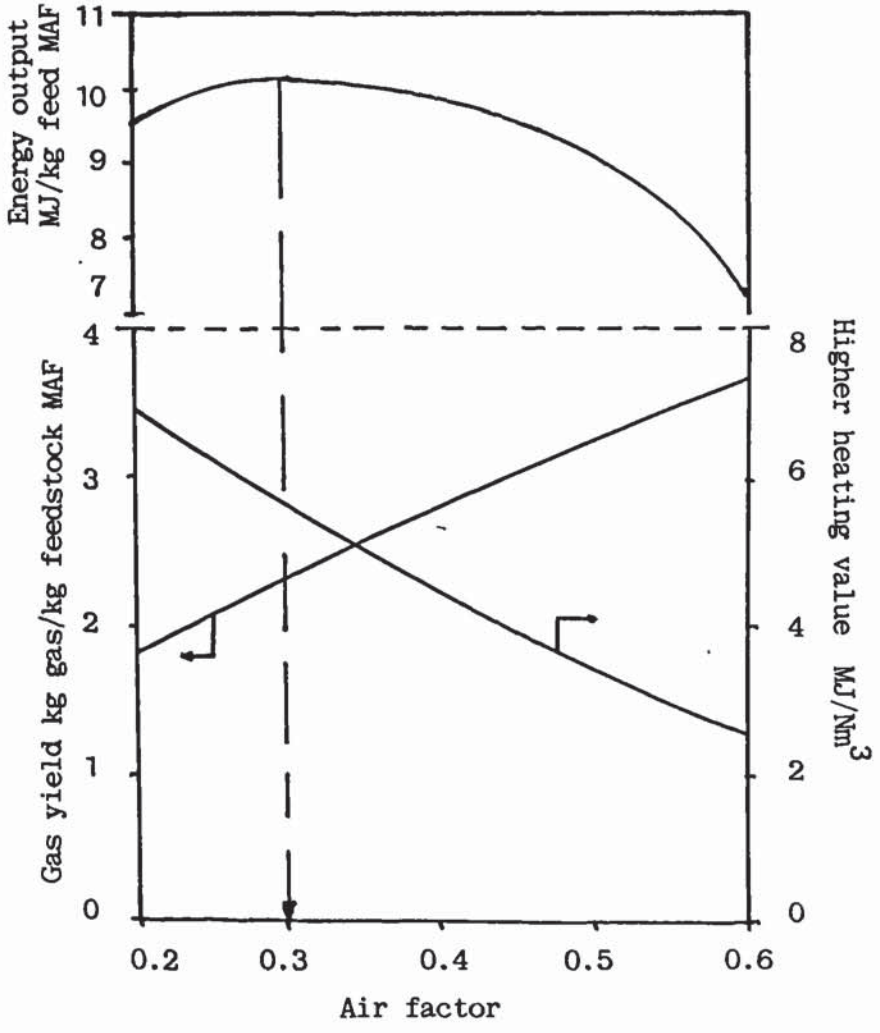

Figure 7.13 : Optimum air factor for maximum energy output.

Table 7.8 : Recommended values of air factor

Application of gas	Air factor	EMCM model			
		HHV	T_{bed}	T_{exit}	Gas yield
		MJ/Nm^3	°C	°C	$\frac{\text{kg gas}}{\text{kg feed MAF}}$
Direct combustion	0.2	6.85	724	651	1.78
Some tar permitted	0.3	5.55	797	737	2.32
No tar permitted	0.4	4.45	848	797	2.80

7.4.6.4 Basis for design

The specification of the independent design variables constitutes the basis for design. In the following sections, a design procedure is developed using the empirical models developed in Chapter 6 as well as other relationships.

The basis for design initially considers the recuperation of the energy content of a well defined feedstock,while the gas is to be combusted directly in a gas burner. This is the most simple case. However, in section 7.4.3.12 the design procedure for other basis of design are also discussed.

Thus the basis of design is developed as follows:

a) from the well define feedstock determine the following:
   feedstock flowrate per hour wet basis.
   moisture content
   ash content
   feedstock flowrate per hour MAF basis.
   elemental analysis of feestock
b) since the gas is to be combusted directly, an air factor (eg. 0.2) can be selectedfrom Table 7.8.

7.4.6.5 Determination of air flowrate

In this step, the air flowrate required to achieve the desired air factor is determined. The air flowrate is required for the specification of the

compressor, distributor et al. It is calculated on the basis of the definition of air factor (see section 5.2.1 and equation 5.2.), as given by equation 7.4.

$$G_{air} = S \times (wt\%\ C \times 11.48 + wt\%\ H \times 34.19 - wt\%\ O \times 4.31) \times G_{feedstock\ MAF}$$

equation 7.4

where S = air factor

Note: In case the elemental composition of the feedstock is not available and it cannot be determined otherwise, an approximation can be made by assuming that the feedstock consists of cellulose only. 1 kg of cellulose requires 5.102 kg air for complete combustion (see section 5.2.1). Thus in this case equation 7.4 becomes:

$$G_{air} = S \times 5.102 \times G_{feedstock\ MAF}$$ equation 7.5

Equation 7.5 gives the mass flowrate of air in kg/h. Dividing the mass flowrate by the density of air - 1.293 kg/m^3 (189) - the volumetric flowrate of air can also be calculated.

7.4.6.6 Determination of the performance of the fluidized bed gasifier

By the above steps, the mass and/or volumetric flowrates of the reactants (feedstock and air) can be determined. The next step is the determination of the mass and/or volumetric flowrates of the products: gas, fly ash and condensate. These can define the specifications of any downstream unit such as cyclones, gas scrubbers as well as any condensate purification system or disposal facilities.

The empirical models developed in Chapter 6 provide the basis for the determination of these parameters. However, the yields of gas and condensate are calculated in relation to the feedstock flowrate and the units are always of the form:

kg component/ kg feedstock (MAF)

Thus, for the determination of the product gas and condensate flowrate the empirical models must be applied for the air factor specified in the basis of

design (see section 7.4.3.4). The procedure for the application of the two models was demonstrated in section 6.5 (see also Table 6.5).

7.4.6.7 Calculation of the mass and volumetric flowrates of product gas and condensate

In order to calculate the mass flowrates of these components, their respective yields must be multiplied by the feedstock flowrate. Thus:

Mass flowrate of i = Yield of i x Feedstock flowrate MAF equation 7.6

where i = product gas or condensate.

The volumetric product gas flowrate in Nm^3/h can be calculated by dividing the mass flowrate by the average specific weight of the gas (1.27 kg/Nm^3, see section 5.7.1). The volumetric condensate flowrate can be determined by dividing the mass flowrate by the density of the condensate (985 kg/m^3, see section 5.83).

7.4.6.8 Calculation of the fly ash flowrate

Calculate the ash input to the reactor by multiplying the feedstock flowrate by the ash content of the feedstock. Multiply this value by 100/30 = 3.33, since it was found that the fly ash had a carbon content of 70 wt% (see section 5.8.2). This gives the fly ash flowrate at the outlet of the reactor in kg/h. The volumetric fly ash flowrate can be determined by dividing the mass flowrate by the bulk density of the fly ash (210 kg/m^3, see section 5.8.2).

Therefore by applying the steps described in sections 7.4.3.4 to 7.4.3.7, the mass and volumetric flowrates of the reactants and the products of the gasification process can be determined. The bed dimensions as well as the overall dimensions of the reactor are required in order to complete the design of the reactor. These are determined in the following sections.

7.4.6.9 Determination of bed dimensions

The dimensions of the fluidized bed are very important and are needed to ensure good fluidization. Nevertheless the compression costs must also be considered in the selection of the bed dimensions. In order to determine the

cross sectional area of the bed, the maximum specific capacity of the system (mass flowrate of feedstock per unit time, unit cross sectional area) is used. The cross sectional area of the bed is calculated by dividing the mass flowrate of the feedstock by the maximum specific capacity of the system:

$$\text{cross sectional area of bed} = \frac{\text{feedstock flowrate}}{\text{maximum specific capacity}} \qquad \text{equation 7.7}$$

The maximum specific capacity obtained in this work (note: this was limited by the maximum capacity of the feeding unit) was 711 kg/hm^2 MAF (see section 5.14). Only one work was found in the literature where a maximum specific capacity of 880 kg/hm^2 MAF was quoted (91). However, since little information was provided on how this maximum specific capacity was obtained, it was decided to consider 711 kg/hm^2 MAF as maximum specific capacity of the fluidized bed reactor. This value also provides a safety margin as larger beds are determined in comparison to the value from the literature.

The diameter of the bed can be determined from the cross sectional area of the bed. For fluidized beds with cross sectional area less than 5 m^2, it is recommended that circular configuration is used, while for cross-sectional area larger than 5 m^2 square configuration can also be used (273).

The determination of the bed diameter on the basis of equation 7.7 provides the minimum acceptable bed diameter. It is therefore recommended to increase the bed diameter by a safety margin of 10%.

The bed height can be calculated from the empirical relationship:

$$\frac{\text{Bed diameter}}{\text{Bed height}} = 1.33 \qquad \text{equation 7.8}$$

with a maximum value of 1 m. This limitation is necessary to ensure that the compression costs of the air would not be excessive.

7.4.6.10 Determination of reactor dimensions

The overall reactor dimensions are necessary for the specifications for construction. In chemical reactor engineering science, the volume of the

reactor and the flowrates of the reactants and products are related by the retention time of the reactants and/or products (185):

$$R_T = \frac{V_r}{Q_{gas}} \qquad \text{equation 7.9}$$

where R_T = retention time
V_r = volume of the reactor
and Q_{gas} = volumetric flowrate of the gas.

The average flowrate of the gas at reactor conditions is (see section 5.21):

$$Q_{gas.av.} = \frac{1}{2} \times \left[Q_{air} \times \frac{(T_B + 273)}{273} + Q_{gas} \times \frac{(T_O \times 273)}{273} \right] \qquad \text{equation 7.10}$$

where $Q_{gas,av.}$ = average gas flowrate
Q_{air} = air flowrate
Q_{gas} = product gas flowrate
T_B = temperature of the bed
and T_O = temperature at the outlet of the reactor.

The volume of the reactor can be calculated by first applying equation 7.10 and then assuming a retention time.

The retention time can be selected on the basis of the application of the product gas. Thus, if the gas is to be combusted directly, then the importance of retention time is significantly reduced (see section 5.21.1) and low values - 10-15 s - are acceptable. However, if high concentration of tar is undisarable, then higher retention times must be selected to minimize tar by providing longer residence time in the reactor. The same is true when a high carbon conversion efficiency is required. The recommended retention times according to the application of the product gas are given in Table 7.9 .

Table 7.9 Recommended retention time of gas

Application of gas	Retention time of gas s
Direct combustion	10-15
Some tar permitted	15-20
No tar permitted	20-25

From the total volume of the reactor, the volume of the bed must be substracted in order to determine the volume of the freeboard. It is recommended to select an expanded freeboard configuration in order to minimize elutriation of char and sand particles (see section 2.5.6.8). In general the freeboard diameter can be increased as follows (see section 3.7.4):

$d_f = d_b \times 1.5$ equation 7.11

where d_f = freeboard diameter
d_b = bed diameter

The dimensions of the reactor can then be calculated since the bed height, the bed diameter, the volume of the reactor and the diameter of the freeboard are known. The hight of the frustum of the right conical part is not of any significant importance and can be selected so that the angle of the frustum satisfies equation 7.12:

$20 < a_f < 70°$ equation 7.12

where a_f = angle of frustum.

This inclination allows for the return to the bed of all particles falling on the frustum.

7.4.6.11 Openings, measuring ports and instrumentation

In general the following openings must be foreseen on the reactor wall:
a) inlet of feedstock
b) outlet of gas
c) inlet of air to the distributor
d) ports for measuring instruments (eg. thermocouples).
It is recommended that an observation port at the top of the reactor and a manhole are also provided.

The inlet of the feedstock can be specified according to the feeding system specifications. No special considerations are necessary. In case of wood chips or other feedstock of similar dimensions the feeding port should be

placed just above the surface of the bed at fluidization condition. However, in case of sawdust or other fine material, the feeding inlet should be placed just above the distributor to ensure that sufficient residence time is provided to gasify the feedstock, in the bed (see section 2.4.3.7).

The outlet of the gas should be at the top of the reactor. No special considerations are required except that the diameter of the pipe should be large enough to minimize pressure drop.

The observation port should be designed on the top of the reactor and provisions made to protect the viewing glass from tars by a moveable gate. This can help in determining the operating state of the reactor (e.g. sintering). .

The manhole should be designed just above the surface of the bed at static conditions. This is necessary for access in the reactor in case of problems (such as bed sintering) or to inspect and clean the distributor. In case of pipe grid distributors, the manhole can also be below the distributor since the bed material could be retrieved through the distributor.

Measuring ports are necessary to provide access in the reactor of instruments such as thermocouples. The measuring ports of the following instrumention is required:

a) It is recomended that a minimum of three thermocouples be foreseen, one in the middle of the bed, a second just above the surface of the bed at actual conditions of fluidization and the third close to the exit of the gas. However, it is desirable to have two more thermocouples, one just above the distributor and the other in the middle of the freeboard for a more accurate temperature profile.

b) The pressure drop over the bed and over the distributor must be measured. The former indicates whether there is built up of foreign material in the bed (eg. stones, ash et al.) while the latter indicates whether the orifices of the distributor are getting blocked by sand or other particles. The pressure in the freeboard must also be measured in order to provide information about downstream processing and the feeding system.

7.4.6.12 Discussion

The design procedure developed in section 7.4.3 can determine on the basis of the objectives of the plant all the necessary parameters for a detailed design. This is demonstrated in Chapter 8. For safety and contigency reasons it is recommended to consider a turn down ratio of 1:3. This would ensure satisfactory operation in cases of problems either upstream (feedstock not in sufficient quantities) or downstream (breakdown of equipment) the reactor.

By assuming a turn down ratio of 1:3 and by applying the procedure and equations described in sections 3.3 to 3.7 and summarized in Table 7.10, the fluidized bed reactor can be designed and the design verified, by calculating the residence time of gas flowing interstitially (which indicates whether sufficient time is provided for the gas to react) and the fraction of bubble gas in contact with particles (which represent a contact efficiency).

The equipment and operating costs can be estimated from the results obtained. These in turn can provide an economic objective function for optimization.

Table 7.10 Design procedure for fluidized beds

Step	Thesis section	Procedure	Equation
Design of distributor	3.3.2	-calculate pressure drop over bed	$\Delta P_{bed} = \rho_b \times h_b$
		-calc. min pressure drop over distributor	$\Delta P_d^{min} = \text{Max}(0.1\ \Delta P^{bed};$ 35cm H_2O; 100 $\Delta P_{expansion}$ into vessel) 3.5
		-calculate Reynolds number for total flow approaching distributor	$R_{et} = \frac{d_r\ \rho_g\ U_o}{\mu g}$
		-find out orifice coefficient for R_{et}	Use a reference C'_d, R_{et} figure
		-calculate velocity of gas through the orifices	$U_{or} = \frac{C'_d\ (2g_c\ \Delta P_d)^{1/2}}{\rho_g}$ 3.6

Table 7.10 - continued

		-calculate open area of distributor which should be less than 10%	U_o/U_{or}	
		-calculate number of orifices by selecting orifice diameter	$N_{or} = \frac{U_o}{A_{or}\, U_{or}}$	3.7
Pressure drop for the compressor	3.3.3	- calculate pressure drop over bed at conditions of minimum fluidization	$\Delta P_{bed} = H(1-e_{mf})(\rho_s-\rho_g)g$	3.8
		- calculate total pressure drop for the compressor	$\Delta P_{total} = \Delta P_{distr.} + \Delta P_{bed}$	3.9
Particle size of sand	3.3.4	- ensure efficient fluidization	$U/U_{mf} \geq 2.5$	3.14
		- minimum fluidization velocity	$U_{mf} = 0.805\times10^{-3}\times g\times d_p^{1.83}\times (\rho_s-\rho_g)^{0.94}\times\mu^{-0.88}$	3.12
		- volumetric flowrate	$Q = U\times A$	3.15
			or combining 3.14 and 3.15 $Q = 2.5\, U_{mf} \times A$	3.16
		- calculate particle size of sand	substitute 3.12 in 3.16 and solve for d_p	
Fluidization parameters	3.4	calculate:- minimum fluidization velocity	use equation 3.12.	
		- Reynolds no at min.fluid. velocity	$R_{emf} = \frac{d_p\, \rho_g\, U_{mf}}{\mu_g}$	3.17
		- particles terminal falling velocity	for $R_{emf} < 1$, $U_T = 70\times U_{mf}$	3.18
		to obtain efficient operation of bed determine the operational velocity with the restrictions:	$U_{op} \geq 2.5\, U_{mf}$ at bottom of bed	3.19
			$U_{op} < 0.5\, U_T$ at top of bed	3.20
		size of bubbles.	$d = g^{-1/4}(U-U_{mf})^{1/2}(h+h_o)^{3/4}$	3.22
		to avoid slugging	$\frac{d_b}{d_B} \geq 2$	3.24

Table 7.10 - continued

Design verification	3.6	-calculate the amount of gas flowing interstitially and compare it to the total flow of gas	$Q_{ig} = U_{mf} A_r$	3.25
		- calculate the residence time of gas in the bed. This will indicate whether sufficient time for reaction is provided	$(t_r)_{i=} \frac{h_{bed}}{U_{mf}}$	3.26
		- calculate the bubble velocity	$U_B = \sqrt{g}\, d_B/2 + (U - U_{mf})$	3.27
		- calculate the residence time of bubbles in the bed	$(t_r)_B = \frac{h_{bed}}{U_B}$	3.28
		- find the ratio of bubble velocity to interstitial gas velocity (for sand e = 0.5)	$a = e^{\frac{U_B}{U_{mf}}}$	3.29
		-find the fraction of bubble gas in contact with particles	$\frac{V_{CP}}{V_B} = \frac{1.17}{a-1}$	3.30
		this is an approximation of the contact efficiency which schould not be less than 10%.	$\frac{V_{CP}}{V_B} \geq 0.1$	-

The same nomenclature as in Chapter 3 is valid.

7.4.6.13 Design procedure based on the energy requirements of plants

This basis of design considers the energy requirements of a plant that must be satisfied by the gas produced from the the gasification facility. Thus, the basis of design is the number (x) of MJ/h needed to operate the downstream plant. Depending on the type of conversion system from gas to energy and assuming that the EMCM model is applicable, from Table 7.6, the desired

higher heating value of the gas can be selected. The volumetric flowrate of product gas needed to produce X MJ/h is calculated by equation 7.13 :

$$G_{gas} = \frac{E}{H.H.V.} \qquad \text{equation 7.13}$$

where E is the energy requirements.

Then the designer has the task to determine the feedstock flowrate that could produce this amount of gas by gasification. This can be determined by using equation 7.6 and selecting a value for the gas yield from Table 7.6 so that the gas yield corresponds to the selected higher heating value. This accordingly also defines the air factor. From this point on the design procedure can be applied in the same way as for the previous procedure, since the air factor, the feedstock flowrate, the gas yield, the gas flowrates and the higher heating value of the gas are known.

Alternatively, the designer can select a different gas yield (it is recommended that a gas yield value of 2.5 kg gas/kg feed MAF be selected since this was the realistic optimum obtained in this work (see Table 6.3)), then determine the air factor from equation 7.14 (obtained by solving equation 6.8 for the air factor):

$$S = \left[\frac{Y}{5.087}\right]^{1/0.6536} \qquad \text{equation 7.14}$$

This air factor will result in a different value of higher heating value of gas, which will change the gas flowrate required to produce the necessary energy for the plant (see equation 7.13). Likewise an optimization process can be established by selecting different values for the gas yield. Similarly, all the other parameters of the design can be determined in the same way as with the procedure developed previously.

7.4.6.14 Consideration of other objectives and design requirements

When other design requirements such as operating temperature, higher heating value of product gas or thermal efficiency have to be considered in the design, the design engineer must make a choice of the overruling

requirement. In case it is the availability of feedstock or the energy requirements of the plant, the corresponding procedure can be followed as developed in this chapter. Otherwise the design engineer should base the procedure on the new requirement and then proceed to determine the air factor required for that performance. Then the procedure can follow sections 7.4.6.5 to 7.4.6.11, while the limits discussed and given in Table 7.8 and 7.9 must be considered.

7.4.7 Design procedure for the hot gas cyclone

The design procedure for the hot gas cyclone can follow the procedure summarized in Appendix III. This has been proven satisfactory for the requirements of fluidized bed reactors. Otherwise commercially available cyclones can be obtained when the gas flowrate, temperature and particulate load can be provided.

7.5 CONCLUSIONS

A design procedure was developed for air gasification plants. This procedure considers feeding system, fluidized bed gasifier and hot gas cyclone. For the former it is recommended to rely on commercially proven systems which can operate at low over- pressures. For the fluidized bed gasifiers a design procedure was developed based on the empirical model developed in Chapter 6. With this procedure it is possible to specify the exact dimensions of the reactor. The procedure is flexible so that several alternative objectives can be considered and incorporated in the design. The cyclone can be designed by standard procedures.

CHAPTER EIGHT : CONCEPTUAL DESIGN OF A FLUIDIZED BED GASIFICATION PLANT

8.1. SCOPE OF PLANT

8.1.1 Introduction

During the early stages of the programme, negociations were held between Vyncke Warmtetechniek N.V. and SPANO N.V., the particle board manufacturer who supplied the feedstock used in the fluidized bed gasifier, for the eventual purchace of a fluidized bed gasification plant. SPANO N.V., the largest particle board manufacturer in West Flanders was concerned about its high energy bills and the biomass residues produced at its plant(mainly bark and wood waste), which posed environmental problems. Some of it was sold while the rest had to be discarded.

It was envisaged that with the quantities of biomass residues available it would be possible to retrofit both of its process heaters (14,644 MJ/h net output each) from natural gas to producer gas. The heaters produced hot air at about 540°C for the driers of the plant, to dry the chopped wood before processing to particle board.

SPANO N.V. finally opted for a classical biomass combustion system, since the fluidized bed gasification process was still at the early stages of development (beginning 1982).

It was decided to use this case as the basis for the case study since it represents a realistic problem.

8.1.2 Basis of design

The case study calls for the design of a fluidized bed gasification plant to provide for the energy requirements of two process heaters. The net output of each heater is 14,644 MJ/h. The feedstock available is a mixture of bark and wood residues and sufficient quantities exist. The feedstock is produced by the particle board plant and there is space availability for the gasification plant within the limits of the particle board plant. Hence, transportation of the feedstock does not have to be considered. Utilities are readily available at the particle board plant as well as process air for instrumentation. The

product gas is to be combusted in the comnbustion chamber of the process heaters. The plant operates 6,000 h/y.

8.1.3 Feedstock

The biomass residues at SPANO N.V. was a mixture of bark and woodwaste each at about 50 wt% (295). The wood waste had very similar properties and composition as with the feedstock used in this work. For the bark fraction a characterization was made at the Free University of Brussels as well as at Depauw-Stokoe N.V. The results of both analyses are summarized in Table 8.1.

Table 8.1 : Characterization of bark residues from SPANO N.V.

		V.U.B.(1)	D.S.(2)	Average
1) Moisture content wt%		11.1	13.8	12.45
2) Ash/inerts content wt%		23.5	28.5	26
3) Calorific value MJ/kg dry basis			12.0	12.0
bark only		15.6		
as received > 0.71 mm		10.0		
as received > 0.42 mm		8.7		
4) Elemental analysis (MAF) wt%				
	C		52.5	52.5
	H		6.6	6.6
	O		40.3	40.3
	N		0.76	0.76
	S		0.02	0.02
5) Bulk density	kg/m^3	248		248
6) Sieve analysis	mm	wt%	Ash wt%(3)	
10.5 - 8.5		31.8	20.6	31.8
8.5 - 6.7		8.4	14.5	8.4
6.7 - 4.7		8.2	12.9	8.2
4.7 - 3.3		8.4	20.1	8.4
3.3 - 2.0		8.8	-	8.8
2.0 - 0.71		14.1	27.1	14.1
0.71 - 0.42		5.2	31.8	5.2
0.4 - 0.25		6.0	42.8	6.0
0.25 - 0.18		7.2	-	7.2
< 0.18		1.9	52.0	1.9

(1) VUB = Free University of Brussels

(2) DS = Depauw-Stokoe N.V.

(3) Ash wt% in fraction of bark.

The high ash/inerts content of the bark was due to high content of soil and sand. Apparently, the trees originated in the "Kempen", the area of Belgium

close to the boarder with the Netherlands. After harvesting the trees, the trunks were pulled on the sandy soil before being loaded on trunks and therefore a lot of inerts was captured in the cavities of the bark. Thus the properties and characteristics of the feedstock available was a combination of these of the bark and these of the chopped wood used in the experiments. Table 8.2 summarizes the characteristics of the residuces available at SPANO N.V

Table 8.2 : Characteristics of the available feedstock (mixture of chopped wood and bark) at SPANO N.V.

1) Moisture content	wt%		12.0	
2) Ash content	wt%		13.80	
3) Calorific value dry basis	MJ/kg		15.00	
4) Elemental analysis (MAF)	wt%	C	48.85	
		H	6.10	
		O	44.60	
		N	0.39	
		S	0.01	
5) size(approximate)	mm	0- 10	10. 75	wt%
		1-30	45.60	
		30-50	30.05	
		50-70	7.65	
		70-150	5.95	

8.1.4 Process specifications

According to SPANO N.V., the particle board process can tolerate low loads (0.01 kg/Nm3) of ash in the driers without any negative effects on the quality of the final particle board. However, high ash loads are not permissible. Therefore a hot gas cyclone must be foreseen for particulates removal. The gasification plant must therefore consist of a feeding system, a fluidized bed gasifier and a hot gas cyclone.

The two heaters are placed in parallel; however, the place for the installation of the fluidized bed gasifier was selected at about 50m from the heaters at the personnel car parking. This location has the advantage that it is very close to the source of the feedstock. There was also space available close to the heaters; however, the feedstock had to be transported from its source to the plant.

It was decided that it is more easy and less expensive to transport the product gas over the 50m distance than to have to transport the feedstock around the plant (either by truck or conveyor belt).

Thus, the process has to consider an excess energy supply to the heaters to account for the heat losses in transporting the product gas over this distance and other losses over the heaters. However, the actual transport, distribution and combustion of the product gas in the two heaters is considered beyond the scope of the thesis and are not examined any further in this chapter.

8.2 PROCESS AND PLANT CIRCUIT DESCRIPTION

The process flow diagram (see Figure 8.1) shows the various process streams associated with the gasification system and the major equipment items. The conceptual design considers the plant from the wood storage and reception up to the cyclone included. Downstream the cyclone, the gas is to be fed to the process heaters of SPANO N.V. The description of all stream numbers is given in Table 8.3. The feedstock is removed from its source by a fork lift equipped with a bucket (front-end loader). It is then fed to the fluidized bed gasifier by means of a screw feeder. Silica sand is used as the inert bed in the fluidized bed. The inert bed is fluidized by air supplied through a distributor by means of an air compressor. The feedstock is gasified to produce the product gas.

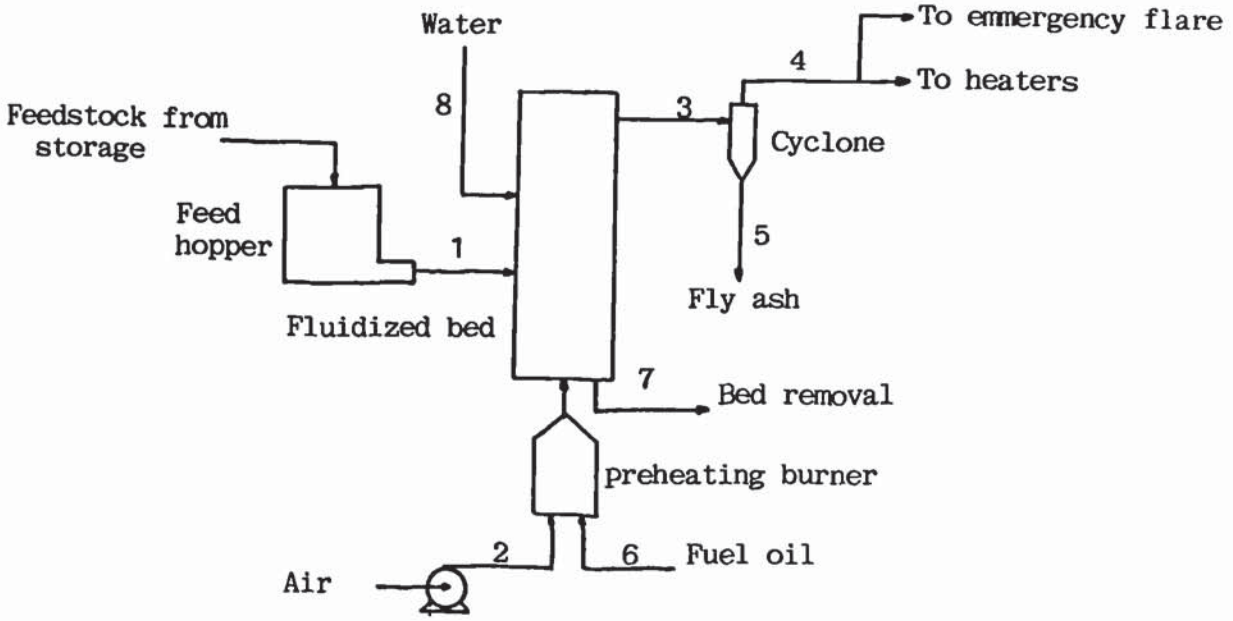

Figure 8.1 : Process flow diagram

The product gas is passed through a cyclone to remove substantial part of fly ash and fine sand elutriated from the bed. The product gas is fed to process heaters while the cyclone discharge is discarded.

Due to the high ash/inerts content of the feedstock, there is an accumulation of inerts in the bed. Thus, in order to avoid de-fluidization part of the bed is continuously removed so that a constant bed heigh is maintained.

When starting up from cold, a preheating burner/combustion chamber fired with oil is used to preheat the fluidized bed.

An emergency flare and pilot flame are provided in case of downstream problems at the process heaters to combust the gas.

Table 8.3 : Stream number and description

Stream no.	Description
1	Feedstock feed to fluidized bed
2	Air feed by compressor to the fluidized bed
3	Hot product gas to cyclone
4	Hot raw gas to process heaters
5	Cyclone discharge
6	Oil fuel supply (start up)
7	Continuous removal of bed material
8	Cooling water (shut down)

8.3 PROCESS DESIGN

The design must consider a fluidized bed gasification system capable of delivering gas with an energy output of:

14644 x 2 = 29288 MJ/h.

Since the moisture content of the feedstock is 12 wt%, the EMCM model is applicable (see sections 6.3 and 6.4.1). An air factor of 0.3 (see section 7.4.6.3) is selected so that the process will result to maximum energy output.

8.3.1 Determination of product gas, feedstock and air flowrate

8.3.1.1 Product gas

The sensible energy of the gas and the sensible and latent heat of steam are not considered in the determination of the gas flowrate required to provide

this energy. This extra amount of energy is for safety margin, which should be at least 20% (296) in excess of the net output requirements, to account for the energy losses in transporting the gas, in the heaters et al. Following the procedure outlined in section 7.4.6.13 and from equation 7.13 and Table 7.8 the volumetric flowrate of gas required for the minimum specified energy output is (see equation 7.13):

$$Q_{gas} = \frac{E}{HHV}$$

$$= \frac{29288}{5.55} = 5277.1 \ Nm^3/h.$$

The specific weight of the product gas is 1.27 (see section 7.4.6.7) thus

$$G_{gas} = Q_{gas} \times p_{gas} \qquad \text{equation 8.1}$$

where G_{gas} = mass flowrate of product gas
Q_{gas} = volumetric flowrate of product gas
p_{gas} = specific weight of the product gas

and $G_{gas} = 5277.1 \times 1.27 = 6701.9$ kg/h.

8.3.1.2 Feedstock

From section 7.4.6.7 and equation 7.6 the feedstock flowrate required to produce this amount of gas is (from Table 7.8: $Y_{gas} = 2.32$):

Mass flowrate of gas = yield of gas x feedstock flowrate

or $G_{gas} = Y_{gas} \times G_{feed(MAF)}$

or $$G_{feed(MAF)} = \frac{G_{gas}}{Y_{gas}}$$

$$= \frac{6701.9}{2.32} = 2888.7 \text{ kg feedstock (MAF)/h}$$

The feedstock flowrate on as received basis is determined as follows:

$$G_{feed} = \frac{G_{feed(MAF)}}{1-M\%-A\%} \qquad \text{equation 8.2}$$

where M = moisture content wt%
A = ash content wt%

Substituting the moisture and ash contents from Table 8.2, equation 8.1 gives :

$$G_{feed} = \frac{2688.7}{1-0.12-0.138} = 3893.1 \text{ kg/h}$$

By using the bulk density of the feed from Table 8.1, the volumetric flowrate becomes:

$Q_{feed\,(MAF)}$ = 15.7 m^3/h.

8.3.1.3 Air

The air flowrate is determined as discussed in section 7.4.6.5, by using equation 7.4.:

$$G_{air} = S \times (wt\%\ C \times 11.48 + wt\%\ H \times 34.19 - wt\%\ O \times 4.31) \times G_{feed(MAF)}$$

$$G_{air} = 0.3 \times (0.489 \times 11.48 + 0.061 \times 34.19 - 0.446 \times 4.31) \times 2688.7$$
$$= 5009.0 \text{ kg/h}.$$

$$\text{or } Q_{air} = \frac{5009}{1.293} = 3873.9 \text{ } Nm^3/h.$$

8.3.1.4 Performance of the fluidized bed gasifier

The performance of the gasifier can be determined by applying the EMCM model (see Table 6.2). The results are summarized in Table 8.4.

Table 8.4 : Performance of gasifier at an air factor of 0.3

HHV	=	5.55	MJ/Nm^3
Y	=	2.32	kg gas/kg feed(MAF)
n	=	59.20	%
T_B	=	797	°C
T_E	=	737	°C
X_{CON}	=	0.326	kg condensate/kg feed (MAF)
H_R	=	8.20	MJ/kg
Y_{H2}	=	0.015	kg H_2/kg feed (MAF)
Y_{CH4}	=	0.063	kg CH_4/kg feed (MAF)
Y_{CO}	=	0.324	kg CO/kg feed (MAF)
Y_{C2}	=	0.032	kg C_2/kg feed (MAF)
Y_{CO2}	=	0.657	kg CO_2/kg feed (MAF)

8.3.2 Mass and volumetric flowrates of all other components

Following the procedure described in section 7.4.6.7, the flowrates of the products of the gasification process can be calculated.

8.3.2.1 Steam

$$G_{st} = Y_{CON} \times G_{feedMAF} \qquad \text{equation 8.3}$$

$$= 0.326 \times 2888.7 = 941.7 \text{ kg/h}$$

$$Q_{st} = \frac{G_{st}}{\rho_{CON}} \qquad \text{equation 8.4}$$

$$= \frac{941.7}{0.8113} = 1161 \text{ Nm}^3/\text{h} = 4296 \text{ m}^3/\text{h at } 737\,^{\circ}\text{C}.$$

In this work it was found that the condensate contained dissolved hydrocarbons. Therefore, the amount of carbon that would dissolve in the condensate (in the form of higher molecular weight hydrocarbons) is:

$$G_C = G_{steam} \times X_C \qquad \text{equation 8.5}$$

where X_C = 0.013 kg C/kg steam (see section 5.8.3).

$G_C = 941.7 \times 0.013 = 12.24$ kg C/h.

8.3.2.2 Gas components

The same procedure can be applied for the components of the gas and the results are summarized in Table 8.5. In the nitrogen balance, the nitrogen of the feed is also included, while sulphur is negligible and therefore is excluded.

Table 8.5 : Mass and volumetric flowrates of gas components

Component	Flowrate	
	Mass kg/h	Volumetric Nm^3/h
H_2	43.3	482.5
CH_4	182.0	253.4
CO	935.9	748.7
C_2	92.4	70.5
CO_2	1897.9	960.0
N_2 (balance)	3550.4	2761.5
Total	6701.9	5277.1

The specific gravity of this gas is:

$$\rho_g = \frac{6701.9}{5277.1} = 1.27 \text{ kg/Nm}^3.$$

The gas composition in terms of weight % and volume % is given in Table 8.6.

Table 8.6 : Gas composition

Component	Weight %	Volume %
H_2	0.65	9.14
CH_4	2.72	4.82
CO	13.96	14.19
C_2	1.38	1.34
CO_2	28.32	18.19
N_2	52.97	52.32
Total	100.00	100.00

8.3.2.3 Ash/Inerts

The data on fly ash from this work cannot be used directly in this case study, since the feedstock has a very high content of inerts (13.8 wt%). Experience

has shown (102, 108) that with similar feedstocks (Ipicia bark, 24 wt% ash/inerts) 52.9 wt% of the ash/inerts accumulated in the bed. Those experiments were carried out at 3.67 kg/h feedstock. In the air factor range of 0.2-0.6, the average accumulation of inerts in the bed was 0.466 kg/h, while the rest of the inerts was elutriated with the fly ash. This resulted in relatively low carbon content of the fly ash (an average of 14.0 wt%). These data will be used in the design as they are more representative for bark containing feedstocks.

The ash/inerts input in the reactor is:

$$G_{ash} = G_{feed} \times \text{Ash content} \qquad \text{equation 8.5}$$
$$= 3893.1 \times 0.138 = 537.2 \text{ kg/h.}$$

From this quantity, the larger and heavier particles (about 53%) accumulate in the bed and have to be removed continuously:

$$G_{ash,\,acc.} = G_{ash} \times 0.53 \qquad \text{equation 8.6}$$
$$= 537.2 \times 0.53 = 284.7 \text{ kg/h}$$

It is envisaged that the inerts removed from the bed will contain some char. In the same work (102) it was found that the bed section just above the distributor contained about 2 wt% char. Thus:

$$G_{bed,rem} = G_{ash,acc} \times 1.02$$
$$= 284.7 \times 1.02 = 290.4 \text{ kg/h.} \qquad \text{equation 8.7}$$

Since the material being removed from the bed is mainly sand, it is assumed that it has the same bulk density as silica sand, $\rho = 2444$ kg/m^3 (187). Thus:

$$G_{bed,\,rem} = \frac{290.4}{2444} = 0.12 \text{ m}^3\text{/h.} \qquad \text{equation 8.8}$$

The balance of fine particles is elutriated from the reactor. In addition, the elutriated fly ash has a carbon content of 14.0 wt%.

$$G_{ash,el} = G_{ash} \times 0.47$$

$$= 537.2 \times 0.47 = 252.5 \text{ kg/h.}$$

$G_{fly\ ash} = G_{ash,el} \times 1.14$ equation 8.9

$= 252.5 \times 1.14 = 287.8$ kg/h

The bulk density of the fly ash is 210 kg/m³ (see section 5); therefore:.

$$Q_{fly\ ash} = \frac{287.8}{210} = 1.4\ m^3/h.$$

8.3.2.4 Summary of reactants and products flowrates

The flowrates of the reactants and the products are summarized in Table 8.7.

Table 8.7 : Summary of reactants and products flowrates of the fluidized bed gasifier.

1. Reactants	kg/h	Nm³/h	m³/h
Feedstock (MAF)	2888.7	-	11.6
Feedstock (as received)	3893.1	-	15.7
Air	5009.0	3873.9	-
2. Products			
Total gas (cool, dry, ash free)	6701.9	5277.1	-
H_2	43.3	482.5	-
CH_4	182.0	253.9	-
CO	935.9	748.7	-
$(C_2H_4 + C_2H_6)$	92.4	70.5	-
CO_2	1897.9	9160.0	-
N_2	3550.4	2761.5	-
Steam	941.7	1161.0	-
Fly ash elutriated	287.8	-	1.4
Inert removal from bed	290.4	-	0.2

8.4 Mass and energy balances

The mass balance and energy balance over the gasifier are given respectively in Tables 8.8 and 8.9. The mass balance closure based on the data of Table 8.7 was 92.4 %. Since this is a conceptual design, it was necessary to adjust the mass balance. This was made by carrying out a nitrogen balance (see equation 5.28 and section 5.8.1) over the air input and using the gas composition of Table 8.6. The energy balance had to be adjusted accordingly.

Table 8.8 : Mass balance of gasification process

Reactants		Products	
Component	Total kg/h	Component	Total kg/h
Feedstock (MAF)	2888.7	Total gas	7382.2
Water (feed)	467.2	H_2	48.0
Ash (feed)	537.2	CH_4	200.8
Air	5009.0	CO	1030.6
		C_2*	101.9
		CO_2	2090.5
		N_2	3910.4
		Steam	941.7
		Fly ash	287.8
		Bed removal	290.4
Total	8902.1		8902.1

*C_2 assumed to be C_2H_6

Table 8.9 : Energy balance of gasification process

Reactant		Products	
Component	MJ/h	Component	MJ/h
Feedstock	51388	- Heat of combustion of product gas	32809
		- Sensible heat of product gas	6808
		- Sensible and latent heat of steam	3797
		- Heat of combustion of fly ash	1322
		- Sensible heat of fly ash	194
		- Heat of combustion of char in bed removed	191
		- Sensible heat of bed removed	246
		- Heat of combustion of carbon in steam	402
		- Heat loss reactor walls (balance 11 % heat loss)	5619
Total	51388		51388

The heat losses of the reactor (11%) are considered acceptable, since in two commercial projects the heat losses of the gasifier were estimated at 8.8% (115) and 14.3% (247).

The energy supplied to the process heaters is:

Total energy supply = Heat of combustion of product gas + sensible heat of product gas + sensible and latent heat of steam + heat of combustion of fly ash escaping the cyclone + sensible heat of fly ash escaping the cyclone + heat of combustion of carbon in condensate.

equation 8.10

Assuming that the cyclone has an overall particulates removal eficiency of 75% then the total energy supply to the process heaters is 44194 MJ/h. Assuming that the pipe connecting the cyclone to the process heaters has the same insulation as the freeboard of the fluidized bed, then the heat losses are estimated at 107 MJ/h. Therefore the net energy supply to the heaters is 44089 MJ/h.

It can also be assumed that the heat losses through the walls of the heaters are 4% of the input - 1763 MJ/h. Thus the net output at the exit of the heaters (assuming no other losses) is 42323 MJ/h. This is 44.5% in excess of the minimum output requirement of the heaters (for the mass flowrates of Table 8.7, the net output of the heaters is 37905 MJ/h or 29.4% in excess). This excess amount of energy is a reliable safety margin for other energy losses (e.g. efficiency of combustion of product gas,fly ash et al.) and is well above the estimated 20% excess of energy required (see section 8.3.1.1).

The thermal efficiency of the gasification process on the basis of the energy output as defined by equation 8.10 (43636 MJ/h) is 86.0%. However, the thermal efficiency on the basis of the chemical energy of the gas defined by equation 5.18 is 63.8%.

8.5 PLANT AND EQUIPMENT SPECIFICATIONS

8.5.1 Specifications of the fluidized bed gasification process

The specifications of the fluidized bed gasification process therefore are:

a) The fluidized bed reactor has an energy output of 41788 MJ/h; 42.6% in excess of the net output requirements of the process heaters.
b) The maximum energy output is obtained at an air factor of 0.3.
c) For this purpose, 3.89 t/h (as received) or 2.89 t/h (MAF) feedstock and 5009 kg/h or 3874 Nm^3/h air are required.

d) The process produces 7.38 t/h (or 5812.8 m^3/h) gas.

e) The higher heating value of the gas is 5.55 MJ/h. The overall efficiency of the process is 86.0%.

f) The process takes place at 797 °C while the product gas leaves the reactor at 737 °C.

g) The steam flowrate is 941.7 kg/h.

h) The fly ash flowrate is 287.8 kg/h with a carbon content of 14.0 wt% (40.3 kg/h C).

i) Part of the bed is removed continuously at a flowrate of 290.4 kg/h. This contains 2 wt% char (5.8 kg/h char).

8.5.2 Equipment schedule and specifications

In Table 8.10 the schedule and specifications of all equipment needed for the gasification plant are specified.

Table 8.10 : Equipment schedule and specifications

Section	Feeding		Reactor	Auxialiary
Equipment	Feeder	Hopper	Fluidized bed	Compressor
Type	Choked screw	Cylindrical	Expanded free-board.	Centrifugal
Purpose	To feed biomass into fluidized bed	Intermediate storage of feedstock for 0.5 h.	To gasify feed-stock to produce gas.	To compress air to pressure required by the fluidized bed.
Flowrate kg/h	3893.1	3893.1	f)3893.1 a)5009.0 g)7382.2	5009
gas Nm^3/h	-	-	a)3873.9 g)5812.7	3873.9
solids m^3/h	15.7	15.7	f)15.7	-
Temperature °C	Ambient (20)	(20)	b)797, f_r)737.	60
Pressure bar	(1.013)	(1.013)	TD	TD
Material of construction	Mild steel	Mild steel	Mild steel, refractory bricks.	Mild steel

Table 8.10 cont'd

Auxiliary			Gas cleaning	
Heater	Bed screw	Cyclone	Ash collector	Feeder
Direct fired, atomizing oil burner	Constant cross section	Single unit, 75% removal efficiency	Bin, cylindrical	Rotary
To preheat the air during start up	To remove part of the bed	To remove the particulates from the product gas	Intermidiate storage of fly ash for 0.5/h	To remove fly ash from ash bin, inter-mittent operation
TD	290.4	8611.7	215.9	400
	-	6975.3	- -	
	0.2	-	1 -	
600 °(exit)	20	737	i)700 o)80	80
TD	1.013	TD	TD	i)TD o)1.013
Mild steel reactory	Stainless steel	Mild steel, lined with ceramic tiles	Mild steel	Mild steel

where: f) = feedstock; a) = air; g) = gas; b) = bed; fr = freeboard; i) = inlet; o) = outlet
TD) = to be determined by engineering design.

8.6 EQUIPMENT DESIGN

8.6.1 Feeding system

The feeding system consists of two parts: the feeder and the hopper.

8.6.1.1 Feeder system

The design is based on the procedure outlined in Figure 7.11. The properties of the feeedstock have been determined and are given in Table 8.1. Since the feedstock contains relatively large amounts of inerts, it is expected to be abrasive. Thus, a slow moving feeder with minimum of moving components must be selected. It can be envisaged that the feedstock could be screened to reduce sand and dirt content. This is also justified from the ash/inerts content of the lower size fractions of the feedstock (31.8% for the size range

0.71-0.42 mm; increased to 52% for the fraction smaller than 0.18 mm.). However, at this scale of application screening of the feedstock is not cost effective (see section 7.3.2.1).

Since the feedstock is relatively dry (12.45 wt% moisture) and not of resinous origin, it is not expected to be corrosive or sticky.

The fluidized bed process operates at pressures slightly above atmospheric in the freeboard section, with typical values in the range of 60-200 mbar.

From the feeders proposed in section 7.4.5.10, the choked screw meets the above requirements, since it has few moving parts, can operate up to 0.5 bar differential pressure (see Table 7.7) and has relatively low power consumption (see Figure 7.9). On the basis of the feeder requirements, the following specifications can be determined.

Flight diameter	= 0.3 m	(Table 7.7)
Pitch	= 0.15 m	(189)
Speed rpm	= 50	(189)
Power	= 0.5 kw	(Figure 7.9)

8.6.1.2 Hopper

The angle of repose of the feedstock was determined at 65 °. Thus the feedstock is considered as sluggish. However, due to its relatively low moisture content the feedstock has acceptable flowability. This was also confirmed by SPANO N.V. The hopper shall therefore be designed with an angle at the outlet of 80 °.

The hopper has a capacity of 8 m^3 which can supply the feeder for half hour. Its total height shall not exceed 4 m from ground so that it can be filled by a fork lift. Its specifications are:

Volume	=	8 m^3.
Angle at outlet	=	80 °
Diameter of cylinder	=	2.5 m
Height of cylinder	=	1.2 m
Volume of cylinder	=	6 m^3
Diameter of outlet	=	1 m

Height of frustum of right cone = 0.8 m
Volume of frustum of right cone = 2 m^3

8.6.2 Reactor

The design of the fluidized bed is carried out on the basis of the procedure outlined in sections 7.4.6.9-7.4.6.11 (summarized in Table 7.10).

8.6.2.1 Bed dimensions (see section 7.4.6.9)

Applying equation 7.7 with a maximum specific capacity of 711 kg/hm^2 (MAF) gives

$$\text{Cross sectional area of bed} = \frac{2888.7}{711} = 4.06\ m^2 = 4.1\ m^2$$

Since the cross sectional area is below 5 m^2 a cylindrical bed is selected (see section 7.4.6.9).
The diameter of the bed is 2.27 m.
Increasing this value by a safety margin of 10% gives :
d_b = 2.5 m

The bed height is calculated by equation 7.8.

$$\frac{d_b}{h_b} = 1.33 \qquad h_b = \frac{2.5}{1.33} = 1.88\ m$$

This value is above the allowable maximum of 1m and hence it is not acceptable. The height of the bed is than set at 1 m.

8.6.2.2 Reactor dimensions (see 7.4.6.10).

The average flowrate of the gas at reactor conditions is given by equation 7.10. Substituting the appropriate values equation 7.10 gives:

$$Q_{gas,av} = \frac{1}{2} \times \left[3873.9 \times \left(\frac{797+273}{273}\right) + 5812.7 \times \left(\frac{737+273}{273}\right)\right] = 18344\ m^3/h.$$

Since the gas will be combusted directly before cooling, tars pose no problem since, they are burned along with the gas. Therefore a retention time of 10

seconds is acceptable. The volume of the reactor is given by solving equation 7.9 for V_r. Thus:

$V_r = R_T \times Q_{gas}$ equation 8.11

$= 10 \times \frac{18344}{3600} = 50.95\ m = 51\ m$

The volume of the freeboard is given by equation 8.12.

$V_f = V_r - V_b$ equation 8.12

where V_i = volume
$_f$ = freeboard
$_r$ = reactor total
$_b$ = bed

and $V_f = 51 - 4.1 = 46.9\ m^3$.

To allow for good disengagement of entrained bed particles and to minimize the particulate load of the product gas, the diameter of the freeboard will be expanded, according to equation 7.11. Thus :

$d_f = d_b \times 1.5$ (equation 7.11)
$= 2.5 \times 1.5 = 3.75$ m.

The height of the frustum of the right cone is set at 3 m to allow for a gradual reduction. From Figure 8.2 the angle of the frustum is :

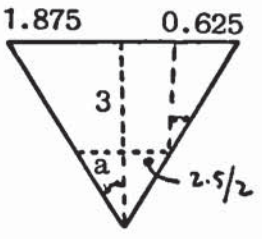

$\sin a = \frac{0.625}{3.06} = 0.21$

or $a = 12^0$

Angle of frustum $= 2 \times 12 = 24^0$

Figure 8.2 Dimensions of frustum of the freeboard.

This angle satisfies equation 7.12 and is considered acceptable.

The volume of the frustum, V_{fr} is

$$V_{fr} = \frac{\pi h}{3}(r_1^2 + r_1 r^2 + r_2^2) \qquad \text{equation 8.12}$$

$$= 23.3 m^3$$

Hence $V_f = V_{fr} + V_c$ equation 8.13

where V_c is the cylindrical part of the freeboard

and $V_c = V_f - V_{fr}$

$$= 23.6 m^3.$$

The overall dimensions of the reactor are given in Figure 8.3.

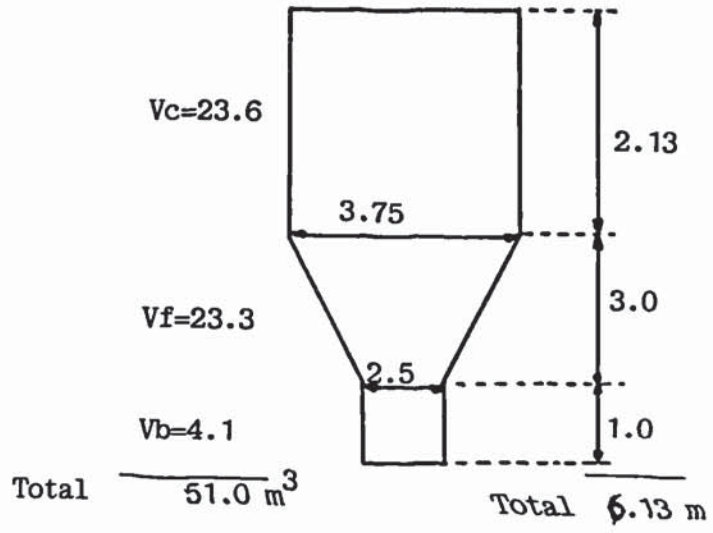

Figure 8.3 : Dimensions of fluidized bed.

8.6.2.3 Design of distributor. (see Appendix II)

The design is based on a turn down ratio of 1/3. The results are summarized in Table 8.11.

Table 8.11 Distributor design

Flowrate of air	= 1291.3 Nm^3/h.
ΔP distributor	= 0.35 m
U_o	= 0.073 m/s
Re	= 13.0×10^3
C_d	= 0.6
U_o	= 43.59 m/s.
U_o/U_{or}	= 0.002 = 0.2 % open area
d_{or}	= 3mm
A_{or}	= 7.06×10^{-6} m
N_{or}	= 237 $/m^2$
$N_{or,a}$	= 116.1

At full capacity of 3873.9 Nm^3 of air:

$Re = 39 \times 10^3$

$$U_{or} = \frac{U_o'}{A_{or} \times N_{or}} = 130.9 \text{ m/s}$$

$\Delta P_d = 315$ cm H_2O

Due to the high ash/inerts content of the feedstock, part of the bed must be removed continuously (see section 8.3.2.3). Since the removal of the bed in this work was very successful, the same concept of distributor is to be used for the fluidized bed of the conceptual plant. The configuration of the distributor is given in Figure 8.4

8.6.2.4 Pressure drop for the air compressor. (see Appendix II).
The pressure drop over the bed is (equation 3.9):

$\Delta P = \Delta P_d + \Delta P_b = 315 + 122 = 437$ cm H_2O (or 0.43 bar).

Considering a safety margin of 15%, then the compressor must supply the air at 500 cm H_2O (0.49 bar). Therefore the pressure in the freeboard and the cyclone is 0.06 bar.

16 pipes of 25 mm (Inconel 600)
Tubes A with 44 orifices each
Tubes b with 74 orifices each
Tubes C with 90 orifices each

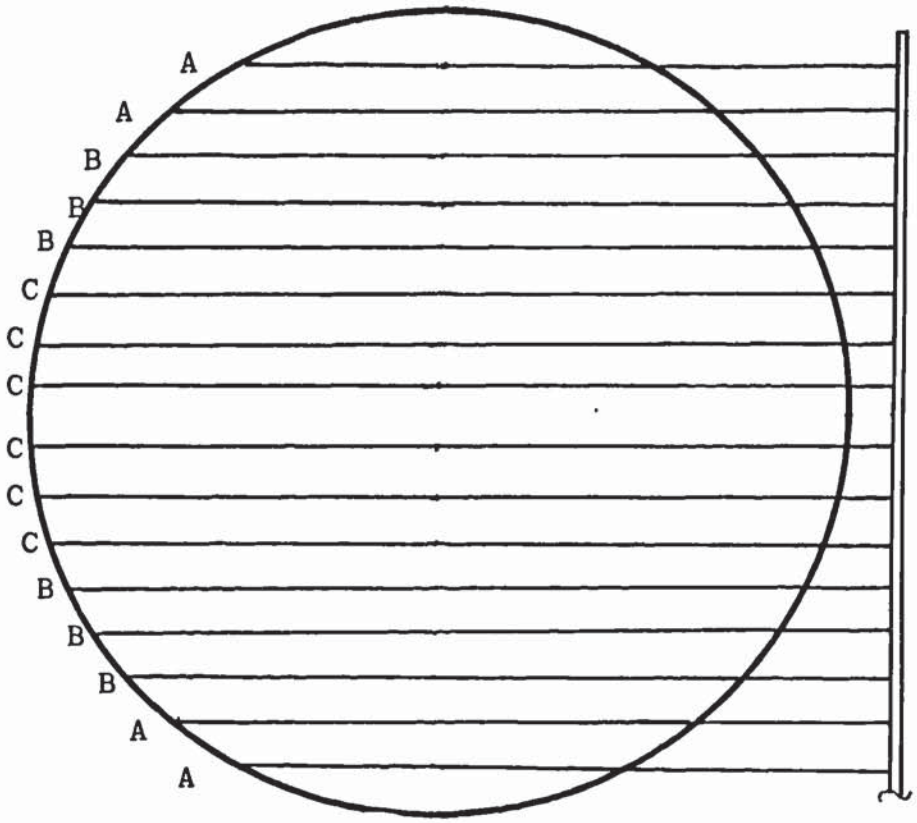

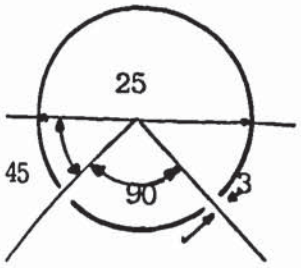

The orifices are drilled in pairs, facing dawnwards to avoid blockage by sand, at 90°

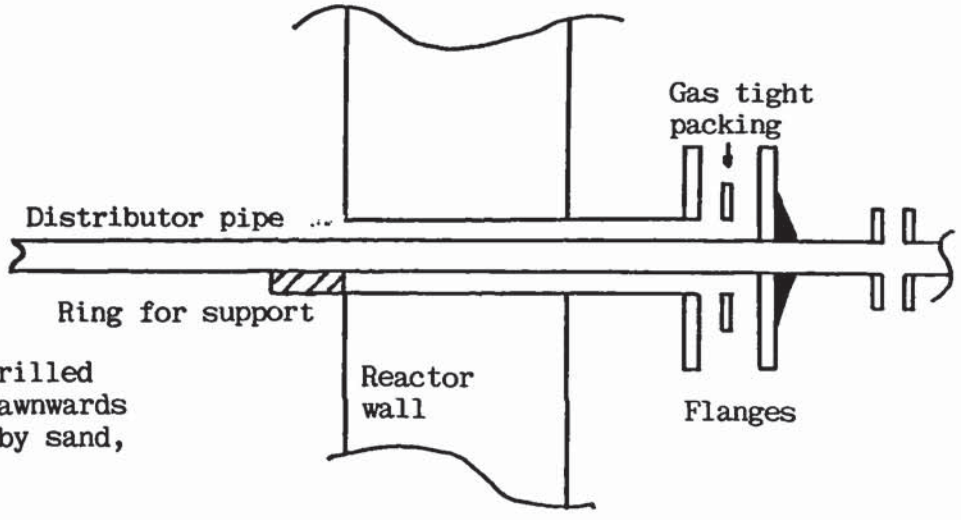

The pipes are introduced through larger pipes of 50 mm supported by flanges. They rest on ring of 50 mm width and are held in place by wells in the reactor wall.

Figure 8.4 Configuration of distributor.

8.6.2.5 Fluidization parameters (see sections 3.3.4, and 3.4)

The fluidization parameters of the reactor are summarized in Table 8.12.

Table 8.12 : Fluidization parameters

d_p = 604×10^{-6} m
U_{mf} = 0.11 m/s
Re_{mf} = 0.5
U_t = 7.7 m/s
$0.275 < U_{op} < 7.7$ m/s
$U_{op\ max}$ = 0.86 m/s acceptable
$U_{op\ min}$ = 0.29 m/s acceptable
$d_{B\ max}$ = 0.59 m. no slugging
$d_{B\ min}$ = 0.29 m. no slugging

The above data show that the fluidized bed will function efficiently. No slugging will take place and the entrainment of bed particles will be acceptable.

8.6.2.6 Design verification (see section 3.6).

The design was verified and the results are summarized in Table 8.13.

Table 8.13 : Verification of design

$(tr)_i$	=	9.1 s
$U_{B\ max}$	=	1.95 m/s
$U_{B\ min}$	=	1.09 m/s
$(tr)_{bmax}$	=	0.51 s
$(tr)_{bmin}$	=	0.92 s
$\theta_{max.}$	=	8.86
θ_{min}	=	4.95
$\frac{V_{op}}{V_B}$ max	=	0.14
$\frac{V_{op}}{V_B}$ min	=	0.29

The above data show that sufficient residence time is provided for the gas flowing interstitially so that the oxygen will be consumed completely. The contact efficiency at maximum (14%) and minimum (29%) flow are acceptable, since a contact efficiency of 10% is usually considered as the minimum acceptable.

8.6.2.7 Openings on the shell of the reactor and insulation

The openings (ports) necessary for the operation of the reactor are listed below:

1) feeding port diameter = 0.35 m
2) outlet of gas diameter = 0.6 m
3) removal of bed diameter = 0.5 m
4) manhole = 0.6x0.6 m
5) observation port diameter = 0.3 m

The bed feeding port is placed above the surface of the bed. Assuming that the maximum expansion of bed under all conditions is 50%, then the feeding port is placed at 1.5 m above the distributor.

The removal of the bed is accomplished through the grid distributor. The base of the reactor is conical and is not insulated in order to accelerate cooling of the bed material. The exit has a diameter of 0.5 m. The height of the conical base is 2 m. The base cone has a volume of $4m^3$. This provides for a retention time of 20 h (volumetric flowrate of bed material = 0.2 m^3/h, see Table 8.7). During this time the bed material will have cooled down to ambient temperature.

The manhole is foreseen at the base cone, so that the orifices and the pipes of the distributor can be inspected easily.

The observation port is placed at the ceiling of the reactor, in order to have a complete view of the reactor.

Two thermocouples, one in the center of the bed (0.5 m above distributor) and the other above the bed (1.6 m above distributor), are foreseen in the bed section. A third one is placed close to the outlet of the gases, at the freeboard. Provisions for pressure measurement (ΔP over bed and operating

pressure at the freeboard) are also foreseen. A detailed diagram of the fluidized bed is shown in Figure 8.5.

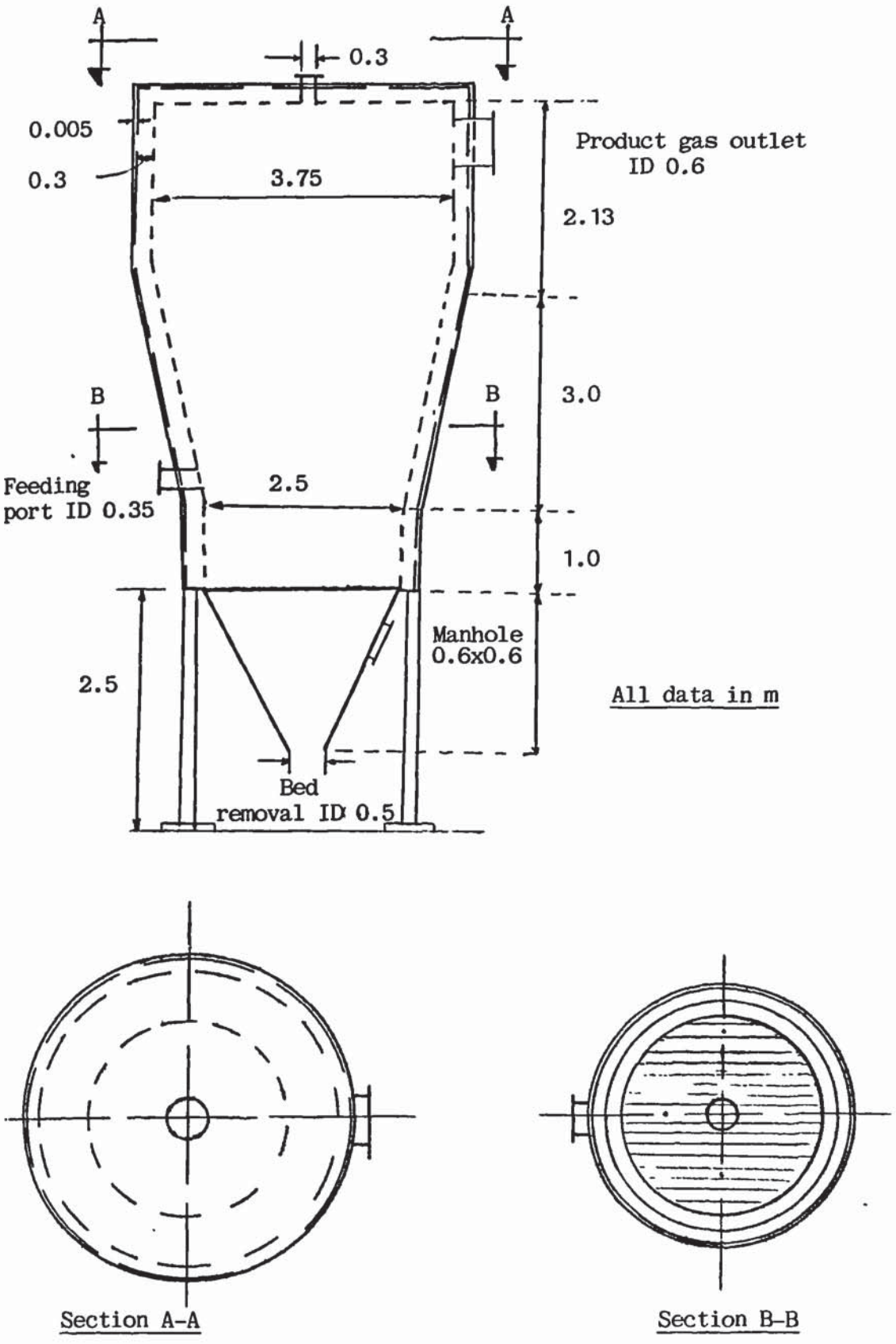

Figure 8.5 : The fluidized bed.

The inner walls of the reactor are fabricated by refractory bricks of 0.3 m total thickness. The shell is made of mild steel and at the outside is covered by another layer of ceramic wool of 0.1 m, protected by galvanised sheets. The temperature on the outside should not exceed 50 °C. The reactor is supported on four legs of 2.5 m height.

8.6.3 Auxiliary equipment for the fluidized bed

8.6.3.1 Compressor

The compressor is of centrifugal type and has to deliver 1.08 m^3/s air at 0.49 bar. Its power consumption is 11.2 Kw at 200 rpm (189).

8.6.3.2 Heater

The heater is a direct fired, atomizing oil burner. The exit temperature of the gas is specified at 600 °C. Thus, the energy required to heat up the air from 60 °C to 600 °C is :

E = 2948 MJ/h

Assuming the oil has a higher heating value of 43 MJ/kg (189), then 68.6 kg/h of oil are required. Its power consumption is 0.07 Kw (189). The fuel oil and power are only consumed during start up.

8.6.3.3 Bed screw

The bed screw has a flight of 0.05 m diameter and a pitch of 0.05 m. Its length is 4 m and is inclined at an angle of 45°. Its power consumption is 0.05 Kw (189). The screw empties the bed material in containers, to facilitate transportation to the dump site.

8.6.4 Gas cleaning

8.6.4.1 Cyclone

The design of the cyclone is on the basis of the procedure given in Appendix III. The following data are obtained:

$A_d = H_c.B_c = 0.48\ m^2$

$D_c = 1.96\ m$
$B_o = 0.49$
$D_c = 0.98$
$H_c = 0.98$
$L_c = 3.92$
$S_o = 0.25$
$S_c = 3.92$
$J_c = 0.49$

The dimensions of the cyclone are given in Figure 8.6.

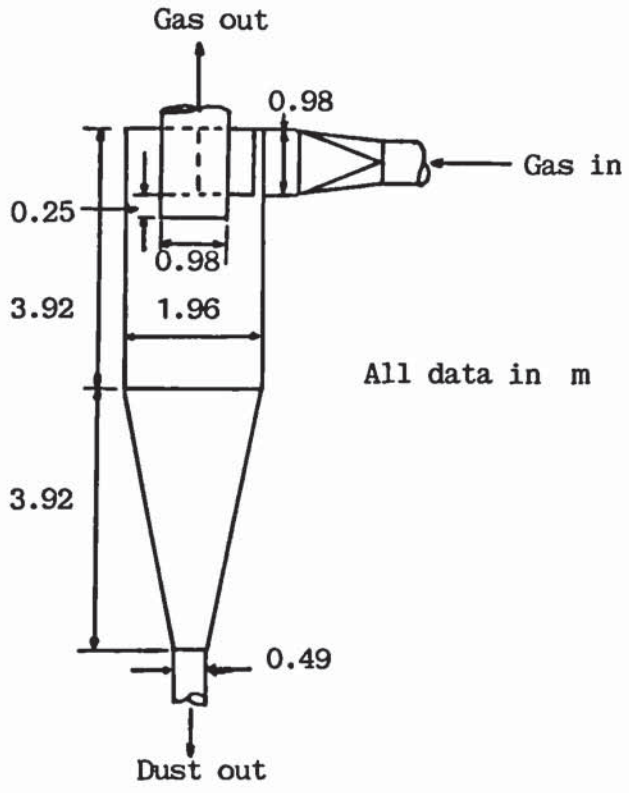

Figure 8.6 : The cyclone

8.6.4.2 Ash collector bin

The bin stores the fly ash which is produced at a rate of 1 m^3/h. To allow sufficient time for the fly ash to cool from about 700 °C to ambient

temperature, the bin has a volume of 3 m^3. Its dimensions are given in Figure 8.7.

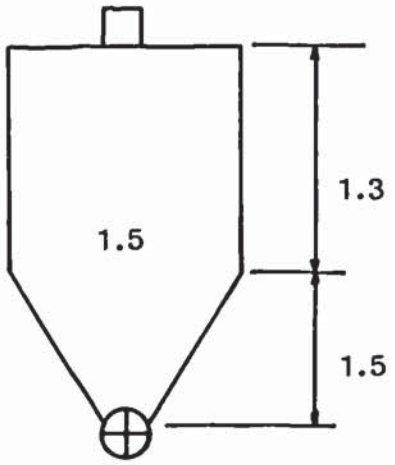

Figure 8.7 : Ash collector bin

8.6.4.3 Fly ash feeder

The diameter and length of the rotary vane valve is 0.2 m and operates at 2.6 rpm. Its power requirements are 0.03 Kw (33). The valve can provide gas tight operation under differential pressure up to 0.5 bar.

8.6.5 Discussion

The diameter of the bed is 2.5 m and its cross sectional area is 4.9 m^2. This size of the fluidized bed requires a second feeding port to ensure good distribution of biomass all over the cross sectional area of the bed (see section 7.4.3.2). However, due to the scale of the process, a second feeding port is not justified on economic grounds. Therefore a spreader will be used to distribute the biomass over the bed area. Spreaders have been developed successfully in the coal industry and are reliable units (294). These are wall mounted units using mechanical flingers. The specifications of the spreader are:

type	= mechanical flinger
lenth of flinger	= 0.6 m

thickness	= 0.005 m
height of flinger	= 0.1 m
no of flingers	= 2
rpm	= 30
power	= 0.05 Kw
material of construction	= stainless steel.

The ash /inerts of the feedstock contained mainly sand (see section 8.1.3) and soil. It is therefore envisaged that the fine sand and soil particles would be entrained and elutriated from the bed, while only the larger sand particles remain in the bed. The larger and heavy particles fall at the bottom of the bed and are removed quickly through the distributor. Only the particles with similar properties (size and density) as with the bed material (design value = 600×10^{-6}m) will remain in the bed.

It is envisaged that the bed material will not have to be replenished with fresh sand of 600×10^{-6}m diameter, but generally a bed will form consisting of only sand provided by the ash/inert fraction of the feedstock. This simplifies the process, otherwise the bed material removed should undergo screening and the fraction of appropriate size should be fed back in the bed.

The engineering design of the process is given in Figure 8.8, while the detailed characterizations of the process streams are summarized in Table 8.14. Figure 8.9 gives the layout of the process and Figure 8.10 the elevation of the plant.

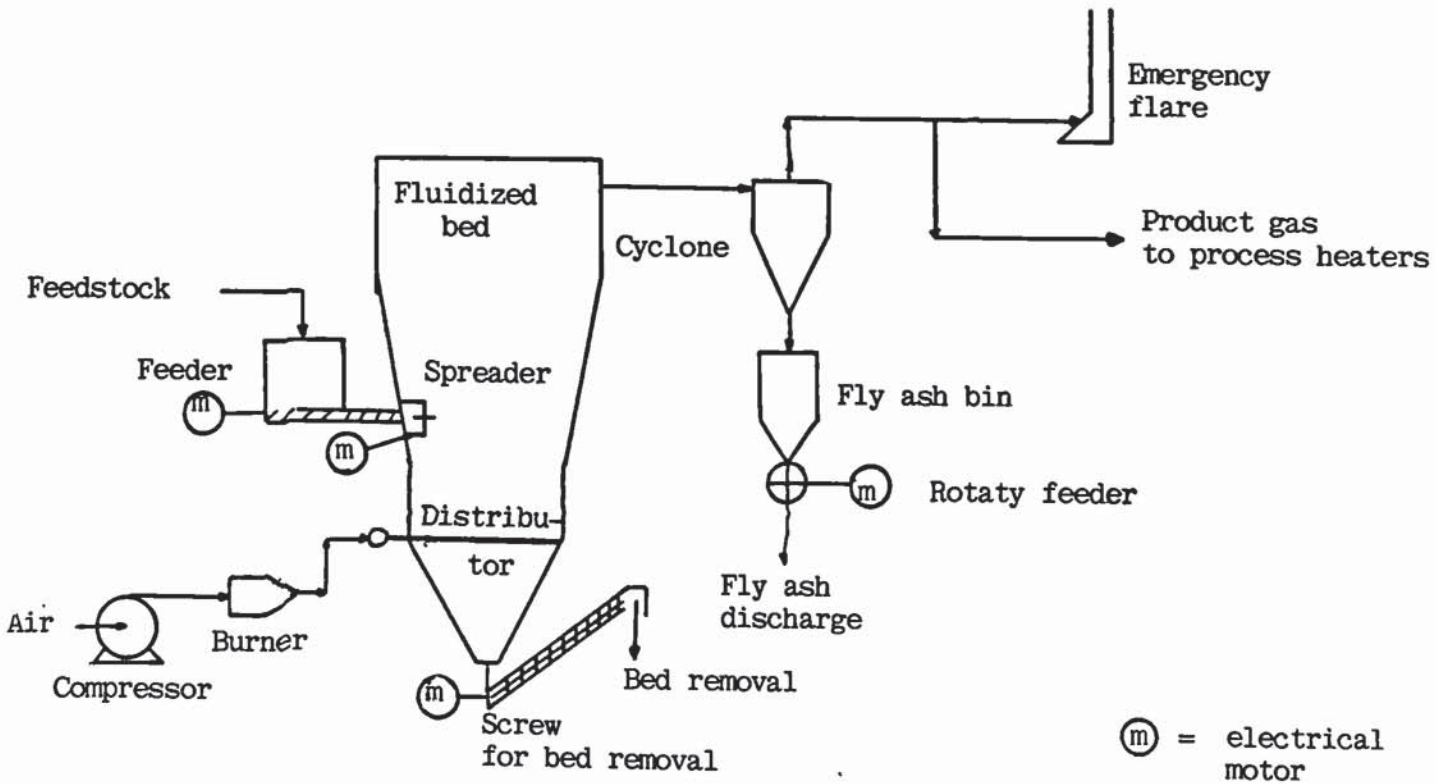

Figure 8.8 : Engineering design

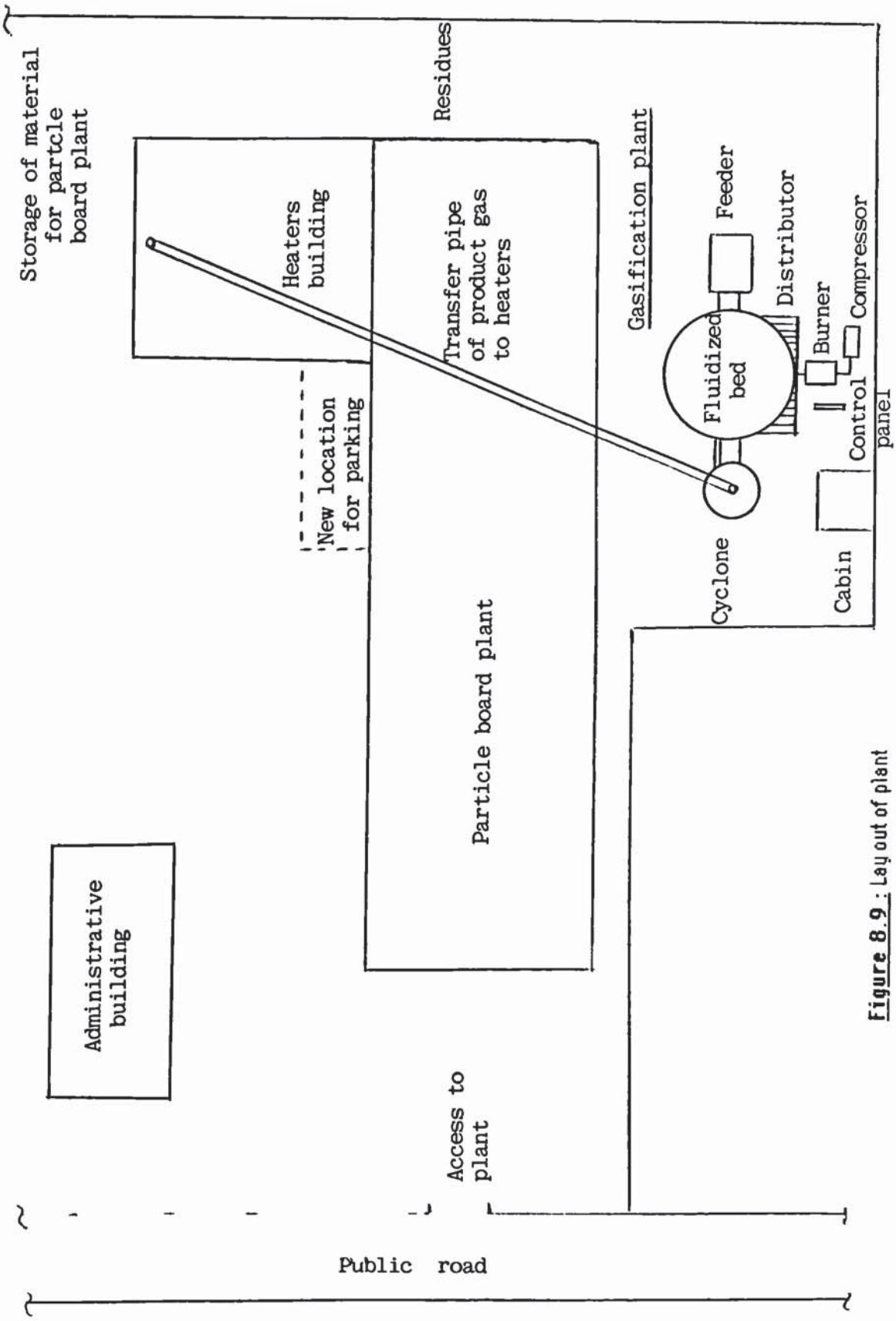

Figure 8.9 : Lay out of plant

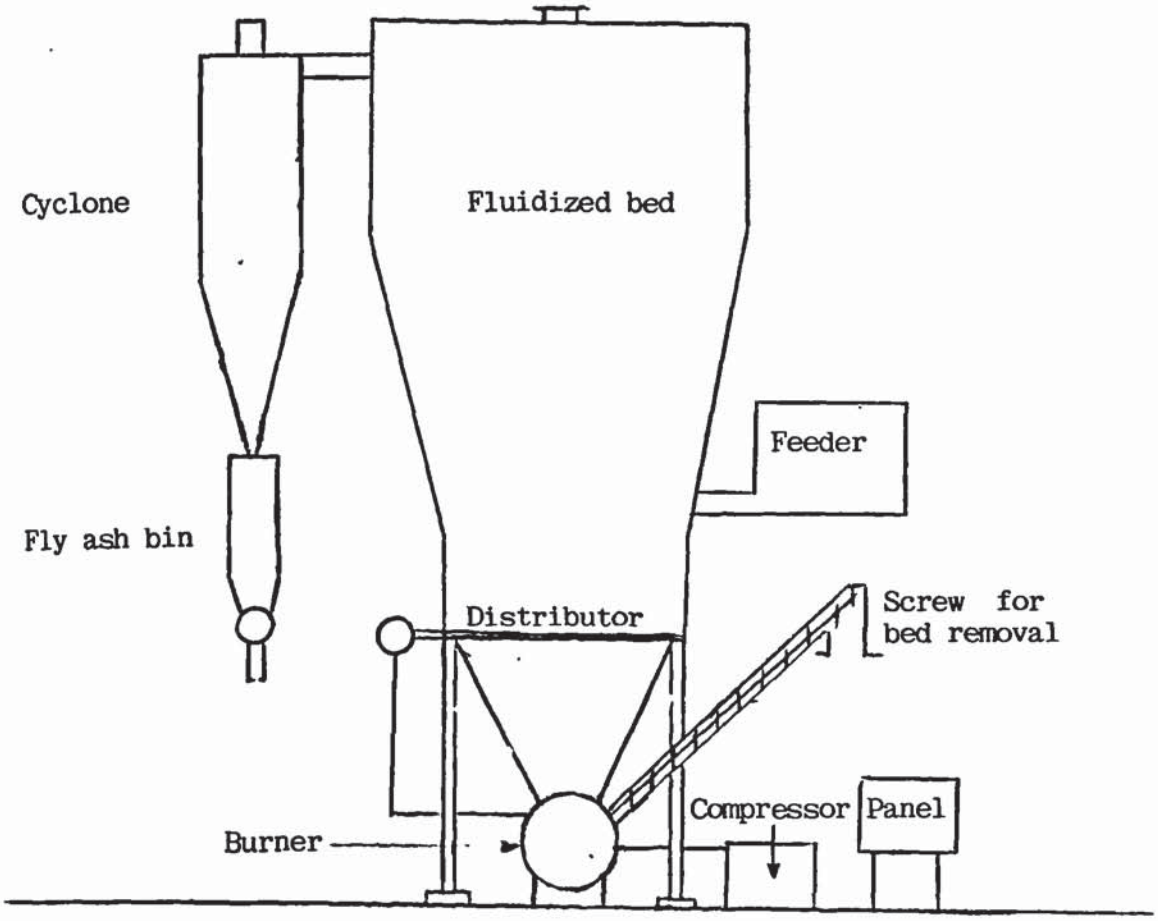

Figure 8.10 : Elevation of plant

Table 8.14 : Process stream characterization of fluidized bed biomass gasification plant.

Stream no.	1	2	3	4	5	6*	7	8
Stream name	Biomass feed	Air feed	Product gas	Gas to heaters	Cyclone ash	Oil fuel	Bed removal	Cooling water
Total weight (kg/h)	3893.1	5009.0	8611.7	8395.8	215.9	68.6	290.4	300
Gas/liquid (kg/h)	467.2	5009.0	8323.9	8323.9	-	68.6	-	300
Solids (kg/h)	3425.9	-	287.8	71.9	215.9	-	290.4	-
Volume (Nm^3/h)	-	3873.9	6975.3	6975.3	-	-	-	-
Temperature (°C)	20	20	737	700	700	20	50	20
Solids (wt%)	88.0	-	3.3	0.85	100	-	100	-
Vol.%								
CO			14.19	14.19				
CO_2			18.19	18.19				
CH_4			4.82	4.82				
C_2H_6	-		1.34	1.34	-	-	-	-
H_2			9.14	9.19				
N_2			52.32	52.32				
O_2			-	-				
Elemental wt%								
C	48.85					86.4		
H	6.10					13.6		
O	44.50					0.01		
N	0.39			-	-	0.01		
S	0.16					0.09		
Ash kg/h	532.2	-	247.5	61.8	185.7	-	284.7	-
Energy content MJ/h	51388	-	45332	44194	1137	2950	437	-

Stream no. 6 is only valid during preheating for start up.

8.7 INSTRUMENTATION AND CONTROL

The controls of the plant are shown in Figure 8.11. Local panel mounted on/off push buttons will be used to activate all motors. Running lights, shutdown switches and alarm indicators are also mounted on the local control units.

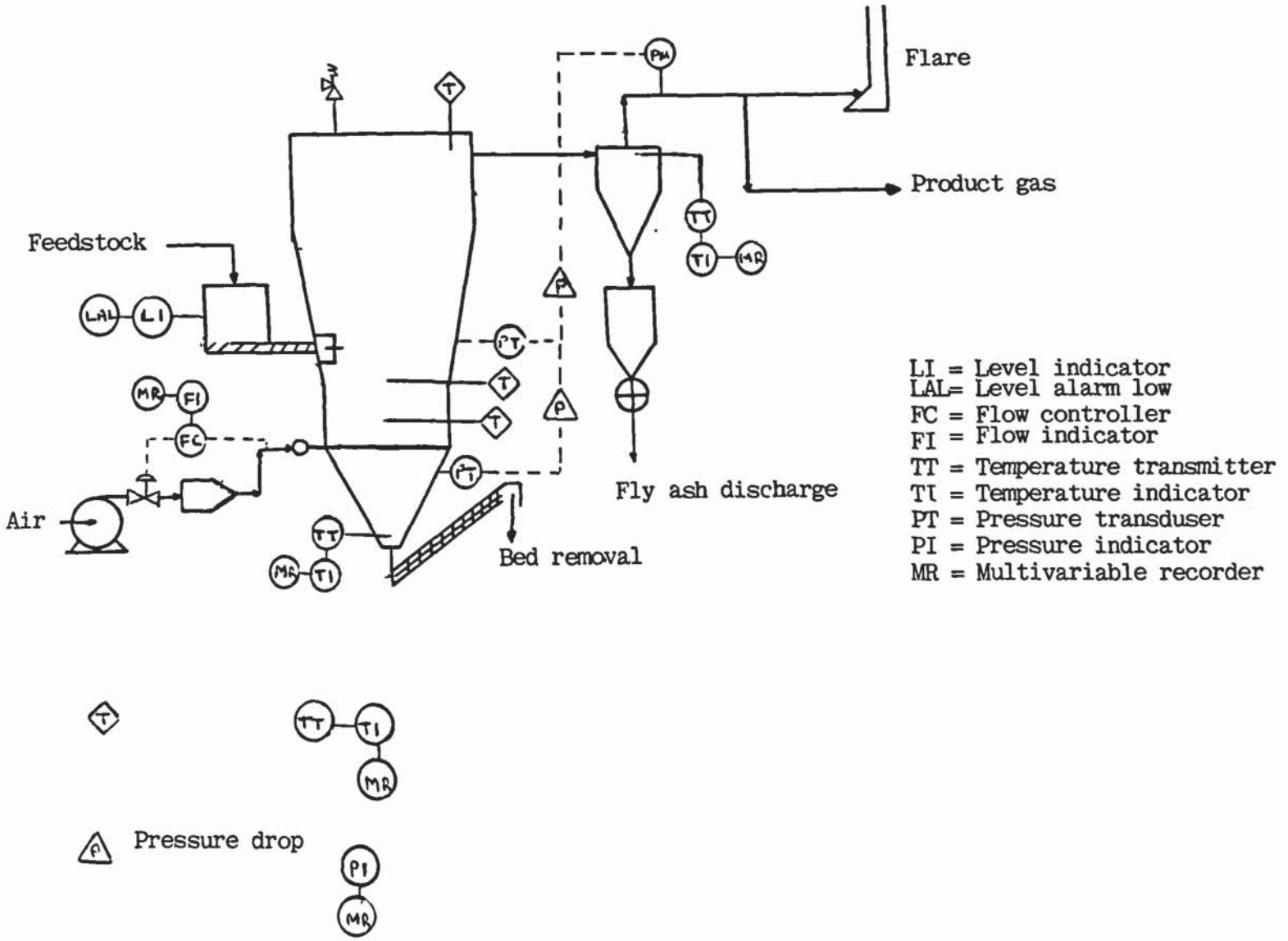

Figure 8.11 : Instrumentation of plant

8.7.1 Feeding system

The controls of the feeding system are to ensure that a continuous and constant supply of feedstock is fed to the gasifier.

The hopper of the feeder is equipped with a level control. The level control measures the level of the feedstock in the hopper and when the level drops below 4 m from the top of the hopper a Low Level Alarm is actuated.

The feeder is calibrated for constant flowrate and a flow/weight control is installed. Since there is a workman responsible for the feeding system, no other controls are necessary. A local control unit is provided.

8.7.2 Fluidized bed gasifier

8.7.2.1 Control strategy

In exothermic reactor system the control strategy is to use the temperature of the reactor as critical parameter (189). For atmospheric pressure fluidized bed gasifiers the control variable is always the temperature, while for pressurized fluidized bed gasifiers the pressure of the system must also be considered.

Because of the rapid equalization of temperatures in fluidized beds,temperature control can be accomplished in a number of ways (189):

a) Feed flow. Control gas flow and/or solids feed rate so that the heat of reaction is removed as sensible heat in off gases and solids or heat supplied by gases or solids
b) Solids circulation. Remove or add heat by circulation of solids.
c) Gas circulation. Recycle gas through heat exchangers to cool or heat.
d) Liquid injection. Add volatile liquid so that the latent heat of evaporation equals excess energy.
e) Cooling or heating surfaces in bed.

The least complex (mechanically), highly reliable and with a fast response control method for the fluidized bed in consideration is the feed flow one.

8.7.2.2 Temperature control

The temperature of the bed must be maintained within the temperature range of 775-825 °C. Lower temperatures result in high concentrations of tar and pyroligneous hydrocarbons in the gas as well as char in the bed. Temperatures above 850 °C may sinter the bed material and decrease the lifetime of the reactor and the measuring instruments in the bed, while disturbing the operation of the process heaters.

The fluidized bed temperature is controlled by controlling the air/feedstock ratio and the uniformity of temperature within the fluidized bed is controlled by having an adequate space velocity through the reactor (by maintaining $U/U_{mf} \geq 2.5$ (see section 5.17). For a given set of operating conditions the feedstock flowrate is fixed, while the amount of air is varied to control and maintain the temperature. Air is selected as the variable parameter, since its flowrate can be changed more rapidly and accurately than that of the feedstock, providing a faster response.

However, since air is also a reactant of the gasification process, large and frequent variations will result in significant fluctuations of the gas composition. For a constant energy output from the gasifier, the gas composition must remain constant. Therefore, a set temperature point of 747 °C (the design temperature) will not be used ; instead the temperature of the bed is left to vary in the range of 775-825 °C without any interference from the operator. In case the temperature of the bed varies beyond the above limits, then the controller will undertake action to bring it back in the above range, by increasing or decreasing the air flowrate. Therefore, the control of the air flowrate is manual.

Two thermocouples, one in the center of the bed (0.5 m above distributor) and the other at 1 m above distributor are foreseen in the bed. Both the instantaneous temperature, as well as the rate of rise of temperature are measured and recorded for both thermocouples.

An alarm is provided which is activated in case the temperature difference measured by the two thermocouples exceeds 20 °C which indicates that either the bed has sintered or a hot spot has been created by uneven distribution of solids. The first response of the operator is to increase the air flowrate (in this case the effect is to increase the U/U_{mf} ratio) by about 10% in order to facilitate mixing. If the temperature difference remains the

same or increases and the pressure drop over the bed drops, this indicates bed agglomeration and/or sintering. The operator should then stop the feedstock feed but maintain the air flow in anticipation that the sinters will fall through the distributor. Care should be taken that the temperature does not exceed 900 °C, since then it is almost certain the bed will sinter. This is a critical situation, since the char hold up in the bed is combusted generating energy and raising the temperature of the bed. Thus, the operator should try to maintain fluidization as long as possible, but always below 900 °C. If indeed the temperature difference is eliminated, then the feedstock feed can be started again. Otherwise the reactor has to be shut down (see section 8.9). A third thermocouple is provided close to the outlet of the product gas. This temperature is measured and recorded.

8.7.2.3 Pressure measurements

The differential pressures below the distributor and in the freeboard are measured and recorded by pressure transdusers. The pressure drop over the bed is also derived from the above measurements and recorded separately.

8.7.3 Cyclone

The temperature of the cyclone is measured and recorded. The differential pressure at the outlet of the cyclone is also measured and record. The pressure drop over the cyclone is derived (by this measurement and the differential pressure of the freeboard) and recorded.

8.7.4 Air flow

The air flowrate is measured and recorded. A local control unit is provided for the air compressor.

8.7.5 Indicators

The temperature of the fluidized bed and the pressure drop over the bed and the cyclone are also indicated on the control panel.

8.7.6 Gas analysis

A gas chromatograph is provided for gas analyses. The specifications of the instrument are the same as those used for this work (see section 4.2.8), with the difference that the instrument is of industrial type and not analytical. Gas samples are taken and analysed every hour.

8.8 START UP AND SHUT DOWN PROCEDURES

8.8.1 Start up procedure

After checking that the feed hopper is full with feedstock and the fly ash receiver bin empty, the compressor is turned on and the air flowrate is set at its maximum. Then the preheating burner is turned on and the bed is left to heat up to 400 °C. At this temperature, intermittent feeding starts. The feeder runs for 5 minutes every 15 minutes (5 on, 10 off) until the temperature of the bed increases to 500 °C. Then the feeding rate is increased and the feeder runs for 10 minutes every 15 minutes (10 on, 5 off) until the temperature increases to 650 °C. Then the desired air flowrate is set on the flow controller and feeding is continuous while the screw for the removal of bed material is activated. The fluidized bed is left to reach steady state.

8.8.2 Shut down procedure

The screw for the removal of the bed is deactivated and the feedstock flowrate is stopped while the air feed is left on. Due to the combustion of the char hold up, the temperature rises and when it reaches 850 °C the air feed is stopped and water is sprayed on the bed surface. When the bed cools down to 800 °C, air is fed again to the reactor and the water supply is maintained until the temperature in the cyclone reaches 150 °C. Then the air feed is stopped to avoid steam condensation in the cyclone and the bed cools down by natural convection. the feeder of the fly ash bin is left on to empty the bin.

8.9 UTILITIES AND SERVICES

8.9.1 Utilities

The utilities required for the operation of the gasification plant are electrical power, water for cooling the reactor and compressed air for the control instruments (see section 8.8). The power requirements of the plant are listed in Table 8.15.

The utilities are readily available at the particle board plant and can be supplied to the gasification plant.

Table 8.15 : Power requirements

Unit	Power kW
Feeder	0.50
Spreader	0.05
Air compressor	11.20
Heater	0.07
Bed screw	0.05
Fly ash feeder	0.03
Total	11.90 kW

8.9.2 Services

The services required for the gasification plant are minimum since it is located in an existing plant.

Access to plant is existing since it would be built in a parking lot already being used by SPANO N.V. Since it is within the limits of the particle board plant security is provided. No building is required for the plant except for a control room. The control room can be a field cabin or can be constructed next to the plant.

An electrical substation is required for the power supply to the plant. Office space is available at the SPANO N.V. facilities and the administration of the gasification plant can be handled by SPANO N.V. Mechanical workshop and related facilities exist at SPANO N.V. and can also service the gasification plant.

One workman and one technician are required for the operation of the plant. The former for operating the fork-lift and supplying feedstock to the feeding hopper and the latter for the control room. Three shifts per day are required to run the plant. Supervision is provided by the technical manager of SPANO N.V.

8.10 HEALTH AND SAFETY CONSIDERATIONS

In this section the hazards of the gasification process are identified and safety measures are taken to provide the maximum protection for personnel with the minimum chance of accident. However, only hazards specific to the gasification plant are discussed, the other general ones such as work accidents due to falls, burns, injured limbs are common for all industrial plants and thus beyond the scope of the thesis.

8.10.1 Hazard analysis

The hazards specific to the gasification process are fire, explosion, poisoning and death from carbon monoxide and the effect of tar on humans.

8.10.2 Fire and explosion hazard elimination

Fire and explosion are associated with combustible gases, liquids and fine dust. For the gasification process the hazards are:

a) ignition fire and explosion of product gas
b) ignition fire and explosion of fly ash

These hazards can be eliminated by avoiding any product gas leaks to the environment. Since the operating pressure in the gasifier, cyclone and transfer pipe is above the ambient pressure, diffusive leaks of air are not possible. Product gas leaks can be addressed in the mechanical design phase, since gas can only leak out at joints and flanges if thermal stress has bent the equipment. This problem can be solved by designing and utilizing extra strong flanges and flexible joints at the manifolds of the fluidized bed and cyclone. A heavy duty pipe will be used to transport the product gas to the heaters. Moreover all electrical equipment on the feeders fluidized bed and cyclone are flame proof. Since static electrical charge can accumulate on the feeder fluidized bed and cyclone, these units are grounded.

In order to avoid explosion due to pressure built up in the fluidized bed (e.g. due to downstream blockage of the cyclone), a pressure relief valve and rapture disk is provided at the ceiling of the fluidized bed gasifier. The pressure relief valve will be activated at 0.098 bar.

The fly ash is emptied from the ash bin via the rotary feeder directly into a closed container in order to avoid any omissions of fly ash. The container has a capacity of 30 m^3, sufficient for at least 24 hours of operation. It is

replaced every day. During replacement the rotary feeder is stopped. The container is closed and is transported by truck to a sanitary landfill for industrial wastes.

With the above measures fire and explosion hazards are eliminated.

8.10.3 Carbon monoxide and tar

Carbon monoxide is a colourless, odourless, tasteless gas that is formed primarily through the incomplete combustion of carbonaceous fuel. The health effects of carbon monoxide are associated with its reaction with hemoglobin in the blood and its subsequent effects on the cardiovascular and central nervous system (298). Exposure to 100 ppm in air results in no poisoning; however, exposure at 500 ppm in air results in poisoning and consequently death. Commonly alarms are set in the range of 200-300 ppm.

Since the mechanical design addresses the problem of gas leaks, carbon monoxide is not a hazard under normal operating conditions. Care must nevertheless be taken during breakdowns, since no personnel may enter the reactor, cyclone, ash bin or transfer pipe without checking for carbon monoxide concentrations. This can be checked by taking gas samples and analysing them in the gas chromatograph or, more simply, by Drågger tubes which instantly give reliable concentrations of carbon monoxide. It has been reported that two technicians died during the CROW project of the University of Missouri Rolla, because they entered the feedstock hopper before checking for carbon monoxide (91).

Tar is thought to be carcinogenic and therefore any contact must be avoided. However this is a minor hazard, since the product gas is not cooled and hence tar does not condense. It can nevertheless be envisaged that tar may deposit on inner surfaces during start up and shut down. Personnel should avoid contact during breakdown and maintenance practices, by appropriate clothing and gloves.

It can be concluded that the gasification plant poses no major hazard to personnel or environment.

8.11 ECONOMIC ANALYSIS

Vyncke Warmtetechniek could not provide any information on the capital cost of the fluidized bed gasifier and related equipment. It is therefore necessary to use data from the literature for the economic analysis. Recently Bridgwater (288) carried out a survey of biomass gasifiers in view of worldwide markets. On the basis of the information provided by several gasifier fabricators he proposed a method by which the costs of the gasification plant can be determined.

8.11.1 Costs

8.11.1.1 Total capital cost

For relatively simple gasifier systems the total plant cost - from the gasifier feeding system to clean gas - is estimated by equation 8.14 (288).

$$£_{1985}\ \text{Capital Cost} = 260{,}000\ (\text{capacity MAF t/h})^{0.65} \qquad \text{equation 8.14}$$

where the capital cost is expressed in 1985 pounds sterling and the capacity in MAF basis.

8.11.1.2 Utilities

The average electricity costs of gasifiers was found equal to £ 0.114/GJ product gas. Since this value does not include the other utilities costs, it was proposed to use a value of £ 0.24/GJ. However, for the gasification plant of this case study the only utility consumed is electricity (the plant also needs oil for start up and cooling water for shut down); therefore a value of £ 0.114/GJ product gas will be used.

8.11.1.3 Maintenance

Yearly maintenance cost is usually estimated as a proportion of the gasifier capital cost. The mean maintenance cost was found to be 2.5% on the total plant cost basis. However, if only fluidized bed gasifiers are considered, then the yearly maintenance cost reduces to 1.9%. Therefore, this value will be used in the economic analysis.

8.11.1.4 Overheads

A fraction of 0.08 of the total plant cost is proposed to cover annual overheads (local tax, insurance) and all head office expences. Payroll overheads have been included in the labour cost.

8.11.1.5 Labour cost

Supervision is provided by the technical manager of SPANO N.V. free of charge. The cost per shift is ± 20,000/y. This includes the cost of two operators per shift. Three shift per day run the plant (plant runs only on week days).

8.11.1.6 Feedstock

SPANO N.V. was selling about half of the residues produced, while the other half had to be discharged. It is assumed that the cost of discharging this residues was equal to the income selling the other half. Thus, the cost of the feedstock for the gasification plant is zero. The results are summarized in Table 8.16.

Table 8.16 : Cost of gasification plant

Item	Recommendation (288)	Cost £
Total capital cost	$£_{1985}\,CC = 260{,}000\,G_{f\,MAF}^{0.65}$	517,104
Utilities	0.144/GJ	22,445
Maintenance	1.9% of CC	9,825
Overheads	8% of CC	41,368
Labour	20,000/shift, year	60,000

8.11.2 Product cost

In order to determine the product cost, the annual capital charges (ACC) are estimated (189). The annual capital charges are the initial plant cost (C)

annualized over the lifetime of the plant (t) at the interest rate (i). Thus, ACC is given by equation 8.15.

$$ACC = \frac{CC \times i}{1-(1+i)^{-t}} \qquad \text{equation 8.15}$$

The expected lifetime of the plant is 10 years, while the interest rate is 10%. The results are summarized in Table 8.17.

Table 8.17 : Product cost

Item	Cost in £
ACC	84,156
Utilities	22,445
Overhead	41,368
Maintenance	9,825
Labour	60,000
Total annual cost	217,794

Total gas output gasifier 44,194 GJ/h x 6000 = 265,164 GJ/h.
Product cost £ 0.82/GJ.

8.11.3 Pay back period

This value has to be compared to energy costs from natural gas at around £ 5.0/GJ. It has been recommended to consider a discount of about 25% as compensation for lower quality (299). Therefore the savings made by the installation of the gasification plant are:

Savings = 5 x 0.75 - 0.82 = £ 2.93/GJ
or on anual basis the savings are £ 776,930.

The payback period (P) is calculated by equation 8.15 (189).

$$P = \frac{CC}{RE} \qquad \text{equation 8.15}$$

where CC = the total plant capital cost

RE = the reveunes (or savings) minus the expenses.

for the case study, P = 0.92 years.

This is considered a good payback period. However, this method of estimating the economic feasibility of a project neglects the potential income after the costs have been regained.

8.11.4 Internal rate of return

This method of project economic feasibility is carried out on the basis of the actual value of the proceeds given by the following equation (189):

$$V = \left[\sum_{t=1}^{t=n} \frac{RE}{(1+i)^t}\right] - CC \qquad \text{equation 8.16}$$

where V = the actual value of the proceeds
t = the number of years
RE = the revenues minus the expenses
CC = total capital cost
n = number of years in which the plant will be amortized
i = interest rate

For gasification plants, it can be assumed that RE s constant, so that V becomes:

$$V = RE\left[\frac{1-(1+i)^{-t}}{i}\right] - CC \qquad \text{equation 8.17}$$

When V = 0, the project yields an interest of i per year. This interest rate is the internal rate of return. To obtain the correct value of i, an assumed value for i is taken and by iteration the best fitting for V = 0 is sought. If the rate of interest on the bank is lower than the internal rate of return, the project can be evaluated positive.

Substituting the appropriate values in equation 8.17, the iteration gives:

V = 0 for i = 105%

Thus the internal rate of return, IRR is 105% which is very high.

8.11.5 Benefits-costs ratio

The benefits-costs ratio (BCR) is a third method of evaluating the economic feasibility of a project. It is calculated by equation 8.18.

$$BCR = \frac{RE}{CC\left(\frac{1}{1-(1+i)^{-t}}\right)} \qquad \text{equation 8.18}$$

The more the BCR of a project is bigger than 1 or smaller than 1, the more the project is respectively appreciated or depreciated concerning the financial aspects. The benifits-costs ratio equals 1 when the value of i is equal to the internal rate of return.

For the case study BCR = 6.6 , hence the project is appreciated.

8.11.6 Sensitivity analysis

Using the case study as a base line, a sensitivity analysis was performed in which the main parameters were varied in turn. The product costs, payback time, internal rate of return and benifits-costs ratio were calculated each time. The results are summarized in Table 8.18.

Table 8.18 : Results of sensitivity analysis

Scenario		Product cost £/GJ	Payback period Y	IRR %	BCR
Case study		0.82	0.92	105	6 6
Lifetime years					
	5	1.02	1.13	84	3.3
	15	0.76	0.87	115	8.7
Interest rate %					
	8	0.79	0.90	112	7.4
	12	0.85	0.95	98	5.9
Operating hours					
h/y	4000	1.23	2.25	45	2.7
	8000	0.67	0.61	165	10.1
Fuel cost £/ton MAF					
	10	1.47	2.41	40	2.5
	15	1.79	12.10	-0.4	-0.5

The capacity of the gasifier was not varied, since it is related to the total energy requirements of the downstream plant. The shifts were not varied, since the operation of the particle board plant is continuous during week days. Project lifes of 5 and 15 years are considered as well as interest rates of 8 and 12%. The operating hours of the base case is 6000 h/y. The effect of higher (8000 h/y) and lower (4000 h/y) operating hours is investigated.

The feedstock cost of the base case is zero. Therefore feedstock costs of 10 and 15 £/tons MAF are considered.

8.11.7 Discussion

The results of the economic analysis indicate that the economics of the proposed gasification plant are very robust. Since the exact cost of the natural gas consumption at the heaters of SPANO N.V. are not known, it was necessary to use a recommended value of £ 5.0/GJ with a 25% discount. If the discount is not considered then the economics become even more attractive.

The strongest effect on total costs was due to the feedstock cost. With a price of £ 10/ton MAF, the gasification plant is still economically sound; however, with a price of £ 25/ton MAF, the process becomes uneconomic.
The length of the annual operating period also has a fairly large effect on the product cost and economics. Nevertheless, it would have to drop to below 2000 h/y before the gasification plant becomes uneconommic.
The effect of life time on the economics is not so profound and the process is still economically viable for a lifetime of 5 years.

The interest rate has a relatively small effect on the economics. The effect of the annual operating period and the cost of the feedstock on the product cost is shown respectively in Figures 8.12 and 8.13

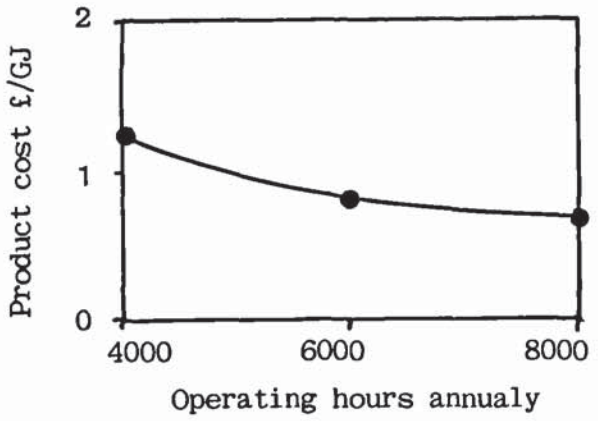

Figure 8.12: Effect of annual operating period on product cost.

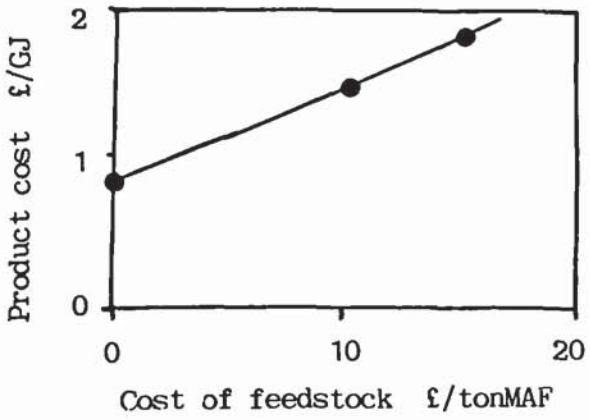

Figure 8.13: Effect of cost of feedstock on product cost

CHAPTER NINE : CONCLUSIONS

9.1 EXPERIMENTS

A fluidized bed process development unit was designed on the basis of a empirical procedure and afterwards constructed. The following conclusions are drawn from the experimental programme described and reported in section 4.5.2 and Chapter 5.

9.1.1 Original design procedure

The procedure by which the process development unit was designed proved adequate for the purpose of designing an experimental facility.

9.1.2 Peripheral equipment and apparatus

Except for the air compressor, the preheating burner and the heat exchanger of the gas sampling line, all other equipment (feeding system, product gas burner and cyclone of gas sampling line) failed in providing trouble free operation. For reliable industrial operation these equipment should be procured commercially from proven systems.

9.1.3 Operation of the fluidized bed

It was easy to operate and control the reactor and its response to the variations of the feedstock and air flowrates were predictable in terms of the operating temperature. No problems were encountered with the fluidized bed reactor.

9.1.4 Fluidization characteristics

In general there was good agreement between the design calculated values and the experimentally measured values of the various fluidization parameters (minimum fluidization velocity, pressure drop, mean particle size of sand).

9.1.5 Gas composition

Eight gas components were identified with concentrations higher than 0.1 Vol.%, namely hydrogen, oxygen, nitrogen, carbon monoxide, carbon dioxide, methane, ethene and ethane. The two last components, although only produced in small amounts, had a significant influence on the higher heating value of the gas, e.g. raising it from an expected 5.3 MJ/Nm^3 to 6.89 MJ/Nm^3.

The equilibrium composition of the water gas shift reaction was appreached only at bed temperatures higher than 900 °C.

9.1.6 Air factor

For reliable and continuous operation as well as for acceptable performance (higher heating values higher than 5 MJ/Nm^3, thermal efficiencies higher than 60%), the air factor should be in the range of 0.25-0.35.

The higher heating value of the gas and thermal efficiency increase at lower values of the air factor, while the gas yield decreases in terms of maximum output of energy. The optimum air factor is 0.3.

9.1.7 Higher heating value of product gas

In most of the experiments (18 out of 29) the higher heating value of the gas exceeded 5 MJ/Nm^3, while the most typical value was 5.5 MJ/Nm^3.

9.1.8 Efficiency

At realistic feedstock flowrates in excess of 160 kg/h (or about 60% of maximum design capacity) the expected efficiency (chemical energy in the gas/energy in the feedstock) is 61%. If the sensible heat of the gas could be recovered or utilized, the overall efficiency would increase to about 80%.

9.1.9 Gas yield

Under realistic operation (see section 8.1.8) the gas yield is expected to be in the range of 1.8 to 3 kg gas per kg feedstock (MAF), while a typical value is 2.6 kg gas per kg feedstock (MAF).

9.1.10 Bed temperature

In the temperature range of 775 to 825 °C satisfactory results in terms of gas composition and tar are expected.

9.1.11 Turn down ratio

The gasifier proved rather flexible since at turn down ratios of 1:3 similar values of the higher heating value of the gas were obtained. However, for industrial applications a turn down ratio of 1:2 is reasonable.

9.1.12 Operational stability

The fluidized bed attains equilibrium (indicated by an almost constant temperature) within about two hours, while for the freeboard about eight

hours are needed. The higher heating value of the gas does not change to any significant extent after two hours of operation.

9.1.13 Feedstock flowrate

Uniform and constant feedstock flowrate is an absolute necessity for stable operation.

9.1.14 Flame burn out

The flame burns out within half a minute from the termination of the feedstock supply to the reactor. The gas composition is very sensitive to uniform constant feedstock flowrate, while the gasification of char seems to be of secondary importance.

9.1.15 Retention time of gas

For industrial applications, acceptable retention times of 10 to 20 seconds are to be expected.

9.2 MASS AND ENERGY BALANCES

The mass and energy balance closures were within acceptable experimental limits. Typical values of total mass balance closures were in the range of 95-105%. The elemental mass balance closures were also satisfactory with average values in the range of 95-98%.

With good feedstock calibration, the unaccounted heat losses were about 9.5% after allowing 2-4% for reactor heat losses, typical figures for which are as high as 5-8%. Other sources suggest 29% as a typical heat loss for reactors of this type and size.

9.3 MODELLING AND DESIGN

It appeared that a comprehensive design procedure incorporating all the following aspects was missing from the literature:

a) a model to predict the performance of a fluidized bed gasifier,

b) a method of determining the fluidization parameters and characteristics for designing the fluidized bed, as well as,

c) a conceptual design of a fluidized bed gasification plant.

Two empirical models were developed by which the performance of fluidized bed gasifiers can be predicted. The first empirical model constant moisture, EMCM, was developed for feedstocks with 10-15 wt% moisture, while the second empirical model moisture, EMM, is for feedstocks with 15-50 wt% moisture. The EMCM is more reliable than the EMM since the latter was based on data from the literature. Feedstocks with moisture higher than 50 wt% must not be used in realistic applications unless dried.

9.4 Case study

The applicability of the design procedure was demonstrated in a case study for the construction of a fluidized bed gasifier to supply energy to two process heaters of an existing facility. For the supply of 44,194 MJ/h, 2888 kg/h MAF feedstock and 3874 Nm^3/h air are required. The process takes place at 800 °C and the higher heating value of the gas is 5.55 MJ/Nm^3, while the overall thermal efficiency is 86 %.

The economics of the process are very robust. On the basis of zero cost for the feedstock the product cost is 0.82 £/GJ and the pay back period is 0.92 years. A sensitivity analysis shows that the cost of feedstock has the strongest influence on the economics with the plant still being economically attractive at a feedstock cost of 10 £/ton MAF. The effect of the annual operating period also has a strong influence on the overall economics; however, the plant becomes uneconomic for annual operating period of less than 2000 h/y. The life time and interest rate have a less profound influence on the economics

CHAPTER TEN : RECOMMENDATIONS FOR FUTURE WORK

10.1 INTRODUCTION

The research results of this work provide a better understanding of fluidized bed air gasification of biomass and provide a frame work for future research in the system design and optimization of this subject. The following recommendations are made for extending and developing this work.

10.2 MOISTURE CONTENT OF FEEDSTOCK

During this work the moisture content was limited to the range of 10-14 wt%. Thus the effect of higher or lower moisture content on the performance of the gasifier needs further investigations. This would greatly improve the reliability of the EMM model developed in Chapter 6, since actual data could be incorporated in the model.

In order to achieve this, it is recommended to obtain fresh chopped wood which should have a moisture content in the range of 50-55 wt %. With this material about four experiments (at different air factors in the range of 0.2-0.5) should be carried out. Then fresh chopped wood should be air dried for several days at moisture contents of about 30 and 40 wt%. At each value of moisture content experiments should also be carried out at otherwise identical conditions as with the experiments with 50 wt% moisture content. All these experiments would supplement the data of this work and would provide sufficient information for the development of a reliable model.

10.3 PARTICLE SIZE OF FEEDSTOCK

Chopped wood was the only feedstock used. The usage of other feedstock with either bigger or smaller particle size and other types of biomass (e.g. wood pellets, rice husks, sawdust) in the fluidized bed would greatly extend and prove the applicability of this unit.

10.4 FEEDING POINT

In this reactor configuration the feeding was above the bed surface. To minimize carry over of light feedstock particles (e.g. sawdust), feeding below the surface of the bed should be tested. However, this is not possible with the present feeding system, since the gas leaks through it would be significant. Indeed with the feeding port in the bed, higher pressure at that point would exist, which would result in gas leaks.

10.5 BED HEIGHT

The static bed height during this work was 0.6 m. No other information was obtained concerning the influence of the bed height on the performance of the reactor.

A more shallow bed would decrease the pressure drop over the bed and hence the compression costs. However, a too shallow bed would result in incomplete fluidization, when the volume of the char bed would significantly exceed the volume of the sand, since char is non-homogeneous and difficult to fluidize. Alternatively, a higher bed can provide more intimate contact between the sand and the char and thus enhance the gasification process.

It is recommended that some experiments be repeated with static bed heights of 0.4 and 0.8 m to test whether any significant influence results. Information from this kind of experiments could also be incorporated in the design procedure, since the height of the bed would become also a design parameter. The designer would then have to select a bed height in accordance with the objectives of the gasification plant.

10.6 SEPARATION AND RECIRCULATION OF FLY ASH

The fly ash produced by the gasifier had a high carbon content (about 70%), which represents a loss of efficiency carbon conversion at about 6-10%. An improvement could be made by separating the fly ash and recirculated bark into the gasifier. For this purpose, the inlet point should be just above the distributor, in order to provide sufficient residence time for the fly ash in the bed for complete gasification.

Alternatively, in applications for direct combustion of the product gas, special gas burners can be chosen, which simultaneously can combust fine particles. With such a burner (300) the loss in carbon conversion efficiency would be balanced by the recuperation of the energy content of the fly ash in the gas burner.

10.7 DETAILED TEMPERATURE PROFILE

Only five thermocouples were used to record temperatures in the reactor. A more detailed temperature profile in and above the bed would prove whether the bed operates isothermally or whether cold and hot spots exist. It would also show whether the mixing of the feedstock is fast enough or whether non-isothermal operation is caused by one feeding port. To achieve this, it is

recommended that movable thermocouples be used under operation with and without feeding.

10.8 HEAT LOSSES THROUGH REACTOR WALLS

The calculated heat losses through the reactor walls of the process development unit are considered low. It is therefore recommended that experiments be carried out to measure them accurately. If the measured heat losses would be higher than the calculated ones, then this would improve the energy balance since the unaccounted heat losses would decrease.

10.9 GAS COMPOSITION PROFILE IN THE REACTOR

A profile of the gas composition in and above the bed would indicate whether the water gas shift reaction attains equilibrium and how this equilibrium is approached. It would also prove whether there is any significant difference of the gas composition, which could be attributed to the cracking of tars and continuing conversion of the fly ash in the freeboard.

It is recommended that a movable insulated water cooled probe (the probe must be water cooled in order to freeze the gas composition at the point of sampling) be used to sample gas from the reactor at various heights.

10.10 LONG DURATION EXPERIMENTS

In order to prove the reliability of the reactor as well as of the peripheral equipment, it is recommended that continuous tests of 1 day, 7 days and 30 days be carried out. These would enhance the understanding of the fluidized bed gasifier and identify possible operational problems. In order to carry out such tests, three shifts of technicians would be required as well as sufficient provisions of feedstock.

10.11 SAMPLING OF BED MATERIAL

The sampling of bed material would give information on the amount of char accumulated in the reactor as well as on the bulk density of the char and the char-sand mixture. Cold fluidization tests could then be carried out to determine the fluidization characteristics of the char-sand mixture. These can be different from the fluidization characteristics of sand, since a significant volume of the bed would consist of char which is larger and lighter than sand.

10.12 ENVIRONMENTAL CONSIDERATIONS

Tests should be made to determine the environmental impact assessment of the gasification process. Thus, it is recommended that the emissions of gaseous pollutants - such as cool nitrogen oxides, carbon monoxide, polychlorinated hydrocarbons et al. - be measured from the exhaust gases of an internal combustion engine or boiler. Similarly, the condensate of the gasifier should be analysed for pH, biological oxygen demand, chemical oxygen demand, phenols et al. Finally, if the fly ash is to be disposed off, an appropriate sanitary landfill for industrial wastes should be selected.

10.13 COMPLETE TREATMENT OF PRODUCT GAS

The results of this work are based on a small fraction of the product gas which was sampled. It is recommended to construct downstream equipment for the complete treatment of the product gas and to check whether any variations are produced with the results of this work.

10.14 CONTINUOUS REMOVAL AND REINJECTION OF BED

Certain feedstocks have a high ash and/or inert content (for example bark, rice husks). Since already provisions are available for bed removal, it is recommended to design and construct a bed separation and injection system and test this for satisfactory operation.

The bed material could be removed by an inclined screw (in order to avoid gas leaks) and transported to a screen. The oversize material should be rejected, while the undersize returned in the bed. This can be achieved with a simple screw feeder through one of the several openings of the reactor. This arrangement is shown in Figure 10.1. Gas leaks through this feeding system can be avoided by always maintaining a height of 1 m packed bed of sand. Dry sand is a free flowing material and no special considerations are necessary for the design of the hopper. The front end loader could be used to feed the hopper of the sand. In industrial applications this can be achieved either by a screw or bucked elevator.

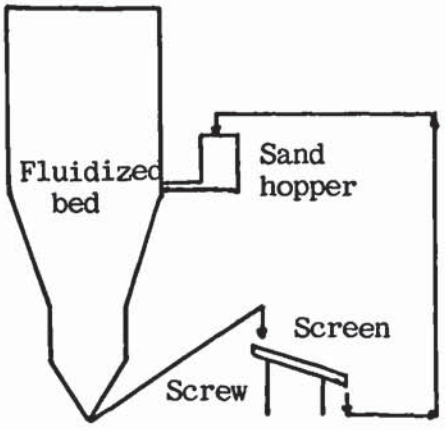

Figure 10.1 : Proposed arrangement for removal, screening and feeding the bed material.

10.15 ECONOMIC DATA

Detailed economic data are necessary for a more accurate economic analysis. It is recommended that informations about the cost of all components of the plant for different capacities be collected.

APPENDIX I - PUBLISHED ARTICLES

The following articles are considered as a relevant part of the thesis and support its argument.

1) J. Schoeters, K. Maniatis, A. Buekens, "fuel gas from agricultural residues in a fluidized bed reactor, Proceedings, 2nd World Congress of Chemical Engineering, Montreal, October 1981.

2) K. Maniatis, A. Buekens, "Practical experience in fluidized bed gasification of biomass", EPE, Revue Energie Primaire, No. 3-4, Vol. XVII, 1982.

3) K. Maniatis, J. Schoeters, A. Buekens", Experimental study of the gasification of Euphorbia Tirrucalli by means of oxygen-steam mixtures, Proceedings, 2nd International Producer Gas Conference, Bandung, March 1985.

References

1. L. WALDHEIM, E. RENSFELT

"Methanol from wood and peat" Proceedings, Biomass to methanol specialist workshop, ed. Reed T.B., SERI/CP-234-1590, 1982.

2. J.W. BLACK

"The pressurized fluidzed bed gasifier in the synthesis of methanol from wood" Ibid.

3. W.H. BLACKADDER, E. RENSFELT

"Synthesis gas from Wood and Peat - The Micro Process", Thermochemical Processing of biomass, Ed. A.V. Bridgwater, Butterworths, 1984.

4. R.S. BICKLE, A.J. EDWARDS, G. MOSS

"Development of the O_2 donor gasifier for conversion of wood to synthesis gas for eventual production of methanol", in Energy from biomass, Vol. 2 Reidel, Dordrecht, 1982.

5. J.P. BABU, M. ONINSCHK, G. KOJOWSKI

"Development of a pressurized fluidized bed biomass gasifier to produce substitute fuels", Proceedings, Fundamentals of thermochemical biomass conversion, Easter Park Colorado, 1983.

6. L. SCHRADER, E. NITSCHKE, H. WILL, A. BERLLIN

"Biomasses as feed for the Rheinbraun HTW-gasification process", Proceedings Energy from biomass and wastes VIII, IGT, Lake Buena Vista, 1984.

7. G. CHEVSOFAME, S.M. LEMASLE

Synthesis gas production from wood by oxygen gasification under pressure, Bio Energy by Coteborg Sweden, 1984.

8. A. STRUB

"The Commission of the European Communities R & D Programme "Energy from biomass", same as in (3).

9. D. KUNII, O. LEVENSPIEL

Fluidization engineering, Wiley, New York 1969.

10. M. GRABOWSKI

"Kinetics of char gasification Reactions, in A survey of biomass gasification", SERI, Golden Colorado April 1980.

11. VAN DER AARSEN et.al,

"Proceedings International Biomass Conversion", Golden, Colorado (1982).

12. DE GROOT, SHAFIZADEH, ibid.

13. EDRICH et.al., ibid.

14. BJERLE et.al.
Tech. Univ. of Lund, Publication 1360, 261, 1980.

15. J. SCHOETERS, K. MANIATIS, A. BUEKENS
"Fuel gas from Agricultural residues in a fluidized bed reactor", Proc. 2nd World Congress of Chemical Engineering, Montreal 1981.

16. A.W. COATS, RED FERN J.P.
Nature, 201, 4914, 1964, p. 68.

17. D. FUNG
"Application of fluid bed technology to the gasification of waste wood", Final report to ENFOR, project C-12, June 1980.

18. W.P. WALAWENDER, S. GANESAN, L.T. FAN
"Steam gasification of manure in a fluid bed - Influence of Limestone as a bed additive".
Energy from biomass and Wastes V, Florides, 1981.

19. M. DECLERCK et.al.
Peper to be presented at the IV IGT Conferences, Lake Buena Vista January 1985.

20. J. SCHOETERS, K. MANIATIS, A. BUEKENS
"Research Project, Kenia-Euphorbia", Final report to ABOS, June 1984.

21. W. COUSINS
"A theoretical study of wood gasification processes" New Zealand J. of Science, Vol. 21, 1978.

22. P. KOSKY AND J. FLOERS
"Global model for countercurrent coal gasifiers", Ind. Eng. Chem. Proc. Res. Dev. 19, 1978.

23. W. GUMZ
"Gas Producers and Blast Furnaces", J. Wiley and Sons Inc., New York, 1950.

24. E. RAMMLER
"Technologie und Chemie der Brounkoh leverwertung", 1962.

25. J. SCHOETERS
"The Fluidized bed gasification charcoal", Ph.D. Thesis, Vrije Universiteit Brussel, 1983.

26. K. MANIATIS, J. SCHOETERS, A. BUEKENS

"Gasification of Refuse derived fuel in a fluidized bed reactor", 6th ISWA Symposium, München, 1984.

27. R. GRAHAM, D. FUNG

"A review of biomass Gasification, The role of catlysis, Eastern, Forrest Products Laboratory, Report OPXZZIE, 1979.

28. D. MITCHELL et.al.

"Methane/Methanol by catalytic Gasification of biomass", CEP, 1980.

29. K. MANIATIS, A. BUEKENS

"Practical experience in fluidized bed gasification of biomass", 1st Producer gas conference, Colombo, Sri Lanka, 1982.

30. R. RAIMERT, P. MEHRLING, C. LINDNER

"Methanol from wood via Lurgi circulating fluidized bed gasification, same as (7).

APPENDIX II - DESIGN OF DISTRIBUTOR FOR THE PROCESS DEVELOPMENT UNIT

II.1 Introduction

The design of the distributor was based on the procedure outlined in section 3.3.2.2.

II.2 Calculation of the minimum pressure drop over the distributor

In fluidized bed reactors envisaged to operate under a certain turn down ratio, it must be ensured that even at the minimum operational gas flowrate the distribution of the gas will be equal across the cross sectional area of the bed. Therefore in the determination of the minimum pressure drop over the distributor, the minimum gas flowrate must be considered.

Assuming no preheating of the fluidizing gas, the pressure drop over the bed is given by equation II.1 (273) :

$$\Delta P_b = \rho_b \times h_b \qquad \text{equation II.1}$$

where ρ_b = bulk density of the bed
and h_b = height of the bed.

Assuming a bulk density of 1300 kg/m^3 for sand, which is a typical value (189), substitution in equation II.1 gives:

$$\Delta P_b = 780 \text{ kg/m}^2 = 78 \text{ cm } H_2O$$

Applying the first term of equation 3.5 (see section 3.3.2.2) as the limiting condition gives :

$$\Delta P_{d\,min} = 0.1 \times \Delta P_b = 7.8 \text{ cm } H_2O.$$

However, this value is well below the minimum acceptable recommended by equation 3.5, 35 cm H_2O.
Thus it was decided to apply the second term of equation 3.5 as the limiting condition;

$$\Delta P_{d\,min} = 35 \text{ cm } H_2O.$$

The third term of equation 3.5, 100 ΔP expansion into vessel, is rarely applied for two reasons: a) the expansion loss of circular and even conical inlets is very small and hence the rearrangement resistance of the gas is negligible; and b) in order to determine the pressure drop due to expansion into the vessel, the velocity of the gas in the orifice must be known (277):

$$\Delta P_{expansion} = \rho_g \frac{(U_{or} - U_v)^2}{2}$$ equation II. 2

or

$$\Delta P_{expansion} = \frac{\rho_g . U_{or}^2}{2} \left[1 - \frac{A_{or}}{A_v}\right]^2$$ equation II. 3

Where U_{or} = velocity of gas in the orifice
U_v = velocity in the vessel
A_v = cross sectional area of the vessel
ρ_g = density of gas
A_{or} = cross sectional area of the orifice

II. 3 Calculation of the Reynolds number for the total flow approaching the distributor.

The Reynolds number is given by equation II. 4 and it is a dimensionless group which characterizes the type of flow between laminar and turbulent (277).

$$Re = \frac{d_r \rho_g U_g}{\mu_g}$$ equation II. 4

where ρ_g = density of gas
μ_g = viscosity of gas
d_r = diameter of reactor
U_g = velocity of gas approaching the distributor

The Reynolds number is of vital importance in the study of fluid flow. Thus numerous relationships are based on this dimensionless group. This is also the case with the coefficient of discharge C_d for an orifice which is a function of the Reynolds number, see Figure II. 1 (36).

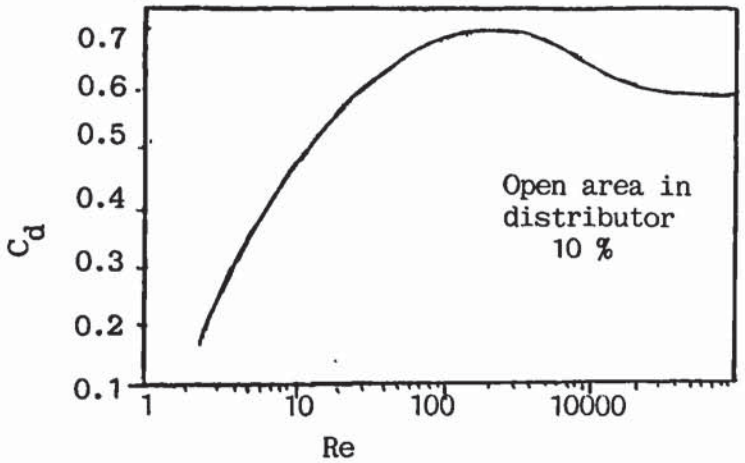

Figure II. 1 : Orifice coefficient versus Reynolds number based on diameter of approach chamber (36).

The orifice coefficient of discharge allows for the friction losses and besides the Reynolds number, it also depends on the roughness of the pipe walls, the exact shape of the orifice, the thickness of the orifice plate and the proximity of bends and valves (277). Thus, in order to determine the coefficient of discharge of the distributor orifices, the Reynolds number must be determined first.

Since efficient fluidization must be ensured at both maximum and minimum air flowrates, the limiting condition is the one at minimum air flowrate. Hence this value will be used in this calculation. By substitution of the following data at normal conditions (189),

$\rho_g = \rho_{air} = 1.293$ kg/Nm^3

$\mu_g = \mu_{air} = 1.8 \times 10^{-5}$ kg/m.s

$d_r = 0.8$ m

$$\text{and } U_o = \frac{Q_{air\ min}}{A_r} = \frac{88.3}{0.502 \times 3600} = 0.049 \text{ m/s}$$

where Q_{air} = minimum volumetric flowrate of air (Table 3.2)
A_r = cross sectional area of the reactor

equation II.4 gives:

Re = 2758

This value of Reynolds number corresponds (from Figure II. 1) to an orifice coefficient C_d of 0.6. It also indicates that the flow is in the transition range from laminar (usually Re < 2000) to turbulent (Re > 4000) flow (277).

II. 4 Calculation of the velocity of the gas through the orifices.

The velocity of the gas through the orifices of the distributor U_{or}, can be calculated at the approach density and temperature by applying equation II..5, (36) (see also equation 3.6, section 3.3.2 2)

$$U_{or} = C_d \left(\frac{2 g_c \Delta P_d}{\rho_g} \right)^{1/2} \qquad \text{equation II. 5}$$

where ρ_g = density of the gas = 1.293 $g/cm^3 \times 10^{-3}$
g_o = conversion factor = 980 $g.cm/g.(s)^2$
ΔP_d = pressure drop over distributor = 35 g/cm^2

Thus, U_{or} = 4359 cm/s = 43.95 m/s

The ratio of gas velocity upstream the distributor over gas velocity through the orifices (U_o/U_{or}) gives the fraction of open area in the distributor plate. This open area, an empirical parameter, signifies the total surface area of the orifices in relation to the surface area of the distributor and in normal applications it is less than 10 % in order to ensure sufficient pressure drop over the distributor. Thus:

$$\frac{U_o}{U_{or}} = \frac{0.049}{43.59} = 0.0011 \text{ or } 0.1\ \% \qquad \text{equation II. 6}$$

Hence the above limitation is met.

Orifices which are too small (<1 mm) are liable to become clogged, whereas those which are too large (> 5 mm) may cause an uneven distributon of gas (273). Taking in account these considerations and with previous experience where different distributors were tested at the laboratory pilot plant (278), the orifice diameter was chosen as 3 mm.

II. 5 Calculation of the number of orifices

The number of orifices per unit distributor area, Nor, can be calculated using equation II. 7 (36).

$$U_o = A_{or}.\ U_{or}.\ N_{or}. \qquad \text{equation II. 7}$$

where U_{or} = velocity of gas through orifice
U_o = velocity of gas approaching distributor
A_{or} = cross sectional area of orifice
N_{or} = number of orifices per unit area

rearranging equation II. 7 gives :

$$N_{or} = \frac{U_o}{A_{or}\, U_{or}} \qquad \text{equation II 8}$$

Substitution of the appropriate values in equation II. 8 gives :

$$N_{or} = \frac{0.048}{7\times10^{-6} \times 43.59} = 160/m^2$$

Hence, the distributor should be constructed with 160 orifices per square meter. Since an even distributon of gas has to be ensured all over the cross-sertional area of the bed, distributors are designed with the same cross-sectional area as the bed. The cross sectional area of the bed A_b under consideration is :

$$A_b = \frac{0.8^2\,\pi}{4} = 0.5027\ m^2 \qquad \text{equation II. 9}$$

The actual number of orifices can be determined by equation II.10

$$N_{or\cdot d} = N_{or} \times A_r \qquad \text{equation II 10}$$

where $N_{or\cdot d}$ is the actual number of orifices on the distributor. Thus,

$$N_{or\cdot d} = 160 \times 0.5027 = 80.4 \text{ or } 80 \text{ orifices}$$

However, this number of orifices was determined for the minimum flowrate of air (see section II.3). Thus, it is necessary to determine the pressure drop over the distributor of the maximum air flowrate as well, to ensure that it would be acceptable in terms of power consumption for the blower. The pressure drop and gas velocity are related according to equation II.11 (277) :

$$\Delta P \propto U^2 \qquad \text{equation II.11}$$

for two different gas velocities under identical flow conditions equation II. 11 becomes :

$$\frac{\Delta P_1}{\Delta P_2} = \frac{(U_1)^2}{(U_2)^2} \qquad \text{equation II.12}$$

or

$$\Delta P_2 = \Delta P_1 \frac{(U_2)^2}{(U_1)^2} \qquad \text{equation II.13}$$

Substituting the appropriate values in equation II.13 with subscript 1 denoting minimum air flowrate and 2 maximum air flowrate, the following result is obtained :

$$\Delta P_{max.} = \Delta P_{min.} \times 3^2$$
$$= 35 \times 9$$
$$= 315 \text{ cm } H_2O$$

II. 6 Discussion

This pressure drop over the distributor at maximum air flowrate is extremely high for the size of the reactor and the compression costs would also be relatively high. Since the reactor would rarely operate at the minimum air flowrate ,but mostly at the maximum air flowrate, it was unreasonable to accept such a high pressure drop. It was therefore decided to overrule the condition of $\Delta P_{d\,min} = 35$ cm H_2O and use instead the first terms of equation 3.5, increased by a factor of two.
Thus equation II.13 was used :

$$\Delta P_{d\,min} = 2 \times 0.1\ \Delta P_b \qquad \text{equation II.13}$$

Using this equation and proceeding as described above the following results are obtained :

$\Delta P_d = 15.6$ cm H_2O (from equation II. 14)

$U_{or} = 29.44$ m/s (from equation II. 5)

$N_{or} = 240$ (from equation II. 8)
and
$N_{or.d} = 120.6 \approx 120$ (from equation II. 10)

Applying once more equation II.13 for the determination of the pressure drop over the distributor at the maximum air flowrate, the following result is obtained :

$\Delta P_d = 140.4$ cm H_2O

This is an acceptable value of pressure drop over the distributor and ensures a good gas distribution over the cross sectional area of the bed. At this condition, the velocity of the gas passing through the orifice is :

$U_{or} = 88$ m/s

II. 7 Conclusions

As demonstrated above, the design of distributors, being the most important component of a fluidized bed, is extremely empirical. The designer is relatively free to select the pressure drop over the distributor as long as equal distribution of gas is achieved, subject to constrains of power consumption for the blower. Thus the relatively arbitrary character of equation II.13 is justified in terms of the basis of design, being a fluidized bed capable of operating with a turn down ratio of 1 : 3.

However, if the basis of design had been either the minimum or the maximum air flowrate only, then equation II.13 would not be justified and the design should follow equation 3.5 (see section 3.3.2.2).

APPENDIX III - DESIGN OF CYCLONE

Cyclone separators are the most widely used type of dust collection equipment. The dust-laden gas enters a cylindrical or conical chamber tangentially and leaves through a central opening. The dust particles, by virtue of their inertia, will tend to move towards the outside wall from which they are led to a receiver. A cyclone is essentially a settling chamber in which gravitational acceleration is replaced by centrifugal acceleration

Cyclones have been employed to remove solids and liquids from gases at temperatures as high as 1000 °C and pressures as high as 500 atm. (189). Cyclones for removing solids from gases are generally applicable when particles of over 5×10^{-6} m are involved.

Although several attempts have been made to design cyclones from fundamental considerations, none has proved satisfactory and their design is largely empirical.

The design of the cyclone used in the sampling gas line was made on basis of an empirical procedure (189). An inlet velocity of 15.2 m/s is recommended. The design is based on this value, the volumetric flowrate of the gas at actual conditions and the diameter of the cylindrical section of the cyclone. The empirical equations shown in Figure III.1 are applied to determine the various dimensions.

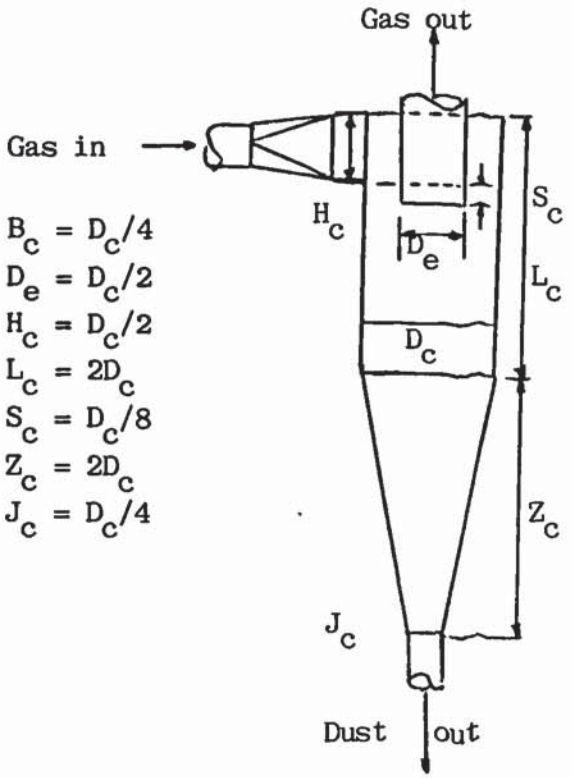

Figure III.1 : Cyclone separator and design proportions

The cyclone was designed for a volumetric gas flowrate of 15 m^3/h at ambient conditions. Thus, considering the recommended inlet velocity and the volumetric gas flowrate, the area of the rectangular inlet duct, A_d, can be found :

$$A_d = \frac{\text{Gas flowrate}}{\text{Gas inlet velocity}} \qquad \text{equation III.1}$$

An operating temperature of 800 °C was assumed. Thus the gas flowrate at operating temperature is :

$$\text{Gas flowrate} = 15 \times \frac{(273 + 800)}{273} \qquad \text{equation III.2}$$

$$= 58.96\ m^3/h = 0.016\ m^3/s$$

Substituting in equation III.1 gives:

$$A_d = \frac{0.016}{15.2} = 0.0011\ m^2$$

By combining equation III.3 and III.5 (see Figure III.1), the cyclone diameter can be determined :

$$A_d = 0.25\ Dc \times 0.5\ D_c$$
$$\text{or} \quad A_d = 0.125\ Dc^2$$
$$\text{or} \quad 0.0011 = 0.125\ D_c^2$$
$$\text{and} \quad D_c = 0.094\ m$$

Substituting this value for D_c in equations III.3 to III.9 the dimensions of the cyclone can be determined. Thus :

$B_c = 0.024\ m$
$D_e = 0.047\ m$
$H_c = 0.047\ m$
$L_c = 0.188\ m$
$S_c = 0.012\ m$
$Z_c = 0.188\ m$
$J_c = 0.024\ m$

The cyclone was constructed by mild steel plate.

APPENDIX IV - CALCULATION OF MASS AND ENERGY BALANCE FOR RUN 38

IV.1 EXPERIMENTAL DATA

IV.1.1. Mass and volumetric flowrates

Air flowrate	=	333.70 Nm^3/h.
Feed flowrate	=	340.00 kg/h.
Condensate flowrate	=	1.36 kg/h.
Fly ash flowrate	=	0.48 kg/h.
Ambient temperature	=	10.00 °C
Ambient pressure	=	1.00 bar.
Flowrate gas samping line	=	13.54 kg/h.

IV.1.2. Feedstock properties

Ash content	=	1.60 wt%.
Moisture content	=	12.00 wt%.
Higher heating value	=	4300.00 kcal/kg.
Elemental analysis	=	C = 45.3 wt%
		H = 5.8 wt%
		O = 48.8 wt%
		N = 0.1 wt%

IV.1.3. Experimental temperatures

Average bed temperature	=	865 °C
Inlet air temperature	=	69 °C
Exit gas temperature	=	775 °C
Freeboard temperature	=	852 °C

IV.1.4. Composition of fly ash and condensate

Carbon content fly ash	=	70 wt%
Tars in condensate	=	0.013 kg C/kg condensate

Note: All other data were taken from the literature (189).

IV.2. PRODUCT GAS COMPOSITION DETERMINED BY GAS CHROMATOGRAPHY

Component	wt.%	Vol.%
H_2	0.72	9.86
O_2	1.57	1.35
N_2	46.80	48.13

CH_4	3.05	5.25
CO	16.41	16.18
CO_2	26.85	16.76
C_2H_4	2.07	2.02
C_2H_6	0.35	0.32
C_3H_6	0.19	0.12

IV.3. CALCULATION OF SPECIFIC WEIGHT OF PRODUCT GAS

ρ_{gas} = H_2vol.% x 0.0899 + O_2vol..% x 1.429 + N_2vol.% x 1.251 + CH_4vol.% x 0.718 + CO vol.% x 1.251 + CO_2vol.% x 1.977 + C_2H_4vol.% x 1.261 + C_2H_6vol.% x 1.357 + C_3H_6vol %x 1.877

= 0.099 x 0.0899 + 0.014 x 1.429 + 0.481 x 1.251 + 0.053 x 0.718 + 0.162 x 1.251 + 0.168 x 1.977 + 0.020 x 1.261 + 0.003 x 1.357 + 0.001 x 1.251

= 1.234 kg/Nm^3

IV.4. CALCULATION OF HIGHER HEATING VALUE OF PRODUCT GAS

HHV = H_2wt% x 141.8 + CH_4wt% x 55.5 + COwt% x 10.11 + C_2H_4wt% x 50.3 + C_2H_6wt% x 51.87 + C_3H_6wt% x 48.92

= 0.007 x 141.8 + 0.03 x 55.5 + 0.164 x 10.11 + 0.021 x 50.3 + 0.004 x 51.87 + 0.002 x 48.92

= 5.68 MJ/kg

HHV = 5.68 x 1.234 = 7.01 MJ/Nm^3.

IV.5. MASS BALANCE

IV.5.1 Input flowrate

Note: Q represents volumetric flow, G represents mass flow.

Mass air flowrate = $Q_{air} \times \rho_{air}$

= 333.70 x 1.293 = 431.47 kg/h.

Feed flowrate = 340.00 kg/h

Total input flowrate = $G_{air} + G_{feed}$ =

431.47 + 340.00 = 771.47 kg/h.

IV.5.2 Ash, moisture and elemental input flowrates

Ash flowrate $G_A = G_{feed} \times \frac{A.C}{100}$

= 340 x 0.016 = 5.44 kg/h

Moisture flowrate $G_M = G_{feed} \times \frac{M.C}{100}$

$= 340 \times 0.12 = 40.8$ kg/h

Feed (MAF) flowrate $= G_{feed} - G_M - G_A$

$= 340 - 40.8 - 5.44 = 293.76$ kg/h

$$O_{input} = G_{air} \times \frac{23.3}{100} + G_{feed\ MAF} \times \frac{O wt\%}{100} + G_M \times \frac{16}{18}$$

$$= 431.47 \times 0.233 + 293.76 \times 0.488 + 40.8 \times \frac{16}{18}$$

$= 100.53 + 143.35 + 36.27$

$= 280.15$ kg/h.

$$N_{input} = G_{air} \times \frac{76.7}{100} + G_{feed\ (MAF)} \times \frac{N wt\%}{100}$$

$= 431.47 \times 0.767 + 293.76 \times 0.0001$

$= 330.94 + 0.03$

$= 330.97$ kg/h.

$$C_{input} = G_{feed\ (MAF)} \times \frac{C wt\%}{100}$$

$= 293.76 \times 0.453$

$= 133.07$ kg/h

$$H_{input} = G_{feed(MAF)} \times \frac{H wt\%}{100} + G_M \times \frac{2}{18}$$

$$= 293.76 \times 0.058 + 40.8 \times \frac{2}{18}$$

$= 17.04 + 4.53$

$= 21.57$ kg/h

IV.5.3 Output flowrates

$$\text{Total gas flowrate} = \frac{\text{total } N_{input}}{N_2 wt\% \text{ in gas}} \times 100$$

$$= \frac{330.97}{48.8} \times 100$$

$= 678.22$ kg/h

H_2 flowrate $= \text{total gas flowrate} \times \frac{H_2 wt\%}{100}$

$= 678.22 \times 0.0072$

$= 4.88$ kg/h.

Similarly

O_2	flowrate	= 10.64 kg/h
N_2	flowrate	= 330.97 kg/h
CH_4	flowrate	= 20.71 kg/h
CO	flowrate	= 111.29 kg/h
CO_2	flowrate	= 182.10 kg/h
C_2H_4	flowrate	= 14.03 kg/h
C_2H_6	flowrate	= 2.37 kg/h
C_3H_6	flowrate	= 1.28 kg/h

Total condensate flowrate $= \frac{\text{total gas flowrate}}{\text{sampling line gas flowrate}} \times$ condensate flowrate

$$G_{con} = \frac{678.22}{13.54} \times 1.3 = 65.10 \text{ kg/h}$$

Similarly

Total fly ash flowrate $= G_{fa} = \frac{678.22}{13.54} \times 0.48 = 24.04$ kg/h

Total output $= G_{gas} + G_{con} + G_{fa}$

$= 678.22 + 65.10 + 24.04$

$= 767.36$ kg/h.

IV.5.4 Elemental and ash output flowrates

$$O_{output} = G_{O2} + G_{CO} \times \frac{16}{28} + G_{CO2} \times \frac{32}{44} + (G_{con} - G_{C,con}) \times \frac{16}{18}$$

$$= 10.64 + 111.29 \times \frac{16}{28} + 182.10 \times \frac{32}{44} + 65.10 - (0.013 \times 65.10) \times \frac{16}{18}$$

$= 263.62$ kg/h

$N_{output} = G_{N2} = 330.97$ kg/h

$$C_{output} = G_{CH4} \times \frac{12}{16} + G_{CO} \times \frac{12}{28} + G_{CO_2} \times \frac{12}{44} + G_{C2H4} \times \frac{24}{28}$$

$$+ G_{C2H6} \times \frac{24}{30} + G_{C3H6} \times \frac{36}{42} + G_{fl} \times Cwt\% \times \frac{G_{con}}{100} \times 0.013$$

$$= 20.71 \times \frac{12}{16} + 111.29 \times \frac{12}{28} + 182.10 \times \frac{12}{44} + 14.03 \times \frac{24}{28}$$

$$+ 2.37 \times \frac{24}{30} + 1.28 \times \frac{36}{42} + 24.04 \times \frac{70}{100} + 65.10 \times 0.013$$

$$= 145.63 \text{ kg/h}$$

$$H_{output} = GH_2 + G_{CH4} \times \frac{4}{16} + G_{C2H4} \times \frac{4}{28} + G_{C2H6} \times \frac{6}{30} +$$

$$G_{C3H6} \times \frac{6}{42} + (G_{con} - G_{C,con}) \times \frac{2}{18}$$

$$= 4.88 + 20.71 \times \frac{4}{16} + 14.03 \times \frac{4}{28} + 2.37 \times \frac{6}{30} + 1.28 \times \frac{6}{42}$$

$$+ (65.10 - 0.85) \frac{2}{18}$$

$$= 19.93 \text{ kg/h}$$

$$Ash_{output} = G_{fl} \times \frac{100 - Cwt\%}{100}$$

$$= 24.04 \times 0.3 = 7.21 \text{ kg/h.}$$

IV.5.5 Balance

$$\text{Total} = \frac{\text{total output flowrate}}{\text{total input flowrate}} \times 100 = 99.46$$

$$O_{balance} = \frac{263.62}{280.15} \times 100 = 94.10$$

$$N_{balance} = \frac{330.97}{330.97} \times 100.00 = 100.00$$

$$C_{balance} = \frac{145.63}{133.07} \times 100 = 109.43$$

$$H_{balance} = \frac{19.93}{21.57} \times 100 = 92.40$$

IV.6. ENERGY BALANCE

IV.6.1 Input

Sensible heat in air = $G_{air} \times C_{pair} \times (T_{inlet} - 20)$
where C_p = mean heat capacity, KJ/kg °C

$H_{S,air}$ = (431,47 x 1.09 x (69-20))/1000
= 23.04 MJ/h

Energy in feedstock = $G_{feedMAF} \times HHV_{feed}$
= (293.76 x 4300 x 4.189))1000
= 5291.41 MJ/h

Total input = Energy in feedstock + sensible heat in air
= 5291.41 + 23.04 = 5314.46 MJ/h.

IV.6.2 Output

Sensible heat in gas = $G_i \times C_{Pi} \times (T_e-20)/1000$
= (G_{H2} x 14.86 + G_{02} x 1.02 + G_{N2} x 1.11 + G_{CH4} x 3.74 +
G_{CO} x 1.12 + G_{CO2} x 1.11 + G_{C2H4} x 2.81 + G_{C2H6} x 3.35 +
+ G_{C3H6} x 2.80) x (T_e-20)/1000
= (4.88 x 14.86 + 10.64 x 1.02 + 330.97 x 1.11 + 20.71 x 3.74 +
111.29 x 1.12 + 182.10 x 1.11 + 14.03 x 2.81 + 2.37 x 3.35 +
1.28 x 2.8) x (775-20)/1000
= 683.73 MJ/h

Sensible and latent heat in steam = $G_{con} \times C_{P,H20,l} \times (100-20)$
+ $G_{con} \times C_{P,H20,g} \times (T_e-100) + G_{con} \times L_{H20}$
= (65.1 x 4.19 x 80 + 65.1 x 2.09 x 6.75)/1000 + 6.51 x 2.26
= 260.92 MJ/h

Sensible heat in fly ash = $G_{fa} \times C_{Pfa} \times (T_e-20)/1000$
= 24.04 x 0.94 x 755/1000
= 17.06 MJ/h

$$\text{Heat loss reactor walls} = \frac{(T_f-20) \times S_f \times K_f}{d_o} +$$

$$+ \frac{(T_b-20) \times S_b \times K_b}{d_o} + \frac{(T_o-20) \times S_c}{K_c}$$

where T_i = temperature of freeboard
S_i = surface
ki = heat transfer coefficient
d_o = outside diameter
i = f freeboard
b bed
o outlet
c ceiling of reactor
R = thermal resistance

$$H_1 = \frac{(852 + 775)/2 - 20 \times 15.33 \times 0.6313}{1.6} + \frac{(865 - 20) \times 6.28 \times 0.3125}{1.6}$$

$$+ \frac{(775-20) \times 1.13}{1.0144} \times 4$$

$$= (4799.6 + 1036.4 + 841.0) \times 4$$
$$= 26708 \text{ kcal/h}$$
$$= 111.88 \text{ MJ/h}$$

Energy in gas $= G_{gas} \times HHV_{gas}$
$= 678.22 \times 5.68$
$= 3852.28$ MJ/h

Energy in tar and fly ash $= G_{tar} \times HHV_{tar} + G_{fa} \times HHV_{fa}$
$= 0.85 \times 23.3 + 16.83 \times 32.81$
$= 19.8 + 552.2$
$= 572$ MJ/h.

Total output = sensible heat in gas + sensible and latent heat in steam
+ sensible heat in fly ash + heat loss reactor walls +
+ energy in gas + energy in tar and fly ash
$= 683.73 + 113.81 + 17.06 + 260.92 + 3852.28 + 572$
$= 5499.8$ MJ/h

Unaccounted heat loss = Total input - Total output
$= 5314.46 - 5499.8$
$= 185.34$

Balance $= \frac{\text{Total output}}{\text{Total input}} \times 100 = 103.48.$

APPENDIX V - COMPUTER PRINT OUTS

In this Appendix the computer print outs of the results of runs 13-38 are presented. These include the gas composition and calorific value, the reaction parameters and temperature profile in the fluidized bed and the mass and energy balances.

MATERIAL :CH WOOD R13 DATE :6/5/82 NUMBER :11-14

ASH CONTENT = 1.00WT %
MOISTURE CONTENT = 12.00WT %
HIGHER HEATING VALUE = 4300.0KCAL/KG

GAS COMPOSITION

	WEIGHT %	VOLUME %
H2	0.26	3.82
O2	0.00	0.00
N2	64.23	67.24
CH4	1.52	2.78
CO	9.03	9.45
CO2	24.46	16.20
C2H4	0.42	0.43
C2H6	0.07	0.07
C3H6	0.00	0.00
C4H6	0.00	0.00

METHANE RATIO = 1.13 HYDROGEN RATIO = 1.11

HIGHER HEATING VALUE

2.38	MJ/KG	568.2	KCAL/KG
3.11	MJ/NM3	744.1	KCAL/NM3

LOWER HEATING VALUE

2.22	MJ/KG	530.7	KCAL/KG
2.91	MJ/NM3	696.0	KCAL/NM3

SPECIFIC WEIGHT = 1.310 KG/NM3

AIR FACTOR "S"= 0.532

REACTION PARAMETERS

FLOWRATE AIR (NM3/HR; 0 C,1ATM)=	143.00
AIR PRESSURE (BAR REL) =	0.30
FLOWRATE OXYGEN (NM3/HR) =	0.00
OXYGEN PRESSURE (BAR REL) =	0.00
FLOWRATE STEAM (KG/HR) =	0.00
FLOWRATE SOLIDS (KG/HR) =	78.00
FLOWRATE NITROGEN (L/HR)	0.00
AMBIENT TEMPERATURE (C) =	10.00
FLOWRATE CONDENSATE (KG/HR) =	2.00
FLOWRATE FLY ASH (KG/HR) =	0.27
FLOWRATE CHAR (KG/HR) =	0.00
AMBIENT PRESSURE (BAR) =	1.00

TEMPERATURES

REACTOR TEMPERATURE =	860 C
TEMPERATURE PREHEATER =	0 C
TEMPERATURE INLET GAS =	47 C
T11 =	845 C
T10 =	883 C
T9 =	863 C
T5 =	696 C

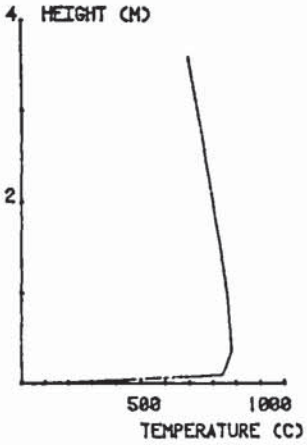

	KG/HR	C KG/HR	H KG/HR	O KG/HR	N KG/HR	ASH KG/HR
AIR	184.96	0.00	0.00	43.10	141.86	0.00
OXYGEN	0.00	0.00	0.00	0.00	0.00	0.00
NITROGEN	0.00	0.00	0.00	0.00	0.00	0.00
STEAM	0.00	0.00	0.00	0.00	0.00	0.00
SOLIDS MAF	67.99	30.53	3.91	32.30	0.01	0.00
MOISTURE	9.36	0.00	1.04	8.32	0.00	0.00
ASH	1.25	0.00	0.00	0.00	0.00	1.25
TOTAL	263.6	30.53	4.95	84.30	141.89	1.25
TOTAL GAS	228.89	0.00	0.00	0.00	0.00	0.00
H2	0.58	0.00	0.58	0.00	0.00	0.00
O2	0.00	0.00	0.00	0.00	0.00	0.00
N2	141.89	0.00	0.00	0.00	141.89	0.00
CH4	3.36	2.52	0.84	0.00	0.00	0.00
CO	18.94	8.56	0.00	11.39	0.00	0.00
CO2	54.04	14.75	0.00	39.28	0.00	0.00
C2H4	0.93	0.79	0.13	0.00	0.00	0.00
C2H6	0.16	0.13	0.03	0.00	0.00	0.00
C3H6	0.00	0.00	0.00	0.00	0.00	0.00
C4H6	0.00	0.00	0.00	0.00	0.00	0.00
CONDENSATE	40.07	0.52	4.44	35.11	0.00	0.00
FLY ASH	3.00	2.67	0.00	0.00	0.00	1.20
CHAR	0.00	0.00	0.00	0.00	0.00	0.00
TOTAL	264.83	29.94	6.03	85.78	141.89	1.198
BALANCE	100.4	98.07	121.67	101.75	100.00	95.984

TARS IN COND= 0.58 TARS IN GAS= 0.09KG/KG

THERMAL EFFICIENCY = 43.91 %

Y=3.28
X=0.59

THERMAL BALANCE

HEAT OF REACTION (MJ/KG)	11.57	MJ/KG
IN		
SENSIBLE HEAT IN GAS	5.44	MJ/H
SENSIBLE & LATENT HEAT IN STEAM	0.00	MJ/H
HEAT IN FEEDSTOCK	1213.91	MJ/H
TOTAL IN	1219.36	MJ/H
OUT		
SENSIBLE HEAT IN GAS	178.58	MJ/H
SENSIBLE & LATENT HEAT IN STEAM	153.91	MJ/H
SENSIBLE HEAT IN FLY ASH	2.46	MJ/H
SENSIBLE HEAT IN CHAR	0.00	MJ/H
HEAT LOSS REACTOR WALLS	106.35	MJ/H
ENERGY IN GAS	525.35	MJ/H
ENERGY IN TARS & FLY ASH	101.06	MJ/H
TOTAL OUT	1067.68	MJ/H
HEAT LOSS (BY DIFFERENCE)	151.66	MJ/H

% HEAT LOSS HV1 = 10.796 %

MATERIAL :CH WOOD R14 DATE :6/5/82 NUMBER :AVER

ASH CONTENT = 1.60WT %
MOISTURE CONTENT = 12.00WT %
HIGHER HEATING VALUE = 4300.0KCAL/KG

GAS COMPOSITION

	WEIGHT %	VOLUME %
H2	0.31	4.47
O2	0.00	0.00
N2	58.69	60.74
CH4	2.33	4.20
CO	13.24	13.71
CO2	24.80	16.24
C2H4	0.52	0.53
C2H6	0.11	0.11
C3H6	0.00	0.00
C4H6	0.00	0.00

METHANE RATIO = 0.06 HYDROGEN RATIO = 0.06

HIGHER HEATING VALUE

3.39	MJ/KG	809.9	KCAL/KG
4.39	MJ/NM3	1048.6	KCAL/NM3

LOWER HEATING VALUE

3.17	MJ/KG	758.1	KCAL/KG
4.11	MJ/NM3	981.6	KCAL/NM3

SPECIFIC WEIGHT = 1.295 KG/NM3

AIR FACTOR "S"= 0.379

REACTION PARAMETERS

FLOWRATE AIR (NM3/HR; 0 C,1ATM)=	101.72
AIR PRESSURE (BAR REL) =	0.35
FLOWRATE OXYGEN (NM3/HR) =	0.00
OXYGEN PRESSURE (BAR REL) =	0.00
FLOWRATE STEAM (KG/HR) =	0.00
FLOWRATE SOLIDS (KG/HR) =	76.00
FLOWRATE NITROGEN (L/HR)	0.00
AMBIENT TEMPERATURE (C) =	10.00
FLOWRATE CONDENSATE (KG/HR) =	2.00
FLOWRATE FLY ASH (KG/HR) =	0.27
FLOWRATE CHAR (KG/HR) =	0.00
AMBIENT PRESSURE (BAR) =	1.00

TEMPERATURES

REACTOR TEMPERATURE =	774 C
TEMPERATURE PREHEATER =	0 C
TEMPERATURE INLET GAS =	39 C
T11 = 739 C	
T10 = 811 C	
T9 = 773 C	
T5 = 678 C	

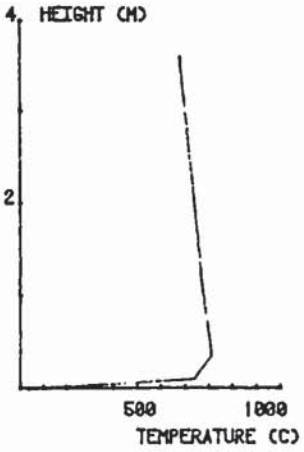

	KG/HR	C KG/HR	H KG/HR	O KG/HR	N KG/HR	ASH KG/HR
AIR	131.52	0.00	0.00	30.64	100.88	0.00
OXYGEN	0.00	0.00	0.00	0.00	0.00	0.00
NITROGEN	0.00	0.00	0.00	0.00	0.00	0.00
STEAM	0.00	0.00	0.00	0.00	0.00	0.00
SOLIDS MAF	67.39	30.53	3.91	32.68	0.01	0.00
MOISTURE	9.36	0.00	1.04	8.32	0.00	0.00
ASH	1.25	0.00	0.00	0.00	0.00	1.25
TOTAL	209.5	30.53	4.95	71.84	100.88	1.25
TOTAL GAS	171.91	0.00	0.00	0.00	0.00	0.00
H2	0.53	0.00	0.53	0.00	0.00	0.00
O2	0.00	0.00	0.00	0.00	0.00	0.00
N2	100.88	0.00	0.00	0.00	100.88	0.00
CH4	4.00	3.00	1.00	0.00	0.00	0.00
CO	22.77	9.77	0.00	13.00	0.00	0.00
CO2	42.64	11.64	0.00	31.00	0.00	0.00
C2H4	0.89	0.76	0.13	0.00	0.00	0.00
C2H6	0.20	0.16	0.04	0.00	0.00	0.00
C3H6	0.00	0.00	0.00	0.00	0.00	0.00
C4H6	0.00	0.00	0.00	0.00	0.00	0.00
CONDENSATE	31.46	0.41	3.49	27.56	0.00	0.00
FLY ASH	2.97	2.85	0.00	0.00	0.00	0.92
CHAR	0.00	0.00	0.00	0.00	0.00	0.00
TOTAL	286.34	27.78	5.19	71.56	100.88	0.921
BALANCE	98.5	91.01	104.90	99.60	100.00	73.775

TARS IN COND= 0.46 TARS IN GAS= 0.10KG/KG

THERMAL EFFICIENCY = 48.04 %

Y=2.55
X=0.47

THERMAL BALANCE

HEAT OF REACTION (MJ/KG)	18.07	MJ/KG
IN		
SENSIBLE HEAT IN GAS	2.72	MJ/H
SENSIBLE & LATENT HEAT IN STEAM	0.00	MJ/H
HEAT IN FEEDSTOCK	1213.91	MJ/H
TOTAL IN	1216.64	MJ/H
OUT		
SENSIBLE HEAT IN GAS	138.74	MJ/H
SENSIBLE & LATENT HEAT IN STEAM	119.65	MJ/H
SENSIBLE HEAT IN FLY ASH	1.64	MJ/H
SENSIBLE HEAT IN CHAR	0.00	MJ/H
HEAT LOSS REACTOR WALLS	99.26	MJ/H
ENERGY IN GAS	582.77	MJ/H
ENERGY IN TARS & FLY ASH	77.89	MJ/H
TOTAL OUT	1020.18	MJ/H
HEAT LOSS (BY DIFFERENCE)	196.46	MJ/H

% HEAT LOSS HV1 = 13.983 %

MATERIAL :CH WOOD R15 DATE :7/5/82 NUMBER :6-9

ASH CONTENT = 1.00WT %
MOISTURE CONTENT = 12.00WT %
HIGHER HEATING VALUE = 4300.0KCAL/KG

GAS COMPOSITION

	WEIGHT %	VOLUME %
H2	0.24	3.57
O2	0.00	0.00
N2	65.82	70.00
CH4	2.96	1.77
CO	6.01	6.39
CO2	26.66	17.94
C2H4	0.31	0.33
C2H6	0.00	0.00
C3H6	0.00	0.00
C4H6	0.00	0.00

METHANE RATIO = 0.00 HYDROGEN RATIO = 0.64

HIGHER HEATING VALUE

1.64	MJ/KG	390.6	KCAL/KG
2.16	MJ/NM3	520.0	KCAL/NM3

LOWER HEATING VALUE

1.52	MJ/KG	363.4	KCAL/KG
2.02	MJ/NM3	483.6	KCAL/NM3

SPECIFIC WEIGHT = 1.330 KG/NM3

AIR FACTOR "S"= 0.702

REACTION PARAMETERS

FLOWRATE AIR (NM3/HR; 0 C,1ATM)=	166.49
AIR PRESSURE (BAR REL) =	0.44
FLOWRATE OXYGEN (NM3/HR) =	0.00
OXYGEN PRESSURE (BAR REL) =	0.00
FLOWRATE STEAM (KG/HR) =	0.00
FLOWRATE SOLIDS (KG/HR) =	78.00
FLOWRATE NITROGEN (L/HR)	0.00
AMBIENT TEMPERATURE (C) =	10.00
FLOWRATE CONDENSATE (KG/HR) =	1.52
FLOWRATE FLY ASH (KG/HR) =	0.13
FLOWRATE CHAR (KG/HR) =	0.00
AMBIENT PRESSURE (BAR) =	1.00

TEMPERATURES

REACTOR TEMPERATURE =	942 C
TEMPERATURE PREHEATER =	0 C
TEMPERATURE INLET GAS =	50 C
T11 = 923 C	
T10 = 944 C	
T9 = 960 C	
T5 = 770 C	

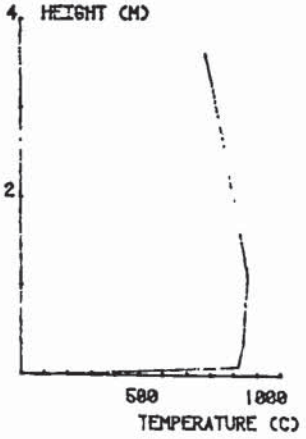

	KG/HR	C KG/HR	H KG/HR	O KG/HR	N KG/HR	ASH KG/HR
AIR	243.72	0.00	0.00	56.79	186.93	0.00
OXYGEN	0.00	0.00	0.00	0.00	0.00	0.00
NITROGEN	0.00	0.00	0.00	0.00	0.00	0.00
STEAM	0.00	0.00	0.00	0.00	0.00	0.00
SOLIDS MAF	67.39	30.53	3.91	32.68	0.01	0.00
MOISTURE	9.36	0.00	1.04	8.32	0.00	0.00
ASH	1.25	0.00	0.00	0.00	0.00	1.25
TOTAL	321 ?	30.53	4.95	97.99	186.94	1.25
TOTAL GAS	284.02	0.00	0.00	0.00	0.00	0.00
H2	0.68	0.00	0.68	0.00	0.00	0.00
O2	0.00	0.00	0.00	0.00	0.00	0.00
N2	186.94	0.00	0.00	0.00	186.94	0.00
CH4	2.71	2.04	0.68	0.00	0.00	0.00
CO	17.87	7.32	0.00	9.75	0.00	0.00
CO2	75.73	20.67	0.00	55.06	0.00	0.00
C2H4	0.88	0.76	0.13	0.00	0.00	0.00
C2H6	0.00	0.00	0.00	0.00	0.00	0.00
C3H6	0.00	0.00	0.00	0.00	0.00	0.00
C4H6	0.00	0.00	0.00	0.00	0.00	0.00
CONDENSATE	37.29	0.48	4.14	32.67	0.00	0.00
FLY ASH	3.19	1.59	0.00	0.00	0.00	1.59
CHAR	0.00	0.00	0.00	0.00	0.00	0.00
TOTAL	324.51	32.67	5.63	97.48	186.94	1.595
BALANCE	100.9	107.07	113.71	99.47	100.00	127.798

TARS IN COND= 0.54 TARS IN GAS= 0.36KG/KG

THERMAL EFFICIENCY = 98.91 %

Y=4.21
X=0.55

THERMAL BALANCE

HEAT OF REACTION (MJ/KG)	12.16	MJ/KG
IN		
SENSIBLE HEAT IN GAS	10.36	MJ/H
SENSIBLE & LATENT HEAT IN STEAM	0.00	MJ/H
HEAT IN FEEDSTOCK	1213.91	MJ/H
TOTAL IN	1224.27	MJ/H
OUT		
SENSIBLE HEAT IN GAS	253.12	MJ/H
SENSIBLE & LATENT HEAT IN STEAM	149.71	MJ/H
SENSIBLE HEAT IN FLY ASH	2.26	MJ/H
SENSIBLE HEAT IN CHAR	0.00	MJ/H
HEAT LOSS REACTOR WALLS	119.22	MJ/H
ENERGY IN GAS	464.67	MJ/H
ENERGY IN TARS & FLY ASH	64.96	MJ/H
TOTAL OUT	1053.94	MJ/H
HEAT LOSS (BY DIFFERENCE)	170.33	MJ/H

% HEAT LOSS HV1 = 12.123 %

MATERIAL :CH WOOD R16 DATE :7/5/82 NUMBER :7-10

ASH CONTENT = 1.60WT %
MOISTURE CONTENT = 12.00WT %
HIGHER HEATING VALUE = 4300.8KCAL/KG

GAS COMPOSITION

	WEIGHT %	VOLUME %
H2	0.00	0.85
O2	0.00	0.00
N2	74.36	81.12
CH4	0.21	0.40
CO	0.29	0.31
CO2	25.00	17.31
C2H4	0.00	0.00
C2H6	0.00	0.00
C3H6	0.00	0.00
C4H8	0.00	0.00

METHANE RATIO = 0.00 HYDROGEN RATIO = 0.00

HIGHER HEATING VALUE

0.23	MJ/KG	53.9	KCAL/KG
0.31	MJ/NM3	73.5	KCAL/NM3

LOWER HEATING VALUE

0.20	MJ/KG	46.2	KCAL/KG
0.28	MJ/NM3	66.8	KCAL/NM3

SPECIFIC WEIGHT = 1.365 KG/NM3

AIR FACTOR 'S'= 0.000

REACTION PARAMETERS

FLOWRATE AIR (NM3/HR; 0 C,1ATM)=	233.27
AIR PRESSURE (BAR REL) =	0.50
FLOWRATE OXYGEN (NM3/HR) =	0.00
OXYGEN PRESSURE (BAR REL) =	0.00
FLOWRATE STEAM (KG/HR) =	0.00
FLOWRATE SOLIDS (KG/HR) =	78.00
FLOWRATE NITROGEN (L/HR)	0.00
AMBIENT TEMPERATURE (C) =	15.00
FLOWRATE CONDENSATE (KG/HR) =	1.00
FLOWRATE FLY ASH (KG/HR) =	0.13
FLOWRATE CHAR (KG/HR) =	0.00
AMBIENT PRESSURE (BAR) =	1.00

TEMPERATURES

REACTOR TEMPERATURE =	970 C
TEMPERATURE PREHEATER =	0 C
TEMPERATURE INLET GAS =	50 C
T11 =	959 C
T10 =	964 C
T9 =	982 C
T5 =	911 C

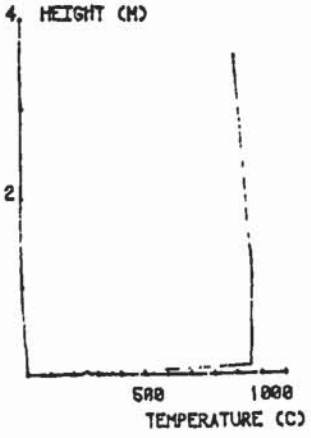

	KG/HR	C KG/HR	H KG/HR	O KG/HR	N KG/HR	ASH KG/HR
AIR	301.62	0.00	0.00	78.26	231.34	0.00
OXYGEN	0.00	0.00	0.00	0.00	0.00	0.00
NITROGEN	0.00	0.00	0.00	0.00	0.00	0.00
STEAM	0.00	0.00	0.00	0.00	0.00	0.00
SOLIDS MAF	67.39	38.53	3.91	32.68	0.01	0.00
MOISTURE	9.36	0.00	1.04	8.32	0.00	0.00
ASH	1.25	0.00	0.00	0.00	0.00	1.25
TOTAL	379.6	38.53	4.95	119.48	231.35	1.25
TOTAL GAS	311.12	0.00	0.00	0.00	0.00	0.00
H2	0.17	0.00	0.17	0.00	0.00	0.00
O2	0.00	0.00	0.00	0.00	0.00	0.00
N2	231.35	0.00	0.00	0.00	231.35	0.00
CH4	0.00	0.49	0.16	0.00	0.00	0.00
CO	0.90	0.36	0.00	0.51	0.00	0.00
CO2	78.04	21.30	0.00	56.73	0.00	0.00
C2H4	0.00	0.00	0.00	0.00	0.00	0.00
C2H6	0.00	0.00	0.00	0.00	0.00	0.00
C3H6	0.00	0.00	0.00	0.00	0.00	0.00
C4H8	0.00	0.00	0.00	0.00	0.00	0.00
CONDENSATE	36.81	0.48	4.06	32.25	0.00	0.00
FLY ASH	2.00	1.44	0.00	0.00	0.00	1.44
CHAR	0.00	0.00	0.00	0.00	0.00	0.00
TOTAL	350.81	24.18	4.42	89.50	231.35	1.441
BALANCE	92.4	76.95	89.36	88.35	100.00	115.502

TARS IN COND= 0.54 TARS IN GAS= 0.00KG/KG

THERMAL EFFICIENCY = 5.76 %

Y=4.62
X=0.55

THERMAL BALANCE

HEAT OF REACTION (MJ/KG)	16.33	MJ/KG
IN		
SENSIBLE HEAT IN GAS	12.62	MJ/H
SENSIBLE & LATENT HEAT IN STEAM	0.00	MJ/H
HEAT IN FEEDSTOCK	1213.91	MJ/H
TOTAL IN	1226.73	MJ/H
OUT		
SENSIBLE HEAT IN GAS	311.97	MJ/H
SENSIBLE & LATENT HEAT IN STEAM	157.93	MJ/H
SENSIBLE HEAT IN FLY ASH	2.41	MJ/H
SENSIBLE HEAT IN CHAR	0.00	MJ/H
HEAT LOSS REACTOR WALLS	139.00	MJ/H
ENERGY IN GAS	78.16	MJ/H
ENERGY IN TARS & FLY ASH	59.76	MJ/H
TOTAL OUT	731.78	MJ/H
HEAT LOSS (BY DIFFERENCE)	495.83	MJ/H

% HEAT LOSS HV1 = 35.233 %

MATERIAL :CH WOOD R18 DATE :18/5/82 NUMBER :AVER

ASH CONTENT = 1.60WT %
MOISTURE CONTENT = 12.00WT %
HIGHER HEATING VALUE = 4300.8KCAL/KG

GAS COMPOSITION

	WEIGHT %	VOLUME %
H2	8.38	4.34
O2	0.00	0.00
N2	62.58	65.46
CH4	1.45	2.64
CO	9.59	10.84
CO2	25.78	17.89
C2H4	0.39	0.34
C2H6	0.00	0.00
C3H8	0.00	0.00
C4H10	0.00	0.00

METHANE RATIO = 1.65 HYDROGEN RATIO = 1.56

HIGHER HEATING VALUE
2.39 MJ/KG 570.6 KCAL/KG
3.13 MJ/NM3 746.1 KCAL/NM3

LOWER HEATING VALUE
2.23 MJ/KG 533.2 KCAL/KG
2.93 MJ/NM3 698.9 KCAL/NM3

SPECIFIC WEIGHT = 1.311 KG/NM3

AIR FACTOR "S"= 0.415

REACTION PARAMETERS

FLOWRATE AIR (NM3/HR, 0 C,1ATM)= 228.70
AIR PRESSURE (BAR REL) = 0.41
FLOWRATE OXYGEN (NM3/HR) = 0.00
OXYGEN PRESSURE (BAR REL) = 0.00
FLOWRATE STEAM (KG/HR) = 0.00
FLOWRATE SOLIDS (KG/HR) = 100.00
FLOWRATE NITROGEN (L/HR) 0.00
AMBIENT TEMPERATURE (C) = 15.00
FLOWRATE CONDENSATE (KG/HR) = 2.00
FLOWRATE FLY ASH (KG/HR) = 3.31
FLOWRATE CHAR (KG/HR) = 0.00
AMBIENT PRESSURE (BAR) = 1.00

TEMPERATURES

REACTOR TEMPERATURE = 917 C
TEMPERATURE PREHEATER = 0 C
TEMPERATURE INLET GAS = 64 C
T11 = 919 C
T10 = 921 C
T9 = 895 C
T5 = 723 C

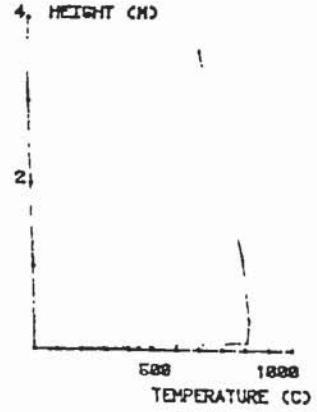

	KG/HR	C KG/HR	H KG/HR	O KG/HR	N KG/HR	ASH KG/HR
AIR	295.71	0.00	0.00	66.90	226.81	0.00
OXYGEN	0.00	0.00	0.00	0.00	0.00	0.00
NITROGEN	0.00	0.00	0.00	0.00	0.00	0.00
STEAM	0.00	0.00	0.00	0.00	0.00	0.00
SOLIDS MAF	136.24	62.62	6.82	67.46	0.01	0.00
MOISTURE	19.20	0.00	2.13	17.07	0.00	0.00
ASH	2.56	0.00	0.00	0.00	0.00	2.56
TOTAL	455.7	62.62	10.15	153.43	226.82	2.56
TOTAL GAS	362.90	0.00	0.00	0.00	0.00	0.00
H2	1.00	0.00	1.00	0.00	0.00	0.00
O2	0.00	0.00	0.00	0.00	0.00	0.00
N2	226.62	0.00	0.00	0.00	226.62	0.00
CH4	5.25	3.93	1.31	0.00	0.00	0.00
CO	34.76	14.92	0.00	19.86	0.00	0.00
CO2	93.57	25.54	0.00	68.02	0.00	0.00
C2H4	1.19	1.02	0.17	0.00	0.00	0.00
C2H6	0.21	0.17	0.04	0.00	0.00	0.00
C3H8	0.00	0.00	0.00	0.00	0.00	0.00
C4H6	0.00	0.00	0.00	0.00	0.00	0.00
CONDENSATE	63.61	0.63	7.00	55.90	0.00	0.00
FLY ASH	2.69	0.62	0.00	0.00	0.00	3.07
CHAR	0.00	0.00	0.00	0.00	0.00	0.00
TOTAL	436.60	53.24	9.68	143.79	226.62	3.066
BALANCE	95.8.	85.02	95.41	93.71	100.00	119.765

IN COND= 0.93 TARS IN GAS= 1.36KG/KG

THERMAL EFFICIENCY = 34.65 %

Y=2.63
X=0.46

THERMAL BALANCE

HEAT OF REACTION (MJ/KG)	18.67	MJ/KG
IN		
SENSIBLE HEAT IN GAS	14.18	MJ/H
SENSIBLE & LATENT HEAT IN STEAM	0.00	MJ/H
HEAT IN FEEDSTOCK	2490.00	MJ/H
TOTAL IN	2504.20	MJ/H
OUT		
SENSIBLE HEAT IN GAS	386.34	MJ/H
SENSIBLE & LATENT HEAT IN STEAM	248.67	MJ/H
SENSIBLE HEAT IN FLY ASH	6.54	MJ/H
SENSIBLE HEAT IN CHAR	0.00	MJ/H
HEAT LOSS REACTOR WALLS	111.52	MJ/H
ENERGY IN GAS	657.26	MJ/H
ENERGY IN TARS & FLY ASH	245.51	MJ/H
TOTAL OUT	1784.83	MJ/H
HEAT LOSS (BY DIFFERENCE)	719.62	MJ/H

% HEAT LOSS HV1 = 24.969 %

MATERIAL :CH WOOD R19 DATE :19/5/82 NUMBER :AVER

ASH CONTENT = 1.60WT %
MOISTURE CONTENT = 12.00WT %
HIGHER HEATING VALUE = 4300.0KCAL/KG

GAS COMPOSITION

	WEIGHT %	VOLUME %
H2	8.46	6.64
O2	0.00	0.00
N2	53.37	55.00
CH4	1.96	3.56
CO	11.62	12.16
CO2	32.11	21.26
C2H4	0.40	0.42
C2H6	0.00	0.00
C3H8	0.00	0.00
C4H10	0.00	0.00

METHANE RATIO = 1.77 HYDROGEN RATIO = 0.00

HIGHER HEATING VALUE
3.16 MJ/KG 754.6 KCAL/KG
4.14 MJ/NM3 988.0 KCAL/NM3

LOWER HEATING VALUE
2.94 MJ/KG 701.2 KCAL/KG
3.84 MJ/NM3 916.1 KCAL/NM3

SPECIFIC WEIGHT = 1.300 KG/NM3

AIR FACTOR "S"= 0.340

REACTION PARAMETERS

FLOWRATE AIR (NM3/HR; 0 C,1ATM)= 167.42
AIR PRESSURE (BAR REL) = 0.41
FLOWRATE OXYGEN (NM3/HR) = 0.00
OXYGEN PRESSURE (BAR REL) = 0.00
FLOWRATE STEAM (KG/HR) = 0.00
FLOWRATE SOLIDS (KG/HR) = 100.00
FLOWRATE NITROGEN (L/HR) 0.00
AMBIENT TEMPERATURE (C) = 15.00
FLOWRATE CONDENSATE (KG/HR) = 2.20
FLOWRATE FLY ASH (KG/HR) = 0.32
FLOWRATE CHAR (KG/HR) = 0.00
AMBIENT PRESSURE (BAR) = 1.00

TEMPERATURES

REACTOR TEMPERATURE = 627 C
TEMPERATURE PREHEATER = 0 C
TEMPERATURE INLET GAS = 51 C
T11 = 617 C
T10 = 657 C
T9 = 709 C
T5 = 691 C

	KG/HR	C KG/HR	H KG/HR	O KG/HR	N KG/HR	ASH KG/HR
AIR	242.33	0.00	0.00	58.46	185.87	0.00
OXYGEN	0.00	0.00	0.00	0.00	0.00	0.00
NITROGEN	0.00	0.00	0.00	0.00	0.00	0.00
STEAM	0.00	0.00	0.00	0.00	0.00	0.00
SOLIDS WAF	138.24	62.62	6.82	67.46	0.91	0.00
MOISTURE	19.20	0.00	2.13	17.07	0.00	0.00
ASH	2.56	0.00	0.00	0.00	0.00	2.56
TOTAL	402.3	62.62	10.15	140.99	186.98	2.56
TOTAL GAS	348.31	0.00	0.00	0.00	0.00	0.00
H2	1.59	0.00	1.59	0.00	0.00	0.00
O2	0.00	0.00	0.00	0.00	0.00	0.00
N2	185.00	0.00	0.00	0.00	185.00	0.00
CH4	6.64	5.13	1.71	0.00	0.00	0.00
CO	48.46	17.36	0.00	23.10	0.00	0.00
CO2	111.63	30.53	0.00	81.30	0.00	0.00
C2H4	1.40	1.20	0.20	0.00	0.00	0.00
C2H6	0.31	0.25	0.06	0.00	0.00	0.00
C3H8	0.00	0.00	0.00	0.00	0.00	0.00
C4H8	0.00	0.00	0.00	0.00	0.00	0.00
CONDENSATE	58.52	0.00	5.00	44.20	0.00	0.00
FLY ASH	7.35	5.07	0.00	0.00	0.00	2.20
CHAR	0.00	0.00	0.00	0.00	0.00	0.00
TOTAL	406.19	60.19	9.16	148.67	185.98	2.276
BALANCE	100.9	96.12	90.20	105.58	100.00	88.992

TARS IN COND= 0.73 TARS IN GAS= 1.79KG/KG

THERMAL EFFICIENCY = 44.21 %

Y=2.52
X=0.37

THERMAL BALANCE

HEAT OF REACTION (MJ/KG)	10.63	MJ/KG
IN		
SENSIBLE HEAT IN GAS	0.10	MJ/H
SENSIBLE & LATENT HEAT IN STEAM	0.00	MJ/H
HEAT IN FEEDSTOCK	2490.00	MJ/H
TOTAL IN	2490.20	MJ/H
OUT		
SENSIBLE HEAT IN GAS	249.70	MJ/H
SENSIBLE & LATENT HEAT IN STEAM	104.00	MJ/H
SENSIBLE HEAT IN FLY ASH	4.01	MJ/H
SENSIBLE HEAT IN CHAR	0.00	MJ/H
HEAT LOSS REACTOR WALLS	95.04	MJ/H
ENERGY IN GAS	1100.10	MJ/H
ENERGY IN TARS & FLY ASH	103.40	MJ/H
TOTAL OUT	1617.33	MJ/H
HEAT LOSS (BY DIFFERENCE)	000.00	MJ/H

% HEAT LOSS HY1 = 23.027 %

MATERIAL =CH WOOD R28 DATE =25/5/82 NUMBER =AYER

ASH CONTENT = 1.60WT %
MOISTURE CONTENT = 12.90WT %
HIGHER HEATING VALUE = 4388.0KCAL/KG

GAS COMPOSITION

	WEIGHT %	VOLUME %
H2	8.27	3.94
O2	0.00	0.00
N2	64.90	60.64
CH4	8.94	1.74
CO	6.46	6.67
CO2	26.63	16.91
C2H4	8.49	9.52
C2H6	0.00	0.00
C3H6	0.00	0.00
C4H8	0.00	0.00

METHANE RATIO = 1.15 HYDROGEN RATIO = 0.97

HIGHER HEATING VALUE
1.65 MJ/KG 441.6 KCAL/KG
2.45 MJ/NM3 585.9 KCAL/NM3

LOWER HEATING VALUE
1.72 MJ/KG 410.6 KCAL/KG
2.28 MJ/NM3 545.0 KCAL/NM3

SPECIFIC WEIGHT = 1.327 KG/NM3

AIR FACTOR 'S'= 0.500

REACTION PARAMETERS

FLOWRATE AIR (NM3/HR; 0 C,1ATM)= 275.79
AIR PRESSURE (BAR REL) = 0.52
FLOWRATE OXYGEN (NM3/HR) = 0.00
OXYGEN PRESSURE (BAR REL) = 0.00
FLOWRATE STEAM (KG/HR) = 0.00
FLOWRATE SOLIDS (KG/HR) = 100.00
FLOWRATE NITROGEN (L/HR) 0.00
AMBIENT TEMPERATURE (C) = 20.00
FLOWRATE CONDENSATE (KG/HR) = 1.53
FLOWRATE FLY ASH (KG/HR) = 0.33
FLOWRATE CHAR (KG/HR) = 0.00
AMBIENT PRESSURE (BAR) = 1.00

TEMPERATURES

REACTOR TEMPERATURE = 900 C
TEMPERATURE PREHEATER = 0 C
TEMPERATURE INLET GAS = 65 C
T11 = 905 C
T10 = 1002 C
T9 = 1013 C
T5 = 620 C

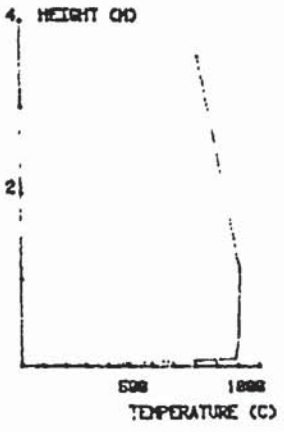

	KG/HR	C KG/HR	H KG/HR	O KG/HR	N KG/HR	ASH KG/HR
AIR	358.60	0.00	0.00	65.80	273.51	0.00
OXYGEN	0.00	0.00	0.00	0.00	0.00	0.00
NITROGEN	0.00	0.00	0.00	0.00	0.00	0.00
STEAM	0.00	0.00	0.00	0.00	0.00	0.00
SOLIDS MAF	138.24	62.62	6.82	64.46	0.81	0.00
MOISTURE	19.20	0.00	2.13	17.07	0.00	0.00
ASH	2.56	0.00	0.00	0.00	0.00	2.56
TOTAL	516.6	62.62	10.15	168.42	273.52	2.56
TOTAL GAS	421.43	0.00	0.00	0.00	0.00	0.00
H2	1.12	0.00	1.12	0.00	0.00	0.00
O2	0.00	0.00	0.00	0.00	0.00	0.00
N2	273.52	0.00	0.00	0.00	273.52	0.00
CH4	3.36	2.57	0.00	0.00	0.00	0.00
CO	27.36	11.71	0.00	15.59	0.00	0.00
CO2	113.00	30.67	0.00	82.21	0.00	0.00
C2H4	2.00	1.79	0.30	0.00	0.00	0.00
C2H6	0.57	0.29	0.07	0.00	0.00	0.00
C3H6	0.00	0.00	0.00	0.00	0.00	0.00
C4H8	0.00	0.00	0.00	0.00	0.00	0.00
CONDENSATE	49.37	9.64	5.46	43.25	0.00	0.00
FLY ASH	10.00	7.30	0.00	0.00	0.00	3.31
CHAR	0.00	0.00	0.00	0.00	0.00	0.00
TOTAL	481.40	55.03	7.90	141.05	273.52	3.305
BALANCE	93.2	88.03	78.44	84.28	100.00	129.105

TARS IN COND= 0.72 TARS IN GAS= 1.00KG/KG

THERMAL EFFICIENCY = 31.30 %

Y=3.05
X=0.36

THERMAL BALANCE

HEAT OF REACTION (MJ/KG)	10.03	MJ/KG
IN		
SENSIBLE HEAT IN GAS	17.49	MJ/H
SENSIBLE & LATENT HEAT IN STEAM	0.00	MJ/H
HEAT IN FEEDSTOCK	2490.00	MJ/H
TOTAL IN	2507.57	MJ/H
OUT		
SENSIBLE HEAT IN GAS	396.04	MJ/H
SENSIBLE & LATENT HEAT IN STEAM	202.40	MJ/H
SENSIBLE HEAT IN FLY ASH	0.02	MJ/H
SENSIBLE HEAT IN CHAR	0.00	MJ/H
HEAT LOSS REACTOR WALLS	125.00	MJ/H
ENERGY IN GAS	776.05	MJ/H
ENERGY IN TARS & FLY ASH	250.00	MJ/H
TOTAL OUT	1771.00	MJ/H
HEAT LOSS (BY DIFFERENCE)	735.50	MJ/H

% HEAT LOSS HV1 = 25.522 %

MATERIAL :CH WOOD R21 DATE :25/6/92 NUMBER :AVER

ASH CONTENT = 1.60WT %
MOISTURE CONTENT = 12.80WT %
HIGHER HEATING VALUE = 4988.0KCAL/KG

GAS COMPOSITION

	VEIGHT %	VOLUME %
H2	0.67	9.29
O2	0.00	0.00
N2	52.42	51.67
CH4	3.89	5.33
CO	16.17	16.00
CO2	27.84	16.06
C2H4	0.40	0.40
C2H6	0.10	0.09
C3H8	0.00	0.00
C4H10	0.00	0.00

METHANE RATIO = 0.96 HYDROGEN RATIO = 0.92

HIGHER HEATING VALUE
4.59 MJ/KG 1097.2 KCAL/KG
5.69 MJ/NM3 1358.3 KCAL/NM3

LOWER HEATING VALUE
4.26 MJ/KG 1017.0 KCAL/KG
5.27 MJ/NM3 1259.1 KCAL/NM3

SPECIFIC WEIGHT = 1.236 KG/NM3

AIR FACTOR "S"= 0.264

REACTION PARAMETERS

FLOWRATE AIR (NM3/HR, 0 C,1ATM)=	145.25
AIR PRESSURE (BAR REL) =	0.40
FLOWRATE OXYGEN (NM3/HR) =	0.00
OXYGEN PRESSURE (BAR REL) =	0.00
FLOWRATE STEAM (KG/HR) =	0.00
FLOWRATE SOLIDS (KG/HR) =	100.00
FLOWRATE NITROGEN (L/HR)	0.00
AMBIENT TEMPERATURE (C) =	20.00
FLOWRATE CONDENSATE (KG/HR) =	2.12
FLOWRATE FLY ASH (KG/HR) =	0.30
FLOWRATE CHAR (KG/HR) =	0.00
AMBIENT PRESSURE (BAR) =	1.00

TEMPERATURES

REACTOR TEMPERATURE =	817 C
TEMPERATURE PREHEATER =	0 C
TEMPERATURE INLET GAS =	52 C
T11 = 816 C	
T10 = 815 C	
T9 = 801 C	
T5 = 747 C	

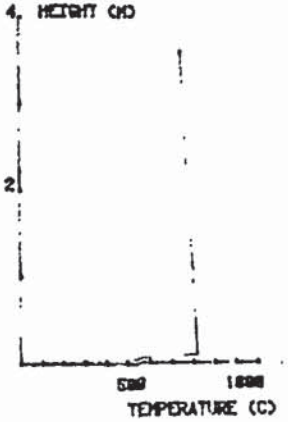

	KG/HR	C KG/HR	H KG/HR	O KG/HR	N KG/HR	ASH KG/HR
AIR	187.81	0.00	0.00	43.76	144.05	0.00
OXYGEN	0.00	0.00	0.00	0.00	0.00	0.00
NITROGEN	0.00	0.00	0.00	0.00	0.00	0.00
STEAM	0.00	0.00	0.00	0.00	0.00	0.00
SOLIDS MAF	136.24	62.62	8.82	64.46	0.81	0.00
MOISTURE	19.20	0.00	2.13	17.07	0.00	0.00
ASH	2.50	0.00	0.00	0.00	0.00	2.50
TOTAL	347.8	62.62	10.15	128.29	144.05	2.50
TOTAL GAS	274.65	0.00	0.00	0.00	0.00	0.00
H2	1.95	0.00	1.85	0.00	0.00	0.00
O2	0.00	0.00	0.00	0.00	0.00	0.00
N2	144.00	0.00	0.00	0.00	144.00	0.00
CH4	8.40	6.57	2.12	0.00	0.00	0.00
CO	44.44	19.00	0.00	25.37	0.00	0.00
CO2	74.44	20.32	0.00	54.12	0.00	0.00
C2H4	1.20	1.20	0.10	0.00	0.00	0.00
C2H6	0.20	0.22	0.00	0.00	0.00	0.00
C3H8	0.00	0.00	0.00	0.00	0.00	0.00
C4H10	0.00	0.00	0.00	0.00	0.00	0.00
CONDENSATE	43.25	0.00	4.00	37.00	0.00	0.00
FLY ASH	0.12	0.02	0.00	0.00	0.00	0.10
CHAR	0.00	0.00	0.00	0.00	0.00	0.00
TOTAL	324.21	51.00	9.01	117.30	144.00	1.007
BALANCE	93.2	82.01	88.01	91.49	100.00	74.100

TARS IN COND= 0.03 TARS IN GAS= 2.10KG/KG

THERMAL EFFICIENCY = 50.73 %

Y=1.99
X=0.31

THERMAL BALANCE

HEAT OF REACTION (MJ/KG)	0.02	MJ/KG
IN		
SENSIBLE HEAT IN GAS	0.55	MJ/H
SENSIBLE & LATENT HEAT IN STEAM	0.00	MJ/H
HEAT IN FEEDSTOCK	2498.00	MJ/H
TOTAL IN	2498.03	MJ/H
OUT		
SENSIBLE HEAT IN GAS	258.93	MJ/H
SENSIBLE & LATENT HEAT IN STEAM	170.72	MJ/H
SENSIBLE HEAT IN FLY ASH	4.10	MJ/H
SENSIBLE HEAT IN CHAR	0.00	MJ/H
HEAT LOSS REACTOR WALLS	100.57	MJ/H
ENERGY IN GAS	1202.33	MJ/H
ENERGY IN TARS & FLY ASH	153.10	MJ/H
TOTAL OUT	1955.72	MJ/H
HEAT LOSS (BY DIFFERENCE)	540.01	MJ/H

% HEAT LOSS HV1 = 10.700 %

MATERIAL :CH WOOD R22 DATE :28/6/82 NUMBER :4-6

ASH CONTENT = 1.00WT %
MOISTURE CONTENT = 12.90WT %
HIGHER HEATING VALUE = 4300.0KCAL/KG

GAS COMPOSITION

	WEIGHT %	VOLUME %
H2	2.77	19.53
O2	0.07	0.00
N2	54.13	52.06
CH4	2.65	4.66
CO	14.63	14.51
CO2	20.92	10.67
C2H4	0.35	0.34
C2H6	0.66	0.87
C3H8	0.00	0.00
C4H8	0.00	0.00

METHANE RATIO = 1.07 HYDROGEN RATIO = 1.06

HIGHER HEATING VALUE
4.39 MJ/KG 1049.4 KCAL/KG
5.38 MJ/NM3 1284.5 KCAL/NM3

LOWER HEATING VALUE
4.05 MJ/KG 966.3 KCAL/KG
4.96 MJ/NM3 1185.3 KCAL/NM3

SPECIFIC WEIGHT = 1.224 KG/NM3

AIR FACTOR "S"= 0.259

REACTION PARAMETERS

FLOWRATE AIR (NM3/HR, @ C,1ATM)=	167.42
AIR PRESSURE (BAR REL) =	0.41
FLOWRATE OXYGEN (NM3/HR) =	0.00
OXYGEN PRESSURE (BAR REL) =	0.00
FLOWRATE STEAM (KG/HR) =	0.00
FLOWRATE SOLIDS (KG/HR) =	218.00
FLOWRATE NITROGEN (L/HR)	0.00
AMBIENT TEMPERATURE (C) =	20.00
FLOWRATE CONDENSATE (KG/HR) =	2.36
FLOWRATE FLY ASH (KG/HR) =	0.30
FLOWRATE CHAR (KG/HR) =	0.00
AMBIENT PRESSURE (BAR) =	1.00

TEMPERATURES

REACTOR TEMPERATURE =	774 C
TEMPERATURE PREHEATER =	0 C
TEMPERATURE INLET GAS =	40 C
T11 = 778 C	
T10 = 778 C	
T9 = 762 C	
T5 = 617 C	

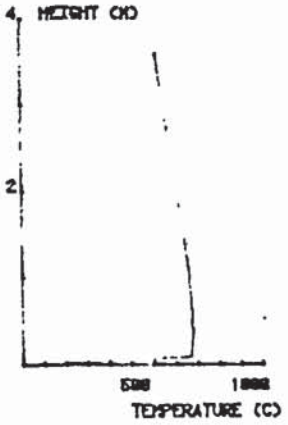

	KG/HR	C KG/HR	H KG/HR	O KG/HR	N KG/HR	ASH KG/HR
AIR	242.33	0.00	0.00	58.46	185.87	0.00
OXYGEN	0.00	0.00	0.00	0.00	0.00	0.00
NITROGEN	0.00	0.00	0.00	0.00	0.00	0.00
STEAM	0.00	0.00	0.00	0.00	0.00	0.00
SOLIDS MAF	181.44	82.19	10.52	88.54	0.82	0.00
MOISTURE	25.20	0.00	2.00	22.40	0.00	0.00
ASH	3.36	0.00	0.00	0.00	0.00	3.36
TOTAL	452.3	82.19	13.52	169.40	185.00	3.36
TOTAL GAS	343.41	0.00	0.00	0.00	0.00	0.00
H2	2.00	0.00	2.00	0.00	0.00	0.00
O2	0.24	0.00	0.00	0.24	0.00	0.00
N2	185.69	0.00	0.00	0.00	185.69	0.00
CH4	9.70	7.34	2.45	0.00	0.00	0.00
CO	50.92	21.84	0.00	29.00	0.00	0.00
CO2	92.46	25.24	0.00	67.22	0.00	0.00
C2H4	1.10	1.02	0.17	0.00	0.00	0.00
C2H6	0.20	0.21	0.05	0.00	0.00	0.00
C3H8	0.00	0.00	0.00	0.00	0.00	0.00
C4H8	0.00	0.00	0.00	0.00	0.00	0.00
CONDENSATE	63.49	0.03	7.04	55.02	0.00	0.00
FLY ASH	0.07	5.73	0.00	0.00	0.00	2.34
CHAR	0.00	0.00	0.00	0.00	0.00	0.00
TOTAL	414.97	82.22	12.37	152.15	185.69	2.341
BALANCE	91.8	75.78	92.00	90.9	100.00	69.658

TARS IN COND= 0.02 TARS IN GAS= 2.40KG/KG

THERMAL EFFICIENCY = 46.10 %

Y=1.89
X=0.35

THERMAL BALANCE

HEAT OF REACTION (MJ/KG)	9.31	MJ/KG
IN		
SENSIBLE HEAT IN GAS	7.06	MJ/H
SENSIBLE & LATENT HEAT IN STEAM	0.00	MJ/H
HEAT IN FEEDSTOCK	3200.22	MJ/H
TOTAL IN	3275.00	MJ/H
OUT		
SENSIBLE HEAT IN GAS	200.59	MJ/H
SENSIBLE & LATENT HEAT IN STEAM	233.37	MJ/H
SENSIBLE HEAT IN FLY ASH	4.53	MJ/H
SENSIBLE HEAT IN CHAR	0.00	MJ/H
HEAT LOSS REACTOR WALLS	94.00	MJ/H
ENERGY IN GAS	1500.50	MJ/H
ENERGY IN TARS & FLY ASH	289.51	MJ/H
TOTAL OUT	2317.00	MJ/H
HEAT LOSS (BY DIFFERENCE)	958.00	MJ/H

% HEAT LOSS HV1 = 25.349 %

MATERIAL =CH WOOD R23 DATE =26/6/82 NUMBER =AVER

ASH CONTENT = 1.60WT %
MOISTURE CONTENT = 12.00WT %
HIGHER HEATING VALUE = 4300.0KCAL/KG

GAS COMPOSITION

	WEIGHT %	VOLUME %
H2	8.78	18.56
O2	8.00	8.00
N2	53.11	51.66
CH4	3.17	5.38
CO	16.25	15.61
CO2	26.28	16.18
C2H4	8.34	8.33
C2H6	8.86	8.87
C3H8	8.00	8.00
C4H8	8.00	8.00

METHANE RATIO = 8.94 HYDROGEN RATIO = 8.94

HIGHER HEATING VALUE

4.72	MJ/KG	1127.6	KCAL/KG
5.75	MJ/NM3	1372.6	KCAL/NM3

LOWER HEATING VALUE

4.36	MJ/KG	1042.8	KCAL/KG
5.31	MJ/NM3	1268.4	KCAL/NM3

SPECIFIC WEIGHT = 1.217 KG/NM3

AIR FACTOR "S"= 8.228

REACTION PARAMETERS

FLOWRATE AIR (NM3/HR, 2 C,1ATM)=	166.88
AIR PRESSURE (BAR REL) =	8.48
FLOWRATE OXYGEN (NM3/HR) =	8.88
OXYGEN PRESSURE (BAR REL) =	8.88
FLOWRATE STEAM (KG/HR) =	8.88
FLOWRATE SOLIDS (KG/HR) =	218.88
FLOWRATE NITROGEN (L/HR)	8.88
AMBIENT TEMPERATURE (C) =	28.88
FLOWRATE CONDENSATE (KG/HR) =	1.58
FLOWRATE FLY ASH (KG/HR) =	8.36
FLOWRATE CHAR (KG/HR) =	8.82
AMBIENT PRESSURE (BAR) =	1.88

TEMPERATURES

REACTOR TEMPERATURE =	796 C
TEMPERATURE PREHEATER =	8 C
TEMPERATURE INLET GAS =	51 C
T11 = 797 C	
T18 = 881 C	
T9 = 782 C	
T5 = 664 C	

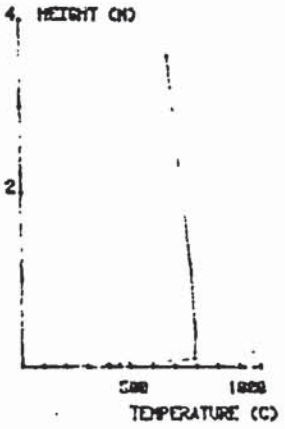

	KG/HR	C KG/HR	H KG/HR	O KG/HR	N KG/HR	ASH KG/HR
AIR	214.64	8.88	8.88	58.81	164.63	8.88
OXYGEN	8.88	8.88	8.88	8.88	8.88	8.88
NITROGEN	8.88	8.88	8.88	8.88	8.88	8.88
STEAM	8.88	8.88	8.88	8.88	8.88	8.88
SOLIDS MAF	181.44	82.19	18.52	88.54	8.82	8.88
MOISTURE	25.28	8.88	2.88	22.48	8.88	8.88
ASH	3.56	8.88	8.88	8.88	8.88	3.56
TOTAL	424.6	82.19	13.52	161.03	164.65	3.56
TOTAL GAS	318.81	8.88	8.88	8.82	8.88	8.88
H2	2.42	8.88	2.42	8.88	8.88	8.88
O2	8.88	8.88	8.88	8.88	8.88	8.88
N2	164.65	8.88	8.82	8.88	164.65	8.88
CH4	8.84	7.38	2.46	8.88	8.88	8.88
CO	58.36	21.88	8.88	28.78	8.88	8.28
CO2	81.46	22.24	8.88	59.22	8.88	8.88
C2H4	1.88	8.81	8.15	8.88	8.88	8.88
C2H6	8.25	8.19	8.85	8.88	8.88	8.88
C3H8	8.88	8.88	8.88	8.88	8.88	8.88
C4H8	8.88	8.88	8.88	8.88	8.88	8.88
CONDENSATE	36.24	8.47	4.82	31.76	8.88	8.38
FLY ASH	6.78	8.16	8.88	8.88	8.88	2.52
CHAR	8.88	8.88	8.88	8.88	8.88	8.88
TOTAL	354.95	58.88	9.18	119.73	164.65	2.523
BALANCE	83.6	71.74	68.28	74.35	188.88	75.877

TARS IN COND= 8.63 TARS IN GAS= 2.48KG/KG

THERMAL EFFICIENCY = 44.81 %

Y=1.71
X=0.20

THERMAL BALANCE

HEAT OF REACTION (MJ/KG)	7.55	MJ/KG
IN		
SENSIBLE HEAT IN GAS	7.25	MJ/H
SENSIBLE & LATENT HEAT IN STEAM	8.88	MJ/H
HEAT IN FEEDSTOCK	3268.22	MJ/H
TOTAL IN	3275.48	MJ/H
OUT		
SENSIBLE HEAT IN GAS	289.62	MJ/H
SENSIBLE & LATENT HEAT IN STEAM	138.58	MJ/H
SENSIBLE HEAT IN FLY ASH	5.43	MJ/H
SENSIBLE HEAT IN CHAR	8.88	MJ/H
HEAT LOSS REACTOR WALLS	188.67	MJ/H
ENERGY IN GAS	1463.28	MJ/H
ENERGY IN TARS & FLY ASH	214.91	MJ/H
TOTAL OUT	2192.21	MJ/H
HEAT LOSS (BY DIFFERENCE)	1083.27	MJ/H

% HEAT LOSS HV1 = 28.838 %

MATERIAL =CH WOOD /24 DATE =27/6/82 NUMBER =AVER

ASH CONTENT = 1.60WT %
MOISTURE CONTENT = 12.00WT %
HIGHER HEATING VALUE = 4300.0KCAL/KG

GAS COMPOSITION

	VEIGHT %	VOLUME %
H2	0.54	7.58
O2	0.00	0.00
N2	60.62	61.07
CH4	1.29	3.49
CO	11.44	11.52
CO2	24.73	15.77
C2H4	0.92	0.52
C2H6	0.07	0.07
C3H6	0.00	0.00
C4H8	0.00	0.00

METHANE RATIO = 0.56 HYDROGEN RATIO = 0.05

HIGHER HEATING VALUE
3.22 MJ/KG 768.2 KCAL/KG
4.05 MJ/NM3 968.2 KCAL/NM3

LOWER HEATING VALUE
2.98 MJ/KG 711.1 KCAL/KG
3.75 MJ/NM3 896.3 KCAL/NM3

SPECIFIC WEIGHT = 1.200 KG/NM3

AIR FACTOR "S"= 0.304

REACTION PARAMETERS

FLOWRATE AIR CNM3/HR, 0 C,1ATM=	277.00
AIR PRESSURE (BAR REL) =	0.50
FLOWRATE OXYGEN CNM3/HR) =	0.00
OXYGEN PRESSURE (BAR REL) =	0.00
FLOWRATE STEAM (KG/HR) =	0.00
FLOWRATE SOLIDS (KG/HR) =	210.00
FLOWRATE NITROGEN (L/HR)	0.00
AMBIENT TEMPERATURE (C) =	20.00
FLOWRATE CONDENSATE (KG/HR) =	1.00
FLOWRATE FLY ASH (KG/HR) =	0.36
FLOWRATE CHAR (KG/HR) =	0.00
AMBIENT PRESSURE (BAR) =	1.00

TEMPERATURES

REACTOR TEMPERATURE =	927 C
TEMPERATURE PREHEATER =	0 C
TEMPERATURE INLET GAS =	50 C
T11 =	923 C
T10 =	950 C
T9 =	911 C
T5 =	703 C

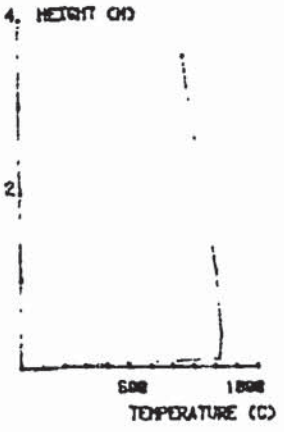

	KG/HR	C KG/HR	H KG/HR	O KG/HR	N KG/HR	ASH KG/HR
AIR	359.30	0.00	0.00	69.72	275.58	0.00
OXYGEN	0.00	0.00	0.00	0.00	0.00	0.00
NITROGEN	0.00	0.00	0.00	0.00	0.00	0.00
STEAM	0.00	0.00	0.00	0.00	0.00	0.00
SOLIDS VAF	181.44	82.19	10.52	88.54	0.02	0.00
MOISTURE	25.20	0.00	2.80	22.40	0.00	0.00
ASH	3.36	0.00	0.00	0.00	0.00	3.36
TOTAL	569.3	82.19	13.32	194.66	275.60	3.36
TOTAL GAS	454.64	0.00	0.00	0.00	0.00	0.00
H2	2.43	0.00	2.43	0.00	0.00	0.00
O2	1.36	0.00	0.00	0.00	0.00	0.00
N2	275.60	0.00	0.00	0.00	275.60	0.00
CH4	9.04	6.78	2.26	0.00	0.00	0.00
CO	51.00	22.30	0.00	29.00	0.00	0.00
CO2	112.45	30.70	0.00	81.75	0.00	0.00
C2H4	1.45	1.24	0.21	0.00	0.00	0.00
C2H6	0.32	0.26	0.06	0.00	0.00	0.00
C3H6	0.00	0.00	0.00	0.00	0.00	0.00
C4H8	0.00	0.00	0.00	0.00	0.00	0.00
CONDENSATE	44.36	0.50	4.02	36.00	0.00	0.00
FLY ASH	15.97	11.34	0.00	0.00	0.00	4.63
CHAR	0.00	0.00	0.00	0.00	0.00	0.00
TOTAL	514.97	73.20	9.09	151.00	275.60	4.631
BALANCE	90 5	89.05	74.21	34.5%	100.00	137.63

TARS IN COND= 0.04 TARS IN GAS= 2.20GR/KG

THERMAL EFFICIENCY = 44.76 %

Y=2.51
X=0.24

THERMAL BALANCE

HEAT OF REACTION CMJ/KG)	0.21	MJ/KG
IN		
SENSIBLE HEAT IN GAS	15.27	MJ/H
SENSIBLE & LATENT HEAT IN STEAM	0.00	MJ/H
HEAT IN FEEDSTOCK	3268.22	MJ/H
TOTAL IN	3283.50	MJ/H
OUT		
SENSIBLE HEAT IN GAS	428.14	MJ/H
SENSIBLE & LATENT HEAT IN STEAM	176.50	MJ/H
SENSIBLE HEAT IN FLY ASH	11.15	MJ/H
SENSIBLE HEAT IN CHAR	0.00	MJ/H
HEAT LOSS REACTOR WALLS	115.31	MJ/H
ENERGY IN GAS	1461.96	MJ/H
ENERGY IN TARS & FLY ASH	367.85	MJ/H
TOTAL OUT	2572.19	MJ/H
HEAT LOSS CBY DIFFERENCE)	711.31	MJ/H

% HEAT LOSS HV1 = 18.604 %

MATERIAL =CH WOOD R25 DATE =27/6/82 NUMBER =AVER

ASH CONTENT = 1.60WT %
MOISTURE CONTENT = 12.90WT %
HIGHER HEATING VALUE = 4386.9KCAL/KG

GAS COMPOSITION

	WEIGHT %	VOLUME %
H2	3.74	18.86
O2	0.14	0.12
N2	58.21	54.69
CH4	2.74	4.66
CO	14.84	14.49
CO2	24.93	15.48
C2H4	0.32	0.31
C2H6	0.07	0.06
C3H6	0.00	0.00
C4H6	0.00	0.00

METHANE RATIO = 0.07 HYDROGEN RATIO = 0.66

HIGHER HEATING VALUE
4.27 MJ/KG 1019.6 KCAL/KG
5.21 MJ/NM3 1245.6 KCAL/NM3

LOWER HEATING VALUE
3.94 MJ/KG 942.2 KCAL/KG
4.62 MJ/NM3 1158.6 KCAL/NM3

SPECIFIC WEIGHT = 1.221 KG/NM3

AIR FACTOR "S"= 0.328

REACTION PARAMETERS

FLOWRATE AIR (NM3/HR, 0 C,1ATM)= 231.18
AIR PRESSURE (BAR REL) = 0.45
FLOWRATE OXYGEN (NM3/HR) = 0.00
OXYGEN PRESSURE (BAR REL) = 0.00
FLOWRATE STEAM (KG/HR) = 0.00
FLOWRATE SOLIDS (KG/HR) = 218.00
FLOWRATE NITROGEN (L/HR) 0.00
AMBIENT TEMPERATURE (C) = 20.00
FLOWRATE CONDENSATE (KG/HR) = 1.35
FLOWRATE FLY ASH (KG/HR) = 0.36
FLOWRATE CHAR (KG/HR) = 0.00
AMBIENT PRESSURE (BAR) = 1.00

TEMPERATURES

REACTOR TEMPERATURE = 876 C
TEMPERATURE PREHEATER = 0 C
TEMPERATURE INLET GAS = 50 C
T11 = 871 C
T10 = 880 C
T9 = 861 C
T5 = 777 C

	KG/HR	C KG/HR	H KG/HR	O KG/HR	N KG/HR	ASH KG/HR
AIR	298.91	0.00	0.00	69.65	229.27	0.00
OXYGEN	0.00	0.00	0.00	0.00	0.00	0.00
NITROGEN	0.00	0.00	0.00	0.00	0.00	0.00
STEAM	0.00	0.00	0.00	0.00	0.00	0.00
SOLIDS MAF	181.44	82.19	10.52	82.54	0.82	0.00
MOISTURE	25.20	0.00	2.80	22.40	0.00	0.00
ASH	3.50	0.00	0.00	0.00	0.00	3.50
TOTAL	508.9	82.19	13.32	180.54	229.28	3.50
TOTAL GAS	487.67	0.00	0.00	0.00	0.00	0.00
H2	3.82	0.00	3.82	0.00	0.00	0.00
O2	0.67	0.00	0.00	0.67	0.00	0.00
N2	229.28	0.00	0.00	0.00	229.28	0.00
CH4	11.16	8.37	2.79	0.00	0.00	0.00
CO	60.55	25.96	0.00	34.57	0.00	0.00
CO2	181.69	27.76	0.00	73.93	0.00	0.00
C2H4	1.31	1.13	0.19	0.00	0.00	0.00
C2H6	0.29	0.29	0.00	0.00	0.00	0.00
C3H6	0.00	0.00	0.00	0.00	0.00	0.00
C4H6	0.00	0.00	0.00	0.00	0.00	0.00
CONDENSATE	58.51	0.00	5.00	44.25	0.00	0.00
FLY ASH	13.47	9.58	0.00	0.00	0.00	3.91
CHAR	0.00	0.00	0.00	0.00	0.00	0.00
TOTAL	471.65	73.00	11.00	153.32	229.28	3.900
BALANCE	92.7	89.05	87.53	84.9	100.00	110.25?

TARS IN COND= 0.73 TARS IN GAS= 2.73KG/KG

THERMAL EFFICIENCY = 53.31 %

Y=2.56
X=0.32

THERMAL BALANCE

HEAT OF REACTION (MJ/KG)	7.10	MJ/KG
IN		
SENSIBLE HEAT IN GAS	11.73	MJ/H
SENSIBLE & LATENT HEAT IN STEAM	0.00	MJ/H
HEAT IN FEEDSTOCK	3268.22	MJ/H
TOTAL IN	3279.86	MJ/H
OUT		
SENSIBLE HEAT IN GAS	396.99	MJ/H
SENSIBLE & LATENT HEAT IN STEAM	292.56	MJ/H
SENSIBLE HEAT IN FLY ASH	9.50	MJ/H
SENSIBLE HEAT IN CHAR	0.00	MJ/H
HEAT LOSS REACTOR WALLS	112.78	MJ/H
ENERGY IN GAS	1741.87	MJ/H
ENERGY IN TARS & FLY ASH	330.67	MJ/H
TOTAL OUT	2795.77	MJ/H
HEAT LOSS (BY DIFFERENCE)	484.10	MJ/H

% HEAT LOSS H/1 = 12.880 %

MATERIAL :CH WOOD R26 DATE :21/6/82 NUMBER :VUB

ASH CONTENT = 1.60WT %
MOISTURE CONTENT = 12.00WT %
HIGHER HEATING VALUE = 4300.0KCAL/KG

GAS COMPOSITION

	WEIGHT %	VOLUME %
H2	0.70	9.74
O2	0.70	0.66
N2	50.05	50.01
CH4	2.05	4.94
CO	19.62	19.75
CO2	20.77	16.11
C2H4	1.61	1.70
C2H6	0.43	0.32
C3H8	0.00	0.00
C4H8	0.00	0.00

METHANE RATIO = 0.94 HYDROGEN RATIO = 0.93

HIGHER HEATING VALUE
5.10 MJ/KG 1219.4 KCAL/KG
6.35 MJ/NM3 1516.0 KCAL/NM3

LOWER HEATING VALUE
4.72 MJ/KG 1127.6 KCAL/KG
5.00 MJ/NM3 1403.7 KCAL/NM3

SPECIFIC WEIGHT = 1.245 KG/NM3

AIR FACTOR "S"= 0.260

REACTION PARAMETERS

FLOWRATE AIR (NM3/HR; 0 C,1ATM)= 210.34
AIR PRESSURE (BAR REL) = 0.70
FLOWRATE OXYGEN (NM3/HR) = 0.00
OXYGEN PRESSURE (BAR REL) = 0.00
FLOWRATE STEAM (KG/HR) = 0.00
FLOWRATE SOLIDS (KG/HR) = 220.00
FLOWRATE NITROGEN (L/HR) 0.00
AMBIENT TEMPERATURE (C) = 15.00
FLOWRATE CONDENSATE (KG/HR) = 9.15
FLOWRATE FLY ASH (KG/HR) = 0.30
FLOWRATE CHAR (KG/HR) = 0.00
AMBIENT PRESSURE (BAR) = 1.00

TEMPERATURES

REACTOR TEMPERATURE = 746 C
TEMPERATURE PREHEATER = 0 C
TEMPERATURE INLET GAS = 62 C
T11 = 740 C
T10 = 752 C
T9 = 709 C
T5 = 501 C

	KG/HR	C KG/HR	H KG/HR	O KG/HR	N KG/HR	ASH KG/HR
AIR	262.31	0.00	0.00	65.70	210.53	0.00
OXYGEN	0.00	0.00	0.00	0.00	0.00	0.00
NITROGEN	0.00	0.00	0.00	0.00	0.00	0.00
STEAM	0.00	0.00	0.00	0.00	0.00	0.00
SOLIDS MAF	190.00	66.11	11.02	92.46	0.02	0.00
MOISTURE	26.40	0.00	2.03	23.47	0.00	0.00
ASH	3.52	0.00	0.00	0.00	0.00	3.52
TOTAL	502.3	66.11	13.00	182.00	210.55	3.52
TOTAL GAS	425.02	0.00	0.00	0.00	0.00	0.00
H2	3.00	0.00	3.00	0.00	0.00	0.00
O2	3.30	0.00	0.00	3.30	0.00	0.00
N2	210.55	0.00	0.00	0.00	210.55	0.00
CH4	12.13	9.10	3.03	0.00	0.00	0.00
CO	50.05	25.25	0.00	33.60	0.00	0.00
CO2	122.50	33.44	0.30	89.05	0.00	0.00
C2H4	7.09	6.53	1.10	0.00	0.00	0.00
C2H6	1.01	1.45	0.30	0.00	0.00	0.00
C3H8	0.00	0.00	0.00	0.00	0.00	0.00
C4H8	0.00	0.00	0.00	0.00	0.00	0.00
CONDENSATE	60.30	0.09	7.50	50.09	0.00	0.00
FLY ASH	7.01	5.39	0.03	0.00	0.00	2.42
CHAR	0.00	0.00	0.00	0.00	0.00	0.00
TOTAL	501.90	02.10	15.07	105.05	210.55	2.422
BALANCE	99.9	95.35	100.01	102.11	100.00	00.005

TARS IN COND= 0.00 TARS IN GAS= 3.02KG/KG

THERMAL EFFICIENCY = 00.53 %

Y=2.24
X=0.36

THERMAL BALANCE

HEAT OF REACTION (MJ/KG)	0.12	MJ/KG
IN		
SENSIBLE HEAT IN GAS	12.02	MJ/H
SENSIBLE & LATENT HEAT IN STEAM	0.00	MJ/H
HEAT IN FEEDSTOCK	3423.05	MJ/H
TOTAL IN	3436.70	MJ/H
OUT		
SENSIBLE HEAT IN GAS	270.00	MJ/H
SENSIBLE & LATENT HEAT IN STEAM	204.70	MJ/H
SENSIBLE HEAT IN FLY ASH	3.53	MJ/H
SENSIBLE HEAT IN CHAR	0.00	MJ/H
HEAT LOSS REACTOR WALLS	05.10	MJ/H
ENERGY IN GAS	2173.02	MJ/H
ENERGY IN TARS & FLY ASH	200.01	MJ/H
TOTAL OUT	2005.04	MJ/H
HEAT LOSS (BY DIFFERENCE)	470.04	MJ/H

% HEAT LOSS HV1 = 11.001 %

MATERIAL :CH WOOD R27 DATE :23/6/82 NUMBER :VUB/A

ASH CONTENT = 1.60WT %
MOISTURE CONTENT = 12.90WT %
HIGHER HEATING VALUE = 4300.0KCAL/KG

GAS COMPOSITION

	WEIGHT %	VOLUME %
H2	0.75	10.30
O2	0.92	0.60
N2	46.60	46.53
CH4	2.94	5.80
CO	14.67	14.56
CO2	29.76	18.71
C2H4	1.60	1.00
C2H6	0.57	0.33
C3H8	0.00	0.00
C4H8	0.00	0.00

METHANE RATIO = 0.00 HYDROGEN RATIO = 0.00

HIGHER HEATING VALUE

5.21	MJ/KG	1245.5	KCAL/KG
6.46	MJ/NM3	1547.0	KCAL/NM3

LOWER HEATING VALUE

4.82	MJ/KG	1151.0	KCAL/KG
5.99	MJ/NM3	1430.5	KCAL/NM3

SPECIFIC WEIGHT = 1.242 KG/NM3

AIR FACTOR "S"= 0.324

REACTION PARAMETERS

FLOWRATE AIR (NM3/HR; 0 C,1ATM)=	245.40
AIR PRESSURE (BAR REL) =	0.75
FLOWRATE OXYGEN (NM3/HR) =	0.00
OXYGEN PRESSURE (BAR REL) =	0.00
FLOWRATE STEAM (KG/HR) =	0.00
FLOWRATE SOLIDS (KG/HR) =	220.00
FLOWRATE NITROGEN (L/HR)	0.00
AMBIENT TEMPERATURE (C) =	15.00
FLOWRATE CONDENSATE (KG/HR) =	2.00
FLOWRATE FLY ASH (KG/HR) =	0.52
FLOWRATE CHAR (KG/HR) =	0.00
AMBIENT PRESSURE (BAR) =	1.00

TEMPERATURES

REACTOR TEMPERATURE =	768 C
TEMPERATURE PREHEATER =	0 C
TEMPERATURE INLET GAS =	62 C
T11 = 762 C	
T10 = 776 C	
T9 = 762 C	
T5 = 546 C	

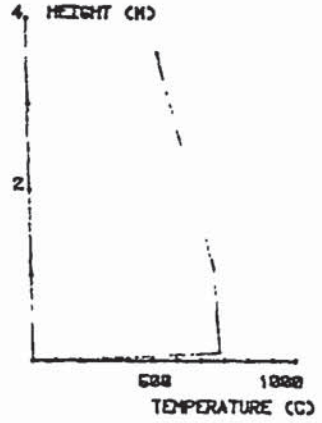

	KG/HR	C KG/HR	H KG/HR	O KG/HR	N KG/HR	ASH KG/HR
AIR	317.42	0.00	0.00	73.96	243.46	0.00
OXYGEN	0.00	0.00	0.00	0.00	0.00	0.00
NITROGEN	0.00	0.00	0.00	0.00	0.00	0.00
STEAM	0.00	0.00	0.00	0.00	0.00	0.00
SOLIDS MAF	198.00	96.11	11.82	92.56	0.02	0.00
MOISTURE	26.40	0.00	2.93	23.47	0.00	0.00
ASH	3.52	0.00	0.00	0.00	0.00	3.52
TOTAL	537.4	96.11	13.96	190.19	243.46	3.52
TOTAL GAS	496.87	0.00	0.00	0.00	0.00	0.00
H2	3.71	0.00	3.71	0.00	0.00	0.00
O2	4.60	0.00	0.00	4.60	0.00	0.00
N2	243.46	0.00	0.00	0.00	243.46	0.00
CH4	14.67	11.00	3.67	0.00	0.00	0.00
CO	73.35	31.34	0.00	41.71	0.00	0.00
CO2	146.32	40.49	0.00	107.83	0.00	0.00
C2H4	8.42	7.21	1.20	0.00	0.00	0.00
C2H6	1.82	1.46	0.36	0.00	0.00	0.00
C3H8	0.00	0.00	0.00	0.00	0.00	0.00
C4H8	0.00	0.00	0.00	0.00	0.00	0.00
CONDENSATE	54.17	0.78	0.21	47.48	0.00	0.00
FLY ASH	6.67	5.96	0.00	0.00	0.00	2.69
CHAR	0.00	0.00	0.00	0.00	0.00	0.00
TOTAL	569.00	96.16	14.96	201.60	243.46	2.687
BALANCE	104.4	114.83	187.17	105.99	188.00	76.328

TARS IN COND= 0.78 TARS IN GAS= 6.36KG/KG

THERMAL EFFICIENCY = 75.90 %

Y=2.62
X=0.29

THERMAL BALANCE

HEAT OF REACTION (MJ/KG)	6.66	MJ/KG
IN		
SENSIBLE HEAT IN GAS	14.53	MJ/H
SENSIBLE & LATENT HEAT IN STEAM	0.00	MJ/H
HEAT IN FEEDSTOCK	3423.65	MJ/H
TOTAL IN	3496.90	MJ/H
OUT		
SENSIBLE HEAT IN GAS	347.78	MJ/H
SENSIBLE & LATENT HEAT IN STEAM	191.07	MJ/H
SENSIBLE HEAT IN FLY ASH	4.29	MJ/H
SENSIBLE HEAT IN CHAR	0.00	MJ/H
HEAT LOSS REACTOR WALLS	69.79	MJ/H
ENERGY IN GAS	2596.65	MJ/H
ENERGY IN TARS & FLY ASH	214.55	MJ/H
TOTAL OUT	3444.24	MJ/H
HEAT LOSS (BY DIFFERENCE)	-5.65	MJ/H

% HEAT LOSS HV1 = -0.146 %

MATERIAL :CH WOOD R28 DATE :28/6/82 NUMBER :AVER

ASH CONTENT = 1.60WT %
MOISTURE CONTENT = 12.00WT %
HIGHER HEATING VALUE = 4300.0KCAL/KG

GAS COMPOSITION

	WEIGHT %	VOLUME %
H2	8.78	18.56
O2	0.00	0.00
N2	52.71	31.68
CH4	2.52	4.31
CO	16.78	16.36
CO2	28.92	16.78
C2H4	0.33	0.29
C2H6	0.37	0.00
C3H8	0.00	0.00
C4H8	0.00	0.00

METHANE RATIO = 1.11 HYDROGEN RATIO = 1.81

HIGHER HEATING VALUE
4.37 MJ/KG 1045.0 KCAL/KG
5.37 MJ/NM3 1281.6 KCAL/NM3

LOWER HEATING VALUE
4.06 MJ/KG 968.6 KCAL/KG
4.97 MJ/NM3 1186.1 KCAL/NM3

SPECIFIC WEIGHT = 1.227 KG/NM3

AIR FACTOR "S"= 0.384

REACTION PARAMETERS

FLOWRATE AIR (NM3/HR, 0 C,1ATM)= 258.47
AIR PRESSURE (BAR REL) = 0.60
FLOWRATE OXYGEN (NM3/HR) = 0.00
OXYGEN PRESSURE (BAR REL) = 0.00
FLOWRATE STEAM (KG/HR) = 0.00
FLOWRATE SOLIDS (KG/HR) = 189.50
FLOWRATE NITROGEN (L/HR) 0.00
AMBIENT TEMPERATURE (C) = 20.00
FLOWRATE CONDENSATE (KG/HR) = 2.00
FLOWRATE FLY ASH (KG/HR) = 0.40
FLOWRATE CHAR (KG/HR) = 0.00
AMBIENT PRESSURE (BAR) = 1.00

TEMPERATURES

REACTOR TEMPERATURE = 811 C
TEMPERATURE PREHEATER = 0 C
TEMPERATURE INLET GAS = 60 C
T11 = 818 C
T18 = 812 C
T9 = 796 C
T5 = 594 C

	KG/HR	C KG/HR	H KG/HR	O KG/HR	N KG/HR	ASH KG/HR
AIR	323.06	0.00	0.00	75.46	248.46	0.00
OXYGEN	0.00	0.00	0.00	0.00	0.00	0.00
NITROGEN	0.00	0.00	0.00	0.00	0.00	0.00
STEAM	0.00	0.00	0.00	0.00	0.00	0.00
SOLIDS MAF	163.73	74.17	9.59	79.90	0.02	0.00
MOISTURE	22.74	0.00	2.52	20.22	0.00	0.00
ASH	3.03	0.00	0.00	0.00	0.00	3.23
TOTAL	513.4	74.17	12.92	175.58	248.41	3.03
TOTAL GAS	471.32	0.00	0.00	0.00	0.00	0.00
H2	3.65	0.00	3.65	0.00	0.00	0.00
O2	0.00	0.00	0.00	0.00	0.00	0.00
N2	248.41	0.00	0.00	0.00	248.41	0.00
CH4	11.69	8.92	2.97	0.00	0.00	0.00
CO	78.73	33.78	0.00	44.96	0.00	0.00
CO2	126.69	34.64	0.32	92.25	0.00	0.00
C2H4	1.42	1.22	0.20	0.00	0.00	0.00
C2H6	0.31	0.25	0.06	0.00	0.00	0.00
C3H8	0.00	0.00	0.00	0.00	0.00	0.00
C4H8	0.00	0.00	0.00	0.00	0.00	0.00
CONDENSATE	51.72	0.07	5.74	45.91	0.00	0.00
FLY ASH	10.34	7.14	0.00	0.00	0.00	3.21
CHAR	0.00	0.00	0.00	0.00	0.00	0.00
TOTAL	533.36	86.61	12.63	182.52	248.41	3.207
BALANCE	103.9	116.78	105.87	103.95	100.00	105.765

TARS IN COND= 0.75 TARS IN GAS= 2.92KG/KG

THERMAL EFFICIENCY = 69.90 %

Y=2.88
X=0.32

THERMAL BALANCE

HEAT OF REACTION (MJ/KG)	7.64	MJ/KG
IN		
SENSIBLE HEAT IN GAS	12.71	MJ/H
SENSIBLE & LATENT HEAT IN STEAM	0.00	MJ/H
HEAT IN FEEDSTOCK	2949.18	MJ/H
TOTAL IN	2961.89	MJ/H
OUT		
SENSIBLE HEAT IN GAS	349.33	MJ/H
SENSIBLE & LATENT HEAT IN STEAM	167.69	MJ/H
SENSIBLE HEAT IN FLY ASH	5.58	MJ/H
SENSIBLE HEAT IN CHAR	0.00	MJ/H
HEAT LOSS REACTOR WALLS	95.33	MJ/H
ENERGY IN GAS	2861.73	MJ/H
ENERGY IN TARS & FLY ASH	251.78	MJ/H
TOTAL OUT	2961.91	MJ/H
HEAT LOSS (BY DIFFERENCE)	18.58	MJ/H

% HEAT LOSS HV1 = 0.310 %

MATERIAL :CH WOOD R29 DATE :18/8/82 NUMBER :AVER

ASH CONTENT = 1.60WT %
MOISTURE CONTENT = 14.10WT %
HIGHER HEATING VALUE = 4308.0KCAL/KG

GAS COMPOSITION

	WEIGHT %	VOLUME %
H2	0.63	0.94
O2	0.95	0.95
N2	44.52	45.64
CH4	3.48	6.86
CO	13.65	14.23
CO2	34.76	22.56
C2H4	1.06	1.06
C2H6	0.39	0.37
C3H8	0.33	0.23
C4H8	0.29	0.85

METHANE RATIO = 1.04 HYDROGEN RATIO = 1.05

HIGHER HEATING VALUE
5.12 MJ/KG 1223.1 KCAL/KG
6.57 MJ/NM3 1568.9 KCAL/NM3

LOWER HEATING VALUE
4.73 MJ/KG 1130.9 KCAL/KG
6.07 MJ/NM3 1450.6 KCAL/NM3

SPECIFIC WEIGHT = 1.269 KG/NM3

AIR FACTOR "S"= 0.259

REACTION PARAMETERS

FLOWRATE AIR (NM3/HR; 0 C,1ATM)=	246.00
AIR PRESSURE (BAR REL) =	0.05
FLOWRATE OXYGEN (NM3/HR) =	0.00
OXYGEN PRESSURE (BAR REL) =	0.00
FLOWRATE STEAM (KG/HR) =	0.00
FLOWRATE SOLIDS (KG/HR) =	285.00
FLOWRATE NITROGEN (L/HR)	0.00
AMBIENT TEMPERATURE (C) =	20.00
FLOWRATE CONDENSATE (KG/HR) =	2.00
FLOWRATE FLY ASH (KG/HR) =	8.32
FLOWRATE CHAR (KG/HR) =	0.00
AMBIENT PRESSURE (BAR) =	1.00

TEMPERATURES

REACTOR TEMPERATURE =	786 C
TEMPERATURE PREHEATER =	0 C
TEMPERATURE INLET GAS =	60 C
T11 =	787 C
T10 =	795 C
T9 =	695 C
T5 =	585 C

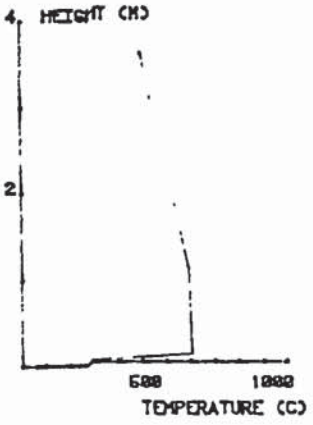

	KG/HR	C KG/HR	H KG/HR	O KG/HR	N KG/HR	ASH KG/HR
AIR	328.67	0.00	0.00	74.72	245.95	0.00
OXYGEN	0.00	0.00	0.00	0.00	0.00	0.00
NITROGEN	0.00	0.00	0.00	0.00	0.00	0.00
STEAM	0.00	0.00	0.00	0.00	0.00	0.00
SOLIDS MAF	248.28	106.64	13.23	121.15	0.02	0.00
MOISTURE	40.19	0.00	4.46	35.72	0.00	0.00
ASH	4.56	0.00	0.00	0.00	0.00	4.56
TOTAL	605 ±	106.64	16.48	231.54	245.97	4.56
TOTAL GAS	552.54	0.00	0.00	0.00	0.00	0.00
H2	3.46	0.00	3.46	0.00	0.00	0.00
O2	5.25	0.00	0.00	5.25	0.00	0.00
N2	245.97	0.00	0.00	0.00	245.97	0.00
CH4	16.79	14.18	4.73	0.00	0.00	0.00
CO	76.53	32.83	0.00	43.79	0.00	0.00
CO2	192.15	52.46	0.00	139.78	0.00	0.00
C2H4	5.66	5.04	0.64	0.00	0.00	0.00
C2H6	2.16	1.73	0.43	0.00	0.00	0.00
C3H8	1.82	1.56	0.26	0.00	0.00	0.00
C4H8	8.51	8.45	0.06	0.00	0.00	0.00
CONDENSATE	64.46	9.64	7.15	56.47	0.00	0.00
FLY ASH	18.31	7.12	0.00	0.00	0.00	3.28
CHAR	0.00	0.00	0.00	0.00	0.00	0.00
TOTAL	627.31	116.13	16.98	245.12	245.97	3.197
BALANCE	103.6	106.78	91.67	105.84	100.00	78.113

TARS IN COND= 8.94 TARS IN GAS=12.85KG/KG

THERMAL EFFICIENCY = 65.42 %

Y=2.29
X=0.27

THERMAL BALANCE

HEAT OF REACTION (MJ/KG)	8.21	MJ/KG
IN		
SENSIBLE HEAT IN GAS	13.96	MJ/H
SENSIBLE & LATENT HEAT IN STEAM	0.00	MJ/H
HEAT IN FEEDSTOCK	4327.64	MJ/H
TOTAL IN	4341.62	MJ/H
OUT		
SENSIBLE HEAT IN GAS	358.59	MJ/H
SENSIBLE & LATENT HEAT IN STEAM	221.84	MJ/H
SENSIBLE HEAT IN FLY ASH	4.78	MJ/H
SENSIBLE HEAT IN CHAR	0.00	MJ/H
HEAT LOSS REACTOR WALLS	81.84	MJ/H
ENERGY IN GAS	2629.81	MJ/H
ENERGY IN TARS & FLY ASH	255.31	MJ/H
TOTAL OUT	3743.48	MJ/H
HEAT LOSS (BY DIFFERENCE)	598.22	MJ/H

% HEAT LOSS HV1 = 11.653 %

MATERIAL :CH WOOD RSB DATE :12/8/82 NUMBER :AVER

ASH CONTENT = 1.68WT %
MOISTURE CONTENT = 14.18WT %
HIGHER HEATING VALUE = 4300.0KCAL/KG

GAS COMPOSITION:

	WEIGHT %	VOLUME %
H2	9.64	9.85
O2	2.14	1.91
N2	59.86	51.06
CH4	2.52	4.48
CO	10.67	11.00
CO2	32.15	20.76
C2H4	1.15	1.16
C2H6	0.60	0.47
C3H6	0.00	0.00
C4H8	0.00	0.00

METHANE RATIO = 1.00 HYDROGEN RATIO = 0.96

HIGHER HEATING VALUE

4.24	MJ/KG	1011.3	KCAL/KG
5.41	MJ/NM3	1292.8	KCAL/NM3

LOWER HEATING VALUE

3.90	MJ/KG	932.8	KCAL/KG
4.36	MJ/NM3	1100.2	KCAL/NM3

SPECIFIC WEIGHT = 1.277 KG/NM3

AIR FACTOR "S"= 0.320

REACTION PARAMETERS

FLOWRATE AIR (NM3/HR) @ C,1ATM)=	380.44
AIR PRESSURE (BAR REL) =	1.00
FLOWRATE OXYGEN (NM3/HR) =	0.00
OXYGEN PRESSURE (BAR REL) =	0.00
FLOWRATE STEAM (KG/HR) =	0.00
FLOWRATE SOLIDS (KG/HR) =	279.00
FLOWRATE NITROGEN (L/HR)	0.00
AMBIENT TEMPERATURE (C) =	20.00
FLOWRATE CONDENSATE (KG/HR) =	2.00
FLOWRATE FLY ASH (KG/HR) =	0.32
FLOWRATE CHAR (KG/HR) =	0.00
AMBIENT PRESSURE (BAR) =	1.00

TEMPERATURES

REACTOR TEMPERATURE =	722 C
TEMPERATURE PREHEATER =	0 C
TEMPERATURE INLET GAS =	67 C
T11 =	720 C
T18 =	723 C
T9 =	736 C
T5 =	480 C

	KG/HR	C KG/HR	H KG/HR	O KG/HR	N KG/HR	ASH KG/HR
AIR	386.47	0.00	0.00	90.51	297.96	0.00
OXYGEN	0.00	0.00	0.00	0.00	0.00	0.00
NITROGEN	0.00	0.00	0.00	0.00	0.00	0.00
STEAM	0.00	0.00	0.00	0.00	0.00	0.00
SOLIDS WAF	295.20	186.54	13.64	114.74	0.02	0.00
MOISTURE	39.34	0.00	4.37	34.97	0.00	0.00
ASH	4.46	0.00	0.00	0.00	0.00	4.46
TOTAL	667.5	186.54	18.01	240.25	297.98	4.46
TOTAL GAS	595.43	0.00	0.00	0.00	0.00	0.00
H2	3.79	0.00	3.79	0.00	0.00	0.00
O2	12.72	0.00	0.00	12.72	0.00	0.00
N2	297.98	0.00	0.00	0.00	297.96	0.00
CH4	15.00	11.25	3.75	0.00	0.00	0.00
CO	64.71	27.76	0.00	36.95	0.00	0.00
CO2	191.42	52.20	0.00	139.10	0.00	0.00
C2H4	6.84	5.86	0.96	0.00	0.00	0.00
C2H6	2.96	2.37	0.59	0.00	0.00	0.00
C3H6	0.00	0.00	0.00	0.00	0.00	0.00
C4H8	0.00	0.00	0.00	0.00	0.00	0.00
CONDENSATE	73.00	0.96	6.19	64.72	0.00	0.00
FLY ASH	11.62	6.16	0.00	0.00	0.00	3.66
CHAR	0.00	0.00	0.00	0.00	0.00	0.00
TOTAL	681.12	186.62	17.31	253.55	297.96	3.664
BALANCE	102.0	101.04	96.11	105.53	100.00	82.067

TARS IN COND= 1.07 TARS IN GAS= 9.57KG/KG

THERMAL EFFICIENCY = 59.58 %

Y=2.53
X=0.31

THERMAL BALANCE

HEAT OF REACTION (MJ/KG)	6.78	MJ/KG
IN		
SENSIBLE HEAT IN GAS	19.99	MJ/H
SENSIBLE & LATENT HEAT IN STEAM	0.00	MJ/H
HEAT IN FEEDSTOCK	4236.53	MJ/H
TOTAL IN	4256.43	MJ/H
OUT		
SENSIBLE HEAT IN GAS	354.33	MJ/H
SENSIBLE & LATENT HEAT IN STEAM	258.48	MJ/H
SENSIBLE HEAT IN FLY ASH	5.11	MJ/H
SENSIBLE HEAT IN CHAR	0.00	MJ/H
HEAT LOSS REACTOR WALLS	81.19	MJ/H
ENERGY IN GAS	2522.15	MJ/H
ENERGY IN TARS & FLY ASH	292.62	MJ/H
TOTAL OUT	3585.81	MJ/H
HEAT LOSS (BY DIFFERENCE)	768.63	MJ/H

% HEAT LOSS HV1 = 14.936 %

MATERIAL :CH WOOD R31 DATE :13/6/82 NUMBER :1.3

ASH CONTENT = 1.60WT %
MOISTURE CONTENT = 14.10WT %
HIGHER HEATING VALUE = 4388.8KCAL/KG

GAS COMPOSITION

	WEIGHT %	VOLUME %
H2	8.61	6.51
O2	5.43	5.89
N2	57.26	57.16
CH4	2.87	3.68
CO	9.58	9.46
CO2	23.87	14.56
C2H4	1.46	1.45
C2H6	8.14	8.13
C3H8	8.85	8.83
C4H6	8.88	8.88

METHANE RATIO = 8.83 HYDROGEN RATIO = 8.89

HIGHER HEATING VALUE

3.61	MJ/KG	889.3	KCAL/KG
4.75	MJ/NM3	1136.1	KCAL/NM3

LOWER HEATING VALUE

3.51	MJ/KG	837.7	KCAL/KG
4.36	MJ/NM3	1045.7	KCAL/NM3

SPECIFIC WEIGHT = 1.246 KG/NM3

AIR FACTOR "S"= 8.376

REACTION PARAMETERS

FLOWRATE AIR (NM3/HR, 8 C, 1ATM)=	357.34
AIR PRESSURE (BAR REL) =	1.80
FLOWRATE OXYGEN (NM3/HR) =	8.80
OXYGEN PRESSURE (BAR REL) =	8.80
FLOWRATE STEAM (KG/HR) =	8.88
FLOWRATE SOLIDS (KG/HR) =	283.80
FLOWRATE NITROGEN (L/HR)	8.88
AMBIENT TEMPERATURE (C) =	28.80
FLOWRATE CONDENSATE (KG/HR) =	2.28
FLOWRATE FLY ASH (KG/HR) =	8.32
FLOWRATE CHAR (KG/HR) =	8.80
AMBIENT PRESSURE (BAR) =	1.80

TEMPERATURES

REACTOR TEMPERATURE =	883 C
TEMPERATURE PREHEATER =	8 C
TEMPERATURE INLET GAS =	65 C
T11 =	883 C
T18 =	883 C
T9 =	798 C
T5 =	588 C

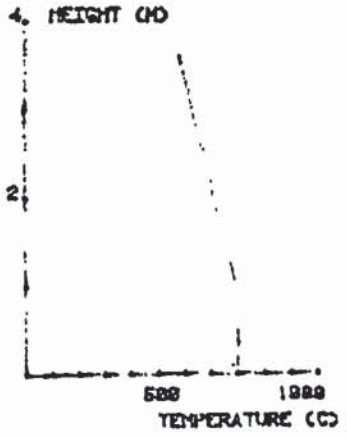

	KG/HR	C KG/HR	H KG/HR	O KG/HR	N KG/HR	ASH KG/HR
AIR	462.84	8.88	8.88	187.65	354.34	8.88
OXYGEN	8.88	8.88	8.88	8.88	8.88	8.88
NITROGEN	8.88	8.88	8.88	8.88	8.88	8.88
STEAM	8.88	8.88	8.88	8.88	8.88	8.88
SOLIDS MAF	234.57	186.87	13.84	116.42	8.82	8.88
MOISTURE	39.88	8.88	4.43	35.47	8.88	8.88
ASH	4.53	8.88	8.88	8.88	8.88	4.53
TOTAL	745.8-	195.87	18.27	279.5%	354.48	4.53
TOTAL GAS	618.73	8.88	8.88	8.88	8.82	8.88
H2	3.78	8.88	3.78	8.88	8.88	8.88
O2	36.87	8.88	8.88	36.87	8.88	8.88
N2	354.48	8.88	8.88	8.88	354.48	8.88
CH4	12.68	3.68	3.28	8.88	8.88	8.88
CO	58.77	25.21	8.88	33.56	8.88	8.88
CO2	142.72	38.96	8.88	183.76	8.88	8.88
C2H4	8.85	7.78	1.28	8.88	8.88	8.88
C2H6	2.84	8.87	8.17	8.88	8.88	8.88
C3H8	8.28	2.24	8.84	8.88	8.88	8.88
C4H6	8.88	8.88	8.88	8.88	8.88	8.88
CONDENSATE	81.16	1.98	9.88	71.18	8.88	8.88
FLY ASH	11.61	6.15	8.88	8.88	8.88	3.66
CHAR	8.88	8.88	8.88	8.88	8.88	8.82
TOTAL	711.62	81.65	17.52	244.48	354.48	3.668
BALANCE	95.5	84.69	96.79	94.19	188.87	88.823

TARS IN COND= 1.16 TARS IN GAS= 6.95KG/KG

THERMAL EFFICIENCY = 64.84 %

Y=2.59
X=0.34

THERMAL BALANCE

HEAT OF REACTION (MJ/KG)	8.34	MJ/KG
IN		
SENSIBLE HEAT IN GAS	22.88	MJ/H
SENSIBLE & LATENT HEAT IN STEAM	8.88	MJ/H
HEAT IN FEEDSTOCK	4297.27	MJ/H
TOTAL IN	4319.85	MJ/H
OUT		
SENSIBLE HEAT IN GAS	446.38	MJ/H
SENSIBLE & LATENT HEAT IN STEAM	283.87	MJ/H
SENSIBLE HEAT IN FLY ASH	6.28	MJ/H
SENSIBLE HEAT IN CHAR	8.88	MJ/H
HEAT LOSS REACTOR WALLS	84.36	MJ/H
ENERGY IN GAS	2355.88	MJ/H
ENERGY IN TARS & FLY ASH	284.76	MJ/H
TOTAL OUT	3488.88	MJ/H
HEAT LOSS (BY DIFFERENCE)	831.85	MJ/H

% HEAT LOSS MV1 = 16.382 %

MATERIAL :CH WOOD R32 DATE :28/6/82 NUMBER :3.4.5

ASH CONTENT = 1.60WT %
MOISTURE CONTENT = 14.10WT %
HIGHER HEATING VALUE = +4300.0KCAL/KG

GAS COMPOSITION

	WEIGHT %	VOLUME %
H2	0.60	0.92
O2	2.47	2.17
N2	56.42	56.51
CH4	2.35	4.11
CO	11.55	11.57
CO2	25.30	16.84
C2H4	1.86	1.87
C2H6	0.24	0.22
C3H6	0.00	0.00
C4H6	0.00	0.00

METHANE RATIO = 0.04 HYDROGEN RATIO = 0.04

HIGHER HEATING VALUE
3.96 MJ/KG 951.7 KCAL/KG
4.89 MJ/NM3 1192.7 KCAL/NM3

LOWER HEATING VALUE
3.68 MJ/KG 879.4 KCAL/KG
4.61 MJ/NM3 1102.0 KCAL/NM3

SPECIFIC WEIGHT = 1.253 KG/NM3

AIR FACTJR "S"= 0.373

REACTION PARAMETERS

FLOWRATE AIR (NM3/HR; 0 C,1ATM)= 347.64
AIR PRESSURE (BAR REL) = 1.00
FLOWRATE OXYGEN (NM3/HR) = 0.00
OXYGEN PRESSURE (BAR REL) = 0.00
FLOWRATE STEAM (KG/HR) = 0.00
FLOWRATE SOLIDS (KG/HR) = 277.50
FLOWRATE NITROGEN (L/HR) 0.00
AMBIENT TEMPERATURE (C) = 10.00
FLOWRATE CONDENSATE (KG/HR) = 1.00
FLOWRATE FLY ASH (KG/HR) = 0.30
FLOWRATE CHAR (KG/HR) = 0.00
AMBIENT PRESSURE (BAR) = 1.00

TEMPERATURES

REACTOR TEMPERATURE = 837 C
TEMPERATURE PREHEATER = 0 C
TEMPERATURE INLET GAS = 83 C
T11 = 836 C
T10 = 836 C
T9 = 817 C
T5 = 648 C

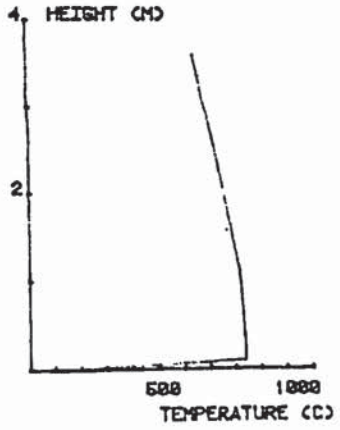

	KG/HR	C KG/HR	H KG/HR	O KG/HR	N KG/HR	ASH KG/HR
AIR	449.50	0.00	0.00	104.73	344.77	0.00
OXYGEN	0.00	0.00	0.00	0.00	0.00	0.00
NITROGEN	0.00	0.00	0.00	0.00	0.00	0.00
STEAM	0.00	0.00	0.00	0.00	0.00	0.00
SOLIDS MAF	233.03	105.97	13.57	114.16	0.02	0.00
MOISTURE	39.13	0.00	4.34	34.76	0.00	0.00
ASH	4.44	0.00	0.00	0.00	0.00	4.44
TOTAL	727.0	105.97	17.91	253.67	344.79	4.44
TOTAL GAS	611.10	0.00	0.00	0.00	0.00	0.00
H2	3.65	0.00	3.65	0.00	0.00	0.00
O2	15.00	0.00	0.00	15.00	0.00	0.00
N2	344.79	0.00	0.00	0.00	344.79	0.00
CH4	14.38	10.79	3.60	0.00	0.00	0.00
CO	70.59	30.26	0.00	40.31	0.00	0.00
CO2	154.63	42.21	0.00	112.42	0.00	0.00
C2H4	6.56	5.64	0.94	0.00	0.00	0.00
C2H6	1.45	1.16	0.29	0.00	0.00	0.00
C3H6	0.00	0.00	0.00	0.00	0.00	0.00
C4H6	0.00	0.00	0.00	0.00	0.00	0.00
CONDENSATE	67.00	0.00	9.74	77.10	0.00	0.00
FLY ASH	13.00	9.57	0.00	0.00	0.00	4.30
CHAR	0.00	0.00	0.00	0.00	0.00	0.00
TOTAL	712.00	100.52	16.21	245.00	344.79	4.298
BALANCE	98.1	94.00	101.00	9658	100.00	96.797

TARS IN COND= 0.00 TARS IN GAS= 3.00KG/[redacted] HR.

THERMAL EFFICIENCY = 67.62 %

Y=2.61
X=0.38

THERMAL BALANCE

HEAT OF REACTION (MJ/KG)	0.27	MJ/KG
IN		
SENSIBLE HEAT IN GAS	30.87	MJ/H
SENSIBLE & LATENT HEAT IN STEAM	0.00	MJ/H
HEAT IN FEEDSTOCK	4213.76	MJ/H
TOTAL IN	4244.62	MJ/H
OUT		
SENSIBLE HEAT IN GAS	489.91	MJ/H
SENSIBLE & LATENT HEAT IN STEAM	326.43	MJ/H
SENSIBLE HEAT IN FLY ASH	6.16	MJ/H
SENSIBLE HEAT IN CHAR	0.00	MJ/H
HEAT LOSS REACTOR WALLS	100.73	MJ/H
ENERGY IN GAS	2434.64	MJ/H
ENERGY IN TARS & FLY ASH	336.73	MJ/H
TOTAL OUT	3698.62	MJ/H
HEAT LOSS (BY DIFFERENCE)	545.00	MJ/H

% HEAT LOSS HV1 = 10.919 %

MATERIAL :CH WOOD RSS DATE :28/8/82 NUMBER :2.4

ASH CONTENT = 1.60W/T %
MOISTURE CONTENT = 14.10W/T %
HIGHER HEATING VALUE = 4398.0KCAL/KG

GAS COMPOSITION

	WEIGHT %	VOLUME %
H2	8.79	18.94
O2	8.66	8.57
N2	49.75	49.45
CH4	2.66	4.96
CO	13.85	12.97
CO2	31.52	19.63
C2H4	8.96	8.97
C2H6	8.26	8.24
C3H6	8.12	8.86
C4H6	8.88	8.88

METHANE RATIO = 1.88 HYDROGEN RATIO = 1.82

HIGHER HEATING VALUE

4.72	MJ/KG	1128.6	KCAL/KG
5.66	MJ/NM3	1498.6	KCAL/NM3

LOWER HEATING VALUE

4.34	MJ/KG	1037.8	KCAL/KG
5.49	MJ/NM3	1289.4	KCAL/NM3

SPECIFIC WEIGHT = 1.243 KG/NM3

AIR FACTOR "S"= 8.328

REACTION PARAMETERS

FLOWRATE AIR (NM3/HR; 8 C,1ATM)=	385.62
AIR PRESSURE (BAR REL) =	1.28
FLOWRATE OXYGEN (NM3/HR) =	8.88
OXYGEN PRESSURE (BAR REL) =	8.88
FLOWRATE STEAM (KG/HR) =	8.88
FLOWRATE SOLIDS (KG/HR) =	277.88
FLOWRATE NITROGEN (L/HR)	8.88
AMBIENT TEMPERATURE (C) =	18.88
FLOWRATE CONDENSATE (KG/HR) =	2.88
FLOWRATE FLY ASH (KG/HR) =	8.38
FLOWRATE CHAR (KG/HR) =	8.88
AMBIENT PRESSURE (BAR) =	1.88

TEMPERATURES

REACTOR TEMPERATURE =	814 C
TEMPERATURE PREHEATER =	8 C
TEMPERATURE INLET GAS =	75 C
T11 = 814 C	
T18 = 813 C	
T9 = 838 C	
T5 = 718 C	

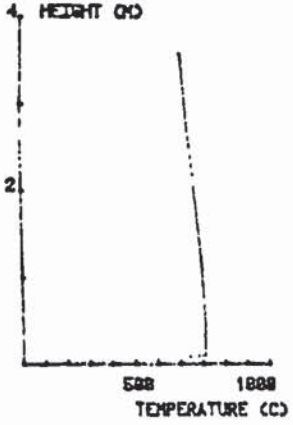

	KG/HR	C KG/HR	H KG/HR	O KG/HR	N KG/HR	ASH KG/HR
AIR	386.17	8.88	8.88	82.86	383.18	8.88
OXYGEN	8.88	8.88	8.88	8.88	8.88	8.88
NITROGEN	8.88	8.88	8.88	8.88	8.88	8.88
STEAM	8.88	8.88	8.88	8.88	8.88	8.88
SOLIDS MAF	233.51	185.78	13.54	(13,95	8.82	8.88
MOISTURE	38.88	8.88	4.34	34.72	8.88	8.88
ASH	4.43	8.88	8.88	8.88	8.88	4.43
TOTAL	672.2	185.78	17.88	240.75	383.12	4.43
TOTAL GAS	888.25	8.88	8.88	8.88	8.88	8.88
H2	4.82	8.88	4.82	8.88	8.88	8.88
O2	4.88	8.88	8.88	4.88	8.88	8.88
N2	383.12	8.88	8.28	8.88	383.12	8.88
CH4	17.43	13.88	4.36	8.88	8.88	8.88
CO	78.63	34.12	8.88	45.41	8.88	8.88
CO2	182.86	52.43	8.88	139.62	8.88	8.88
C2H4	5.97	5.12	8.85	8.88	8.88	8.88
C2H6	1.58	1.28	8.32	8.88	8.88	8.88
C3H6	8.74	8.63	8.11	8.88	8.88	8.88
C4H6	8.88	8.88	8.88	8.88	8.88	8.88
CONDENSATE	83.84	8.84	9.38	73.78	8.88	8.88
FLY ASH	12.88	8.34	8.88	8.88	8.88	3.75
CHAR	8.88	8.88	8.88	8.88	8.88	8.88
TOTAL	785.18	116.82	19.75	282.74	383.12	3.748
BALANCE	104.9	188.48	118.48	109.13	188.88	84.585

TARS IN COND= 8.84 TARS IN GAS= 8.5083/NM HR

THERMAL EFFICIENCY = 88.38 %

Y=2.61
X=0.36

THERMAL BALANCE

HEAT OF REACTION (MJ/KG)	7.77	MJ/KG
IN		
SENSIBLE HEAT IN GAS	23.69	MJ/H
SENSIBLE & LATENT HEAT IN STEAM	8.88	MJ/H
HEAT IN FEEDSTOCK	4206.16	MJ/H
TOTAL IN	4229.85	MJ/H
OUT		
SENSIBLE HEAT IN GAS	553.16	MJ/H
SENSIBLE & LATENT HEAT IN STEAM	324.48	MJ/H
SENSIBLE HEAT IN FLY ASH	7.84	MJ/H
SENSIBLE HEAT IN CHAR	8.88	MJ/H
HEAT LOSS REACTOR WALLS	183.69	MJ/H
ENERGY IN GAS	2873.27	MJ/H
ENERGY IN TARS & FLY ASH	296.61	MJ/H
TOTAL OUT	4158.85	MJ/H
HEAT LOSS (BY DIFFERENCE)	71.88	MJ/H

% HEAT LOSS HV1 = 1.439 %

MATERIAL :CH WOOD R34 DATE :23/8/82 NUMBER :4,5

ASH CONTENT = 1.60WT %
MOISTURE CONTENT = 14.10WT %
HIGHER HEATING VALUE = 4300.0KCAL/KG

GAS COMPOSITION

	WEIGHT %	VOLUME %
H2	8.51	7.41
O2	3.53	3.22
N2	51.67	53.79
CH4	1.76	3.19
CO	18.36	18.60
CO2	30.96	20.40
C2H4	0.78	0.60
C2H6	0.35	0.34
C3H6	0.07	0.05
C4H6	0.00	0.00

METHANE RATIO = 0.02 HYDROGEN RATIO = 1.11

HIGHER HEATING VALUE
3.36 MJ/KG 802.5 KCAL/KG
4.36 MJ/NM3 1045.2 KCAL/NM3

LOWER HEATING VALUE
3.11 MJ/KG 742.6 KCAL/KG
4.05 MJ/NM3 967.5 KCAL/NM3

SPECIFIC WEIGHT = 1.303 KG/NM3

AIR FACTOR "S"= 0.321

REACTION PARAMETERS

FLOWRATE AIR (NM3/HR; 0 C,1ATM)=	250.35
AIR PRESSURE (BAR REL) =	0.02
FLOWRATE OXYGEN (NM3/HR) =	0.00
OXYGEN PRESSURE (BAR REL) =	0.00
FLOWRATE STEAM (KG/HR) =	0.00
FLOWRATE SOLIDS (KG/HR) =	232.00
FLOWRATE NITROGEN (L/HR) =	0.00
AMBIENT TEMPERATURE (C) =	16.00
FLOWRATE CONDENSATE (KG/HR) =	2.60
FLOWRATE FLY ASH (KG/HR) =	0.26
FLOWRATE CHAR (KG/HR) =	0.00
AMBIENT PRESSURE (BAR) =	1.00

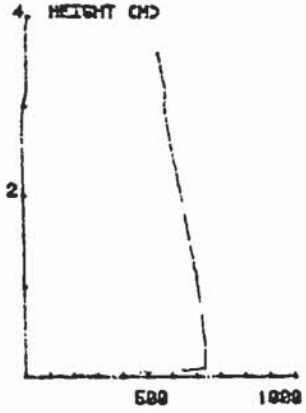

TEMPERATURES

REACTOR TEMPERATURE =	735 C
TEMPERATURE PREHEATER =	0 C
TEMPERATURE INLET GAS =	63 C
T11 = 735 C	
T10 = 735 C	
T9 = 706 C	
T5 = 545 C	

	KG/HR	C KG/HR	H KG/HR	O KG/HR	N KG/HR	ASH KG/HR
AIR	323.78	0.00	0.00	75.42	248.28	0.00
OXYGEN	0.00	0.00	0.00	0.00	0.00	0.00
NITROGEN	0.00	0.00	0.00	0.00	0.00	0.00
STEAM	0.00	0.00	0.00	0.00	0.00	0.00
SOLIDS MAF	196.58	66.68	11.34	95.44	0.82	0.00
MOISTURE	32.71	0.00	3.63	29.08	0.00	0.00
ASH	3.71	0.00	0.00	0.00	0.00	3.71
TOTAL	555.7	66.68	14.97	199.94	248.38	3.71
TOTAL GAS	489.58	0.00	0.00	0.00	0.00	0.00
H2	2.46	0.00	2.46	0.00	0.00	0.00
O2	16.96	0.00	0.00	16.96	0.00	0.00
N2	246.38	0.00	0.00	0.00	246.38	0.00
CH4	8.46	6.35	2.12	0.00	0.00	0.00
CO	49.86	21.39	0.00	28.47	0.00	0.00
CO2	148.77	40.62	0.00	108.16	0.00	0.00
C2H4	3.73	3.19	0.53	0.00	0.00	0.00
C2H6	1.69	1.35	0.34	0.00	0.00	0.00
C3H6	0.35	0.30	0.05	0.00	0.00	0.00
C4H6	0.00	0.00	0.00	0.00	0.00	0.00
CONDENSATE	90.73	0.91	10.07	79.76	0.00	0.00
FLY ASH	6.43	5.81	0.00	0.00	0.00	2.61
CHAR	0.00	0.00	0.00	0.00	0.00	0.00
TOTAL	579.74	79.92	15.56	293.35	248.38	2.612
BALANCE	104.3	98.28	183.91	116.7	188.38	78.361

TARS IN COND= 1.81 TARS IN GAS= 3.14KG/NM3 WG

THERMAL EFFICIENCY = 45.86 %

Y=2.96
X=0.46

THERMAL BALANCE

HEAT OF REACTION (MJ/KG)	11.46	MJ/KG
IN		
SENSIBLE HEAT IN GAS	15.17	MJ/H
SENSIBLE & LATENT HEAT IN STEAM	0.00	MJ/H
HEAT IN FEEDSTOCK	3522.85	MJ/H
TOTAL IN	3538.02	MJ/H
OUT		
SENSIBLE HEAT IN GAS	314.85	MJ/H
SENSIBLE & LATENT HEAT IN STEAM	319.85	MJ/H
SENSIBLE HEAT IN FLY ASH	4.16	MJ/H
SENSIBLE HEAT IN CHAR	0.00	MJ/H
HEAT LOSS REACTOR WALLS	65.00	MJ/H
ENERGY IN GAS	1614.36	MJ/H
ENERGY IN TARS & FLY ASH	214.37	MJ/H
TOTAL OUT	2552.68	MJ/H
HEAT LOSS (BY DIFFERENCE)	985.34	MJ/H

% HEAT LOSS HV1 = 23.576 %

MATERIAL :CH WOOD R36 DATE :23/6/82 NUMBER :1.2

ASH CONTENT = 1.60WT %
MOISTURE CONTENT = 14.18WT %
HIGHER HEATING VALUE = 4300.0KCAL/KG

GAS COMPOSITION

	WEIGHT %	VOLUME %
H2	0.63	0.91
O2	0.83	0.74
N2	49.69	58.83
CH4	2.61	4.64
CO	12.16	12.41
CO2	32.23	20.65
C2H4	1.65	1.66
C2H6	0.34	0.32
C3H6	0.84	0.83
C4H6	0.00	0.00

METHANE RATIO = 1.00 HYDROGEN RATIO = 0.00

HIGHER HEATING VALUE

4.00	MJ/KG	1098.1	KCAL/KG
5.00	MJ/NM3	1399.0	KCAL/NM3

LOWER HEATING VALUE

4.25	MJ/KG	1015.1	KCAL/KG
5.42	MJ/NM3	1294.0	KCAL/NM3

SPECIFIC WEIGHT = 1.275 KG/NM3

AIR FACTOR "S"= 0.267

REACTION PARAMETERS

FLOWRATE AIR (NM3/HR; 0 C,1ATM)=	282.66
AIR PRESSURE (BAR REL) =	0.75
FLOWRATE OXYGEN (NM3/HR) =	0.00
OXYGEN PRESSURE (BAR REL) =	0.00
FLOWRATE STEAM (KG/HR) =	0.00
FLOWRATE SOLIDS (KG/HR) =	226.00
FLOWRATE NITROGEN (L/HR)	0.00
AMBIENT TEMPERATURE (C) =	16.00
FLOWRATE CONDENSATE (KG/HR) =	2.50
FLOWRATE FLY ASH (KG/HR) =	0.50
FLOWRATE CHAR (KG/HR) =	0.00
AMBIENT PRESSURE (BAR) =	1.00

TEMPERATURES

REACTOR TEMPERATURE =	600 C
TEMPERATURE PREHEATER =	0 C
TEMPERATURE INLET GAS =	60 C
T11 = 698 C	
T10 = 699 C	
T9 = 660 C	
T5 = 593 C	

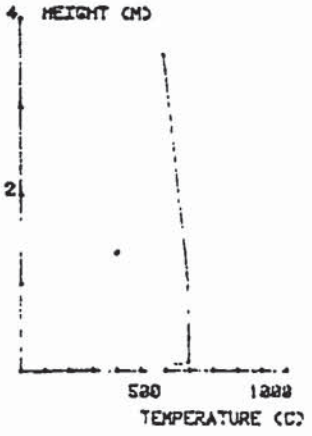

	KG/HR	C KG/HR	H KG/HR	O KG/HR	N KG/HR	ASH KG/HR
AIR	282.66	0.00	0.00	61.06	201.00	0.00
OXYGEN	0.00	0.00	0.00	0.00	0.00	0.00
NITROGEN	0.00	0.00	0.00	0.00	0.00	0.00
STEAM	0.00	0.00	0.00	0.00	0.00	0.00
SOLIDS MAF	198.52	86.38	11.86	92.44	0.02	0.00
MOISTURE	31.67	0.00	3.54	28.33	0.00	0.00
ASH	3.62	0.00	0.00	0.00	0.00	3.62
TOTAL	482.1	86.30	14.59	182.36	201.02	3.62
TOTAL GAS	484.56	0.00	0.00	0.00	0.00	0.00
H2	2.54	0.00	2.54	0.00	0.00	0.00
O2	3.36	0.00	0.00	3.36	0.00	0.00
N2	201.02	0.00	0.00	0.00	201.02	0.00
CH4	18.57	7.92	2.64	0.00	0.00	0.00
CO	49.29	21.14	0.00	28.14	0.00	0.00
CO2	129.58	35.38	0.00	94.20	0.00	0.00
C2H4	6.66	5.71	0.95	0.00	0.00	0.00
C2H6	1.36	1.09	0.27	0.00	0.00	0.00
C3H6	0.15	0.15	0.03	0.00	0.00	0.00
C4H6	0.00	0.00	0.00	0.00	0.00	0.00
CONDENSATE	69.96	9.78	7.76	61.52	0.00	0.00
FLY ASH	5.48	5.79	0.00	0.00	0.00	2.00
CHAR	0.00	0.00	0.00	0.00	0.00	0.00
TOTAL	482.00	77.69	14.29	187.24	201.02	2.000
BALANCE	98.9	90.25	97.33	102.67	100.00	71.994

TARS IN COND= 0.76 TARS IN GAS= 4.38KG/KG

THERMAL EFFICIENCY = 54.23 %

Y=2.12
X=0.37

THERMAL BALANCE

HEAT OF REACTION (MJ/KG)	9.34	MJ/KG
IN		
SENSIBLE HEAT IN GAS	11.43	MJ/H
SENSIBLE & LATENT HEAT IN STEAM	0.00	MJ/H
HEAT IN FEEDSTOCK	3431.74	MJ/H
TOTAL IN	3443.17	MJ/H
OUT		
SENSIBLE HEAT IN GAS	381.51	MJ/H
SENSIBLE & LATENT HEAT IN STEAM	253.72	MJ/H
SENSIBLE HEAT IN FLY ASH	4.52	MJ/H
SENSIBLE HEAT IN CHAR	0.00	MJ/H
HEAT LOSS REACTOR WALLS	67.50	MJ/H
ENERGY IN GAS	1859.70	MJ/H
ENERGY IN TARS & FLY ASH	206.95	MJ/H
TOTAL OUT	2715.40	MJ/H
HEAT LOSS (BY DIFFERENCE)	727.77	MJ/H

% HEAT LOSS HV1 = 17.877 %

Run 36

	1.68WT %
MOISTURE CONTENT =	14.18WT %
HIGHER HEATING VALUE =	4388.8KCAL/KG

GAS COMPOSITION

	WEIGHT %	VOLUME %
H2	8.97	11.74
O2	8.81	8.52
N2	48.34	47.81
CH4	3.24	5.43
CO	14.34	14.53
CO2	23.83	17.31
C2H4	1.37	1.38
C2H6	8.38	8.26
C3H6	8.27	8.84
C4H8	8.28	8.88

METHANE RATIO = 3.36 HYDROGEN RATIO = 8.34

HIGHER HEATING VALUE

5.71	MJ/KG	1364.4 KCAL/KG
8.35	MJ/NM3	1668.8 KCAL/NM3

LOWER HEATING VALUE

5.27	MJ/KG	1256.8 KCAL/KG
6.41	MJ/NM3	1531.3 KCAL/NM3

SPECIFIC WEIGHT = 1.217 KG/NM3

AIR FACTOR "S"= 2.322

REACTION PARAMETERS

FLOWRATE AIR (NM3/HR; 8 C,1ATM)=	243.24
AIR PRESSURE (BAR REL) =	8.62
FLOWRATE OXYGEN (NM3/HR) =	8.28
OXYGEN PRESSURE (BAR REL) =	8.28
FLOWRATE STEAM (KG/HR) =	2.28
FLOWRATE SOLIDS (KG/HR) =	238.88
FLOWRATE NITROGEN (L/HR)	8.88
AMBIENT TEMPERATURE (C) =	15.88
FLOWRATE CONDENSATE (KG/HR) =	2.88
FLOWRATE FLY ASH (KG/HR) =	8.38
FLOWRATE CHAR (KG/HR) =	8.88
AMBIENT PRESSURE (BAR) =	1.88

TEMPERATURES

REACTOR TEMPERATURE =	788 C
TEMPERATURE PREHEATER =	8 C
TEMPERATURE INLET GAS =	64 C
T11 = 781 C	
T18 = 782 C	
T2 = 755 C	
T5 = 678 C	

	KG/HR	C KG/HR	H KG/HR	O KG/HR	N KG/HR	ASH KG/HR
AIR	322.36	8.88	8.28	75.29	247.17	8.28
OXYGEN	2.88	2.88	8.88	8.22	8.23	8.88
NITROGEN	2.88	2.88	8.88	8.88	8.28	8.88
STEAM	8.88	8.28	8.88	8.88	8.88	8.88
SOLIDS DAF	123.68	97.83	11.25	96.68	8.52	8.88
MOISTURE	32.43	8.88	3.68	28.83	8.88	8.88
ASH	3.69	8.88	8.88	8.28	8.82	3.69
TOTAL	572.3	97.83	14.45	266.58	247.13	3.68
TOTAL GAS	585.13	8.88	8.82	8.28	8.83	8.88
H2	4.36	8.88	4.36	8.88	8.88	8.88
O2	8.86	8.88	8.88	3.86	8.88	8.88
N2	247.19	8.88	8.88	8.88	247.13	8.88
CH4	16.35	12.27	4.28	8.88	8.88	8.88
CO	75.44	32.36	8.88	43.08	8.88	8.88
CO2	142.34	48.12	8.88	126.83	8.88	8.88
C2H4	8.33	8.51	1.42	8.88	8.88	8.88
C2H6	1.49	1.19	8.38	8.88	8.88	8.88
C3H8	8.34	8.23	8.86	8.88	8.28	8.88
C4H8	8.88	8.88	8.88	8.28	8.88	8.88
CONDENSATE	72.76	8.36	8.27	63.75	8.88	8.88
FLY ASH	12.31	7.75	8.88	2.28	8.88	3.17
CHAR	8.28	8.88	8.88	8.28	8.88	8.88
TOTAL	568.81	125.43	16.31	218.71	247.13	3.165
BALANCE	106.6	117.76	123.32	108.04	130.32	96.333

TARS IN COND= 1.36 TARS IN GAS= 7.36KG/KG H-7

THERMAL EFFICIENCY = 82.67 %

Y=2.60
X=0.38

THERMAL BALANCE 82.67

HEAT OF REACTION (KJ/KG)	6.34	MJ/KG
IN:		
SENSIBLE HEAT IN GAS	15.46	MJ/H
SENSIBLE & LATENT HEAT IN STEAM	8.88	MJ/H
HEAT IN FEEDSTOCK	3432.48	MJ/H
TOTAL IN	3587.34	MJ/H
OUT		
SENSIBLE HEAT IN GAS	460.26	MJ/H
SENSIBLE & LATENT HEAT IN STEAM	276.73	MJ/H
SENSIBLE HEAT IN FLY ASH	8.75	MJ/H
SENSIBLE HEAT IN CHAR	8.08	MJ/H
HEAT LOSS REACTOR WALLS	34.96	MJ/H
ENERGY IN GAS	2586.84	MJ/H
ENERGY IN TARS & FLY ASH	276.66	MJ/H
TOTAL OUT	3396.75	MJ/H
HEAT LOSS (BY DIFFERENCE)	-447.42	MJ/H

% Heat loss — 13.9

MATERIAL :CH WOOD R37 DATE :14/10/82 NUMBER :AVER

ASH CONTENT = 1.60WT %
MOISTURE CONTENT = 12.00WT %
HIGHER HEATING VALUE = 4300.0KCAL/KG

GAS COMPOSITION

	WEIGHT %	VOLUME %
H2	0.68	9.48
O2	0.83	0.73
N2	49.00	48.99
CH4	2.75	4.79
CO	15.34	15.34
CO2	28.69	18.15
C2H4	2.14	2.12
C2H6	0.36	0.33
C3H6	0.21	0.14
C4H8	0.00	0.00

METHANE RATIO = 1.81 HYDROGEN RATIO = 0.99

HIGHER HEATING VALUE
5.40 MJ/KG 1291.2 KCAL/KG
6.76 MJ/NM3 1615.1 KCAL/NM3

LOWER HEATING VALUE
5.02 MJ/KG 1198.7 KCAL/KG
6.28 MJ/NM3 1498.9 KCAL/NM3

SPECIFIC WEIGHT = 1.251 KG/NM3

AIR FACTOR "S"= 0.289

REACTION PARAMETERS

FLOWRATE AIR (NM3/HR; 0 C,1ATM)=	338.86
AIR PRESSURE (BAR REL) =	0.42
FLOWRATE OXYGEN (NM3/HR) =	0.00
OXYGEN PRESSURE (BAR REL) =	0.00
FLOWRATE STEAM (KG/HR) =	0.00
FLOWRATE SOLIDS (KG/HR) =	340.00
FLOWRATE NITROGEN (L/HR)	0.00
AMBIENT TEMPERATURE (C) =	10.00
FLOWRATE CONDENSATE (KG/HR) =	1.91
FLOWRATE FLY ASH (KG/HR) =	0.50
FLOWRATE CHAR (KG/HR) =	0.00
AMBIENT PRESSURE (BAR) =	1.00

TEMPERATURES

REACTOR TEMPERATURE =	871 C
TEMPERATURE PREHEATER =	0 C
TEMPERATURE INLET GAS =	56 C
T11 = 873 C	
T10 = 870 C	
T9 = 859 C	
T5 = 771 C	

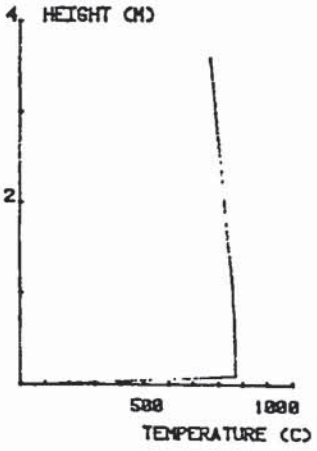

	KG/HR	KG/HR	H KG/HR	O KG/HR	N KG/HR	ASH KG/HR
AIR	438.14	0.	0.00	102.00	336.85	0.00
OXYGEN	0.00	0.	0.00	0.00	0.00	0.00
NITROGEN	0.00	0.00	0.00	0.00	0.00	0.00
STEAM	0.00	0.00	0.00	0.00	0.00	0.00
SOLIDS MAF	285.76	133.07	17.04	141.41	0.03	0.00
MOISTURE	40.00	0.00	4.53	36.27	0.00	0.00
ASH	5.44	0.00	0.00	0.00	0.00	5.44
TOTAL	778.1	133.07	21.57	281.72	336.88	5.44
TOTAL GAS	685.93	0.00	0.00	0.00	0.00	0.00
H2	4.64	0.00	4.64	0.00	0.00	0.00
O2	5.78	0.00	0.00	5.78	0.00	0.00
N2	336.00	0.00	0.00	0.00	336.00	0.00
CH4	18.86	14.14	4.71	0.00	0.00	0.00
CO	185.21	45.14	0.00	60.00	0.00	0.00
CO2	196.00	53.73	0.00	143.07	0.00	0.00
C2H4	14.69	12.59	2.10	0.00	0.00	0.00
C2H6	2.49	1.99	0.50	0.00	0.00	0.00
C3H6	1.46	1.25	0.21	0.00	0.00	0.00
C4H8	0.00	0.00	0.00	0.00	0.00	0.00
CONDENSATE	82.81	1.87	9.16	72.37	0.00	0.00
FLY ASH	21.63	15.14	0.00	0.00	0.00	6.49
CHAR	0.00	0.00	0.00	0.00	0.00	0.00
TOTAL	798.17	145.05	21.32	281.22	336.00	6.488
BALANCE	101 5	109.00	98.87	9981	100.00	119.269

TARS IN COND= 1.28 TARS IN GAS= 0.00KG/HR

THERMAL EFFICIENCY = 78.12 %

Y=2.34
X=0.28

THERMAL BALANCE

HEAT OF REACTION (MJ/KG)	6.67	MJ/KG
IN		
SENSIBLE HEAT IN GAS	17.19	MJ/H
SENSIBLE & LATENT HEAT IN STEAM	0.00	MJ/H
HEAT IN FEEDSTOCK	5291.41	MJ/H
TOTAL IN	5308.60	MJ/H
OUT		
SENSIBLE HEAT IN GAS	679.85	MJ/H
SENSIBLE & LATENT HEAT IN STEAM	330.24	MJ/H
SENSIBLE HEAT IN FLY ASH	15.27	MJ/H
SENSIBLE HEAT IN CHAR	0.00	MJ/H
HEAT LOSS REACTOR WALLS	112.88	MJ/H
ENERGY IN GAS	3787.45	MJ/H
ENERGY IN TARS & FLY ASH	524.66	MJ/H
TOTAL OUT	5368.75	MJ/H
HEAT LOSS (BY DIFFERENCE)	-60.15	MJ/H

% HEAT LOSS HV1 = -0.982 %

MATERIAL :CH WOOD R36 DATE :15/10/82 NUMBER :AVER

ASH CONTENT = 1.60WT %
MOISTURE CONTENT = 12.00WT %
HIGHER HEATING VALUE = 4300.0KCAL/KG

GAS COMPOSITION

	WEIGHT %	VOLUME %
H2	0.72	9.66
O2	1.57	1.35
N2	48.80	48.19
CH4	3.85	5.25
CO	16.41	16.18
CO2	26.85	16.76
C2H4	2.07	2.02
C2H6	0.35	0.32
C3H6	0.10	0.12
C4H6	0.00	0.00

METHANE RATIO = 1.00 HYDROGEN RATIO = 1.83

HIGHER HEATING VALUE

5.68	MJ/KG	1357.9	KCAL/KG
7.01	MJ/NM3	1675.5	KCAL/NM3

LOWER HEATING VALUE

5.27	MJ/KG	1260.1	KCAL/KG
6.51	MJ/NM3	1554.8	KCAL/NM3

SPECIFIC WEIGHT = 1.234 KG/NM3

AIR FACTOR "S"= 0.285

REACTION PARAMETERS

FLOWRATE AIR (NM3/HR, 0 C,1ATM)=	333.78
AIR PRESSURE (BAR REL) =	0.42
FLOWRATE OXYGEN (NM3/HR) =	0.00
OXYGEN PRESSURE (BAR REL) =	0.00
FLOWRATE STEAM (KG/HR) =	0.00
FLOWRATE SOLIDS (KG/HR) =	340.00
FLOWRATE NITROGEN (L/HR)	0.00
AMBIENT TEMPERATURE (C) =	10.00
FLOWRATE CONDENSATE (KG/HR) =	1.30
FLOWRATE FLY ASH (KG/HR) =	0.48
FLOWRATE CHAR (KG/HR) =	0.00
AMBIENT PRESSURE (BAR) =	1.00

TEMPERATURES

REACTOR TEMPERATURE =	865 C
TEMPERATURE PREHEATER =	0 C
TEMPERATURE INLET GAS =	60 C
T11 = 865 C	
T10 = 864 C	
T9 = 862 C	
T5 = 775 C	

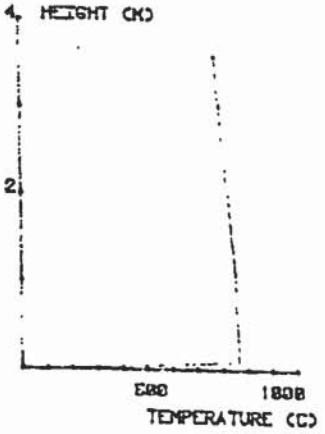

	KG/HR	C KG/HR	H KG/HR	O KG/HR	N KG/HR	ASH KG/HR
AIR	431.47	0.00	0.00	100.53	330.94	0.00
OXYGEN	0.00	0.00	0.00	0.00	0.00	0.00
NITROGEN	0.00	0.00	0.00	0.00	0.00	0.00
STEAM	0.00	0.00	0.00	0.00	0.00	0.00
SOLIDS MAF	283.76	133.87	17.04	143.35	0.03	0.00
MOISTURE	48.00	0.00	4.53	36.27	0.00	0.00
ASH	5.44	0.00	0.00	0.00	0.00	5.44
TOTAL	771.5	133.87	21.57	280.15	330.97	5.44
TOTAL GAS	678.25	0.00	0.00	0.00	0.00	0.00
H2	4.87	0.00	4.87	0.00	0.00	0.00
O2	18.64	0.00	0.00	18.64	0.00	0.00
N2	330.97	0.00	0.00	0.00	330.97	0.00
CH4	28.72	15.54	5.18	0.00	0.00	0.00
CO	111.29	47.74	0.00	63.55	0.00	0.00
CO2	182.12	49.72	0.00	132.48	0.00	0.00
C2H4	14.82	12.81	2.00	0.00	0.00	0.00
C2H6	2.36	1.89	0.47	0.00	0.00	0.00
C3H6	1.27	1.00	0.16	0.00	0.00	0.00
C4H6	0.00	0.00	0.00	0.00	0.00	0.00
CONDENSATE	65.18	0.65	7.22	57.03	0.00	0.00
FLY ASH	24.04	16.63	0.00	0.00	0.00	7.21
CHAR	0.00	0.00	0.00	0.00	0.00	0.00
TOTAL	767.39	145.00	19.93	283.62	330.97	7.211
BALANCE	99.5	109.46	92.41	94.10	100.00	132.559

TARS IN COND= 0.95 TARS IN GAS= 0.00KG/HR

THERMAL EFFICIENCY = 72.91 %

Y=2.31

X=0.22

THERMAL BALANCE

HEAT OF REACTION (MJ/KG)	0.17	MJ/KG
IN		
SENSIBLE HEAT IN GAS	23.04	MJ/H
SENSIBLE & LATENT HEAT IN STEAM	0.00	MJ/H
HEAT IN FEEDSTOCK	5291.41	MJ/H
TOTAL IN	5314.46	MJ/H
OUT		
SENSIBLE HEAT IN GAS	681.17	MJ/H
SENSIBLE & LATENT HEAT IN STEAM	289.79	MJ/H
SENSIBLE HEAT IN FLY ASH	17.86	MJ/H
SENSIBLE HEAT IN CHAR	0.00	MJ/H
HEAT LOSS REACTOR WALLS	111.00	MJ/H
ENERGY IN GAS	3855.34	MJ/H
ENERGY IN TARS & FLY ASH	574.11	MJ/H
TOTAL OUT	5580.95	MJ/H
HEAT LOSS (BY DIFFERENCE)	-185.00	MJ/H

% HEAT LOSS HV1 = -3.035 %

APPENDIX VI - PROGRAMME MASS - ENERGY BALANCES

This Appendix presents the programme written to carry out the calculations for the mass balance and the energy balance.

```
100 PAGE
110 PRINT "=========================================================="
120 PRINT "MASS AND ENERGY BALANCE FOR GASIFICATION FB VYNCKE"
130 PRINT "=========================================================="
140 PRINT
150 PRINT
160 INIT
170 DIM B(5),C(15),R(13),M(13),G(13),D(15),A(3),E(16),P(11)
180 PRINT "MATERIAL TYPE ?"
190 INPUT A$
200 PRINT "DATE OF EXPERIMENTS ?"
210 INPUT B$
220 PRINT "NUMBER OF GC ANALYSIS ?"
230 INPUT C$
240 PRINT "MATERIAL CHARACTERISTICS"
250 PRINT USING "24""-""";
260 PRINT "ASH CONTENT (WT %) ?"
270 INPUT A(1)
280 PRINT "MOISTURE CONTENT (WT %) ?"
290 INPUT A(2)
300 PRINT "HIGHER HEATING VALUE SOLIDS (KCAL/KG) ?"
310 INPUT A(3)
320 C=0
330 B=0
340 D=0
350 T=0
360 PRINT "MOLECULAR SIEVE ANALYSIS"
370 PRINT USING "24""-""";
380 PRINT "H2,O2,N2,CH4,CO ?"
390 INPUT B
400 PRINT "CHROMOSORB ANALYSYS"
410 PRINT USING "19""-""";
420 PRINT "H2,COMP,CH4,CO2,C2H4,C2H6,C3H6,C4H6?"
430 INPUT C(1),C(2),C(3),C(4),C(5),C(6),C(12),C(13)
440 PRINT "C TARS/C CH4 ?"
450 INPUT C(14)
460 PAGE
470 PRINT "FLOWRATES"
480 PRINT USING "9""-""";
490 PRINT "FLOWRATE AIR (M3/HR) ?"
500 INPUT D(1)
510 PRINT "AIR PRESSURE (BAR RELATIVE = MANO READING !!!!!!!!!!)"
520 INPUT D(2)
530 PRINT "FLOWRATE OXYGEN (M3/HR) ?"
540 INPUT D(3)
550 PRINT "OXYGEN PRESSURE (BAR REL !!!!!!!!!!!!!)"
560 INPUT D(4)
570 PRINT "FLOWRATE STEAM (KG/HR) ?"
580 INPUT D(5)
590 PRINT "FLOWRATE SOLIDS (KG/HR) ?"
600 INPUT D(6)
610 PRINT "FLOWRATE NITROGEN (LITER/HR) ?"
620 INPUT D(7)
630 PRINT "FLOWRATE CONDENSATE (KG/HR) ?"
640 INPUT D(9)
650 PRINT "FLOWRATE FLY-ASH (KG/HR) ?"
660 INPUT D(10)
```

```
670 PRINT "FLOWRATE CHAR (KG/HR) ?"
680 INPUT D(11)
690 PRINT "AMBIENT TEMPERATURE (C) ?"
700 INPUT D(8)
710 PRINT "AMBIENT PRESSURE (BAR) !!!!!!!!!!!!!!!!!!!!"
720 INPUT D(12)
730 PRINT "GAS FLOWRATE OF SAMPLING LINE KG/HR?"
740 INPUT D(13)
750 PRINT "C IN CONDENSATE KG/KG ?"
760 INPUT D(14)
770 PRINT "AIR TEMPERATURE (C) ?"
780 INPUT D(15)
790 PAGE
800 PRINT "TEMPERATURES"
810 PRINT USING "12""-""":
820 PRINT "T REACTOR ?"
830 INPUT E(13)
840 PRINT "T PREHEATER ?"
850 INPUT E(15)
860 PRINT "T INLET GASES ?"
870 INPUT E(12)
880 PRINT "T 11 ?"
890 INPUT E(11)
900 PRINT "T 10 ?"
910 INPUT E(10)
920 PRINT "T 9 ?"
930 INPUT E(9)
940 PRINT "T 5 ? (EXIT REACTOR)"
950 INPUT E(5)
960 K=C(2)/(B(2)+B(3)+B(5))
970 FOR I=1 TO 5
980 C(I+6)=K*B(I)
990 NEXT I
1000 FOR J=1 TO 13
1010 READ R(J)
1020 DATA 0.00362,1,0.105,1,0.251,0.221,0.00362,0.489,0.564,0.105,0.58
1030 DATA 0.311,0.262
1040 C(J)=R(J)*C(J)
1050 NEXT J
1060 FOR J=1 TO 13
1070 READ M(J)
1080 DAT 0.0899,1,0.718,1.977,1.261,1.357,0.0899,1.429,1.251,0.718,1.25
1090 DATA 1.877,2.413
1100 G(J)=C(J)/M(J)
1110 NEXT J
1120 T1=C(4)+C(5)+C(6)+C(7)+C(8)+C(9)+C(10)+C(11)+C(12)+C(13)
1130 T2=G(4)+G(5)+G(6)+G(7)+G(8)+G(9)+G(10)+G(11)+G(12)+G(13)
1140 FOR I=1 TO 13
1150 C(I)=C(I)*100/T1
1160 G(I)=G(I)*100/T2
1170 NEXT I
1180
1190 REM
1200 P(1)=C(3)/C(10)
1210 REM
1220 P(10)=C(1)/C(7)
1230 REM HIGHER HEATING VALUE
```

```
1240 R1=G(4)*1.977+G(5)*1.261+G(6)*1.357+G(7)*0.0899+G(8)*1.429
1250 R1=R1+G(9)*1.251+G(10)*0.718+G(11)*1.251+G(12)*1.877+G(13)*2.413
1260 R1=R1/100
1270 P(2)=C(5)*50.3+C(6)*51.87+C(7)*141.8+C(10)*55.5+C(11)*10.11
1280 P(2)=(P(2)+C(12)*48.92+C(13)*47.69)/100
1290 P(3)=P(2)*1000/4.186
1300 P(4)=P(2)*R1
1310 P(5)=P(3)*R1
1320 REM LOWER HEATING VALUE
1330 P(6)=C(5)*47.2+C(6)*47.5+C(7)*120+C(10)*50.01+C(11)*10.11
1340 P(6)=(P(6)+C(12)*45.78+C(13)*45.25)/100
1350 P(7)=P(6)*1000/4.186
1360 P(8)=P(6)*R1
1370 P(9)=P(7)*R1
1380 PAGE
1390 PRINT USING 1400:A$,B$,C$
1400 IMAGE 2X,"MATERIAL :",12A,5X,"DATE :",10A,"NUMBER :",10A,/,/
1410 PRINT USING 1420:A(1)
1420 IMAGE 2X,"ASH CONTENT =",30T,4D.2D,"WT %"
1430 PRINT USING 1440:A(2)
1440 IMAGE 2X,"MOISTURE CONTENT =",30T,4D.2D,"WT %"
1450 PRINT USING 1460:A(3)
1460 IMAGE 2X,"HIGHER HEATING VALUE =",29T,5D.1D,"KCAL/KG",/
1470 PRINT "GAS COMPOSITION"
1480 PRINT USING "15""-""";
1490 PRINT USING 1500:"WEIGHT %","VOLUME %"
1500 IMAGE 19X,8A,5X,8A
1510 FOR J=7 TO 11
1520 READ D$
1530 DATA "H2","O2","N2","CH4","CO"
1540 PRINT USING 1560:D$,C(J),G(J)
1550 NEXT J
1560 IMAGE 5X,5A,5X,6D.2D,5X,6D.2D
1570 FOR J=4 TO 6
1580 READ D$
1590 DATA "CO2","C2H4","C2H6"
1600 PRINT USING 1560:D$,C(J),G(J)
1610 NEXT J
1620 FOR J=12 TO 13
1630 READ D$
1640 DATA "C3H6","C4H6"
1650 PRINT USING 1560:D$,C(J),G(J)
1660 NEXT J
1670 PRINT USING 1680:P(1),P(10)
1680 IMAGE /,"METHANE RATIO = ",4D.2D,"HYDROGEN RATIO = ",4D.2D,/
1690 PRINT "HIGHER HEATING VALUE"
1700 PRINT USING 1720:P(2),P(3)
1710 PRINT USING 1730:P(4),P(5)
1720 IMAGE 5X,3D.2D,15T,"MJ/KG",34T,5D.1D,45T"KCAL/KG"
1730 IMAGE 5X,3D.2D,15T,"MJ/NM3",34T,5D.1D,45T,"KCAL/NM3",/
1740 PRINT "LOWER HEATING VALUE"
1750 PRINT USING 1720:P(6),P(7)
1760 PRINT USING 1730:P(8),P(9)
1770 PRINT USING 1780:R1
1780 IMAGE   "SPECIFIC WEIGHT =     ",2D.3D," KG/NM3"
1790 PRINT "DO YOU WANT A LISTING OF THE REACTION PARAMETERS,"
1800 PRINT "REACTOR TEMPERATURES AND MASS BALANCE ?"
```

```
1810 PRINT "YES OR NO"
1820 INPUT G$
1830 PAGE
1840 IF G$="NO" THEN 6560
1850 PAGE
1860 PRINT USING 1870;"REACTION PARAMETERS"
1870 IMAGE /,25A
1880 PRINT USING "19""-""";
1890 FOR I=1 TO 11
1900 READ J$
1910 DATA "FLOWRATE AIR (M3/HR) = ","AIR PRESSURE (BAR ABS) = "
1920 DATA "FLOWRATE OXYGEN (M3/HR) = ","OXYGEN PRESSURE (BAR ABS) ="
1930 DATA "FLOWRATE STEAM (KG/HR) = ","FLOWRATE SOLIDS (KG/HR) = "
1940 DATA "FLOWRATE NITROGEN (LITER/HR) = "
1950 DATA "AMBIENT TEMPERATURE (C) = ","FLOWRATE CONDENSATE (KG/HR) ="
1960 DATA "FLOWRATE FLY ASH (KG/HR) = ","FLOWRATE CHAR (KG/HR) = "
1970 PRINT USING 1980;J$,D(I)
1980 IMAGE 2X,32A,35T,4D.2D
1990 NEXT I
2000 WINDOW 0,1100,0,4
2010 VIEWPORT 82,125,20,70
2020 AXIS 100,1
2030 MOVE 950,-0.3
2040 PRINT "1000"
2050 MOVE 450,-0.3
2060 PRINT "500"
2070 MOVE -150,2
2080 PRINT "2"
2090 MOVE -50,4
2100 PRINT "4 "
2110 MOVE 100,4
2120 PRINT "HEIGHT (M)"
2130 MOVE 500,-0.6
2140 PRINT "TEMPERATURE (C)"
2150 MOVE E(12),0
2160 DRAW E(11),0.02
2170 DRAW E(10),0.2
2180 DRAW E(9),1.06
2190 DRAW E(5),3.6
2200 VIEWPORT 0,130,0,100
2210 PRINT USING 2220;
2220 IMAGE  5(/,)
2230 PRINT "TEMPERATURES"
2240 PRINT USING "12""-""";
2250 PRINT USING 2260;E(13)
2260 IMAGE 2X,"REACTOR TEMPERATURE = ",32T,4D," C",
2270 PRINT USING 2280;E(15)
2280 IMAGE 2X,"TEMPERATURE PREHEATER = ",32T,4D," C"
2290 PRINT USING 2300;E(12)
2300 IMAGE 2X,"TEMPERATURE INLET GAS = ",32T,4D," C"
2310 PRINT USING 2320;E(11),E(10)
2320 IMAGE 2X,"T11 =",15T,4D," C",/,2X,"T10 =",15T,4D," C"
2330 PRINT USING 2340;E(9),E(5)
2340 IMAGE 2X,"T9  =",15T,4D," C",/,2X,"T5  =",15T,4D," C"
2350 DIM F(4),H(4),Q(8,6),S(18,6)
2360 PRINT "IS AN ELEMENTARY ANALYSIS OF THE SOLID FEED AVAILABLE ?"
2370 PRINT "YES OR NO ?"
```

```
2380 INPUT E$
2390 PAGE
2400 IF E$="NO" THEN 2540
2410 PRINT "INPUT ELEMENTARY ANALYSIS : %C,%H,%O,%N"
2420 INPUT F
2430 PRINT "IS THE CARBON CONTENT OF FLY ASH OR CHAR AVAILABLE ?"
2440 PRINT "YES OR NO ?"
2450 INPUT F$
2460 IF F$="NO" THEN 2590
2470 PRINT "INPUT CARBON CONTENT FLY ASH (WT%)"
2480 INPUT H(1)
2490 H(2)=100-H(1)
2500 PRINT "CARBON CONTENT CHAR (WT %)"
2510 INPUT H(3)
2520 H(4)=100-H(3)
2530 GO TO 2630
2540 F(1)=44.44
2550 F(2)=6.22
2560 F(3)=49.34
2570 F(4)=0
2580 GO TO 2430
2590 H(1)=0
2600 H(2)=100
2610 H(3)=0
2620 H(4)=100
2630 Q=0
2640 S=0
2650 REM TOTAL IN
2660 D(1)=D(1)*SQR((D(12)+D(2))/1.481)
2670 D(1)=D(1)*SQR(353/(273+D(15)))
2680 Q(1,1)=1.293*D(1)
2690 D(3)=D(3)*SQR(2.4/(D(12)+D(4)))*(D(12)+D(4))/1.013
2700 D(3)=D(3)*SQR((273+D(8))/293)*273/(273+D(8))
2710 Q(2,1)=1.429*D(3)
2720 D(7)=D(7)*1.017*D(12)/1.013
2730 D(7)=D(7)*273/(273+D(8))
2740 Q(3,1)=1.251*D(7)/1000
2750 Q(4,1)=D(5)
2760 Q(5,1)=D(6)*(100-A(1)-A(2))/100
2770 Q(6,1)=A(2)*D(6)/100
2780 Q(7,1)=A(1)*D(6)/100
2790 Q(8,1)=Q(1,1)+Q(2,1)+Q(3,1)+Q(4,1)+D(6)
2800 REM CARBON IN
2810 Q(5,2)=Q(5,1)*F(1)/100
2820 Q(8,2)=Q(5,2)
2830 REM HYDROGEN IN
2840 Q(4,3)=Q(4,1)*0.111
2850 Q(5,3)=Q(5,1)*F(2)/100
2860 Q(6,3)=Q(6,1)*0.111
2870 Q(8,3)=Q(4,3)+Q(5,3)+Q(6,3)
2880 REM OXYGEN IN
2890 Q(1,4)=Q(1,1)*0.233
2900 Q(2,4)=Q(2,1)
2910 Q(4,4)=Q(4,1)*0.889
2920 Q(5,4)=Q(5,1)*F(3)/100
2930 Q(6,4)=Q(6,1)*0.889
2940 Q(8,4)=Q(1,4)+Q(2,4)+Q(4,4)+Q(5,4)+Q(6,4)
```

```
2950 REM NITROGEN IN
2960 Q(1,5)=Q(1,1)*0.767
2970 Q(3,5)=Q(3,1)
2980 Q(5,5)=Q(5,1)*F(4)/100
2990 Q(8,5)=Q(1,5)+Q(3,5)+Q(5,5)
3000 REM ASH IN
3010 Q(7,6)=Q(7,1)
3020 Q(8,6)=Q(7,1)
3030 REM TOTAL OUT
3040 S(1,1)=Q(8,5)/C(9)*100
3050 S(2,1)=S(1,1)*C(7)/100
3060 S(3,1)=S(1,1)*C(8)/100
3070 S(4,1)=Q(8,5)
3080 S(5,1)=S(1,1)*C(10)/100
3090 S(6,1)=S(1,1)*C(11)/100
3100 S(7,1)=S(1,1)*C(4)/100
3110 S(8,1)=S(1,1)*C(5)/100
3120 S(9,1)=S(1,1)*C(6)/100
3130 S(10,1)=S(1,1)*C(12)/100
3140 S(11,1)=S(1,1)*C(13)/100
3150 S(12,1)=D(9)* S(1,1)/ D(13)
3160 S(13,1)=D(10)* S(1,1)/ D(13)
3170 S(14,1)=D(11)* S(1,1)/ D(13)
3180 S(15,1)=S(1,1)+S(12,1)+S(13,1)+S(14,1)
3190 REM CARBON OUT
3200 S(5,2)=S(5,1)*0.75
3210 S(6,2)=S(6,1)*0.429
3220 S(7,2)=S(7,1)*0.273
3230 S(8,2)=S(8,1)*0.857
3240 S(9,2)=S(9,1)*0.8
3250 S(10,2)=S(10,1)*0.857
3260 S(11,2)=S(11,1)*0.888
3270 S(13,2)=S(13,1)*H(1)/100
3280 S(14,2)=S(14,1)*H(3)/100
3290 S(12,2)=S(12,1)*D(14)
3300 S(15,2)=S(5,2)+S(6,2)+S(7,2)+S(8,2)+S(9,2)+S(11,2)+S(12,2)+S(10,2)
3310 S(15,2)=S(15,2)+S(13,2)+S(14,2)
3320 REM HYDROGEN OUT
3330 S(2,3)=S(2,1)
3340 S(5,3)=S(5,1)*0.25
3350 S(8,3)=S(8,1)*0.143
3360 S(9,3)=S(9,1)*0.2
3370 S(10,3)=S(10,1)*0.143
3380 S(11,3)=S(11,1)*0.111
3390 S(12,3)=(S(12,1)-S(12,2)-S(12,2)*0.118)*0.111+S(12,2)*0.118
3400 S(15,3)=S(2,3)+S(5,3)+S(8,3)+S(9,3)+S(10,3)+S(11,3)+S(12,3)
3410 REM OXYGEN OUT
3420 S(3,4)=S(3,1)
3430 S(6,4)=S(6,1)*0.571
3440 S(7,4)=S(7,1)*0.727
3450 S(12,4)=(S(12,1)-S(12,2)-S(12,2)*0.118)*0.889
3460 S(15,4)=S(3,4)+S(6,4)+S(7,4)+S(10,4)
3470 REM NITROGEN OUT
3480 S(4,5)=S(4,1)
3490 S(15,5)=S(4,1)
3500 REM ASH OUT
3510 S(13,6)=S(13,1)*H(2)/100
```

```
3520 S(14,6)=S(14,1)*H(4)/100
3530 S(15,6)=S(13,6)+S(14,6)
3540 REM BALANCE
3550 S(16,1)=S(15,1)*100/Q(8,1)
3560 S(16,2)=S(15,2)*100/Q(8,2)
3570 S(16,3)=S(15,3)*100/Q(8,3)
3580 S(16,4)=S(15,4)*100/Q(8,4)
3590 S(16,5)=S(15,5)*100/Q(8,5)
3600 S(16,6)=S(15,6)*100/Q(8,6)
3610
3620
3630
3640
3650 REM TARS IN CONDENSATE
3660 S(18,1)=S(12,2)+S(12,2)*0.118
3670
3680
3690
3700 REM THERMAL EFFICIENCY
3710 T1=S(1,1)*P(3)*100/(Q(5,1)*A(3))
3720 REM AIR FACTOR
3730 W1=(Q(1,1)+Q(2,1)*4.308)/(Q(5,2)*11.48+Q(5,3)*34.194-4.308*Q(5,4))
3740 REM    PRINT
3750 PAGE
3760 PRINT USING 3770:"C","H","O","N","ASH"
3770 IMAGE 24X,5(4X,5A),/
3780 PRINT USING 3790:"KG/HR","KG/HR","KG/HR","KG/HR","KG/HR","KG/HR"
3790 IMAGE 16X,6(2X,7A),/
3800 FOR I=1 TO 7
3810 READ J$
3820 DATA "AIR","OXYGEN","NITROGEN","STEAM","SOLIDS WAF","MOISTURE"
3830 DATA "ASH"
3840 PRINT USING 3850:J$,Q(I,1),Q(I,2),Q(I,3),Q(I,4),Q(I,5),Q(I,6)
3850 IMAGE 2X,12A,6(2X,3D.2D)
3860 NEXT I
3870 PRINT USING "70""-""";
3880 PRINT USING 3890:"TOTAL",Q(8,1),Q(8,2),Q(8,3),Q(8,4),Q(8,5),Q(8,6)
3890 IMAGE     2X,12A,6(2X,3D.2D),/
3900 FOR I=1 TO 14
3910 READ J$
3920 DATA "TOTAL GAS","H2","O2","N2","CH4","CO","CO2","C2H4","C2H6"
3930 DATA "C3H6","C4H6","CONDENSATE","FLY ASH","CHAR"
3940 PRINT USING 3850:J$,S(I,1),S(I,2),S(I,3),S(I,4),S(I,5),S(I,6)
3950 NEXT I
3960 PRINT USING "70""-""";
3970 PRINT USING 4020:"TOTAL",S(15,1),S(15,2),S(15,3),S(15,4),S(15,5)
3980 PRINT USING 4030:S(15,6)
3990 PRINT USING "72""-""";
4000 PRINT USING 4020:"BALANCE",S(16,1),S(16,2),S(16,3),S(16,4),S(16,5)
4010 PRINT USING 4030:S(16,6)
4020 IMAGE    2X,12A,5(2X,3D.2D),S
4030 IMAGE 2X,3D.2D
4040 PRINT USING 4050:T1,P(11)
4050 IMAGE 2X,"THERMAL EFFICIENCY = ",3D.2D," %"
4055 PRINT "_____"
4056 PRINT "TARS IN CONDENSATE=",S(18,1),"KG/KG"
```

```
4057
4060 PRINT "DO YOU WANT A LISTING OF THE THERMAL BALANCE ?"
4070 PRINT "YES OR NO"
4080 INPUT J$
4090 IF J$="YES" THEN 4110
4100 END
4110 DIM X(3),Y(15),Z(16)
4120 X(1)=Q(5,1)-Q(5,5)
4130 X(2)=Q(1,4)+Q(2,1)
4140 X(3)=Q(4,1)+Q(6,1)
4150 M1=0
4160 FOR I=2 TO 4
4170 M1=M1 MAX S(16,I)
4180 NEXT I
4190 M1=M1/100
4200 FOR I=1 TO 14
4210 Y(I)=S(I,1)/M1
4220 NEXT I
4230 Y(13)=Y(13)*H(1)/100+Y(14)*H(3)/100
4240 H1=(Q(5,1)+Q(6,1)+Q(7,1))*A(3)*4.189/1000-Y(2)*141.8-Y(5)*55.5
4250 H1=H1-Y(6)*10.11-Y(8)*50.3-Y(9)*51.87-Y(10)*48.92-Y(11)*47.69
4260 H1=(H1-Y(13)*32.81)/(Q(5,1)+Q(6,1)+Q(7,1))
4270 PAGE
4280 PRINT USING 4520:"REACTION HEAT = ",H1
4290 Z(13)=Q(5,1)*A(3)*4.189/1000
4300 Z(1)=1.09*(E(12)-20)*(Q(1,1)+Q(2,1)+Q(3,1))/1000
4310 Z(2)=4.19*(100-20)*Q(4,1)/1000+2.26*Q(4,1)
4320 Z(2)=Z(2)+2.09*(E(12)-100)*Q(4,1)/1000
4330 Z(3)=H1*(Q(5,1)+Q(6,1)+Q(7,1))
4340 Z(4)=0
4350 Z(5)=14.86*S(2,1)+1.02*S(3,1)+1.11*S(4,1)+3.74*S(5,1)+1.12*S(6,1)
4360 Z(5)=(Z(5)+1.11*S(7,1)+2.81*S(8,1)+3.35*S(9,1))*(E(5)-20)/1000
4370 Z(6)=4.19*(100-20)*S(12,1)/1000+2.26*S(12,1)
4380 Z(6)=Z(6)+2.09*(E(5)-100)*S(12,1)/1000
4390 Z(7)=0.94*S(13,1)*(E(5)-20)/1000
4400 Z(8)=0.94*S(14,1)*(E(13)-20)/1000
4410 Z(12)=((E(9)+E(5))/2-20)/(1.584*1.6)*15.33
4420 Z(12)=Z(12)+(E(13)-20)/(3.2*1.6)*6.28
4430 Z(12)=Z(12)+(E(5)-20)/1.0144*1.13
4440 Z(12)=Z(12)*0.004189
4450 Z(14)=P(2)*S(1,1)
4455 Z(15)=S(13,2)*32.81+S(18,1)*23.3
4460 Z(9)=Z(1)+Z(2)+Z(13)-Z(5)-Z(6)-Z(7)-Z(8)-Z(12)-Z(14)-Z(15)
4480 Z(10)=100*Z(9)/(A(3)*(Q(5,1)+Q(6,1)+Q(7,1))+Z(1)+Z(2))
4490 Z(10)=Z(10)*1000/4.189
4500 X1=Z(1)+Z(2)+Z(13)
4510 X2=Z(5)+Z(6)+Z(7)+Z(8)+Z(12)+Z(14)+Z(15)
4520 IMAGE40A,4D.2D,5OT,"MJ/HR"
4530 PRINT USING 4520:"AIR IN ",Z(1)
4540 PRINT USING 4520:"STEAM IN ",Z(2)
4550 PRINT USING 4520:"FEEDSTOCK IN  ",Z(13)
4560 PRINT USING 4520:"TOTAL IN  ",X1
4570 PRINT USING 4520:"ENERGY IN GAS ",Z(14)
4580 PRINT USING 4520:"GAS OUT ",Z(5)
4590 PRINT USING 4520:"STEAM OUT ",Z(6)
4600 PRINT USING 4520:"FLY ASH OUT ",Z(7)
4610 PRINT USING 4520:"CHAR OUT ",Z(8)
```

```
4620 PRINT USING 4520:"heat loss reactor walls ",Z(12)
4630 PRINT USING 4520:"TOTAL OUT ",X2
4640 PRINT USING 4520:"HEAT LOSS ",Z(9)
4650 PRINT "% HEAT LOSS (HV1) = ",Z(10),"%"
4660 PRINT "-----------------------------------------------------------------"
4665 PRINT USING 4520:"ENERGY IN TARS & ASH=",Z(15)
4670 PRINT "DO YOU WANT A PRINT-OUT OF THE RESULTS ON THE PLOTTER ?"
4680 PRINT "YES OR NO"
4690 INPUT G$
4700 PAGE
4710 IF G$="YES" THEN 4730
4720 GO TO 6560
4730 PAGE
4740 PRINT "DO YOU WANT A PRINT-OUT OF THE GAS COMPOSITION ?"
4750 PRINT "YES OR NO ?"
4760 INPUT G$
4770 IF G$="YES" THEN 4820
4780 FOR I=1 TO 8
4790 READ G$
4800 NEXT I
4810 GO TO 5240
4820 PRINT @1: USING 4830:A$,B$,C$
4830 IMAGE 2X,"MATERIAL :",12A,5X,"DATE :",10A,"NUMBER :",10A,/,/
4840 PRINT @1: USING 4850:A(1)
4850 IMAGE 2X,"ASH CONTENT =",30T,4D.2D,"WT %"
4860 PRINT @1: USING 4870:A(2)
4870 IMAGE 2X,"MOISTURE CONTENT =",30T,4D.2D,"WT %"
4880 PRINT @1: USING 4890:A(3)
4890 IMAGE 2X,"HIGHER HEATING VALUE =",29T,5D.1D,"KCAL/KG",/
4900 PRINT @1:"GAS COMPOSITION"
4910 PRINT @1: USING "15""-""":
4920 PRINT @1: USING 4930:"WEIGHT %","VOLUME %"
4930 IMAGE 19X,8A,5X,8A
4940 FOR J=7 TO 11
4950 READ D$
4960 DATA "H2","O2","N2","CH4","CO"
4970 PRINT @1: USING 4990:D$,C(J),G(J)
4980 NEXT J
4990 IMAGE 5X,5A,5X,6D.2D,5X,6D.2D
5000 FOR J=4 TO 6
5010 READ D$
5020 DATA "CO2","C2H4","C2H6"
5030 PRINT @1: USING 4990:D$,C(J),G(J)
5040 NEXT J
5050 FOR J=12 TO 13
5060 READ D$
5070 DATA "C3H6","C4H6"
5080 PRINT @1: USING 4990:D$,C(J),G(J)
5090 NEXT J
5100 PRINT @1: USING 5110:P(1),P(10)
5110 IMAGE /,"METHANE RATIO = ",4D.2D,30T,"HYDROGEN RATIO = ",4D.2D,/
5120 PRINT @1:"HIGHER HEATING VALUE"
5130 PRINT @1: USING 5150:P(2),P(3)
5140 PRINT @1: USING 5160:P(4),P(5)
5150 IMAGE 5X,3D.2D,15T,"MJ/KG",34T,5D.1D,45T"KCAL/KG"
5160 IMAGE 5X,3D.2D,15T,"MJ/NM3",34T,5D.1D,45T,"KCAL/NM3",/
5170 PRINT @1:"LOWER HEATING VALUE"
```

```
5180 PRINT @1: USING 5150:P(6),P(7)
5190 PRINT @1: USING 5160:P(8),P(9)
5200 PRINT @1: USING 5210:R1
5210 IMAGE "SPECIFIC WEIGHT =  ",2D.3D," KG/NM3",/,/
5220 PRINT @1: USING 5230:W1
5230 IMAGE "AIR FACTOR ""S""=   ",1D.3D
5240 PRINT "DO YOU WANT A PRINT-OUT OF THE REACTION PARAMETERS "
5250 PRINT "AND REACTOR TEMPERATURES ?"
5260 PRINT "YES OR NO ?"
5270 INPUT G$
5280 IF G$="YES" THEN 5330
5290 FOR I=1 TO 11
5300 READ G$
5310 NEXT I
5320 GO TO 5840
5330 PAGE
5340 PRINT @1: USING 5350:"REACTION PARAMETERS"
5350 IMAGE /,25A
5360 PRINT @1: USING "19""-""";
5370 FOR I=1 TO 12
5380 READ J$
5390 DATA "FLOWRATE AIR (NM3/HR; 0 C,1ATM)=","AIR PRESSURE (BAR REL) = "
5400 DATA "FLOWRATE OXYGEN (NM3/HR) = ","OXYGEN PRESSURE (BAR REL) ="
5410 DATA "FLOWRATE STEAM (KG/HR) = ","FLOWRATE SOLIDS (KG/HR) = "
5420 DATA "FLOWRATE NITROGEN (L/HR)"
5430 DATA "AMBIENT TEMPERATURE (C) = ","FLOWRATE CONDENSATE (KG/HR) ="
5440 DATA "FLOWRATE FLY ASH (KG/HR) = ","FLOWRATE CHAR (KG/HR) = "
5450 DATA "AMBIENT PRESSURE (BAR) ="
5460 PRINT @1: USING 5470:J$,D(I)
5470 IMAGE 2X,32A,35T,4D.2D
5480 NEXT I
5490 WINDOW 0,1100,0,4
5500 VIEWPORT 82,125,20,70
5510 AXIS @1:100,1
5520 MOVE @1:950,-0.3
5530 PRINT @1:"1000"
5540 MOVE @1:450,-0.3
5550 PRINT @1:"500"
5560 MOVE @1:-150,2
5570 PRINT @1:"  2"
5580 MOVE @1:-50,4
5590 PRINT @1:"4 "
5600 MOVE @1:100,4
5610 PRINT @1:"HEIGHT (M)"
5620 MOVE @1:500,-0.6
5630 PRINT @1:"TEMPERATURE (C)"
5640 MOVE @1:E(12),0
5650 DRAW @1:E(11),0.1
5660 DRAW @1:E(10),0.36
5670 DRAW @1:E(9),1.09
5680 DRAW @1:E(5),3.6
5690 VIEWPORT 0,130,0,100
5700 PRINT @1: USING 5710:
5710 IMAGE  5(/,)
5720 PRINT @1:"TEMPERATURES"
5730 PRINT @1: USING "12""-""";
5740 PRINT @1: USING 5750:E(13)
```

```
5750 IMAGE 2X,"REACTOR TEMPERATURE = ",32T,4D," C",
5760 PRINT @1: USING 5770:E(15)
5770 IMAGE 2X,"TEMPERATURE PREHEATER = ",32T,4D," C"
5780 PRINT @1: USING 5790:E(12)
5790 IMAGE 2X,"TEMPERATURE INLET GAS = ",32T,4D," C"
5800 PRINT @1: USING 5810:E(11),E(10)
5810 IMAGE 2X,"T11 =",15T,4D," C",/,2X,"T10 =",15T,4D," C"
5820 PRINT @1: USING 5830:E(9),E(5)
5830 IMAGE 2X,"T9  =",15T,4D," C",/,2X,"T5  =",15T,4D," C"
5840 PRINT "DO YOU WANT A PRINT-OUT OF THE MASS BALANCE ?"
5850 PRINT "YES OR NO ?"
5860 INPUT G$
5870 IF G$="YES" THEN 5890
5880 GO TO 6200
5890 PAGE
5900 PRINT @1: USING 5910:"C","H","O","N","ASH"
5910 IMAGE 24X,5(4X,5A),/
5920 PRI @1: USI 5930:"KG/HR","KG/HR","KG/HR","KG/HR","KG/HR","KG/HR"
5930 IMAGE 16X,6(2X,7A),/,/
5940 FOR I=1 TO 7
5950 READ J$
5960 DATA "AIR","OXYGEN","NITROGEN","STEAM","SOLIDS WAF","MOISTURE"
5970 DATA "ASH"
5980 PRINT @1: USING 5990:J$,Q(I,1),Q(I,2),Q(I,3),Q(I,4),Q(I,5),Q(I,6)
5990 IMAGE 2X,12A,6(2X,3D.2D)
6000 NEXT I
6010 PRINT @1: USING "70""-""";
6020 PRI @1: USI 6030:"TOTAL",Q(8,1),Q(8,2),Q(8,3),Q(8,4),Q(8,5),Q(8,6)
6030 IMAGE     2X,12A,6(2X,3D.2D),/,/
6040 FOR I=1 TO 14
6050 READ J$
6060 DATA "TOTAL GAS","H2","O2","N2","CH4","CO","CO2","C2H4","C2H6"
6070 DATA "C3H6","C4H6","CONDENSATE","FLY ASH","CHAR"
6080 PRINT @1: USING 5990:J$,S(I,1),S(I,2),S(I,3),S(I,4),S(I,5),S(I,6)
6090 NEXT I
6100 PRINT @1: USING "70""-""";
6110 PRI @1: USI 6160:"TOTAL",S(15,1),S(15,2),S(15,3),S(15,4),S(15,5)
6120 PRINT @1: USING 6170:S(15,6)
6130 PRINT @1: USING "70""-""";
6140 PRI @1: USI 6160:"BALANCE",S(16,1),S(16,2),S(16,3),S(16,4),S(16,5)
6150 PRINT @1: USING 6170:S(16,6)
6160 IMAGE    2X,12A,5(2X,3D.2D),S
6170 IMAGE 2X,3D.3D
6172 PRINT @1:"-------------------------------------------------------"
6174 PRINT @1:"TARS IN CONDENSATE=",S(18,1),"KG/KG"
6175 PRINT @1:"TARS IN GAS=",S(17,1),"KG/KG"
6180 PRINT @1:.USING 6190:T1,P(11)
6190 IMAGE /,2X,"THERMAL EFFICIENCY = ",3D,2D," %","TAR RATIO=",3D.3D
6200 PRI "DO YOU WANT A PRINT OUT OF THE THERMAL BALANCE ON THE PLOTTER"
6210 PRINT "YES OR NO ?"
6220 INPUT J$
6230 IF J$="YES" THEN 6250
6240 GO TO 6560
6250 PRINT @1:"THERMAL BALANCE"
6260 PRINT @1:"---------------"
6270 PRINT @1:
6280 PRINT @1: USING 6290:"HEAT OF REACTION (MJ/KG)",H1
6290 IMAGE 40A,3D.2D,50T,"MJ/KG"
```

```
6300 IMAGE 40A,4D.2D,5OT,"MJ/H "
6310 PRINT @1:
6320 PRINT @1:"IN"
6330 PRINT @1:
6340 PRINT @1: USING 6300:"SENSIBLE HEAT IN GAS              ",Z(1)
6350 PRINT @1: USING 6300:"SENSIBLE & LATENT HEAT IN STEAM ",Z(2)
6360 PRINT @1: USING 6300:"HEAT IN FEEDSTOCK                ",Z(13)
6370 PRINT @1:
6380 PRINT @1: USING 6300:"TOTAL IN  ",X1
6390 PRINT @1:
6400 PRINT @1:"OUT"
6410 PRINT @1:
6420 PRINT @1: USING 6300:"SENSIBLE HEAT IN GAS              ",Z(5)
6430 PRINT @1: USING 6300:"SENSIBLE & LATENT HEAT IN STEAM ",Z(6)
6440 PRINT @1: USING 6300:"SENSIBLE HEAT IN FLY ASH         ",Z(7)
6450 PRINT @1: USING 6300:"SENSIBLE HEAT IN CHAR            ",Z(8)
6460 PRINT @1: USING 6300:"HEAT LOSS REACTOR WALLS          ",Z(12)
6470 PRINT @1: USING 6300:"ENERGY IN GAS                    ",Z(14)
6475 PRINT @1: USING 6300:"ENERGY IN TARS & GAS             ",Z(15)
6480 PRINT @1:
6490 PRINT @1: USING 6300:"TOTAL OUT ",X2
6500 PRINT @1:
6510 PRINT @1: USING 6300:"HEAT LOSS (BY DIFFERENCE)        ",Z(9)
6520 PRINT @1: USING 6540:Z(10)
6530 PRINT @1: USING 6550:Z(11)
6540 IMAGE //,"% HEAT LOSS  HV1 = ",2D.3D," %"/
6550 PRINT @1: USING 6300:"ENERGY IN TARS & GAS             ",Z(15
6560 PRINT "END OF PROGRAMME"
6570 PRINT "TYPE ""RUN"" TO RECOMMENCE PROGRAMME."
```

APPENDIX VII - THERMODYNAMIC MODEL : PROGRAMME AND RESULTS

This Appendix presents the programme written for the thermodynamic model and the results of its application for the individual runs.

In order to facilitate the execution of the subroutine, CALFUN (M, N, F, X), used for the solution of the system of eight equations, the input data (feedstock flowrate and blast flowrate) were divided by 100.

Since this model was developed for ashless gasification, the ash was subtracted from the feedstock flowrate. The moisture of the feed was also subtracted from the feedstock flowrate and was added to the blast as steam. Thus,for example for run 20 (feedstock flowrate 160 kg/h, air flowrate 356.6 kg/h, basis 1 h).

Feedstock	= 160.0 kg	Air	= 356.60 kg
Moisture	= 19.2 kg	Steam	= 19.20
Ash	= 2.25		
Feedstock MAF = 138.55 kg		Blast	= 375.8

Thus input data:

Feedstock flowrate	= 1.386	Kg/h
Blast flowrate	= 3.758	"
Steam	= 5.1	wt%
O_2	= 22.1	"
N_2	= 72.78	"

The most important results of the thermodynamic production are summarized in Table A.VII.1 along with the air factor and bed temperature.

Table A.VII.1 : Results for the individual runs.

Run	S -	T °C	, HHV MJ/Nm^3	η %	Y_{H2O} kg H_2O/kg MAF feed
3	0.53	860	2.56	48.7	0.37
14	0.38	774	4.23	64.0	0.24
15	0.7	942	1.34	31.0	0.51
16	0.87	970	0.50	13.7	0.61
18	0.42	917	3.79	60.8	0.31
19	0.34	827	4.85	68.7	0.24
20	0.50	986	2.86	52.0	0.39
21	0.26	817	6.13	75.4	0.19
22	0.25	774	6.21	75.7	0.17
23	0.23	799	7.06	80.2	0.15
24	0.38	927	4.19	64.1	0.30
25	0.32	876	5.27	71.9	0.23
26	0.29	746	5.83	74.9	0.18
27	0.32	780	5.60	73.1	0.21
28	0.38	811	4.18	63.9	0.26
29	0.26	706	5.60	71.4	0.19
30	0.32	722	5.13	69.1	0.21
31	0.38	803	4.29	63.6	0.27
32	0.37	837	4.45	62.5	0.18
33	0.33	814	5.01	68.5	0.24
34	0.32	735	5.13	69.2	0.22
35	0.27	699	6.11	74.3	0.17
36	0.33	760	5.10	68.9	0.22
37	0.29	871	5.86	76.1	0.19
38	0.29	865	5.95	76.6	0.19

```
      PROGRAM EQUIL1(INPUT,OUTPUT,TAPE1)

      ********************************************************************

       EQUILIBRIUM CALCULATION OF SOLIDS GASIFICATION

       ************************************************************
      THIS PROGRAM CALCULATES EQUILIBRIUM COMPOSITION OF A PRODUCT GAS
      FROM THE GASIFICATION OF A FEEDSTOCK OF KNOWN ELEMENTAL ANALYSIS
      (WT%, C,H,O,N) BY A BLAST GAS COMPOSED OF AIR AND STEAM ON THE
      BASIS OF THE FOLLOWING HOMOGENEOUS REACTIONS AND EQUILIBRIA :


               H2O   +   CO    =    CO2   +   H2     KW = [CO2][H2]/[H2O][CO]

               2CO   + 2H2     =    CO2   + CH4     KMG= [CO][CH4]/[CO]**2[H2]**2

      THE EQUILIBRIUM CONSTANTS ARE CALCULATED ACCORDING TO GUMZ.

      OUTPUT :  GAS COMPOSITION (WT% AND VOL%) AS FUNCTION OF T (500 ->
                1300 C).

      ********************************************************************


      REAL X(8),H,DMAX,ACC,W(500),F(8)
      INTEGER M,N,MAXFUN,IPRINT
      REAL KW(12),KMG(12),RO(6),FEED(4),GAS(3),FUEL,GASIN,T(12),
     *CIN,HIN,OIN,NIN,V(6),A(12,7)

      INTEGER I

      COMMON/NR1/KW,KMG,RO,CIN,HIN,OIN,NIN,I

      FEEDSTOCK FLOWRATE (KG/H)

      FUEL=1.29

      GAS FLOWRATE (KG/H)
      GASIN=5.83

      COMPOSITION FEEDSTOCK /C,H,O,N  WT FRACTION/

      DATA FEED/.84,.033,.082,0./

      COMPOSITION GAS /H2O,O2,N2  WT FRACTION/
      DATA GAS/.31,.156,.534/

      PRINT 100
      PRINT 110
      PRINT 120
      PRINT 200,(FEED(J),J=1,4)
      PRINT 250,FUEL
      PRINT 300,(GAS(J),J=1,3)
      PRINT 350,GASIN
      PRINT 370
      PRINT 400

  100 FORMAT(       5X,*EQUILIBRIUM COMPOSITION OF GAS*)
  110 FORMAT(5X,*-------------------------*/)
  120 FORMAT(5X,*ASHLESS GASIFICATION*//)
  200 FORMAT(5X,*COMPOSITION FEEDSTOCK /WT%/*//,
     *5X,*CARBON    =*,2PF10.3/,5X,*HYDROGEN  =*,2PF9.3/,
     *5X,*OXYGEN    =*,2PF10.3/,5X,*NITROGEN =*,2PF10.3/)
  250 FORMAT(5X,*FLOWRATE OF FEEDSTOCK /KG/H/=*,F10.3///)
  300 FORMAT(5X,*COMPOSITION GAS IN /WT%/*//,
     *5X,*H2O =*,2PF10.3/,5X,*O2 =*,2PF11.3/,5X,*N2 =*,2PF11.3/)
  350 FORMAT(5X,*FLOWRATE OF BLAST /KG/H/ =*,F10.3///)
  370 FORMAT(5X,*GAS COMPOSITION /VOL%/*//)
  380 FORMAT(//5X,*GAS COMPOSITION /WT%/*//)
  400 FORMAT(T4,*T*,T12,*N2*,T22,*H2*,T32,*CO2*,T42,*CO*,T52,*CH4*
     *,T62,*H2O*,T72,*GAS KG/H*)
```

```
      DO 1000I=1,12

      INITIALISATION OPTIMISATION PARAMETERS

      N=8
      M=8

      GAS COMPOSITION (N2,H2,CO2,CO,CH4,H2O  WT FRACTION)

      X(1)=.2
      X(2)=.2
      X(3)=.2
      X(4)=.1
      X(5)=.1
      X(6)=.2

      PRODUCED GAS (KG/H)

      X(7)=GASIN

      SPECIFIC WEIGHT OF PRODUCED GAS (KG/H)

      X(8)=1.

      OPTIMISATION PARAMETERS

      H=1.E-4
      DMAX=10.
      ACC=1.E-13
      MAXFUN=100
      IPRINT=0

      DATA

      HOMOGENEOUS WATER GAS SHIFT REACTION

      DATA KW/2.55284,1.95859,1.54923,1.25719,1.04217,.8801,.755
     *.65741,.57929,.46469,.38696,.33284/

      HOMOGENEOUS METHANISATION

      DATA KMG/4.9,.704,.123,.0256,.00617,.0017,.000514,.000173,
     *.0000634,.0000107,.0000023,.000000608/

      SPECIFIC WEIGHT

      DATA RO/1.2507,.0898,1.9768,1.2501,.7167,.806/

      TEMPERATURES

      DATA T/600,650,700,750,800,850,900,950,1000,1100,1200,1300/


      CIN=FUEL*FEED(1)
      HIN=FUEL*FEED(2)+GASIN*GAS(1)*.125
      OIN=FUEL*FEED(3)+GASIN*(GAS(2)+.8889*GAS(1))
      NIN=FUEL*FEED(4)+GASIN*GAS(3)

      CALL VA05A(M,N,F,X,H,DMAX,ACC,MAXFUN,IPRINT,W)

      DO 700 K=1,6
      V(K)=X(K)*X(8)/RO(K)
  700 CONTINUE


      PRINT 500,T(I),(V(J),J=1,6),X(7)
  500 FORMAT(I5,2P6F10.3,3X,0PF10.3)

      DO 800 K=1,7
      A(I,K)=X(K)
  800 CONTINUE

 1000 CONTINUE

      PRINT 380
      PRINT 400
      PRINT 500,(T(I),(A(I,J),J=1,7),I=1,12)
```

```
      END


      SUBROUTINE CALFUN(M,N,F,X)

      REAL F(8),X(8)
      INTEGER M,N
      REAL KW(12),KMG(12),RO(6),CIN,HIN,OIN,NIN
      INTEGER I

      COMMON/NR1/KW,KMG,RO,CIN,HIN,OIN,NIN,I


      F(1)=.2727*X(3)+.4286*X(4)+.75*X(5)-CIN/X(7)
      F(2)=X(2)+.25*X(5)+.1111*X(6)-HIN/X(7)
      F(3)=.7273*X(3)+.5714*X(4)+.8889*X(6)-OIN/X(7)
      F(4)=X(1)-NIN/X(7)
      F(5)=X(1)+X(2)+X(3)+X(4)+X(5)+X(6)-1
      F(6)=X(3)*X(2)-KW(I)*.1762*X(4)*X(6)
      F(7)=(X(3)*X(5)-KMG(I)*112.4*(X(2)*X(4)*X(8))**2)*10
      F(8)=X(1)/RO(1)+X(2)/RO(2)+X(3)/RO(3)+X(4)/RO(4)+X(5)/RO(5)
     *+X(6)/RO(6)-1./X(8)

      RETURN


      END


          UCLP, 5B, DEFTERM, 0.198KLNS.
```

EQUILIBRIUM COMPOSITION OF GAS RUN 13

ASHLESS GASIFICATION

COMPOSITION FEEDSTOCK /WT%/

CARBON = 45.300
HYDROGEN = 5.800
OXYGEN = 48.800
NITROGEN = 0.000

FLOWRATE OF FEEDSTOCK /KG/H/= .675

COMPOSITION GAS IN /WT%/

H2O = 4.800
O2 = 22.200
N2 = 73.000

FLOWRATE OF BLAST /KG/H/ = 1.944

GAS COMPOSITION /VOL%/

T	N2	H2	CO2	CO	CH4	H2O	GAS KG/H
600	50.369	13.653	16.598	8.258	.375	10.748	2.620
650	50.064	13.515	15.548	9.463	.074	11.336	2.620
700	50.001	12.926	14.780	10.264	.015	12.014	2.620
750	49.987	12.305	14.125	10.927	.003	12.652	2.620
800	49.982	11.728	13.541	11.514	.001	13.233	2.620
850	49.979	11.204	13.016	12.042	.000	13.759	2.620
900	49.977	10.731	12.542	12.518	.000	14.233	2.620
950	49.975	10.303	12.114	12.947	.000	14.661	2.620
1000	49.973	9.915	11.727	13.336	.000	15.049	2.620
1100	49.970	9.248	11.060	14.005	.000	15.716	2.620
1200	49.968	8.705	10.517	14.550	.000	16.260	2.620
1300	49.966	8.267	10.079	14.990	.000	16.698	2.620

GAS COMPOSITION /WT%/

T	N2	H2	CO2	CO	CH4	H2O	GAS KG/H
600	54.173	1.054	28.215	8.877	.231	7.449	2.620
650	54.173	1.050	26.592	10.235	.046	7.905	2.620
700	54.173	1.006	25.310	11.114	.009	8.388	2.620
750	54.173	.958	24.196	11.836	.002	8.836	2.620
800	54.173	.913	23.197	12.474	.001	9.243	2.620
850	54.173	.872	22.298	13.046	.000	9.611	2.620
900	54.173	.835	21.487	13.562	.000	9.942	2.620
950	54.173	.802	20.755	14.028	.000	10.242	2.620
1000	54.173	.772	20.092	14.450	.000	10.513	2.620
1100	54.173	.720	18.952	15.176	.000	10.980	2.620
1200	54.173	.678	18.022	15.767	.000	11.360	2.620
1300	54.173	.644	17.272	16.244	.000	11.667	2.620

10.18.43.UCLP, 5B, OEFTERM, 0.198KLNS.

EQUILIBRIUM COMPOSITION OF GAS RUN 14

ASHLESS GASIFICATION

COMPOSITION FEEDSTOCK /WT%/

CARBON = 45.300
HYDROGEN = 5.800
OXYGEN = 48.800
NITROGEN = 0.000

FLOWRATE OF FEEDSTOCK /KG/H/= .675

COMPOSITION GAS IN /WT%/

H2O = 6.600
O2 = 21.800
N2 = 71.600

FLOWRATE OF BLAST /KG/H/ = 1.409

GAS COMPOSITION /VOL%/

T	N2	H2	CO2	CO	CH4	H2O	GAS KG/H
600	42.900	18.037	15.887	12.736	1.627	8.813	2.085
650	41.912	19.444	13.911	15.213	.443	9.077	2.085
700	41.622	19.319	12.801	16.471	.097	9.690	2.085
750	41.557	18.749	12.018	17.288	.022	10.366	2.085
800	41.541	18.135	11.357	17.958	.006	11.004	2.085
850	41.535	17.559	10.771	18.548	.002	11.585	2.085
900	41.532	17.035	10.244	19.077	.001	12.111	2.085
950	41.530	16.561	9.770	19.553	.000	12.585	2.085
1000	41.529	16.132	9.341	19.984	.000	13.015	2.085
1100	41.526	15.394	8.604	20.723	.000	13.753	2.085
1200	41.524	14.795	8.006	21.324	.000	14.352	2.085
1300	41.522	14.312	7.524	21.807	-.000	14.835	2.085

GAS COMPOSITION /WT%/

T	N2	H2	CO2	CO	CH4	H2O	GAS KG/H
600	48.395	1.461	28.326	14.360	1.052	6.406	2.085
650	48.395	1.612	25.389	17.557	.293	6.755	2.085
700	48.395	1.613	23.525	19.142	.065	7.261	2.085
750	48.395	1.568	22.120	20.123	.015	7.779	2.085
800	48.395	1.517	20.912	20.911	.004	8.261	2.085
850	48.395	1.469	19.836	21.601	.001	8.699	2.085
900	48.395	1.425	18.867	22.218	.000	9.094	2.085
950	48.395	1.386	17.994	22.774	.000	9.451	2.085
1000	48.395	1.350	17.205	23.277	.000	9.774	2.085
1100	48.395	1.288	15.849	24.139	.000	10.329	2.085
1200	48.395	1.238	14.747	24.840	.000	10.780	2.085
1300	48.395	1.198	13.860	25.405	-.000	11.143	2.085

10.45.58.UCLP, 5B, DEFTERM, 0.132KLNS.

EQUILIBRIUM COMPOSITION OF GAS RUN 15

ASHLESS GASIFICATION

COMPOSITION FEEDSTOCK /WT%/

CARBON = 45.300
HYDROGEN = 5.800
OXYGEN = 48.800
NITROGEN = 0.000

FLOWRATE OF FEEDSTOCK /KG/H/= .675

COMPOSITION GAS IN /WT%/

H2O = 3.700
O2 = 22.400
N2 = 73.900

FLOWRATE OF BLAST /KG/H/ = 2.531

GAS COMPOSITION /VOL%/

T	N2	H2	CO2	CO	CH4	H2O
600	56.890	8.401	17.238	4.328	.038	13.105
650	56.852	7.915	16.654	4.933	.006	13.640
700	56.843	7.413	16.136	5.456	.001	14.150
750	56.840	6.950	15.669	5.926	.000	14.616
800	56.838	6.528	15.246	6.350	.000	15.038
850	56.836	6.147	14.865	6.733	.000	15.417
900	56.834	5.803	14.522	7.078	.000	15.763
950	56.832	5.494	14.212	7.389	.000	16.073
1000	56.831	5.215	13.933	7.669	.000	16.353
1100	56.828	4.737	13.455	8.149	.000	16.831
1200	56.826	4.351	13.070	8.536	.000	17.217
1300	56.825	4.043	12.762	8.845	.000	17.525

GAS COMPOSITION /WT%/

T	N2	H2	CO2	CO	CH4	H2O
600	58.329	.618	27.935	4.436	.022	8.659
650	58.329	.583	27.006	5.059	.004	9.019
700	58.329	.546	26.170	5.596	.001	9.357
750	58.329	.512	25.415	6.078	.000	9.666
800	58.329	.481	24.730	6.514	.000	9.945
850	58.329	.453	24.113	6.906	.000	10.198
900	58.329	.428	23.556	7.261	.000	10.426
950	58.329	.405	23.056	7.580	.000	10.631
1000	58.329	.384	22.603	7.867	.000	10.816
1100	58.329	.349	21.829	8.380	.000	11.133
1200	58.329	.321	21.204	8.757	.000	11.387
1300	58.329	.298	20.705	9.075	.000	11.592

09.54.31.UCLP, 5B, DEFTERM, 0.132KLNS.

EQUILIBRIUM COMPOSITION OF GAS RUN 16

ASHLESS GASIFICATION

COMPOSITION OF FEEDSTOCK /WT%/

CARBON = 45.300
HYDROGEN = 5.800
OXYGEN = 48.800
NITROGEN = 0.000

FLOWRATE OF FEEDSTOCK /KG/H/= .675

COMPOSITION GAS IN /WT%/

H2O = 3.000
O2 = 22.600
N2 = 74.400

FLOWRATE OF BLAST /KG/H/ = 3.111

GAS COMPOSITION /VOL%/

T	N2	H2	CO2	CO	CH4	H2O	GAS KG/H
600	61.992	3.455	17.487	1.522	.001	15.543	3.787
650	61.990	3.199	17.229	1.781	.000	15.800	3.787
700	61.988	2.959	16.989	2.023	.000	16.041	3.787
750	61.987	2.738	16.767	2.245	-.000	16.262	3.787
800	61.986	2.536	16.565	2.448	-.000	16.464	3.787
850	61.985	2.354	16.383	2.632	-.000	16.647	3.787
900	61.984	2.190	16.219	2.797	-.000	16.811	3.787
950	61.983	2.043	16.072	2.944	-.000	16.958	3.787
1000	61.982	1.911	15.940	3.077	-.000	17.090	3.787
1100	61.981	1.689	15.718	3.300	-.000	17.312	3.787
1200	61.980	1.514	15.542	3.476	-.000	17.488	3.787
1300	61.979	1.377	15.405	3.614	.000	17.625	3.787

GAS COMPOSITION /WT%/

T	N2	H2	CO2	CO	CH4	H2O	GAS KG/H
600	61.125	.245	27.253	1.500	.000	9.877	3.787
650	61.125	.227	26.852	1.756	.000	10.040	3.787
700	61.125	.210	26.478	1.994	.000	10.193	3.787
750	61.125	.194	26.133	2.213	-.000	10.334	3.787
800	61.125	.180	25.819	2.413	-.000	10.463	3.787
850	61.125	.167	25.535	2.594	-.000	10.579	3.787
900	61.125	.155	25.279	2.757	-.000	10.684	3.787
950	61.125	.145	25.051	2.902	-.000	10.777	3.787
1000	61.125	.135	24.845	3.033	-.000	10.861	3.787
1100	61.125	.120	24.500	3.253	-.000	11.003	3.787
1200	61.125	.107	24.227	3.426	-.000	11.115	3.787
1300	61.125	.097	24.013	3.562	.000	11.202	3.787

14.34.18.UCLP, 5B, OEFTERM, 0.128KLNS.

EQUILIBRIUM COMPOSITION OF GAS RUN 18

ASHLESS GASIFICATION

COMPOSITION OF FEEDSTOCK /WT%/

CARBON = 45.300
HYDROGEN = 5.800
OXYGEN = 48.800
NITROGEN = 0.000

FLOWRATE OF FEEDSTOCK /KG/H/= 1.386

COMPOSITION GAS IN /WT%/

H2O = 6.100
O2 = 21.900
N2 = 72.000

FLOWRATE OF BLAST /KG/H/ = 3.149

GAS COMPOSITION /VOL%/

T	N2	H2	CO2	CO	CH4	H2O	GAS KG/H
600	44.796	17.102	16.034	11.615	1.206	9.247	4.536
650	44.000	18.028	14.335	13.718	.300	9.618	4.536
700	43.790	17.710	13.331	14.830	.064	10.275	4.536
750	43.744	17.098	12.577	15.608	.014	10.958	4.536
800	43.732	16.478	11.927	16.265	.004	11.593	4.536
850	43.728	15.905	11.347	16.848	.001	12.170	4.536
900	43.725	15.385	10.826	17.372	.000	12.692	4.536
950	43.723	14.914	10.355	17.845	.000	13.163	4.536
1000	43.721	14.488	9.929	18.272	.000	13.589	4.536
1100	43.718	13.755	9.197	19.007	.000	14.322	4.536
1200	43.716	13.159	8.602	19.605	.000	14.919	4.536
1300	43.714	12.678	8.121	20.087	-.000	15.400	4.536

GAS COMPOSITION /WT%/

T	N2	H2	CO2	CO	CH4	H2O	GAS KG/H
600	49.981	1.370	28.276	12.953	.771	6.649	4.536
650	49.981	1.470	25.737	15.575	.195	7.040	4.536
700	49.981	1.451	24.050	16.918	.042	7.558	4.536
750	49.981	1.403	22.713	17.825	.009	8.069	4.536
800	49.981	1.352	21.545	18.580	.002	8.539	4.536
850	49.981	1.305	20.500	19.249	.001	8.964	4.536
900	49.981	1.263	19.558	19.848	.000	9.349	4.536
950	49.981	1.224	18.709	20.389	.000	9.697	4.536
1000	49.981	1.189	17.940	20.878	.000	10.011	4.536
1100	49.981	1.129	16.619	21.719	.000	10.552	4.536
1200	49.981	1.080	15.544	22.403	.000	10.992	4.536
1300	49.981	1.041	14.676	22.955	-.000	11.347	4.536

10.45.23.UCLP, 5B, DEFTERM, 0.128KLNS.

EQUILIBRIUM COMPOSITION OF GAS

RUN 19

ASHLESS GASIFICATION

COMPOSITION FEEDSTOCK /WT%/

CARBON = 45.300
HYDROGEN = 5.800
OXYGEN = 48.800
NITROGEN = 0.000

FLOWRATE OF FEEDSTOCK /KG/H/= 1.386

COMPOSITION GAS IN /WT%/

H2O = 7.300
O2 = 21.600
N2 = 71.100

FLOWRATE OF BLAST /KG/H/ = 2.615

GAS COMPOSITION /VOL%/

T	N2	H2	CO2	CO	CH4	H2O	GAS KG/H
600	40.674	19.016	15.722	14.021	2.215	8.351	4.002
650	39.465	21.028	13.400	16.957	.668	8.483	4.002
700	39.062	21.204	12.139	18.423	.155	9.018	4.002
750	38.967	20.716	11.321	19.290	.036	9.669	4.002
800	38.944	20.123	10.654	19.970	.009	10.300	4.002
850	38.937	19.554	10.067	20.561	.003	10.878	4.002
900	38.934	19.033	9.542	21.089	.001	11.401	4.002
950	38.931	18.562	9.069	21.563	.000	11.874	4.002
1000	38.930	18.135	8.643	21.992	.000	12.301	4.002
1100	38.927	17.402	7.911	22.726	.000	13.034	4.002
1200	38.925	16.808	7.318	23.321	.000	13.628	4.002
1300	38.923	16.331	6.842	23.798	-.000	14.105	4.002

GAS COMPOSITION /WT%/

T	N2	H2	CO2	CO	CH4	H2O	GAS KG/H
600	46.455	1.559	28.382	16.007	1.450	6.147	4.002
650	46.455	1.777	24.931	19.951	.450	6.435	4.002
700	46.455	1.811	22.818	21.899	.105	6.911	4.002
750	46.455	1.773	21.332	22.986	.025	7.429	4.002
800	46.455	1.724	20.087	23.810	.006	7.918	4.002
850	46.455	1.675	18.985	24.519	.002	8.364	4.002
900	46.455	1.631	17.996	25.151	.001	8.767	4.002
950	46.455	1.590	17.105	25.718	.000	9.131	4.002
1000	46.455	1.554	16.301	26.230	.000	9.460	4.002
1100	46.455	1.491	14.922	27.108	.000	10.024	4.002
1200	46.455	1.440	13.804	27.819	.000	10.482	4.002
1300	46.455	1.399	12.907	28.390	-.000	10.849	4.002

09.54.59.UCLP, 5B, DEFTERM, 0.132KLNS.

EQUILIBRIUM COMPOSITION OF GAS RUN 20

ASHLESS GASIFICATION

COMPOSITION OF FEEDSTOCK /WT%/

CARBON = 45.300
HYDROGEN = 5.800
OXYGEN = 48.800
NITROGEN = 0.000

FLOWRATE OF FEEDSTOCK /KG/H/= 1.386

COMPOSITION GAS IN /WT%/

H2O = 5.100
O2 = 22.100
N2 = 72.800

FLOWRATE OF BLAST /KG/H/ = 3.758

GAS COMPOSITION /VOL%/

T	N2	H2	CO2	CO	CH4	H2O	GAS KG/H
600	48.936	14.657	16.419	9.156	.537	10.294	5.145
650	48.520	14.737	15.225	10.562	.112	10.845	5.145
700	48.430	14.182	14.402	11.431	.022	11.532	5.145
750	48.410	13.549	13.718	12.127	.005	12.191	5.145
800	48.404	12.953	13.111	12.737	.001	12.793	5.145
850	48.401	12.410	12.566	13.285	.000	13.337	5.145
900	48.398	11.919	12.075	13.779	.000	13.829	5.145
950	48.396	11.476	11.631	14.224	.000	14.273	5.145
1000	48.395	11.074	11.230	14.627	.000	14.675	5.145
1100	48.392	10.382	10.539	15.321	.000	15.367	5.145
1200	48.389	9.818	9.975	15.886	-.000	15.931	5.145
1300	48.387	9.363	9.520	16.343	-.000	16.386	5.145

GAS COMPOSITION /WT%/

T	N2	H2	CO2	CO	CH4	H2O	GAS KG/H
600	53.172	1.143	28.198	9.944	.335	7.208	5.145
650	53.172	1.160	26.371	11.569	.070	7.659	5.145
700	53.172	1.118	24.993	12.544	.014	8.159	5.145
750	53.172	1.069	23.815	13.313	.003	8.629	5.145
800	53.172	1.022	22.765	13.985	.001	9.056	5.145
850	53.172	.979	21.820	14.588	.000	9.442	5.145
900	53.172	.940	20.967	15.130	.000	9.791	5.145
950	53.172	.905	20.198	15.620	.000	10.106	5.145
1000	53.172	.874	19.501	16.063	.000	10.391	5.145
1100	53.172	.819	18.302	16.826	.000	10.881	5.145
1200	53.172	.775	17.325	17.448	-.000	11.281	5.145
1300	53.172	.739	16.535	17.950	-.000	11.604	5.145

14.46.32.UCLP, 5B, OEFTERM, 0.128KLNS.

EQUILIBRIUM COMPOSITION OF GAS RUN 21

ASHLESS GASIFICATION

COMPOSITION OF FEEDSTOCK /WT%/

CARBON = 45.300
HYDROGEN = 5.800
OXYGEN = 48.800
NITROGEN = 0.000

FLOWRATE OF FEEDSTOCK /KG/H/= 1.386

COMPOSITION GAS IN /WT%/

H2O = 9.300
O2 = 22.100
N2 = 69.600

FLOWRATE OF BLAST /KG/H/ = 2.070

GAS COMPOSITION /VOL%/

T	N2	H2	CO2	CO	CH4	H2O	GAS KG/H
600	35.453	20.770	15.848	16.485	3.624	7.820	3.478
650	33.916	23.965	12.790	20.324	1.306	7.699	3.478
700	33.276	24.913	11.137	22.303	.341	8.029	3.478
750	33.103	24.684	10.214	23.315	.083	8.600	3.478
800	33.061	24.166	9.531	24.020	.022	9.200	3.478
850	33.049	23.624	8.950	24.609	.006	9.761	3.478
900	33.045	23.119	8.434	25.128	.002	10.273	3.478
950	33.042	22.659	7.971	25.592	.001	10.734	3.478
1000	33.041	22.243	7.555	26.010	.000	11.151	3.478
1100	33.039	21.531	6.843	26.724	.000	11.863	3.478
1200	33.037	20.956	6.270	27.299	.000	12.438	3.478
1300	33.036	20.498	5.813	27.758	.000	12.896	3.478

GAS COMPOSITION /WT%/

T	N2	H2	CO2	CO	CH4	H2O	GAS KG/H
600	41.424	1.742	29.266	19.252	2.426	5.888	3.478
650	41.424	2.102	24.690	24.811	.914	6.060	3.478
700	41.424	2.227	21.914	27.751	.243	6.441	3.478
750	41.424	2.218	20.201	29.162	.060	6.936	3.478
800	41.424	2.174	18.876	30.082	.016	7.429	3.478
850	41.424	2.126	17.731	30.830	.005	7.885	3.478
900	41.424	2.081	16.710	31.485	.001	8.299	3.478
950	41.424	2.040	15.795	32.069	.001	8.672	3.478
1000	41.424	2.002	14.970	32.594	.000	9.009	3.478
1100	41.424	1.938	13.562	33.491	.000	9.586	3.478
1200	41.424	1.887	12.426	34.213	.000	10.050	3.478
1300	41.424	1.845	11.520	34.789	.000	10.421	3.478

14.50.56.UCLP, 5B, OEFTERM, 0.128KLNS.

EQUILIBRIUM COMPOSITION OF GAS RUN 22

ASHLESS GASIFICATION

COMPOSITION OF FEEDSTOCK /WT%/

CARBON = 45.300
HYDROGEN = 5.800
OXYGEN = 48.800
NITROGEN = 0.000

FLOWRATE OF FEEDSTOCK /KG/H/= 1.818

COMPOSITION GAS IN /WT%/

H2O = 9.400
O2 = 22.100
N2 = 69.500

FLOWRATE OF BLAST /KG/H/ = 2.675

GAS COMPOSITION /VOL%/

T	N2	H2	CO2	CO	CH4	H2O	GAS KG/H
600	35.148	20.851	15.842	16.661	3.732	7.765	4.521
650	33.592	24.125	12.735	20.559	1.360	7.629	4.521
700	32.935	25.136	11.052	22.576	.358	7.942	4.521
750	32 755	24.932	10.121	23.599	.088	8.504	4.521
800	32.711	24.422	9.439	24.305	.023	9.100	4.521
850	32.699	23.885	8.859	24.892	.007	9.658	4.521
900	32.694	23.382	8.345	25.409	.002	10.167	4.521
950	32.692	22.925	7.885	25.871	.001	10.626	4.521
1000	32.691	22.510	7.470	26.287	.000	11.041	4.521
1100	32.688	21.802	6.762	26.998	.000	11.750	4.521
1200	32.687	21.230	6.192	27.570	.000	12.321	4.521
1300	32.685	20.775	5.738	28.026	-.000	12.777	4.521

GAS COMPOSITION /WT%/

T	N2	H2	CO2	CO	CH4	H2O	GAS KG/H
600	41.118	1.751	29.292	19.482	2.502	5.854	4.521
650	41.118	2.120	24.637	25.153	.954	6.018	4.521
700	41.118	2.253	21.810	28.172	.256	6.390	4.521
750	41.118	2.247	20.082	29.610	.063	6.880	4.521
800	41.118	2.204	18.753	30.537	.017	7.371	4.521
850	41.118	2.156	17.608	31.286	.005	7.827	4.521
900	41.118	2.111	16.589	31.940	.002	8.240	4.521
950	41.118	2.070	15.674	32.524	.001	8.613	4.521
1000	41.118	2.033	14.851	33.048	.000	8.950	4.521
1100	41.118	1.969	13.444	33.943	.000	9.525	4.521
1200	41.118	1.918	12.311	34.664	.000	9.989	4.521
1300	41.118	1.876	11.408	35.239	-.000	10.358	4.521

11.23.18.UCLP, 5B, OEFTERM, 0.128KLNS.

EQUILIBRIUM COMPOSITION OF GAS RUN 23

ASHLESS GASIFICATION

COMPOSITION OF FEEDSTOCK /WT%/

CARBON = 45.300
HYDROGEN = 5.800
OXYGEN = 48.800
NITROGEN = 0.000

FLOWRATE OF FEEDSTOCK /KG/H/= 1.818

COMPOSITION GAS IN /WT%/

H2O = 10.500
O2 = 20.800
N2 = 68.600

FLOWRATE OF BLAST /KG/H/ = 2.398

GAS COMPOSITION /VOL%/

T	N2	H2	CO2	CO	CH4	H2O	GAS KG/h
600	32.954	21.470	15.469	18.132	4.800	7.175	4.215
650	31.228	25.458	11.956	22.523	1.936	6.899	4.215
700	30.398	27.110	10.004	24.897	.560	7.031	4.215
750	30.145	27.200	9.002	26.029	.142	7.482	4.215
800	30.081	26.802	8.332	26.732	.038	8.015	4.215
850	30.063	26.322	7.783	27.291	.011	8.529	4.215
900	30.058	25.860	7.302	27.775	.004	9.001	4.215
950	30.055	25.437	6.873	28.206	.001	9.428	4.215
1000	30.053	25.052	6.488	28.593	.000	9.813	4.215
1100	30.051	24.397	5.833	29.250	.000	10.469	4.215
1200	30.050	23.870	5.308	29.777	.000	10.995	4.215
1300	30.049	23.453	4.891	30.195	.000	11.413	4.215

GAS COMPOSITION /WT%/

T	N2	H2	CO2	CO	CH4	H2O	GAS KG/H
600	39.025	1.826	28.955	21.462	3.257	5.475	4.215
650	39.025	2.284	23.615	28.133	1.386	5.556	4.215
700	39.025	2.499	20.300	31.947	.412	5.817	4.215
750	39.025	2.528	18.419	33.680	.106	6.242	4.215
800	39.025	2.497	17.085	34.664	.028	6.701	4.215
850	39.025	2.453	15.969	35.409	.008	7.135	4.215
900	39.025	2.411	14.985	36.045	.003	7.531	4.215
950	39.025	2.371	14.106	36.607	.001	7.889	4.215
1000	39.025	2.336	13.316	37.111	.000	8.211	4.215
1100	39.025	2.275	11.973	37.966	.000	8.761	4.215
1200	39.025	2.226	10.895	38.652	.000	9.202	4.215
1300	39.025	2.187	10.040	39.196	.000	9.552	4.215

11.23.55.UCLP, 5B, DEFTERM, 0.128KLNS.

EQUILIBRIUM COMPOSITION OF GAS RUN 24

ASHLESS GASIFICATION

COMPOSITION OF FEEDSTOCK /WT%/

CARBON = 45.300
HYDROGEN = 5.800
OXYGEN = 48.800
NITROGEN = 0.000

FLOWRATE OF FEEDSTOCK /KG/H/= 1.818

COMPOSITION GAS IN /WT%/

H2O = 6.600
O2 = 21.800
N2 = 71.700

FLOWRATE OF BLAST /KG/H/ = 3.845

GAS COMPOSITION /VOL%/

T	N2	H2	CO2	CO	CH4	H2O	GAS KG/H
600	43.167	17.926	15.906	12.537	1.556	8.908	5.669
650	42.210	19.254	13.978	14.952	.417	9.189	5.669
700	41.934	19.094	12.885	16.186	.091	9.810	5.669
750	41.872	18.515	12.106	16.997	.021	10.488	5.669
800	41.857	17.899	11.446	17.666	.005	11.127	5.669
850	41.851	17.323	10.860	18.256	.002	11.708	5.669
900	41.849	16.799	10.334	18.785	.001	12.234	5.669
950	41.847	16.324	9.859	19.261	.000	12.709	5.669
1000	41.845	15.895	9.430	19.692	.000	13.138	5.669
1100	41.842	15.157	8.693	20.431	.000	13.877	5.669
1200	41.840	14.558	8.094	21.032	.000	14.476	5.669
1300	41.838	14.075	7.612	21.516	.000	14.959	5.669

GAS COMPOSITION /WT%/

T	N2	H2	CO2	CO	CH4	H2O	GAS KG/H
600	48.634	1.450	28.325	14.118	1.004	6.468	5.669
650	48.634	1.593	25.455	17.219	.276	6.823	5.669
700	48.634	1.590	23.619	18.763	.061	7.332	5.669
750	48.634	1.544	22.224	19.733	.014	7.851	5.669
800	48.634	1.493	21.021	20.517	.004	8.331	5.669
850	48.634	1.445	19.947	21.204	.001	8.768	5.669
900	48.634	1.402	18.981	21.820	.000	9.162	5.669
950	48.634	1.362	18.110	22.375	.000	9.519	5.669
1000	48.634	1.326	17.323	22.876	.000	9.841	5.669
1100	48.634	1.265	15.970	23.737	.000	10.394	5.669
1200	48.634	1.215	14.871	24.436	.000	10.844	5.669
1300	48.634	1.175	13.986	24.999	.000	11.206	5.669

11.25.33.UCLP, 5B, DEFTERM, 0.128KLNS.

EQUILIBRIUM COMPOSITION OF GAS RUN 25

ASHLESS GASIFICATION

COMPOSITION OF FEEDSTOCK /WT%/

CARBON = 45.300
HYDROGEN = 5.800
OXYGEN = 48.800
NITROGEN = 0.000

FLOWRATE OF FEEDSTOCK /KG/H/= 1.818

COMPOSITION GAS IN /WT%/

H2O = 7.800
O2 = 20.800
N2 = 71.400

FLOWRATE OF BLAST /KG/H/ = 3.241

GAS COMPOSITION /VOL%/

T	N2	H2	CO2	CO	CH4	H2O	GAS KG/H
600	39.704	19.519	15.342	14.855	2.684	7.896	5.061
650	38.333	21.974	12.793	18.101	.870	7.929	5.061
700	37.833	22.425	11.424	19.724	.211	8.383	5.061
750	37.709	22.032	10.589	20.623	.050	8.997	5.061
800	37.679	21.474	9.930	21.298	.013	9.606	5.061
850	37.670	20.925	9.356	21.877	.004	10.167	5.061
900	37.667	20.419	8.844	22.392	.001	10.677	5.061
950	37.665	19.960	8.384	22.854	.000	11.137	5.061
1000	37.663	19.545	7.969	23.271	.000	11.552	5.061
1100	37.660	18.834	7.258	23.984	.000	12.264	5.061
1200	37.658	18.258	6.684	24.560	.000	12.839	5.061
1300	37.657	17.798	6.224	25.021	-.000	13.300	5.061

GAS COMPOSITION /WT%/

T	N2	H2	CO2	CO	CH4	H2O	GAS KG/H
600	45.726	1.614	27.928	17.100	1.772	5.860	5.061
650	45.726	1.882	24.120	21.581	.595	6.095	5.061
700	45.726	1.946	21.824	23.828	.146	6.530	5.061
750	45.726	1.918	20.294	24.996	.035	7.031	5.061
800	45.726	1.871	19.046	25.835	.009	7.512	5.061
850	45.726	1.824	17.951	26.543	.003	7.953	5.061
900	45.726	1.780	16.970	27.170	.001	8.353	5.061
950	45.726	1.740	16.088	27.733	.000	8.713	5.061
1000	45.726	1.704	15.292	28.239	.000	9.039	5.061
1100	45.726	1.642	13.929	29.107	.000	9.596	5.061
1200	45.726	1.592	12.828	29.807	.000	10.047	5.061
1300	45.726	1.552	11.946	30.369	-.000	10.408	5.061

11.28.36.UCLP, 5B, DEFTERM, 0.128KLNS.

EQUILIBRIUM COMPOSITION OF GAS RUN. 26

ASHLESS GASIFICATION

COMPOSITION FEEDSTOCK /WT%/

CARBON = 45.300
HYDROGEN = 5.800
OXYGEN = 48.800
NITROGEN = 0.000

FLOWRATE OF FEEDSTOCK /KG/H/= 1.905

COMPOSITION GAS IN /WT%/

H2O = 8.600
O2 = 21.300
N2 = 70.100

FLOWRATE OF BLAST /KG/H/ = 3.087

GAS COMPOSITION /VOL%/

T	N2	H2	CO2	CO	CH4	H2O	GAS KG/H
600	37.301	20.259	15.586	15.808	3.224	7.823	4.774
650	35.819	23.156	12.743	19.404	1.115	7.763	4.774
700	35.233	23.094	11.215	21.231	.282	8.146	4.774
750	35.080	23.593	10.331	22.193	.068	8.736	4.774
800	35.043	23.057	9.660	22.884	.018	9.338	4.774
850	35.032	22.513	9.083	23.467	.005	9.899	4.774
900	35.028	22.008	8.569	23.984	.002	10.409	4.774
950	35.026	21.548	8.108	24.447	.001	10.870	4.774
1000	35.025	21.133	7.693	24.864	.000	11.286	4.774
1100	35.022	20.422	6.982	25.576	.000	11.997	4.774
1200	35.020	19.848	6.410	26.151	.000	12.571	4.774
1300	35.019	19.390	5.952	26.610	.000	13.029	4.774

GAS COMPOSITION /WT%/

T	N2	H2	CO2	CO	CH4	H2O	GAS KG/H
600	43.334	1.690	28.618	18.355	2.146	5.857	4.774
650	43.334	2.011	24.366	23.463	.773	6.053	4.774
700	43.334	2.110	21.801	26.100	.199	6.457	4.774
750	43.334	2.092	20.171	27.401	.048	6.954	4.774
800	43.334	2.047	18.881	28.284	.013	7.442	4.774
850	43.334	1.999	17.758	29.014	.004	7.891	4.774
900	43.334	1.955	16.755	29.656	.001	8.299	4.774
950	43.334	1.914	15.855	30.231	.000	8.666	4.774
1000	43.334	1.877	15.043	30.748	.000	8.998	4.774
1100	43.334	1.814	13.655	31.631	.000	9.566	4.774
1200	43.334	1.763	12.536	32.343	.000	10.024	4.774
1300	43.334	1.723	11.641	32.912	.000	10.390	4.774

09.48.58.UCLP, 5B, DEFTERM, 0.132KLNS.

EQUILIBRIUM COMPOSITION OF GAS RUN 27

ASHLESS GASIFICATION

COMPOSITION OF FEEDSTOCK /WT%/

CARBON = 45.300
HYDROGEN = 5.800
OXYGEN = 48.800
NITROGEN = 0.000

FLOWRATE OF FEEDSTOCK /KG/H/= 1.905

COMPOSITION GAS IN /WT%/

H2O = 7.000
O2 = 21.500
N2 = 70.800

FLOWRATE OF BLAST /KG/H/ = 3.138

GAS COMPOSITION /VOL%/

T	N2	H2	CO2	CO	CH4	H2O	GAS KG/H
600	38.400	19.576	15.394	16.141	3.177	7.312	5.022
650	36.892	22.437	12.564	19.710	1.096	7.302	5.022
700	36.298	23.171	11.059	21.507	.276	7.689	5.022
750	36.144	22.881	10.196	22.446	.066	8.267	5.022
800	36.106	22.360	9.543	23.119	.017	8.855	5.022
850	36.096	21.829	8.980	23.688	.005	9.402	5.022
900	36.092	21.337	8.479	24.192	.002	9.899	5.022
950	36.089	20.888	8.028	24.644	.001	10.349	5.022
1000	36.088	20.482	7.622	25.052	.000	10.756	5.022
1100	36.086	19.786	6.927	25.750	.000	11.452	5.022
1200	36.084	19.223	6.365	26.313	.000	12.015	5.022
1300	36.082	18.773	5.916	26.764	-.000	12.465	5.022

GAS COMPOSITION /WT%/

T	N2	H2	CO2	CO	CH4	H2O	GAS KG/H
600	44.238	1.619	28.030	18.586	2.098	5.429	5.022
650	44.238	1.932	23.812	23.623	.753	5.642	5.022
700	44.238	2.028	21.303	26.200	.193	6.039	5.022
750	44.238	2.011	19.725	27.460	.046	6.520	5.022
800	44.238	1.967	18.479	28.312	.012	6.991	5.022
850	44.238	1.921	17.395	29.017	.004	7.426	5.022
900	44.238	1.878	16.425	29.638	.001	7.819	5.022
950	44.238	1.838	15.554	30.194	.000	8.175	5.022
1000	44.238	1.803	14.767	30.695	.000	8.497	5.022
1100	44.238	1.742	13.421	31.552	.000	9.048	5.022
1200	44.238	1.692	12.334	32.244	.000	9.493	5.022
1300	44.238	1.653	11.463	32.798	-.000	9.849	5.022

11.32.56.UCLP, 5B, DEFTERM, 0.128KLNS.

EQUILIBRIUM COMPOSITION OF GAS RUN 28

ASHLESS GASIFICATION

COMPOSITION FEEDSTOCK /WT%/

CARBON = 45.300
HYDROGEN = 5.800
OXYGEN = 48.800
NITROGEN = 0.000

FLOWRATE OF FEEDSTOCK /KG/H/= 1.636

COMPOSITION GAS IN /WT%/

H2O = 6.500
O2 = 21.800
N2 = 71.700

FLOWRATE OF BLAST /KG/H/ = 3.466

GAS COMPOSITION /VOL%/

T	N2	H2	CO2	CO	CH4	H2O	GAS KG/H
600	43.246	17.880	15.899	12.551	1.552	8.871	5 103
650	42.289	19.205	13.972	14.964	.416	9.154	5.103
700	42.013	19.044	12.881	16.196	.091	9.775	5.103
750	41.952	18.466	12.103	17.006	.021	10.453	5.103
800	41.936	17.850	11.444	17.673	.005	11.090	5.103
850	41.931	17.275	10.859	18.262	.002	11.671	5.103
900	41.928	16.752	10.333	18.790	.000	12.196	5.103
950	41.926	16.278	9.857	19.266	.000	12.670	5.103
1000	41.924	15.849	9.431	19.696	.000	13.099	5.103
1100	41.922	15.113	8.695	20.435	.000	13.836	5.103
1200	41.919	14.514	8.097	21.035	.000	14.435	5.103
1300	41.917	14.031	7.615	21.518	.000	14.918	5.103

GAS COMPOSITION /WT%/

T	N2	H2	CO2	CO	CH4	H2O	GAS KG/H
600	48.695	1.446	28.295	14.126	1.001	6.437	5.103
650	48.695	1.588	25.428	17.222	.275	6.793	5.103
700	48.695	1.585	23.596	18.762	.060	7.301	5.103
750	48.695	1.539	22.204	17.729	.014	7.819	5 103
800	48.695	1.488	21.003	20.512	.004	8.299	5.103
850	48.695	1.440	19.932	21.198	.001	8.734	5.103
900	48.695	1.397	18.968	21.812	.000	9.128	5.103
950	48.695	1.357	18.097	22.366	.000	9.483	5.103
1000	48.695	1.322	17.313	22.866	.000	9.805	5.103
1100	48.695	1.260	15.963	23.725	.000	10.357	5.103
1200	48.695	1.210	14.866	24.423	.000	10.806	5.103
1300	48.695	1.170	13.982	24.985	.000	11.168	5.103

20.25.53.UCLP, 5B, OEFTERM, 0.132KLNS.

EQUILIBRIUM COMPOSITION OF GAS RUN29

ASHLESS GASIFICATION

COMPOSITION FEEDSTOCK /WT%/

CARBON = 45.300
HYDROGEN = 5.800
OXYGEN = 48.800
NITROGEN = 0.000

FLOWRATE OF FEEDSTOCK /KG/H/= 2.409

COMPOSITION GAS IN /WT%/

H2O = 10.000
O2 = 21.000
N2 = 69.000

FLOWRATE OF BLAST /KG/H/ = 4.011

GAS COMPOSITION /VOL%/

T	N2	H2	CO2	CO	CH4	H2O	GAS KG/H
600	36.887	20.728	15.808	15.030	3.008	8.539	6.420
650	35.495	23.449	13.083	18.492	1.012	8.469	6.420
700	34.963	24.041	11.602	20.256	.251	8.887	6.420
750	34.827	23.674	10.714	21.216	.060	9.508	6.420
800	34.794	23.105	10.025	21.924	.016	10.136	6.420
850	34.785	22.538	9.429	22.526	.005	10.718	6.420
900	34.781	22.015	8.898	23.060	.001	11.246	6.420
950	34.779	21.540	8.421	23.538	.001	11.721	6.420
1000	34.777	21.111	7.992	23.968	.000	12.151	6.420
1100	34.775	20.377	7.259	24.704	.000	12.885	6.420
1200	34.773	19.785	6.668	25.297	.000	13.477	6.420
1300	34.772	19.312	6.196	25.770	.000	13.950	6.420

GAS COMPOSITION /WT%/

T	N2	H2	CO2	CO	CH4	H2O	GAS KG/H
600	43.088	1.738	29.185	17.548	2.013	6.428	6.420
650	43.088	2.044	25.102	22.437	.704	6.626	6.420
700	43.088	2.127	22.598	24.951	.178	7.058	6.420
750	43.088	2.103	20.950	26.235	.043	7.581	6.420
800	43.088	2.054	19.621	27.136	.011	8.089	6.420
850	43.088	2.004	18.460	27.889	.003	8.556	6.420
900	43.088	1.958	17.422	28.553	.001	8.978	6.420
950	43.088	1.916	16.490	29.147	.000	9.358	6.420
1000	43.088	1.878	15.651	29.682	.000	9.702	6.420
1100	43.088	1.813	14.217	30.594	.000	10.288	6.420
1200	43.088	1.760	13.060	31.330	.000	10.762	6.420
1300	43.088	1.718	12.136	31.918	.000	11.140	6.420

09.32.47.UCLP, 5B, DEFTERM, 0.132KLNS.

EQUILIBRIUM COMPOSITION OF GAS RUN 30

ASHLESS GASIFICATION

COMPOSITION FEEDSTOCK /WT%/

CARBON = 45.300
HYDROGEN = 5.800
OXYGEN = 48.800
NITROGEN = 0.000

FLOWRATE OF FEEDSTOCK /KG/H/= 2.358

COMPOSITION GAS IN /WT%/

H2O = 9.200
O2 = 21.100
N2 = 69.700

FLOWRATE OF BLAST /KG/H/ = 4.270

GAS COMPOSITION /VOL%/

T	N2	H2	CO2	CO	CH4	H2O	GAS KG/H
600	38.811	20.018	15.827	14.069	2.455	8.820	6.639
650	37.559	22.257	13.388	17.167	.767	8.861	6.639
700	37.123	22.545	12.055	18.732	.182	9.364	6.639
750	37.017	22.078	11.204	19.639	.043	10.018	6.639
800	36.992	21.480	10.519	20.339	.011	10.659	6.639
850	36.984	20.902	9.920	20.943	.003	11.248	6.639
900	36.981	20.371	9.384	21.481	.001	11.782	6.639
950	36.978	19.891	8.903	21.964	.000	12.263	6.639
1000	36.977	19.457	8.469	22.400	.000	12.697	6.639
1100	36.974	18.713	7.726	23.145	.000	13.441	6.639
1200	36.972	18.112	7.126	23.748	.000	14.043	6.639
1300	36.971	17.630	6.645	24.230	.000	14.524	6.639

GAS COMPOSITION /WT%/

T	N2	H2	CO2	CO	CH4	H2O	GAS KG/H
600	44.912	1.663	28.947	16.272	1.628	6.578	6.639
650	44.912	1.911	25.304	20.519	.526	6.828	6.639
700	44.912	1.958	23.051	22.652	.126	7.301	6.639
750	44.912	1.923	21.486	23.816	.030	7.833	6.639
800	44.912	1.872	20.186	24.681	.008	8.340	6.639
850	44.912	1.822	19.040	25.420	.002	8.803	6.639
900	44.912	1.776	18.014	26.076	.001	9.221	6.639
950	44.912	1.735	17.091	26.664	.000	9.598	6.639
1000	44.912	1.697	16.258	27.194	.000	9.939	6.639
1100	44.912	1.632	14.833	28.101	.000	10.522	6.639
1200	44.912	1.580	13.681	28.834	.000	10.993	6.639
1300	44.912	1.538	12.759	29.421	.000	11.371	6.639

11.46.03.UCLP, 5B, DEFTERM, 0.132KLNS.

EQUILIBRIUM COMPOSITION OF GAS RUN 31

ASHLESS GASIFICATION

COMPOSITION OF FEEDSTOCK /WT%/

CARBON = 45.300
HYDROGEN = 5.800
OXYGEN = 48.800
NITROGEN = 0.000

FLOWRATE OF FEEDSTOCK /KG/H/= 2.392

COMPOSITION GAS IN /WT%/

H2O = 8.000
O2 = 21.400
N2 = 70.600

FLOWRATE OF BLAST /KG/H/ = 5.019

GAS COMPOSITION /VOL%/

T	N2	H2	CO2	CO	CH4	H2O	GAS KG/H
600	42.045	18.590	15.990	12.314	1.606	9.455	7.414
650	41.088	19.972	14.042	14.765	.436	9.697	7.414
700	40.808	19.824	12.926	16.029	.096	10.317	7.414
750	40.745	19.237	12.129	16.859	.022	11.007	7.414
800	40.730	18.608	11.455	17.543	.006	11.658	7.414
850	40.724	18.021	10.857	18.145	.002	12.251	7.414
900	40.721	17.487	10.320	18.684	.001	12.787	7.414
950	40.719	17.004	9.837	19.169	.000	13.271	7.414
1000	40.717	16.566	9.400	19.608	.000	13.708	7.414
1100	40.715	15.816	8.650	20.360	.000	14.459	7.414
1200	40.712	15.207	8.042	20.971	.000	15.068	7.414
1300	40.711	14.717	7.553	21.462	-.000	15.558	7.414

GAS COMPOSITION /WT%/

T	N2	H2	CO2	CO	CH4	H2O	GAS KG/H
600	47.792	1.517	28.728	13.991	1.046	6.926	7.414
650	47.792	1.668	25.815	17.166	.291	7.269	7.414
700	47.792	1.667	23.926	18.763	.064	7.787	7.414
750	47.792	1.620	22.487	19.766	.015	8.320	7.414
800	47.792	1.568	21.245	20.575	.004	8.816	7.414
850	47.792	1.518	20.139	21.284	.001	9.265	7.414
900	47.792	1.474	19.144	21.918	.000	9.672	7.414
950	47.792	1.433	18.248	22.488	.000	10.038	7.414
1000	47.792	1.396	17.439	23.004	.000	10.369	7.414
1100	47.792	1.333	16.049	23.888	.000	10.938	7.414
1200	47.792	1.282	14.921	24.605	.000	11.399	7.414
1300	47.792	1.240	14.014	25.183	-.000	11.771	7.414

11.36.11.UCLP, 5B, OEFTERM, 0.128KLNS.

EQUILIBRIUM COMPOSITION OF GAS RUN 32

ASHLESS GASIFICATION

COMPOSITION FEEDSTOCK /WT%/

CARBON = 45.300
HYDROGEN = 5.800
OXYGEN = 48.800
NITROGEN = 0.000

FLOWRATE OF FEEDSTOCK /KG/H/= 2.341

COMPOSITION GAS IN /WT%/

H2O = .800
O2 = 21.400
N2 = 70.600

FLOWRATE OF BLAST /KG/H/ = 4.886

GAS COMPOSITION /VOL%/

T	N2	H2	CO2	CO	CH4	H2O	GAS KG/H
600	45.597	15.910	14.817	15.735	2.072	5.868	6.873
650	44.314	17.811	12.556	18.554	.612	6.153	6.873
700	43.896	18.009	11.403	19.889	.138	6.664	6.873
750	43.800	17.593	10.684	20.651	.032	7.240	6.873
800	43.777	17.077	10.102	21.244	.008	7.791	6.873
850	43.770	16.579	9.588	21.762	.002	8.299	6.873
900	43.767	16.120	9.125	22.227	.001	8.761	6.873
950	43.765	15.701	8.706	22.648	.000	9.180	6.873
1000	43.763	15.321	8.326	23.029	.000	9.561	6.873
1100	43.761	14.665	7.670	23.687	.000	10.217	6.873
1200	43.759	14.129	7.135	24.224	.000	10.753	6.873
1300	43.757	13.697	6.703	24.657	.000	11.186	6.873

GAS COMPOSITION /WT%/

T	N2	H2	CO2	CO	CH4	H2O	GAS KG/H
600	50.186	1.257	25.777	17.310	1.307	4.162	6.873
650	50.186	1.448	22.474	21.003	.397	4.491	6.873
700	50.186	1.478	20.606	22.728	.091	4.910	6.873
750	50.186	1.447	19.350	23.650	.021	5.346	6.873
800	50.186	1.406	18.304	24.342	.005	5.756	6.873
850	50.186	1.365	17.376	24.940	.002	6.132	6.873
900	50.186	1.327	16.537	25.475	.000	6.474	6.873
950	50.186	1.293	15.779	25.958	.000	6.784	6.873
1000	50.186	1.262	15.090	26.396	.000	7.065	6.873
1100	50.186	1.208	13.903	27.152	.000	7.551	6.873
1200	50.186	1.163	12.934	27.769	.000	7.948	6.873
1300	50.186	1.128	12.151	28.266	.000	8.268	6.873

11.38.22.UCLP, 5B, OEFTERM, 0.132KLNS.

EQUILIBRIUM COMPOSITION OF GAS RUN 33

ASHLESS GASIFICATION

COMPOSITION FEEDSTOCK /WT%/

CARBON = 45.300
HYDROGEN = 5.800
OXYGEN = 48.800
NITROGEN = 0.000

FLOWRATE OF FEEDSTOCK /KG/H/= 2.341

COMPOSITION GAS IN /WT%/

H2O = 9.000
O2 = 21.200
N2 = 69.800

FLOWRATE OF BLAST /KG/H/ = 4.343

GAS COMPOSITION /VOL%/

T	N2	H2	CO2	CO	CH4	H2O	GAS KG/H
600	39.282	19.816	15.870	13.796	2.307	8.928	6.687
650	38.075	21.915	13.510	16.792	.705	9.002	6.687
700	37.667	22.122	12.214	18.304	.165	9.528	6.687
750	37.549	21.631	11.372	19.199	.039	10.191	6.687
800	37.545	21.025	10.687	19.897	.010	10.835	6.687
850	37.538	20.443	10.087	20.502	.003	11.427	6.687
900	37.535	19.911	9.549	21.042	.001	11.962	6.687
950	37.533	19.428	9.066	21.527	.000	12.445	6.687
1000	37.531	18.992	8.631	21.964	.000	12.881	6.687
1100	37.529	18.245	7.885	22.713	.000	13.628	6.687
1200	37.526	17.641	7.281	23.319	.000	14.233	6.687
1300	37.525	17.156	6.797	23.804	.000	14.717	6.687

GAS COMPOSITION /WT%/

T	N2	H2	CO2	CO	CH4	H2O	GAS KG/H
600	45.332	1.642	28.947	15.913	1.526	6.640	6.687
650	45.332	1.873	25.424	19.982	.481	6.907	6.687
700	45.332	1.912	23.234	22.019	.114	7.390	6.687
750	45.332	1.874	21.688	23.154	.027	7.924	6.687
800	45.332	1.823	20.395	24.012	.007	8.431	6.687
850	45.332	1.773	19.253	24.747	.002	8.893	6.687
900	45.332	1.727	18.229	25.401	.001	9.310	6.687
950	45.332	1.685	17.308	25.988	.000	9.687	6.687
1000	45.332	1.647	16.477	26.517	.000	10.027	6.687
1100	45.332	1.582	15.053	27.423	.000	10.609	6.687
1200	45.332	1.530	13.902	28.156	.000	11.080	6.687
1300	45.332	1.488	12.979	28.743	.000	11.458	6.687

10.49.59.UCLP, 5B, OEFTERM, 0 132KLNS.

EQUILIBRIUM COMPOSITION OF GAS RUN 34

ASHLESS GASIFICATION

COMPOSITION FEEDSTOCK /WT%/

CARBON = 45.300
HYDROGEN = 5.800
OXYGEN = 48.800
NITROGEN = 0.000

FLOWRATE OF FEEDSTOCK /KG/H/= 1.961

COMPOSITION GAS IN /WT%/

H2O = 9.100
O2 = 21.200
N2 = 69.700

FLOWRATE OF BLAST /KG/H/ = 3.564

GAS COMPOSITION /VOL%/

T	N2	H2	CO2	CO	CH4	H2O	GAS KG/H
600	38.868	19.968	15.855	14.053	2.433	8.824	5.528
650	37.623	22.184	13.425	17.138	.758	8.872	5.528
700	37.191	22.459	12.096	18.695	.179	9.379	5.528
750	37.087	21.989	11.247	19.600	.042	10.035	5.528
800	37.061	21.389	10.562	20.300	.011	10.677	5.528
850	37.054	20.810	9.962	20.905	.003	11.267	5.528
900	37.050	20.279	9.426	21.443	.001	11.801	5.528
950	37.048	19.798	8.944	21.927	.000	12.282	5.528
1000	37.047	19.363	8.509	22.363	.000	12.717	5.528
1100	37.044	18.618	7.766	23.110	.000	13.462	5.528
1200	37.042	18.016	7.164	23.713	.000	14.065	5.528
1300	37.040	17.534	6.683	24.196	.000	14.547	5.528

GAS COMPOSITION /WT%/

T	N2	H2	CO2	CO	CH4	H2O	GAS KG/H
600	44.941	1.658	28.975	16.241	1.612	6.575	5.528
650	44.941	1.903	25.347	20.462	.519	6.830	5.528
700	44.941	1.949	23.103	22.580	.124	7.304	5.528
750	44.941	1.913	21.541	23.740	.029	7.837	5.528
800	44.941	1.862	20.242	24.604	.008	8.343	5.528
850	44.941	1.812	19.097	25.342	.002	8.806	5.528
900	44.941	1.766	18.071	25.998	.001	9.224	5.528
950	44.941	1.724	17.140	26.586	.000	9.601	5.528
1000	44.941	1.687	16.315	27.116	.000	9.942	5.528
1100	44.941	1.622	14.890	28.022	.000	10.525	5.528
1200	44.941	1.569	13.738	28.756	.000	10.996	5.528
1300	44.941	1.527	12.815	29.343	.000	11.374	5.528

10.33.19.UCLP, 5B, OEFTERM, 0.132KLNS.

EQUILIBRIUM COMPOSITION OF GAS RUN 35

ASHLESS GASIFICATION

COMPOSITION FEEDSTOCK /WT%/

CARBON = 45.300
HYDROGEN = 5.600
OXYGEN = 48.800
NITROGEN = 0.000

FLOWRATE OF FEEDSTOCK /KG/H/= 1.910

COMPOSITION GAS IN /WT%/

H2O = 10.800
O2 = 20.800
N2 = 68.400

FLOWRATE OF BLAST /KG/H/ = 2.940

GAS COMPOSITION /VOL%/

T	N2	H2	CO2	CO	CH4	H2O	GAS KG/H
600	35.187	21.305	15.769	15.899	3.564	8.276	4.853
650	33.681	24.465	12.781	19.687	1.278	8.109	4.853
700	33.058	25.375	11.154	21.648	.338	8.436	4.853
750	32.890	25.124	10.225	22.664	.081	9.015	4.853
800	32.849	24.593	9.535	23.377	.021	9.624	4.853
850	32.837	24.044	8.946	23.973	.006	10.193	4.853
900	32.833	23.532	8.423	24.499	.002	10.711	4.853
950	32.831	23.066	7.956	24.969	.001	11.178	4.853
1000	32.829	22.646	7.535	25.391	.000	11.599	4.853
1100	32.827	21.927	6.817	26.111	.000	12.318	4.853
1200	32.825	21.349	6.240	26.690	.000	12.896	4.853
1300	32.824	20.888	5.780	27.152	.000	13.357	4.853

GAS COMPOSITION /WT%/

T	N2	H2	CO2	CO	CH4	H2O	GAS KG/H
600	41.442	1.802	29.354	18.716	2.406	6.282	4.853
650	41.442	2.161	24.855	24.211	.901	6.430	4.853
700	41.442	2.284	22.094	27.126	.239	6.815	4.853
750	41.442	2.273	20.363	28.543	.059	7.320	4.853
800	41.442	2.228	19.013	29.478	.015	7.825	4.853
850	41.442	2.179	17.844	30.240	.005	8.290	4.853
900	41.442	2.133	16.804	30.907	.001	8.712	4.853
950	41.442	2.091	15.872	31.502	.001	9.093	4.853
1000	41.442	2.053	15.033	32.037	.000	9.436	4.853
1100	41.442	1.988	13.602	32.947	.000	10.021	4.853
1200	41.442	1.935	12.451	33.680	.000	10.492	4.853
1300	41.442	1.893	11.533	34.264	.000	10.868	4.853

10.22.51.UCLP, 5B, DEFTERM, 0.132KLNS.

EQUILIBRIUM COMPOSITION OF GAS RUN 36

ASHLESS GASIFICATION

COMPOSITION OF FEEDSTOCK /WT%/

CARBON = 45.300
HYDROGEN = 5.800
OXYGEN = 48.800
NITROGEN = 0.000

FLOWRATE OF FEEDSTOCK /KG/H/= 1.944

COMPOSITION GAS IN /WT%/

H2O = 9.100
O2 = 21.200
N2 = 69.600

FLOWRATE OF BLAST /KG/H/ = 3.547

GAS COMPOSITION /VOL%/

T	N2	H2	CO2	CO	CH4	H2O	GAS KG/H
600	38.900	19.956	15.872	14.004	2.410	8.859	5.490
650	37.662	22.151	13.454	17.074	.748	8.911	5.490
700	37.235	22.413	12.130	18.623	.177	9.422	5.490
750	37.132	21.938	11.281	19.527	.042	10.080	5.490
800	37.107	21.336	10.595	20.227	.011	10.723	5.490
850	37.099	20.756	9.995	20.833	.003	11.314	5.490
900	37.096	20.224	9.458	21.372	.001	11.848	5.490
950	37.094	19.743	8.976	21.857	.000	12.331	5.490
1000	37.092	19.307	8.540	22.293	.000	12.766	5.490
1100	37.090	18.561	7.795	23.041	.000	13.512	5.490
1200	37.088	17.958	7.193	23.645	.000	14.116	5.490
1300	37.086	17.475	6.711	24.130	.000	14.599	5.490

GAS COMPOSITION /WT%/

T	N2	H2	CO2	CO	CH4	H2O	GAS KG/H
600	44.967	1.656	29.000	16.180	1.597	6.599	5.490
650	44.967	1.899	25.389	20.376	.512	6.857	5.490
700	44.967	1.943	23.154	22.480	.122	7.333	5.490
750	44.967	1.907	21.593	23.636	.029	7.867	5.490
800	44.967	1.856	20.294	24.500	.008	8.374	5.490
850	44.967	1.806	19.148	25.239	.002	8.837	5.490
900	44.967	1.760	18.121	25.895	.001	9.256	5.490
950	44.967	1.718	17.197	26.483	.000	9.633	5.490
1000	44.967	1.681	16.364	27.014	.000	9.974	5.490
1100	44.967	1.616	14.938	27.921	.000	10.557	5.490
1200	44.967	1.563	13.784	28.655	.000	11.030	5.490
1300	44.967	1.521	12.860	29.243	.000	11.408	5.490

1. 40. 40. UCLP, 5B, OEFTERM, 0. 128KLNS.

EQUILIBRIUM COMPOSITION OF GAS RUN 37

ASHLESS GASIFICATION

COMPOSITION FEEDSTOCK /WT%/

CARBON = 45.300
HYDROGEN = 5.000
OXYGEN = 48.600
NITROGEN = 0.000

FLOWRATE OF FEEDSTOCK /KG/H/= 2.991

COMPOSITION GAS IN /WT%/

H2O = 7.600
O2 = 21.500
N2 = 70.900

FLOWRATE OF BLAST /KG/H/ = 4.741

GAS COMPOSITION /VOL%/

T	N2	H2	CO2	CO	CH4	H2O	GAS KG/H
600	37.549	19.914	15.397	16.424	3.404	7.312	7.734
650	35.998	22.952	12.464	20.123	1.205	7.258	7.734
700	35.366	23.814	10.896	22.004	.310	7.611	7.734
750	35.199	23.570	10.015	22.968	.075	8.174	7.734
800	35.158	23.062	9.358	23.646	.020	8.756	7.734
850	35.147	22.536	8.796	24.215	.006	9.301	7.734
900	35.142	22.046	8.296	24.717	.002	9.796	7.734
950	35.140	21.600	7.848	25.168	.001	10.244	7.734
1000	35.138	21.196	7.443	25.574	.000	10.648	7.734
1100	35.136	20.504	6.752	26.267	.000	11.341	7.734
1200	35.134	19.945	6.194	26.827	.000	11.900	7.734
1300	35.133	19.499	5.749	27.274	.000	12.346	7.734

GAS COMPOSITION /WT%/

T	N2	H2	CO2	CO	CH4	H2O	GAS KG/H
600	43.462	1.655	28.169	19.002	2.258	5.455	7.734
650	43.462	1.990	23.784	24.284	.833	5.647	7.734
700	43.462	2.101	21.163	27.028	.218	6.027	7.734
750	43.462	2.090	19.545	28.347	.053	6.504	7.734
800	43.462	2.047	18.284	29.217	.014	6.976	7.734
850	43.462	2.001	17.192	29.929	.004	7.412	7.734
900	43.462	1.958	16.217	30.555	.001	7.807	7.734
950	43.462	1.918	15.341	31.113	.000	8.165	7.734
1000	43.462	1.882	14.551	31.616	.000	8.488	7.734
1100	43.462	1.821	13.201	32.476	.000	9.040	7.734
1200	43.462	1.771	12.111	33.169	.000	9.486	7.734
1300	43.462	1.732	11.240	33.723	.000	9.843	7.734

10.17.44.UCLP, 5B, DEFTERM, 0.132KLNS.

EQUILIBRIUM COMPOSITION OF GAS RUN 38

ASHLESS GASIFICATION

COMPOSITION FEEDSTOCK /WT%/

CARBON = 45.300
HYDROGEN = 5.800
OXYGEN = 48.800
NITROGEN = 0.000

FLOWRATE OF FEEDSTOCK /KG/H/= 2.991

COMPOSITION GAS IN /WT%/

H2O = 7.700
O2 = 21.500
N2 = 70.800

FLOWRATE OF BLAST /KG/H/ = 4.675

GAS COMPOSITION /VOL%/

T	N2	H2	CO2	CO	CH4	H2O	GAS KG/H
600	37.245	20.001	15.395	16.587	3.502	7.271	7.668
650	35.675	23.114	12.415	20.341	1.253	7.202	7.668
700	35.026	24.032	10.820	22.257	.325	7.540	7.668
750	34.852	23.010	9.931	23.232	.079	8.095	7.668
800	34.810	23.310	9.274	23.911	.021	8.675	7.668
850	34.798	22.788	8.714	24.478	.006	9.216	7.668
900	34.794	22.300	8.216	24.979	.002	9.710	7.668
950	34.791	21.855	7.769	25.428	.001	10.156	7.668
1000	34.790	21.453	7.366	25.832	.000	10.559	7.668
1100	34.787	20.764	6.678	26.523	.000	11.249	7.668
1200	34.786	20.207	6.122	27.080	.000	11.805	7.668
1300	34.784	19.763	5.679	27.525	.000	12.249	7.668

GAS COMPOSITION /WT%/

T	N2	H2	CO2	CO	CH4	H2O	GAS KG/H
600	43.165	1.664	28.200	19.214	2.326	5.431	7.668
650	43.165	2.008	23.742	24.600	.869	5.616	7.668
700	43.165	2.126	21.075	27.416	.230	5.988	7.668
750	43.165	2.117	19.441	28.759	.056	6.461	7.668
800	43.165	2.075	18.177	29.636	.015	6.932	7.668
850	43.165	2.030	17.084	30.349	.004	7.367	7.668
900	43.165	1.986	16.110	30.974	.001	7.763	7.668
950	43.165	1.947	15.235	31.533	.000	8.120	7.668
1000	43.165	1.911	14.445	32.035	.000	8.443	7.668
1100	43.165	1.850	13.096	32.894	.000	8.995	7.668
1200	43.165	1.800	12.008	33.587	.000	9.440	7.668
1300	43.165	1.761	11.138	34.140	.000	9.796	7.668

10.10.18.UCLP, 5B, OEFTERM, 0 132KLINS.

APPENDIX VIII - CORRELATIONS OF EMPIRICAL MODEL

This Appendix gives all correlations examined in the development of the empirical models. Table A.VIII.1 lists all linear correlations and the corresponding coefficient of correlation. Tables A.VIII.2 - A.VIII.4 list the non linear correlations. For these, the best fit was given by the function which minimized the final sum of squares.

Table A. VIII. 1 : Linear correlations.

Correlation		Coefficient
N	$= 83.038 - 79.556\ S$	-0.685
X_{con}	$= 0.1723 + 0.5114\ S$	0.729
H_R	$= 4.429 + 12.561\ S$	0.815
Y_{H2}	$= 0.0216 - 0.0206\ S$	-0.626
Y_{CH4}	$= 0.0873 - 0.082\ S$	-0.720
Y_{CO}	$= 0.4356 - 0.3710\ S$	-0.644
Y_{C2}	$= 0.0487 - 0.0562\ S$	0.414
Y_{CO2}	$= 0.3852 + 0.9068\ S$	0.802
HHV	$= 16.463 - 0.014\ T_B$	-0.683
N	$= 153.2 - 0.121\ T_B$	0.577
T_o	$= -298.6 + 1.174\ T_B$	0.851
HHV	$= 6.51 - 0.0844\ M$	0.941
N	$= 8.02 + 9.288\ HHV$	0.910

Table A. VIII. 2 : Non linear correlation for air factor (x) and higher heating value (y).

Equation type	Final sum of squares	Standard deviation	Parameters a value	a error	b value	b error	c value	c error	Partial correlation a-b	a-c	c-b
$Y = a + \frac{b}{\log x}$	26.71	1.102	5.970	0.3158	0.3983	0.0750	-	-	0.7019	-	-
$Y = a + \frac{b}{x}$	19.41	0.9393	-0.2019	0.7135	1.705	0.2487	-	-	-0.9671	-	-
$Y = a \times b$	19.37	0.9382	1.749	0.3589	-0.9449	0.1722	-	-	0.9822	-	-
$Y = \frac{1}{a + b \log x}$	18.90	0.9268	0.0250	0.0354	0.5274	0.1171	-	-	-0.9799	-	-
$Y = a + b \log x$	14.48	0.8114	0.1719	0.5750	-10.31	1.228	-	-	0.9576	-	-
$Y + a x^b + cx$	13.75	0.8095	6.151	3.249	-0.1804	0.3101	-6.983	4.070	0.9946	-0.9871	-0.9689
$Y = a + b \log x + cx$	13.75	0.8086	5.322	4.831	-3932	6.065	-6.088	5.669	0.9954	-0.9924	-.09794

Table A. VIII. 3 : Non-linear correlation for air factor (x) and gas yield (y).

Equation	Final sum of squares	Standard deviation	Parameters a value	a error	b value	b error	c value	c error	Partial correlation a-b	b-c	c-b
$Y = \frac{1}{a+b^x}$	1.616	0.2711	0.5274	0.0169	-0.3721	0.0261	-	-	-0.9172	-	-
$Y = ab^x$	1.181	0.2317	1.611	0.0683	3.574	0.3064	-	-	-0.9121	-	-
$Y = a+b\log x$	0.9901	0.2121	4.683	0.1503	4.536	0.3211	-	-	0.9576	-	-
$Y = ax^b + cx$	0.9368	0.2063	6.518	19.71	0.7226	0.6997	-1.433	19.95	0.999	-0.999	-0.999
$Y = ax^b + cx$	0.9298	0.2056	5.0823	0.1970	0.6092	0.1337	-0.0441	0.1061	0.5162	0.2734	0.9578
$Y = a+b\log x + cx$	0.9256	0.2051	2.595	1.223	0.8632	0.6663	2.483	1.436	0.9955	-0.9929	-0.9796
$Y = ax^b$	0.8654	0.1983	5.087	0.1865	0.6536	0.03858	-	-	0.9139	-	-

Table A. VIII. 4 : Non-linear correlation for air factor (x) and bed temperature (y).

Equation	Final sum of squares	Standard deviation	Parameters a value	a error	b value	b error	Partial correlation
$Y = \frac{1}{a+b^x}$	86685.5	61.391	0.0019	4.49 E-5	-4.63 E-4	9.76 E-5	-0.916
$Y = ab^x$	84877.3	60.715	704.3	27.14	1.519	0.138	-0.924
$Y = \frac{x}{a+b^x}$	79480.6	58.785	1.03 E-4	2.105 E-5	9.13 E-4	6.03 E-5	-0.958
$Y = axb$	79016.3	58.613	1022.3	45.815	0.208	0.0426	0.948
$Y = a+b \log x$	78739.4	58.510	1012.2	41.368	414.88	87.804	0.959

APPENDIX IX : CALCULATION OF BURN OUT TIME

When a batch of solids burns, the oxygen is progressively consumed from the distributor, while a fraction always bypasses through the bed in bubbles. The rate of combustion can be controlled by the oxygen transfer from bubble to dense phase, the mechanism of reaction at the active char surface or both.

The burning rate can be equated to the oxygen feed rate, minus the rate of oxygen leaving the dense phase, minus the rate of oxygen leaving the bubble phase. Thus, assuming full backmixing of the dense phase (294):

$$\frac{dM_C}{dt} = UAC_o - UAC_p - UA(C_o-C_p)ze^{-x} = (C_o-C_p)\,\Delta\,[U-(U-U_{mf})e^{-x}] \text{ kmol/s}$$

equation IX.1

where
- M_C = kmol of char in batch
- U = superficial gas velocity
- A = cross sectional area
- C_o = concentration of oxygen in inlet air
- C_p = concentration of oxygen in dense phase
- z = function of gas velocity = $\frac{U-U_{mf}}{U}$
- X = bubble exchange factor
- U_{mf} = minimum fluidization velocity

Some oxygen breakthrough is inevitable unless x---> OO and C_P = 0, when the burning rate equals the oxygen supply rate. The particle reaction rate is:

$$\frac{dM_C}{d_t} = N_p\, h_c\, A_p\, C_p\, J$$

equation IX.2

where
- N_p = number of particles
- h_C = mass transfer coefficient
- A_p = area of particle surface
- J = mechanism factor, 1 for carbon dioxide formation at the surface and 2 for carbon monoxide formation.

Therefore :

$$\frac{dM_C}{dt} = N_P\, Sh\, D\pi d_c\, J\, C_p$$

equation IX.3

where
- Sh = Shrewood number = $h_o\, d_c/D$
- D = mass diffusion coefficient
- d_c = char particle size.

Eliminating C_p we obtain:

$$\frac{dM_o}{d_t} = \frac{C_o}{L + (n/d_c)} \qquad \text{equation IX 4}$$

where $L = \dfrac{1}{A\,[U-(U-U_{mf})e^{-x}]}$

and $$n = \frac{1}{N_p\, D\, Sh\, \pi\, J}$$

In order to find the burn out time of a batch of char of uniform size, we note that:

$$\frac{dM_c}{d_t} \quad \frac{N_P \pi \rho_c d_c^2}{24} \quad \frac{dd_c}{d_t} \qquad \text{equation IX.6}$$

However

$$\frac{dd_c}{d_t} = \frac{C_o}{f d_c^2 L + n f d_c} \qquad \text{equation IX. 7}$$

where

$$f = \frac{N_P \pi \rho_c}{24} \qquad \text{equation IX.8}$$

Therefore :

$$t = \frac{1/3 L f d_c^3 + 1/2\ nf d_c^2}{C_o} \qquad \text{equation IX.9}$$

or

$$t = \frac{LM_o}{C_o} + \frac{\rho_c d_c^2}{48\ D\, Sh\, J\, C_o} \qquad \text{equation IX.10}$$

where M_o is the initial mass of C (kmol).

The derivation of equation IX.10 is an oversimplification, assuming that the reaction is diffusion limited, elutriation is negligible, the two phase theory of fluidization applies, the char particles are of uniform size and properties etc. However, equation IX.10 is useful in estimating burn out time.

Data :	M_o	=	8.25 kg = 0.867 kmol	assuming char is 100% carbon (see section 5.16.1).
	C_o	=	1.16×10^{-3} kmol/m^3	(calculated)
	ρ_c	=	150 kg/m^3	(255)
	d_o	=	0.04 m	(see section 5.16.1).
	D	=	320×10^{-6} m^2/s	(294)
	Sh	=	$\frac{h_o d_o}{D}$	
	h_o	=	0.027 m/s	(255)
	J	=	1 or 2	
	X	=	1	(294)
	U	=	0.64 m/s	(calculated)
	U_{mf}	=	0.16 m/s	(see section 5.4.3).

Substituting the appropriate values in equation IX.5 gives

$$L = 4.28 \ s/m^3$$

Similarly for the Shrewood number gives:

$$Sh = 3.38$$

Substituting these in equation IX.10 gives:

$$t = 6520 \ s = 108.6 \ min \text{ for } J=1$$

and $$t = 4528 \ s = 75.5 \ min \text{ for } J=2.$$

REFERENCES

1. P.H. Bourdeau, G.L. Ferrero, "Introduction and general presentation of the R&D programme on recycling of urban and industrial waste" in Anaerobic digestion and carbohydrate hydrolysis of waste, eds. G.L. Ferrero, M.P. Ferranti, H. Naveau, Elsevier applied science publishers, 1984.
2. World Bank, "Energy in the developing countries". August 1980.
3. M. Carpentier, "Waste management in the European Community", European Conference waste manag. CEC, Wembley England, June 1980, ed. J. Woole, D. Reidel publishing company 1981.
4. H.R. Bungay, Chapt.4, "Thermochemical processes" in Energy, The biomass options, A Wiley - Intersc. Public., New York, 1981.
5. W. Verstraete, "Biotechnological processes in environmental technology", Lab. general and applied microbial ecology, State University of Gent, 1984.
6. D.O. Hall, "Biomass for energy - Fuels now and in the future", in Biogas utilization, ed. W.A. Cole, NATO Adance Study Institute, Plenum Press, N.Y., 1983.
7. P. Chartier, "Prospect for energy from biomass in the E.C." 1st Eur. Conf. on Energy from Biomass, Brighton, England, November 1980, eds. W. Palz, P. Chartier, D.E. Hall, Applied Science Publishers, Ltd. 1981.
8. J.W. Tatom, F. Harahap, S. Sasmojo, "Third World applications of pyrolysis of agricultural and forestry wastes. Prox. Thermal Conv. of solid wastes and biomass, Div. Env. Chem. Am. Chem. Soc. Washington D.C., September 1979.
9. D.A. Tillman, "Wood as an energy resource", Acad. Press, N. Y., 1978.
10. D.L. Klass, "Energy from biomass and wastes: 1980 Update", Energy from biomass and wastes VII, Lake Buena Vista, Fl., Jan. 1984.
11. S.M. Kohan, "Basic principles of thermochemical conversion" Chapter 8, Biomass Conversion Processes for energy and fuels, eds. S.S. Sofer, O.R. Zaborsky, Plenum Publishing Corporation, 1981.
12. E.J. Soltes, T.J. Elder, "Pyrolysis" Chapter 5 in Organic Chemicals from biomass, ed. I.S. Goldstein, CRC Press Inc. 1§981.
13. D.L. Brink, "Gasification" Chapter 4, ibid.
14. E. Wan, M.P.E. Cheng, "A comparison of thermochemical gasification technologies for biomass" Energy from biomass and wastes III. Auust 1978, Washington D.C.
15. J. Schoeters, Ph.D. Thesis, Free University of Brussels 1983.
16. T.B. Reed, "Types of gasifiers and gasifier design considerations". Ch. 8, A Survey of biomass gasification, Vol.III. Seri April 1980.
17. A. Buekens, H. Masson, "A review of biomass gasification", Proc. 2nd world recycling conference Manilla, 121-138, 1879.
18. K. Maniatis, A. Beukens, M. Rosid, "Biomass gasification an overview" Proc. World Energy Conference, Jakarta, 8,9 May 1985.
19. A.V. Bridgwater, private communication.

20. Vyncke Warmtetechniek, Practical measurements during Vyncke, VUB IWONL R&D Programme. Internal report, May 1983.
21. R. Overend, "Wood gasification an overview". Proc. FPRS Seattle Conference, 1979.
22. W.P.M. van Swaaij, "Gasification - The process and the technology" Resources and Cons., 7: 337-349, 198.
23. T.B. Reed, M. Markson, "Biomass gasification reaction velocities", in Fundamentals of thermochemical biomass conversion, ed. R.P. Overend, T.D. Milne, K.K. Mudge, Elsevier applied science publishers, 1985.
24. R.N. Shand, A.V. Bridgwater, "Fuel from biomass: Status and new modelling approaches" in Thermochemical processing of biomass, ed. A.V. Bridgwater, Butterworths 1984.
25. M.J. Groeneveld, J.J. Hos, "Gasification of solid wastes (1-50 mm) in an annular co-current moving bed gasifier" Producer gas conference, Sri Lanka, November 1982.
26. I.E. Cruz, "Studies on the Practical application of Producer gas from agricultural residues as supplementary fuel for diesel engines", Proc. Thermal conversion of solid wastes and biomass, Washington D.C. September 1979.
27. J.P. Goss, R.H. Coppocic, "Producing gas from crop residues", California Agriculture 34, 5, 1980.
28. L. Linanki, G. Thessen, "Gasification of agricultural residues in a downdraft gasifier", Proc., 2nd International Producer Gas Conference, Bandung, March 1985.
29. K. Maniatis, A. Beukens, "Producer gas for small and large scale irrigation in rural areas", Proc., 5th World congress, International water resources association, Water resources for rural areas and their communities, Brussels 1985.
30. L.K. Mudge and C.A. Rohrmann, "Gasification of solid waste fuels in a fixed bed gasifier", Thermal Conversion of solid wastes and biomass, Div. Env. Chem. Am. Chem. Soc. Washington D.C., September 1979.
31. J.C. Arbo, Dynecology Inc. "The simplex coal and bioass gasification process" Energy from biomass and wastes, IGT conference, January 1980.
32. M. Leuchs, "Measurements of a counter current gasifier in connection with an engine of 125 kw electrical power", Energy brom biomass, 2nd EC conference, Berlin 1982.
33. Levelton Associates Ltd. "Status of biomass feeder technology" ENFOR, 1982.
34. J. Fletcher, R. Wright, "Development of modular biomass gasification and combustion systems", Thermal conversion of solid wastes and biomass, Div. Env. Chem. Am. Chem. Soc. Washington DC, September 1979.
35. V.K. Mathur, R.R. Caughey, "Fuel gas from wood waste" AICHE Symposium series No. 185, Vol. 76, 85-90, 1980.

36. D. Kunii, O. Levenspiel, "Fluidization engineering" R.E. Krieger Publsihing Co., Huntington New York, 1977.
37. J.F. Davidson, D. Harrison, "Fluidized particles" Cambridge University-Press, 1963.
38. J.G. Yates, "Fundamentals of fluidized bed chemical processes" Butterworths 1983.
39. R.D. Twoomy, H.F. Johnstone, Chem. Eng. Progress 48, 220, 1952.
40. J.R. Grase, R. Clift, Chem. Eng. Science 29, 327, 1974.
41. D. Park, O. Leenspiel, T.J. Fitzgerald, "A comparison of the plume model with currently used models for atmospheric fluid bed combustion", Chem. Eng. Science Vol. 35, 295-301, 1980.
42. K. Kato, C.V. Wen, "Bubble assemblage model for fluidized bed catalytic reactors" Chem. Eng. Science, 24, 1351-1369, 1969.
43. C.V. Wen, L.H. Chen, "Fluidized bed freeboard phenomena, entrainment and elutiation" AICHE Journal Vol. 28, 117-125, 1982.
44. J. Werther, "Mathematical modelling of fluidized bed reactors", International chemical engineering, Vol. 20, No. 4, 529-540, 1980.
45. K. Vismanathan, "Semicompartmental Approach to fluidized bed reactor modelling-application to catalytic reactors" Ind. Eng. Chem. Fundam., 21, 352-360, 1982.
46. W.G. May, Chem. Enging. Prog. 55(12), 49, 1959.
47. J.J. van Deemter, Chem. Enging. Sci. 13. 143, 1961.
48. P.N. Rowe in "Fluidization" Soc. Chem. Ind. London 15, 1963.
49. P.L. Rose Ph.D. Thesis, Cambridge University 1983.
50. J.R. Grace, "Fluidized bed reactor modelling: an overview" A.C.S. Symposium series No. 168 Chemical reactors, ed. H.S. Fogler, 1981.
51. P.N. Rowe, Proc. 2nd Int. Conf. Reaction Enging., Amsterdam 29, 1972.
52. D.L. Pyle, Proc. 1st Int. Conf. Reaction Enging., Washington D.C., 106, 1975.
53. C. Chavarie, J.P. Grace, Ind. Enging. Chem. Fund., 14, 75-86, 1975.
54. S. Sundaresan, N.R. Amundson, "Studies in char gasification III, The Combustion zone", Chem. Eng. Sci., 24, 259-264, 1979.
55. A.W. Weimer, B.E. Clough, "The Influence of Jetting-emulsion mass and heat interchange in a fluidized bed coal gasifier", in Recent advances in fluidization, AICHE Symp. Series, No. 205, Vol. 7.7,1981.
56. Wen-Ching Yang, "Jet penetration in a pressurized fluidized bed", Ind. Eng. Chem. Fundamentals, 20,297, 1981.
57. P.W. Kehoe, Ph.D. Thesis, Cambridge University, 1969.
58. M. Leva, C.Y. Wen, in "Fluidization", Eds. J.F. Davidson, D. Harrison, Chapter 14, Academic Press, London 1971.
59. M.S. Dimitri, R.P. Jongedijk, H.C. Lewis, "Distillation of fluidized hardwood", Chemical Engineering, 124-125, December 1948.
60. A.H. Vroom, "Bark pyrolysis by fluidization techniques", Pulp and paper magazine of Canada, 121-124, April 1952.

61. L.W. Morgan, G.M. Armstrong, H.C. Lewis. "Distillation of hardwood in a fluidized bed", Chemical Engineering Progress 49, 2, 98-101, 1953.
62. W.W. Shuster, "Partial Oxidation of solid organic wastes", Research Grant No. EC-00263 final report to U.S. Department of health education and welfare, 1970.
63. Varian Inc., "Fundamentals of gas analysis by gas chromatography", Varian Associates Inc., Paolo Alto, 1977.
64. M. Graboski, R. Bain, "Properties of biomass relevant to gasification" Chapter 3, in Surey of biomass gasification, SERI, 1979.
65. J.E. Halligan, K.L. Herzog, H.W. Parker, "Synthesis gas from bovine wastes", Ind. Eng. Chem. Process. Res. Devel., Vol. 14, No. 1, 1975.
66. S.R. Beek, W.J. Huffman, J.E. Halligan, B.C. Landeene, C.S. Lin,R. Ravi, R.A. Bartsch, P.E. Hillman, "Partial oxidation - pyrolysis of cattle feedlot manure in the SGPM reactor", final report, US, DOE, Solar Energy, Contract E (29-2)-3779, November 1977.
67. S.R. Beek, W.J. Huffman,B.C. Landeene, J.E. Halligan, "Pilot plant results for partial oxidation of cattle feedlot manure", Ind. Eng. Chem. Process design. Devel., Vol. 18, 328, April, 1979.
68. S.R. Beek, M.J. Wang, "Wood gasification in a fluidized bed", ibid. 19, 312, 1980.
69. S.R. Beek, M.J. Wang, J.A. Hightower, "Gasification of oak sawdust, mesquite, corn stover and cotton gin trash in a countercurrent fluidized bed pilot reactor", A.C.J. Symposium series, No.144, Biomass as a non fossil fuel source, ed. D.L. Klass, 1981.
70. Saskatchewan Power Corp., "Evaluation of wood gasifier at Hudson bay Saskatchewan", ENFOR Project C-8, May 1979.
71. Saskatchewan Power Corp., :Pilot Plant Investigation of a wood gasifier for generation of electricity", ENFOR Project C-29, June 1980.
72. K. Salo, H. Filey, B. Asplund, "Gasification of milled peat in a fluidized bed" 6th International peat congress proc., M.I. Duluth, USA, 1980.
73. E. Ekman, D. Asplund, "A review of research on peat gasification in Finland", Ind. Symposium on Gas Liquefaction, Katatowia, 1979.
74. D.V. Punwani, S.Weil, C.J. Pyrcioch, S.P. Nandi, "Peat char gasification-laboratory and PDU-scale studies", Journal of Energy, Vol. 5, No.5, 276-280, October 1981.
75. M. Lin, O. Martiner, D.W. Duncan, "Gasification of wood waste and coal", presented at 1977 Spring Conference, Canadian pulp and paper association, The Empress, Victoria, June 1977.
76. J.W. Black, K.G. Bircher, K.A. Chrisholin, "The fluidized bed gasification of solid wastes and biomass. The CIL program", Thermal conversion of solid wastes and biomass, Div. Env. Chem. Am. Chem. Soc., Washington DC, September 1979.
77. R.S. Burton, R.C. Bailie, "Fluid bed pyrolysis of solid wastes materials", Combustion, 13-19 February 1974.

78. J.W. Black, K.G. Bircher, K.A. Chrisholin, "The fluidized bed gasification of solid wastes and biomass: The CIL program", Thermal conversion of solid wastes and biomass, Div. Env. Chem. Am. Chem. Soc., Washington DC, September 1979.
79. F.T. Garey, G. Gurnik, "Application of a fluidized bed gasifier to conversion of forest biomass to an energy source", Proc. Biotechnology, Ottawa 1980.
80. G. Gurnik, K.O. Luke, D.C. Pollock, "Application of a fluidized bed gasifier to conversion of forest biomass to an energy source", Report to ENFOR, 1980.
81. K.G. Bircher, "Economics of an 80MM BTU/H wood gasifier installation", Energy from biomass and wastes VI, January 1982.
82. Vyncke Warmtetechniek: Practical measurements-Internal report, May 1983.
83. P.K. Raman, W.P. Walawender, L.T. Fan, "Gasification of feedlot manure in a fluidized bed reactor. The effect of temperature", Ind. Eng. Chem., Process design and development, 623-629, 1980, 10.
84. W.P. Walawender, P.K. Raman, L.T. Fan, "Gasification of carbonaceous materials in a fluidized bed reactor", Proc., Bio-Energy 1980, Atlanta Georgia, USA, April 1980.
85. P.T. Raman, W.P. Walawender, V. Shimizu, L.T. Fan, "Gasification of corn stover in a fluidized bed", Agricultural Energy, Vol. 2, ASAE, National Energy Symposium, 1980.
86. P.T. Raman, W.P. Walawender, L.T. Fan, "Gasification of feedlot manure in a fluidized bed effects of superficial gas velocity and feed size fraction", Fuels from biomass and wastes, eds. D.L. Klass, G.V. Emert, Ann Arbor Science, 1981.
87. D.A. Hoveland, W.P. Walawender, L.T. Fan, F.S. Lai, "Experimental study of the steam gasification of grain dust in a fluidized bed reactor", AIAE 1981 winter meeting, Chicago Illinois, December 1981.
88. W.P. Walawender, S. Ganesan, L.T. Fan, "Steam gasification of manure in a fluid bed. Influence of linestone as bed additive", Energy from Biomass and Wastes V, Lake Buena Vista, Florida, January 1981.
89. W.P. Walawender, D.A. Hoveland, L.T. Fan, "Steam gasification of Alpha cellulose in a fluid bed reactor", Fundamentals of thermochemical biomass conversion conference Estes park Colorado, October 1982.
90. N.E. Welch, "Status of the Missouri Rolla fluidized bed gasifier probram", Proc. Technology and economics of wood residue gasification, 10th Texas Industrial wood Seminar, March 1979.
91. V. Flaningan, M. Findley, Y. Omirtag, H. Sineath, N.M. Welch, "Gasification research on wood GROW", Low Energy gas Production - Phase I" DOE report, March 1981.
92. M. Findley, V. Flanigan, H. Sineath, "Phase II, GROW Project", Proc., 13th Biomass Thermochemical contractors meeting. Arlington, Virginia. October 1981.

93. V. Flanigan, J.E. Shimon, A. Punyakumleard, "Low BTUY Gas from a small scale fluidized bed reactor using sawdust feeds", Energy from biomass and wastes VII, Lake Buena Vista Fl., January 1982.
94. W. O'Neill, V. Flanigan, "Small fluidized gasifier using charred biomass", Producer gas technical conference Sri Lanka, November 1982.
95. F.G. van den Aarsen, A.A.C.M. Beenackers, W.P.M. van Swaaij, "Concurrent moving bed and fluidized bed biomass gasification", EC Contractors' Meeting at Brussels, Energy from biomass, May 1982.
96. F.G. van den Aarsen, A.A.C.M. Beenackers, W.P.M. van Swaaij, "Thermochemical gasification in a pilot plant fluidized bed wood gasifier", Energy from biomass, 2nd CEC conference, Berlin. September 1982.
97. F.G. van den Aarsen, A.A.C.M. Beenackers, W.P.M. van Swaaij, "Performance of a rice husk fueled fluidized bed pilot plant fasifier", Producer gas technical Conference, Sri Lanka, November 1982.
98. T.C. Chou, K.T. Chang, "Gasification of bagasse in the presence of a pilot flame in a modified fluidized bed", Ind. Eng. Chem. Process design and development, 20, 161-165, 1981.
99. F.E. Moreno, Private communication, June 1982.
100. F.E. Moreno, J.R. Goss, "Fluidized bed gasification of high ash agricultural wastes to producce process heat and electrical power". Energy from biomass and wastes VII, IGT Conf., January 1983.
101. G. Salvi, E. Zanella, "Gasificazione in letto fluidizzato di biomass escarti industriali", La Rivista del combustibili, Vol. 37, 11-12, 291, 1983.
102. K. Maniatis, J. Schoeters, A. Buekens, Reports for Vyncke Warmetechniek, No. 1-4 and 8.
103. J. Cherian, V. Flanigan, "Effect of operating conditions on gas quality and conversion efficiency of a fluidized bed gasifier", Proc. Energy from biomass and wastes VIII, Lake Buena Vista, Fl. January 1983.
104. J. Schoeters, A. Buekens,"Experimental studies in a laboratory-scale fluidized bed reactor", Proc. Fluidized combustion conference, Cape Town, January 1981.
105. J. Schoeters, K. Maniatis, A. Buekens. "Fuel gas from agricultural residues in a fluidized bed reactor", Proc. 2nd World Congress of chemical engineering, Montreal, October 1981.
106. H. Masson, J. Schoeters, A. Buekens. "Gasification of biomass in a fluidized bed some fundamental investigations about the reactor performance", Proc. 2nd MER symposium, Antwerp, October 1981.
107. K. Maniatis, J. Schoeters, A. Buekens. "Biomass gasification in a fluidized bed reactor", Proc. 6th International Industrial wood energy forum, Washington D.C., March 1983.

108. K. Maniatis, A. Buekens, "Practical experience in fluidized bed gasification of biomass", Proc. Producer gas technical conference, Sri Lanka, November 1982.
109. R. Desrosiers, Chapter 6, in Survey of Biomass Gasification, Volume II, SERI 1979.
110. E. Rensfelt, "Practical achievements in biomass gasification", Proc., Bio-energy 1984, Göteburg, 1984.
111. V. Flanigan, W. O'Neill, "Development of a low cost fluidized bed gasifier-gas engine system for use in remote areas", Energy from biomass and wastes VIII, Lake Buena Vista, Florida, 1984.
112. K. Maniatis, J. Schoeters, A. Buekens. "Gasification of refuse derived fuel in a fluidized bed reactor", ISWA Symposium, Munich, May 1984.
113. J. Schoeters, "Charcoal gasification in a fluidized bed" to be published.
114. J. Black, Private communication, "Tests with Omnifuel gasifier" in The state of the art in biomass gasification in Canada and California, by K. Maniatis, December 1981.
115. INCO Metals company, "Application of fluid bed technology to the gasification of waste wood", Volume I, Report to ENFOR, June 1980.
116. K. Maniatis, J. Schoeters, A. Buekens. "Experimental study of the gasification of Euphorbia Tirrucalli by means of oxygen/steam mixtures", 2nd International Producer gas conference, Bandung, March 1985.
117. M. Graboski, R. Bain, "Properties of biomass relevant to gasification", Survey of biomass gasification, Vol. II Seri Colorado, 1979.
118. T. Miles, "Biomass preparation for Thermochemical Conversion" Chapter 5, in Thermochemical processing of biomass, ed. A.V. Bridgwater, Butterworth, London, 1984.
119. E. Lipinsky, "Pretreatment of biomass for thermochemical biomass conversion", in Fundamentals of thermochemical biomass conversion, ed. R. Overend, T. Milne, L. Mudge, Elsevier Ap. Sc. Pub., London, 1985.
120. D. Huffman, Private communication, Forintek Canada, October 1981.
121. D. Huffman,"Gasification research and comercialization in Canada", Industrial wood Energy forum 83, Nashville TN, September 1983.
122. R. Lang, D. Wang. California Energy commission, private communication, Sacramento, October 1981.
123. M. Murphy. "Case history of the design, start up and operation of a 54 mm BTU/H fluidized bed gasifier for steam production from wood and biomass residue". Proc. Energy from Biomass and wastes VIII, IGT, Lake Buena Vista, January 1984.
124. Eisenmann Umwelttechnik, private communication and company leaflet, ISWA, Munich, 1984.
125. A.V. Bridgwater, private communication 1986.

126. A.A.C.M. Beenackers, W.P.M. van Swaaij, "Gasification of biomass, a state of the Art review", Thermochemical Processing of Biomass, ed. A.V. Bridgwater, Butterworths, London, 1984.
127. S.M. Kohan, P. Barkhordar, "Mission Analysis for the federal fuels from biomass program", Volume IV, SERI International, 1979.
128. R. Reimert, P. Mehzling, C. Lindner, "Methanol from wood via Lurgi circulating fluidized bed gasification", Bio-energy 1984, Göteborg Sweden, June 1984.
129. J.M. Lemasle, "Methanol from wood", in Thermochemical processing of Biomass, ed. A.V. Bridgwater, Butterworths, London, 1984.
130. G. Chrysostome, J.M. Lemasle, "Syngas production from wood by oxygen gasification under pressure", Bio-energy 1984, Göteborg Sweden, June 1984.
131. W.H. Blackadder, E. Rensfelt, "Synthesis gas from wood and peat - The Mino process" ibid.
132. L. Waldheim, E. Rensfelt, "Methanol from wood and peat", Proc., Biomass to methanol specialist workshop, ed. T.B. Reed, SERI/CP-234-1590, 1982.
133. L. Schrader, E. Nitschke, H. Will, A. Bellin, "Biomass as feed for the Rheinbraun HTW-Gasification Process", Proc., Energy from Biomass and Wastes VIII, Lake Buena Vista, Fl., January 1984.
134. A. Bellin, H.J. Scharf, L. Schrader, H. Teggers, "Application of Rheinbraun HTW-Gasification Process to biomass feedstocks", Proc. Bio-energy 1984, Göteborg, June 1984.
135. J.W. Black, "The pressurized fluidized bed gasfifier in the synthesis of methanol from wood", Proc. Biomass to methanol specialist workshop, ed. T.B. Reed, SERI/Cp-234-1590, 1982.
136. S.P. Batu, M. Onischak, G. Kosowski, "Development of a pressurized fluidized bed biomass gasifier to produce substitute fuels", 13th Biomass thermochemical contractors meeting, Arligton, Virginia, 1981.
137. G. Moss, A.I. Edwards, Private communication during the 1st European Workshop on Thermochemical Processing of biomass, University of Aston in Birmingham, 1983.
138. A.A.C.M. Beenackers, K. Maniatis, "Conclusions of the workshop on evaluation of thermochemical gasification reactors for biomass", Chapter 21, in Thermochemical processing of biomass, ed. A.V. Bridgwater, Butterworths, London, 1984.
139. C. Lindner, R. Reimert, "Gasification of wod in the circulating fluidized bed: Methanol production route". In Energy from Biomass, Vol. 2, eds. W. Palz, G. Grassi, Reidel, Dordrecht, 1982.
140. R. Reimert, D. Mehzling, C. Lindner, "Methanol from wood via Lurgi circulating fluidized bed gasification", Lurgi, commercial leaflet, 1984.
141. Methanol, The Lurgi low pressure methanol process, Lurgi Express Information Q 1414.

142. R.S. Bickle, A.S. Edwards, G. Moss, "Development of the O_2 donor gasifier for conversion of wood to synthesis gas for eventual production of methanol", in Energy from Biomass, Vol. 2, eds. W. Palz, G. Grassi, Reidel, Dordrecht, 1982.

143. O.H. Brandon, G.H. King, O.V. Kinsey, "The role of thermochemical processing in biomass exploitation", Ch. 2, in Thermochemical Processing of biomass, ed. A.V. Bridgwater, Butterworths, London, 1984.

144. A.V. Bridgwater, "The thermochemical processing system", Chapter 3, ibid.

145. L. Liinaki, N. Lindman, S.O. Sjöborg, E. Strom, "Methane yield from biomass gasification at high temperature and pressure", in Fundamentals of thermochemical biomass conversion, eds. R.P. Overend, T.A. Milne, L.K. Mudge, Elsevier, London, 1985.

146. P. Janesch, O. De Santi, "Synthesis gas obtained from biomass", in Energy from biomass, Vol. 2, Eds. W. Palz, G. Grassi, Reidel Dordrecht, 1982.

147. H.F. Feldmann, P.S. Choi, M.A. Paisley, J.P. Chankan, C.J. Robb, O.W. Folsom, B.C. Kim, "Steam gasification of wood in a multi solid fluidized bed gasifier", Energy from biomass and wastes V, Lake Buena Vista, Florida, 1981.

148. H.F. Feldmann, M.A. Paisley, B.C. Kim, H.R. Appelbaum, "Gasification of forest residues to produce a methane rich gas", 13th biomass Thermochemical Contractors meeting, Arligton, Virginia, 1981.

149. R. Holmes, D. Gibbs, R. Davis, "Synthetic fuel from wood using steam and air", in Energy from Biomass, Vol. 2, eds. W. Palz, G. Grassi, Reidel Dordrecht, 1982.

150. A. Bary, H.A. Masson, P. Debaub, "Synthetic fuel from biomass: The AVSA dual fluid bed combustor - gasifier project", ibid.

151. R.C. Bailie, "Result from comercial-demonstration pyrolysis facilities extended to producing synfuels from biomass", Energy from biomass and wastes V, IGT, 1981.

152. M. Kagayama, M. Igarashi, N. Hasegama, J. Fukuda, "Gasification of solid waste in duel fluidized bed reactors", ACS Symposium Series 130, September 1979.

153. D.S. Scott, J. Piskorz, "Thermal flash pyrolysis of wood ", Proc. Am. Chem. Soc. Symposium on Energy from biomass, Las Vegas, August 1980.

154. D.S. Scott, J. Piskorz, "The flash pyrolysis of Aspen Poplar Wood", The Canadian journal of chemical engineering, Vol. 60,666, October 1982.

155. D.S. Scott, J. Piskorz, "Continuous flash pyrolysis of wood for production of liquid fuels", Energy from biomass and wastes VII, January 1983.

156. D.S. Scott, J. Piskorz, "The continuous flash pyrolysis of biomass", The Canadian Journal of chemical engineering Vol. 62, 404, June 1984.

157. R. Rensfelt, G. Blomkvist, C. Eastrom, S. Engstrom, B. Esperas, L. Liinanki, "Basic gasification studies for development of biomass Medium-Btu gasification processes", Energy from biomass and wastes, IGT, 1978.

158. K. Maniatis, unpublished authors data on flash pyrolysis of biomass in a pyroprobe.

159. T. Funazukuri, R. Hudgins, P. Silveston, "Prediction of volatile products from thermal conversion of cellulose oby correlation with carbon oxides in the gas", Energy from biomass and wastes VIII, Lake Buena Vista, 1984.

160. T. Funazukuri, R. Hudgins, P. Silveston, "Flash Pyrolysis of cellulose in a Micro fluidized bed", Preprints, Am. Chem. Soc. Div. Fuel. Chemistry, Vol. 29, No. 6, Philadelphia 1984.

161. D. Kunzru, M. Ali, "Pyrolysis of bovine waste" Fuel, Vol. 60, 447-451, May 1981.

162. A. Sakoda, M. Sadakata, T. Koya, T. Furusawa, D. Kunii, "Gasification of biomass in a fluidized bed", The chemical eng. journal, 22, 221-227, 1981.

163. J. Kuester. "Diesel fuel from biomass", Energy from biomass and wastes VIII, Lake Buena Vista, February 1984.

164. J. Kuester, C. Fernander, T. Wang, G. Heath, "Liquid hydrocarbon fuel potential of agricultural materials" in fundamentals of thermochemical biomass conversion, ed. R. Overend, T. Milne, L.Mudge, Elsevier Ap. Sc. Publishers, 875-896, 1985.

165. W. Walawender, S. Ganasan, L. Fan, "Steam Gasification of manure in a fluid bed influence of limestone as a bed additive", Energy from biomass and wastes V, IGT, 1981.

166. M. Declerck, P. Smets, J. Smets, J. Roman, "Development of an Integrated energy plantation in Kenya utilizing Euphorbia production", Proc., Energy from biomass wastes IX, IGT, 1985 and communication of Traditional Eng. Dept. of Metallurgy to the Free University of Brussels.

167. J. Schoeters, K. Maniatis, A. Buekens, "Gasification experiments, final report, Research project Kenya-Euphorbia" for the General Directorate of Development Aid of the Belgian Ministry of Foreign Affairs, June 1984.

168. R. Carten, "Catalytic Conversion of biomass to fuels". Catalytica Associates Inc. Publication, 1979.

169a. P. Graham, D.P.C. Fung, "A review of biomass gasification. The role of catalysis" Report OPx221E, Forintek Canada Corp. 1979.

169b. J.L. Cox, G.W. Willson, E.J. Hoffman, "Conversion of organic wastes to fuel gas". J. Env. Eng. Div. 100, (EE3), 717-731, Amer. Chem. Soc. 1974.

170. W.P. Haynes, S.J. Gasoir, A.J. Forney, "Catalysis of coal gasification at elevated pressure", Preprints, A.C.S. Div. fuel chemistry, 18 (2) 29-42, 1972.

171. D.P.C. Fung, V. Tsughigya, K. Suni, "Thermal degradation of cellulose and levoglucosan - the effect of inorganic salts", Wood science, 5, (1), 38-43, 1972.
172. R. Ross, P. Fung, "Catalytic Conversion of woodbarks to fuel gases", Ind. Eng. Chem. Prod. Res. Dev., 20, 197-203, 1981.
173. W.K. Lewis, E.R. Gilliland, H. Hipkin, "Carbon steam reactions at low temperatures", Ind. Eng. Chem. 45 (8), 1697-1703, 1953.
174. S. Prahacs, H.G. Barclay, S.P. Bhatia, "A study of the possibilities of producing synthetic tonnage chemicals from lignocellulosic residues", Pulp paper Mg. Canada, 72 (6), 69-83, 1971.
175. L. Mudge, L. Sealock, S. Weber, "Catalyzed steam gasification of biomass", J. of analytical and applied pyrolysis, 1, 165-1§75, 1979.
176. L. Mudge, E. Baker, D. Mitchell, H. Brown, R. Robertus, "Catalytic steam gasification of biomass for methanol and methane production", Energy from biomass and wastes VII, IGT conference, 1983.
177. E. Baker, M. Brown, "Catalytic steam gasification of bagasse for the production of methanol". Ibid, VII, 1984.
178. L. Mudge, E. Baker, D. Mitchell, "Catalytic generation of methanol synthesis gas from wood", Energy from biomass and wastes IX, 1985.
179. E. Baker, L. Mudge, W. Wilcox, "Catalysis of gas phase reactions in steam gasification of biomass" Fundamentals of Thermochemical processing of biomass, eds. R. Overend, T. Milne, L. Mudge, Elsevier applied science publishers, New York, 1985.
180. D.P.C. Fung, R. Graham, "The role of catalysis in wood gasification", Proc. Thermal conversion of solid wastes and biomass. Div. Env. Chem. Am. Chem. Soc. Washington, D.C., September 1979.
181. M.H.I. Rei, S.J. Yang, C.H. Hong, "The catalytic crackingof rice husk for olefins or for hydrogen rich synthesis gas", Proc. 2nd World Congress of Chemical Engineering, Montreal, October 1981.
182. W.Y. Wen, "Mechanisms of alkali metal catalysis in the gasification of coal, char or graphite", Catalysis reviews Science and Engineering, 22 (1), 1-28, 1980.
183. M. Rose, "Chemical reactor design in practice", Elsevier Scientific Publishing company, 1981.
184. A. Buekens, J. Schoeters, "Modelling of biomass gasification, In Fundamentals of thermochemical biomass conversion, eds. D.P. Overend, T.A. Milne, L.K. Mudge, Elsevier, 1985.
185. O. Levenspiel, "Chemical reaction Engineering", 2nd edition, J. Wiley and Sons, 1972.
186. D. Bukur, H. Caram, N. Amundson, "Chemical reactor theory a review", ed. L. Lapidus and N. Amundson, Practice-Hall, Englewood Cliffs, N.J. 1977.
187. M.J. Antal, "Synthesis gas production from organic wastes by "pyrolysis/steam reforming". In Energy from biomass and waste ed. D.E. Klass, Washington D.C., 1978.

188. E. Smith, "Reactors: Some Design Perspectives", Chapter 15. Thermochemical Processing of Biomass, ed. A.V. Bridgwater, Butterworths, London, 1984.
189. P.H. Perry, C. Chilton, "Chemical Engineers Handbook", McGraw Hill Kogakusha, 5th ed. 1973.
190. D.Q. Kern, "Process heat transfer", Int. Student ed. McCraw Hill International, 1965.
191. W. McCabe, J. Smith, "Unit operations of chemical engineering", McGraw Hill book company, New York, 1967.
192. G. Barton, "Specification of standard biomass materials for thermochemical research", in Fundamentals of thermochemical biomass conversion, eds. R. Overend, T. Milne, L. Mudge, Elsevier applied science publication, London 1985.
193. T. Milne, "Pyrolysis the thermal behaviour of biomass below 600 °C" Chapter 5, Vol. II, Survey of biomass gasification, SERI, Golden, Colorado 1979.
194. F. Shafizadeh, "Pyrolytic reactions and products of biomass". In Fundamentals of thermochemical biomass conversion, eds. R. Overend, T. Milne, L. Mudge, Elsevier applied science publishers, London, 1985.
195. R. Chan, B.B. Krieger, "Modelling of physical and chemical processes during pyrolysis of a large biomass pellet with experimental verification", Am. Chem. Soc., Div. fuel chem., vol. 28, No. 5. Washington D.C., August 1983.
196. M.J. Antal Jr., "The effects of residence time, temperature and pressure fuel source, D.E. Klass ed. A.C.S. Symposium series 144, A.C.S., 1982.
197. I.S. Goldstein, "Composition of biomass", Chapter 2 in Oreganic Chemicals from biomass, C.R.C. Press Inc. 1981.
198. P.C. Lewellen, W.A. Peters, J.B. Howard, "Cellulose pyrolysis kinetics and char formation mechanism", 16th International symposium on Combustion, Cambridge Mass. 1976.
199. M.J. Antal Jr., "Biomass pyrolysis : A review of the literature, part. 1 - carbohydrate pyrolysis", Advances in solar energy, American Solar Energy Society, Boulder, N. York, 1983.
200. M. Graboski, "Kinetics of char gasification reactions", Chapter 7, A survey of Biomass gasification, SERI Golden, Colorado, 1979.
201. F. Shafizadeh, "Introduction to pyrolysis of biomass". Journal of analytical and applied pyrolysis, 3, 283, 1982.
202. F. Shafizadeh, "Pyrolysis and combustion of cellulosic materials", Advan Carbohydr. Chemistry 23, 419, 1968.
203. A.J. Stamm, "Thermal degradation of wood and cellulose", Industrial and engineering chemistry, 48, 413, 1956.
204. H. Saluma, S. Munakala, S. Sugawara, "Volatile products of cellulose pyrolysis", Agricultural and biological chemistry, 45, 2, 443-451, 1981.

205. F.J. Kilzer, A. Broido, "Speculations on the nature of cellulose pyrolysis", Pyrodynamics, 2, 151-163, 1965.
206. D.F. Arseneau, "Competitive reactions in thermal decomposition of cellulose" Can. J. Chem. 49, 632-638, 1971.
207. A.G.W. Bradbury, Y. Sakai, F. Shafizadeh, "A kinetic model for pyrolysis of cellulose", Journal of applied polymer science, vol. 23, 3271-3280, 1979.
208. A. Broido, "Kinetics of solid phase cellulose pyrolysis", in Thermal uses and properties of carbohydrates and lignins, ed. F. Shafizadeh et al., Academic Press, 1976.
209. M.R. Hajaligol, J.B. Howard, J.P. Longwell, W.A. Peters, "Product compositions and kinetics for rapid pyrolysis of cellulose, Ind. Eng. Chem. Proces Des. Dev. 21, 457-465, 1982.
210. J.N. Barooah, V.D. Long, "Rates of thermal decomposition of some carbonaceous materials in a fluidized bed", Fuel, vol. 55, 116-120, 1976.
211. C. Fairbridge, R.A. Ross, S.P. Sood, "A kinetic and surface study of the thermal decomposition of cellulose powder in inert and oxidizing atmospheres", Journal of applied polymer science, vol. 22, 497-510, 1978.
212. G.M. Simmons, M. Sanchez, "High temperature gasification kinetics of biomass pyrolysis" J. Anal. Appl. Pyrolysis, 3, 161-171, 1981.
213. P. Fang, "Thermogravimetric analysis of loblolly pine bark componants", Wood and fibre, 7, 136, 1975.
214. F. Shafizadeh, "Thermal degradation of Xylan and related model compounds", Carbohydrate research", 25, 23, 1972.
215. L. Wise, E. Jahn, "Wood Chemistry", 2nd ed. Reinhold, N.York, 1952.
216. G. Allan, T. Mattila, "High energy degradation" Chapt. 14 in Lignins, accurence, formation, structure and reactions, eds. K.V. Sarkanen, C.H. Ludwig, Wiley-Inter Science, 1971.
217. N.J. Sundaram, M. Sleinberg, P.T. Fallon, "Flash pyrolysis of biomass with reactive and non reactive gases", in Fundaments of thermochemical biomass conversion, eds. R. Overend, T. Milne, L. Mudge, Elsevier, 1985.
218. R.C.R. Chan, M. Kelbon, B.B. Krieger, "Product formation in the pyrolysis of large wood particles", ibid.
219. C. Roy, B. Caumia, D. Brouillard, M. Menard, "The pyrolysis under vacuum of Aspen Poplar", ibid.
220. F.P. Petrocelli, M.T. Klein, "Simulation of kraft lignin pyrolysis", ibid.
221. T.L. Nunn, J.B. Howard, J.P. Longwell, W.A. Peters, "Studies in the rapid pyrolysis of sweet Gum hardwood", ibid.
222. G. Rose, R. Zabransky, "Devolatilization of Maple Hardwood", ibid.
223. S.A. Milne, M.N.Soltys, "The direct, Mass Spectrometric study of the primary and secondary pyrolysis behaviour of biomass and its constituents", ibid.
224. G.M. Simmons, W.H. Lee, "Kinetics of gas formation fro cellulose and wood pyrolysis", ibid.

225. R.G. Graham, M.A. Bergouguon, L. Mok, H. de Lasa, "Fast pyrolysis of biomass using solid heat carriers", ibid.
226. A.E. Lipska-Quinn, S.H.Zeronian, K.M. McGee, "Thermal degradation of rice straw and its components", ibid.
227. D. Pyle, C. Zaror, "Models for the low temperature Pyrolysis of wood particles", Chap. 12, Thermochemical Processing of Biomass ed. A.V. Bridgwater, Butterworths, London, 1984.
228. M. Groeneveld, Ph. D. thesis, Twente University of Technology, the Netherlands, 1980.
229. O. Hougen, K. Watson, R. Ragatz, "Chemical Process Principles", Part. 1, 2nd ed. Wiley Intern. Ed. London, 1954.
230. J.M. Smith, H.C. van Ness, "Introduction to chemical engineering thermodynamics", 3rd ed., McGraw Hill, 1975.
231. W. Gumz, "Gas producers and blast furnaces", John Wiley and Sons, N. York, 1950.
232. P. Belleville, R. Capart, "A model for predicting outlet gas concentrations from a wood gasifier", Chapter 13, Thermochemical Processing of biomass, ed. A.V. Bridgwater. Butterworths, London, 1984.
233. E. Rammler, "Technologie und chemie der Braunkohleverwertung" 1962.
234. W. Cousins, "A theoretical study of wood gasification processes", New Zealand Journal of Science, Vol. 21, 1978, 175-183.
235. D. Bacon, J. Downie, J. Hsu, J. Peters, "Modelling of fluidized bed wood gasifiers", Fundamentals of Thermochemical biomass conversion, eds. R. Overend, T. Milne, L. Mudge, Elsevier, 1985.
236. J. Gibbins, H. Wilson. "Equilibrium modelling - A cheap and efective aid to gasifier system design and analysis". Energy money materials and engineering 1. Chem. E. Symposium Series No. 78, Pergamon Press, 1982.
237. A.V. Bridgwater, R. Shand, "Biomass processing simulation - gasification system", Presented at Contractors meeting on biomass processing, UK Energy technology support unit, Department of Energy, november 1983.
238. C. Von Federsdroff, and M. Elliott, "Coal gasification", in Chemistry of coal utilization, ed. H.W. Lowry 892. J. Wiley, New York, 1963.
239. Chemical reaction Engineering, 3rd. year coarse in chemical engineering, University College London, 1977.
240. P. Walker, F. Rusinko, L. Austin, "Gas reactions of carbon", Adv. Catal. Vol. II, ed. D. Elen, 134, Academic Press, N. York, 1959.
241. M. Mulcaly, I. Smith, "Kinetics of combustion of pulverized fuel: A review of theory and experiments", Rev. Pure Appl. Chem. 19, 81, 1969.
242. J. Richardson, J.Zrekely, Trans. I. Chem. E. 39, 212, 1961.
243. J. Johnson, "Kinetics of Bituminous coal char gasification with gases containing steam and H_2", Adv. Chem. Ser. No. 131, 145, 1974.

244. M. Kawahata, P. Walker, "Mode of Porosity Development in activated Anthracite", Proc. 5th Carbon conf. 11, 251, 1963.
245. P. Walker, R. Forest, C. Wright, "Surface Area studies of carbon-carbon dioxide reaction", Ind. Eng. Chem. 45, 1703, 1953.
246. K. Hashimarto, P. Silvestor, "Gasification" Part I, AIChEJ. 19, 259, 1973.
247. K. Hashimato, P. Silvestor, "Gasification" Part II, ibid 19, 268, 1973.
248. A. Putta, C. Wen, R. Reid. "Reactivity of coal and char. 1. In CO_2 atmosphere", Ind. Eng. Chem. Proces Design Develop 16, 20, 1977.
249. B. Srynivas, N. Amundson, "A single Particle Char Gasification Model", AIChEJ 26, 3, 1980.
250. C. Wen, S. Tone, "Coal conversion reaction engineering", Chapt. 3, Chemical reaction engineering reviews, Houston 1976.
251. F. Bonner, J. Turkevich, J. American, Chemical Society Vol. 73, 561, 1951.
252. M. Meutser, S. Ergun, "A study of the carbon dioxide-carbon oxygen exchange" USBM Bulletin 664.
253. S. Nandi, M. Onischak, "Gasification of chars obtained from Maple and Jalk pine woods, Energy from biomass and Wastes, VI IGT, 1982.
254. R. Edrich, T. Bradley, M. Graboski, "The gasification of panderosa pine charcoal", In Fundamentals of thermochemical biomas conversion, eds. R. Overend, T. Milne, L. Mudge, Elsevier, 1985.
255. F.G. van den Aarsen, A.A.C.M. Beenackers, W.P.M. van Swaaij, "Wood Pyrolysis and carbon dioxide char gasification kinetics in a fluidized bed", ibid.
256. I. Bierle, J.C. Berggren, H. Eklund, O. Svensson, "Kinetijka studierl turmovac, förgasningsförsök I fluidiserad bado Av Kol och biomassa", Technical University of Lund, Publication 1360 261, 1980.
257. W.F. de Groot, L.Shafizadeh, "Kinetics of wood gasification by carbon dioxide and steam", in Fundamentals of thermochemical biomass conversion", eds. R. Overend, T. Milne, L. Mudge, Elsevier, 1985.
258. N. Laurendeau, "Heterogeneous kinetics of coal char gasification" in Progress in Energy Combustion Science, Vol. 4, 221, 1978.
259. F. Shafizadeh, "Basic Principles of direct combustion" Ch. 6 in Biomass conversion processes for energy and fuels", eds. S. Sofer, O. Zaborsky, Plenum Publishing Corp., 1981.
260. C. Rao, "Fluidized bed combustion technology a review", Combustion Science and Technology, Vol. 16, 215, 1977.
261. K. Yoshida, D. Kunii, "Complex reaction in fluidized beds, simulation of gasification", J. Chem. Eng. Japan, Vol. 7, No. 1, 1974.
262. S. Mori, M. Kurita, S. Hiraoka, I. Yamadas, "Analysis of the fluidized bed coal gasifier". Presented at Japan-China Symp. on fluidization, China April, 18982.
263. A. Weimer, D. Clough, "Modelling a low pressure steam-oxygen fluidized bed coal gasifying reactor", Chem. Eng. Sc. Vol. 36,549-567, 1981.

265. H. Caram, N. Amundson, "Fluidized bed gasification reactor modelling. Model Description and numerical results for a single bed". Ind. Eng. Chem. Process. Des. Dev. Vol. 18, No. 1, 1979.
265. J.Wether, "Bubble growth in large diameter fluidized beds", in Fluidization Technology, Vol. II, ed. D.L. Keairns, McGraw Hill, London, 1975.
266. L.A. Behie, M.A. Bergougnon, O.G. Baker, "Mass transfer from a grit jet in a large gas fluidized bed", ibid.
267. F.G. van den Aarsen, A.C.M. Beenackers, W.P.M. van Swaaij, "Modelling of a fluidized bed gasifier", E.C. contractors meeting, 1983.
268. P.K. Raman, W.P. Walawender, L.T. Fan, C. Chang, "Mathematical model for the fluidized bed gasification of biomass materials. Application to feedlot manure", Ind. Eng. C. Process Des. Dev. 20, 686-692, 1981.
269. C. Chang, L.T. Fan, W.P. Walawender, "Dynamic modelling of biomass gasification in a fluidized bed". In Fluidization and fluid particle systems, AIChE Symp. series No. 234, Vol. 80, 1983.
270. D. Bacon, J. Downie, I. Hsu, J. Peters, "Modelling of fluidized bed wood gasifier", Report to ENFOR, 1983.
271. V. Biba, J. Mkacak, E. Klose, J. Malecha, Industrial Engineering Chemistry, Process Design Development, Vol. 17, 92, 1978.
272. S. Sundaresan, N. Amundson, "Studies in char gasifciation, parts I, II, III, Chem. Eng. Science, Vol. 34, 345-364, 1979.
273. P.N. Rowe, Undergraduate course notes on fluidization, Department of Chemical Engineering, University College London, 1977.
274. J. Schoeters, Private communication, unpublished results, internal report, V.U.B., 1980.
275. F.A. Zenz, D.F.Othmer, "Fluidization and fluid-particle systems", Reinhold Publishing Corp. New York, 1960.
276. D.R. Richardson, Chemical Engineering 68, 83, May 1961.
277. J.M. Coulson, J.F. Richardson, "Chemical Engineering" Vol. 1, Pergamon Press London, 1970.
278. Internal V.U.B. report on testing various types of distributors
279. M. Leva, "Fluidization", McGraw Hill, New York, 1979.
280. B.D. Patridge, P.N. Rowe, "Bubble Phenomena in fluidized beds", Trans. Inst. Chem. Eng. 44, 335, 1966.
281. P.N. Rowe, A.W. Nienow, A.J. Agbim, "The mechanisms by which particles segregrate in gas fluidized beds-binary system of near spherical particles", Trans. Inst. Chem. Eng. 50, 310, 1972.
282. L.G. Gibilaro, P.N. Rowe, "A model for a segregating gas fluidized bed", Chem. Eng. Science, Vol. 29, 1403-1412, 1974.
283. P.N. Rowe, A.W. Nienow, in "Fluidization", Undergraduate course, University College London, 1977, also published.
284. K. Maniatis, "The minimum fluidization velocity of mixtures of particles of different size but of same density", 3rd year research thesis, University College London, 1977.

285. G. Socrates, "Thermodynamics and statistical mechanics", Butterworths, London, 1971.
286. FAO, "Charcoal making", Forestry paper 41.
287. D.M. Himmelblau, "Process analysis by statistical methods", John Willey and Sons Inc. New York, 1968.
288. A.V. Bridgwater, J.M. Double, D.M. Earp, "Technical and market assessment of biomass gasification in the UK", Vol. 1, Report to energy technology support unit, agreement no. E/5A/CON/1167/1338.
289. G.A. Weisgerber, S.P. Van der Heijden, "Cleaning wood gas for combustion", Canadian electrical association, report no. 4400-1979-1-Alternate energy, 1980.
290. MW. First, G.A. Jonson, R. Dennis, "Performance characteristics of wet collectors", Harvard Air Cleansing laboratory report, NYO 1587, 1953.
291. J. Davidson, "Coal combustion in fluidized bed reactors", presented at the 7th Annual general meeting of the European branch of the Institution of Chemical Engineers, The Hague, 1982.
292. R.C. Johnson, "Biomass feedstocks", data of Levelton Associates Ltd. Vancouver.
293. T.R. Miles, "Biomass preparation for thermochemical conversion, Ch. 5, in Thermochemical processing of biomass, ed. A.V. Bridgwater, Butterworths, 1984.
294. J. Broughton, J.R. Howard, "Combustion of coal in fluidized beds", Ch. 2 in Fluidized beds, combustion and applications, ed. J.R. Howard, Applied science publishers, London 1983.
295. K. Maniatis, "Characterization of waste arisings at SPANO N.V.", report to Vyncke Warmtetechniek, December 1981.
296. Vyncke Warmtetechniek, private communication, SPANO N.V. - Gazovif retrofit project, January 1982.
297. H.B. Mason, W.M. Toy, "Program development and design for gasifier central plant wood gasification and boiler retrofit to fire low BTU gases at the central heating and cooling plant, Sacramento, California", ACUREX final report 80-50/EE, April 1980.
298. N.I. Sax, "Dangerous Properties of Industrial Materials", 4th ed. Van Nostrand Reinhold Company, N.York 1975.
299. A.V. Bridgwater, "Worldwide markets for biomass gasification systems", Private communication 1986.
300. Coen Burner. Private communication 1986.